Photochemistry of Heterocycles

Maurizio D'Auria, Ambra Guarnaccio,
Rocco Racioppi, Sonia Stoia, Lucia Emanuele

PHOTOCHEMISTRY OF HETEROCYCLES

PHOTOCHEMISTRY OF HETEROCYCLES

MAURIZIO D'AURIA
University of Basilicata, Potenza, Italy

AMBRA GUARNACCIO
Institute of Structure of Matter (ISM) at the CNR-ISM, Tito Scalo, Italy

ROCCO RACIOPPI
University of Basilicata, Potenza, Italy

SONIA STOIA
ITT "16 Agosto 1860", Corleto Perticara, Potenza, Italy

LUCIA EMANUELE
Department of Art and Restoration, University of Dubrovnik, Dubrovnik, Croatia

ELSEVIER

Notices

Knowledge and best practice in this field are constantly changing. As new research and experience broaden our understanding, changes in research methods, professional practices, or medical treatment may become necessary.

Practitioners and researchers must always rely on their own experience and knowledge in evaluating and using any information, methods, compounds, or experiments described herein. In using such information or methods they should be mindful of their own safety and the safety of others, including parties for whom they have a professional responsibility.

To the fullest extent of the law, neither the Publisher nor the authors, contributors, or editors, assume any liability for any injury and/or damage to persons or property as a matter of products liability, negligence or otherwise, or from any use or operation of any methods, products, instructions, or ideas contained in the material herein.

For Information on all Elsevier publications
visit our website at https://www.elsevier.com/books-and-journals

Working together
to grow libraries in
developing countries

www.elsevier.com • www.bookaid.org

Contents

Preface

Ole Buchardt served as the editor of a volume bearing the title *Photochemistry of Heterocyclic Compounds* (J. Wiley & Sons, 1976) in 1976. After this book, nothing has been published in this regard. Over the last forty-six years, many things have changed, especially heterocyclic compounds and their photochemical behavior. For example, the current electronic devices use LEDs where heterocyclic compounds and their fluorescence emission are used. The photochromism of dietheroarylethene derivatives has been studied in detail, and many possible applications in the field of information storage or simply for the preparation of photochromic lenses are discussed. The conversion of sunlight into electricity is mainly based on the chemistry of heterocyclic compounds. The study of the photochemical behavior of a drug is mainly derived from the different possibilities of administering the drug. Heterocyclic compounds are used in many agricultural products, and their photochemical decomposition can have significant effects on the environment.

A gap of 46 years is such a long time period in terms of radical change of perspectives. Hence, this book is our humble contribution to update the existing literature on this topic.

Maurizio D'Auria

1

Photochemical synthesis of heterocyclic compounds

1

1.1 Introduction

Heterocyclic compounds are of enormous interest, especially in pharmaceutical chemistry. In fact, the majority of current drugs contains a heterocyclic ring. Despite the great importance of these compounds, only few methods exist for the synthesis of heterocycles using photochemical method though photochemical reactions are often easy to realize, clean, and environmentally benign. Among the various methods to build a heterocycle, cyclization of linear compounds, [x + y] cyclization and ring closure are the major ones. The research in this field has significantly increased compared to the past, to discover new methods and clarify the reaction mechanisms.

The aim of this chapter is to explore the photochemical synthetic methods for the synthesis of the most common heterocyclic compounds.

1.2 Azetidines

1.2.1 Synthesis by aza Paternò–Buchi reaction

The aza Paternò–Buchi reaction is a photochemical reaction between an alkene and an imine or an oxime. Not much information exists in the literature about this reaction. Becker et al. developed a method for an intra molecular aza Paternò–Buchi reaction in which in the same molecules a double bond and an oxime are present to obtain a bicyclic azetidine (Fig. 1.1).[1]

Usually, these reactions are difficult, because the preferred reaction is the *E/Z* isomerization of imine or oxime, and are limited to rigid systems with irradiation with high energy UV radiation. The use of a catalyst (PF_6) permits to use visible light via a triplet energy transfer to the double bond of the alkene. Control reactions revealed that both light and photocatalyst were necessary for the [2 + 2] photocycloaddition to proceed.

Other substrates with the same basic structure were investigated. In every case, the reaction procedes well with high yield (up to 98%) and excellent diastereoselectivity (20:1). Furthermore, it is independent from the *E/Z* configuration of the oxime.[2]

In 2020, the same research group pointed its attention to intermolecular aza Paternò–Buchi reactions.[3] The first difficulty encountered was that the excited alkene has a too short lifetime before reacting with an oxime. So, the choice was to select a cyclic oxime that cannot give *E/Z* isomerization (Fig. 1.2).
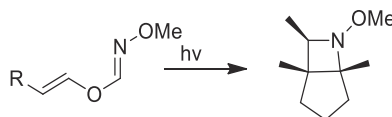
FIGURE 1.1   Intramolecular aza Paternò–Buchi reaction.
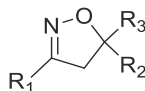
FIGURE 1.2   Cyclic oxime.

The catalyst of choice was always PF_6. An example is given in the Scheme 1.1.
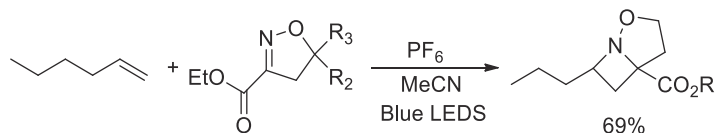
SCHEME 1.1   Azetidine from cyclic oxime.

Many azetidines were synthesized in this way, in some cases with excellent regio and diastereoselectivity.

1.2.2 Synthesis by intramolecular closure of N-formil-α-oxoamides

Irradiation of a benzene solution of *N*-formyl-*N*-methylbenzoylformamide with a high pressure mercury lamp gave a cyclization product, 3-hydroxy-1-methyl-3-phenylazetidine-2,4-dione.[4] When other *N*-formyl-α-oxoamides were irradiated under the same conditions, the corresponding cyclic imides were obtained (Scheme 1.2).

R = Me, Et, *n*-Pr, Bz, Ph
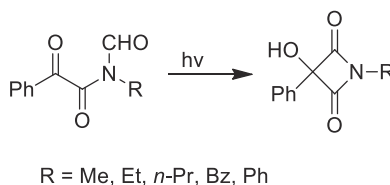
SCHEME 1.2   Intramolecular closure of *N*-formil-α-oxoamides.

The formation of azetidine is rationalized in terms of hydrogen abstraction by the ketone carbonyl from the formyl group and subsequent cyclization of the resulting 1,4 diradical (Fig. 1.3).

1.2.3 Synthesis by Norris-Yang rearrangement

Another simple way to construct 3-hydroxy azetidines is described by Baxendale et al.[5] A simple acyclic 2-amino ketone following photochemical excitation involving a n → π* transition with formation of a diradical that abstracts a proton from one of the available sites (usually the δ-proton) leading to a new diradical which can combine to form the cyclic product (Scheme 1.3).
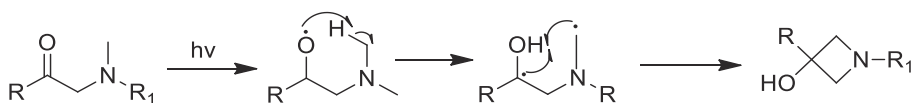
SCHEME 1.3   Norris-Yang rearrangment.

Performing the reaction in batch, often long reaction times and very dilute conditions are necessary. So the reaction was performed with a flow reactor at a speed of 1 mL/min. This permits to obtain conversion up to 95% and isolated yields of 70%/80%. Concerning the used wavelength an analysis of UV spectra shows that the n → π* transition corresponds to about 300 nm so a suitable filter was used. About the chosen substrate, the authors find the best results when nitrogen is derivatized as sulfonamide (Fig. 1.4).

R = Me, Et, *n*-Pr, Bz, Ph
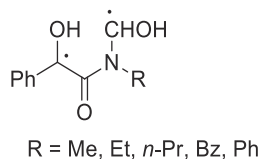
FIGURE 1.3   Diradical intermediate in the reaction of Scheme 1.2.
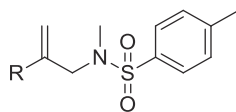
FIGURE 1.4 Sulfonamide used in Scheme 1.3.

About 30 compounds of this kind were prepared and submitted to photochemical reaction. The isolated yields vary from moderate to excellent. The lowest yields were obtained when R was an orto chloro or bromo phenyl. Maybe, it can be due to a lack of planarity in the transition state between phenyl and carbonyl.

1.2.4 Reaction between fullerene and formamidines

Fullerene (C60) is a very interesting molecule, non only for its shape, but also for the possibility that fuctionalized fullerenes could have biological activity.[6] The authors report novel fullerene derivatives having an azetidinimine framework and characterized the product. The reaction (Scheme 1.4) was performed using *N,N'*-bis(2,2-dialkylphenyl)formamidines and a wavelength > 400 nm.

1a: R_1 = R_2 = H
1b: R_1 = H, R_2 = Me
1c: R_1 = R_2 = Me
1d: R_1 = R_2 = Et
1e: R_1 = R_2 = *i*-Pr
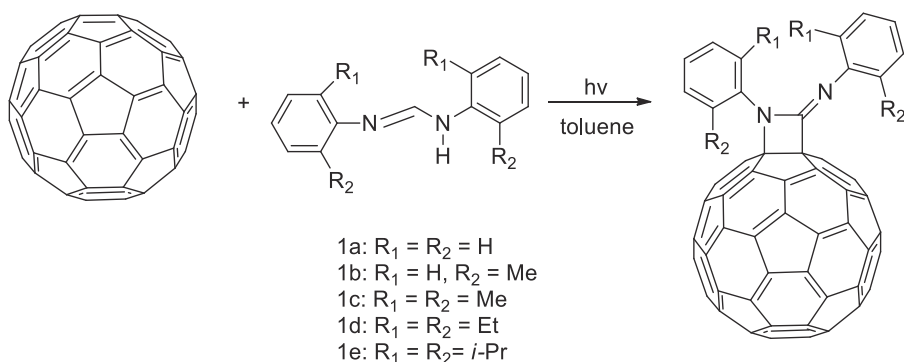
SCHEME 1.4 Reaction of fullerene.

The reaction did not proceed when **1a** or **1b** was used because of their poor solubility in the solvent that was used (toluene). Moreover, the reaction did not proceed in the absence of oxygen.

In this regard, the reaction mechanism can be proposed as shown in Scheme 1.5. Initially, a single electron transfer occurred from the formation of a stable C60 anion radical and an amidinium cation radical through an electron transfer from a formamidine. Once generated, the C60 anion radical reduces molecular oxygen to generate superoxide anion radical. C60 and an amidinium cation react together to form a protonated intermediate. The superoxide anion then deprotonated radical; the resulting O_2H^- must be a sufficiently powerful oxidant to convert the intermediate into azetidinimine.
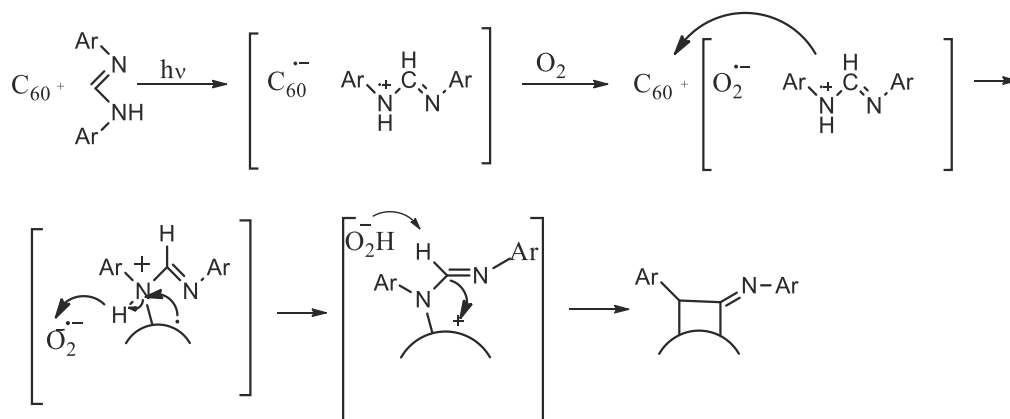
SCHEME 1.5 Mechanism of the reaction.

1.2.5 Synthesis by ciclization of amino ketones

Azetidines can also prepared in optically pure form starting from amino ketones.[6] After a series of synthetic steps, compound A was prepared and submitted to irradiation to obtain an azetidine with configuration *2R* (Scheme 1.6).
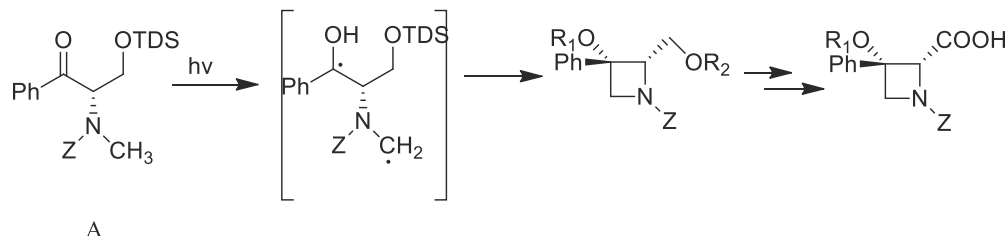
SCHEME 1.6   Azetidines from amino ketones.

For the synthesis of *2S* enantiomer, it was started from serine, that was submitted to a series of synthetic steps: in analogous matter, it is possible to obtain the enantiomer of the azetidine carboxylic acid with configuration *2S* (Scheme 1.6).

1.3 Aziridines

1.3.1 Synthesis by rearrangement of pyridinium salts

Aziridine can be obtained by rearrangement of pyridinium salts also in a diastereoselective manner.[7,8] An example is outlined below (Scheme 1.7).
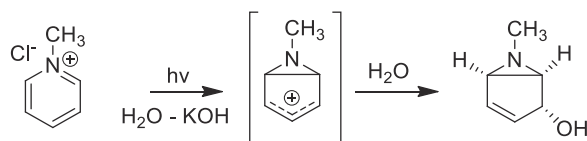
SCHEME 1.7   Rearrangment of pyridinium salts.

If the aziridine is treated with a nucleofile, in some cases it is possible the opening of aziridine ring to afford a cyclopentene (Scheme 1.8).
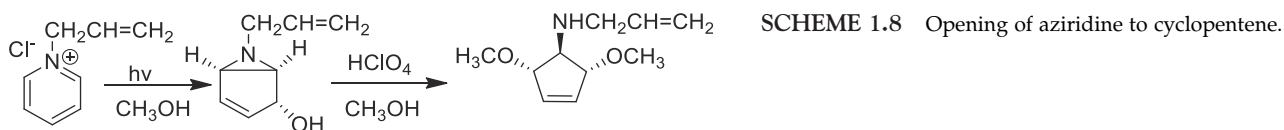
SCHEME 1.8   Opening of aziridine to cyclopentene.

The reaction works well also with tetrahydroquinolines (Fig. 1.5).
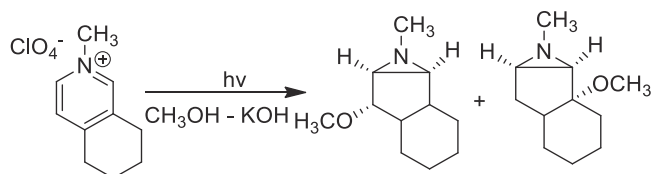
FIGURE 1.5   Reaction of tetrahydroquinolines.
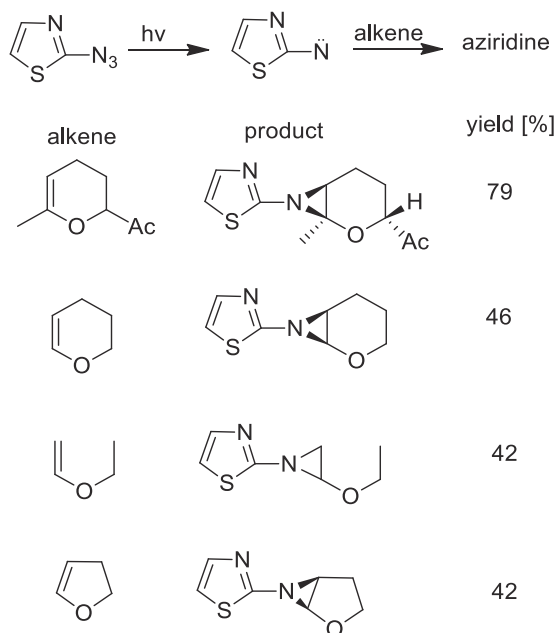
FIGURE 1.6   Synthesis of aziridines from enol ethers.
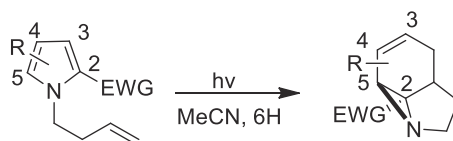
FIGURE 1.7   Aziridines from homoallyl pyrroles.

The reaction furnishes almost exclusively aziridines in the case in which reaction is performed in a basic medium. Thus, it allows to minimize the ring opening to cyclopentene.

1.3.2 Synthesis by insertion of nitrene into double bonds

When 2-azido-1,3-thiazole reacts with a double bond, a triplet nitrene is formed, which can insert in the double bond to form an aziridine.[9] The reaction works particularly with enol ethers (Fig. 1.6).

1.3.3 Synthesis from homoallylpyrroles

In 2016, Blackam and coworkers synthesized a set of homoallylpirroles, with the aim to obtain a methatesis reaction, as it happened for pyrroles alkyl substituted with a longer chain.[10] With their great surprise the products obtained were aziridine. In the figure below is obtained the general outcome of reaction (Fig. 1.7).

The reaction proceeds with good yields. The only requirement is the presence of an EWG group in position 2 of pyrroles. Varying the grade of substitution, it is possible to obtain very complex molecules with quaternary centers. A proposed mechanism is the following: the excitation of the generic pyrrole substituted with an EWG at C2 results in an initial [2 + 2] cycloaddition across the C2−C3 bond to give a cyclobutane. Then the formation of a biradical happens, and this latter undergoes C2−C5 to afford the aziridine (Scheme 1.9).

SCHEME 1.9   Mechanism of the reaction.

The reaction is scalable-up. Using a battery of flow reactors, it is possible to obtain up to 100 g per day of aziridine.

1.3.4 Synthesis by rearrangement of triazolines

Usually, photochemical reactions are performed in solution. De Loera et al. tried instead to make the reaction in solid phase.[11] The reaction starts from a triazoline to obtain, after loss of nitrogen, an aziridine. The reaction can be followed monitoring the development of gaseous nitrogen. The mechanism of denitrogenation of triazoline is reported in the Scheme 1.10.
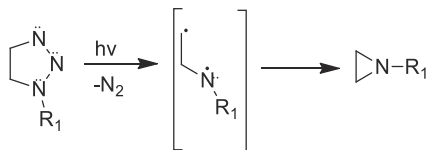
SCHEME 1.10   Mechanism of the reaction.

The triazolines were obtained by [1,1] dipolar cycloaddition between maleimide and substitute phenylazides, and then irradiated with a medium pressure Hg lamp whit a quartz filter (Scheme 1.11 and 1.12).
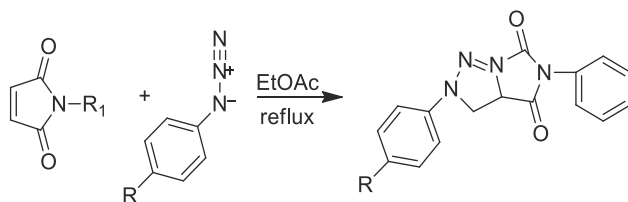
SCHEME 1.11   [1,1] dipolar cycloaddition between maleimide and substitute phenylazides.
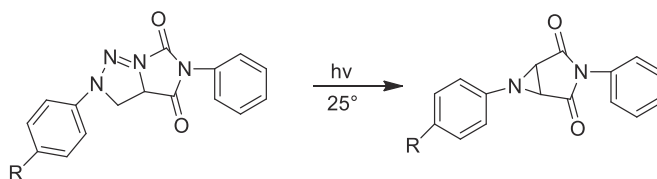
SCHEME 1.12   Obtaining of the aziridine.

1.3.5 Synthesis of aziridines by visible-light induced decarboxylative cyclization of N-aryl glycines and diazo compounds

The authors envisioned that the visible-light photoredox-mediated decarboxylation of *N*-aryl glicine would afford an α-amino alkyl radical which could be further oxidized in the presence of oxygen to generated active imine.[12] The attack of imine by diazo compounds would lead to intermediate A. Intermediate A containing a negative amine anion might undergo an *exo-tet* cyclization, which ultimately form aziridine as the product (Fig. 1.8). The reaction is complete after 60 min with a yield of 80%.

After various tentative, the authors found the best condition for the reaction: Rose Bengal as catalyst, methanol, O_2, r.t and blue LEDS.

FIGURE 1.8   Reaction of *N*-arylglicine.

2a: R = 4-MeC$_6$H$_4$

2b: R = 2-NO$_2$C$_6$H$_4$

2c: R = Py
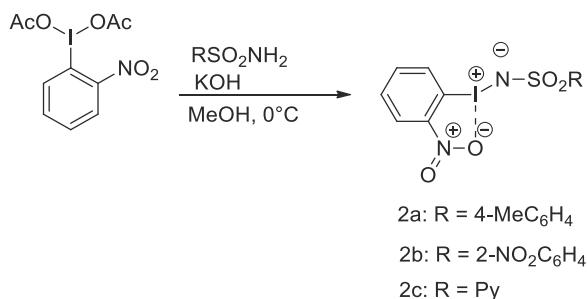
FIGURE 1.9 Synthesis of iminoiodinanes.
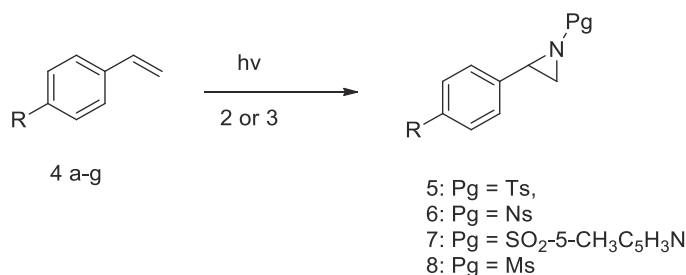
FIGURE 1.10 Synthesis of aziridines *via* imidoiodinanes.

4 a-g

5: Pg = Ts,
6: Pg = Ns
7: Pg = SO$_2$-5-CH$_3$C$_5$H$_3$N
8: Pg = Ms

1.3.6 *Photoinduced aziridination of alkenes with N-sulfonyliminoiodinane*

N-Sulfonyliminoiodinanes are powerful catalysts for the photoinduced aziridination of alkenes. They can easily synthesized from 2-nitroiodobenzene diacetate and the corresponding sulfonamide (Fig. 1.9).[13]

In the same way were synthesized iminoiodinane **3a-c** (Scheme 1.13).

3a: Pg = Ts
3b: Pg = Ns

3c:
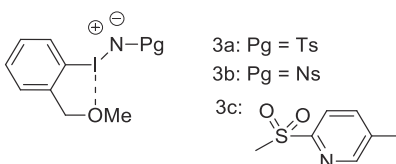
SCHEME 1.13 Synthesis of iminoiodinane.

With these reactants in hand, the authors tried photochemical reaction at 0°C with LEDs at 375 nm (Fig. 1.10).

The reaction of styrene **4a** with **3a** gave aziridine **5a** in 73% yield, while the same reaction with **2a** improved chemical yield up to 98%. Other examples are reported in Scheme 1.14.

SCHEME 1.14 Other examples.

5b, 72%
with 2a

5c, 55%
with 2a

8c, 68%
with 2a

5d, 44%
with 2a
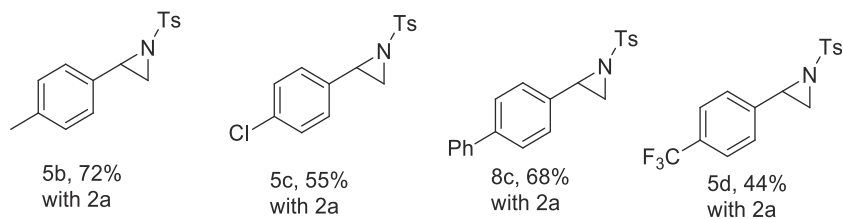
1.3.7 *Photochemical aziridination of fullerenes*

Fullerenes are very interesting compounds from a chemistry of heterocycles point of view because they are able to incorporate heteroatoms by reactions of cycloadditions.[14,15] In particular, fullerene can thermally

incorporate aryl azides to give triazolines which in turn can photochemically extrude nitrogen to give aziridino-fullerene (Scheme 1.15).
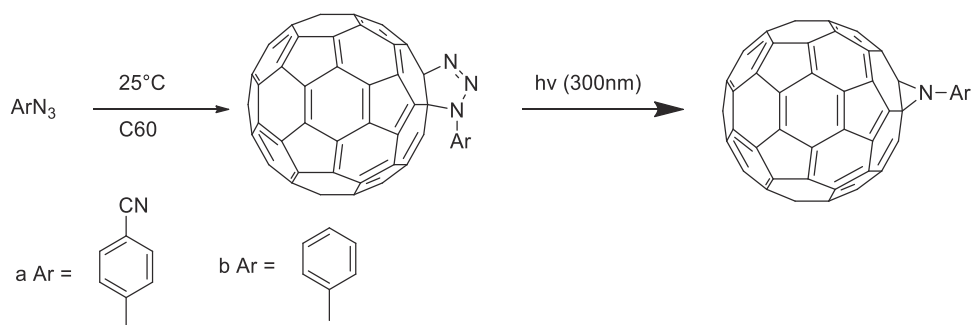
SCHEME 1.15   Synthesis of azidofullerenes.

The aziridination process was not disturbed by the introduction of group such an alkyl, ester, ketone, and fluorine.

1.3.8 Synthesis from sugar derivatives and azides

Amino sugars are component of vary compounds of great importance in medicine. Among these, daunosamine and ristosamine are component of a family of antibiotics (Fig. 1.11).

Many syntheses exist of these compounds, but only in one case an aziridine is present in a crucial synthetic step.[16] The synthetic passages for the synthesis of daunosamine glicoside are showed in Scheme 1.16.
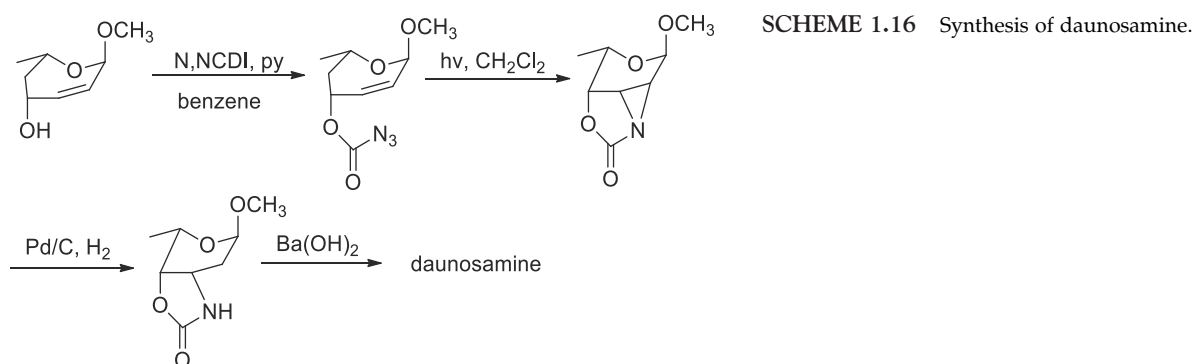
SCHEME 1.16   Synthesis of daunosamine.

1.3.9 Synthesis from azides by photocatalysis

In a work concerning the synthesis of pyrrole derivatives, certain particular substrates, with a double bond near an azide group, can react to give aziridines, at the condition that be used the appropriate photocatalyst [Ir (df(CF$_3$)(ppy)$_2$(dtb bpy)]PF$_6$ (Scheme 1.17).[17]
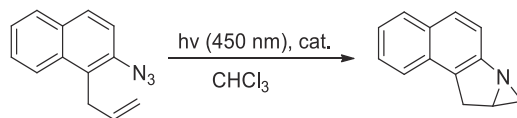
SCHEME 1.17   Pyrrole derivatives from azido group.
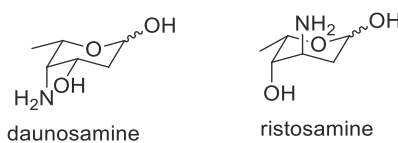
FIGURE 1.11   Daunosamine and ristosamine.

1.3.10 Synthesis from azidoformates

Aziridines can also be obtained by azidoformates. It interesting to note that when the substituent in *ortho* position in the phenyl ring is H or alkyl the products obtained are amido esters (Fig. 1.12).[18]

On the contrary, when the substituent is an allyl, the reaction takes a completely different way with formation of aziridines (Fig. 1.13). Other examples are reported in Fig. 1.14.

1.4 Diazepines and benzodiazepines

1.4.1 Synthesis from 4-pyridyl azides

Among the three isomers of diazepines, only 1,2- and 1,3-diazepines are well known in the literature. The synthesis of less substituted 6H-1,4-diazepines from 4-pyridyl azides by irradiation in the presence of methoxide ion has been described. The starting 4-azidopyridines were prepared from the corresponding 4-chloropyridines by treatment with hydrazine hydrate followed by diazotization (Fig. 1.15).[19]
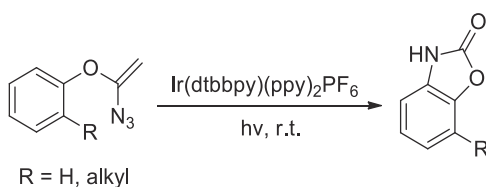
FIGURE 1.12   Reaction of azidoformates.
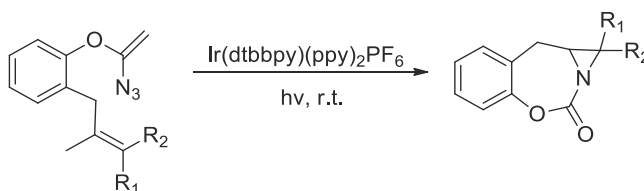
FIGURE 1.13   Azidoformate having an allyl group.
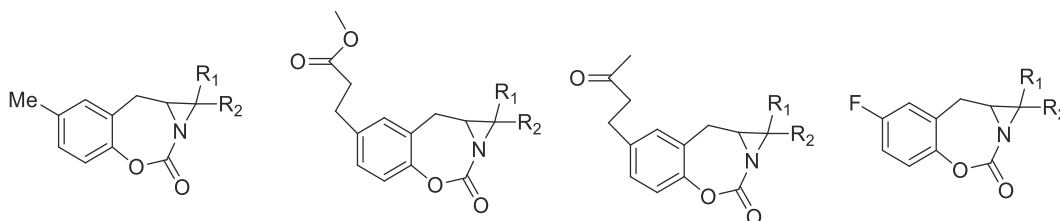
FIGURE 1.14   Other examples of the synthesis of aziridines through azidoformates.
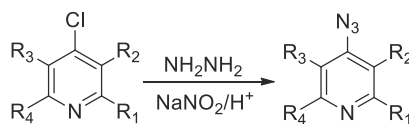
a: $R_1 = R_2 = R_3 = R_4 = H$
b: $R_1 = Me$; $R_2 = R_3 = R_4 = H$
c: $R_1 = H$; $R_2 = Me$; $R_3 = R_4 = H$
d: $R_1 = Me$; $R_2 = R_3 = H$; $R_4 = Me$
e: $R_1 = H$; $R_2 = R_3 = Me$; $R_4 = H$

FIGURE 1.15   Diazotization of pyridine derivatives.
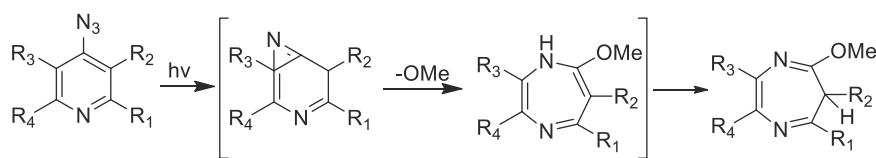
FIGURE 1.16   Synthesis of 1,4-diazepines.
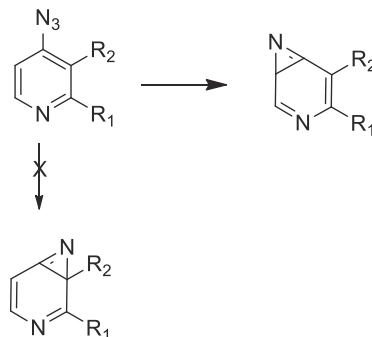
FIGURE 1.17   Possible intermediates in the synthesis of 1,4-diazepines.

Irradiation (400 W, high pressure Hg lamp; pyrex filter) (Fig. 1.16) of the azides resulted in the formation of the desired 6H-1,4-diazepines in 35%−70% yields, as the sole ring expansion products.

Unsymmetrical azides may ring close in either of two direction to afford two isomeric products. However, the authors observed the formation of a sole product as depicted in Fig. 1.17.

In the same way, the authors synthesized some 1H-2,4-benzodiazepines.[20] The synthetic routes to the starting 4-azidoquinolines are depicted in the Scheme 1.18.
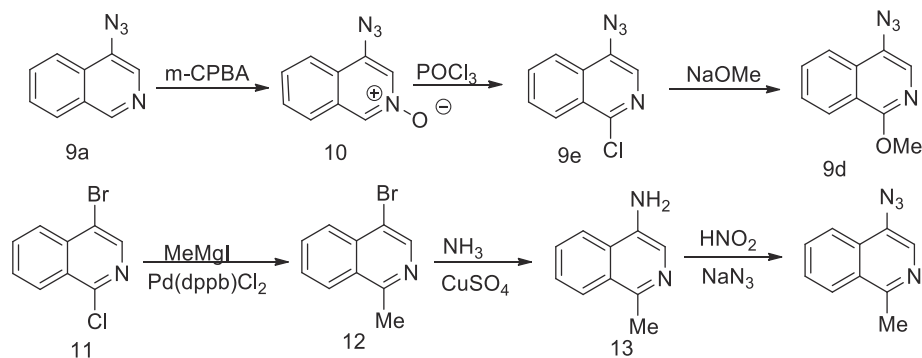
SCHEME 1.18   Synthesis of the starting azidoquinolines.

Irradiation of the azides (9a-e) in methanol-dioxane containing sodium methoxide for 30−40 min resulted in the formation of the desired 2,4-benzodiazepines (14a-e) in 45%−70% yields, as the sole ring-expansion products. In the case of the 1-chloroisoquinoline (9e), the chlorine atom was replaced by methoxide under the present basic reaction condition to afford the same 1-methoxydiazepine (14d) as that obtained from 9d. The mechanism of formation of benzodiazepines is reported in Scheme 1.19.
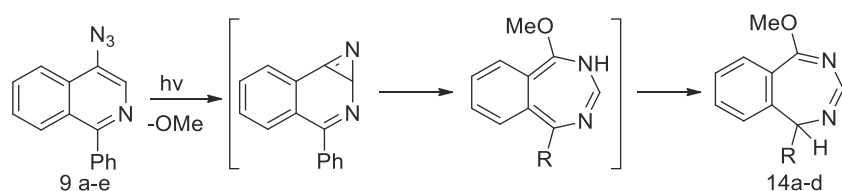
SCHEME 1.19   Mechanism of the reaction.
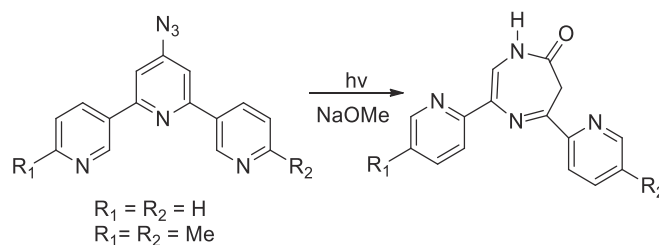
FIGURE 1.18   Synthesis of diazepinones.

Azido terpyridines can photochemically converted in diazepinones (Fig. 1.18).[21] If R_1 is different from R_2, both isomers of diazepinones were obtained.

1.5 Furans

1.5.1 Furans from α-bromo-β-dicarbonyl compounds and alkynes

An unusual reaction permits to obtain furans from α-bromo-β-dicarbonyls and alkynes.[22] The reaction occurs with visible light and a complex of iridium as catalyst, according to the Scheme 1.20.
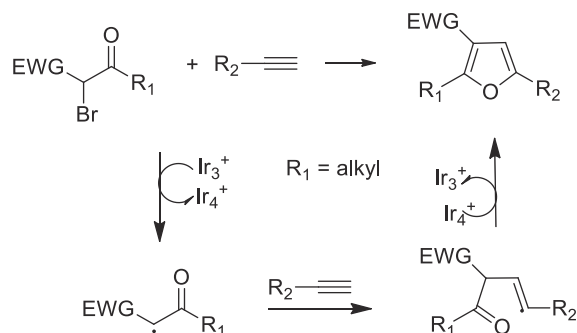
SCHEME 1.20   Furans from α-bromo-β-dicarbonyls and alkynes.

The reaction works well if R_1 is an alkyl while, if it is an aryl, a naphthol is obtained. Another example is reported in Scheme 1.21. The yields vary from good (40%−50%) to excellent (80%−90%).
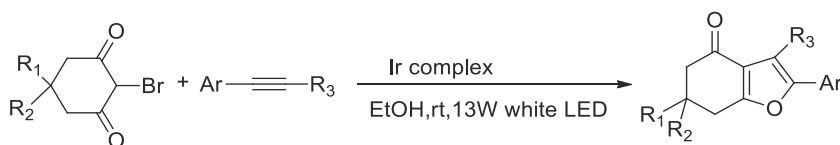
SCHEME 1.21   Another example.

1.5.2 Benzofurans from 2-chlorophenols and alkynes

2-Substituted benzofurans were synthesized by a one-step metal-free photochemical reaction between 2-chlorophenol derivatives and terminal alkynes by tandem formation of an aryl−C and a C−O bond via an aryl cation intermediate.[23] A reasonable mechanism for this reaction is depicted in Scheme 1.22.
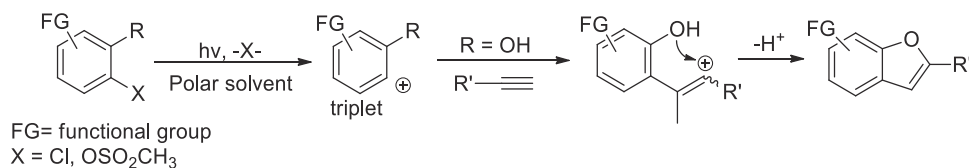
SCHEME 1.22   Reaction of 2-chlorophenol derivatives.

The first part of this study aimed to individuate the condition for a successful synthesis by using the reaction of 2-chlorophenol in presence of 1-hexyne under different conditions. The best solvent revealed to be 5:1 MeCN/water in presence of acetone which acts as a triplet sensitizer. This consents to maximize the yields (42%−49%) and to minimize the formation of the main by-product (phenol). The yield of benzofurans further increased when starting from 4-*t*-butyl-2-chlorophenol. Furthermore, good yields (up to 85%) were obtained when oxygen based substituent, such a methoxy or an hydroxyl group, were introduced. Finally, acceptable yields were obtained also by using trimethylacetylene instead of 1-hexyne.

1.5.3 Dihydro and tetrahydrofurans from cyclopropane derivatives

The photochemistry of cyclopropane involves mainly the *cis-trans* isomerization. In few cases, with suitable substituents, a ring expansion could happen to cyclopentenes or furan derivatives.[24] A series of derivatives starting from ethyl chrysantemates was sinthesized (Fig. 1.19).

When the reaction is triplet sensitized with benzophenone, compound **16** gives only recovered material and a cyclopentene. The same was observed with **16b**, **16c**, and **16d**, that, besides cyclopentene, affords also furan derivatives **19** and **20** (Fig. 1.20).

Oxime **16e** does not react, giving only a mixture of diastereoisomers. Alcohol **16f** gives a mixture of highly polar compounds which does not were identified. It was also tried to make the reaction without sensitizer. **16a** furnishes a mixture of stereoisomer of the starting product and a 19% of 2-furanone **21** (Fig. 1.21).

Ketone **16d** does not give the cyclopentene derivative observed in in the triplet-sensitized reaction but produces the tetrahydrofuran **20** (19%) along with starting material.

15a: R = H
15b R = Et

16a,17a,18a: R = CO₂Et
16b,17b,18b: R = CO₂H
16c,17c,18c R = CHO
16d,17d, 18d: R = COMe
16e,17e,18e: R = CH=NOH
16f,17f: R = CH₂OH
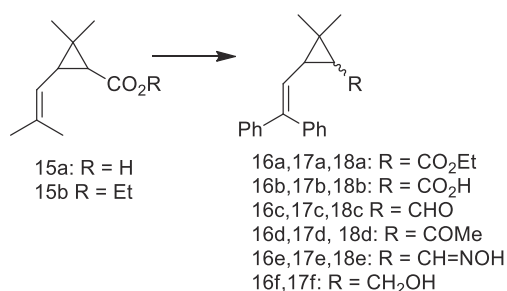
FIGURE 1.19   Derivatives of chrisanthemates.

19a: R = H
19b R = Me

20a: R = H
20b R = Me
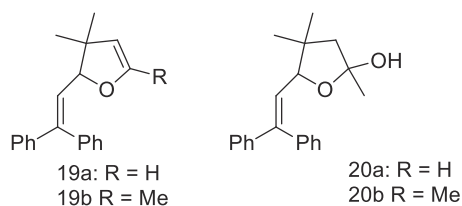
FIGURE 1.20   Dihydro and tetrahydrofurans from cyclopropane derivatives.

21
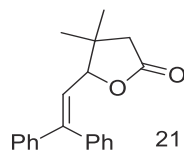
FIGURE 1.21   2-Furanone obtained from **16a**.
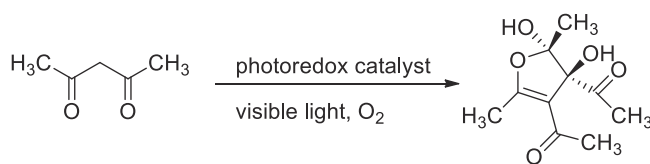
FIGURE 1.22   Dimerization of acetylacetone.
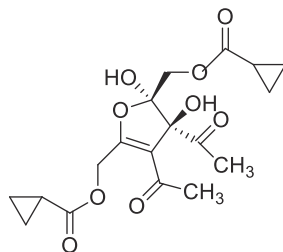
FIGURE 1.23   A more complex example.

1.5.4 Dihydrofuran from photodimerization of β-carbonyl ketones

Highly functionalized furans can be obtained by aerobic oxidative dimerizative annulations of β-carbonyl ketones (Fig. 1.22).[25]

A plausible mechanism of reaction should be that reported in Scheme 1.23.
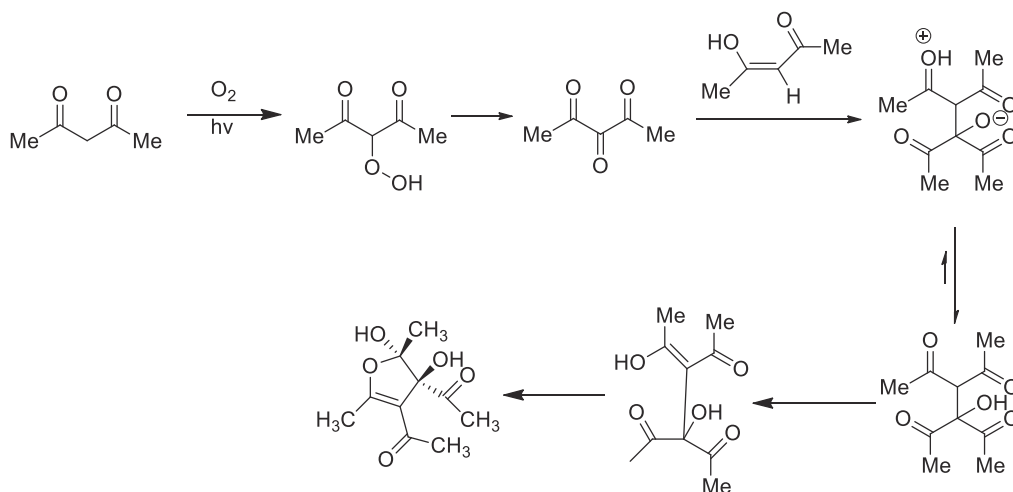
SCHEME 1.23   Mechanism of the reaction.

The reaction occurs irradiating the mixture with blue LEDs under oxygen, and, in some cases, excellent yields can be obtained adding 4 Å molecular sieves. Another example of this procedure is reported in Fig. 1.23.

1.5.5 Tetrasubstituted furans from silylenolethers and α-bromo diketones

The same authors that obtained furans from α-bromo-β-dicarbonyl compounds and alkynes used instead of alkynes silyl enol ethers (Scheme 1.24).[26]
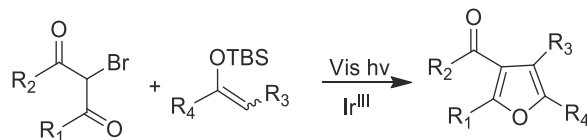
SCHEME 1.24   Reaction with silyl enol ethers.

This way some problems observed in the previous reactions have been avoided, including the fact that it is necessary to utilize a terminal alkyne to have an acceptable yield. Regarding the photocatalyst, the best was (Ir[df(CF$_3$)ppy]$_2$(bpy))PF$_6$. The reaction was performed in methanol containing Na$_2$HPO$_4$, to obtain tetrasubstituted furans with good yields.

1.5.6 Synthesis of 5H-furanones from substituted cyclobutenones

A photochemical rearrangment of cyclobutenones can be realized in near quantitative yields using a continuous flow reactor and low-energy lamps.[27] The reaction proceeds by an intermediate ketene as shown in Scheme 1.25.
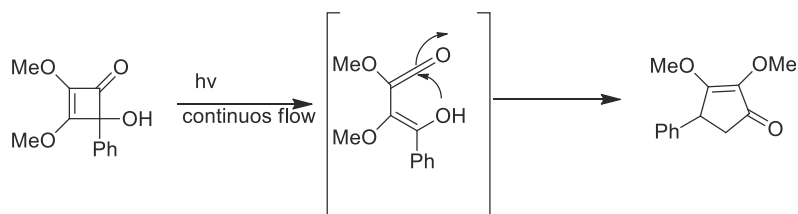
SCHEME 1.25   Rearrangment of cyclobutenones.

The yields of this reaction are comparable to those described in literature (medium-good). However, replacing the current solvent with acetonitrile raise up the yields to nearly quantitative values. The yields in all cases are very satisfactory, regardless of the nature of substituent.

1.5.7 Photochemical catalytical synthesis of dihydrofurans from vinyl and aryl cyclopropanes

The Fe-catalyzed Cloke–Wilson rearrangement is a reaction that can be performed on vinyl and arylcyclopropanes catalyzed by a complex of Fe (Fig. 1.24).[28] This reaction can be obtained in both thermal or photochemical way.

The used catalyst was Bu$_4$[Fe(CO)$_3$NO)]. The best conditions for the reaction were MeCN as solvent, room temperature, and a 180 nm Hg lamp, although in some cases the reaction works also with a 23 W lamp. It was demonstrated that this reaction is a non-decarbonilative process, that is, the iron complex does not lose CO. It was also demonstrated that the reaction is enantioselective (Fig. 1.25).

1.5.8 Tetrahydrofurans from cyclobutanones and nitrile compounds

Structurally modified nucleosides in which a methylene carbon replaces the oxygen of furanose (carbocyclic nucleosides) have been investigated for their medicinal properties. The glycoside bond becomes more resistant to
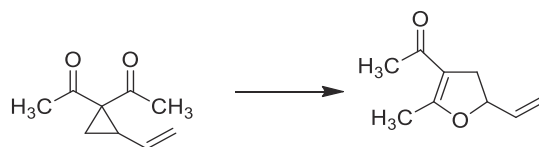
FIGURE 1.24   Cloke–Wilson rearrangment.
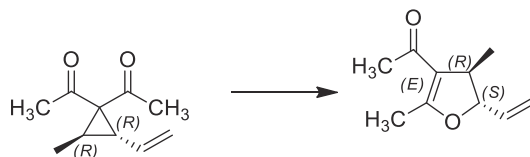
FIGURE 1.25   Enantioselectivity of the Cloke–Wilson rearrangement.

nucleoside phosphorylase and hydrolase degradation. The photochemical isomerization of cyclobutanones to the corresponding oxacarbene has been used as a synthetic route to nucleosides (Scheme 1.26).[29]
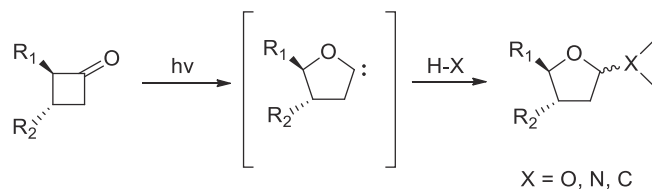
SCHEME 1.26　Isomerization of cyclobutanones.

The generated carbene can react with HCN or malononitrile to afford the corresponding derivatives (Scheme 1.27).

SCHEME 1.27　Reaction of carbene with HCN or malononitrile.

R = TBDMS
R$_1$ = H, Me
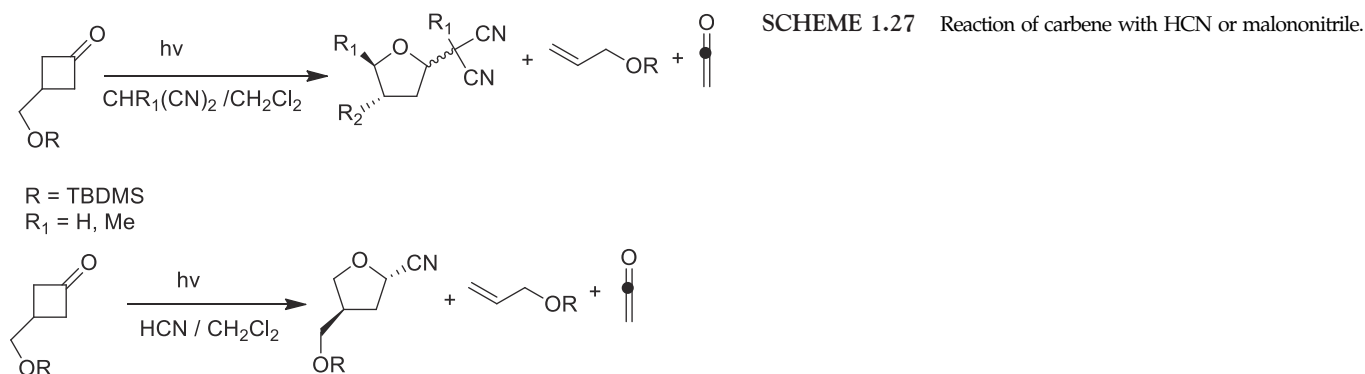
A series of subsequent chemical transformation (not photochemical) allows to obtain a modified nucleotide (Fig. 1.26).

1.5.9 Reaction of propargyl derivatives with alkenes

Acetylenic α-diketones can react, via intermediate carbenes, with alkenes to afford furan derivatives (Scheme 1.28).[30]

R' = R" = CH$_3$
R' = C$_6$H$_5$　R" = CH$_3$
R' = CH$_3$　R' '= C$_6$H$_5$
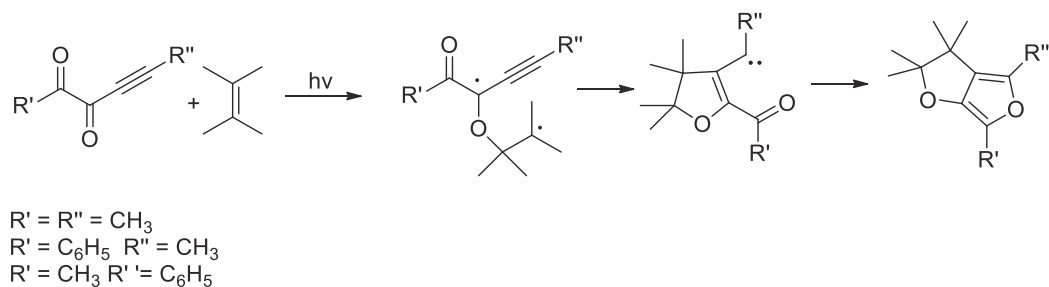
SCHEME 1.28　Reaction of acetylenic diketones.
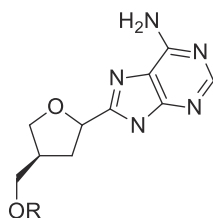
FIGURE 1.26　A modified nucleotide.
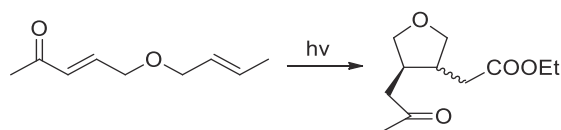
FIGURE 1.27   Tetrahydrofuran from α,β-unsaturated ketone.

The same reaction happens with isobutylene (Scheme 1.29).
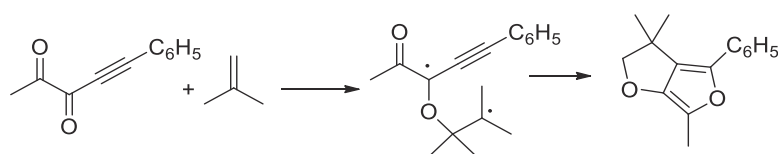
SCHEME 1.29   Reaction of isobutylene.

1.5.10 Tetrahydrofurans from α,β-unsaturated ketones

In a work devoted to study the formation of vary compounds by oxidoreductive cycles, there is only one example of formation of a tetrahydrofuran, while the other compounds are carbocyclic derivatives (Fig. 1.27).[31]

1.5.11 γ-Lactones from allylic alcohols and α,β-unsaturated keto ester

The selective divergent all-photochemical syntheses of levulinate and butanolide derivatives using simple starting materials has been reported.[32] Following a UV-A photoinduced cross-methathesis reaction, UV-C irradiation generated the desired products. Phenanthrene acts as an UV-C modulator: its presence or not directs the reaction toward butenolides or levulinates (Scheme 1.30).
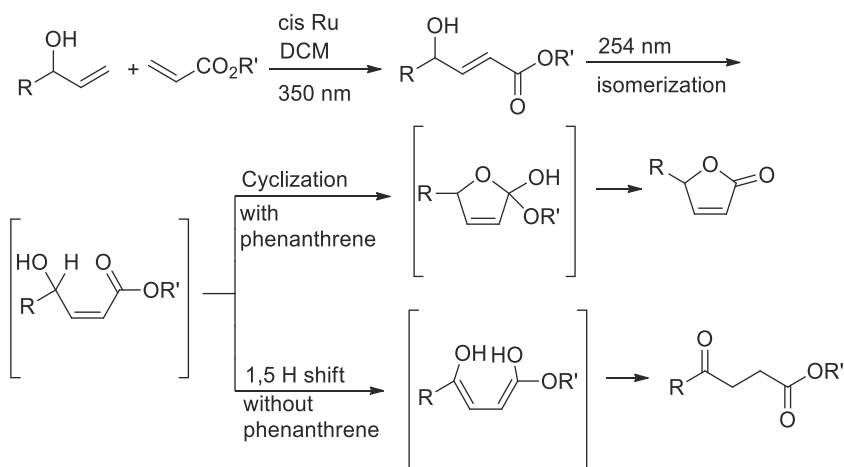
SCHEME   1.30   Cross   methatesis   and butenolides.

The first reaction (metathesis) needs the use if a *cis*-Ru(I) complex which, anyway, does not work well with more complex substrates. In this case it can be used a *cis*-Ru(II) complex.

1.5.12 Synthesis from cinnamic acid and ketones

Among recent procedures to obtain furans in photochemical way it is interesting the work of Rai et al., which is based of cinnamic acid, a ketone and nanoparticles of $CoFe_2O_4$.[33] Moreover, the reaction is performed in water, and that is a greener alternative to the use of solvents. The general scheme for the reaction is depicted in Scheme 1.31.

R = H, Me, Et, Ph
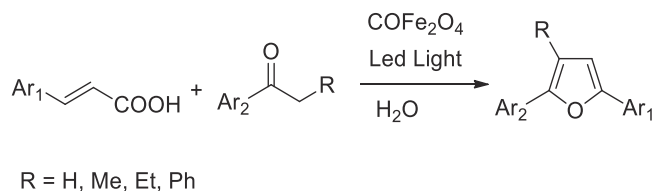
SCHEME 1.31   Reaction between cinnamic acid and ketones.
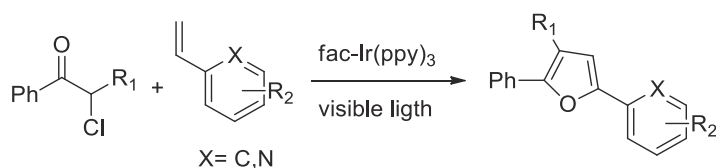
FIGURE 1.28 The reaction of α-chloro ketones with alkenes.

X= C,N
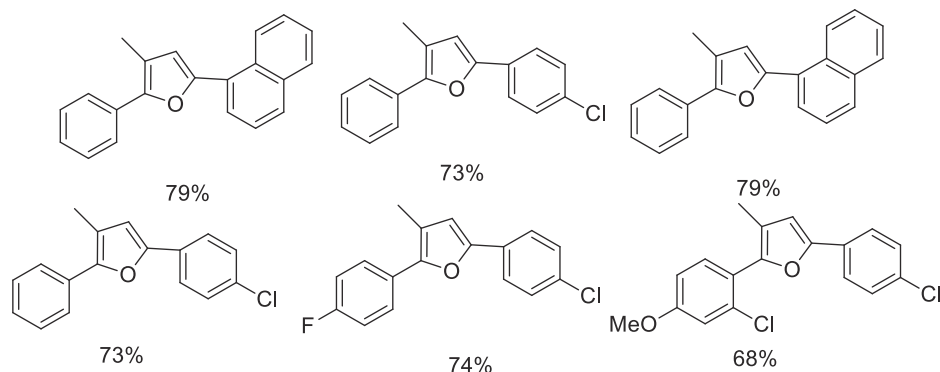
FIGURE 1.29 Examples of products obtained in the reaction of Fig. 1.28.

79%

73%

79%

73%

74%

68%

The yields are very high (80%−90%). In some experiments, the reaction can happen also without catalyst or irradiation, but the yields are lower. Interestingly, the catalyst can be recycled and reused up to seven times without loss of catalytic activity.

1.5.13 Synthesis from α-chloro alkyl ketones and styrenes

A simple, environmentally benign, and general method for the synthesis of substituted furans starting from a-chloroketones, styrene, a photocatalyst, an oxidant and a base has been recently reported (Fig. 1.28).[34]

It was first found the best condition using 2-chloro-1-phenyl-propan-1-one and styrene in MeCN, the photocatalysis, and various oxidant and bases. The better yields were obtained in DMSO, the same catalyst, 2,6 lutidine as base, $K_2S_2O_8$ as oxidant. In this case, the yield of 84% has been obtained. Later, they tried with substituted styrenes and α-chloro aryl ketones. The yields vary between good and excellent. Some examples are reported in Fig. 1.29.

A possible mechanism for this reaction is based on single electron transfer (SET) (Scheme 1.32).
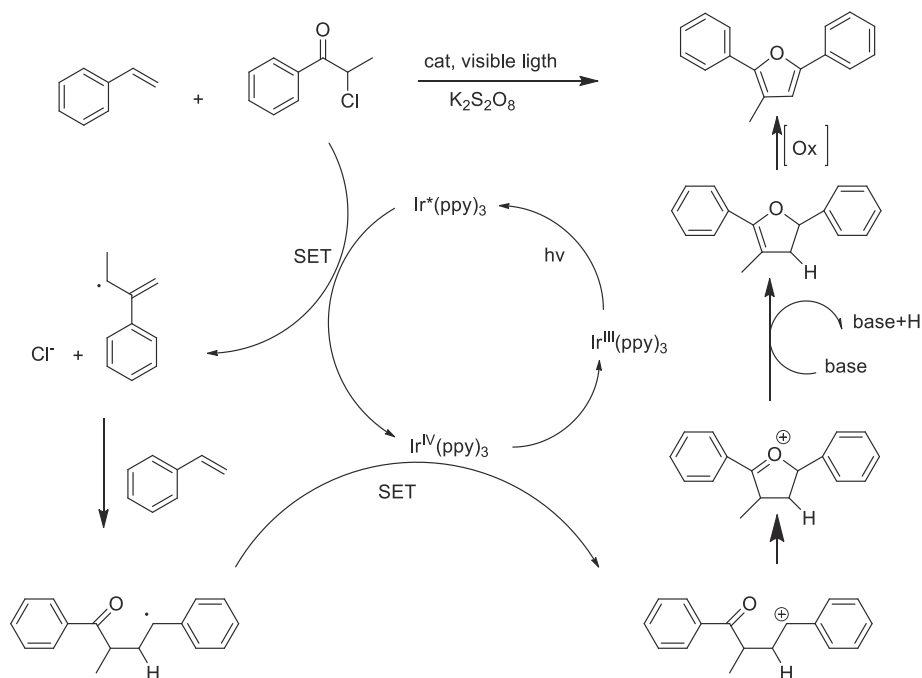
SCHEME 1.32 Mechanism of the reaction.

1.5.14 Synthesis by isomerization of alkenes

Alkenes, obtained easily by cross methatesis, can isomerizes from *E* to *Z* and then aromatize to furans (Scheme 1.33).[35]

SCHEME 1.33   Cross methatesis.
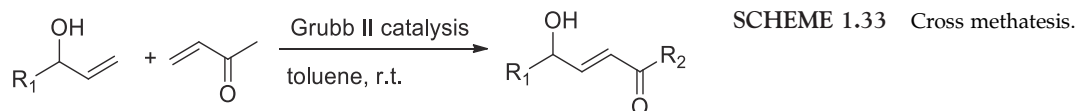
With these olefins in hands, the authors optimized the conditions. The best yields were obtained in hexane/chloroform, eventually adding one equivalent of pyridine (Scheme 1.34).

SCHEME 1.34   Ring closure.
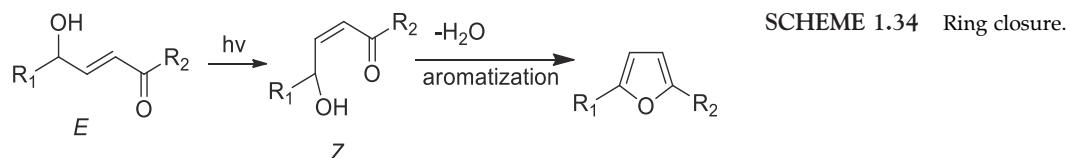
The photochemical irradiation sequence demonstrated excellent functional group tolerance. THP and cyclic acetal protecting group show yield of 95% and 98%. Boc-protected amines gave yields of 93%. (Scheme 1.35).

SCHEME 1.35   Other examples.
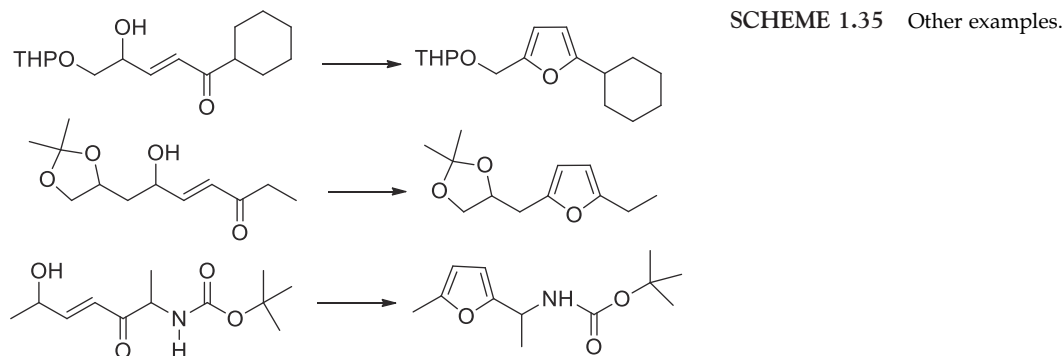
1.6 Imidazoles and derivatives

1.6.1 Synthesis of an imidazole intermediated by HCN

Hydrogen cyanide chemistry is believed to be an important part of the abiotic synthesis of organic material, including nucleobases and aminoacids. HCN in oligomerization into the tetramer *cis*-2,3-diaminomaleonitrile (*cis* DAMN, **21**) which may be converted photochemically into an imidazole intermediate (4-amino-1H-imidazole-5-carbonitrile, (AICN, **22**) (Scheme 1.36).

SCHEME 1.36   Synthesis of an imidazole intermediate from HCN.
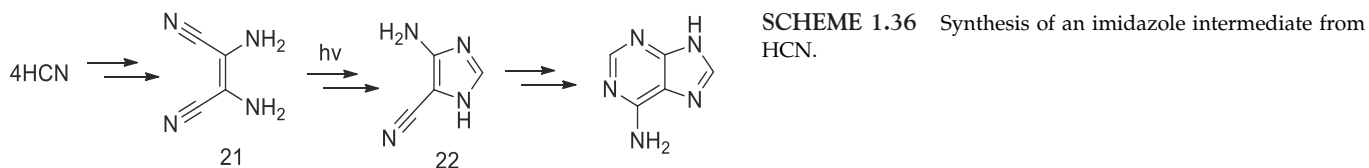
The reaction was examined in detail, and various mechanisms were proposed and after ruled out. Now it was proposed a unique set of steps that is the only one sequence that is compatible with the experimental conditions.[36]

The reaction DAMN → AICN is very robust. It was observed in a variety of solvent, and at diverse concentration and temperatures. The author's results about the mechanism of the reaction are depicted in Scheme 1.37.

SCHEME 1.37   Mechanism of the reaction.
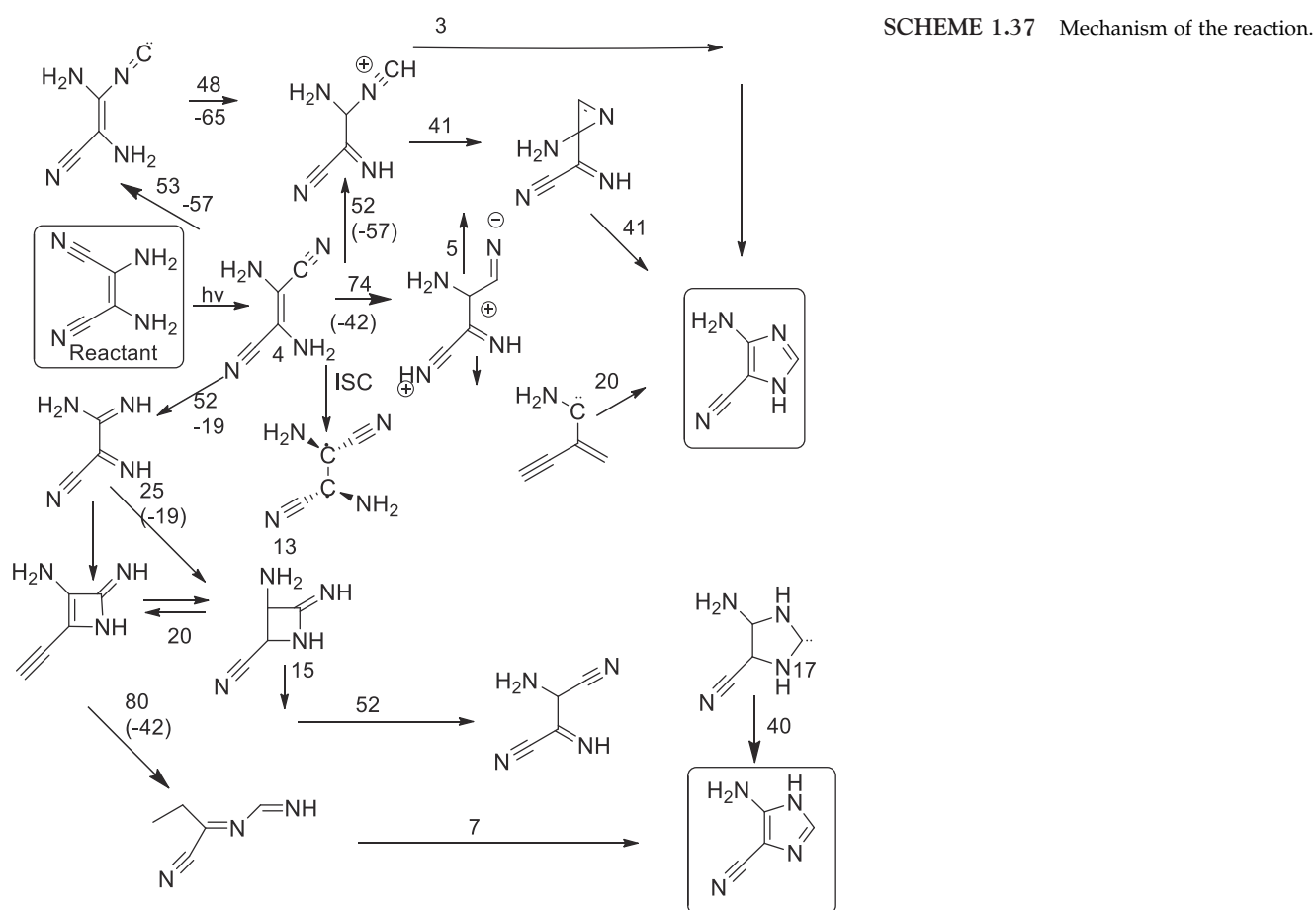
The values near the arrow are the computed free energies of activation in kcal mol^{-1} for the ground state reaction. When an excited state reaction is relevant, the corresponding energy barrier is given in parenthesis.

1.6.2 Synthesis of dihydroimidazoles from pyridinium salts and an alkene

Imidazoles derivatives (imidazolines) can also be synthesized from an alkene and a pyridinium salt.[37] The best conditions to realize this reaction are acetonitrile as solvent, 1 mol% Ir(ppy)$_3$ as catalyst, 20°C, blue LEDS (Scheme 1.38).
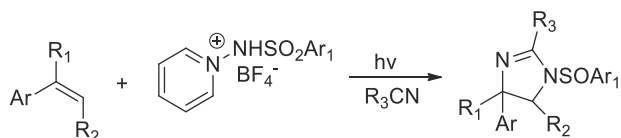
SCHEME 1.38   Synthesis of dihydroimidazoles from pyridinium salts and an alkene.

Fig. 1.30 reported some examples of this interesting reaction. As it can be seen, the yields are more than satisfactory.
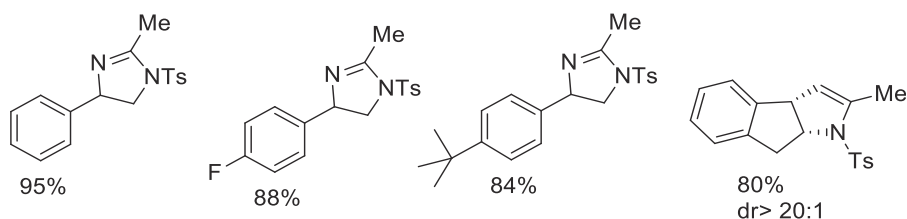
FIGURE 1.30   Examples of products obtained in the reaction of Scheme 1.38.

95%

88%

84%

80%
dr> 20:1

1.6.3 Synthesis of an imidazolinone by cyclization of a linear compound

Another way to obtain imidazole derivatives is the cyclization of an aminoacid derivative, based on N−H/C (sp^3)−H dehydrogenation.[38] The reaction conditions were optimized using PIFA [bis(trifluoroacetoxy)-iodobenzene] in 1,2-dichloroethane at 0°C. Scheme 1.39 reports an example of phenylalanine derivative readily prepared from the aminoacid and dibenzilamine.
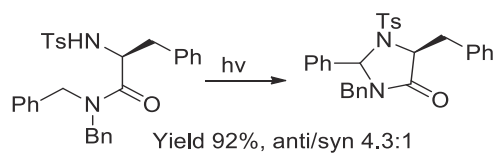
SCHEME 1.39   Cyclization of an aminoacid derivative.

Substrates derived from alkyl containing aminoacid such as alanine, leucine and valine gave the corresponding product in 75%−96% yields. When protected glutamic acid was reacted, the product reported in Fig. 1.31 was obtained in high yields.

The hydroxyl group of serine was tolerated under the oxidative coupling condition and the product was obtained in moderate yield (48%) (Fig. 1.32).

Two substrates prepared from unnatural aminoacids, namely D-α-phenylglycine and α,α-dimethylglicine, also underwent dehydrogenative C−N bond formation to give the desired product (63% and 77% yields, respectively) (Fig. 1.33).

1.6.4 Synthesis of purines by irradiation of urea/acetylene

In a study made to understand the origin of life on earth, a 0.1 M solution of urea in ultrapure water was subjected to freeze − thaw cycles (beginning from the eutectic point of the urea/water system, −21°C to +5°C) in a sealed reactor under a pure acetylene atmosphere for three weeks.[39] The system was irradiated with UV light (254 nm) for the first 72 h. After the end of experiment, the reactor content was allowed to warm to room temperature for analysis by GC−Ms. Many products were formed, but the most important are those reported in Scheme 1.40. Anyway, the mechanism of formation of these products remain still unclear.
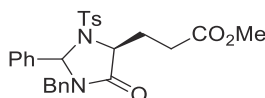
FIGURE 1.31   The product obtained irradiating protected glutamic acid derivative.
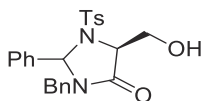
FIGURE 1.32   Product obtained irradiating protected serine.
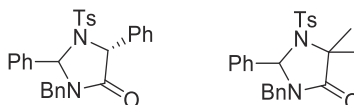
FIGURE 1.33   Products obtained irradiating D-α-phenylglycine and α,α-dimethylglicine.
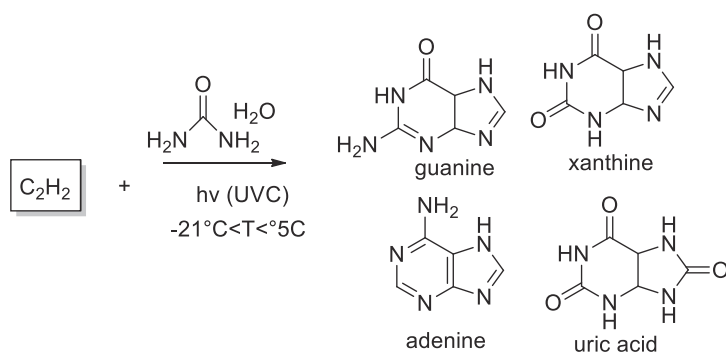
SCHEME 1.40 Synthesis of nucleoside bases from urea and acetylene.

1.6.5 *One pot synthesis from aldehydes, α-aminonitriles and isoxazoles*

When an isoxazole, an α-aminonitrile and an aldehyde were mixed together and irradiated, they afforded a highly substituted imidazole (Scheme 1.41).[40]
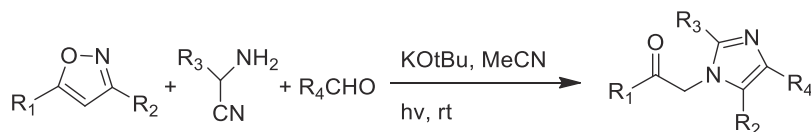
SCHEME 1.41 One pot synthesis from aldehydes, α-aminonitriles and isoxazoles.

Some examples illustrating the scope of the reaction (Fig. 1.34).

1.6.6 *Reaction of N-(1-methylpyrimidin-2-one)pyridinium chloride. Contraction to an imidazolidinone*

Scheme 1.42.
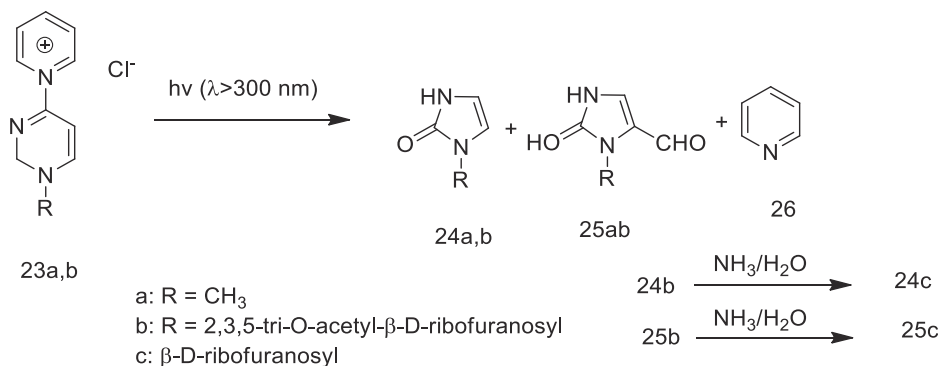
SCHEME 1.42 Contraction to an imidazolidinone.

a: R = CH$_3$
b: R = 2,3,5-tri-O-acetyl-β-D-ribofuranosyl
c: β-D-ribofuranosyl
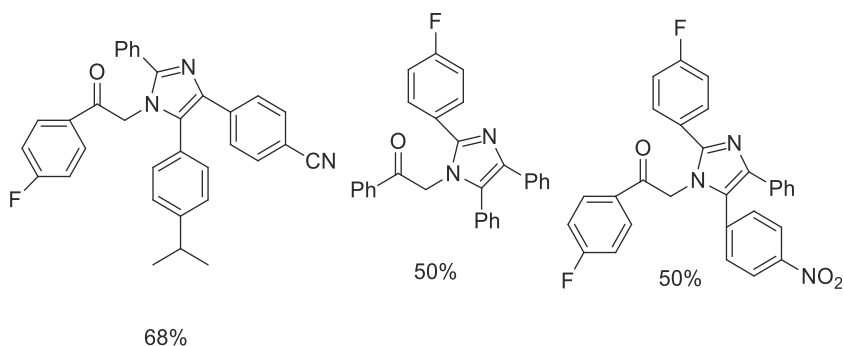
FIGURE 1.34 Products obtained in the reaction of Scheme 1.41.

68%

50%

50%

When an aqueous solution of **23a** was irradiated with near UV (>300 nm), in the absence of oxygen, irradiation results in a gradual disappearance of the absorption band with a maximum at $\lambda = 330$ nm, characteristic of *N*-(pyrimid-2-one-4-yl)pyridinium cations, with concomitant formation of new absorption band at $\lambda = 280$ nm.[41] Careful analysis by HPLC and NMR showed the formation of three main photoproducts **24a**, **25a**, and **26** (Scheme 1.42). The chemical yields of the imidazolinone photoproduct depend on the pH of the irradiated solution. The aldehyde **25a** is the mayor product when irradiation is performed in water (pH 6.5) and the ratio **24a**/**25a** increases significantly when the irradiation of **23a** is performed in slightly basic solution (pH 8.2). In the case of pyridinium salt **23b** derived from 2′,3′,5′-tri-O-acetyluridine, the irradiation was performed in water to avoid decomposition. The expected photoproducts **24b** and **25b** were obtained in moderate yields. During the work-up of the irradiated solution of **23b** in a preparative scale experiment, both photoproducts, **24b** and **25b** were found to undergo partial deacetylation. Therefore, they were fully deprotected and characterized as **24c** and **25c**. The reaction was also tried on other compounds (Fig. 1.35), but none of them underwent ring contraction.

1.7 Synthesis of oxadiazoles

1.7.1 1,2,4 Oxadiazoles from 2H-azirines and nitrosoarenes

Not much material exists in the literature about the synthesis of oxadiazoles by photochemistry. One example consists in the reaction of azirines with nitrosoarenes.[42] For the reaction to come, it is necessary absence of oxygen, a photoredox catalyst (9-mesityl-10-methylacridinium perchlorate), and irradiation with blue LEDs. Control experiments revealed that in absence of one of these elements the reaction does not work. The mechanism seems to be a formal [3 + 2] cycloaddition after a single electron transfer (Scheme 1.43).
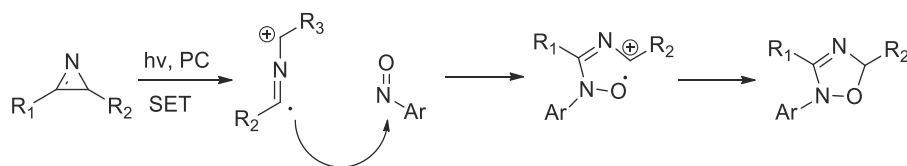
SCHEME 1.43 Mechanism of the reaction.

To explore the scope of the reaction, a series of substituted azirines was prepared to react with nitrosobenzene. As can be seen, both electron-rich (Me, Et, OMe, OPh) and electron deficient substituents (F, Cl), at *para* position were suitable for this photocatalytic transformation, providing the corresponding 1,2,4-oxadiazoles in good yields. The R_1 group could also be replaced by an alkyl substituent (es: butyl), but with lowering of the yield (21%). Fig. 1.36 reports an example of the reaction product obtained by using this approach.
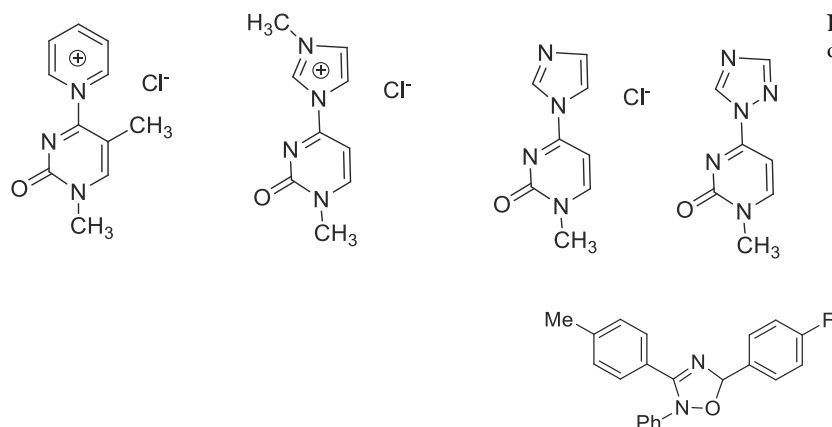
FIGURE 1.35 Other substrates used in the reaction of *N*-(1-methylpyrimidin-2-one)pyridinium chloride.

FIGURE 1.36 An example of the reaction product in the reaction of azirines with nitrosoarenes.
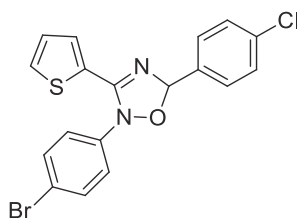
FIGURE 1.37   An example of the reaction product in the reaction of azirines with substituted nitrosoarenes.
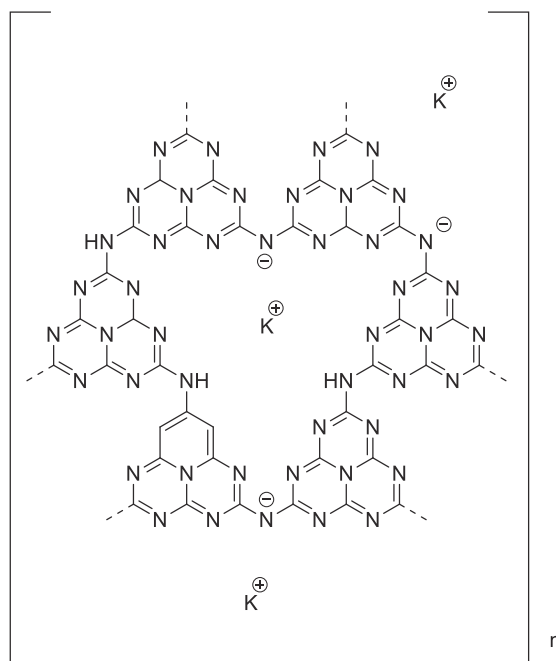
FIGURE 1.38   K-PHI.

It is also possible to perform variation on the nitrosoarenes. An example is given in the Fig. 1.37.
In these reactions, nitrosoarenes substituted in *ortho* position provided lower yields, probably due to steric effects.

1.7.2 Photooxidation of N-acylhydrazones to 1,3,4-oxadiazoles

Another interesting method to obtain 1,3,4-oxadiazoles is the catalytic photooxidation of *N*-acylhydrazones.[43]
For the reaction to occur, it is necessary a catalyst (a solid nitride) (see Fig. 1.38), an oxidant (S_8, that works better than oxygen) and irradiation with blue LEDs (Scheme 1.44).
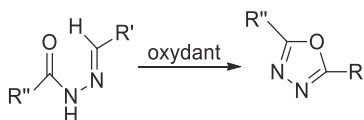
SCHEME 1.44   Catalytic photooxidation of *N*-acylhydrazones.

Control experiments showed that in absence of irradiation or catalyst the reaction does not take place. Moreover, the catalyst (easy separable from the reaction mixture because solid) can be reused. Fig. 1.39 collects some examples of the products that can be obtained by using this procedure.
Derivatives of nicotinohydrazide derivatives undergo the same reaction.
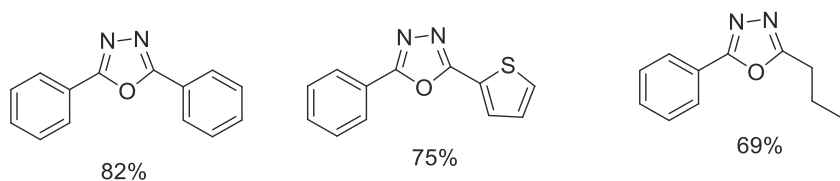
FIGURE 1.39 Examples of products that can be obtained in the reaction of N-acylhydrazones.

82%　　　　　75%　　　　　69%

1.8 Synthesis of oxazoles and related systems

1.8.1 Synthesis of oxazoles by conversion of 1-acyl triazoles

A method to obtain oxazoles consists by irradiation or flash vacuum photolysis of acyl triazoles or acyl isoxazoles (Scheme 1.45).[44]
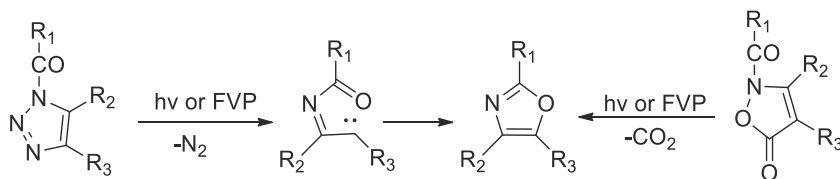
SCHEME 1.45 Irradiation of acyl triazoles.

The yields of isolated oxazole are significantly better than those obtained from triazoles where such information is available. Moreover, in the case of acyl-isoxazoles, the reaction can be iterated (Scheme 1.46).
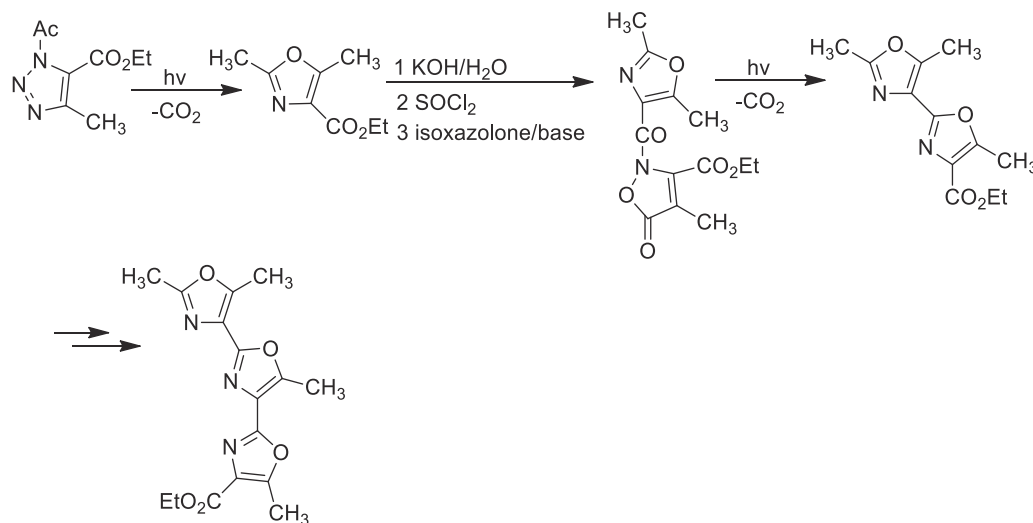
SCHEME 1.46 Iteration of the reaction.

1.8.2 Synthesis from α-bromoketones and benzylamines

A simple and elegant method to obtain oxazoles consist into mix together a α-bromoketone and a benzylamine with the adding of a metal catalyst and an additive in an appropriate solvent. The reaction conditions were first optimized by authors using bromoacetophenone and benzylamine (Scheme 1.47).[45]
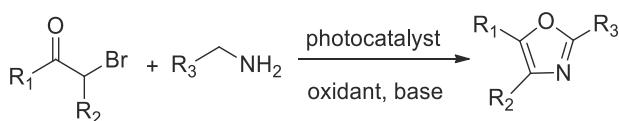
SCHEME 1.47 Synthesis from α-bromoketones and benzylamines.
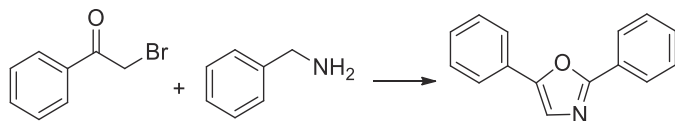
After various attempts, the best conditions were found as follows: catalyst: [Ru(bpy)$_3$]Cl$_2$, additive: CCl$_3$Br, base: K$_3$PO$_4$, solvent: DMF, light source: blue LEDs 7 W.

Bromoacetophenones containing both electron donating and electron-withdrawing substituents underwent cyclization with benzylamine to afford the corresponding 2,5-disubstituted oxazole in moderate to excellent yields. On the other hand, α-bromoester such as ethyl 2-bromoacetate and diethyl 2-bromomalonate were poor substrates for the transformation. Subsequently, the reactivity was explored using various benzylamine derivatives with 2-bromoacetophenone. The reaction afforded the corresponding oxazoles in high yields. However, reaction of allylamine, propargylamine, and alkylamines did not furnish the desired oxazole.

Furthermore, to verify the applicability of the methodology to the synthesis of biologically active natural products, the synthesis of texaline was attempted, an antimycobacterial agent (Scheme 1.48). The yield was good (71%).
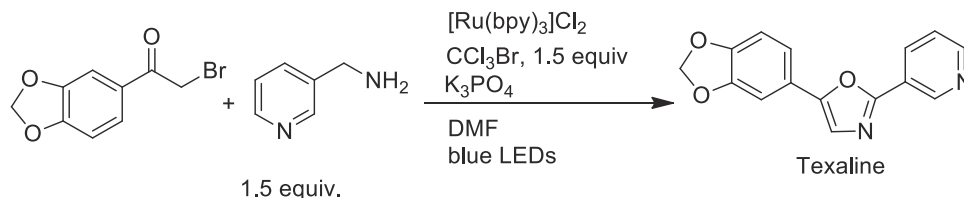
SCHEME 1.48   Synthesis of texaline.

1.8.3 Three components condensation of silylenolethers, fluoroalkyl halides and chiral aminoalcohols to obtain oxazolidines

The described reaction requires the presence of a silylenolether, a fluoroalkyl halide and a chiral aninoalcohol. The irradiation in the presence of a photocatalyst allowed the formation of an oxazolidine (Scheme 1.49). First, the authors tried to find the best condition to perform the reaction.[46]
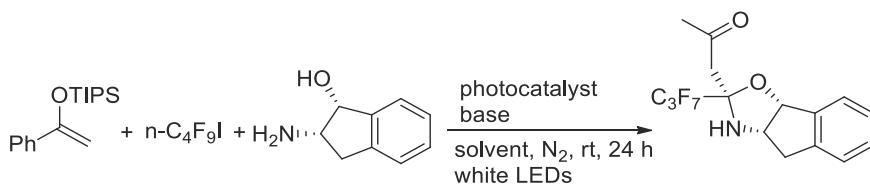
SCHEME 1.49   Three components condensation of silylenolethers, fluoroalkyl halides and chiral aminoalcohols.

After various attemps, as best photocatalyst, acriflavine was chosen (Fig. 1.40).

Notably, all the reactions proceeded with excellent diastereoselectivity (20:1 Dr), which probably could be attributed to the cis mode of chiral amino alcohol. Subsequently, the reactivity was tested on silylenolethers bearing a substituent on phenyl group (Scheme 1.50).
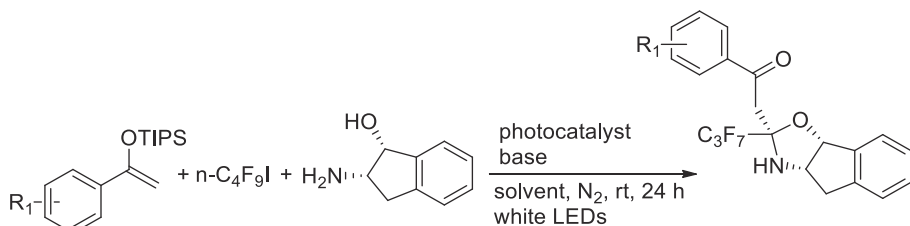
SCHEME 1.50   Silylenolethers bearing a substituent on phenyl group.
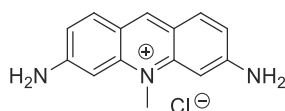
FIGURE 1.40   Acriflavine.

The reaction works well with both electron donating group either and withdrawing groups. The yields vary from 48% to 68%, and the diastereomeric ratio is excellent ($>20:1$). The reaction was also tried replacing the phenyl group with naphthalene, benzothiophene and pyridine, and works equally well. Only with an alkyl group as substituent no reaction takes place. Furthermore, variation on the amino alcohol was examined, according to Scheme 1.51. Also in this case, the reaction worked well, as showed in the same, while, by using some other diamines or aminoalcohols, no reaction occurred.

SCHEME 1.51   More examples.
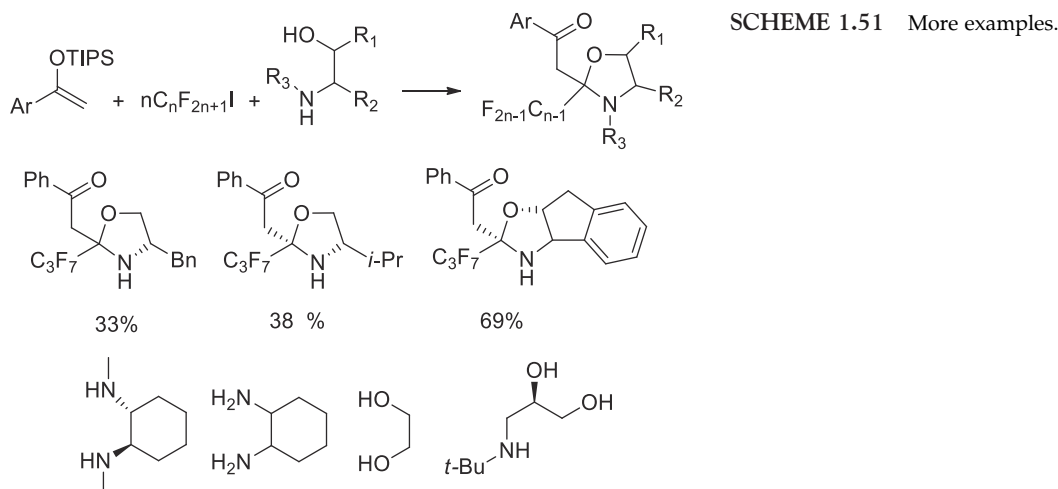
1.8.4 Oxazolidinones from propargylic amines and CO_2

A visible-light-promoted metal-free carboxilative cyclization of propargylic amines with CO_2 was shown to offer *exo*-iodo-methylene-2-oxazolidinones.[47]

To validate this hypothesis, the carboxylative cyclization of *N*-benzylprop-2-yn-1-amine with CO_2 was initially selected as the model reaction under a 300 W xenon lamp. This reaction in absence of base failed, indicating the base is necessary. Organic bases gave better result that inorganic bases. The yields grow up also increasing the pressure of CO_2. As catalyst, tetramethylguanidine (TMG) gave the best results (Scheme 1.52).
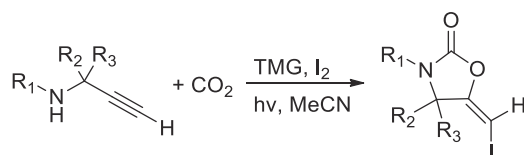
SCHEME 1.52   Carboxilative cyclization of propargylic amines with CO_2.

Firstly, a methyl substituent at the *para*, *ortho* and *meta* position of the phenyl ring was tested, demonstrating that steric effect was negligible. Also electron withdrawing groups or electron donating group gave good yields. A pyridine ring works equally well. In addition, propargylic amines with other substituents except an *N*-benzyl group are compatible with the reaction, and the corresponding iodine-functionalized 2-oxazolidinones were obtained in moderate yields. Some examples of the obtained products are reported in Fig. 1.41.
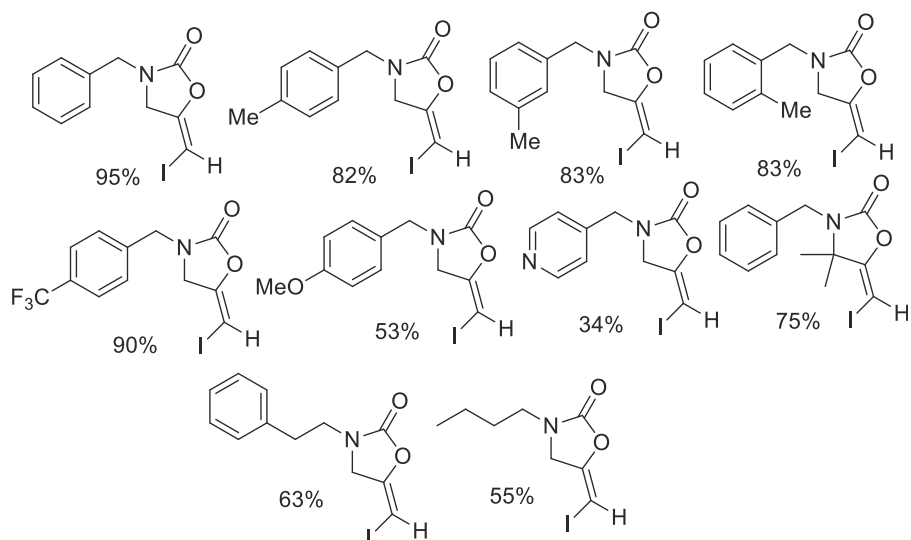
FIGURE 1.41 Some products obtained in the reaction of propargylic amines with carbon dioxide.

1.8.5 Conversion of benzoil formamides to oxazolidin 4-ones

One of the more important challenges in photochemistry is the possibility to perform reaction that give enantiomerically pure products. Jesurai et al. have tried this starting with atropochiral benzoyl formamides (Fig. 1.42).[48]

This compound presents atropoisomerism because of the restricted rotation around the N−C(aryl) bond. Photoirradiation of optically pure atropisomers was performed using a medium pressure Hg lamp with Pyrex cut-off and cooling the vessel. An hypotetic mechanism of the reaction is depicted in Scheme 1.53.
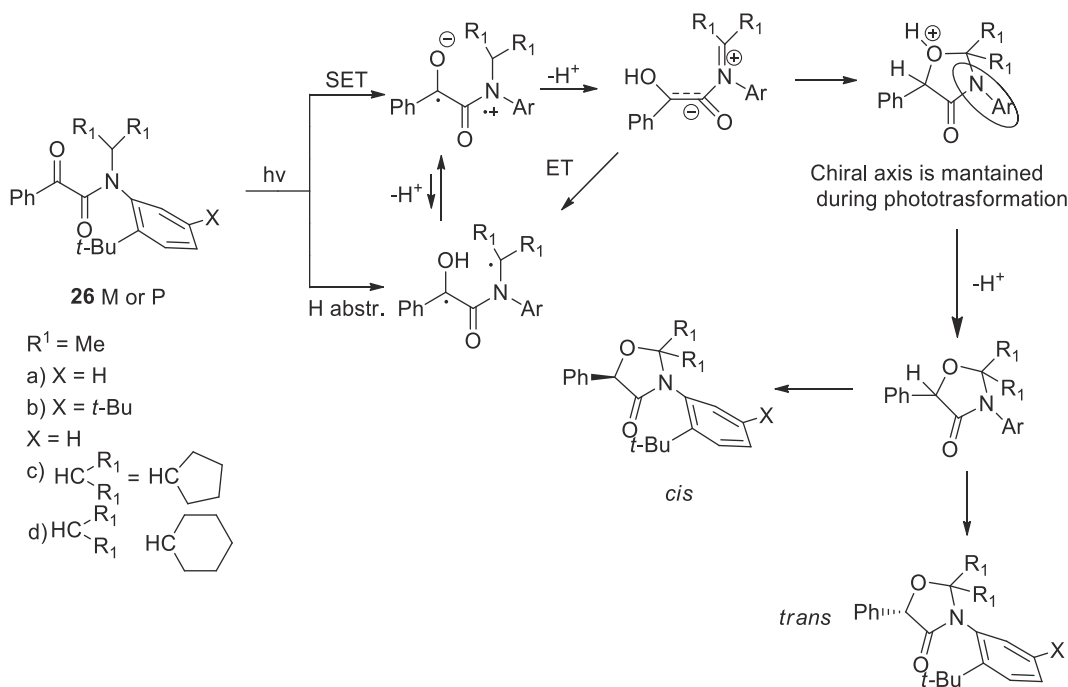
SCHEME 1.53 Mechanism of the reaction.
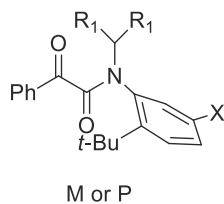
FIGURE 1.42 Atropochiral benzoyl formamides.
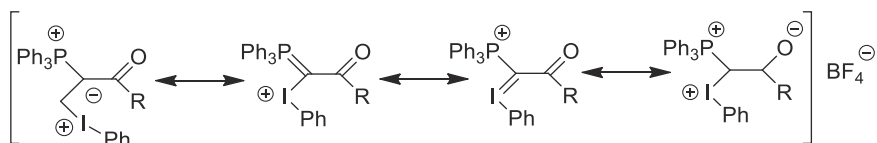
FIGURE 1.43 Resonance structures of the ylide.

All the reactions of **26a-d** show an elevate enantioselectivity, up to 99%. This is a bit strange, because one of the intermediates is near planar in one configuration. A weak aspect of this reaction is the scarce diastereoselectivity, with diasereoselectivity around 65% for the *cis* isomer, and 35% for the *trans* isomer.

1.8.6 Synthesis of phosphonium substituted oxazoles from phosphonium-iodonium ylides

The work of Wittig on carbonyl olefination has prompted a considerable research on other types of ylides, especially on phosphonium-iodonium ylides. Such ylides are best described by resonance structures in Fig. 1.43.[49]

These resonance formulae show that ylide contains several reaction centers, which represent a molecule with separate charges on the P, I, and O atoms. Analysis of the ylide structural peculiarities allowed to conceive the ylide as possible pseudo dipole for the synthesis of five-member heterocycles (Scheme 1.54).

SCHEME 1.54 Mechanism of reaction of the ylide.

27a R = OC$_2$H$_5$
28a R = OCH$_3$
29a R = C$_6$H$_5$
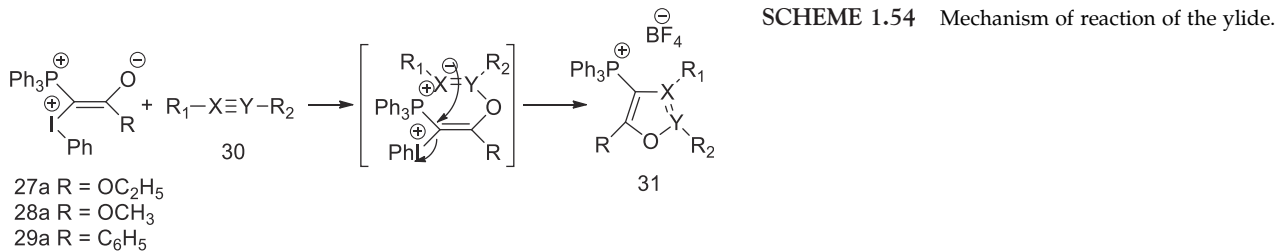
The reaction was attempted in acetonitrile as thermal reaction at various temperatures, but these attempts were unsuccessful. Only adding dimethylacetilene dicarboxylate (DMAD) **31a** was obtained in 30% yield at 80°C. Anyway, it was observed that the reaction was tremendously accelerated under irradiation conditions to yield **31** (Scheme 1.54).

Analogously, the methoxycarbonyl-substituted ylide **28a** reacts under photochemical conditions with acetonitrile and propionitrile to afford the corresponding oxazoles.

1.8.7 Synthesis from azirines and aldehydes

Another easy way to obtain trisubstituted oxazoles is the photoredox catalysis between an azirine and an aldehyde (Scheme 1.55).[50]
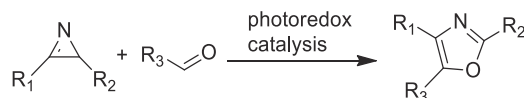
SCHEME 1.55 Reaction between an azirine and an aldehyde.
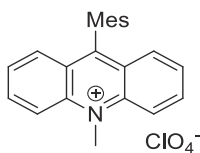
FIGURE 1.44 PC-I.
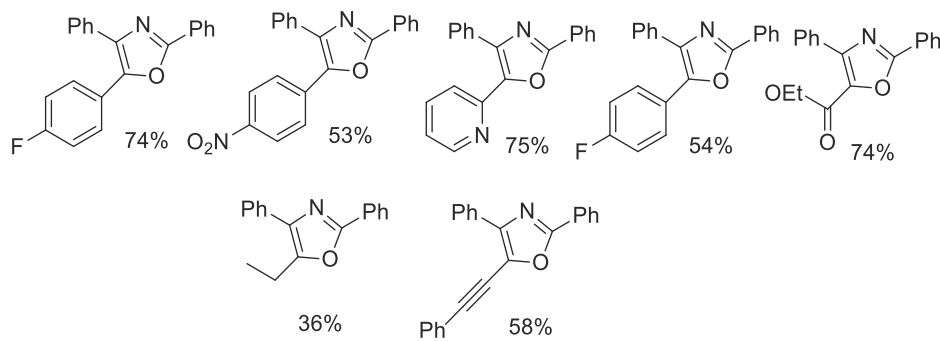
FIGURE 1.45 Obtained products in the reaction of Scheme 1.55.

First, the authors tried to find the best conditions to maximize the yields of the reaction. The best photocatalyst was PC-I (Fig. 1.44).

As additives 4 Å molecular sieves and Li_2CO_3 were used. This way, the yields raised up to 77%. It is also possible to change the substituent on the aldehyde (R_3) to obtain other oxazoles (Fig. 1.45).

A plausible reaction mechanism is depicted in Scheme 1.56.
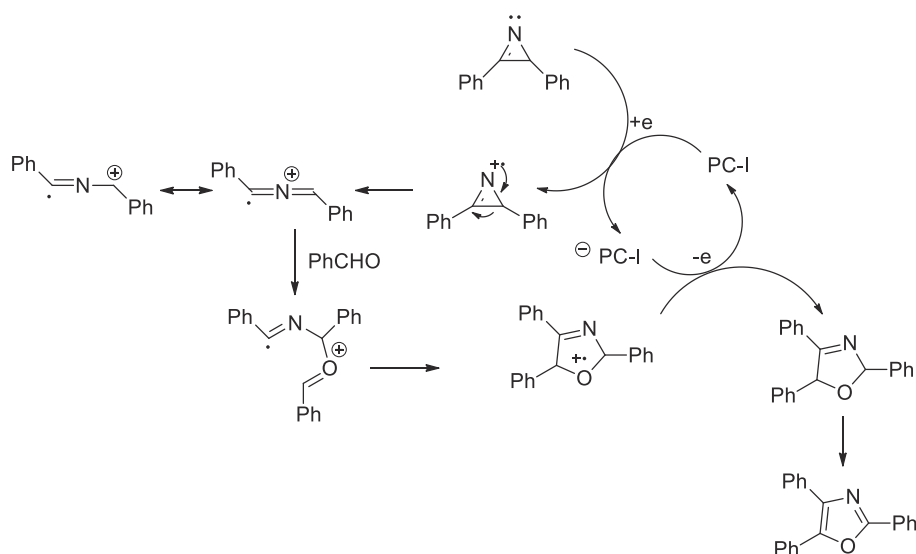
SCHEME 1.56 Mechanism of the reaction.

1.9 Oxetanes: the Paternò Büchi reaction

1.9.1 Exo-oxetanes from carbonyl compounds with vinylene carbonates

Oxetanes, strained four-membered ethers, have attracted considerable attention, not only because of their biological activity, but also as synthetic intermediates. Photochemical 2 + 2 cycloaddition reaction of carbonyl
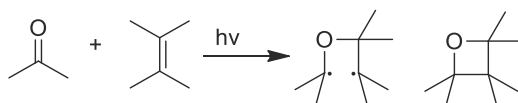
FIGURE 1.46   The Paternò-Büchi reaction.

35
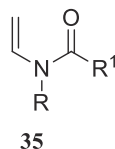
a R = H, R^1 = H   e R = Me, R^1 = OtBu
b R = H, R^1 = Me   f R = Bn, R^1 = OtBu
c R = Bn, R^1 = Me g R = Bn, R^1 = OCH$_2$CH$_2$TMS
d R = Pr, R^1 = Me   h R,R^1 = CH$_2$CH$_2$CH$_2$

FIGURE 1.47   *N*-acyl enamines.

compounds with alkenes, the Paternò-Büchi (PB) reaction, is a most promising method for preparing a wide variety of the synthetic useful strained compounds (Fig. 1.46).

Authors proposed recently a reasonable mechanism for the *exo* selective formation of bicyclic oxetane in PB reactions of benzaldehyde with furan derivatives. Thus, the stereoelectronic, that is, the interaction of a lone pair of electrons on the oxygen atom with the C−O σ* orbital, confers significant stability on the conformer that is the precursor of the *exo*-oxetane (Scheme 1.57).[51]

a: R$_1$ = R$_2$ = Ph
b: R$_1$ = Ph, R$_2$= H
c: R$_1$ = Ac, R$_2$ = Me
d: R$_1$ =CO$_2$Et, R$_2$ = Ph
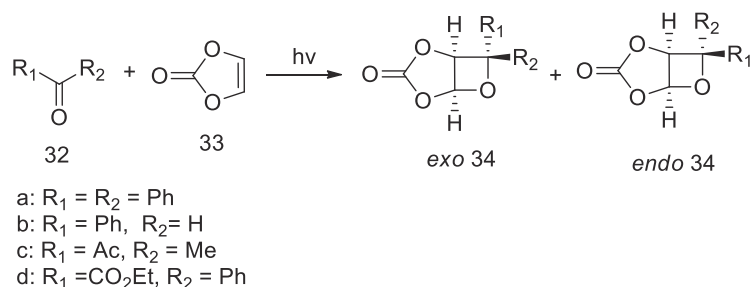
SCHEME 1.57   Examples and mechanism of the reaction.
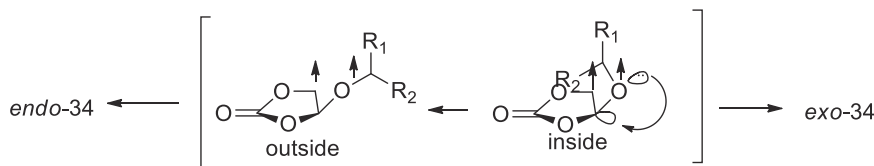
The reaction was performed in acetonitrile with a high pressure mercury lamp through a Pyrex filter (>290 nm). The yields are good except for **32d**. The ratio *exo-endo* was almost superior to 90:10.

1.9.2 *Photocycloaddition of* N-*acyl enamines to aldehydes*

The structures of the alkene components used in this study are shown in the Fig. 1.47.

The Paternò-Büchi reaction of *N*-acyl enamines **35** was first studied with benzaldehyde as the carbonyl substrate. A clean photocycloaddition was observed, which yielded the corresponding 3-amino oxetane **36**.[52]
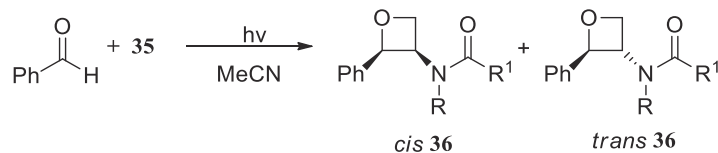
The oxetanes were formed with good-to-excellent diastereoselectivity in favor of the *cis* product (d.r. 70−90).

For a mechanistic explanation of the high simple diastereoselectivity recorded in the enamide photocycloaddition, the authors rely on the picture of a stepwise formation of the oxetane ring (Scheme 1.58). Initial O−C bond formation by attack of the photoexcited aldehyde in its triplet nπ* state at the alkene is succeeded by the C−C bond forming step, which occurs after intersystem crossing (ISC). Indeed, it is known that the irradiation of aromatic carbonyl compound results in an efficient conversion to the corresponding nπ* triplet states T_1 via fast ISC step, and O−C bond formation has been shown to be the first in the Paternò-Büchi reaction of electron rich alkenes leading to a biradical intermediate (^{3}D).
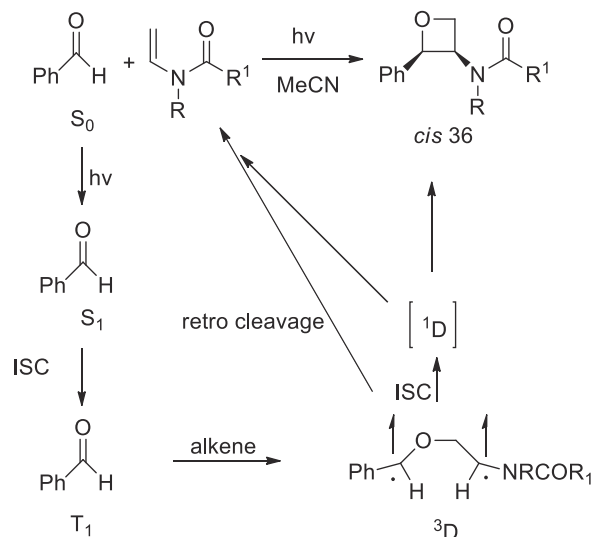
SCHEME 1.58   Mechanism of the reaction.

1.9.3 Oxetanes from carbonyl compounds and 2,5 dimethyl-4-isobutyl-oxazoles

The Paternò-Büchi reaction can be a very useful process because in many cases the obtained oxetanes can be opened to afford polyfunctionalized linear compounds. In this view, Bondock et al. performed a PB reaction for the obtaining of α-amino-β-hydroxyketones (Scheme 1.59).[53]
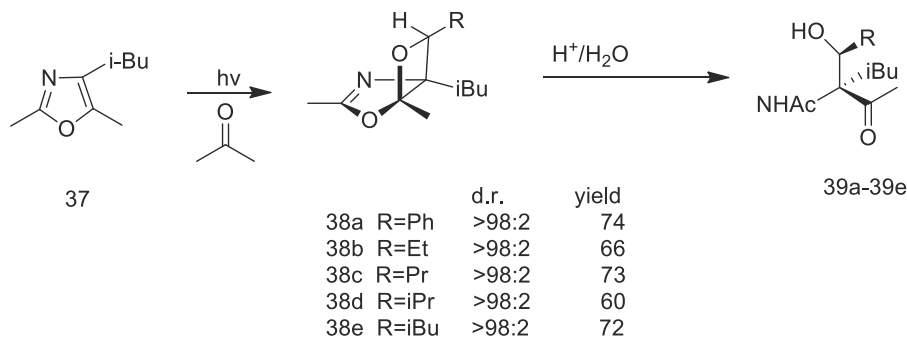
SCHEME 1.59   Oxetanes from carbonyl compounds and 2,5 dimethyl-4-isobutyl-oxazoles.

		d.r.	yield
38a	R=Ph	>98:2	74
38b	R=Et	>98:2	66
38c	R=Pr	>98:2	73
38d	R=iPr	>98:2	60
38e	R=iBu	>98:2	72

In all cases, only the regioisomers **39a-39e** were formed with excellent (*exo*) diastereoselectivity in good yields.

To evaluate the influence of steric as well as electronic factor on the stereoselectivity of the PB reaction of oxazole with aliphatic as well as aromatic α-ketoester, the photocycloaddition of **37** with methyl pyruvate, methyltrimethylpyruvates, and different types of alkyl phenylglyoxylates were investigated.

		exo:endo	yield
40a	R_1 = Me, R_2 = Me	98:2	85
40b	R_1 = tBu, R_2 = Me	98:2	79
40c	R_1 = Ph, R_2 = Me	71:29	86
40d	R_1 = Ph, R_2 = Et	67:33	78
40e	R_1 = Ph, R_2 = Et	55:45	80
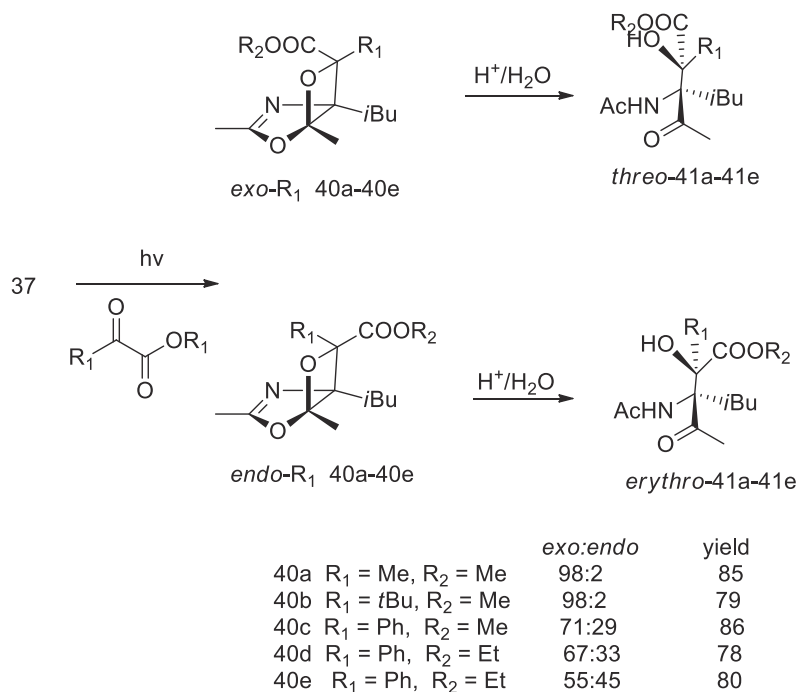
As it can easily be seen, the ratio *exo:endo* tends to diminish when R_1 = Ph. This may be due to the steric hindrance of the large phenyl group.

1.9.4 Reaction of 2,3-dihydrofuran

The irradiation of 2,3-dihydrofuran in benzene with benzophenone gave adduct **42** (Fig. 1.48).

The selectivity depended on 2,3-dihydrofuran concentration:[53,54] this behavior was explained with a switch from a triplet mechanism to a singlet mechanism at higher concentration. This behavior can be explained. The best interaction between the frontier orbitals is that from the LSOMO of acetaldehyde and the HOMO of 2,3-dihydrofuran. The atomic coefficients on the olefinic carbon atoms in 2,3-dihydrofuran were −0.26 at C−2 and −0.38 at C−3. The atomic coefficient on the oxygen atom in the LSOMO of singlet excited acetaldehyde was 0.48, while the atomic coefficient at the C−1 of the acetaldehyde was 0.49.[55−58]

The nature of the LUMO of 2,3-dihydrofuran excludes the possibility of a concerted mechanism. The reaction has to provide for the formation of extremely labile singlet biradical. In this case, the oxygen atom of acetaldehyde has to attack the C−3 carbon atom in 2,3-dihydrofuran to give the more stable biradical intermediate. The reaction, in this case, allowed the formation of only the *exo* isomer. In the triplet state, the main interaction is that between the LSOMO of the triplet state acetaldehyde and the HOMO of the dihydrofuran. This interaction leads to the formation of the corresponding CC biradical intermediate (Scheme 1.60).

SCHEME 1.60   Molecular orbitals in the 2,3 dihydrofuran.

FIGURE 1.48   Reaction of dihydrofuran.

The HSOMO on the biradical intermediate was mainly localized on the aromatic ring and it is extended to the radical carbon. The LSOMO was mainly localized on the dihydrofuran ring. The coupling between the radical carbons in these two orbitals was possible (the atomic orbitals involved can superimpose themselves) only if the *endo* isomer was formed.

1.9.5 Reaction of a silyl derivative of cinnamyl alcohol

The utility of the Paternò-Büchi reaction can be extended also to other systems. Fleming et al. used a trimethyl-silyl derivative of cinnamyl alcohol in the reaction of benzaldehyde (Scheme 1.61).[59,60]

SCHEME 1.61 Reaction of trimethylsilyl derivative of cinnamyl alcohol.

As be easily seen, it is clear that the mayor products is the all *trans* oxetane (isolated in c. a. 20% yield.) It is interesting to note that no other cycloadduct was detected (detection limit <1%). The *cis* and *trans* alkene isomers of the silyl cinnamyl ether are recovered in a 1.6:1 ratio for a combined yield of 67%. This study implicates noncovalent tethering (but not $\pi - \pi$ overlap) for silylated cinnamyl alcohol and benzaldehyde since there is only one stereoisomer obtained and no side reactions. If tethering is involved, then the phenyl groups must be held in opposite directions in the coordinated structure due to steric effects.

1.9.6 Reaction of geraniol derivatives

In the present study, geraniol (**43a**) and its derivatives **43b,c** were chosen to see how the hydroxyl group affects the regioselectivity in the formation of oxetane (Scheme 1.62). They contain the allylic alcohol functionality as well as the unfunctionalized double bond.

SCHEME 1.62 Reactions of geraniol derivatives.

In accordance with the hydroxyl-group directivity, the oxetane formation at the 2,3 double bond should be preferred over the 6,7 one to afford the oxetane **44a** selectively.[61] Instead, at a concentration of 340 mM, the 6,7 oxetane prevails, with a ratio **44a/45a** of c. a. 30/70. At a concentration of 6.8 mM the formation of 45 increased to give nearly the 1:1 mixture of oxetanes **44a** and **45a**. Thus, the regioselectivity was dependent on the concentration of the alcohol. The concentration effect on the selectivity suggests that the intermolecular association of **44a** plays a role in determining the regioselectivity (Scheme 1.63).

SCHEME 1.63   Mechanism of the reaction.

To obtain more information about the hydroxy group effect on the regioselectivity, the PB reaction of the hydroxy protected methyl ether **43b** and acetate **43c** with benzophenone were investigated. The regioselectivity, **44/45** = 15/85−11/89 was not dependent on the concentration of **43b,c**. Thus, the electrophilic oxygen of benzophenone triplet state preferably approaches to the more nucleophilic 6,7 double bond to afford the triplet biradical via the corresponding exciplex.

1.9.7 Reaction with isoxazole derivatives

First, the authors synthesized a variety of isoxazole derivatives, to test their reaction with aldehydes: Scheme 1.64
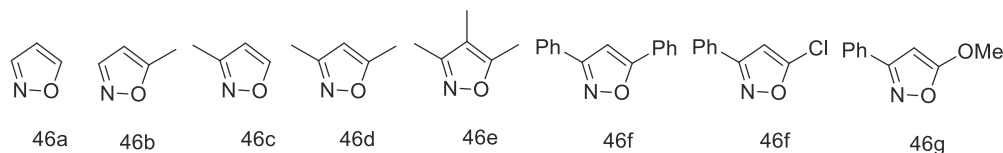
SCHEME 1.64   Synthesized oxazoles.

With these substrates in hand, the photoreaction with benzaldehyde or propionaldehyde was tested.[62]

With propionaldehyde no reaction happened. A possible explanation is that the LUMO energy of propionaldehyde is larger than that of benzaldehyde, so it can be assumed that the energy difference between the isoxazole-HOMO and the aldehyde-LUMO is too large to promote an efficient reaction.

Benzaldehyde reacted, but it was necessary to use a tenfold excess of isoxazole to obtain acceptable yields. Moreover, the reaction was attempted also on substitutes benzaldehydes (Scheme 1.65).
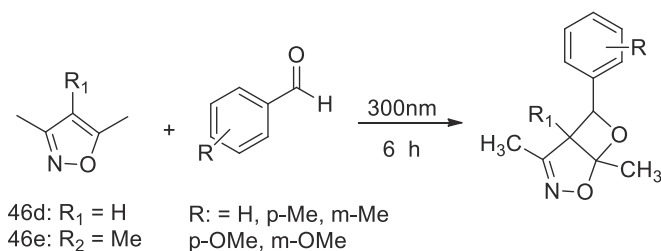
SCHEME 1.65   Photoreaction with benzaldheyde.

First, only **46d** and **46e** reacted with appreciable yields (40%−98%), so the authors pointed their attention only on these two compounds, especially on **46e**. The reaction of **46e** with *p*- and *m*-tolualdehyde showed no change in the reaction conversions compared with benzaldehyde, whilst the conversion of **46d** with these two aldehydes were considerable decreased. Irradiation of **46d** and **46e** with *p*- and *m*-anisaldehyde showed in all cases lower reaction conversions.

The preparative photoreaction of **46e** together with aryl substituted aldehydes was carried out in acetonitrile at −10°C in presence of 10 mol% potassium carbonate (to neutralize traces of acid). In all cases, the regioisomers **47a-c** were formed with excellent (*exo*) diastereoselectivity (>99:1) in moderate yields and high purities (Scheme 1.66).

47a: R = Ph   50%
47b: R = *p*-Tol   35%
47c: R = *m*-Tol   65%
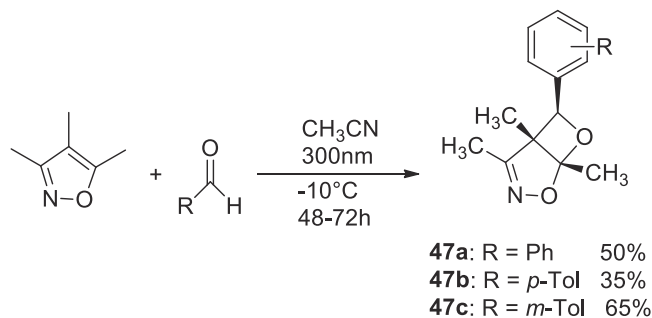
SCHEME 1.66   The reaction.

1.9.8 Synthesis of an elusive oxetane by photoaddition of benzophenone to thiophene in the presence of a Lewis acid

In contrast with furan and its methyl derivatives which readily react with excited carbonyl compounds to yield oxetanes, thiophene and its methyl derivatives were considered until the late 1960s inert to oxetane formation.

Some years ago many attempts carried out to obtain oxetanes from thiophene failed. This behavior suggested the idea that thiophene was perhaps a good quencher of excited carbonyl compound. Later, it was found that, in order for the reaction to take place, it was necessary to substitute at least two methyl groups on the heterocyclic ring. These results could explain the problem qualitatively since substitution of electron donating groups to a conjugated diene system should raise its lowest triplet energy level to a higher value above that of the ground state of the unsubstituted diene.

In view of this situation, we recently turned our attention to the possibility of carrying out successfully the photoaddition reaction to thiophene by the interaction of a ketone-Lewis acid complex with the heterocyclic compound in the presence of light.[63]

The reaction was performed dissolving equimolar quantities of thiophene (0.01 mol) and benzophenone in 10 mL of dried ether containing 0.3 mL of BF_3. The irradiation was carried out for 5 h at 20°C under a nitrogen atmosphere in a quartz immersion photoreactor. After the reaction, the product was separated on silica gel to obtain **48a** (10% yield) and **48b** (90% yield) (Scheme 1.67).
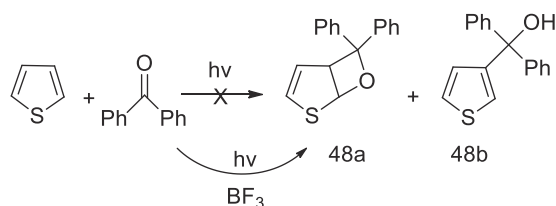
SCHEME 1.67   Synthesis of an elusive oxetane.

Anyway, the oxetane **48a** proved to be very unstable, and rapidly decomposes to **48b**, derived from the opening of the oxetane ring.

1.9.9 Reaction of 2-furylmethanol derivatives

The reaction of allylic alcohols with carbonyl compounds was tested also on 2-furylmethanol derivatives. The presence of large substituents on the carbon bearing the alcoholic function allows a high regioselectivity (Scheme 1.68).[64]
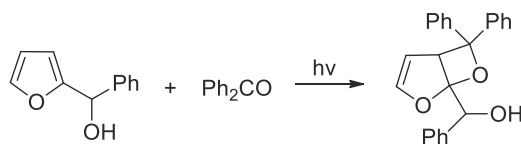
SCHEME 1.68   PB reaction on 2-furylmethanols.

5-Methyl-2-furyl derivatives were used as substrates showing a different regioselectivity. This type of substrates gave a 1:1 mixture of regioisomer, when irradiated in the presence of benzophenone, and a single regioisomer in the presence of benzaldehyde.[65] In agreement with the results obtained with 2-furyl derivatives, the products deriving from the attack on the side bearing the alcoholic function were obtained as s single diastereoisomer, while those deriving from the attack on the side bearing the methyl group were obtained as a mixture of diastereoisomers.

These reactions showed that on furan two possible regioisomer could be obtained. The experimental result showed that, in some cases, the reaction occurred mainly on the side when the hydroxyl group was present, while other reaction showed a completely different regioselectivity. The reason of this behavior can be found in kinetic factors depending on the different stability of the biradical intermediates.

The reaction of 2-furylmethanol derivatives with aliphatic aldehydes and ketones gave the corresponding adducts with high regioselectivity: the reaction occurred on the most hindered side of the substrates. However, no diastereoselectivity was observed.[66] The relative stability of the biradical intermediates was able to explain the regioselectivity of the reaction. A computational study (DFT) showed that the biradical obtained on the most hindered side of the molecule was more stable that the other one.

The diastereoselectivity of the reaction between 2-furylmethanol derivatives and aromatic carbonyl compounds showed that it increased in relation to the nature of the substituent on the carbon bearing the alcoholic function as described by Adam. However, while Adam considered the allylic strain with a methyl group in β-position as the driving force for diastereoselectivity, in this case, a methyl group on the C−3 of the furan ring was not present.

To further explain the observed stereoselectivity, the photochemical behavior of tertiary 2-furylcarbinol was studied.[67] The irradiation of 1-methyl-1-phenyl-1-(2-furyl)methanol with benzaldehyde gave a mixture of two regioisomeric products. The regioisomer on the most hindered side of the molecule was obtained in low yield but it showed a complete diastereisomeric control. On the contrary the main product was a mixture of four diastereomeric products. The reaction of the same compound with benzophenone gave only the product deriving from the attack on the most hindered side of the molecule. This compound was obtained with 48% diastereoisomeric excess.

On the basis of these results an explanation of the stereochemical behavior was attempted.[67] 1-methyl-1-phenyl-1-(2-furyl)methanol showed three conformations. All three conformers were in the range of 1.97 kJ/mol and they did not show a preference. The directing effect exerted by the hydroxyl group is due to the formation of an hydrogen bond between hydroxyl group and the oxygen of the excited carbonyl compound, or it is due to the formation of a complex. This type of interaction could favor the formation of a preferential conformation in the biradical intermediate where the hydroxyl group and and the oxygen of the carbonyl group are near. These conformations could have different energies

for different diastereoisomeric biradicals, giving an explanation of the observed behavior. In the case of 1-methyl-1-phenyl-1-(2-furyl)methanol, if the hydroxyl group drove the attack of the oxygen of the carbonyl group, the conformations of the biradical intermediate represented in Scheme 1.69 were obtained. **B** and **D** were the preferential conformations: calculation on these conformations showed that there was a difference of 13.26 kJ/mol between the energies of these two conformations. In the reaction of the same substrate with benzophenone, the corresponding conformers **B** and **D** showed a difference energy of 7.79 kJ/mol: this difference is in agreement with the observed diastereoselectivity.
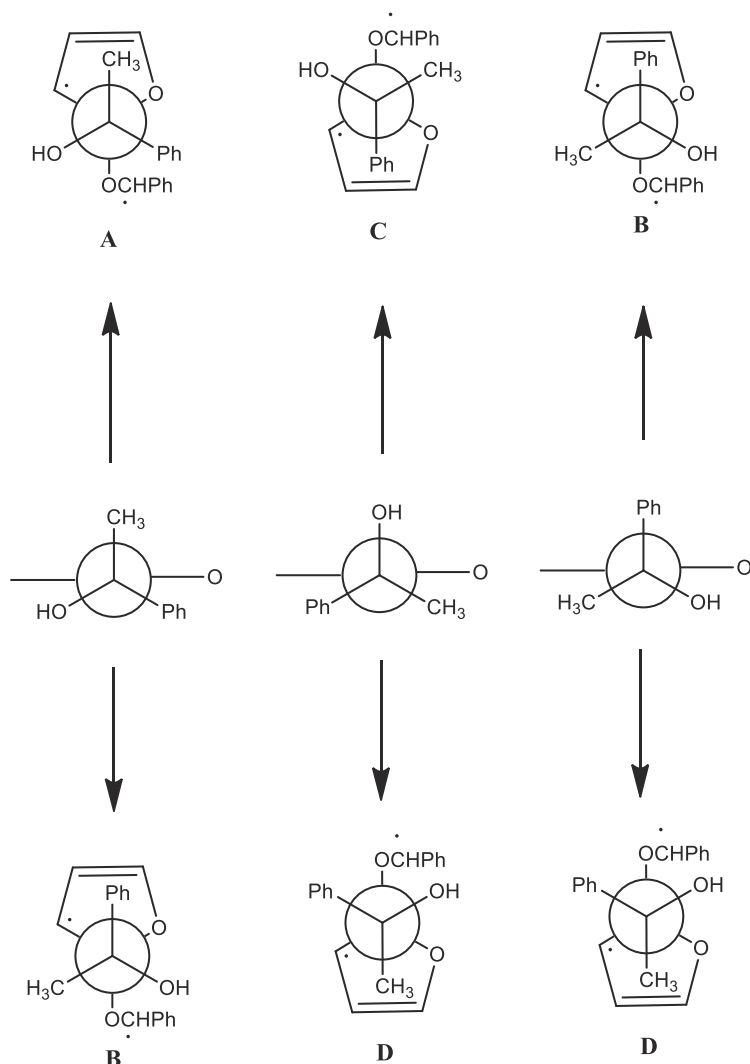
SCHEME 1.69 Conformations of the biradical intermediates.

The above reported results represent all the available on the Paternò-Büchi reaction on pentatomic heterocycles. We can see that, with excepton of furan, there are very few data: in particular, 1. most of the unsubstituted tested compounds differed from furan did not react, 2. only few substituted derivatives showed a significative reactivity toward excited carbonyl compounds.

1.9.10 Reaction of silyl enol ethers

3-(Silyloxy)oxetanes **50** were successfully prepared from silyl enol ethers **49** containing carbon-chlorine, carbon-silicon, or carbon sulfur bonds (Scheme 1.70). Ethers and ester groups were compatible with the reaction. The presence of an alkene moiety was also compatible. When a β-alkyl substitutes silyl enol ether was used, a *trans* relationship between α and β substituent in the oxetane was observed. This result did not depend on the (*E*) or (*Z*) nature of the alkene. The products were obtained with high simple diastereoselectivity (ds 74%−95%).[68]
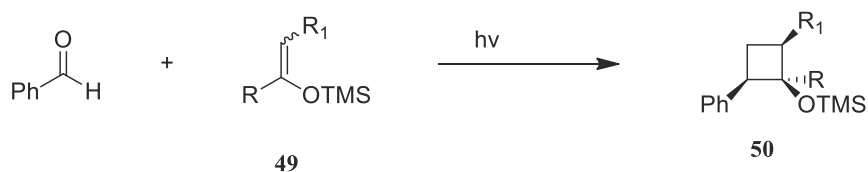
SCHEME 1.70   Reaction of silyl enol ethers.

In the triplet biradical, free rotation leads to the highly preferred, sterically least congested conformation. The further reaction pathway of this species includes ISC and an assumed selection step (cleavage vs. ring closure) at the singlet 1,4 diradical level which accounts for the high simple diastereoselectivity at C−2/C−3.

The presence of a stereogenic center in the β-alkyl group (as in **51**) induced a facial diastereoselectivity. In some cases, high diastereomeric ratios were observed (Scheme 1.71).[69]
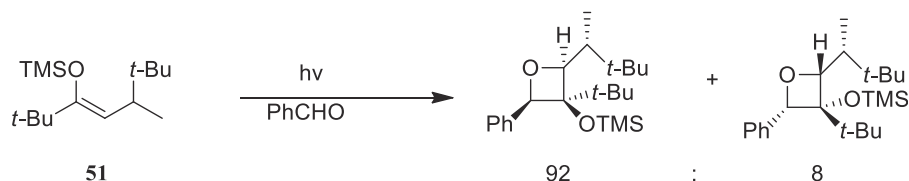
SCHEME 1.71   An example of facial diastereoselectivity.

The diastereoselectivity was probably due to the presence of a conformational preference represented in the Scheme 1.72. This conformation allows the *Si* attack.
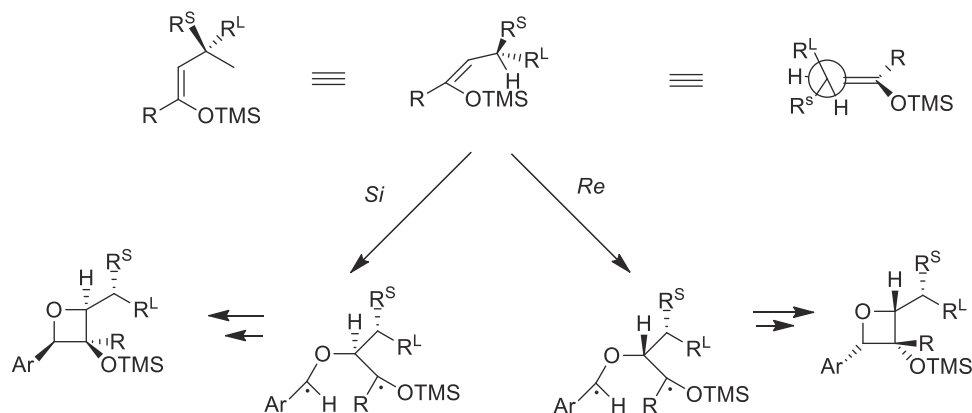
SCHEME 1.72   Conformational preference.

1.10 Piperidines

1.10.1 *Iodine catalyzed* sp³*-H amination*

In a precedent work, the authors synthesized pirrolidines by a iodine-catalyzed Hofmann-Loffler reaction that provided the expected access to pyrrolidines from position-selective C−H functionalization based on intramolecular 1,5 abstraction through a nitrogen centered radical pathway.

In contrast, the related C−H amination strategy toward the piperidine core in significantly more challenging as the required 1,6-H abstraction from nitrogen centered radicals is kinetically disfavored. Consequently, a C−H amination strategy regarding piperidines has remained elusive.

To override the given "innate" preference for pyrrolidine formation, authors decided to pursue condition that would preferentially generate free radicals outside the amidyl radical manifold involved in the Hofmann-Loffler pathway. Within such a scenario, free-radical hydrogen-atom abstraction should address the weakest C−H bond and could be predicted by the introduction of carefully preorganized substitution.[70]
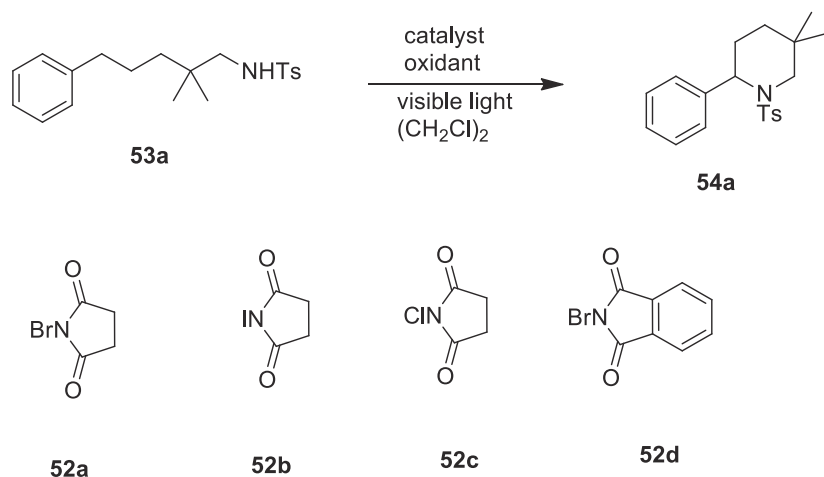
FIGURE 1.49 Iodine-catalyzed piperidine formation.

In the Hofmann-Loffler the used catalyst NIS **1b** provides intermediates for exclusive synthesis of pirrolidine. To avoid this, the less reactive NBS **1a** was used, together with catalytical amounts of iodine (Fig. 1.49).

The reaction was developed with **53a** as the substrate and departed from the observation that a combination of visible-ligth exposure, 5 mol% molecular iodine, and *N*-bromosuccinimide (NBS) **52a** provided a selective transformation to the desired piperidine **54a**. (yield 72%). The subsequent increase in the amount of oxidant to 2 equiv. provided **54a** in 80% yield without detection of the corresponding pyrrolidine. Related iodo and chloro derivatives NIS **52b** and NCL **52c** provided significant decrease reactivity, accompanied by the formation of the undesired pyrrolidine, while *N*-bromophthalimide **52d** gave a comparable yield of 72%.

Under the optimized conditions, the scope of the reaction was explored. The reaction is very robust: it tolerates various protecting groups on nitrogen, as well as several substituent on the aromatic ring. Here below are reported some examples (Scheme 1.73).
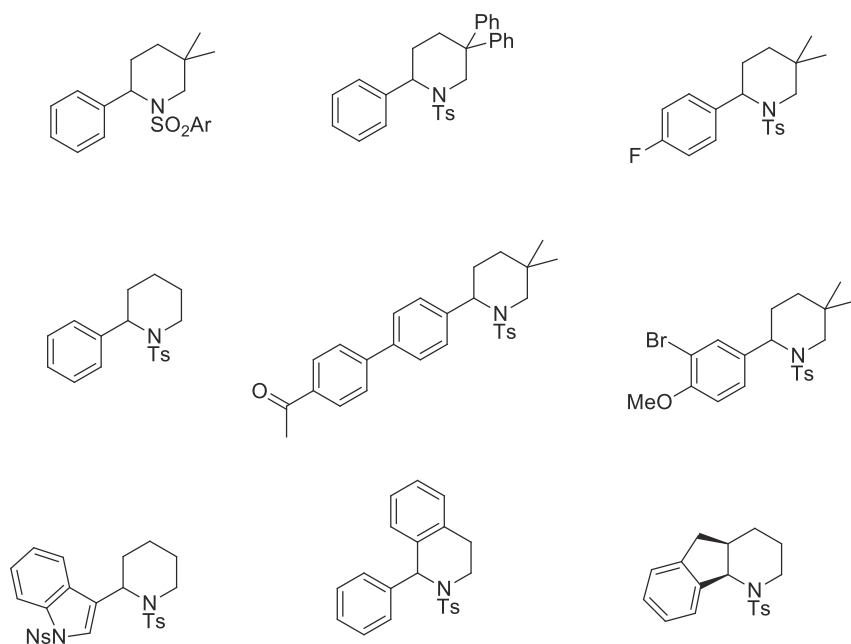
SCHEME 1.73 Some examples of obtained piperidines.

This novel C−H amination reaction is rationalized by the following merger of two catalytic cycles (Scheme 1.74):

SCHEME 1.74   Catalytic cycles.
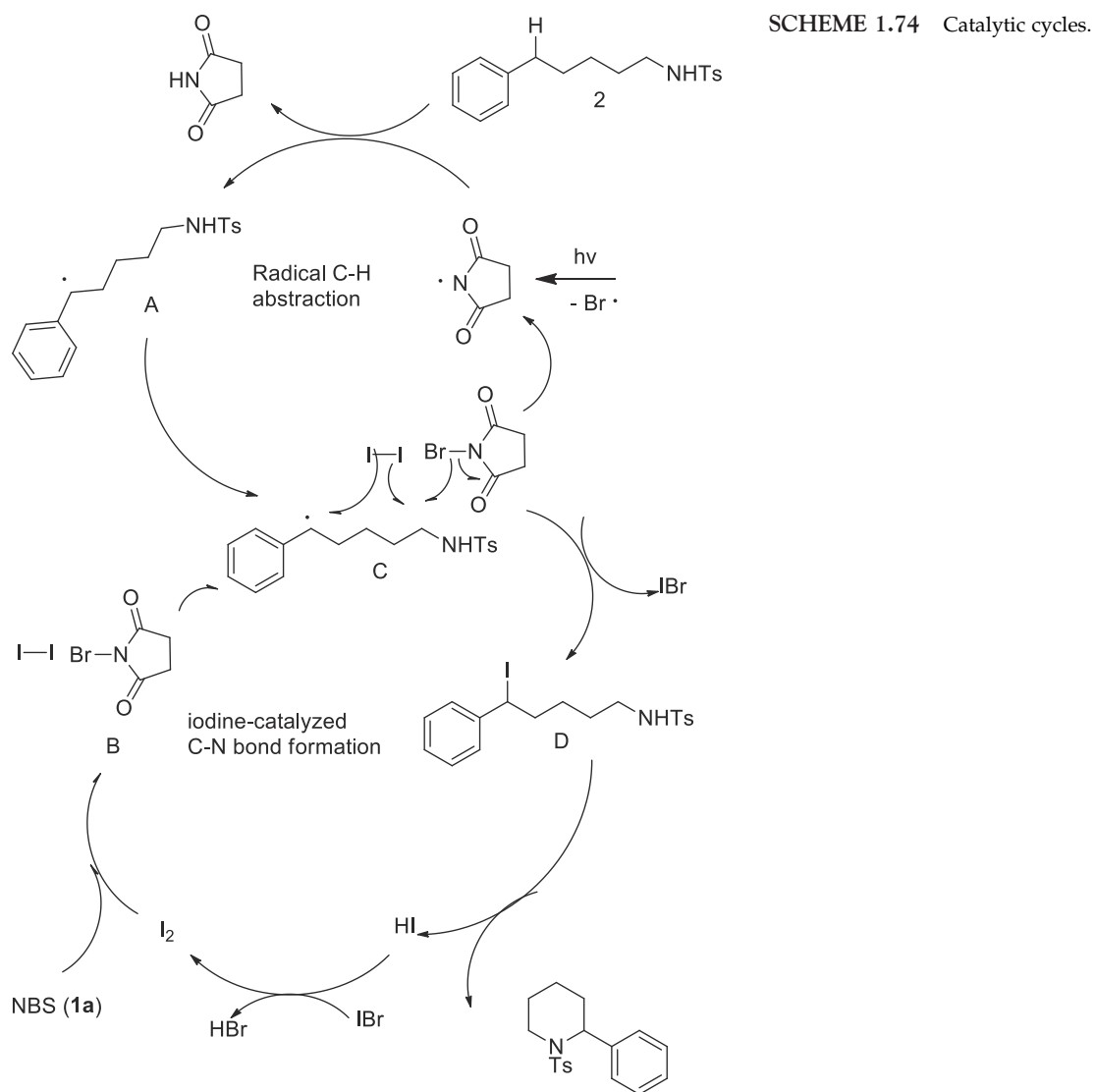
1.10.2 Synthesis from 2,6-diaminopimelic acid to piperidine-2,6-dicarboxylic acid

It has been shown that L-lysine and L-ornithine, natural amino acids, undergo photocatalytic *N*-cyclization into pipecolinic acid (PCA) and proline, respectively, in an aqueous suspension of semiconductor particles, such as titanium(IV) oxide (TiO$_2$) or cadmium(II) sulfide (CdS). As an extention, stereoselective synthesis (Scheme 1.75) of piperidine-2,6-dicarboxylic acid (PDC's) from 2,6-diaminopimelic acid (DAP), a lysine analog having one-more carboxylic group, was studied.[71]

SCHEME 1.75 Synthesis of piperidine-2,6-dicarboxylic acid.

trans   *cis*
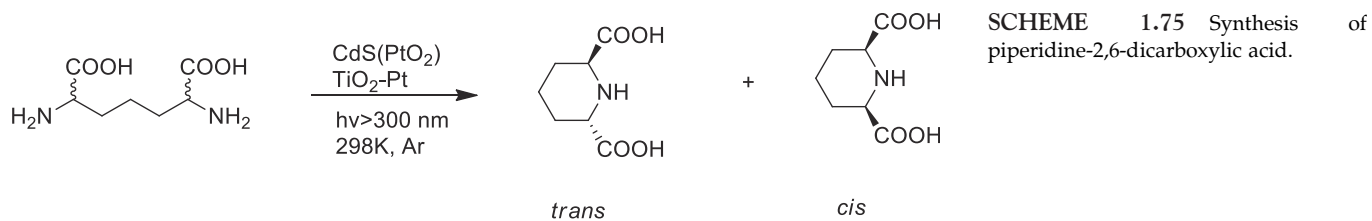
Commercial CdS and TiO$_2$ powders were used with and without pre-treatments. An acqueous solution of DAP (mixture of LL, DD and meso isomer (approx. 1:1:2) and catalyst was placed in a glass tube (transparent at >300 nm) and irradiated at 298 K for 24 h.

The *trans/cis* ratio of PDC dependent on the nature of photocatalysis. Bare CdS particles tend to produce trans-PDC predominantly. On the contrary, in all the cases of PtO$_2$-loaded CdS, the *cis* isomer was produced selectively (*trans/cis* ratio < 0.3).

1.10.3 A photochemical reaction in the synthesis of azasugar derivatives

In a work devoted to the synthesis of azasugars derivatives, useful inhibitors of glycosidases, in one of the steps was utilized a photochemical reaction (Scheme 1.76).[72] Compound **55** was irradiated in 2-propanol in the presence of 1,4-dicyanonaphtalene (DCN) for 2 h to afford, after purification on silica gel, **56** in a yield of 55%.[72] This compound was used to check the inhibition of glycosidases.
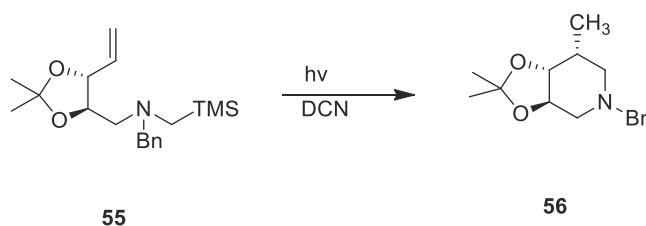
SCHEME 1.76 Photochemical synthesis of an inhibitor of glycosidase.

1.10.4 Piperidines from ring-contaction of N-chlorolactams

Another interesting method to obtain substituted piperidines (and, also, pyrrolidines) is the photochemical rearrangement of *N*-chlorolactams (Scheme 1.77)[73]:
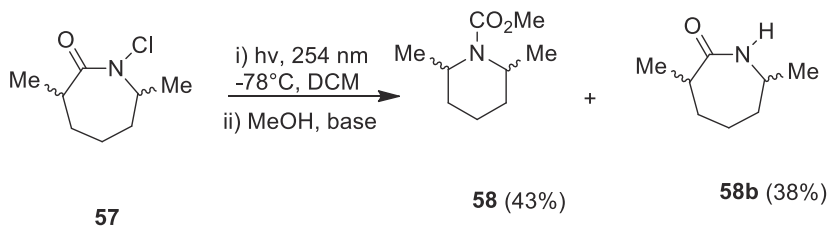
SCHEME 1.77 Ring-contaction of *N*-chlorolactams.

As can be seen, only part of chlorolactams is converted in the substituted piperidine, the rest is converted into the parent lactam. This latter, however, can be re-converted into the chloroderivative and recycled.

Bridged polycyclic molecules rearranged with similar efficiency (Scheme 1.78):
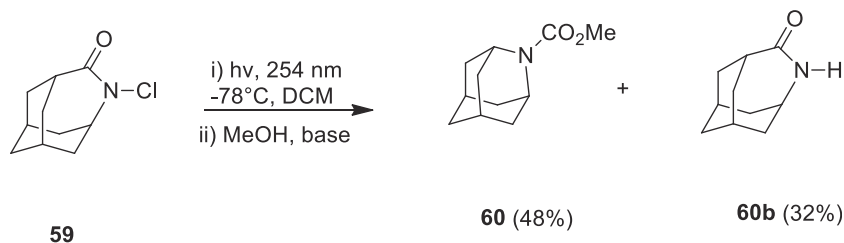
SCHEME 1.78 Rearrangment of bridged polycyclic molecules.

The reaction is stereospecific. From *cis*-**57** the piperidine *cis*-**58** is obtained, and the same for *trans*-**57** (Scheme 1.79).
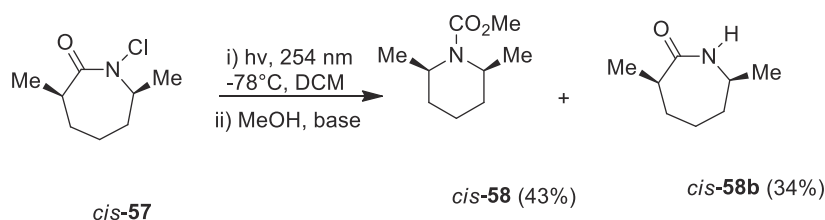
SCHEME 1.79   Stereospecifity of the reaction.

cis-**57**

i) hv, 254 nm
-78°C, DCM

ii) MeOH, base

cis-**58** (43%)

cis-**58b** (34%)

trans-**57**

i) hv, 254 nm
-78°C, DCM

ii) MeOH, base

trans-**58** (55%)

trans-**58b** (33%)
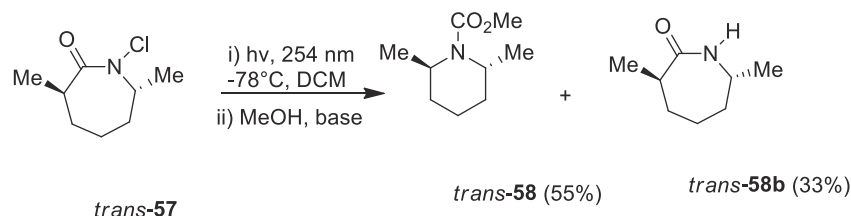
1.10.5 Synthesis of 2-piperidinone catalyzed from a hydrophobic analog of vitamin B$_{12}$

Studying the properties of hydrophobic analogs of vitamin B$_{12}$, obtained as a suspension of vesicles, it was discovered that this system is able to catalyzed ring enlargement of 5-membered cycles (Scheme 1.80).[74]
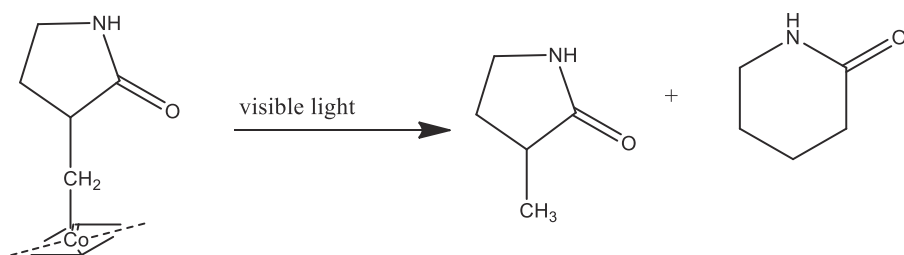
SCHEME 1.80   Ring enlargment of 5-membered cycles.

visible light

1.11 Pyrazoles

1.11.1 Aromatization of 1,3,5 trisubstituted pyrazolines

The synthesis of 1,3,5-trisubstituted-1*H*-pyrazoles is a challenge in organic chemistry, because of the broad spectrum of pharmaceutical activities that these compounds exhibit. Besides chemical methods, also photochemical methods were developed for these syntheses, in particular for the aromatization of 1,3,5 trisubstituted pyrazolines, but they require expensive and/or toxic catalysts or oxidants and prolonged times of reaction. It was developed a simple method that uses visible light and neither catalysts nor oxidants (Scheme 1.81).[75]

light, DCE
catalyst free
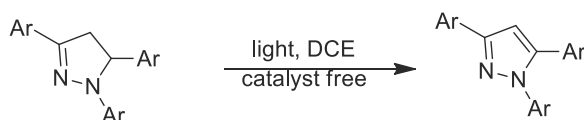
SCHEME 1.81   Aromatization of pyrazolines.
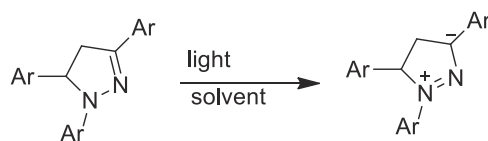
FIGURE 1.50   Intra-molecular charge transfer in pyrazoline.

The key step is an intramolecular charge transfer (ICT) in 1,3,5 trisubstituted pyrazolines, upon excitation by light (Fig. 1.50).

Now, the choice of solvent becomes important. It has been previously reported that DCE has a large electron capture cross section. Hence, DCE was used as a solvent for the oxidation reaction.

The reaction can also performed in sunlight, without any loss of yield, and the yields are good (60%−80%) also if the phenyl groups on the 1,3,5 position are variously substituted.

A plausible mechanism for the light mediated oxidation of 1,3,5-trisubstituted pyrazolines to the corresponding pyrazoles is depicted in Scheme 1.82. Upon irradiation, 1,3,5-trisubstituted pyrazolines **I** initially form the charge separated intermediate species **II**. DCE is known to have large capture cross section and is expected to form a radical anion [DCE$^-$] upon accepting an electron from pyrazoline intermediate **II**, thus generating radical cation **IV** via species **III**. The former radical anion then decomposes into the chlorine radical which abstracts a hydrogen atom radical cationic species **IV** to generate resonance stabilized cations (**V** and **VI**). Abstraction of a proton (H$^+$) from the resonance stabilized cation (**V** and **VI**) results in the formation of pyrazole **VII**.
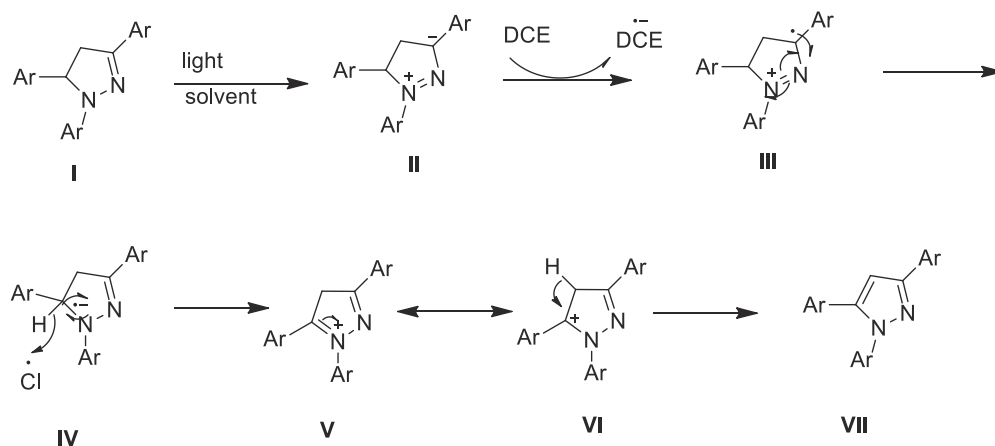
SCHEME 1.82   Mechanism of the reaction.

1.11.2 Photochemical bromination for preparation of mono, bis and fused pyrazole derivatives

In this work, the reaction of NBS with substituted pyrazolinones derivatives (**61a,b**) in CHCl$_3$ at room temperatures in different molar ratio led to the formation of a mixture of mono- and dibromopyrazolinone derivatives (**62a,b, 63a,b**).[76] (Scheme 1.83). In addition, a dibromobispyrazolinone derivative was formed (**64a,b**). Prolonging the time of irradiation, when R = phenyl, only dibromobispyrazolinone derivative was obtained (**64b**), in little yield, while the most of product was a derivative with two pyrazolinone rings linked by a double bond (**65**). This latter product is formed also when R = H, but in this case, the major product is a di-pyrazolo-fused furan derivative (**67**).

SCHEME 1.83 Photochemical bromination for preparation of mono, bis and fused pyrazole derivatives.
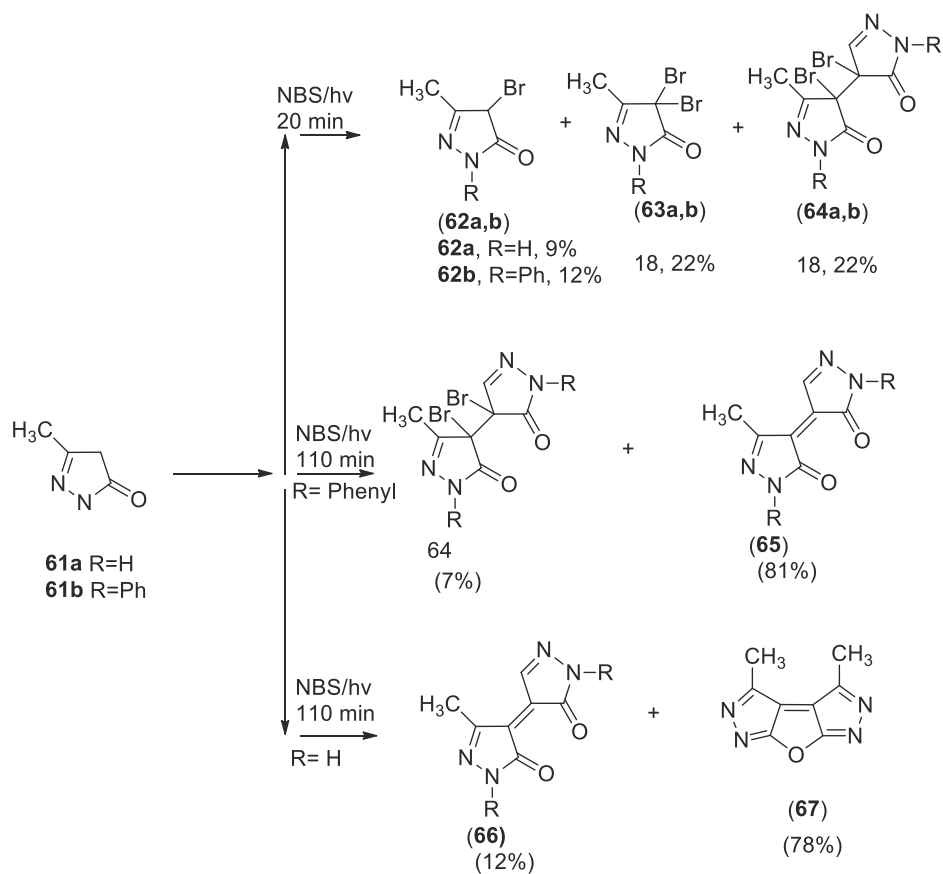
A plausible mechanism for the reaction is depicted in Scheme 1.84. The pirrolydinone forms a bromoradical which dimerizes to **64a**. After, it happens a debromination process that brings to **66**. There is then a dehydration step which affords the furan derivative **67**.

SCHEME 1.84 Mechanism of the reaction.
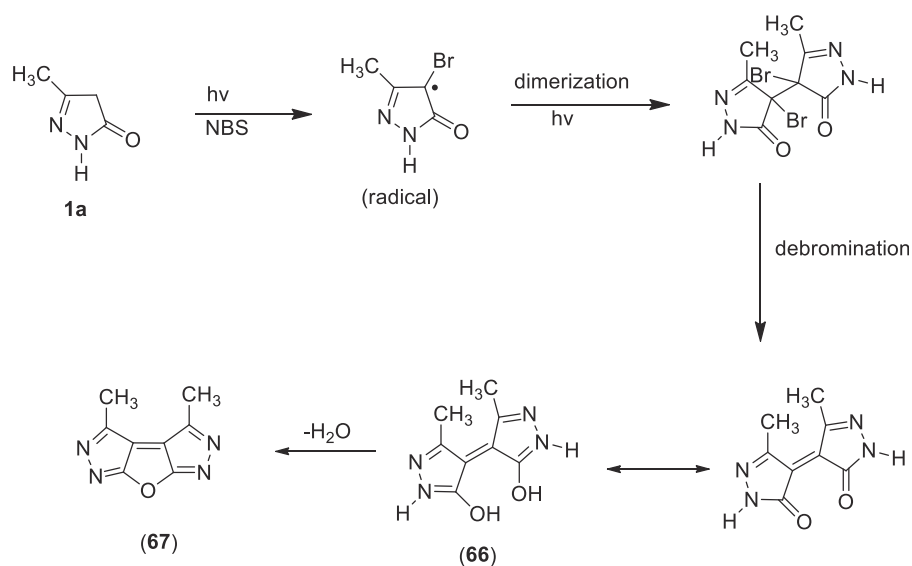
1.11.3 Pyrazoles from hydrazines and Michael acceptors

Pyrazoles skeleton is found in a plethora of compounds, many of these are commercial drugs for various diseases. By far, the most prevalent strategies for constructing pyrazole ring are annulations initiated by the condensation of a monosubstituted hydrazines with a carbonyl, such as cyclocondensation of 1,3-dicarbonyl or $\alpha-\beta$-unsaturated carbonyl compounds with hydrazines. However, these methods usually involve reaction conditions such as high reaction temperatures, microwave irradiation, and hazard oxidant, which are contrary to the concept of green chemistry, and sometimes these can lead to poor regioselectivity. In this context, the authors envisioned that visible light photoredox catalysis (VLPC) can promote transformation of substituted hydrazine to a diazene intermediate which could attack Michael acceptors and cyclize to pyrazoles (Scheme 1.85).[77]
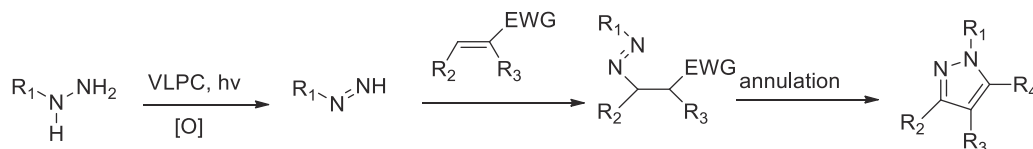
SCHEME 1.85   Pyrazoles from hydrazines and Michael acceptors.

To test this rationale, the authors started their investigation by studying the oxidative annulation between methyl hydrazine (**68a**) and 2-benzylidenemalononitrile (**69a**). The desired product, 5-amino-1-methyl-3-phenyl-1H-pyrazole-4 carbonitrile (**70a**), was furnished in 75% yield (Scheme 1.86) when the reaction proceeded at 25°C in the presence of 2 mol% Ru^{II} (bpy)$_3$Cl$_2$0.6H$_2$O irradiated with a 3 w blue LED in a open vial for 24 h in MeOH. Encouraged by the aforementioned result, other reaction conditions were investigated. The best solvent was acetonitrile, while the other conditions remained the same.

SCHEME 1.86   The reaction.
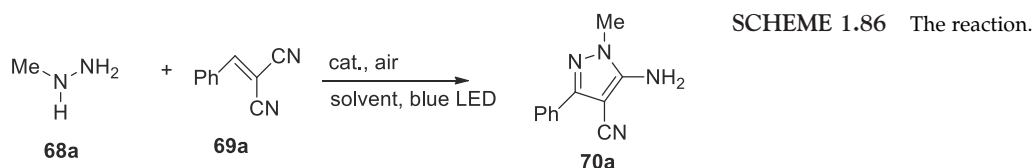
After optimizing the reaction conditions, a wide range of substituted olefins bearing two nitriles were first evaluated in the reaction with methyl hydrazine. Some examples are reported in Scheme 1.87.
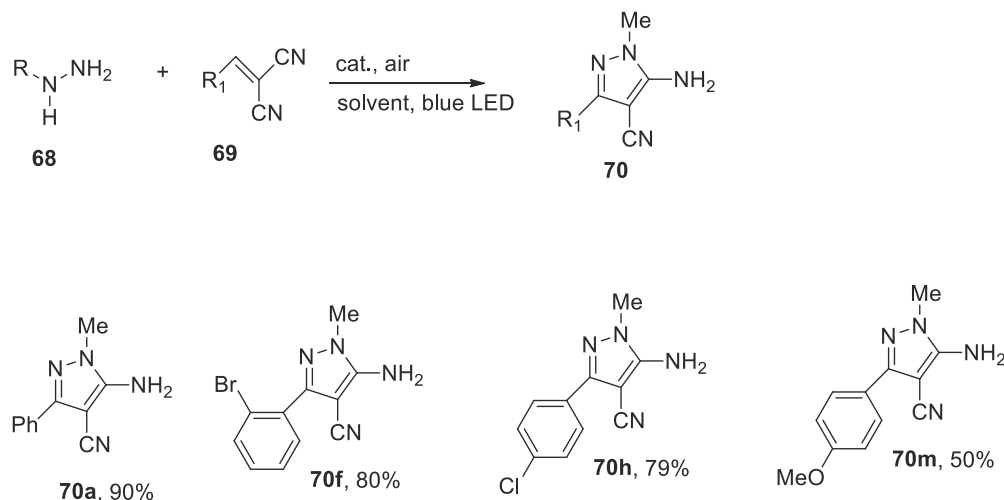
SCHEME 1.87   Some examples of the reaction.

Encouraged by these exciting results, application of this VLPC promoted aerobic annulation to other Michael acceptors was investigated next. Substituted chalcones turned out to be suitable substrates as well as $\alpha - \beta$ unsaturated ketoesters. In the Scheme 1.88 are reported the reaction and some examples of the products.

SCHEME 1.88   More examples.
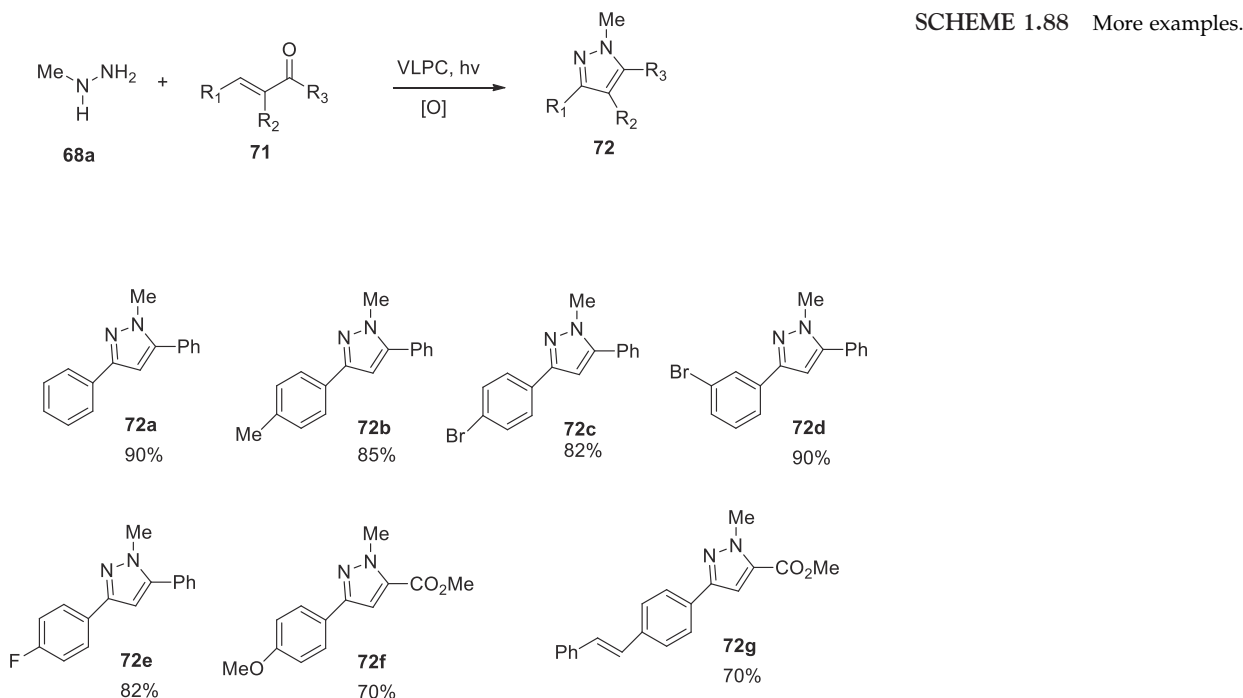
1.11.4 Synthesis of pyrazole derivatives via formal [4 + 1] annulation and aromatization

Visible light photoredox catalysis has recently emerged as a powerful synthetic tool to achieve important organic transfomation. This relay visible light photoredox catalysis can be demonstrated by formal [4 + 1] annulation of hydrazone **A** with diethyl 2-bromomalonate (Scheme 1.89).[78] Three major events are involved in this transformation: (1) photoredox catalyzed oxidative coupling of hydrazone **A** with diethyl 2-bromomalonate via an oxidative quenching cycle to give hydrazone **B**; (2) photo-oxidation of hydrazone **B** to the hydrazinium through a reductive quenching cycle followed by an intramolecular Mannich reaction to provide dihydropyrazole; (3) decarboxylation and photo-oxidation of dihydropyrazole **C** via another reductive quenching cycle to give final pyrazole **D**.
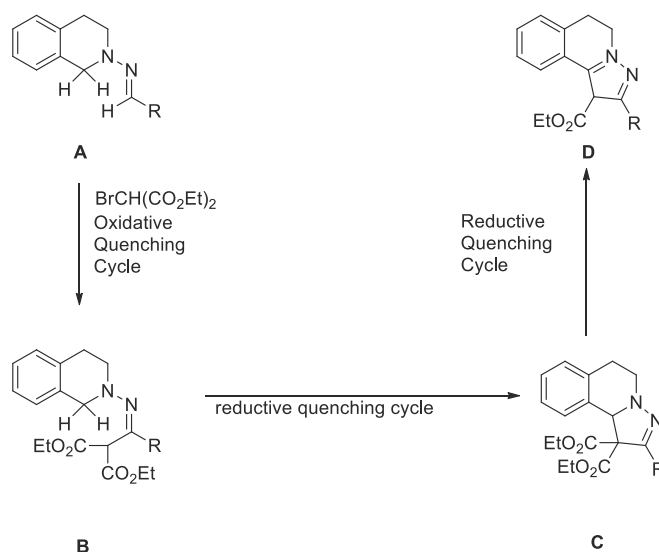
SCHEME 1.89   Annulation of hydrazone **A** with diethyl 2-bromomalonate.

To maximize the yields, the reaction was tried changing various parameters: Fig. 1.51

The best way to perform the reaction was the following: best ratio between **71a** and **72a**: 1:2.5; photocatalyst: [Ir-(ppy)$_2$dtbbpy][PF$_6$]; base K$_2$HPO$_4$ 3 eq.; additive molecular sieves 4 A 100 mg; argon atmosphere; 5 W blue LED irradiation for 16 h.

With the optimized reaction condition estabilished, the scope and limitation of this transformation were explored, using a variety of hydrazones. Some examples are reported in Scheme 1.90.

SCHEME 1.90   Scope of the reaction.
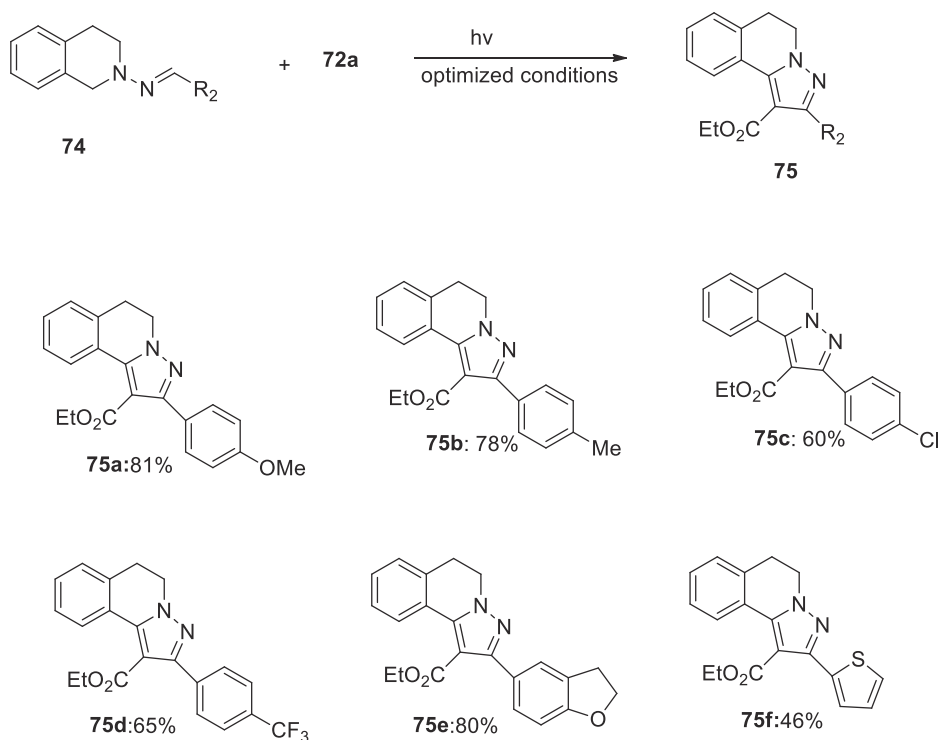
1.11.5 Reaction of hydrazones and α-bromoketones

The authors presented here a strategy which is very actractive, because it shows the good to excellent yield of 1,3,5-trisubstituted pyrazoles under mild condition, short reaction time, and good function group tolerance.[79] The optimized condition to perform the reaction are shown in the figure below: (Fig. 1.52).

FIGURE 1.51   General reaction.

FIGURE 1.52   Reaction with optimized conditions.
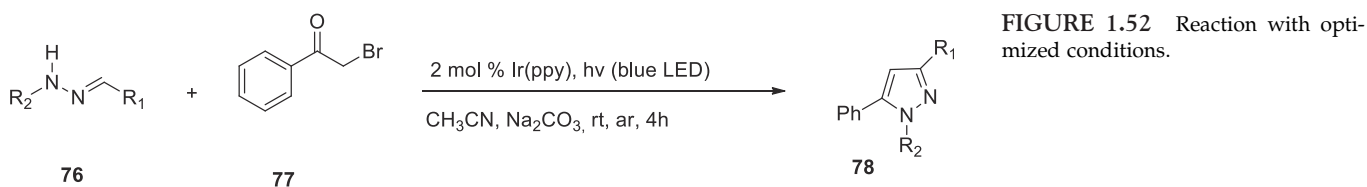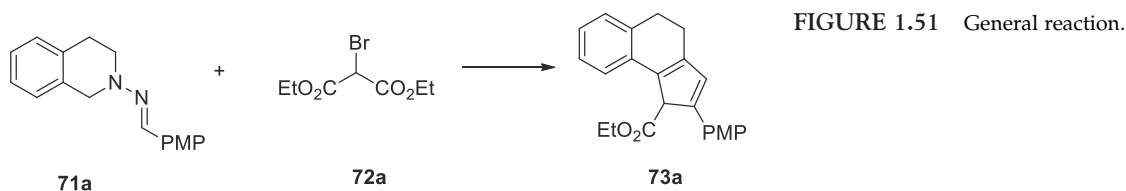
Many pyrazoles can be synthesized in this way. In Scheme 1.91 are shown some of them.

78a, 81%

78b, 60%

78c, 54%

78d, 65%

78e, 72%

78e, 54%
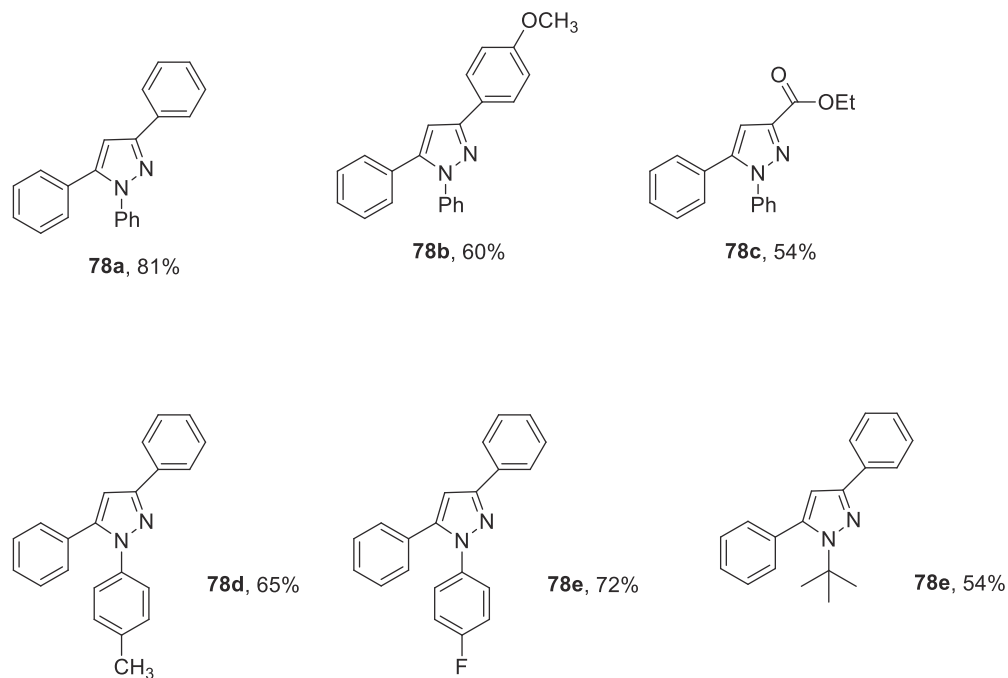
SCHEME 1.91   Some examples of pyrazoles.

Encouraged by these results, the authors tried to do the reaction modifying the structure of α-bromoketone. Even in this case, the reaction proceeds well with yield from moderate to good (Scheme 1.92).

79   **80**

2 mol % Ir(ppy), hv (blue LED)

CH$_3$CN, Na$_2$CO$_3$, rt, ar, 4h

81

81a, 82%

81b, 65%

81c, 65%

81d, 50%

81e, 80%

81f, 72%
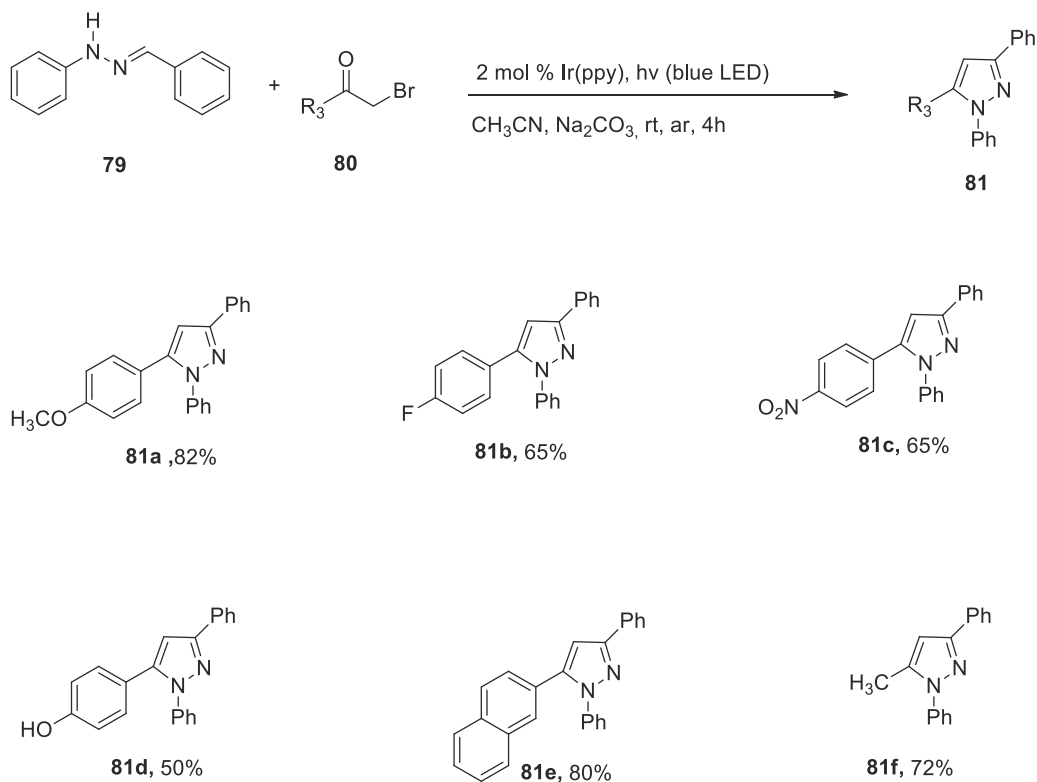
SCHEME 1.92   More examples.
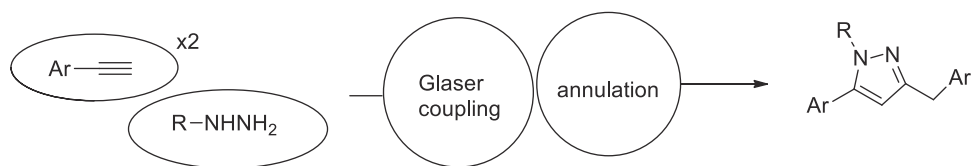
FIGURE 1.53 Diagram of Glaser coupling/annulation.

1.11.6 One pot synthesis of pyrazoles from alkynes and hydrazines

The authors, as continuation of their interest in photocatalysis area, here report a visible-light promoted cascade of Glaser coupling/annulation of alkynes with hydrazines for the synthesis of polysubstituted pyrazoles (Fig. 1.53).[80]

As usual, first, the reaction conditions were optimized using phenylacetylene and hydrazine hydrate as model compounds. After a careful screening, the best conditions were the follows: blue LED 12 W, hydrazine 4 eq., Ru(bpy)$_3$Cl$_2$ 2 mol%, CuI 20 mol%, air (open vial), solvent DMSO.

With the optimize condition in hand, it was explored the reactivity of various aryl acetilenes (**82**) with hydrazine (Scheme 1.93).

SCHEME 1.93 Reaction of acetylenes with hydrazine.
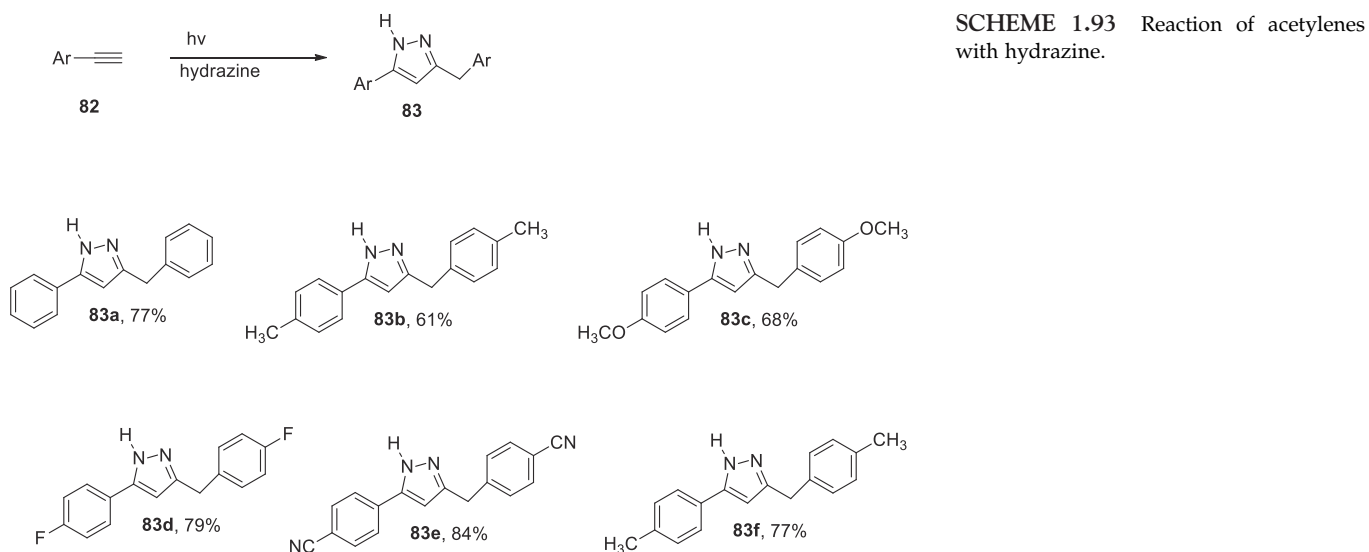
As can be noted, EWG group on the aromating ring gave a yield slighty higher than electron-releasing groups.

The authors then pointed their attention to substituted hydrazines, reacting them with phenylacetylene. Also in this case in the reaction, with few exception, they obtained the expected products with good yields. (Scheme 1.94).

When R = isopropyl or *tert*-butyl the reaction does not happen, probably due to steric hindrance.
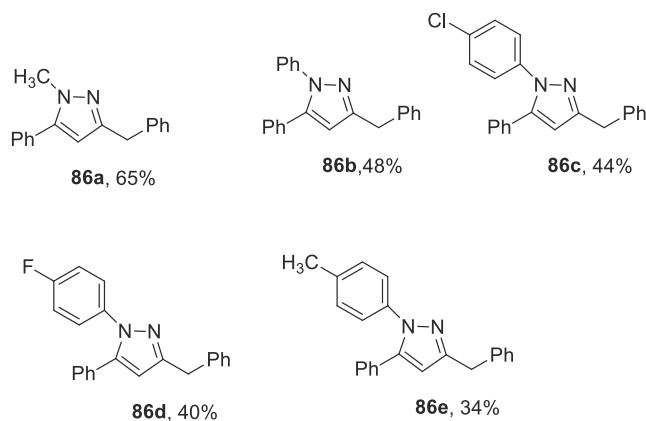
SCHEME 1.94 Reaction of substituted phenylacetylene with substituted hydrazine.

1.11.7 *Sunlight-promoted direct irradiation of N-centered anion: the photocatalyst-free synthesis of pyrazoles*

Zhu et al. developed an interesting method for the synthesis of substituted pyrazoles using direct sunlight irradiation and no photocatalyst. This method is based on the following mechanism (Fig. 1.54) which uses $\alpha-\beta$ unsaturated imines as starting material.

A base abstracts a proton from the group NH forming an anion. This can be excited by light and, after oxidation by air, form the radical **C** which in turn undergo loss of the group Ts and annulation to afford pyrazole.

As usual, the authors tried to optimize the reaction condition to maximize the yield. The optimal conditions are solvent: MeCN; base: K_2CO_3 (1.2 eq.); irradiation by sunlight; air.

In this way many pyrazoles were synthesized: some example are shown in the Scheme 1.95.

SCHEME 1.95   Examples of the reaction.

87a, 98%   **87b**, 89%   **87c**, 84%

87d, 72%   **87e**, 80%   **87f**, 75%

87g, 65%
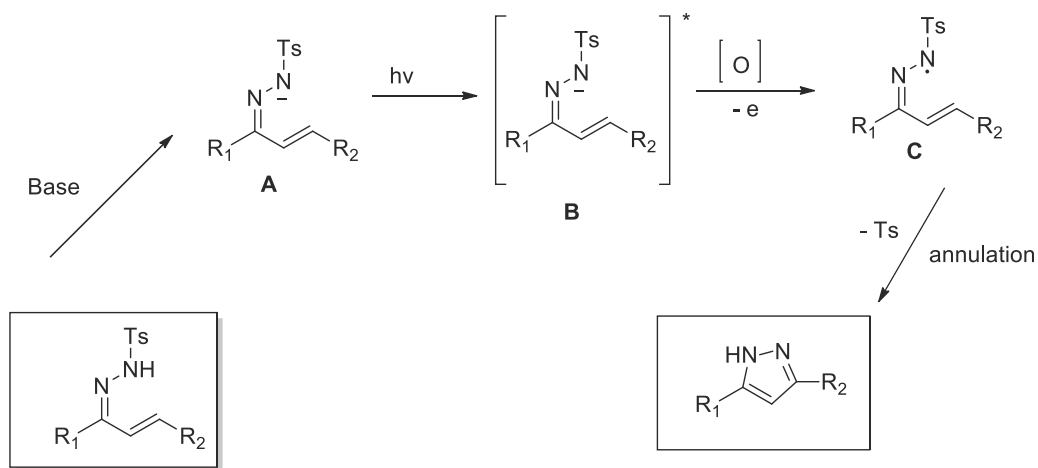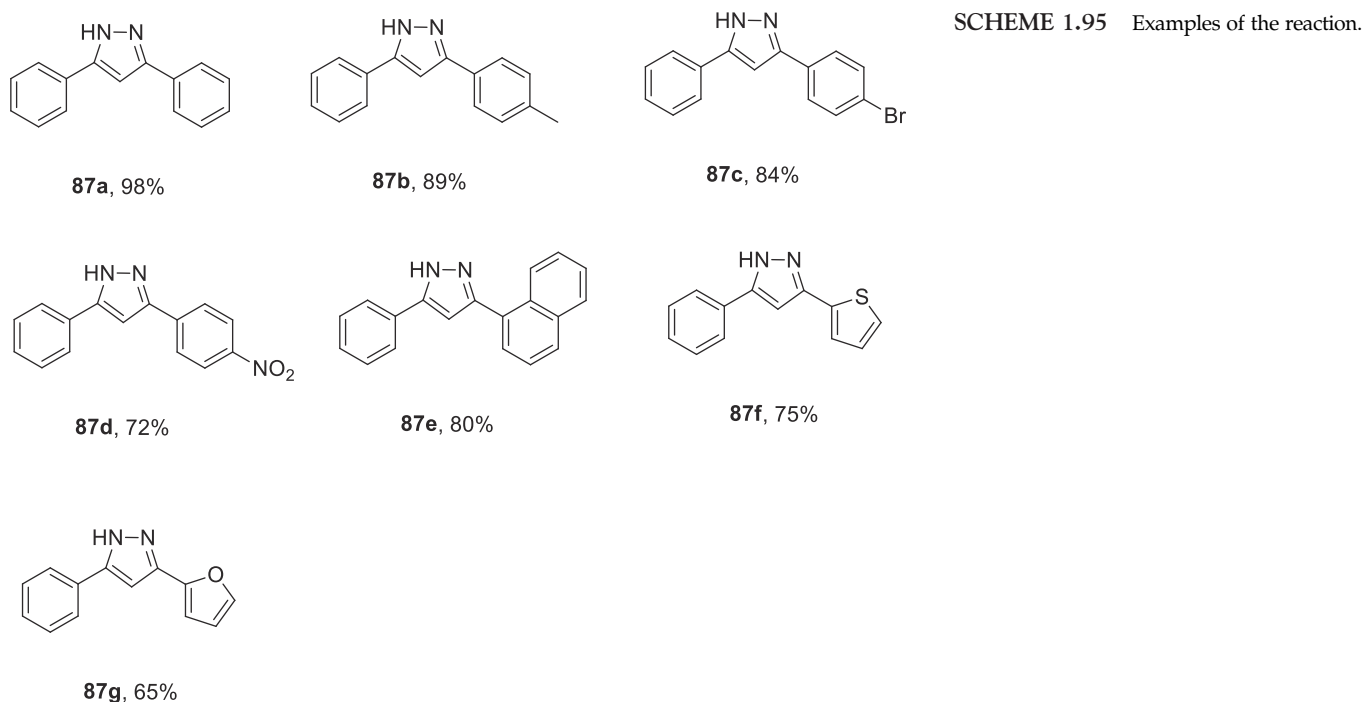
FIGURE 1.54   Mechanism of the reaction.

1.11.8 Efficient photooxidation of aryl (hetaryl)pyrazolines by benzoquinone

Usually, the photo-oxidation of pyrazolines to pyrazoles is performed in perchloroalkanes (CCl_4, C_2Cl_6) which are able to abstract an electron from the excited intermediate. Unfortunately, this method generate acid that may have a negative impact on the course of the reaction. Instead it was used as oxidant benzoquinone (together with molecular oxygen).[81] First, they syntesized a series of (1,5-diaryl-3-pyrazolinyl)coumarines as substrates (Scheme 1.96).
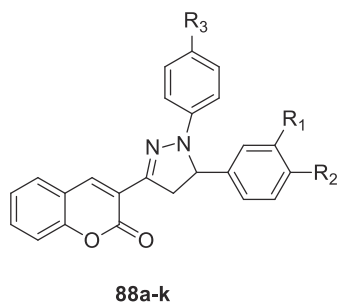
88a: $R_1 = R_2 = R_3 = H$
88b: $R_1 = H$, $R_2 = NMe_2$, $R_3 = F$
88c: $R_1 = H$, $R_2 = NO_2$, $R_3 = Me$
88d: $R_1 = OH$, $R_2 = OMe$, $R_3 = F$
88e: $R_1 = R_2 = H$, $R_3 = Me$
88f: $R_1 = R_2 = H$, $R_3 = F$
88g: $R_1 = R_2 = H$, $R_3 = NO_2$
88h: $R_1 = R_3 = H$, $R_2 = OMe$
88i: $R_1 = R_3 = H$, $R_2 = NO_2$
88j: $R_1 = R_2 = H$, $R_2 = Me$
88k: $R_1 = R_3 = H$, $R_2 = NMe_2$

88a-k

SCHEME 1.96   Synthesis of pyrazolinyl coumarines.

The authors do not report the yield of the single reactions. They stated only that in perchloroalkanes the maximum yield was 67%, while in the presence of benzoquinone the yield can reach 94%.

The best results were obtained with benzoquinone in open air. However, when only air was used, the reaction did not happen.

A mechanism for this reaction was also proposed. This is depicted in Scheme 1.97.
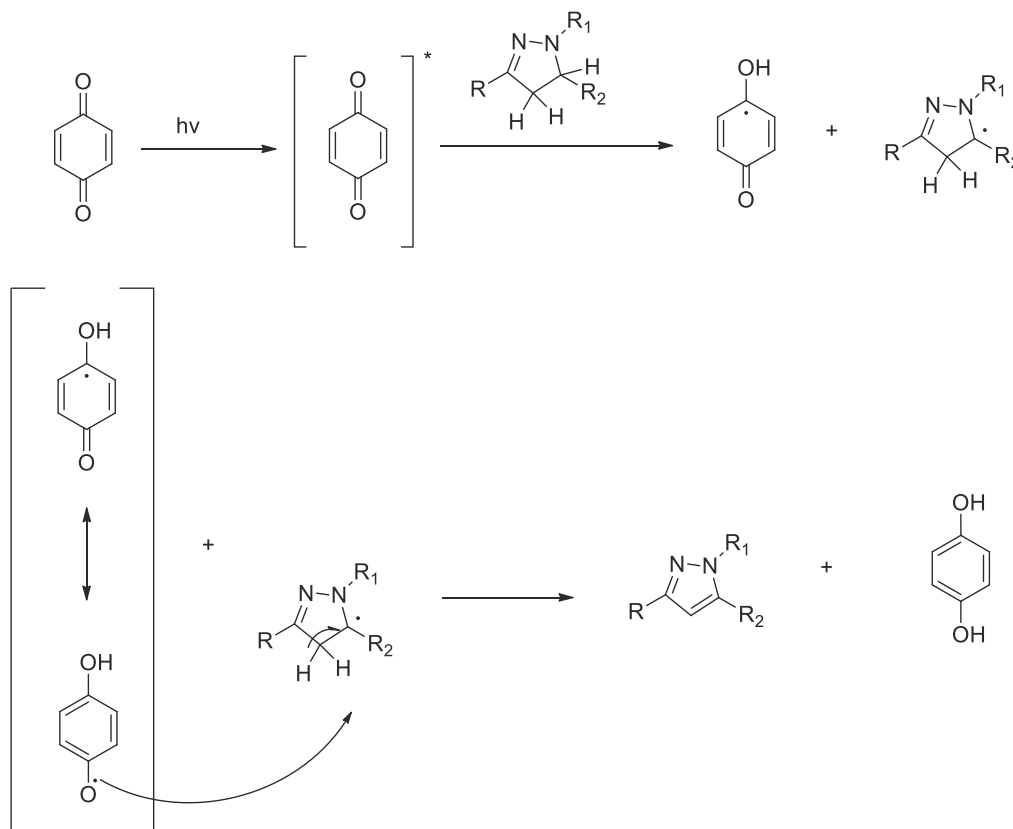
SCHEME 1.97   Mechanism of the reaction.
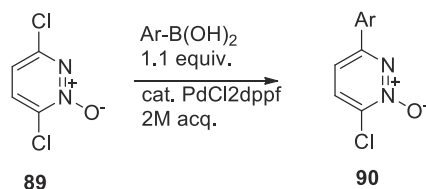
FIGURE 1.55   Suzuki coupling.

1.11.9 Synthesis of pyrazoles via photochemical ring opening of pyridazine N-oxides

An intriguing method to obtain 3,5 substituted pyrazoles is the ring-opening of pyridazines *N*-oxides. However, when these latter compounds were irradiated by UV, no pyrazoles were obtained. In many cases, all what happens is the deoxygenation of *N*-oxide to afford a pyridazine. It was developed an elegant method to obtain the desired pyrazole with complete control of the regiochemistry.[82]

They started from 3,6-dichloro pyridazine *N*-oxide, and performed on this compound the Suzuki coupling (Fig. 1.55).

As can easily be seen, the reaction is highly regioselective: the aryl group goes in position 3. The chlorine in position 6 can be replaced by a nucleophile in an S$_N$Ar reaction. The authors chosed pyrrolidine, and then subjected the obtained compounds to irradiation. The result are summarized in Scheme 1.98.
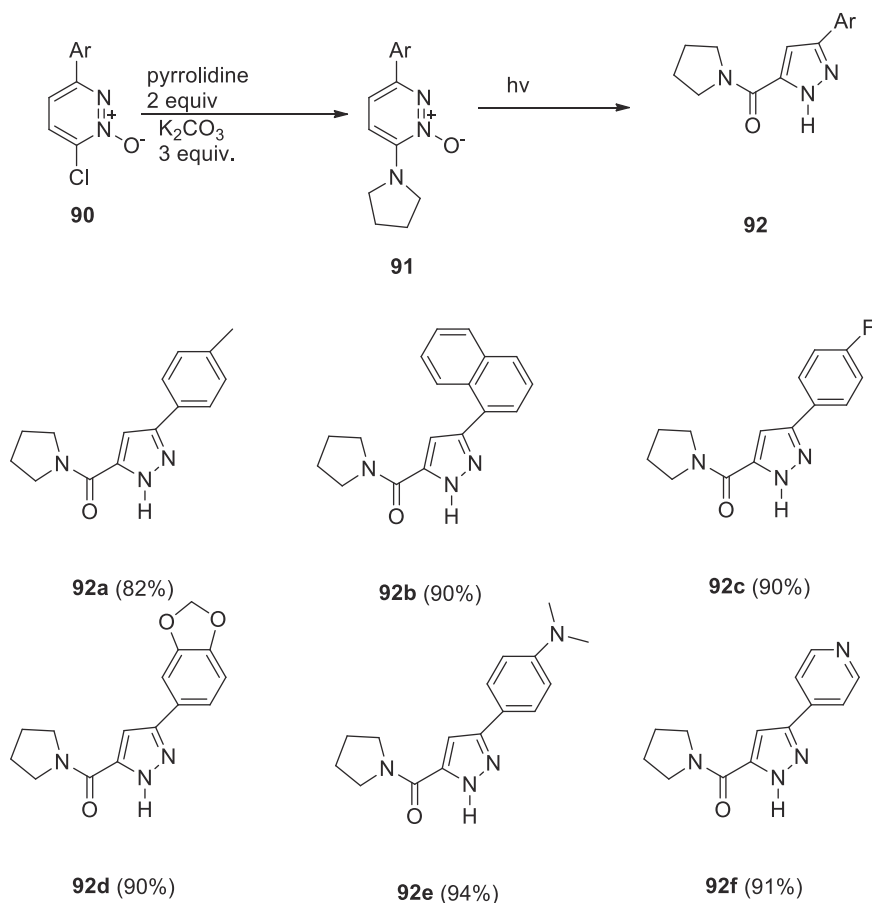
SCHEME 1.98   Obtained compounds.

92a (82%)

92b (90%)

92c (90%)

92d (90%)

92e (94%)

92f (91%)

Encouraged by these results, the authors tried to perform the reaction changing the nucleophile in the second step of the reaction (Scheme 1.99).
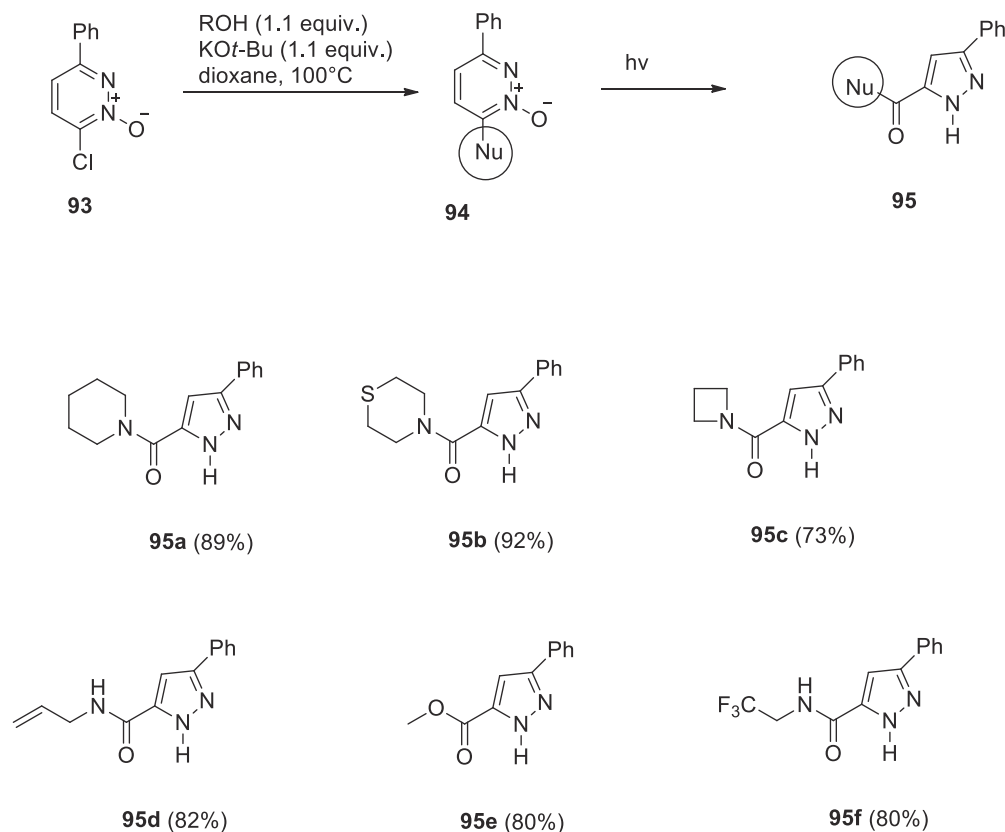
SCHEME 1.99   Change of the nucleophile.

Also in this case, the yield are satisfactory.

1.12 Pyridines

1.12.1 *Pyridines from ring closure of acyloximes*

The rich potential of iminyl radical, generated by both thermal and photochemical methods, is manifested in cyclization reaction. However, the literature on iminyl radical cyclizations is scarce. In most cases, formation of five-membered nitrogen heterocycles rings takes place. Here is described the use on iminyl radical, generated from irradiation of acyloximes, for the preparation of six- membered rings such as phenantridine or isoquinolines (Scheme 1.100).[83]
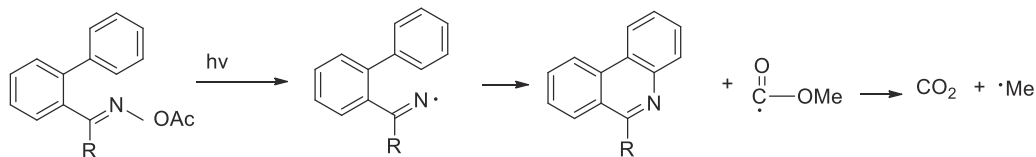
SCHEME 1.100   Reaction of iminyl radical.

The generation of methyl radical has been detected by EPR spectroscopy.

First, it was tried to use a naphthyl group, rather than a phenyl group, as a spacer. When subjected to irradiation in acetonitrile through pyrex glass, **96** gave a 55% yield of benzo[i]phenantridine **97**, after

cyclization of the iminyl radical onto the phenyl ring and the loss of an H-atom to restore the aromaticity (Scheme 1.101).
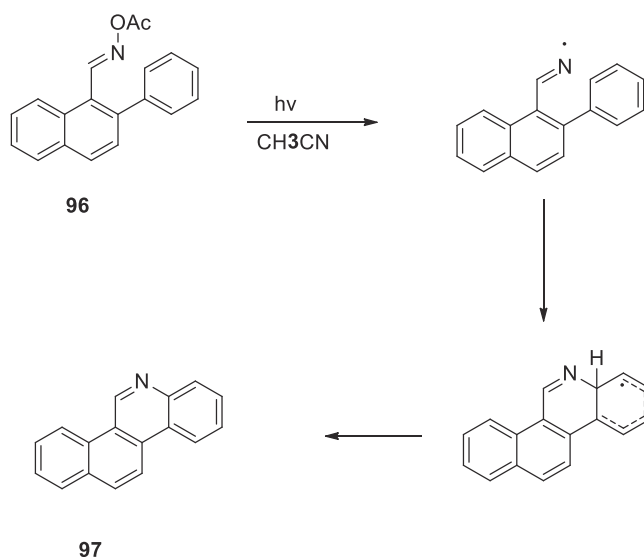
SCHEME 1.101 Phenantridine.

However, the irradiation of indolyl derivative **98** led to the formation of nitrile **99** instead of the expected cyclization product (Scheme 1.102).
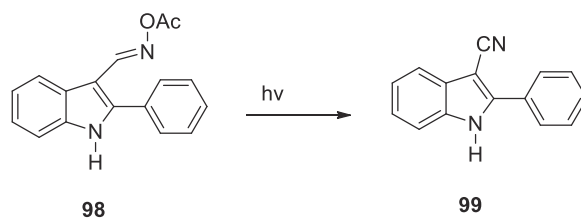
SCHEME 1.102 Formation of a nitrile.

These results suggested that ring closure of intermediate iminyl radical onto phenyl ring supported on a five-member spacer should be slower than that of six-membered one and unable to compete with the formation of nitrile.

It was also explored the iminyl radical ring closure onto heteroaromatic rings. The use of a thiophenyl ring as iminyl radical acceptor led to preparation of thieno[3,2-c]isoquinoline **101** in 56% yield (Scheme 1.103). Next, they
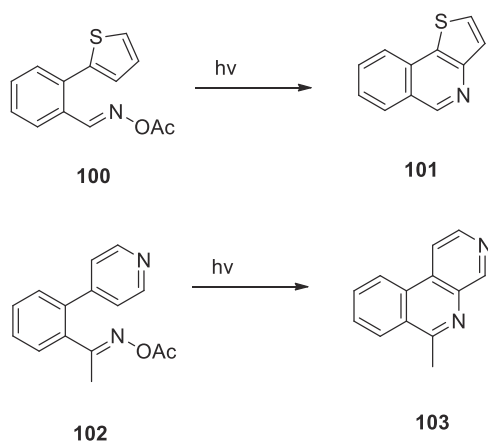
SCHEME 1.103 Iminyl radical ring closure onto heteroaromatic rings.

planned to use this methodology to the iminyl radical closure onto the pyridine ring. Reports of ring closure of C-centered radicals onto pyridine ring are rare and there are not many examples describing the analog reaction for *N*-centered radical either. Scheme 1.5 also shows the results for this process. Iminyl radical, generated from irradiation of **102** in CH$_3$CN, did cyclize onto pyridine, enabling 6-methylbenzo[c][1,7] naphthyridine **103** to be prepared in 90% yield.

1.12.2 Synthesis of naphthyl pyridines from heptadynes and nitriles

Biaryl compounds (such as BINOL or BINAP) have a great importance in organic synthesis because they show atropoisomerism that is, can exist in two enantiomeric forms. Such compounds are of great value as catalysts in enantioselective reaction.

In this work new heterobiaryl systems were synthesized having a pyridine core with the naphthyl linked in position 2 of the pyridine ring.[84] They started with naphthyl heptadynes that, in a photochemical reaction with MeCN or PhCN, afforded the desired heterobiaryls (Scheme 1.104).
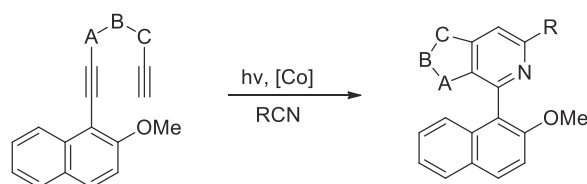
SCHEME 1.104   Synthesis of naphthyl pyridines from heptadynes and nitriles.

The catalyst used was [CpCo(COD)] (COD = 1,5-cyclooctadiene). When performed on diyne **104**, the reaction went better with use of MeCN than PhCN (Scheme 1.105).

104

R = Ph 44%
R = Me 93%

105
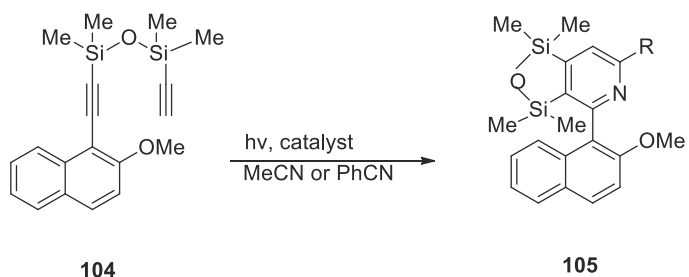
SCHEME 1.105   Another example of this reaction.

In several cases the cyclization was additionally performed under thermal or microwave conditions. However, in the case of lactone **107**, a minor yield was observed under microwave conditions (21%), which can be attributed to the decomposition of the ester moiety under these reaction conditions (Scheme 1.106).

106

MW = 21%
hv = 39%

107
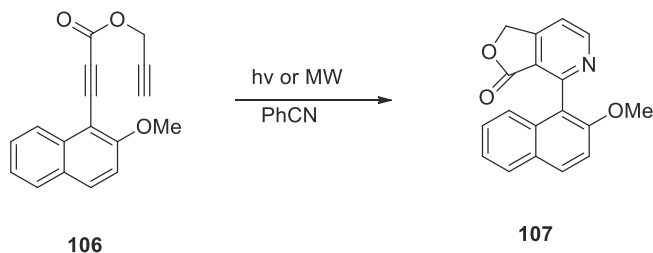
SCHEME 1.106   Another example.

The cyclization of enediyne **108** indeed gave the expected product **109**, containing the exocyclic double bond and only very minor amounts of the internal isomerization product with an endocyclic bouble bond. (Scheme 1.107).
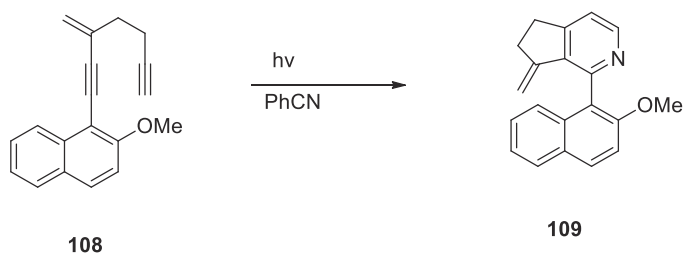
SCHEME 1.107 Cyclization of enediyne 108.

Alcohol 111 was formed as a mixture of diastereomeric atropoisomers due to the presence of the stereogenic carbon atom carring the hydroxyl group (Scheme 1.108).
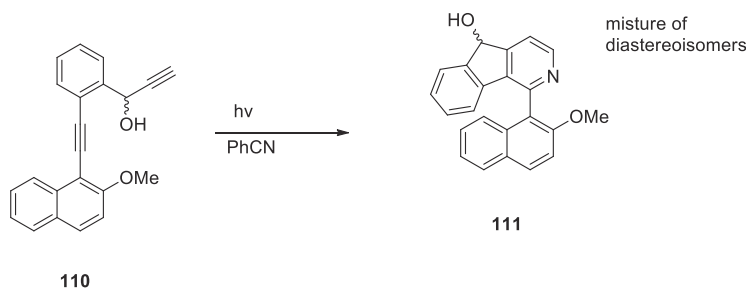
SCHEME 1.108 Reaction leading to a mixture of atropoisomers.

1.12.3 Synthesis of substituted pyridine from aryl ketone and benzylamines

An interesting synthesis of 2,4,6 triaryl substituted pyridines is proposed Fig. 1.56.[85]

First, the authors made many attempts to find the best condition to perform the reaction as follows: aryl ketone, 1.0 equiv.; benzylamine, 3.0 equiv.; catalyst, eosin Y; additive, BF$_3$.Et$_2$O 50%; solvent, MeOH.

Then, to identify which aryl group is derived from which substrate, they performed the same reaction using 1-(p-tolyl)ethanone and benzylamine, yielding 2,4,6 triarylpyridine 112 (Fig. 1.57):

It is clear that the methyl group in **112** arise from the aryl ketone.

With optimized condition in hand, the authors paid their attention to the scope of the substrate. A series of reaction was made. These reactions are all depicted in Scheme 1.109.

The reaction of (p-methoxyphenyl)ethanone with benzyl amine, under the optimized conditions, gave the corresponding 2,4,6-triarylpyridine **115c** in 72% yield. Reaction of electron-withdrawing substituted acetophenones such as (p-fluorophenyl)-, (p-chlorophenyl)-, and (p-bromophenyl) ethanones and benzyl amine afforded good yields of products **115d** (68%), **115e** (68%), and **115f** (64%). However, (p-nitrophenyl)ethanone was unreactive under the reaction conditions. The effect of an electron-donating ortho group was demonstrated by using sterically hindered (o-methoxyphenyl)ethanone as a substrate, which also provided **115m** in 66% yield.

Next, the effect of substituents on the benzyl amine was studied. Thus, the reaction of 4-methoxybenzylamine with (p-chlorophenyl)-, (p-fluorophenyl)-, (p-methylphenyl)-, and (p-methoxyphenyl)ethanone, gave the
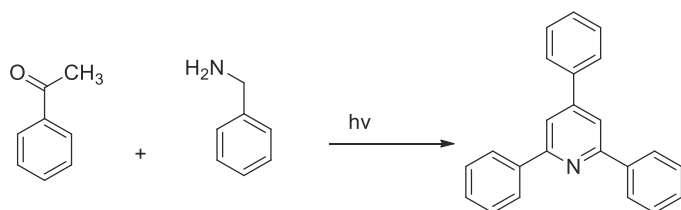
FIGURE 1.56 The general reaction.
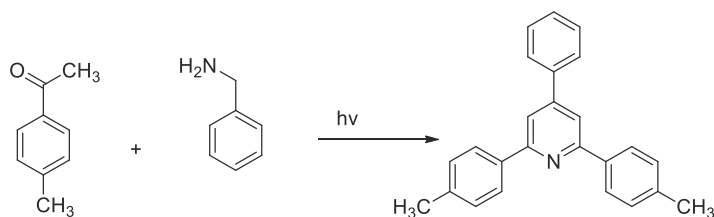
FIGURE 1.57 Reaction of 1-(p-tolyl)ethanone and benzylamine.
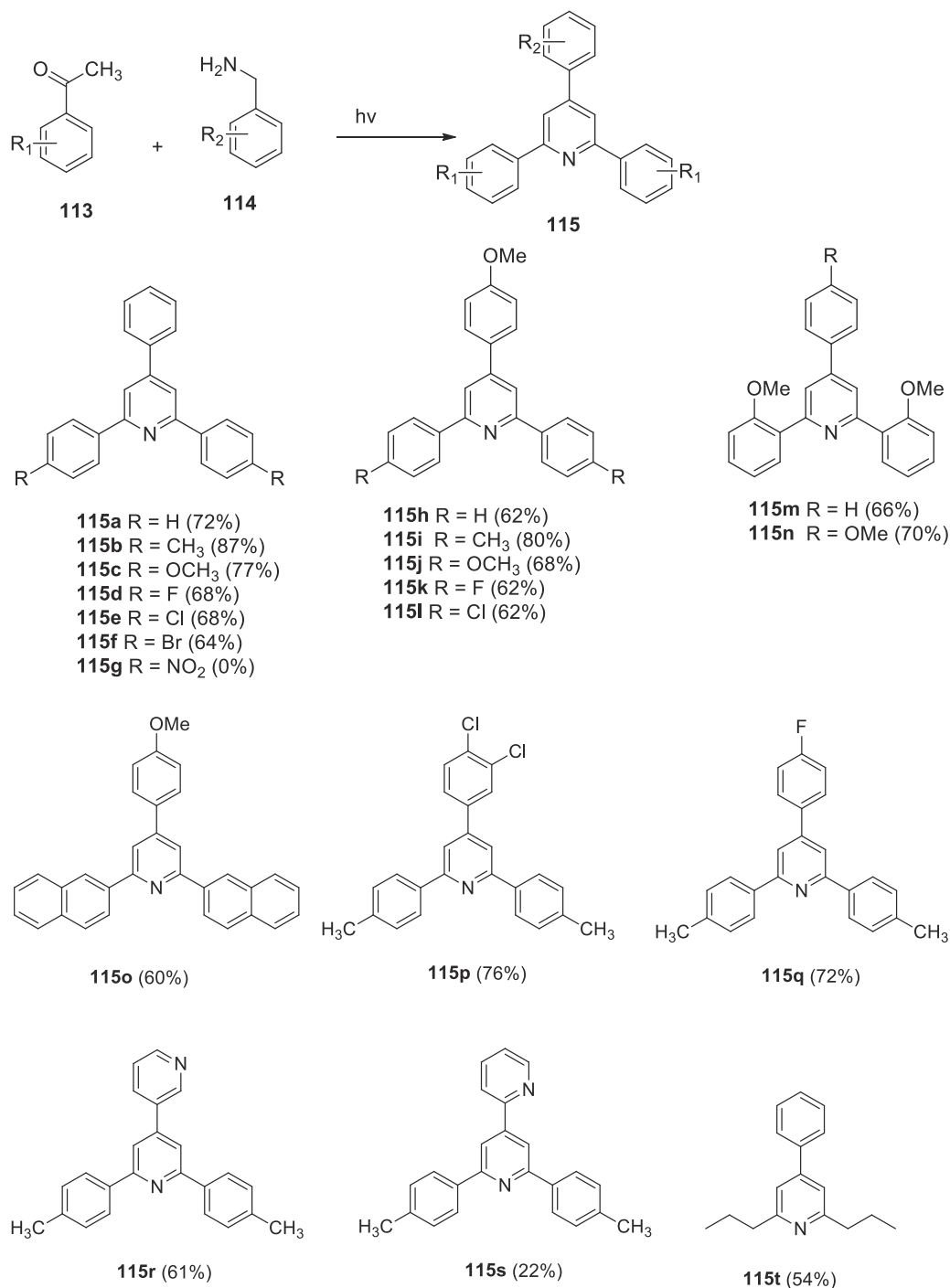
SCHEME 1.109 Scope of the substrate.

corresponding 2,4,6-triaryl pyridines **115h,i** in good yields (62%−80%). The reaction of 4-methoxybenzil amine with 1-(naphthalene -2-yl)ethanone gave **115o** in 60% yield, and the reaction of 3,4-dichlorobenzyl amine and 4-fluorobenzyl amine with 1-(p-tolyl)ethanone provided the corresponding products **115p,q** in 76% and 72% yields, respectively. The scope of the reaction was further studied with aliphatic as well as cyclic ketones. Thus the reaction of pentan-2-one with benzyl amine afforded product **115t** in 54% yield, while the reaction with cyclo-hexanone led to a complex mixture of products. Treatment of 3-picolylamine with (p-methylphenyl)ethanone gave the desired product **115r** in 61% yield.
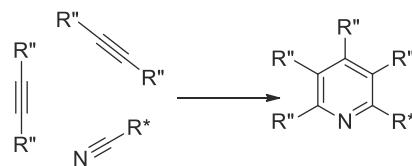
FIGURE 1.58   Cyclocotrimerization of nitriles.

1.12.4 Pyridines from trimerization of two alkenes and a nitrile

A very effective method to prepare substitutes pyridines is the cyclocotrimerization of nitriles with a broad variety of alkynes (Fig. 1.58).[86]

Indeed, this kind of reaction was already performed by two Italian research groups, that made the reaction but in very drastic conditions (ethyne pressure above 10 bar, temperature above 100°C, long reaction times and high catalyst concentration). However, these dramatic reaction conditions usually lead to a noticeable decrease of enantiomerical purity with respect to the starting material (nitrile). Instead, the Co(I)-catalyzed [2 + 2 + 2] cyclo-addition of alkynes with nitriles can be carried out under very mild conditions (ambient temperature and pressure) if the required energy is supplied in the form of light (350−500 nm).

Under irradiation with visible light, the photochemical [2 + 2 + 2] cyclocotrimerization of optical active nitriles with alkynes catalyzed by [cpCo(cod)]($\eta5$ − cyclopentadienyl-$\eta4$-cycloocta-1,5-dienecobalt(I)) can be used to prepare optically active compounds containing a pyridyl moiety. Good to excellent yields are achieved with reaction times between 4 and 6 h working in organic solvents. The results are summarized in Table 1.1.

The photochemical cyclocotrimerization bears the opportunity to improve chemoselectivity: byproducts arising from the homotrimerization of three alkyne molecules can be avoided.

The reaction is very versatile: a dinitrile can react with four molecules of an alkyne to give a product which bears two pyridine moieties (**119b**); furthermore it is not necessary for the alkyne to be a terminal alkyne:

TABLE 1.1   Examples of the reaction.

Nitrile	Alkyne	Obtained pyridine	Yield (%)	e.e. (%)
(-)**116a**	2 ≡	(-)**116b**	82	>99
(-)**117a**	2 ≡	(-)**117b**	68	>99
(+)**118a**	2 ≡	(+)**118b**	89	>99

(Continued)

TABLE 1.1 (*Continued*)
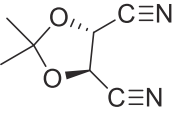
Nitrile	Alkyne	Obtained pyridine	Yield (%)	e.e. (%)
(+)**119a**	4	(+)**119b**	82	>99.5
(-)**120a**	2	(+)**120b**	64	>99.5
(-)**120a**	2	(-)**120c**	83	>99.5
(-)**120a**		(-)**120d**	64	>99.5
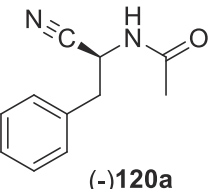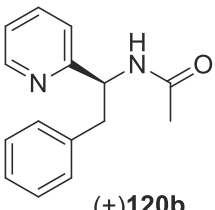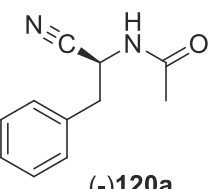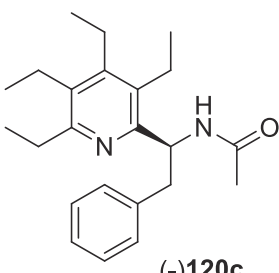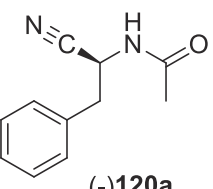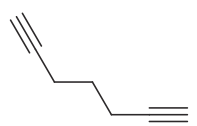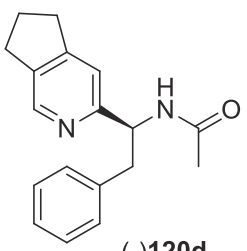
2-butyne reacts with nitrile **120a** to afford a pentasubstituted pyridine (**120c**). It is also possible to use a diyne: 1,6 heptadiyne reacts with **120a** to give **120d** which has a cyclopentane ring fused with pyridine.

1.13 Pyrimidines

1.13.1 Synthesis of benzo-fused pyrimidines- 4-ones from 1,2,4 oxadiazoles

An efficient and generalized photochemical methodology for the preparation of fluorinated quinazolin-4-ones is described.[87] This process, which takes place under irradiation of the oxadiazoles in the presence of sensitizers or triethylamine (TEA), unvolves a photoinduced electron transfer between the excited sensitizer (S) (donor) and the ground state oxadiazole (OXA) (acceptor) or between the excited oxadiazole (acceptor) and the TEA (donor), followed by cyclization of the open chain radical anion intermediate into the final quinazolin-4-one product (Scheme 1.110).

121 → **122**

S = sensitizer   OXA = oxadiazole

e.t. = electron transfer   r.o = ring opening   r.c. = ring closure   b.e.t. = back electron transfer
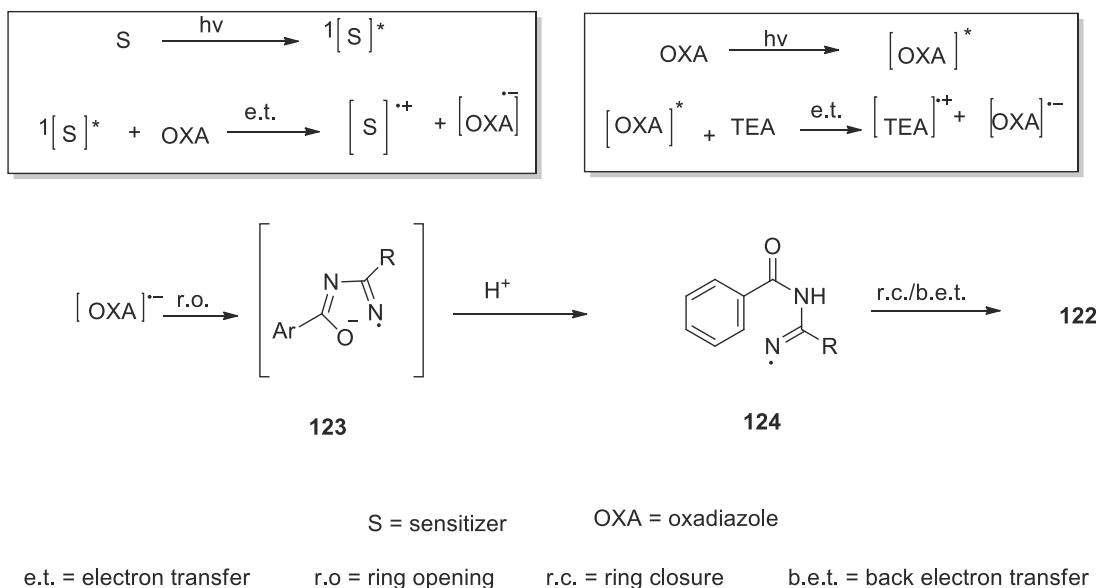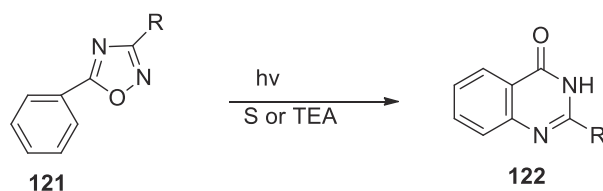
SCHEME 1.110   Mechanism of the reaction.

To realize their project, the authors considered two series of 1,2,4-oxadiazoles: Compounds **125a-d** and compounds **125e-h** (Scheme 1.111). Referring to their previous results on the sensitized photorearrangment of 1,2,4-oxadiazoles, they performed irradiation in the presence of TEA (at $\lambda = 313$ nm) or in presence of pyrene (at $\lambda = 365$ nm).
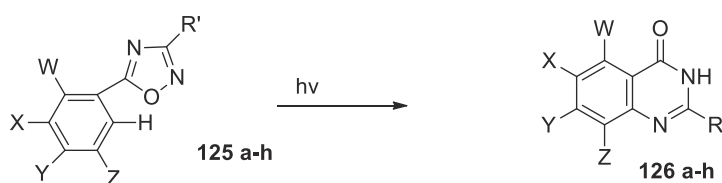
SCHEME 1.111   Examples.

125 a-h → **126 a-h**

a: W,X,Y,Z = H; R' = CF$_3$
b: W,X,Y,Z = H; R' = C$_3$F$_7$
c: W,X,Y,Z = H; R' = C$_7$F$_{15}$
d: W,X,Y,Z = H; R' = C$_6$F$_5$

e: W,X,Y,Z = F; R' = Ph
f: W,X,Y = F; Z = H; R' = Ph
g: W,X,Y,Z = F; R' = Me
h: W,X,Y = F; Z = H; R' = Me

Irradiations performed in the presence of TEA give products in low to moderate yields. So, the procedure was improved trying pyrene as a sensitizer with the advantage of irradiating at a wavelength were both the substrate and the final products do not absorb, thus minimizing photodecomposition processes. In this way, the yields were increased up to 75%. In a separate experiment, the quinazolin-4-ones showed to be unstable under the irradiation conditions, for this reason it was decided to stop the irradiation of the substrate before its complete conversion; chromatographic separation allowed to isolate the product and to recycle the unreacted starting material. It is interesting that, in the case of pentafluorophenyloxadiazole (**127**), the irradiation resulted in the

formation of the reduction product (**129**) only; the corresponding quinazolin-4-one (**126e**) is not observed, likely because of the uneasy displacement of the 2-fluoro substituent on the aromatic ring during the cyclization step of the radical anion intermediate (**128**) (Scheme 1.112).
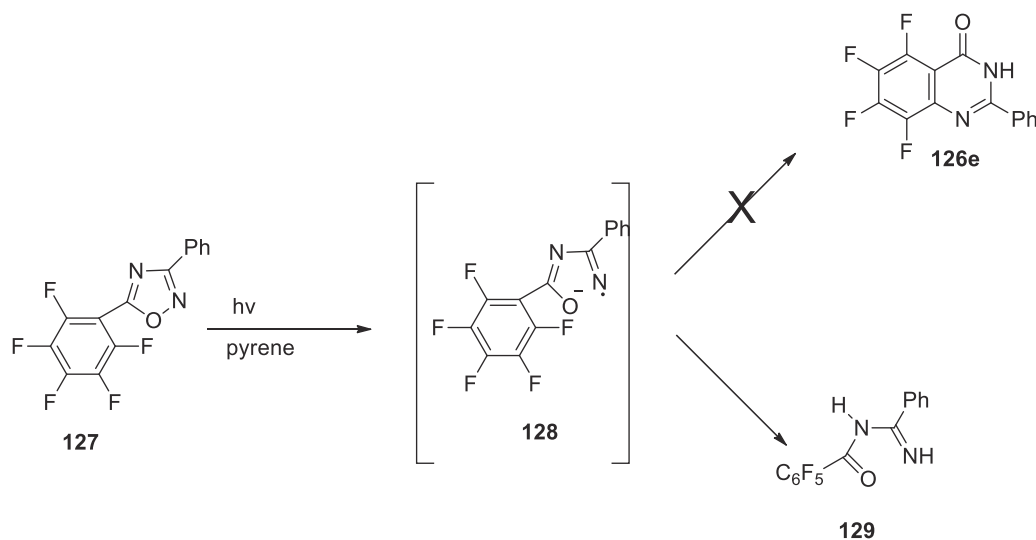
SCHEME 1.112 Formation of the reduction product.

1.13.2 Fluoroalkylates pyrimidines from silyl enol ethers, amidines, and fluoroalkylhalides

Chu and coworkers present an impressive work[88] in which, starting from a silyl enol ether, a iodofluoro alkane and a compound with two nucleophilic sites is possible to obtain fluoroalkylated products, especially pyrimidines (Scheme 1.113).
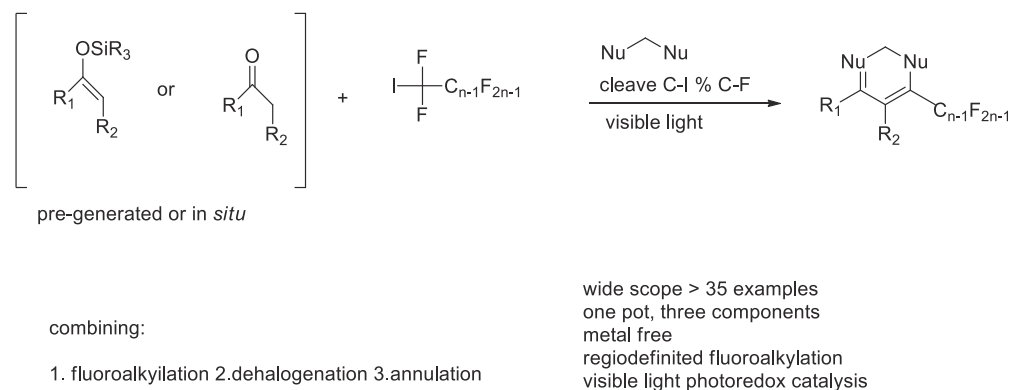
SCHEME 1.113 Obtaining of fluoroalkylated pirimidines.

Such a novel strategy exploits a tandem relay by combining organo-photoredox-catalyzed radical fluoroalkylation, dehalogenation, polar condensation, and synergistic cleavage of two C—F bonds as a means to access fluoroalkylated heterocyclic compounds, such as pyrimidines.

This hypothesis was initially evaluated by treating benzamidine hydrochloride (**130a**) and trimethylsilyl enol ether **131a** with perfluorobutyl iodide (**132a**) in the presence of 3 mol% of Rose bengal and 3.0 equiv. of triethylenediamine (DABCO) in acetonitrile at room temperature under the irradiation of white LEDs for 12 h. The sole use of a visible light photoredox catalyst promoted the desired [3 + 2 + 2] annulation to afford the fluoroalkylated pyrimidine **133a** in 18% yield (Scheme 1.114).

SCHEME 1.114   First attempt.
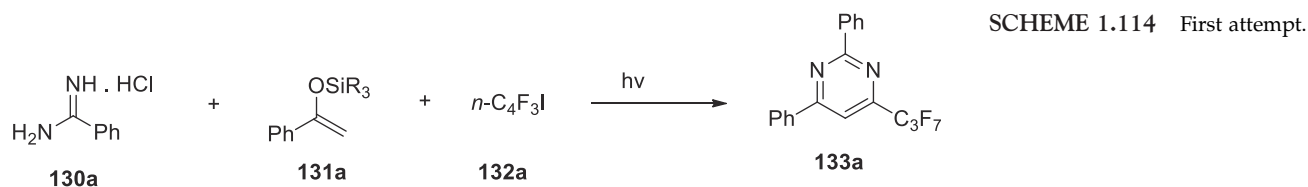
Then the authors, to improve the yield, payed their attention to other catalyst. Eosin was the best catalyst (yield 64%). Moreover, the use of TIPS instead of trimethylsilyl ether improves yields up to 99%.

With the optimal reaction condition in hand, the authors continued their task of exploring the substrate scope of the reaction. As shown in Scheme 1.115, benzamidine containing diverse substituents of varying electronic character and steric hindrance on the phenyl moieties were annulated to afford the corresponding products **133a-f**. In the same manner, the reactions worked equally well with with heteroaryl amidines to afford the heterocyclic variant **133h-i**. As for *C*-alkyl candidates such as formimideamide, acetimidamines, and cyclopropane-carboximidamide they exhibite good reactivity to afford the products **133j-l** in good yields. Remarkably, 1,n-bis nucleophiles of 2-benzimidazolylamine and guanidine hydrochloride were converted into functionalized pyrimidine nuclei in a streamliner manner (Scheme 1.115, **133m-n**).
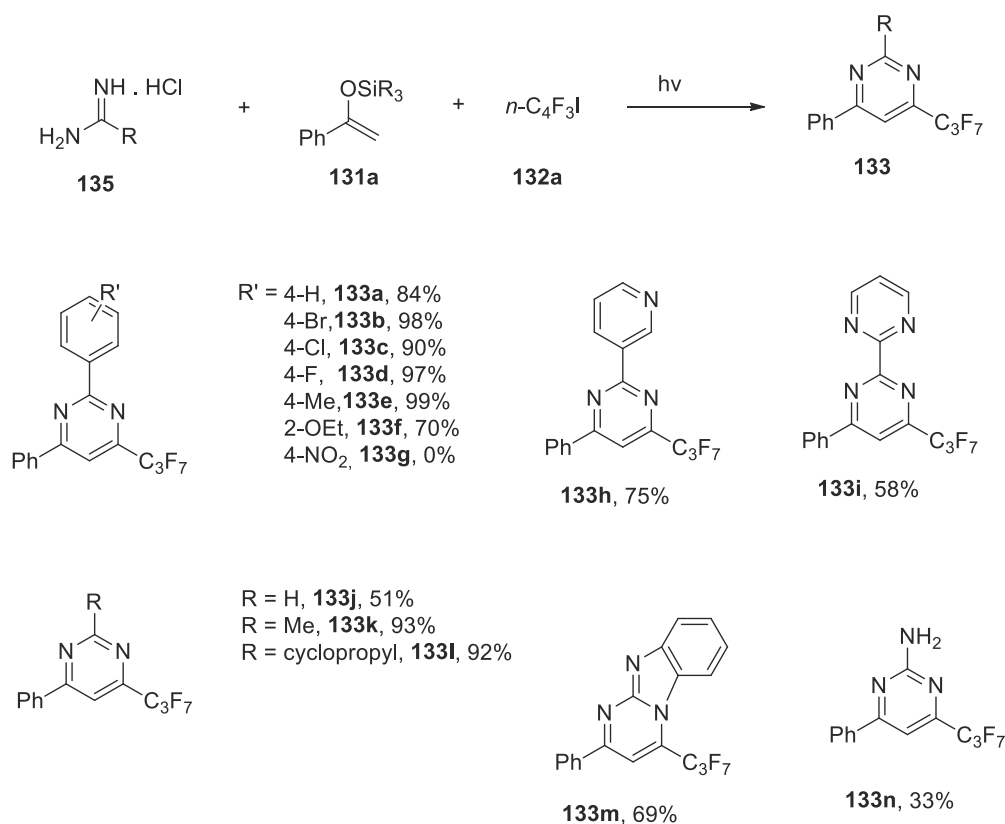
SCHEME 1.115   Substrate scope.

Next, was investigate the substrate scope of this protocol with respect to a series of structurally varied silyl enol ethers, and the results are listed in Scheme 1.116. Both electron-donating (**138a-e**) and electron-withdrawing (**138f-j**) groups on the triisopropyl((1-phenylvinyl)oxy) silanes led to satisfactory yields and thus, a variety of pyrimidines with structural diversity were synthesized. The substrates, featuring the functionalized polycyclic

motifs, such as naphthalene and benzothiophene, were successfully transformed into the fluoroalkylated products **138k** and **138l**, respectively. In addition, the presence of α—substituents in silyl enol ether **137** did not interfere with the intermolecular aromatization, and both cyclic and activated efficiently underwent the trasformation (**138m-n**). The enol silanes derived from aliphatic ketones were also examined, producing **138o** and **138p** in moderate yields with remarkable regioselectivity. The conversion of 3-phenylpropanal to benzylated product **138q** was obtained; this was extremely difficult to achieve through the direct functionalization of pyrimidine at its 5-position. Interestingly, this photocatalytic multicomponent reaction was also employed for the construction of pyrimidine-modified epiandrosterone **138r**.
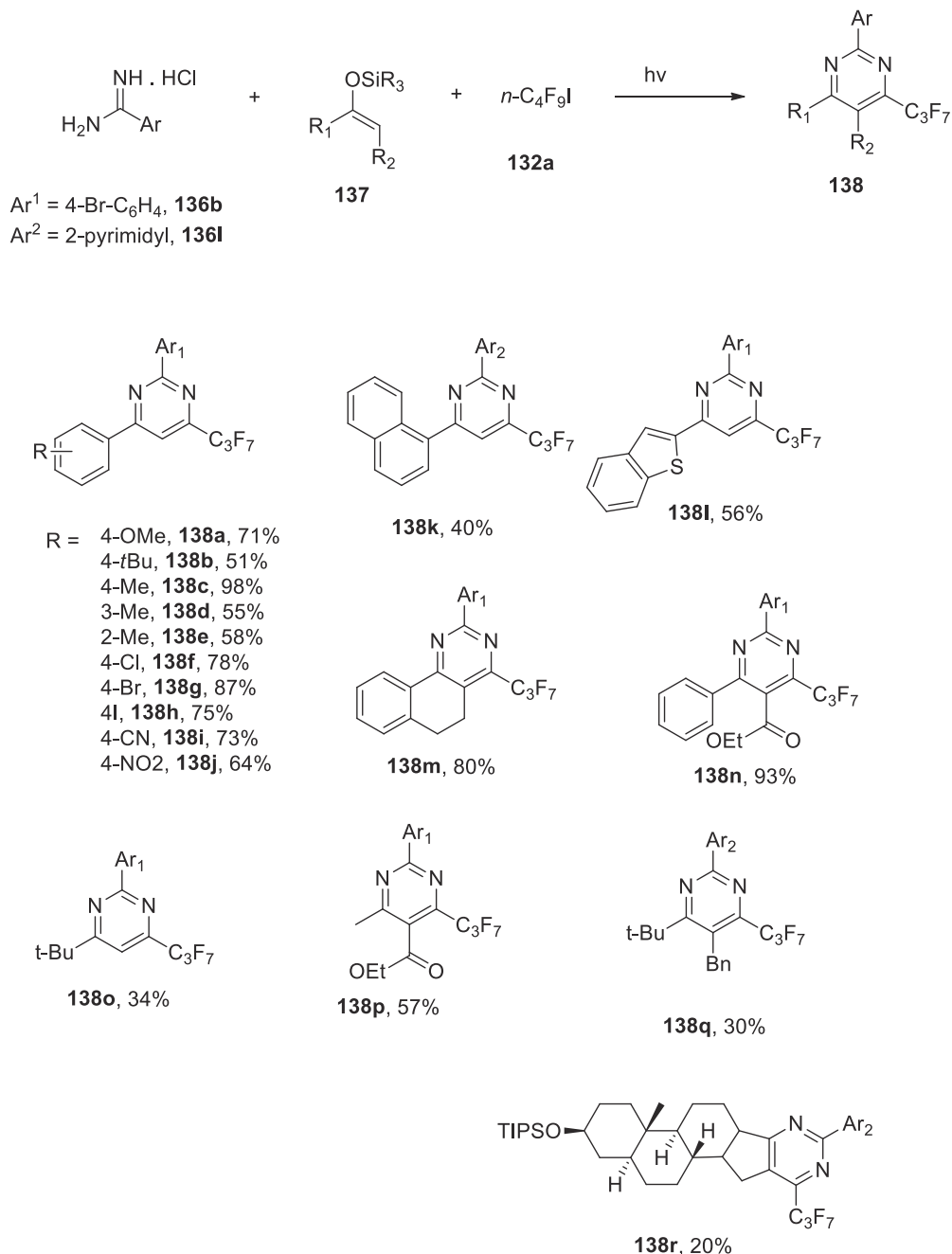
SCHEME 1.116 Scope of the substrate varying the sylil enol ether.

1.13.3 Three component synthesis from active methylene compounds, perfluoroalkyl iodides and guanidines

Strictly correlated to the methodic depicted in the previous paragraph, is the three component synthesis from active methylene compounds, perfluoroalkyl iodides and guanidines.[89] Also in this case, it was first searched for the optimal conditions to perform the reaction (Scheme 1.117).

SCHEME 1.117 Three component synthesis.
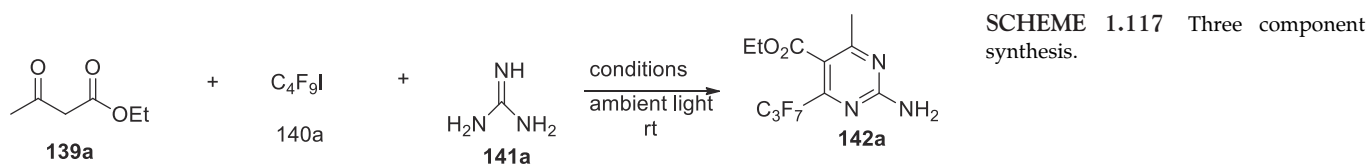
The best condition were: solvent, MeCN; light, ambient light; base NaOH; temperature, r.t. With other bases, as well as organic bases, the yield lowers drastically, while NaOH allows to obtain yield up to 86%.

With the optimize condition in hands, it was set out to study the reaction scope. Initially, a range of active methylene compounds were subjected to the reaction sequence (Scheme 1.118). The reaction of β- ketoesters containing alkyl substituent (R = Me, Et, i-Pr, CF$_3$) with perfluorobutyl iodide **140a** and guanidine **141a** in the presence of NaOH in MeCN proceeded smoothly, giving the corresponding 4-perfluoropropyl pyrimidines **142a-d**. α-aroyl esters (R = H, 4-Me, 4-Meo, 4-F) afforded 6-arylpyrimidines **142e-h** in good to excellent yields. Also β-diketones proved to be suitable substrate. For example, pentane-2,4-dione and dibenzoylmethane furnished 5-acyl-substituted pyrimidines **142i** and **142j** in good yields. However, deacetilation was observed for benzoylacetone, giving trisubstituted pyrimidine **142k** in 48% yield.
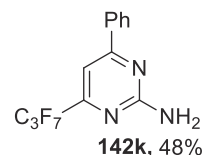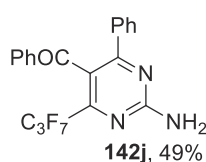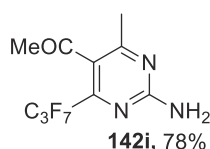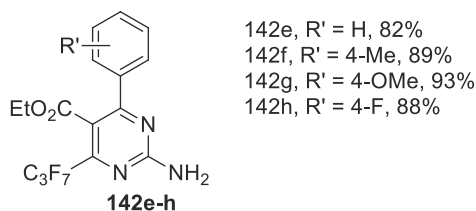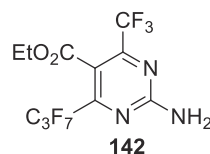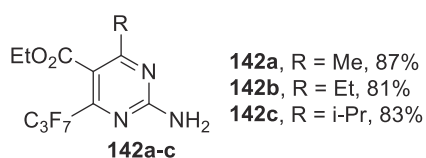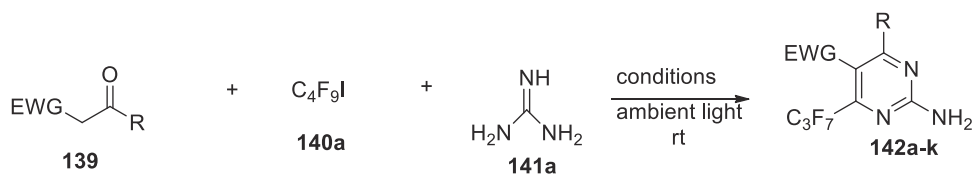
SCHEME 1.118   Reaction scope.

To further examine the scope and utility of this reaction, the scope of guanidine and amidine derivatives was examined by reaction with β-ketoesters and **141a** under otherwise identical conditions. *N*-methyl and *N,N*-dimethylguanidines gave fully substituted pyrimidines **143a** and **143b**. A number of amidines with different steric and electronic properties were appropriate partners. The reaction proceeded efficiently for both alkyl- and arylamidines, affording highly functionalized pyrimidines **5c-n**, in moderate to excellent yields as well as good functional group tolerance (Scheme 1.119).

143a, 55%

143b, 88%

143c, 70%

143d, R = Me, 75%
143e, R = Ph, 91%

143f, X = MeO, 97%
143g, X = Me, 91%
143h, X = Br, 96%
143i, X = F, 94%
143j, X = NO₂, 79%

143k, 56%

143l, 82%

143m, 85%

143n, 57%
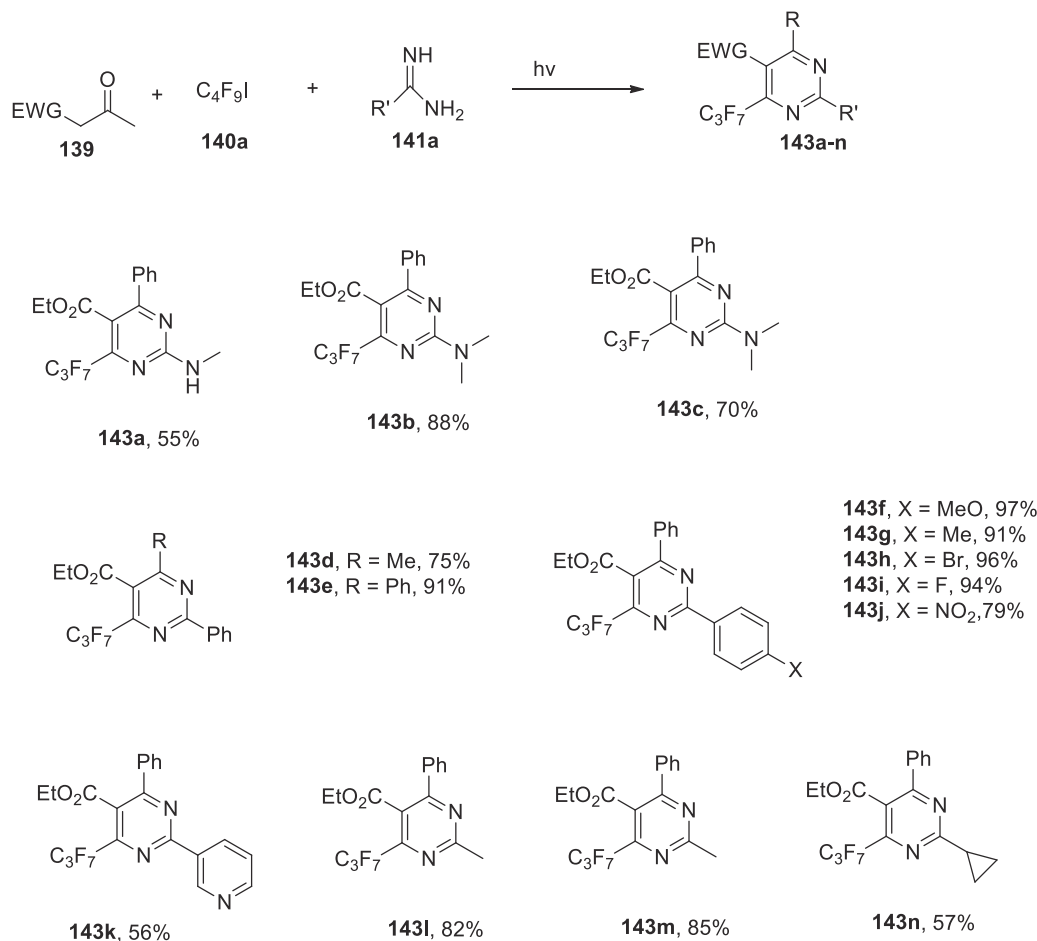
SCHEME 1.119   Further reaction scope.

1.13.4 Synthesis of pyrimidones from 4-allyl-tetrazolones

Tetrazoles and relates tetrazolones are useful intermediates in organic synthesis, for their ability to extrude nitrogen giving various derivatives. The authors first synthesized tetrazolones **144a-c** (Fig. 1.59).[90]
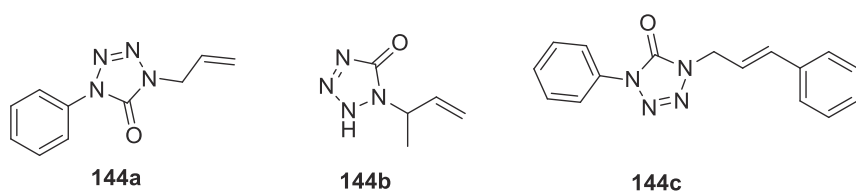
FIGURE 1.59   Tetrazolones.

144a

144b

144c

Photolysis of 4-allyl-tetrazolone **144a** was initially conducted in methanol. A single photoproduct was formed. The choice of solvent was important: in methanol and in general in alcohols the reaction is clear, in other non-alcoholic solvents some by-product can emerge. In Scheme 1.120 is depicted the mechanism of reaction for the three tetrazolones under investigation.

SCHEME 1.120   Mechanism of the reaction.

145a: R = H
145b: R = Me
145c: R = Ph
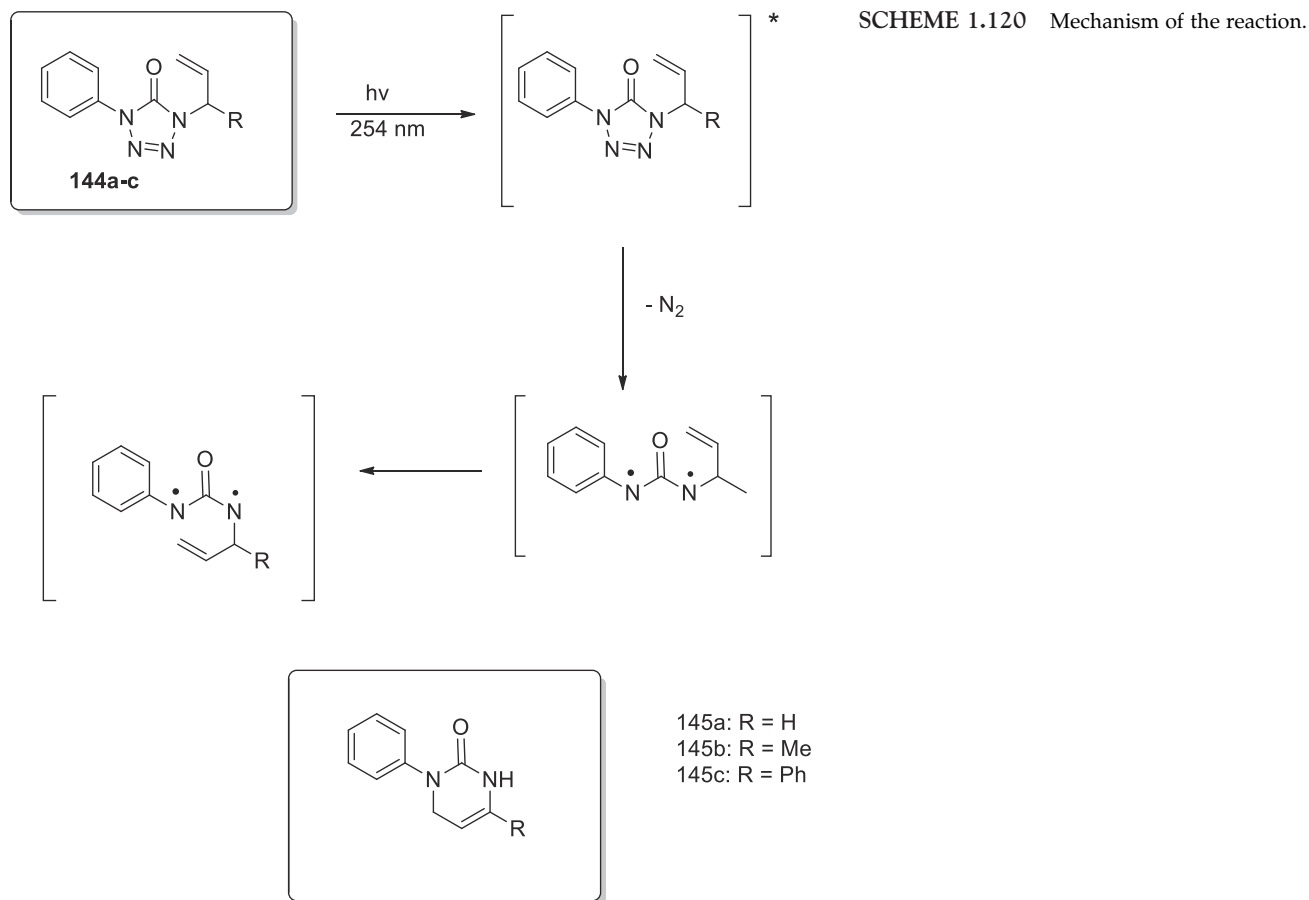
The higher photostability of the primary photoproducts **145a-c** in alcohols against cyclohexane and acetonitrile can be explained based on solvent stabilization. In alcohols, there might be a strong association between the solvent and the photoproduct involving formation of relatively strong hydrogen bonds. Pyrimidones **145a-c** bear several putative atoms capable of forming hydrogen bonds with solvent molecules (Fig. 1.60).

In such conditions, reversible proton transfer could be a fast and efficient mechanism of excited-state quenching, facilitated by steric limitation resulting from the stable cage enclosing the pyrimidinone molecule and
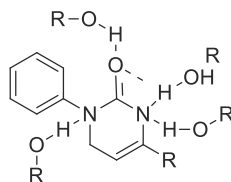
FIGURE 1.60   Solvatation of pyrimidones in alcoholic solution.
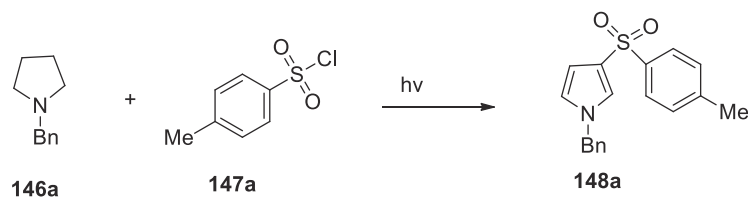
FIGURE 1.61   The reaction.

preventing its photodecomposition. Also, the absorbed energy is more efficiently dissipated through the solvated complex, preventing relaxation through pathways leading photocleavage.

1.14 Pyrroles

1.14.1 Dehydrogenative aromatization and sulfonylation of pyrrolidines

An unusual photochemical conversion of pyrrolidines into pyrroles was casually discovered. The authors, working on photoredox catalyzed sulfonylation of amines, noticed the formation of small amounts of pyrroles. So it was decided to investigate this reaction in more detail (Fig. 1.61).

The comprehensive optimization revealed the following condition: **146a** (0.2 mmol), **147a** (0.6 mmol), catalyst **A** = Ir[dF(CF$_3$)ppy]$_2$(dtbppy)PF$_6$ (2 mol%), base Cs$_2$CO$_3$ (2.5 equiv.) solvent acetonitrile + H$_2$O (3 equiv.), additive KPF$_6$. The base is needed to stabilize iminium ion intermediates, while the addition of water improves the solubility. Control experiments demonstrated that the presence of photocatalyst, base, and visible light are all necessary to attain the 3-substituted pyrrole.

Having a suitable and viable catalyst system, it was decided to explore the scope of these reaction. A series of electronically diversed aryl sulfonyl chloride ranging from electron-rich to electron-deficient group delivered good yield of the desired C3-sulfonylated pyrroles (Scheme 1.121).
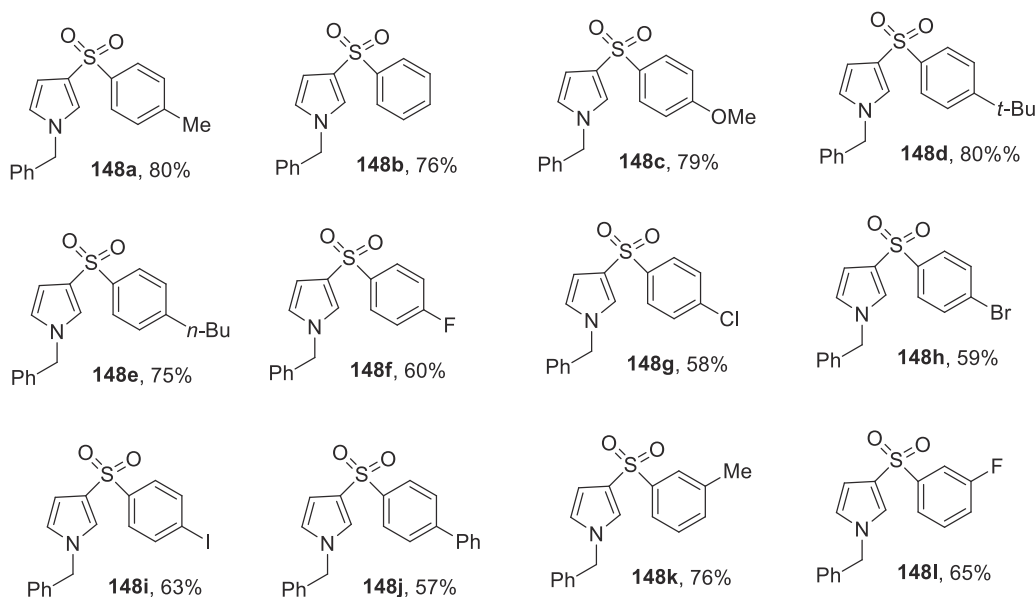
SCHEME 1.121   Scope of the reaction.

Further efforts to extend the scope of the dehydrogenation sulfonylation reaction focused on the variation of the *N*-substitution of the pyrrolidines (Scheme 1.122). *N*-Alkyls bearing primary, secondary, tertiary or ester containing substrates **146b-e** provided the corresponding products. However, *N*-methyl and

N-ethyl substrates react slowly, which may be due to the instability of the intermediary formed radical. Nevertheless, *N*-alkyl groups including *tert*-butyl acetate, ethyl 2-methyl propanoate and 1-(phenylpropan-2-yl) give comparable results to the benzyl-protected derivatives. The yield gradually improved by introducing *N*-benzyl or ester group at the α-position (**149f,g**). This observation is in good agreement with the notion that the generation of radical from benzyl substituted amine is more favorable then aliphatic substituted amine. In addition various benzyl groups regardless of the electronic nature of the aryl ring (**149i-t**) could efficiently be applied. Importantly, benzene fused pyrrolidine could be applied in this protocol and afforded 1-benzyl-5-tosyl-1H indole **149x**.
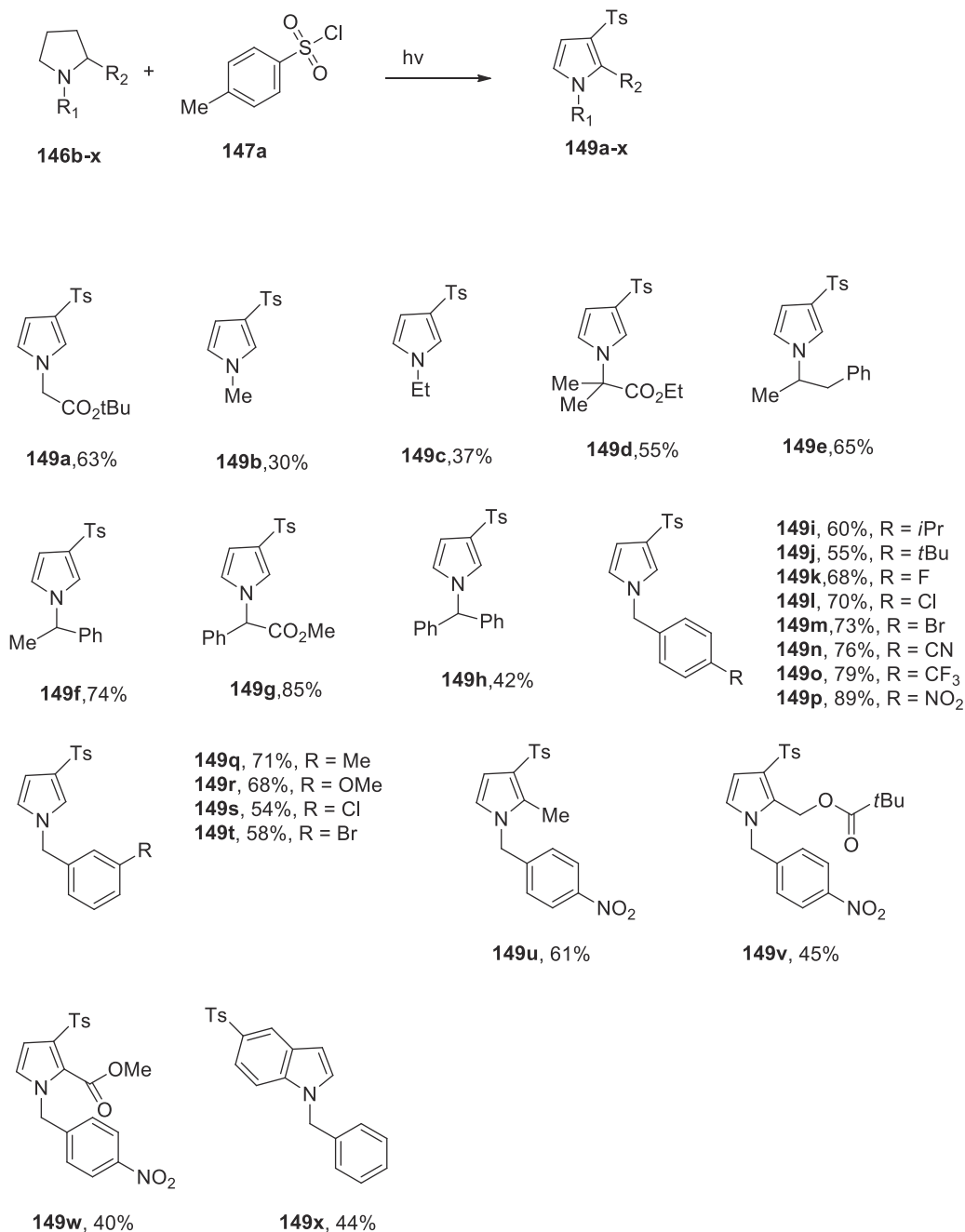
SCHEME 1.122 Scope of the reaction with *N*-variation on pyrrolidines.
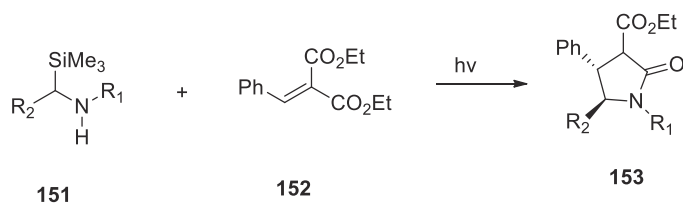
FIGURE 1.62   Reaction of α-silyl secondary amine.

1.14.2 Synthesis of nitrogen heterocycles generated from α-silyl secondary amines under visible light irradiation

In a work intended to study the photochemical reactivity of a-silyl amines with the aim to obtain γ-lactams, the authors extended the research to a possible one-pot syntesis to obtain pyrroles.

The γ-lactams were obtained using a photoredox catalyst derived from rutenium, ([Ru(bpy)$_3$][BF$_4$]$_2$). All reaction of **150** with **151** were carried out in the presence of catalyst in NMP under 14 W white led illumination at 25° for 18 h. Then, the resulting mixture was treated with KOtBu at room temperature for 4 h. (e.g., see Fig. 1.62).

The success in synthesis of γ-lactams prompted the authors to investigated other nitrogen heterocycles such as pyrroles. α − β unsaturated ketones were designed as substrates for the construction of a pyrrole ring. When the reaction of **154** with an α − β-unsaturated ketone derivative (**155**) was examined under similar conditions to the γ-lactam synthesis, dihydropyrrole **156** was obtained in 64% yield (Scheme 1.123). Encouraged by this result, then was successfully developed one pot synthesis of pyrroles by oxidation of dihydropyrroles. After photoreaction of α-silyl secondary amines with **155**, subsequent treatment of the resulting mixture with 2 equiv. of 2,3-dichloro-5,6-dicyano-1,4 benzoquinone (DDQ) at room temperature for 30 min gave the corresponding tri- and tetrasubstituted pyrroles (**157a** and **157b**) in high yields (Scheme 1.123).
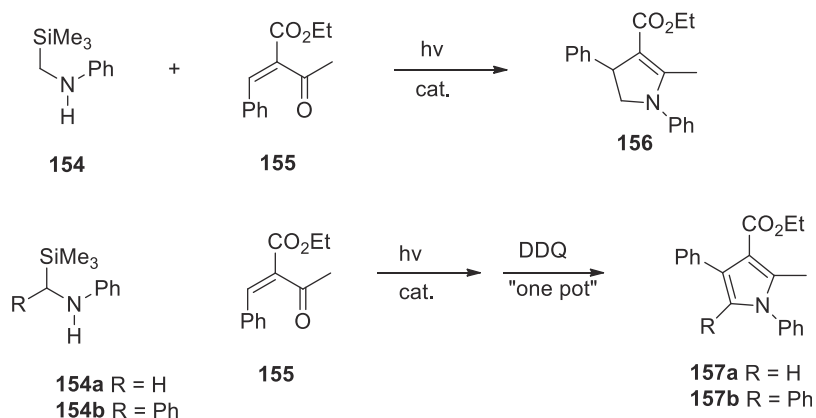
SCHEME 1.123   The reaction.

1.14.3 Synthesis of substituted pyrroles by dimerization of acyl azirines

Here is presented a simple, one pot reaction, to convert isoxazoles into various substituted pyrroles. The reaction consist in two step: a photochemical step in which the isoxazole is converted in an acyl azirine, and a thermal step in which the so generated azirine dimerize to give pirroles (Scheme 1.124).
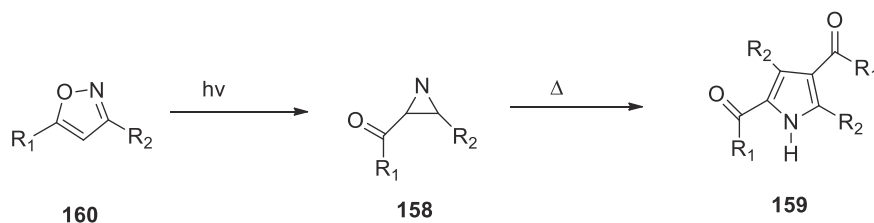
SCHEME 1.124   Conversion of isoxazoles into pyrroles.

First, the authors searched the best catalyst to perform the thermal step. In this case, they started directly from azirine, which is isolable. It was stated to be that the best catalyst was Cu(II)-2-ethyl hexanoate. All in all, the authors discovered that higher yield were obtained making the reaction "one pot" (Scheme 1.125).

SCHEME 1.125   Steps of the reaction.
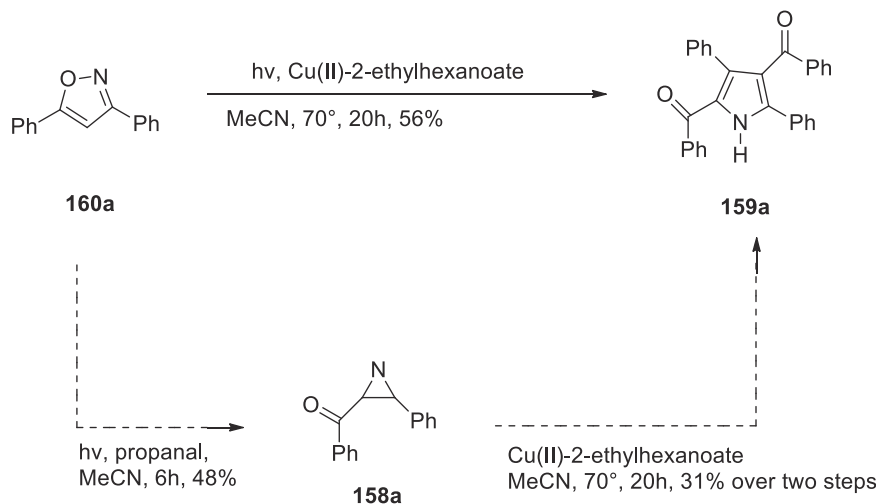
Under the improved reaction conditions, the substrate scope was investigated by applying them to several isoxazoles bearing mostly aromatic substituent on both the 3- and the 5- position, which were previously syntesized using standard methods.

The obtained pyrroles are shown in Table 1.2. The R_1 group in the isoxazoles starting material was varied first by changing the substition pattern of the phenyl group. Replacement of unsubstituted phenyl

TABLE 1.2   Obtained pyrroles.

Entry	Isoxazole	R_1	R_2	Yield
1	160a	Ph	Ph	56
2	160b	4-Tol	Ph	51
3	160c	3-Tol	Ph	46
4	160d	2-Tol	Ph	0
5	160e	4-F-C_6H_4	Ph	47
6	160f	4-Cl-C_6H_4	Ph	45
7	160g	4-Br-C_6H_4	Ph	35
8	160h	4-CF_3-C_6H_4	Ph	39
9	160i	4-MeO_2C-C_6H_4	Ph	33
10	160j	2-naphthyl	Ph	48
11	160k	4-MeO-C_6H_4	Ph	41
12	160l	2-furanyl	Ph	43
13	160m	Me	Ph	19
14	160n	Ph	4-tBu-C_6H_4	57
15	160o	Ph	4-F-C_6H_4	54
16	160p	Ph	4-MeO-C_6H_4	73
17	160q	Ph	4-MeO_2C-C_6H_4	46
18	160r	Ph	pentyl	28

group (**159a**) with both the *p*-tolyl (**159b**) and the *m*-tolyl (**159c**) substituent furnishes the corresponding dimerization product in comparable yields, whereas the reaction failed with the *o*-tolyl substituent (entries 2−4). The introduction of 4′-halogen substituent led to a reduction in yield most pronunced in the case of bromine (entries 5−7), possibly due to a heavy atom effect reduce the lifetime of the S_1-state from which the acylazirine is formed. The incorporation of electron-withdrawing groups resulted in a decreased yield of the dimerization products (entries 8−9). Replacement of the phenyl with a naphthyl group led to very long reaction times and poor yields. The same observation were made when an electronic-donating substituent was attached to the phenyl group (entry 11). The photoisomerization turned out to be very sluggish, possibly due to extensive light absorption by the product formed. We were able to overcome this problem by decreasing the concentration to 0.05 M, which allows more photons to penetrate the reaction mixture resulting in a faster isomerization rate.

Secondly, the R_2-substituent of the isoxazole was varied. Both alkyl and halogens on the phenyl ring were well tolerated (entries 14−15). By introducing an electron-withdrawing substituent, the pyrrole was obtained in a slightly decreased yield (entry 17). Aromatic substituent bearing an electron-donating moiety produced an increased yield (entry 16). The replacement of the aryl moiety in R_2 position with an alkyl group resulted in very long reaction times. Even after 96 h, only partial consumption of the starting material was detected using LC/Ms and pyrrole **159r** was obtained in 28% yield. The UV/Vis spectrum of isoxazole **160r** exhibits a noticeable hypsochromic shift of the absorption maximum (λ_{max} = 240 nm for **160r** in comparison to 270 nm for **160a**) explaining the slow isomerization rate under UV-B irradiation.

1.14.4 Photochemical isomerizations of N-substituted 2-halopyrroles: syntheses of N-substituted 3-halopyrroles

As depicted in Scheme 1.126, when an acetonitrile solution of *N*-benzyl-2-bromopyrrole (**161a**) was irradiated with a 100W-medium pressure Hg lamp for 7 min at room temperature under Ar and then the reaction mixture was separated by Al_2O_3 column, *N*-benzyl-3-bromopyrrole (**162a**, 60%) was obtained as major product with a minor products, *N*-benzylpyrroles (**164a**, 10%) and *N*-benzyl-2,5-dibromopyrrole (**163a**, 10%).

161a X = Br, Y = Bn
161b X = Cl, Y = Bn
161c X = Br, Y = CH$_3$
161d X = Cl, Y = CH$_3$

162a X = Br, Y = Bn
162b X = Cl, Y = Bn

163a X = Br, Y = Bn
163b X = Cl, Y = Bn

164a Y = Bn
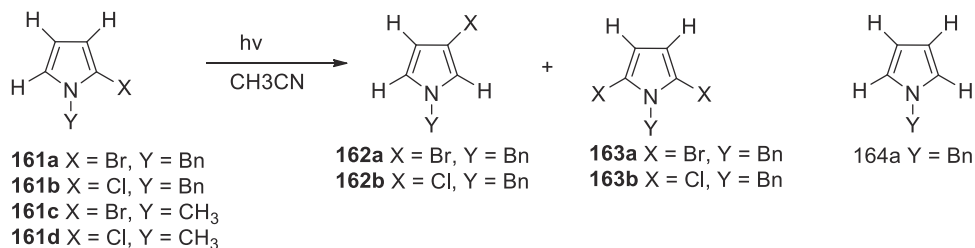
SCHEME 1.126 Obtaining of isomers.

The isomeric pyrrole product, *N*-benzyl-3-chloropyrrole (**162b**) was also obtained from the photoreaction of *N*-benzyl-2-chloropyrrole (**1b**). However, *N*-methyl-2-halopyrroles, **161c** and **161d**, gave tarry products instead of isomeric products. This implies that the phenyl group of **161a** and **161b** is important for the isomerization and blocking for the polymerization. The synthesis of 3-substituted pyrrole is difficult because generally electrophilic halogenation on pyrrole derivative occur at 2-position of the pyrrole due to high electron density of 2- and 5-position of pyrrole. Thus, this method is simple and straightforward for the syntheses of *N*-benzyl-3-halopyrrole.

1.14.5 Synthesis of pentacycles incorporating a pyrrole unit

Pyrrolo[2,1-a] isoquinoline- and coumarin-fused pentacycles constitute the molecular skeleton of the natural products lamellarin alkaloids such as lamellarin D, H, M, N, and α-20 sulfate (Scheme 1.127). These lamellarin alkaloids exhibit a variety of biological activities, such as antitumor, antiviral, antibiotic.

SCHEME 1.127   Lamellarins.

Lamellarin D

Lamellarin H

Lamellarin M

Lamellarin N

Lamellarin α 20-sulfate

Lamellarin core
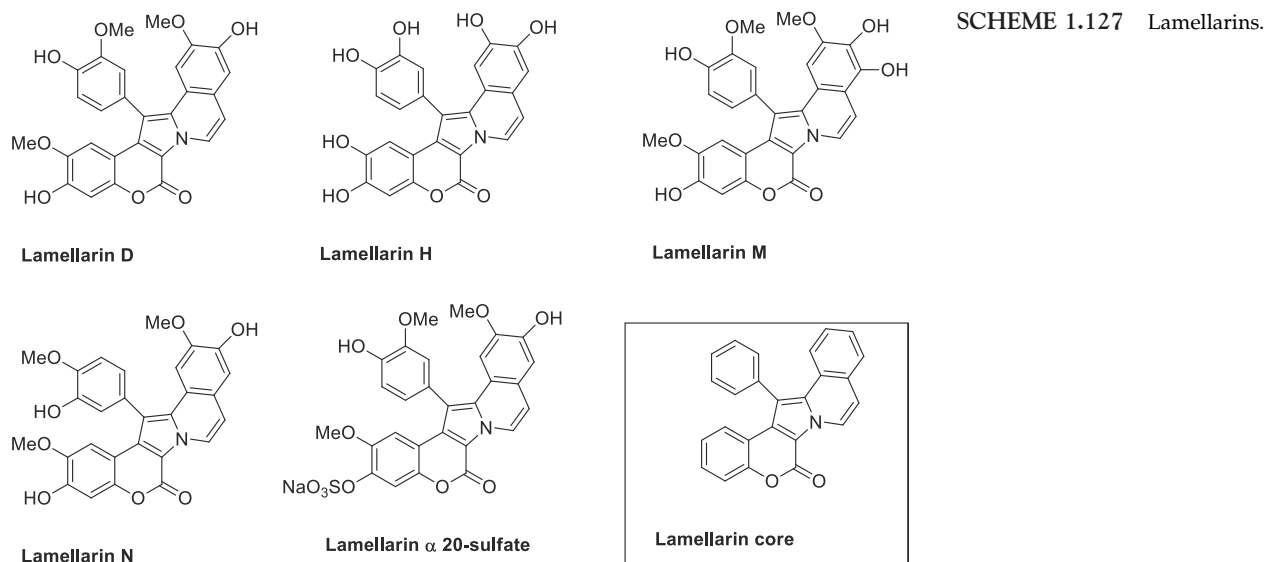
The authors initiated their study by choosing a coumarin-pyrrole-quinoline-fused pentacycle **165** as the first target (Scheme 1.128). The synthesis of **165** involved K_2CO_3-mediated coupling of commercially available 4-chloro-3-nitrocoumarin (**166**) and 2-methylquinoline (**167**) in 1,2-dichloroethane under reflux conditions to give 3-nitro-4-(quinolin-2-ylmethyl)coumarin (**168**) in 50% yield.

SCHEME 1.128   Synthesis of the lamellarin core.

K_2CO_3

DCE, reflux
12h, 50%

166   **167**

168

visible light
MeCN, rt
12h, 95%

165
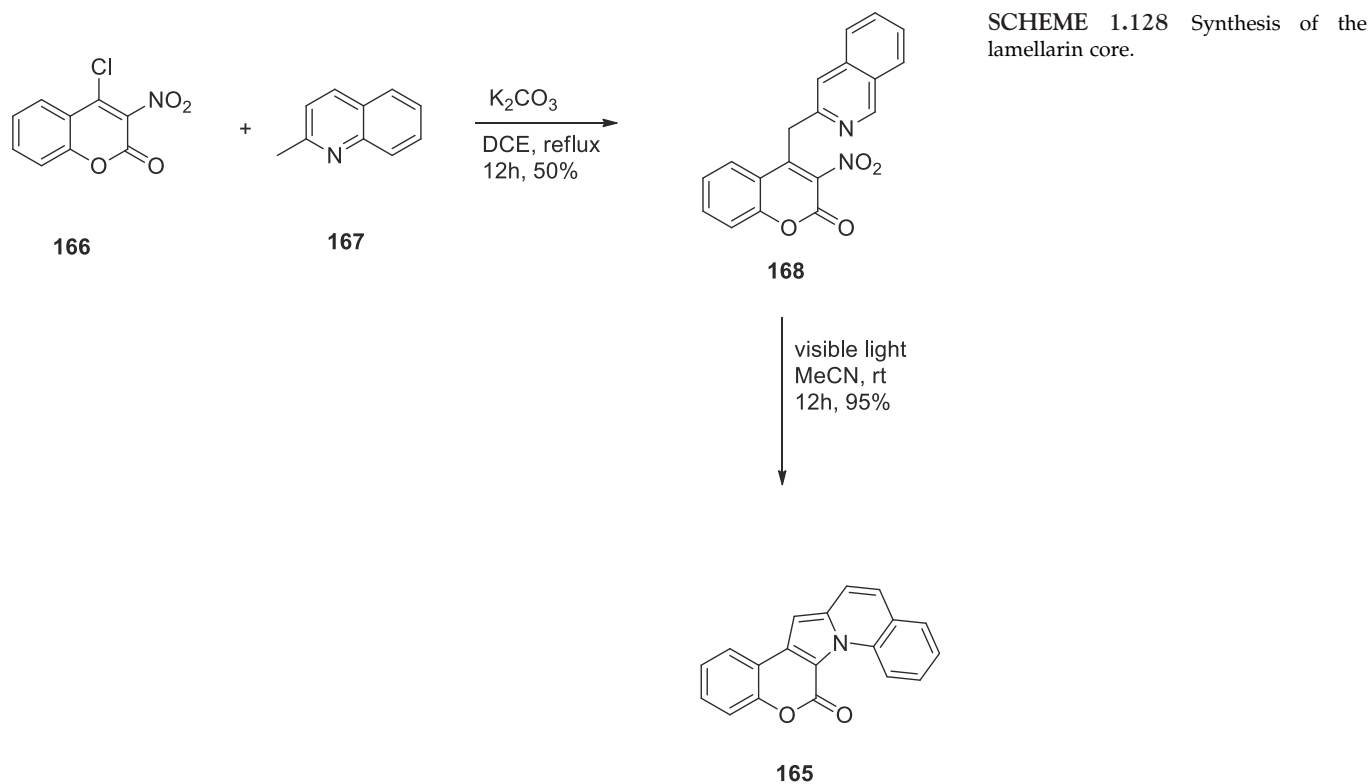
During purification of compound **168**, a new and fluorescent spot on the TLC plate was invariably detected. This observation implied that **168** was light-sensitive and slowly converted into a new product under the

influence of light. Upon exposure to visible light (23 W fluorescent light bulb or blue LEDs) the compound **168** indeed was found to undergo intramolecular cyclization reaction at room temperature to give the pentacycle **165**, quantitatively. No formation of **165** was observed when the reaction was carried out in the dark. This result confirmed that the cyclization of **168** to **165** was promoted by visible light. As for the solvent effect, among several solvents investigated, acetonitrile gave higher conversion in a short time interval. Hence, acetonitrile was used for all subsequent visible-light-mediated reactions.

After the successful synthesis of pentacycle **165**, the authors were focused on the preparation of the coumarin-pyrrole-isoquinoline-fused lamellarin core **166** as shown in Scheme 1.129.

SCHEME 1.129 Pyrrole-isoquinoline-fused lamellarin core.
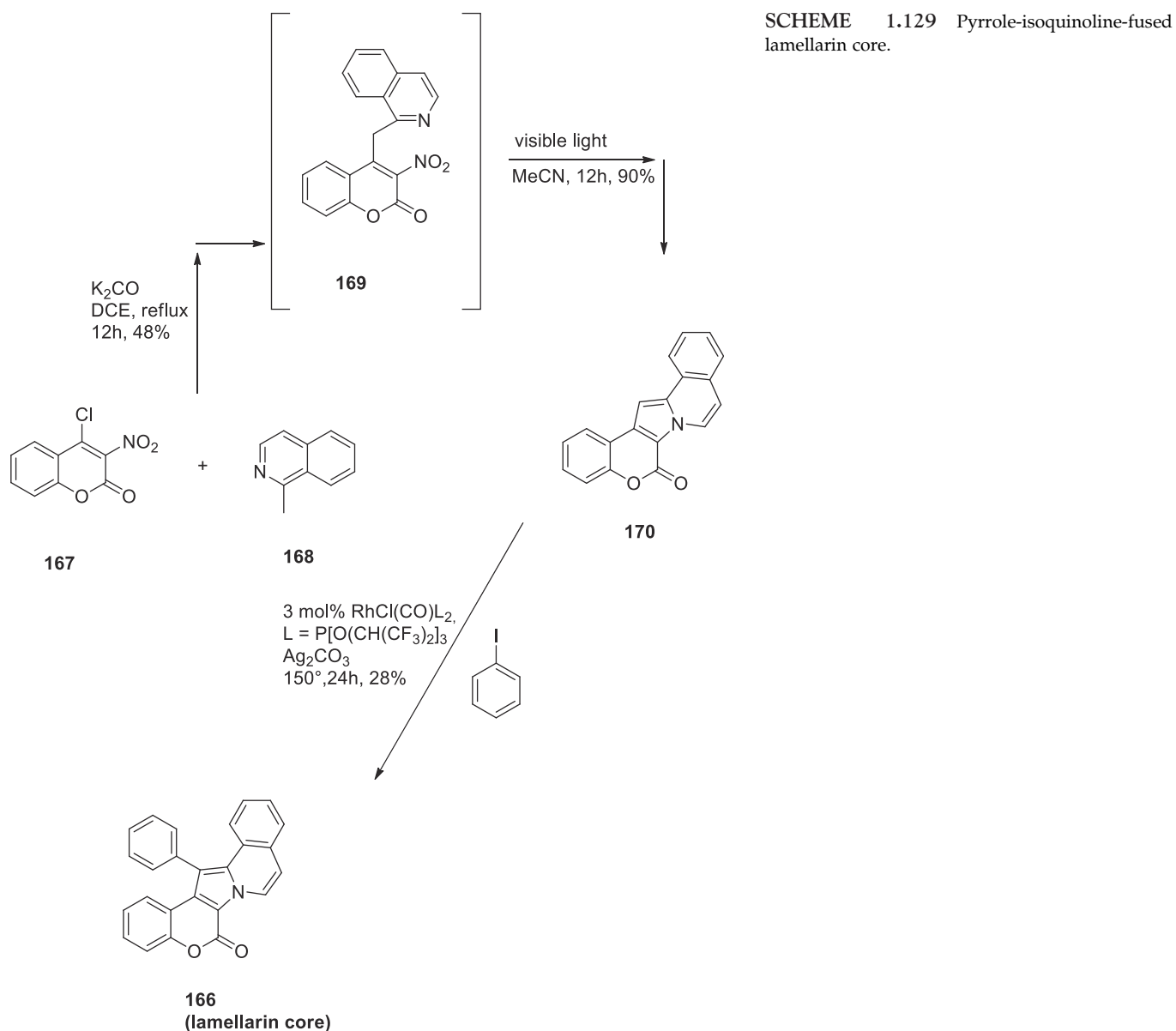
The synthesis started with K_2CO_3 mediated coupling of **167** with 1-methylisoquinoline (**168**) in 1,2-dichloroethane to give 4-(isoquinolin-1-ylmethyl)-3-nitro-2H-chromen-2-one (**169**) in 48% yield. Similar to that of **168**, compound **169** was found to to be highly sensitive to light and readily undergo intramolecular cyclization reaction which made the isolation of **169** in its pure form difficult. Thus, without further characterization, compound **169** was subjected to visible-light promoted cyclization in acetonitrile to afford compound **170** in 90% yield. The subsequent Rh-catalyzed coupling of **170** with iodobenzene in 1,4-dioxane/m-xylene generated lamellarin core **166** in 28% yield.

1.14.6 Synthesis of 1,3,4 trisubstituted pyrroles by condensation of aryl azides and aldheydes

This protocol enable the realization of an unprecedent stoichiometric oxidant-free synthesis of site-selective substituted pyrroles under desirable mild conditions. At the outset of the optimization stage, the authors identified in the arylazide **171a** and phenylacetaldehyde **172a** the model substrates to be condensed under photocatalytic regime (Scheme 1.130). Upon an extensive survey of reaction conditions involving solvent, light source, photosensitizer and additives, the best conditions found are those reported in the Scheme 1.130.

SCHEME 1.130 Synthesis of substituted pyrroles.

PMP = *p*-methoxy phenyl
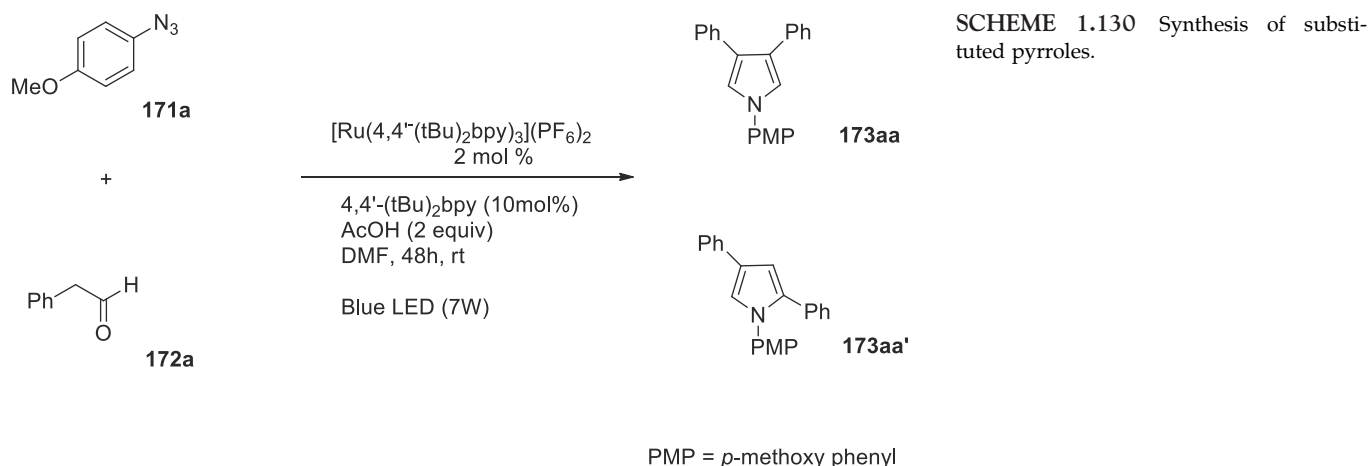
The cumulative yield of **173aa** + **173aa′** was 74%, while their ratio was 87/13. From the data collected some conclusion can be drawn. First, light irradiation proved to be essential (no reaction in the dark). The addition of an external reductant such as morpholine or DIPEA did not affect significantly the reaction course. In contrast, the absence of protic source, the presence of oxygen and removal of 4,4′-(*t*Bu)$_2$bpy as an additive were proven detrimental for the whole protocol. Finally, the replacement of **171a** with *p*-anisidine caused the failure of the protocol; this evidence suggests that the photocatalyzed reduction of the arylazide is critical for generating high energy radical species in the reaction machinery.

With the optimal conditions in hands, the scope and the versatility of the methodology toward the realization of a library of pyrrole derivative were assessed. To this aim, two sets of experiments namely: condensation of different arylazides (**171b-k**) with phenylacetaldehyde **172a** and *p*-MeO-phenylazide (**171a**) with a range of aldehydes (**172b-m**) were carried out and the results reported in Table 1.3 and Scheme 1.131, respectively.

TABLE 1.3   Scope of the reaction: Azide.

Entry	Ar	Yield 3 + 3′ (%)	3/3′
1	C$_6$H$_5$ (**173ba**)	51	90/10
2	4-CH$_3$C$_6$H$_4$(**173ca**)	78	84/16
3	3-CH$_3$C$_6$H$_4$(**173da**)	74	80/20
4	2-OCH$_3$C$_6$H$_4$(**173ea**)	50	83/17
5	4*n*OBuC$_6$H$_4$(**173fa**)	75	83/17
6	3,4(CH$_3$)$_2$C$_6$H$_3$(**173ga**)	47	81/19
7	2,4(CH$_3$)$_2$C$_6$H$_3$(**173ha**)	63	88/12
8	4-FC$_6$H$_4$(**173ia**)	62	85/15
9	3-BrC$_6$H$_4$(**173ja**)	45	80/20
10	4-BrC$_6$H$_4$(**173ka**)	53	80/20
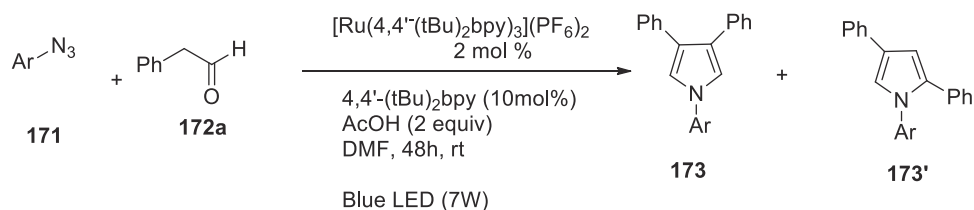
SCHEME 1.131 Reaction of various azides.

Variously substituted arylazides were effectively employed in the synthesis of pyrroles regardless the phenyl substitution pattern. In particular, *ortho*, *meta* and *para* substitutions were efficiently tolerated as well the presence of both electron-rich (**171c-h**) and electron-deficient (**171i-k**) functional groups did not affect the visible-light assisted protocol, delivering the corresponding *N*-aryl-diphenyl-pyrroles **173** in good yields (up to 78%) and moderate to good regioselectivity (**173:173′** up to 90:10). Moreover, mono and disubstitution (**171g** and **171h**) at the *ortho*, *meta* and *para* positions of the aromatic ring were fully compatible with the protocol. In addition, the orthogonal electronic properties of functional groups located at the arenes of the phenylacetaldehyde (EDG: **172b-f** and EWG: **172h-i**) were adequately tolerated (Scheme 1.131). The protocol was also suitable for *ortho*-substituted compounds (yield up to 78% in the case of **172e**). Finally, aliphatic linear aldehydes were also tested under best conditions. Although a moderate yield was observed (30%), the corresponding 3,4-dialkyl-pyrroles **173al** and **173am** were isolated in excellent regioselectivity (up to 94:6) (Scheme 1.132).
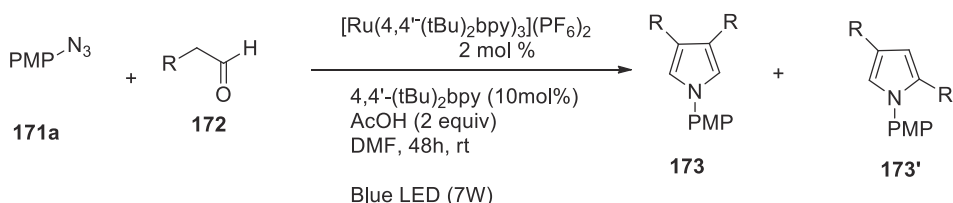
SCHEME 1.132 Scope of the reaction: Aldehyde.
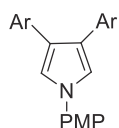
173ab, (Ar: 4-*n*BuOC$_6$H$_4$) Y:51%, (83/17)
173ac, (Ar:4-MeC$_6$H$_4$) Y:78%, (91/9)
173ad, (Ar:3-MeC$_6$H$_4$) Y:51%, (90/10)
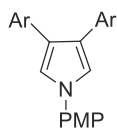
173ae, (Ar:2-MeC$_6$H$_4$) Y:78%, (86/14)
173af, (Ar:2-OMeC$_6$H$_4$) Y:47%,(87/13)
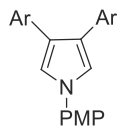
173ag, (Ar: 4-FC$_6$H$_4$) Y:61%,(81/19)
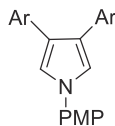
173ah, (Ar: 3-FC$_6$H$_4$) Y:63%,(81/19)
173ai, (Ar: 2-FC$_6$H$_4$) Y:44%,(93/7)
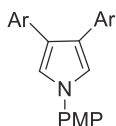
173aj (Ar: 2Me, 4-FC$_6$H$_3$) Y: 77% (92/8)
173ak (Ar: 3,4- (MeO)$_2$C$_6$H$_3$ Y: 72% (20/1)
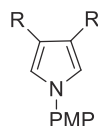
3al (R:*n*C$_3$H$_7$) Y:30% (94/6)
3am (R:*n*C$_3$H$_7$) Y:30% (92/8)

1.15 Pyrrolidines

1.15.1 *Pyrrolydinones from suitable amides and an iridium catalyst*

Olefin hydroamidation is a powerful approach to C−N bond construction, and one that motivate the development of new synthetic methods. Among the most versatile hydroamidation technologies reported to date are those that make use of amidyl radicals. To this end, the authors recently disclosed a catalytic protocol for olefin carboamidation enabled by proton-coupled electron transfer (PCET) activation of aryl amides. In this process, a weak phosphate base and an excited state Ir photocatalyst jointly mediate the homolysis of a strong anilide N−H bond, furnishing a reactive amidyl radical that can undergo addition to a pendant olefin (Scheme 1.133).

SCHEME 1.133   Mechanism of the reaction.
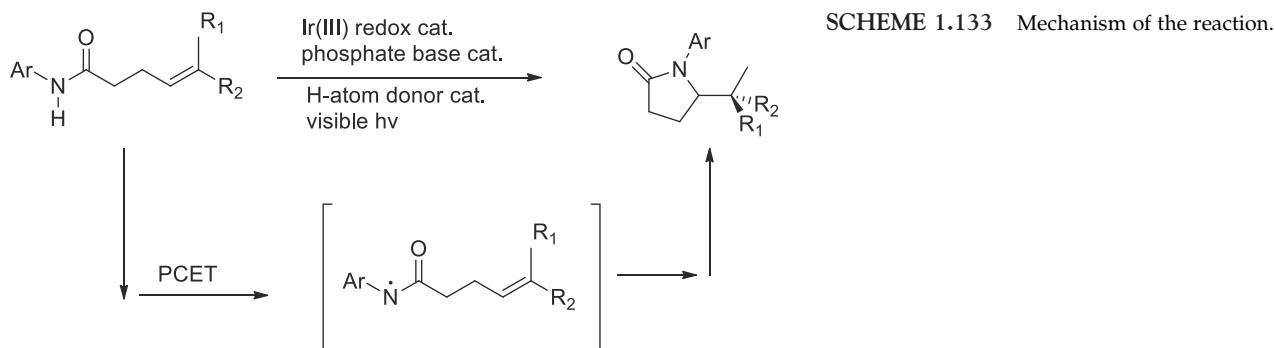
Building on their carboamination protocol, the authors elected[91] to retain the Ir(dF(CF$_3$)-ppy$_2$ (bpy)PF$_6$ photocatalyst and dibutyl phosphate base combination found to be most effective for amidyl generation. Regarding the H-atom donor, after a series of attempts, they found that inclusion of 10% mol of thiophenol producede the desired hydroamidation product in 95% yield.

With these optimized reaction conditions, the authors set out to examine the scope of this new hydroamidation process. (Scheme 1.134)
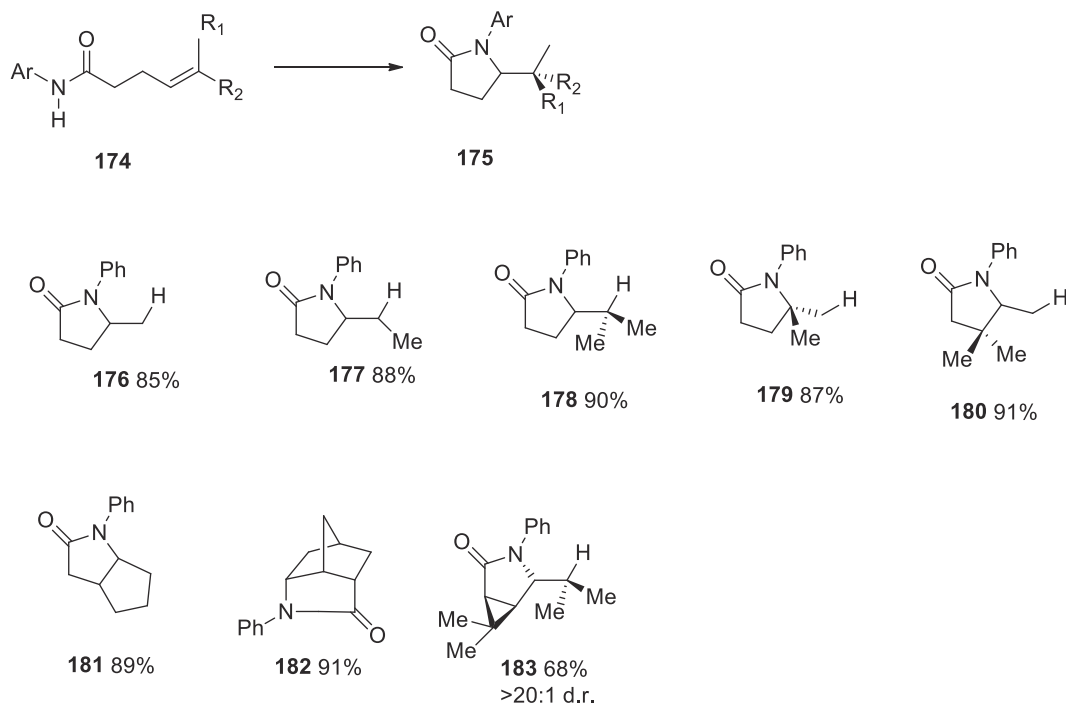
SCHEME 1.134   Scope of the reaction.

On preparative scale, model amide **174** underwent hydroamidation to provide lactam **175** in 85% isolated yield. With respect to the olefin component, a variety of di-, tri-, and tetrasubstituted olefins with different substitution pattern were successfully accomodates (**177**−**179**). Styrenyl acceptors could also be utilized, though an increased loading of the thiophenol (30% mol) was required to achieve optimal yields (**180**). Steric hindrance adjacent to the site of C−N bond formation was also tolerated (**183**). Moreover, hydroamidation of canonical Diels-Alder products could also be accomplished to afford more complex polycyclic structures (**182**). An amide derived from *cis*-chrisanthemic acid was successfully cyclized to deliver a fused 3,5-ring system in good yield and excellent diastereoselectivity.

1.15.2 [3 + 2] Cycloaddition between a cyclopropylketone and an imine

The reaction between a cyclopropylketone and an imine represents a powerful way to obtain densely functionalized pyrrolidines with three chiral centers (Fig. 1.63). The authors embarked in a deep study about the possibility to perform the reaction in a photochemical way, eventually using a photoredox catalyst.[92] They found that, for certain particular substrates, the reaction is possible using as photocatalyst Ir(4-CF$_3$ppy)$_3$ and also a "co-catalyst" Yb(OTf)$_3$ and a dessicant which is MgSO$_4$ (Scheme 1.135).
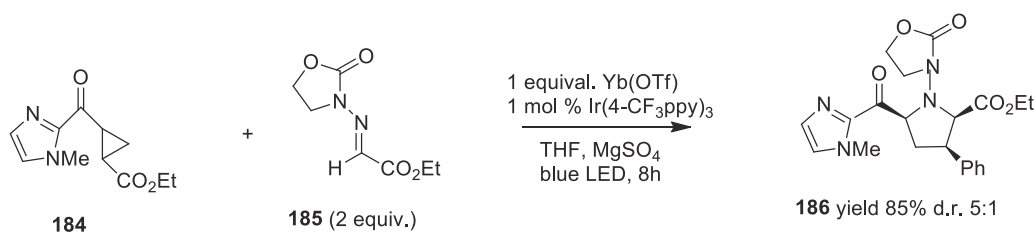
SCHEME 1.135 Conditions to obtain the reaction.

Then the scope of the reaction was explored with various examples (Scheme 1.136).

The scope with respect to the β-aryl substituent was relatively general. Electron-rich aryl rings were well tolerated in good yields and modest diastereoselectivities (**187** and **188**). Very electron-deficient aryl rings were also well tolerated in good yields and good to excellent diastereoselectivities (**189** and **190**). A potentially reactive aryl bromide was well tolerated under these conditions (**191**), and placing steric bulk in the *ortho* position of the aromatic ring was also well tolerated (**192**). Both electron-deficient and electron-rich heteroaryl-substituted cyclopropanes were viable substrates (**193** and **194**), though Lewis basic moieties such as pyridine rings that could compete for the Lewis acid co-catalyst result in reduced yields. Trisubstituted cyclopropanes exhibited excellent regioselectivity and good diastereoselectivities under these conditions (**195**), although these reactions were relatively sluggish. A more electron-deficient cyclopropane derivative with an ester substituent was also a viable substrate in this transformation (**196**). This result highlights the generality that can be accessed by exploiting radical intermediates: both electron-withdrawing and electron donating substituents are well tolerated. As suggested by the earlier experiments exploring redox auxiliares, a 2-pyridyl cyclopropyl ketone also shows productive reactivity in this transformation (**197**). A ketimine derived from ethyl pyruvate showed productive reactivity to generate a quaternary stereocenter (**198**) although the rate of this reaction was significantly diminished.
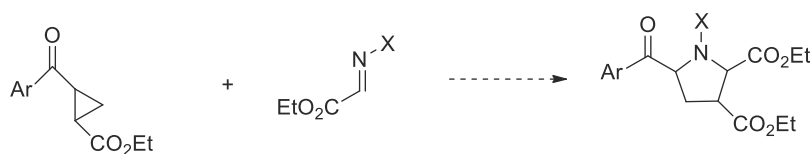
FIGURE 1.63 The reaction

SCHEME 1.136 Scope of the reaction.

187 60% yield, 2:1 d.r.

188 84% yield, 4:1 d.r.

189 85% yield, 5:1 d.r.

190 78% yield, 9:1 d.r.

191 85% yield, 5:1 d.r.

192 75% yield, 4:1 d.r.

193 38% yield, 5:1 d.r.

194 70% yield, 4:1 d.r.

195 40% yield, 7:1 d.r.

196 51% yield, 1:2:1 d.r.

197 40% yield, 20:1 d.r.

198 31% yield, > 10:1 d.r.
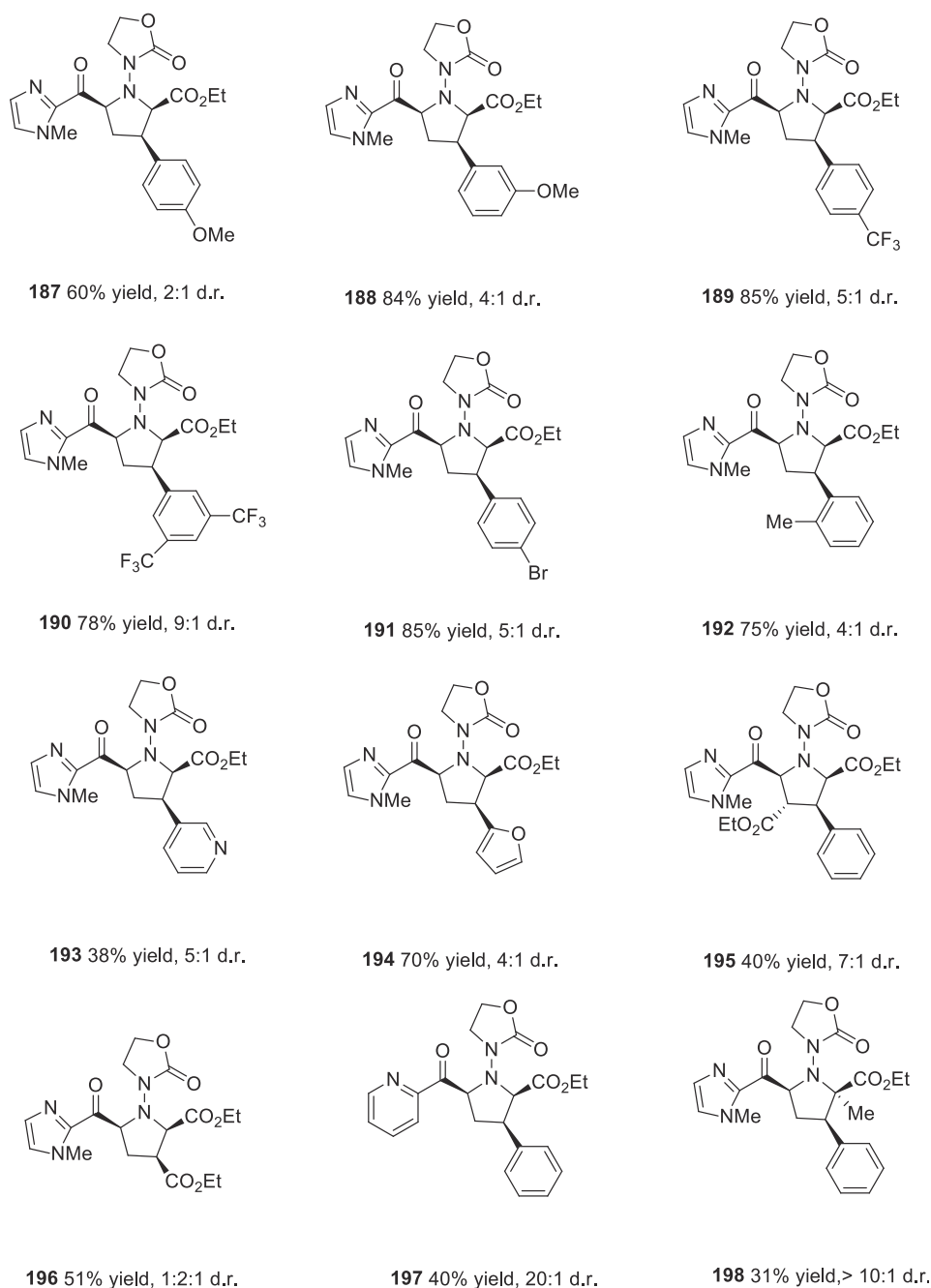
1.15.3 Synthesis of pyrrolidines from alkanes and nitrogen derivatives

The selective replacement of $C_{sp}^3 - H$ with $C_{sp}^3 - N$ bond, a ubiquitous motif in medicinal chemistry, is an intensely pursued research area. The current state of art for intermolecular $C_{sp}^3 - H$ amination is the transition-metal-catalyzed nitrene insertion or transfer chemistry. Another complementary yet unified strategy that has garnered significant momentum recently is the radical-based approach to evoke hydrogen atom transfer (HAT) processes. Despite recent progress in intermolecular C-H amination via HAT, the use of a versatile and convenient nitrogen source is highly desirable with limited examples. During the progress of author's work, they disclose a rare halogen bonding charge-transfer complex induced nitrogen radical formation from sulfonamides to initiate a HAT relay process, a strategy that is not amenable to nitrene-based technology. In turn, multiple $C_{sp}^3 - H$ aminations can take place to convert alkanes into pyrrolidines, a privileged pharmaceutical motif.[93]

Their experiments commenced with finding suitable conditions for the initial benzylamination process. Evaluation of a variety of halogen bond donors revealed that *N*-iodosuccinamide (NIS) was optimal. The two possible courses of reaction is depicted in Scheme 1.137.

SCHEME 1.137 Course of the reaction.
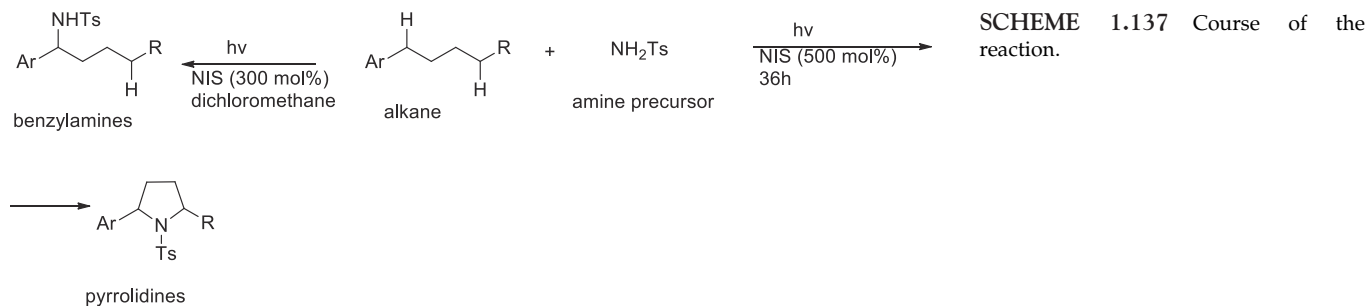
With the first procedure were synthesized 38 examples of different benzylamines. Because the scope of this chapter is to deal with heterocyclic compounds, we report herein only the 9 examples of the obtained pyrrolydines (Scheme 1.138).

SCHEME 1.138 Scope of the reaction.

199 46%   **200** 46%   **201** 64%

202 43%   **203** 43%   **204** 53%

205 52%   **199** 46%

206 48%

from *Celebrex*
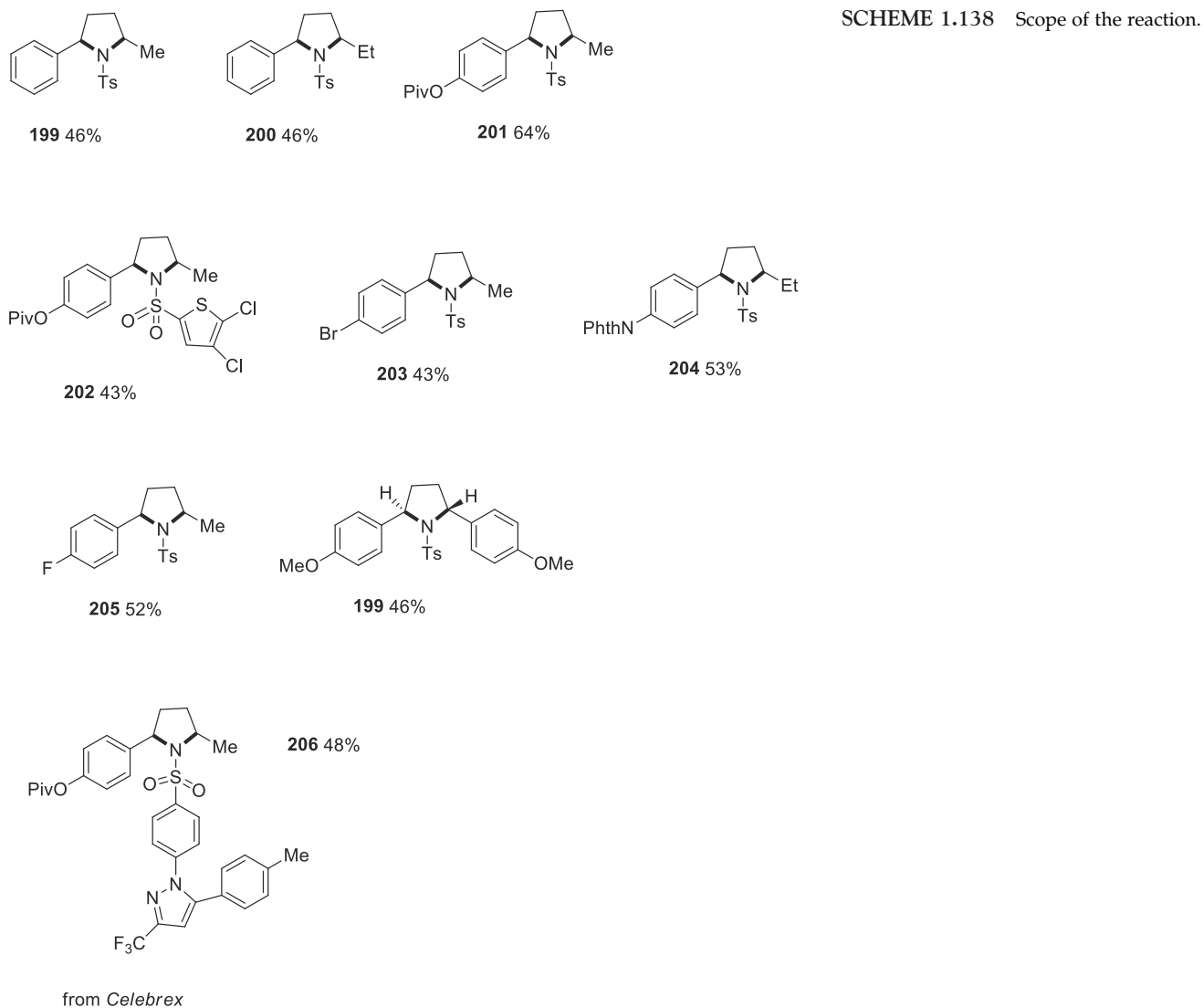
The authors, encouraged by the benzylamine scope, proceeded with *n*-pentylbenzene to test their nitrogen relay strategy. Gratyfingly, the nitrogen relay product − pyrrolidine **199**- was generated in a reasonable 46% yield. Hence, two consecutive amination of C_{sp^3} − H bonds with variable bond dissociation energies, in a single reaction operation, provided a versatile and modular strategy to synthesize pyrrolidines. Excited by this finding, the authors further extended the substrate scope to a range of other pyrrolidine products in moderate yields (Scheme 1.138, products **200**−205). They were delighted to observe that even the drug Celebrex could participate in this reaction, generating the desired pyrrolidine **206** in 48% yield and highlighting the application of this protocol in late-stage pharmaceutical functionalization.

1.15.4 Aroylchlorination of 1,6 dienes to obtain 2-pyrrolidinones

It was developed an atom transfer radical cyclization (ATRC) to develop a method for the aroylchlorination of 1,6-dienes with aroyl chlorides to obtain photochemically under mild conditions functionalized pyrrolidinones (Scheme 1.139).[94]
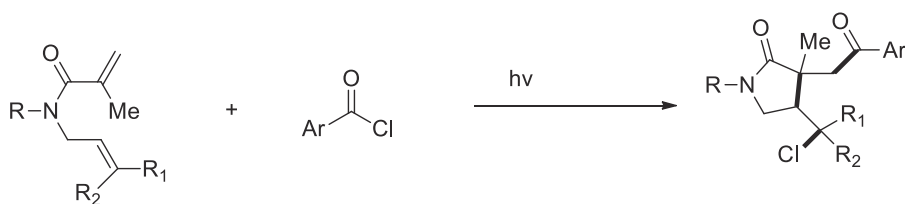
SCHEME 1.139   Aroylchlorination of 1,6 dienes to obtain 2-pyrrolidinones.

First, the authors searched for the best condition to perform the reaction. The choice of photocatalyst was a key factor for carrying out this reaction. Among the various compounds screened, *fac*-Ir (ppy)$_3$ was superior with respect to others to obtain the highest yields. Regarding the base, 2,6-lutidine was essential for the success of the reaction. About the solvents, toluene was the optimal one.

Next, the substrate scope of 1,6-dienes with benzoyl chloride under the optimized reaction condition was evaluated, and the results are presented in Scheme 1.140.

Various *N*-tethered 1,6-dienes were compatible with the reaction. Different groups (-Bn, -Tol, and −Ts) could be used as *N*-tethered 1,6-dienes protecting groups, giving the desired ATRC products (**207**, **208**, and **213**) with moderate to good yields. Likewise, *N*-(but-2-en-1-yl)- *N*-phenylmethacrilamide was also smoothly transformed into the product **209**, which was isolated in 70% yield. When a cyclopentyl or cyclohexyl group was used instead of the terminal dimethyl moiety, these substrates were also well tolerated and efficiently delivered the corresponding products **210** and **211**.

1.15.5 Synthesis of pyrrolidinones fused with a cyclobutane ring

Here is described the synthesis through visible-ligth photocatalysis of novel functionalized tetracyclic scaffolds that incorporate a fused azabicyclo[3.2.0]heptan-2-one motif, which are structurally interesting cores with potential in natural product synthesis and drug discovery.[95] These are unique structures in molecular design due to the high strain energy and conformational rigidity imposed by the cyclobutane ring.

The synthetic approach involves an intramolecular [2 + 2] cycloaddition with concomitant dearomatization of the heterocycle via an energy transfer process promoted by an iridium-based photosensitizer, to build a complex molecular architecture with at least three stereogenic centers from relatively simple, achiral precursors (Fig. 1.64).

To explore the scope of the reaction, the authors had to find the best condition to perform the reaction (photosensitizer, solvent, wavelength, etc.). After a careful screening, they found that the relatively simple, and previous unexploited (Ir[dFppy]$_3$ showed superior efficiency as an energy transfer triplet sensitizer in this [2 + 2] cycloaddition. CH$_3$CN proved to be a better solvent than DMSO for the photocatalyzed process. Quantitative conversion of **214** to **215** was achieved upon prolonged irradiation with 450 nm blue light at a reduced catalyst loading. It was recognized that the visible light absorption maxima of the photocatalyst is closer to 400 nm [λ_{max} (excitation)
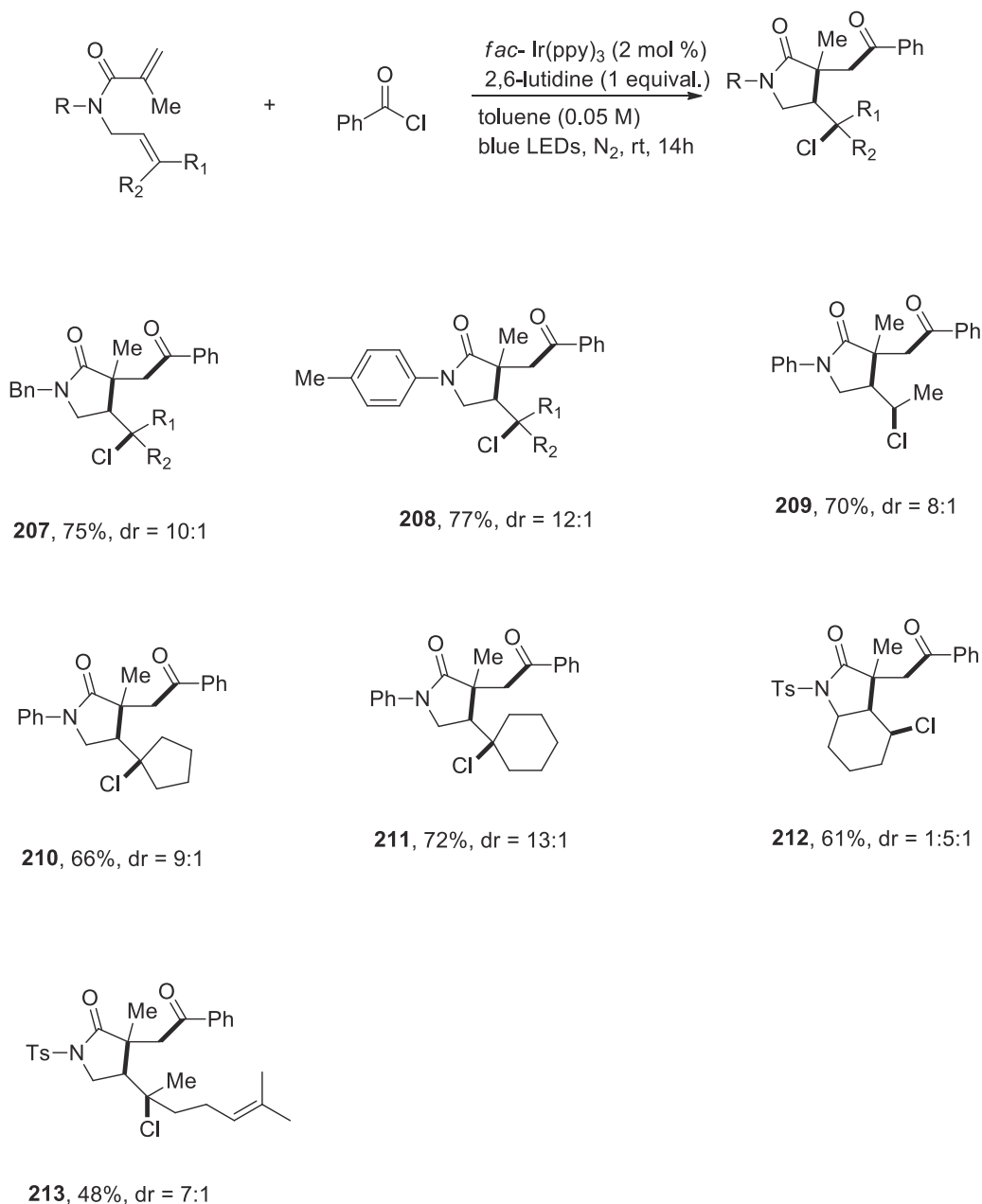
SCHEME 1.140 Substrate scope.

nm = 378]; hence, irradiation with 400 nm purple light appeared to be appropriate. For enhanced practicality, the reaction can be performed with minimal loss of yield without degassing the mixture. Finally, a control experiment in the dark confirmed that the reaction depends on both light and an appropriate photosensitizer.
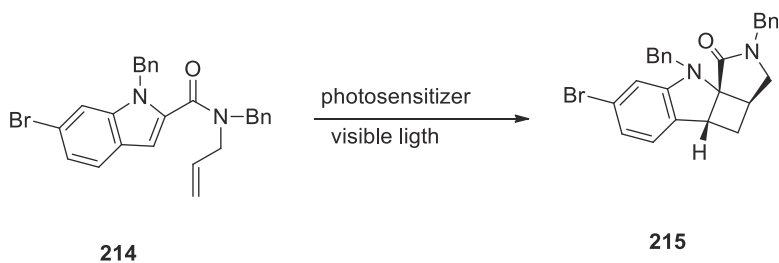
FIGURE 1.64 The reaction.

With the optimized reaction condition in hand, the scope of the reaction was investigated. The versatility of this cycloaddition strategy and the generality of the method are demonstrated by the examples compiled in Scheme 1.141.
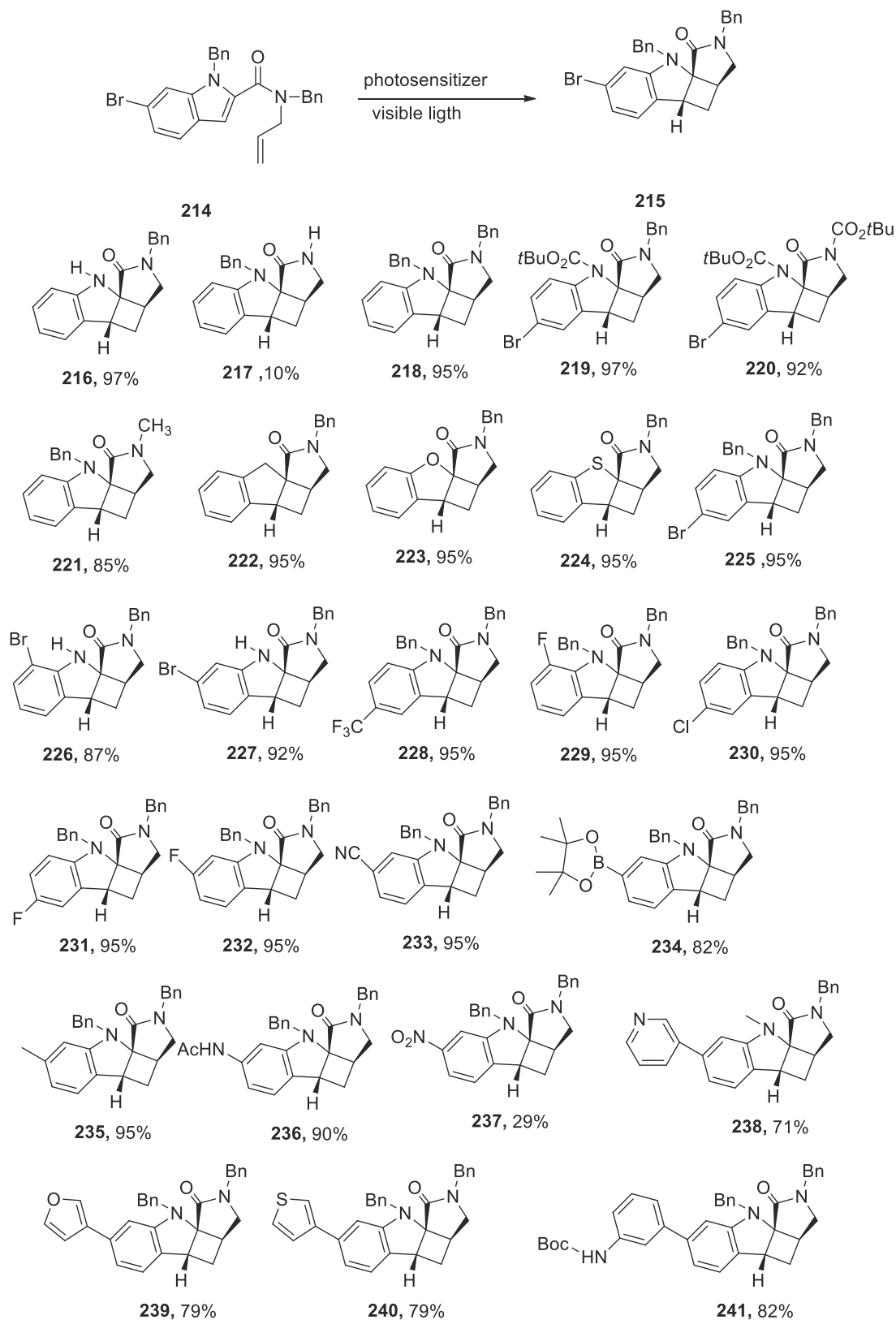
SCHEME 1.141   Scope of the reaction.

The survey was initiated by probing the necessity of having a protecting group on either or both of the indole and carboxamide nitrogen atoms (**216**−**221**). Pleasingly, the presence of a free indole NH had no detrimental effect on the efficiency of the photocycloaddition reaction, affording **216** in 97% yield. By way of contrast, only low amounts of cycloaddition product were obtained when the carboxamide nitrogen was unprotected (**217**). These results suggest that the reaction needs the conformational constraint imparted by substitution at the carboxamide nitrogen to be efficient. The benzylprotecting group can be replaced with a Boc group and an orthogonal protecting group strategy can also be employed with no adverse effect on the yield of the photocycloaddition, as exemplified by **218**−**220**. Capping the carboxamide nitrogen with a methyl group also enabled the cycloaddition reaction (**221**). Analogous to the observation with indoles, *n*-allyl-tetheres indene, benzofuran, and benzothiophene amides readily participated in a cycloaddition to provide the corresponding fused tetracyclic scaffold **222**−**224** in high yields and as a single diastereomers (>95% yield, d.r. >99:1).

Electron-withdrawing and electron-donating groups are tolerated equally well. Most importantly, substituents and functionalities required for either modulating the pharmacological and pharmaceutical properties of drug candidates or providing opportunities for synthetic diversification are all tolerated at the 5-, 6-, and 7- position of the indoline core (**225**−**237**). These moieties include fluorine, chlorine, bromine, carboxyl ester, cyanide, methyl, acetamino, trifluoromethyl, nitro and boronic ester substituents.

An additional aspect of this procedure that is noteworthy is that the installation of heterocycles such as pyridine, furan and thiophene, on the indole substrates remotes of the active center prior to the execution of the photocyclization reaction, has no detrimental effect on the outcome of the cycloaddition reaction (**238**−**240**). Similarly, substituted phenyl ring appended to the core are also energetically permitted in the photocyclization reaction, as exemplified by **241**.

1.16 Thiophenes and benzothiophenes

1.16.1 Cyclization of 2-alkynylanilines with disulfide to afford benzothiophenes

The literature on the photochemical syntheses of thiophenes and benzothiophenes is scarce. One of the most interesting example of such syntheses is that proposed by Xie et al.,[96] which is based on the cyclization of 2-alkynylanilines with disulfide to afford benzothiophenes (Fig. 1.65).

First, a screening was performed on various kinds of oxidant, solvent, and light source, to find the best conditions of reaction. The best yields were obtained with 2 equiv. of H_2O_2, PhCl as solvent and blue LED as light source. It is noticeable that the reaction requires no photocatalyst and no transition metal.

Under the optimized reaction conditions, the scope of the reaction was examined. (Scheme 1.142).

The reactions of various **242** with **243** proceeded well and afforded the desired products **244** in moderate to good yields. A variety of N-2-(phenylethynyl)acetamides (**242**) with electron-donating groups, such as methyl, *n*-propyl, and *n*-butyl, at the *para*-position of the aromatic ring reacted with **243** to afford the desired products (**244a-d**) in 64%−72%, while the reactions of other N-2-(phenylethynyl)acetamides (**242**) with electron-withdrawing groups (F, Cl and Br) at the *para*-position of the phenyl rings with **243** generated the corresponding products (**244e-g**) in 60%−69% yields. It should be noted that N-2-(phenylethynyl)acetamides with a *meta*-substituted aromatic ring also reacted with **243** to generate the corresponding product **244h** in 60% yield. Surprisingly, N-(2-(thiophen-2-ylethynyl)phenyl)acetamide is well tolerated in the reaction and the corresponding product **244i** was generated in 53% yield. However, N-(2-(cyclopropylethynyl)phenyl)acetamide was not tolerated in this transformation. The scope of the disulfide component (**243**) was also examined under the optimized reaction conditions. A series of functional groups on the aromatic rings of the diaryl disulfides were tolerated, leading to the desired products in good yields. Electron-donating groups, such as *p*-CH$_3$ and *p*-phenyl, and electron-withdrawing groups, including *p*-F, *p*-Cl, and *p*-Br, smoothly

FIGURE 1.65   The reaction.

244a, 65% **244b,** 64% **244c,** 72% **244d,** 68%

244e, 69% **244f,** 60% **244g,** 62% **244h,** 60%

244i, 53% **244j,** 0% **244k,** 55% **244l,** 57%

244m, 70% **244n,** 67% **244o,** 65% **244p,** 0%
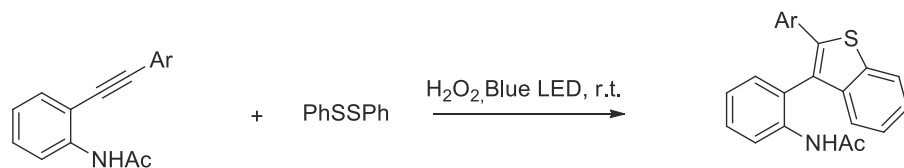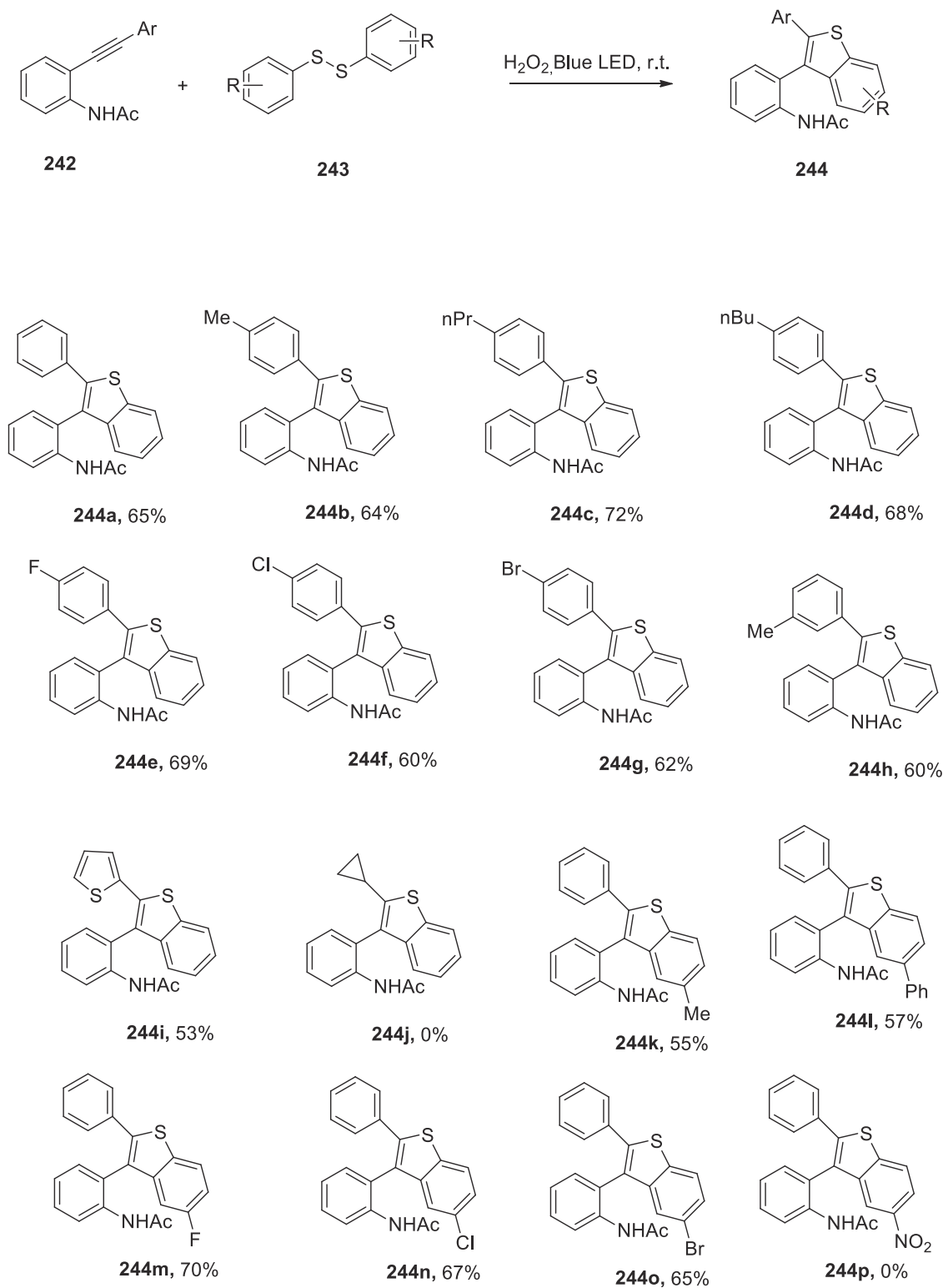
SCHEME 1.142   Scope of the reaction.

underwent the reaction with **242** to generate the anticipated products (**244k-o**) in 55%−70% yields. Unfortunately, 4,4-dinitrodiphenyl disulfide failed to react with **242**, and none of the desired product was detected.

1.16.2 Cyclization of diethynil sulfide to thiophene

The cycloaromatization of enediynes, the Bergman cyclization, has garnered much attention because two highly reactive sp^2 σ-radicals are generated under relatively mild conditions (Scheme 1.143a). An alternative to thermal cycloaromatization is the "photo-Bergman" cyclization, which has been reported for several enediyne derivatives. Here is reported an entirely new variant of this cyclization,[97] namely, the reaction of bis-(phenylethynyl) sulfide and other diethynyl sulfide derivatives (Scheme 1.143b); this constitutes the first five-membered ring cycloaromatization reaction. The reaction course is consistent with the intermediacy of a heretofore inaccessible 2,5-didehydrothiophene, and the product is a 3,4-disubstituted thiophene.

SCHEME 1.143 Cyclization of diethynil sulfide to thiophene.
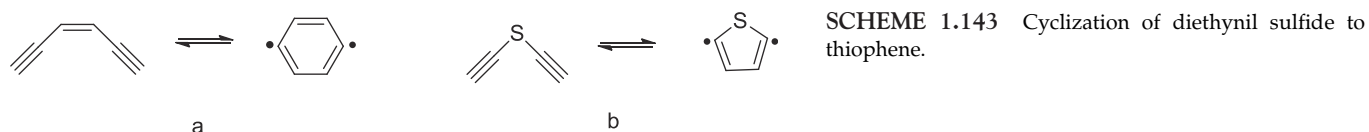
Irradiation of **245a** at 300 nm in hexanes in the presence of 1,4-cyclohexadiene (CHD, 2 mM) as the trapping agent consistently results in the production of two species: 3,4-diphenylthiophene (**246a**) and phenylacetylene (**247a**) in yields of 16 and 33%, respectively (Scheme 1.144). A substantial increase in the concentration of CHD leads to lower yields of **246a** while leaving that of **247a** relatively unchanged. Substituting γ-terpinene as the trapping agent results in similar yields of both **246a** and **247a** compared to CHD. In addition, irradiation of **245a** at 350 nm leads to similar yields and ratios of products, but with a slower rate of reaction.
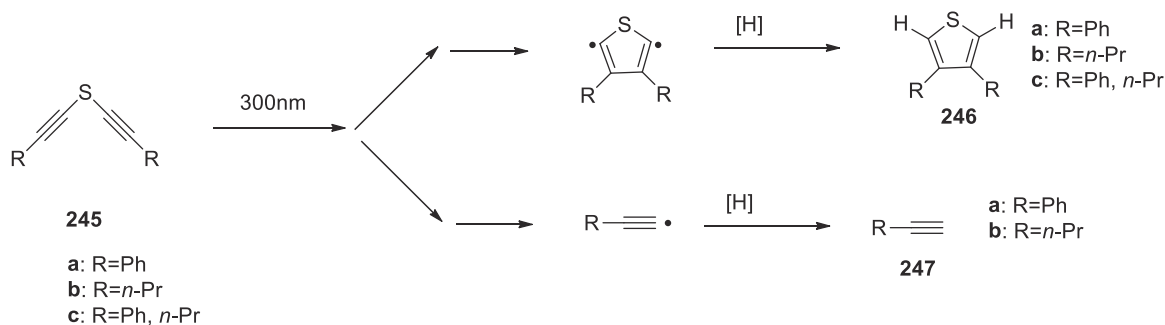
SCHEME 1.144   Products of the reaction.

To explore the generality of this five-membered cycloaromatization, a diethynyl sulfide with two propyl substituents (**245b**) and one with both a propyl and a phenyl substituent (**245c**) were examined. Irradiation of 245b at 300 nm in hexanes with CHD results in the formation of 3,4-dipropylthiophene (**246b**) in 2% yield, reflecting a reduced efficiency of the cyclization with alkyl substituents on the diethynyl sulfide. These effects are still evident in **245c**, which produces 3-phenyl-4-propylthiophene (**246c**) in 3% yield. The rate of consumption of **245b** during irradiation is approximately five times slower when compared to the other substrates and is likely due to the lack of an efficient chromophore.

References

1. Becker, M. R.; Richardson, A. D.; Schindler, C. S. *Nat. Commun.* **2019,** *10*, 1−8.
2. Becker, M. R.; Wearing, E. R.; Schindler, C. S. *Nat. Chem.* **2020,** *12*, 898−905.
3. Aoyama, H.; Sakamoto, M.; Omote, Y. *Chem. Lett.* **1982,** 1211−1212.
4. Ruggeri, M.; Dombrowsky, A. W.; Djuric, S. W.; Baxendale, I. R. *ChemPhotoChem* **2019,** *3*, 1212−1218.
5. Ueda, N.; Nikawa, H.; Takano, Y.; Itshisuka, M. O.; Tsuchiya, T.; Akasaka, T. *Heteroat. Chem.* **2011,** *22*, 3−4.
6. Wessig, P.; Schwarz, J. *Helv. Chim. Acta* **1998,** *81*, 1803−1814.
7. Ling, R.; Yoshida, M.; Mariano, P. S. *J. Org. Chem.* **1996,** *61*, 4439−4449.
8. Damiano, T.; Morton, D.; Nelson, A. *Org. Biomol. Chem.* **2007,** *5*, 2735−2752.
9. D'Auria, M.; Racioppi, R.; Viggiani, L.; Zanirato, P. *Eur. J. Org. Chem.* **2009,** 932−937.
10. Maskill, G.; Knowles, J. P.; Elliot, L. D.; Alder, R. W.; Booker-Milburn, K. I. *Angew. Chem. Int. (Ed.)* **2013,** *52*, 1499−1502.
11. de Loera, D.; Garcia-Garibay, M. A. *Org. Lett.* **2013,** *14*, 3874−3877.

12. Liu, Y.; Dong, X.; Deng, G.; Zhou, L. *Sci. China* **2015,** *59,* 199−202.
13. Masakado, S.; Kobayashi, Y.; Takemoto, Y. C. *Chem. Pharm. Bull.* **2018,** *66,* 688−690.
14. Averdung, J.; Mattay, J. *Tetrahedron* **1996,** *52,* 5407−5420.
15. Okada, M.; Nakahodo, T.; Ishitsuka, T.; Akasaka, T.; Fujie, T.; Yoshimura, T.; Slanina, Z.; Nagase, S. *Chem. Asian J.* **2011,** *6,* 416−423.
16. Mendlik, M. T.; Tao, P.; Hadad, C.; Coleman, S. R.; Lowary, T. L. *J. Org. Chem.* **2006,** *71,* 8059−8070.
17. Farney, E. P.; Yoon, T. P. *Angew. Chem. Int. (Ed.)* **2014,** *53,* 793−797.
18. Zhang, Y.; Dong, X.; Wu, Y.; Li, G.; Lu, H. *Org. Lett.* **2018,** *20,* 4838−4842.
19. Sawanishi, H.; Tajima, K.; Tsuchiya, T. *Chem. Pharm. Bull.* **1987,** *35,* 3175−3181.
20. Sawanishi, H.; Sashida, H.; Tsuchiya, T. *Chem. Pharm. Bull.* **1985,** *33,* 4564−4581.
21. Fallahpour, R. A. *Helv. Chim. Acta* **2000,** *83,* 384−391.
22. Jiang, H.; Cheng, Y.; Zhang, Y.; Yu, S. *Org. Lett.* **2013,** *15,* 4884−4887.
23. Protti, S.; Fagnoni, M.; Albini, A. *J. Org. Chem.* **2012,** *77,* 6473−6479.
24. Armesto, D.; Ortiz, M. J.; Agarrabeitia, A. R. *J. Org. Chem.* **1999,** *64,* 1056−1060.
25. Shang, Z. P.; Zha, G. F.; Chen, X. Q.; Qin, H. L. *Tetrahedron Lett.* **2016,** *57,* 4658−4683.
26. Han, Y. Y.; Jiao, Y. Y.; Ren, D.; Hu, Z.; Shen, S.; Yu, S. *Asian J. Org. Chem.* **2017,** *6,* 414−417.
27. Harrowven, D. C.; Mohamed, M.; Goncalves, T. P.; Whitby, R. J.; Bolien, D.; Sneddon, H. F. *Angew. Chem. Int. (Ed.)* **2012,** *51,* 4405−4408.
28. Lin, C. H.; Pursley, D.; Klein, J. E. M. N.; Teske, J.; Allen, A. J.; Rami, F.; Kohn, A.; Plietker, B. *Chem. Sci.* **2015,** *6,* 7034−7043.
29. Mladenova, G.; Lee-Ruff, E. *Tetrahedron Lett.* **2007,** *48,* 2787−2789.
30. Mukherjee, A. K.; Marghareta, P.; Agosta, W. C. *J. Org. Chem.* **1996,** *61,* 3388−3391.
31. Pandey, G.; Ghorai, M. K.; Hajra, S. *Pure Appl. Chem.* **1996,** *68,* 653−658.
32. Sutar, R. L.; Sen, S.; Eivgi, O.; Segalovich, G.; Schapiro, I.; Reany, O.; Lemcoff, G. *Chem. Sci.* **2018,** *9,* 1368−1374.
33. Verma, F.; Singh, P. K.; Bhardiya, S. R.; Singh, M.; Rai, A.; Rai, V. K. *N. J. Chem.* **2017,** *41,* 4937−4942.
34. Wang, S.; Jia, W. L.; Wang, L.; Liu, Q.; Wu, L. Z. *Chem. Eur. J.* **2016,** *22,* 13794−13798.
35. Walker, J. C. J.; Werrel, S.; Donohoe, T. J. *Chem. Eur. J.* **2019,** *25,* 13114−13118.
36. Boulanger, E.; Anoop, A.; Nachtigallova, D.; Thiel, W.; Barbatti, M. *Angew. Chem. Int. (Ed.)* **2013,** *52,* 8000−8003.
37. Chen, J. Q.; Yu, W. L.; Wei, Y. L.; Li, T. H.; Xu, P. F. *J. Org. Chem.* **2017,** *82,* 243−249.
38. Kanyiva, S. K.; Tane, M.; Shibata, T. *J. Org. Chem.* **2019,** *84,* 12773−12783.
39. Menor-Salvan, C.; Marin-Yaselli, M. *Chem. Eur. J.* **2013,** *19,* 6488−6497.
40. Pusch, S.; Opaz, T. *Org. Lett.* **2014,** *16,* 5430−5433.
41. Wenska, G.; Skalski, B.; Paszyc, S.; Gadiec, Z. *Can. J. Chem.* **1995,** *73,* 2178−2188.
42. Cai, B. G.; Chen, Z. L.; Xu, G. Y.; Xuan, Y.; Xiao, W. J. *Org. Lett.* **2019,** *21,* 4234−4238.
43. Kurpil, B.; Otte, C.; Antonietti, M.; Savateev, A. *Appl. Cat. B: Env.* **2018,** *228,* 97−102.
44. Ang, K. H.; Prager, R. H.; Smith, J. A.; Weber, B.; Williams, C. M. *Tetrahedron Lett.* **1996,** *37,* 675−678.
45. Chatterjee, T.; Cho, J. Y.; Cho, E. J. *J. Org. Chem.* **2016,** *81,* 6995−7000.
46. Chu, X. Q.; Ge, D.; Wang, M. L.; Rao, W.; Loh, T. P.; Shen, Z. L. *Adv. Synth. Catal.* **2019,** *361,* 4082−4090.
47. He, X.; Yao, X. Y.; Chen, K. H.; He, L. N. *ChemSusChem* **2019,** *12,* 5081−5085.
48. Jesuraj, J. L.; Sivaguru, J. *Chem. Commun.* **2010,** *46,* 4791−4793.
49. Matveeva, E. D.; Podrugina, T. A.; Pavlova, A. S.; Mironov, A. V.; Gleiter, R.; Zefirov, N. S. *Eur. J. Org. Chem.* **2009,** 2323−2327.
50. Zeng, T. T.; Xuan, J.; Ding, W.; Wang, K.; Lu, L. Q.; Xiao, W. J. *Org. Lett.* **2015,** *17,* 4070−4073.
51. Abe, M.; Taniguchi, K.; Hayashi, T. *ARKIVOC* **2007,** 58−65 (*viii*).
52. Bach, T.; Schröder, J. *J. Org. Chem.* **1999,** *64,* 1265−1273.
53. Bondock, S.; Griesbeck, A. *Monatshefte für Chem.* **2006,** *137,* 765−777.
54. Silva, M. T.; Braz-Filho, R.; Netto-Ferreira, J. C. *J. Braz. Chem. Soc.* **2000,** *11,* 479−485.
55. Ogata, M.; Watanabe, H.; Kanō. *Tetrahedron Lett.* **1967,** *8,* 533−537.
56. Bondock, S.; Griesbeck, A. G. *Int. J. Photoenergy* **2005,** *7,* 23−25.
57. Griesbeck, A. G.; Fiege, M.; Bondock, S.; Gudipati, M. S. *Org. Lett.* **2000,** *2,* 3623−3625.
58. Griesbeck, A. G. *J. Photosci.* **2003,** *10,* 49−60.
59. Bach, T.; Khater, K. *Tetrahedron* **1994,** *50,* 12319−12328.
60. Bach, T. *Tetrahedron Lett.* **1991,** *32,* 7037−7038.
61. Hisamoto, K.; Hiraga, Y.; Abe, M. *Photochem. Photobiol. Sci.* **2011,** *10,* 1469−1473.
62. Griesbeck, A. G.; Franke, M.; Jörg, N.; Kotaka, H. *Belstein J. Org. Chem.* **2011,** *7,* 127−134.
63. Vargas, F.; Rivas, C.; Navarro, M.; Alvarado, Y. *J. Photochem. Photobiol. A: Chem.* **1996,** *93,* 169−171.
64. D'Auria, M.; Racioppi, R.; Romaniello, G. *Eur. J. Org. Chem.* **2000,** 3265−3272.
65. D'Auria, M.; Racioppi, R. *ARKIVOC* **2000,** *1,* 133−140.
66. D'Auria, M.; Emanuele, L.; Poggi, G.; Racioppi, R.; Romaniello, G. *Tetrahedron* **2002,** *58,* 5045−5051.
67. D'Auria, M.; Emanuele, L.; Racioppi, R. *Photochem. Photobiol. Sci.* **2004,** *3,* 927−932.
68. Bach, T. *Liebigs Ann.* **1995,** 855−865.
69. Bach, T.; Jödicke, K.; Kather, K.; Fröhlich. *J. Am. Chem. Soc.* **1997,** *119,* 2437−2445.
70. Zhang, H.; Muniz, K. *ACS Catal.* **2017,** *7,* 4122−4125.
71. Ohtani, B.; Kusakabe, S.; Okada, K.; Tsuru, S.; Izawa, K.; Amino, Y.; Nishimoto, S. *Tetrahedron Lett.* **1995,** *36* (18), 3189−3192.
72. Pandey, G.; Kapur, M.; Khan, M. I.; Gaikwad, S. M. *Org. Biomol. Chem.* **2003,** *1,* 3321−3326.
73. Winter, D. K.; Drouin, A.; Lessard, J.; Spino, C. *J. Org. Chem.* **2010,** *75* 2610-2610.
74. Murakami, Y.; Hisaeda, Y.; Ohno, T.; Matsuda, Y. *Chem. Lett.* **1988,** 621−624.
75. Annes, S. B.; Rajmohan, R.; Ramesh, S.; Vairaprakash, P. *Tetrahedron Lett.* **2019,** *60,* 150932.
76. Ahmed, S. A.; Awad, I. M. A.; Abdel-Wahab, A. A. *Photochem. Photobiol. Sci.* **2002,** *1,* 84−86.
77. Ding, Y.; Zhang, T.; Chen, Q. Y.; Zhu, C. *Org. Lett.* **2016,** *18,* 4206−4209.

78. Cheng, J.; Li, W.; Duan, Y.; Cheng, Y.; Yu, S.; Zhu, C. *Org. Lett.* **2017,** *19*, 214−217.
79. Fan, X. W.; Lei, T.; Zhou, C.; Meng, Q. Y.; Chen, B.; Tung, C. H.; Wu, L. Z. *J. Org. Chem.* **2016,** *81*, 7127−7133.
80. Meng, Y.; Zhang, T.; Gong, X.; Zhang, M.; Zhu, C. *Tetrahedron Lett.* **2019,** *60*, 171−174.
81. Traven, V. F.; Ivanov, I. V.; Dolotov, S. M.; Semakin, A. N.; Cheptsov, D. A.; Marmigova, Z. Z. *Photochem. Photobiol.* **2019,** *95*, 924−930.
82. Portillo, M.; Maxwell, M. A.; Frederich, J. H. *Org. Lett.* **2016,** *18*, 5142−5145.
83. Alonso, R.; Caballero, A.; Campos, P. J.; Rodrìguez, M. A. *Tetrahedron* **2010,** *66*, 8828−8831.
84. Fischer, F.; Siegle, A. F.; Checinski, M.; Fischer, C.; Kral, K.; Thede, R.; Trapp, O.; Hapke, M. *J. Org. Chem.* **2016,** *81*, 3087−3102.
85. Rohokale, R. S.; Koenig, B.; Dhavale, D. D. *J. Org. Chem.* **2016,** *81*, 7121−7126.
86. Heller, B.; Sundermann, B.; Fischer, C.; You, J.; Chen, W.; Drexler, H. J.; Knochel, P.; Bonrath, W.; Gutnov, A. *J. Org. Chem.* **2003,** *68*, 9221−9225.
87. Buscemi, S.; Pace, A.; Palumbo Piccionello, A.; Pibiri, I.; Vivona, N. *HETEROCYCLES* **2004,** *7*, 1619−1628.
88. Chu, X. Q.; Xie, T.; Li, L.; Ge, D.; Shen, Z. L.; Loh, T. P. *Org. Lett.* **2018,** *20*, 2749−2752.
89. Wang, R.; Guan, W.; Han, Z. B.; Liang, F.; Suga, T.; Nishide, H. *Org. Lett.* **2017,** *19*, 2358−2361.
90. Frija, L. M. T.; Khmelinskii, I. V.; Cristiano, M. L. S. *J. Org. Chem.* **2006,** *71* (3583), 3591.
91. Miller, D. C.; Choi, G. J.; Orbe, H. S.; Knowles, R. R. *J. Am. Chem. Soc.* **2015,** *137*, 13492−13495.
92. Amador, A. G.; Sherbrook, E. M.; Yoon, T. P. *Asian J. Org. Chem.* **2019,** *8*, 978−985.
93. Wu, F.; Ariyarathna, J. P.; Kaur, N.; Alom, N. E.; Kennel, M. L.; Bassiouni, O. H.; Li, W. *Org. Lett.* **2020,** *22*, 2135−2140.
94. Zhao, Q. S.; Xu, G. Q.; Liang, H.; Wang, Z. Y.; Xu, P. F. *Org. Lett.* **2019,** *21*, 8615−8619.
95. Oderinde, M. S.; Mao, E.; Ramirez, A.; Pawluczyk, J.; Jorge, C.; Cornelius, L. A. M.; Kempson, J.; Vetrichelvan, M.; Pitchai, M.; Gupta, A., et al. *J. Am. Chem. Soc.* **2020,** *142*, 3094−3103.
96. Xie, X.; Li, P.; Shi, Q.; Wang, L. *Org. Biomol. Chem.* **2017,** *15*, 7678−7984.
97. Lewis, K. D.; Wenzler, D. L.; Matzger, A. *J. Org.Lett.* **2003,** *5* (13), 2195−2197.

This page intentionally left blank

Photoisomerization of heterocyclic compounds

2.1 Photoisomerization of pentaatomic heterocycles

2.1.1 Isomerization of furan derivatives

2.1.1.1 Furan

The excited singlet states of furan show two Rydberg ($^1A_2(3s)$ and $^1B_1(3p)$) and two π,π^* valence states ($^1B_2(V)$ and $^1A_1(V')$).[1–8] The photolysis of furan (**1**) in gas phase (5−150 mm Hg) in the presence of mercury at 254 nm gave carbon monoxide (**2**) and a fraction containing mainly cyclopropane (**3**) and a very small amount of allene (**4**) or methylacetylene (**5**) (Scheme 2.1).[9] Subsequently, by carrying out the reaction at higher pressure of furan (0.2−1 atm), the same author showed that three new products were obtained.[10–12] The first two compounds (**6** and **7**) were the Diels−Alder adducts obtained by the coupling of furan and cyclopropane, while the third **8** was the Diels−Alder adduct obtained by the coupling of furan and cyclopropane-3-carbaldehyde (Scheme 2.1). None of the reported pro-
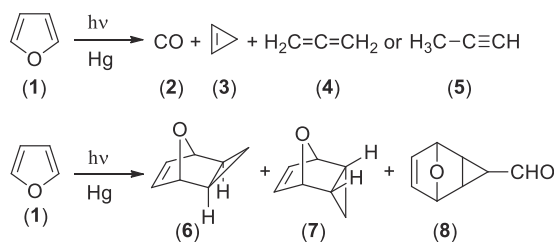
SCHEME 2.1 Reaction products after furan irradiation.

ducts were observed on direct irradiation of furan in solution (cyclopentane as solvent).

These results were justified by assuming that the first photoproduct of the reaction was cyclopropane-3-carbaldehyde. This compound can be obtained via homolytic fission of an O−C$_\alpha$ bond to give the biradical **9**, which then collapses to **10** (Scheme 2.2). In this hypothesis, compound **10** was obtained as an excited species,
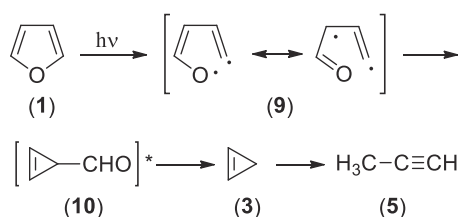
SCHEME 2.2   Proposed mechanism for the degradation product obtained with furan.

allowing further decomposition to cyclopropane. The thermal decomposition of cyclopropane to methylacetylene was known.[13] The author did not consider the possibility that **10** could be excited via direct irradiation at 254 nm. Furthermore, when furan (137 mm Hg) was irradiated in the presence of mercury and methanol (37 mm Hg), the amount of cyclopropane and carbon monoxide in the reaction mixture decreased, while methyl 3-butenoate was obtained as the main product.[10] This product could be generated from vinylketene through addition of methanol. The formation of vinylketene could be a new route to explain the formation of the ring-opening products in the photolysis of furan, but the author did not consider it.

The sensitized reaction on furan led to the formation of a π,π^* triplet state of **1**; then the relaxation of $O-C_\alpha$ bonds can induce, by crossing onto a π,σ^* energy sheet, the formation of a π,σ biradical **9**.[14-16]

In another work, the direct irradiation of furan in gas phase gave carbon monoxide, methylacetylene, and allene, while yclopropane was detected only in traces.[17] The direct irradiation leads to the formation of the excited singlet state, in which case yclopropane is not the main product; then **3** is formed, starting from the excited triplet state. The direct flash photolysis of furan in gas phase gave mass fragments corresponding to C_4H^+, $C_4H_2^+$, $C_4H_3^+$, and $C_4H_4^+$ together with the formation of yclopropane-3-carbaldehyde.[18] This behavior can be explained by assuming that Dewar furan is a precursor of the yclopropane derivative. The irradiation at 214 nm of furan at 10 K gave a complex mixture of products in which carbon monoxide, methylacetylene, allene, vinylketene, formylallene, yclopropane-3-carbaldehyde, and Dewar furan were detected.[19] Furthermore, the irradiation of Dewar furan at 254 nm at 10 K afforded **10**.

Liquid-phase photolysis of furan at room temperature occurred in very low yields (1% conversion), giving a mixture of Diels−Alder adducts deriving from the reaction of yclopropane-3-carbaldehyde and formylallene with furan.[20]

The existence of Dewar furan was confirmed by the generation of this species using both chemical and photochemical methods. In this way, the high reactivity of Dewar furan has been demonstrated to give the corresponding cyclopropenyl derivatives;[21-25] sometimes, the cyclopropenyl derivatives can be converted into the corresponding furan.[26,27] *Ab initio* calculations using STO-3G basis set concluded that Dewar furan has an energy of 318.7 kJ/mol higher than furan.[28]

Semiempirical (PM3) and *ab initio* (6−31 G** basis set) calculations are in agreement with the following hypothesis:[29,30] if the first excited singlet state of a molecule is populated, this molecule can convert into the corresponding triplet state or into the corresponding Dewar isomer. The efficiency of these processes will depend on energetic factors. If the Dewar isomer is formed, an isomeric product is obtained. If the triplet state is formed, cleavage of the $X-C_\alpha$ bond can occur to give ring-opening products, decomposition products, or ring-contraction products. However, if the radical formed after the $X-C_\alpha$ cleavage shows a higher energy than the triplet state, the triplet state will not be able to give the biradical with high efficiency, and then it will be quenched in radiative and nonradiative processes. In this case, the Dewar isomer could be responsible for the isomerization reaction, but the isomerized product will probably be produced in very low quantum yields (Scheme 2.3).
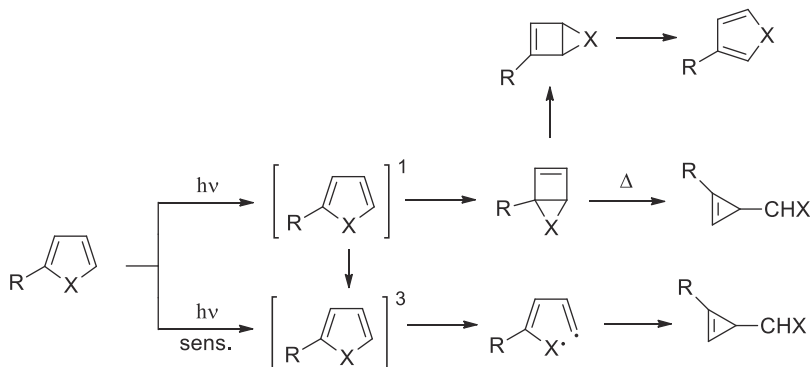
SCHEME 2.3   Proposed mechanism for the photochemical behavior of furan derivatives.
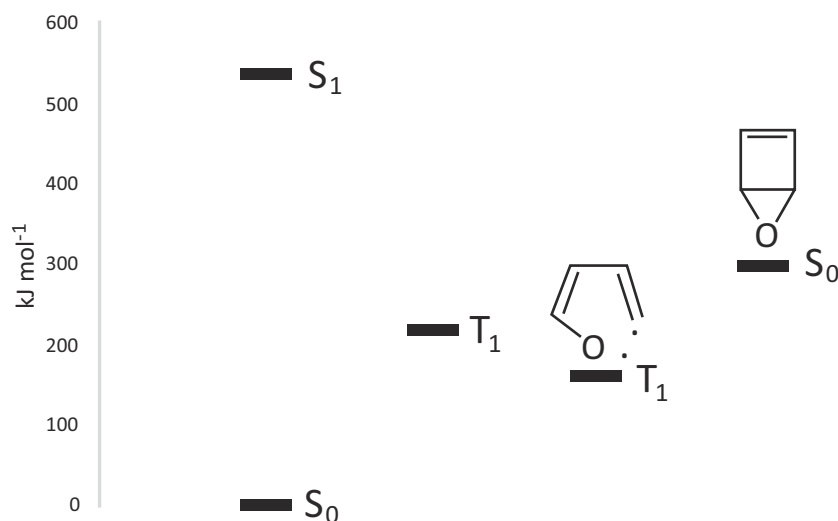
FIGURE 2.1 Relative energy of the excited states of furan and of some reactive intermediates.

Considering furan, in the case of the sensitized reaction, when the excited triplet state is populated, only the formation of the radical intermediate is allowed. This intermediate can evolve to the corresponding cyclopropenyl derivative or to the decomposition products. In the case of direct irradiation, the singlet excited state is populated, hence the formation of the Dewar furan is energetically possible (Fig. 2.1). This result is in agreement both with the evidence for the formation of the Dewar furan in the direct irradiation and with the formation of isomeric furans.

Theoretical studies showed that the deactivation of the singlet state of furan can allow the breaking of the C_α−O bond to give a singlet biradical itermediate.[31−35]

2.1.1.2 Methylfurans

2-Methylfuran, irradiated in the presence of mercury vapor, gave carbon monoxide and a fraction containing 1,3-butadiene and 3-methylcyclopropene (45:55).[9] Subsequently, in both sensitized and direct photolysis of 2-methylfuran, a more complex mixture of products was obtained, where 3-methylfuran was present (Scheme 2.4).[36,37] 3-Methylfuran was the only product when 2-methylfuran was irradiated in diethyl ether.[36]
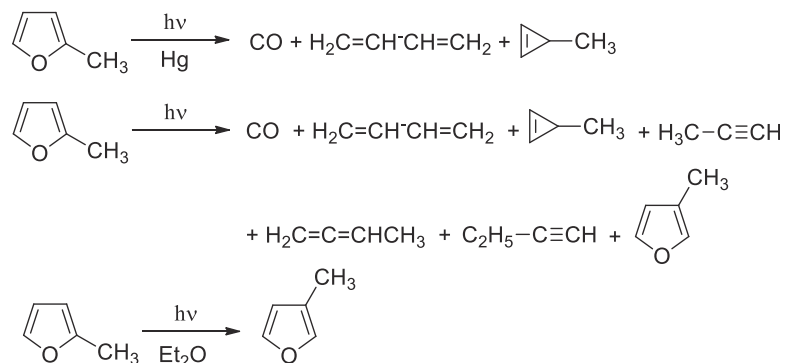
SCHEME 2.4 Reaction product after methylfuran irradiation.

In a theoretical work on this compound (SINDO 1), it was established that excitation takes place to the third excited singlet state. Then, two internal conversion processes cause the system to reach the minimum of the lowest excited singlet state. In this hypothesis, reaction can occur in both excited singlet and triplet state.[38] Some previous authors claimed to predict the direction of the ring contraction. In their opinion, during the reaction the weakest bond is broken, and it is that between O−C_2 and O−C_5.[37,38] Other results (6−31 G**) did not confirm this hypothesis. In this case, the distance between O and C_2 in the triplet state of 2-methylfuran was the same as that between O and C_5.[30]
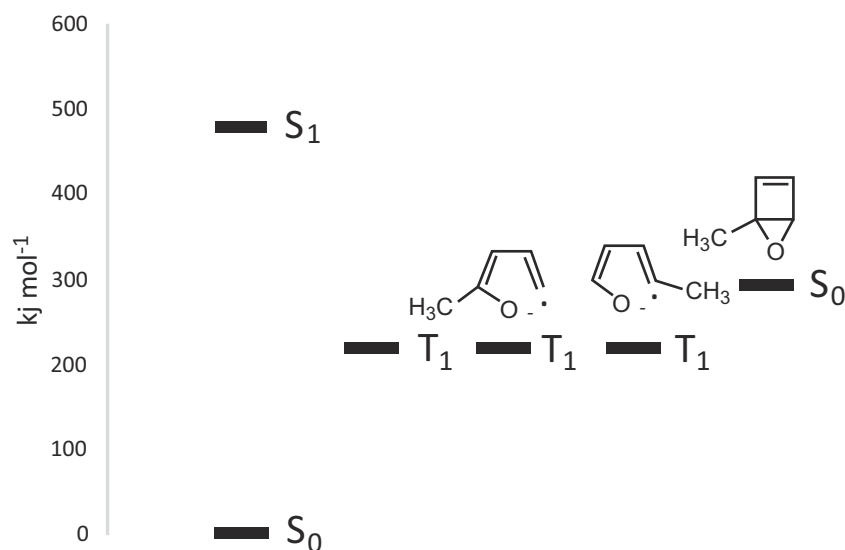
FIGURE 2.2　Relative energy of the excited states of 2-methylfuran and of some reactive intermediates.

Also in this case, the relative energy of all the possible intermediates involved in the photochemical isomerization was calculated.[30] The results are summarized in Fig. 2.2. Also in this case, the sensitized irradiation involves the formation of the biradical. However, it is noteworthy that the fission of $O-C_\alpha$ bond in the triplet state of the molecule is not so favored as in furan. The process should be quite inefficient. The corresponding biradicals show the same energy as that in the triplet state. In this case, then, the formation of a biradical should depend on the activation energy.

A theoretical study on 2-methylfuran isomerization showed that the reaction on the triplet state involved the formation of the cyclopropenyl intermediate.[39]

Mercury-sensitized irradiation of 3-methylfuran gave 2-butyne, 1,2-pentadiene, 1-methylcyclopropene, 1-butyne, and 1,3-butadiene (Scheme 2.5).[36,37] In the direct irradiation, 1-methylcyclopropene was obtained in low yields while both 3-methylcyclopropene and 2-methylfuran appeared (Scheme 2.5).[37]
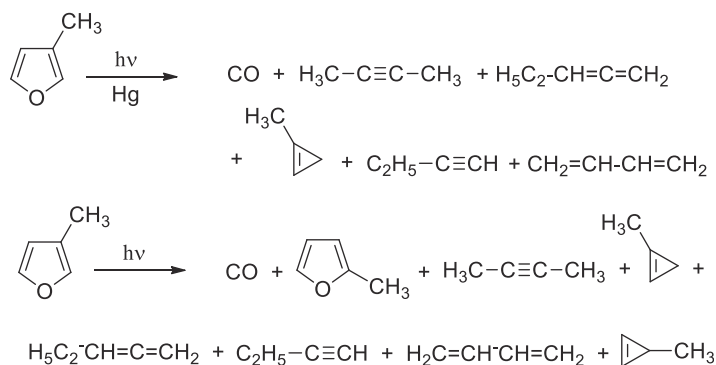
SCHEME 2.5　Irradiation of 3-methylfuran.

2.1.1.3 Alkylfurans

2,4-Dimethylfuran, in a sensitized reaction, gave 1,3-dimethylcyclopropene (the main product), isoprene, *cis*- and *trans*-1,3-pentadiene, 2-pentyne, and 1-methylcyclopropenyl methyl ketone (Scheme 2.6);[37] the ring contraction showed a high selectivity.
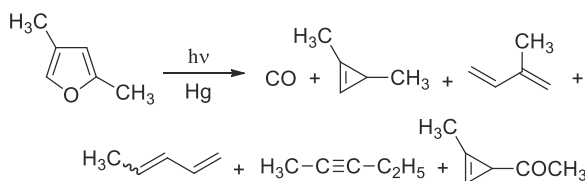
SCHEME 2.6　Irradiation of 2,4-dimethylfuran.

The irradiation of 2,5-dimethylfuran in the presence of mercury vapor gave a complex mixture of products. Carbon monoxide and propene were removed as gaseous products. Then, *cis*- and *trans*-1,3-pentadiene, isoprene, 1,3-dimethylcyclopropene, 2-pentyne, 2-ethyl-5-methylfuran, hexa-3,4-dien-2-one, 1-methyl-3-acetylcyclopropene, and 4-methylcyclopent-2-enone were obtained (Scheme 2.7).[36,40] The most abundant product was the cyclopentenone **19**, the second was the 1,3-pentadiene **12**, while the third product was the cyclopropenyl derivative **18**.
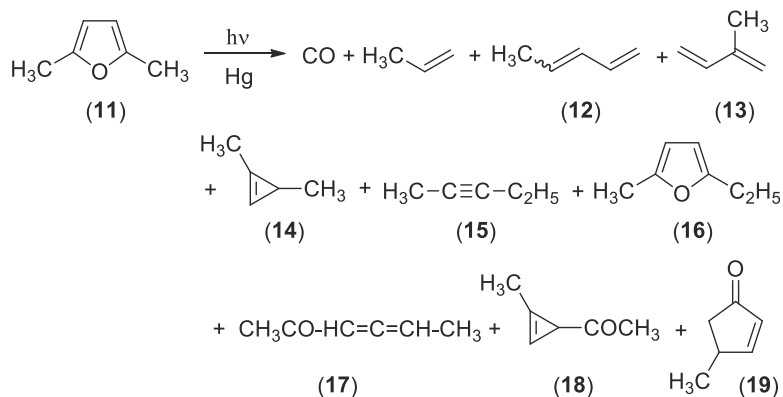
SCHEME 2.7   Irradiation of 2,5-dimethylfuran.

By contrast, direct irradiation of 2,5-dimethylfuran gave 2,4-dimethylfuran as the only isolated product.[36]

The irradiation of 2,5-dimethylfuran in propylamine led to the formation of the corresponding pyrrole. The reaction mechanism can be explained ad depicted in Scheme 2.8.[41,42] It is noteworthy that the irradiation of **18** in butylamine gave a mixture of the analogous *N*-butylpyrroles, in agreement with the proposed mechanism;[43,44] however, the independently synthesized tetrakis(trifluoromethyl)yclopropane derivative of the proposed imine could not be converted into the corresponding pyrrole.[45] The latter result is not in agreement with the mechanism depicted in Scheme 2.8 and gives evidence for one involving the presence of a Dewar furan.
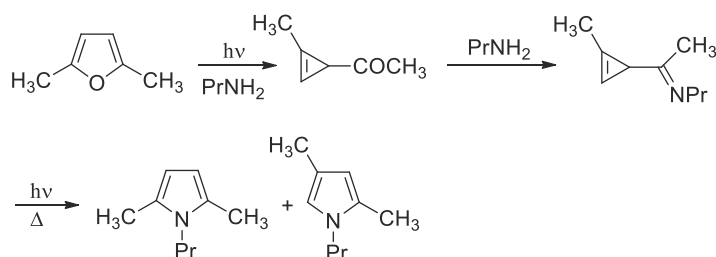
SCHEME 2.8   Irradiation 2,5-dimethylfuran in the presence of an amine.

2,5-Di-*t*-butylfuran (**20**), irradiated in pentane, gave the expected cyclopropenyl ketone **21**, 2,4-di-*t*-butylfuran (**22**), and an allene **23** in low yields (4%, 9%, and 9%, respectively) (Scheme 2.9).[46,47] The irradiation of the cyclopropenyl ketone **21** gave 2,5-di-*t*-butylfuran (**20**) (8%), 2,4-di-*t*-butylfuran (**22**) (13%), and the allene **23** (19%), showing that it was an intermediate in the reaction mixture (Scheme 2.9). The irradiation of 2,4-di-*t*-butylfuran (**22**) gave the corresponding cyclopropenyl derivative **24** (Scheme 2.9).

Finally, 2,3,5-tri-*t*-butylfuran (**25**) gave a cyclopentanone derivative **26** (95%) and a cyclopropenyl derivative **27** (5%) (Scheme 2.9).

The formation of **26** can be explained on the basis of the mechanism depicted in Scheme 2.10, where the irradiation of the cyclopropenyl derivatives **28** induces a radical reaction to give **26**.

Theoretical calculations are in agreement with the experimental results. In fact, the triplet state of **20** can be converted into the corresponding biradical to give the cyclopropenyl derivative (Fig. 2.3).
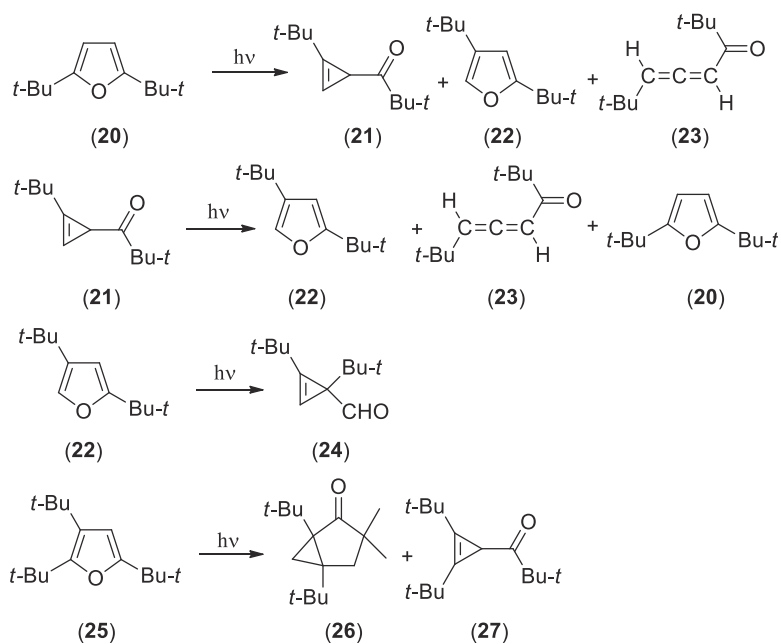
SCHEME 2.9 Irradiation of *t*-butyl substituted furan derivatives.
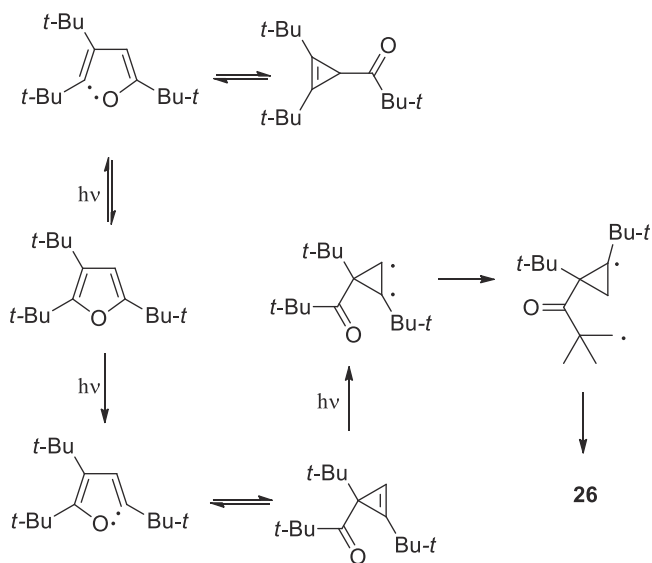
SCHEME 2.10 Proposed mechanism for the photochemical behavior of *t*-butyl substituted furans.
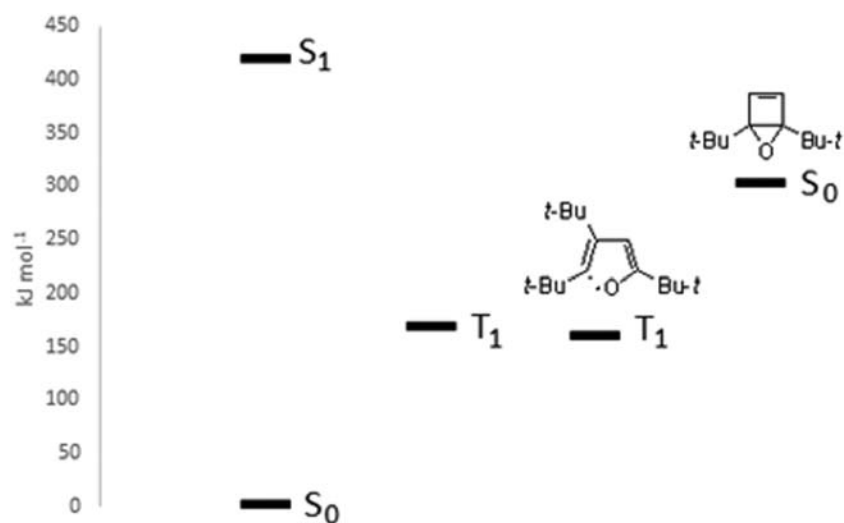
FIGURE 2.3 Relative energy of the excited states of 2,5-di-*t*-butylfuran and of some reactive intermediates.

2.1.1.4 Trimethylsilyl-substituted furans

The irradiation of 2-trimethylsilylfuran (**29**) gave the corresponding ring-opening product **30** in 68% yield (Scheme 2.11).[48] Other trimethylsilyl derivatives showed the same behavior (Scheme 2.11). The allene **32**, obtained starting from the furan **31**, can be thermally converted into 2,4-ditrimethylsilylfuran (**33**). 2,4-ditrimethylsilylfuran and 5-methyl-2-trimethylsilylfuran gave the same type of products (Scheme 2.11).[48]
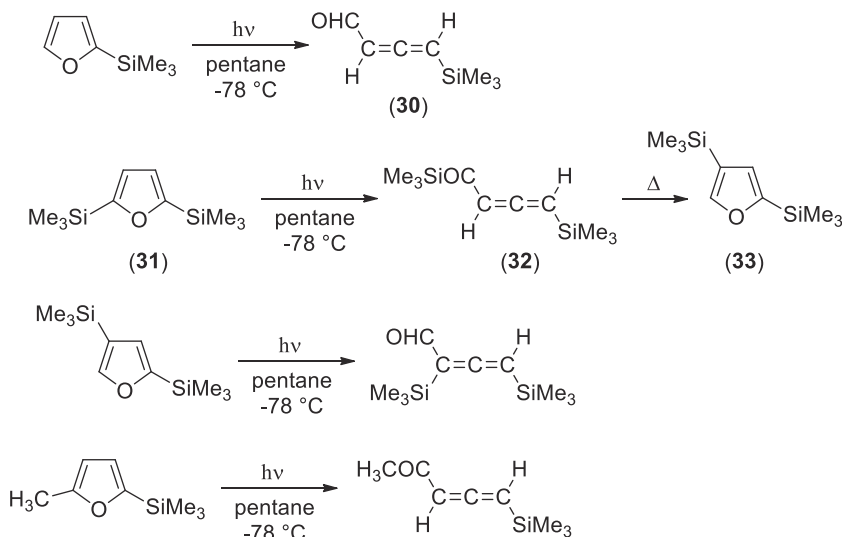
SCHEME 2.11 Photochemical behavior of trimethylsilyl substituted furan derivatives.

The authors, assuming the intervention of a cyclopropenyl intermediate, explained the formation of these types of products. The calculated relative energies of all the possible intermediates involved in the photochemical isomerization are summarized in Fig. 2.4.[30] In this case, the irradiation can involve the excited singlet state, and then the formation of Dewar isomer is possible. As in 2-methylfuran, the fission of a $O-C_\alpha$ bond in the triplet state of the molecule is not so favored as in furan. The corresponding biradicals show the same energy as that in the triplet state. In this case, then, the formation of a biradical should depend on the activation energy.
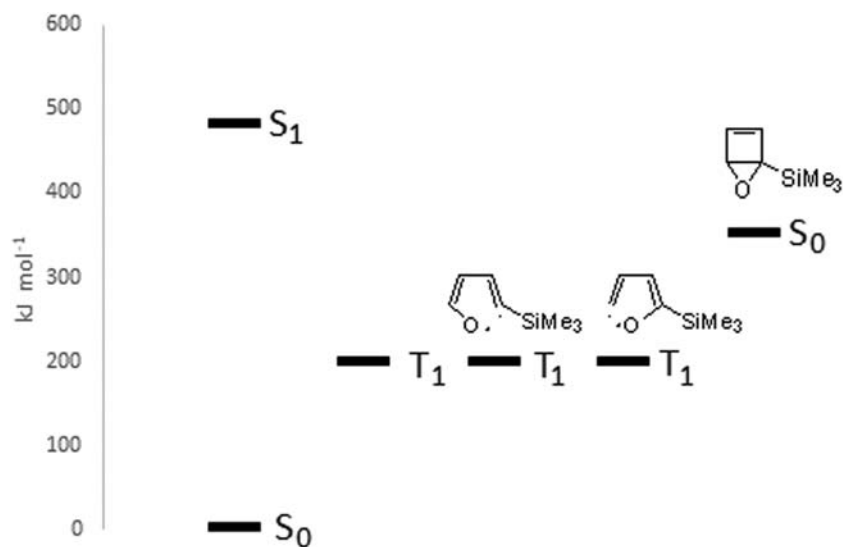
FIGURE 2.4 Relative energy of the excited states of 2-trimethylsilylfuran and of some reactive intermediates.

2.1.1.5 Furans bearing electron-donating or electron-withdrawing groups

The sensitized irradiation of 2-methoxyfuran gave a product **34** derived from the transposition reaction of the methyl group (Scheme 2.12).[49] The 5-methyl derivative **35** was obtained starting from 2-acetoxyfuran (Scheme 2.12).
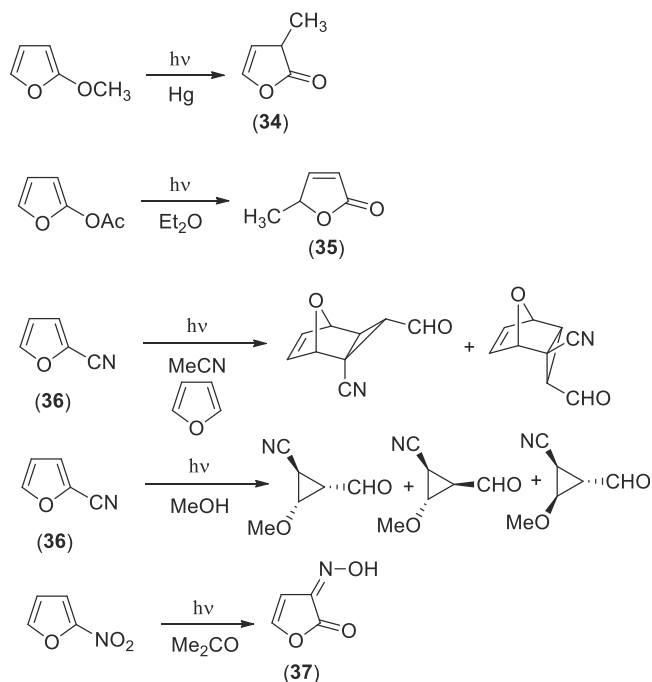
SCHEME 2.12   Photochemical behavior of substituted furans.

Hiraoka and Srinivasan showed that direct irradiation of furan-2-carbaldehyde gave carbon monoxide, methylacetylene, and allene.[17] Subsequently, it was reported that furan, cyclopropane, and acetylene can also be obtained in the direct irradiation of the same molecule at 254 nm.[50] The sensitized irradiation (Hg) of furan-2-carbaldehyde gave carbon monoxide, methylacetylene, cyclopropane, and furan in one report,[17] and carbon monoxide, methylacetylene, allene, acetylene, cyclopropane, and furan in another.[50] Gandini and coworkers found, in contrast with the previous work, that direct and sensitized reactions gave the same mixture of products where furan was present.[50] The only difference they found was that, in the sensitized reaction, a higher quantity of methylacetylene and a lower quantity of furan were obtained than in direct irradiation. The reaction starts from a vibrationally excited π,π^* triplet that decomposes to give CO and furan. More recently, in a work where matrix-isolated furan-2-carbaldehyde were irradiated at $\lambda > 200$ nm, carbon monoxide, furan, cyclopropane-3-carbaldehyde, cyclopropane, and propadiene were detected.[51]

The irradiation of 2-cyanofuran (**36**) in the presence of furan gave the Diels−Alder adducts deriving from furan and the ring-contraction product of **36** (Scheme 2.12).[52] The reaction of 2-cyanofuran in methanol allowed the authors to isolate a possible cyclopropenyl intermediate. In this case, the reaction gives a mixture of isomeric products containing methoxy substituents. These products clearly arise from a cyclopropenyl intermediate through a Michael addition of methanol (Scheme 2.12).[53,54]

The relative energies of all the possible intermediates involved in the photochemical isomerization of 2-cyanofuran are summarized in Fig. 2.5.[30] In this case, the irradiation can involve the excited singlet state, and thus the formation of Dewar isomer is possible. As in furan, the fission of an O−C$_\alpha$ bond in the triplet state of the molecule is favored if the O−C$_2$ bond is broken, By contrast, the fission of the O−C$_5$ bond leads to the formation of a high-energy species.

Finally, while the irradiation of 2-nitrofuran in 2-propanol did not give any interesting product,[55] its irradiation in acetone gave the transposition product **37** (Scheme 2.12).[56] The observed reaction can be explained on the basis of the mechanism depicted in Scheme 2.13.
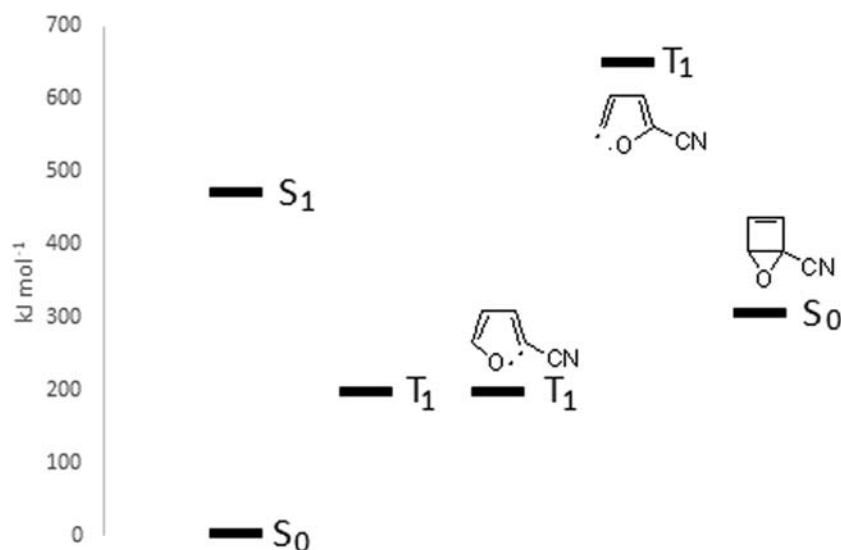
FIGURE 2.5 Relative energy of the excited states of 2-cyanofuran and of some reactive intermediates.
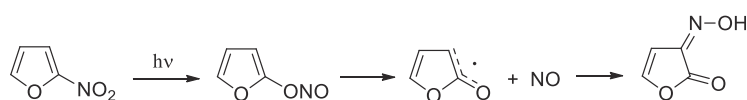
SCHEME 2.13 Photochemical behavior of 2-nitrofuran.

2.1.2 Isomerization of pyrrole

The UV spectrum of the pyrrole in vapor phase showed absorptions at 211.0, 217.0, and 237.5 nm. The absorption at 237.5 nm was identified as relating to a π,π transition, and no decomposition of the starting material was observed.[57] The electronic spectrum of pyrrole has been subjected to many theoretical and experimental studies.,[1,2,4,7,58–77] On irradiation of pyrrole vapor at 214 nm at room temperature, propyne, allene, ethylene, acetylene, and propene were observed as decomposition products in the reaction mixture together with HCN.[78] These authors identified only decomposition products; they did not find isomerization products, as in the vapor phase photochemistry of furan. There are evidences obtained by using femtosecond time resolved spectroscopy that irradiation of pyrrole induced hydrogen atom elimination from the molecule (N−H bond fission).[79] Furthermore, vapor-phase photolysis of 2,5- and 2,4-dimethylpyrroles at 214 and 229 nm showed only hydrogen, methane, and ethane, while no product derived from ring opening was observed.[80] To confirm these experimental data, Dewar pyrrole, generated by photofragmentation of a suitable substrate, was shown to be very unstable in comparison to similar compounds obtained from furans or thiophenes.[28,81] Theoretical calculations on pyrrole are in agreement with the experimental results and showed that decomposition gives acetylene more likely than photoisomerization. Furthermore, they showed that strong electron-donor or -acceptor substituents could modify this behavior.[82]

Irradiation of N-benzylpyrrole gave 2-benzylpyrrole in 28% yield while the 3-isomer was obtained in 9.8%.[83] No interconversion from 2- and 3-isomer was observed.

When (+)-N-(1-phenylethyl)pyrrole was used as a substrate, the same trend was observed. However, only 32% configuration retention was observed when the reaction was performed in methanol. All the data were in agreement with two mechanism hypotheses. The isomerization can occur *via* direct 1,2 and 1,3 migration or *via* the formation of a common intermediate (Scheme 2.14).
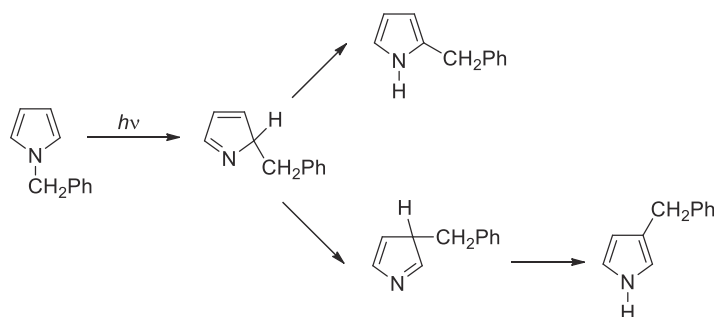
SCHEME 2.14 Isomerization of N-substituted pyrroles.

Similar behavior was observed when *N*-acetylpyrroles were used as the starting material.[84,85] The irradiation of *N*-acetylpyrrole in dioxane at 254 nm gave a mixture of 2- and 3-substituted isomers (Scheme 2.15). The same result has been observed with alkyl substituted pyrroles.
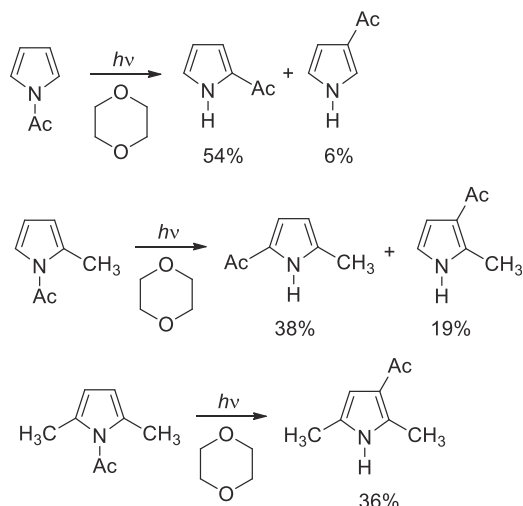
SCHEME 2.15   Isomerization of *N*-acyl substituted pyrroles.
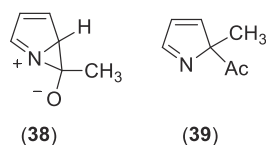
FIGURE 2.6   Possible intermdiates in the photoisomerization of *N*-acylpyrroles.

The formation of the 2-isomer was suggested to involve the formation of a cyclic intermediate **A** (Fig. 2.6).

The 3-isomer can be obtained by direct migration. However, the fact that **39** was not isolate in the photochemical isomerization of *N*-acetyl-2-methylpyrrole may suggest that the 3-isomer was obtained from **39** *via* thermal isomerization. Reactions involving 1,2-migration of type **38** were obtained using as starting materials *N*-oxides (Scheme 2.16).[86,87] The oxaziridine thus obtained can be converted into the corresponding amides through a photochemical isomerization followed by elimination of the substituent at C−2.
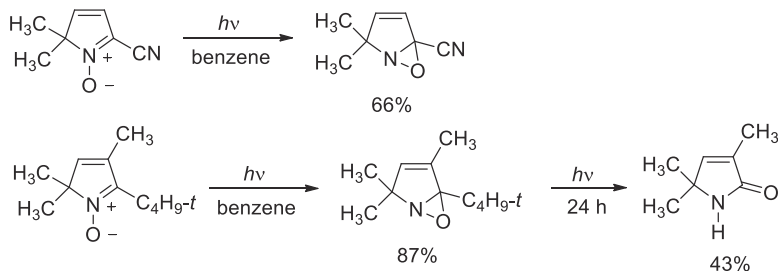
SCHEME 2.16   Isomerization of *N*-oxide pyrrole derivatives.

Flash photolysis experiments on *N*-phenylpyrrole showed that radical species are involved in the reaction.[88] The authors reported the presence of a transient species with absorption at λ 360 nm and τ 0.5 Ms. In *i*-PrOH a second transient species was observed with absorption maximum at 520 nm (τ 0.6 Ms), while after several flashes a band at 290 nm was observed. The transient at 520 nm was identified as the triplet excited state of

N-phenylpyrrole, while the absorption at 360 nm was due to the triplet-triplet transition of biphenyl. This compound could be formed by coupling of the phenyl radical. Finally, the absorption at 290 nm was ascribed to 2-phenylpyrrole formed during the flash.

The photoisomerization of *N*-allylpyrroles has been reported by Patterson (Scheme 2.17).[89] The reaction works well also by using condensed pyrroles.[90,91]
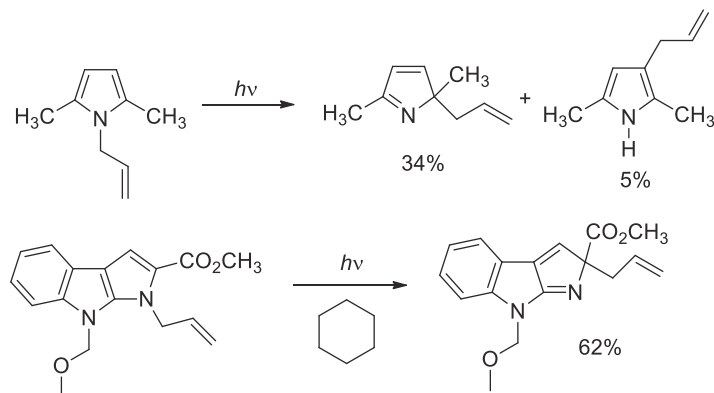
SCHEME 2.17   Isomerization of *N*-allylpyrrole derivatives.

2,4-Diphenylpyrroles derivatives gave an elimination reaction. *N-t*-Butyl and *N*-benzyl derivatives gave the elimination products in very high yields (Scheme 2.18).[92,93]
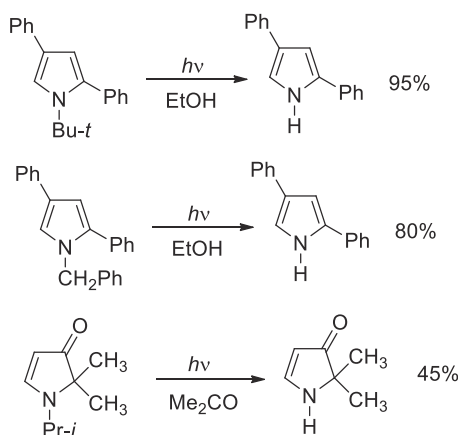
SCHEME 2.18   Photochemical isomerization of *N*-benzyl, *N-t*-butul and *N-i*-proryl pyrrole derivatives.

In 1970 Hiraoka reported that 2-cyanopyrrole, irradiated in methanol with a low-pressure mercury arc for 20 h, gave a mixture of 3-cyanopyrrole and pyrrole-2-carbaldehyde.[94] 1-Methyl-2-cyanopyrrole (**40**) also gave this reaction (Scheme 2.19).[53] In this case, the author isolated the product of the isomerization **41**, the product of the
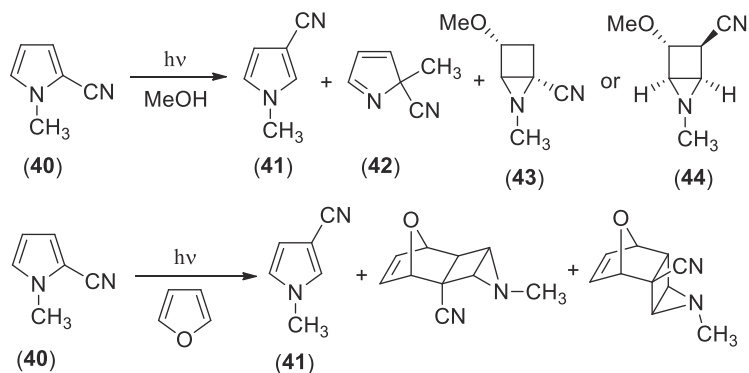
SCHEME   2.19   Isomerization   of   2-cyanopyrrole derivatives.

shift in C−2 of the *N*-methyl group **42**, and a third product that was assumed to be derived from the addition of methanol to the Dewar pyrrole **43**. The reaction depends on the temperature used; in fact, no reaction occurred when the reaction was performed at −68°C. This result was in agreement with the presence of a thermal-activated step.[95] More recently, the nature of this third product was re-evaluated and the structure **44** of Scheme 2.14 was proposed.[95] This structure was also confirmed by performing the reaction in the presence of furan. In this case, 4 + 2 photoadducts were isolated (Scheme 2.19).

All these data seem to be in agreement with a mechanism depicted in Scheme 2.20, where the thermal-activated step is the 1,2-sigmatropic shift between the Dewar pyrroles.
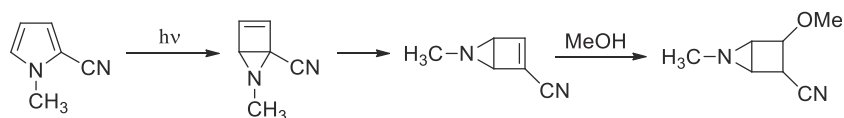
SCHEME 2.20 Proposed mechanism for 2-cyanopyrrole derivatives isomerization.

Similar results were obtained using methyl-substituted 2-cyanopyrroles (Scheme 2.21).[96] All the results can be explained assuming the mechanism depicted in Scheme 2.20. Only the by-product obtained in the irradiation of 5-methyl-2-cyanopyrrole cannot be explained. To explain this product, a subsequent 1,2-sigmatropic shift was postulated (Scheme 2.22).
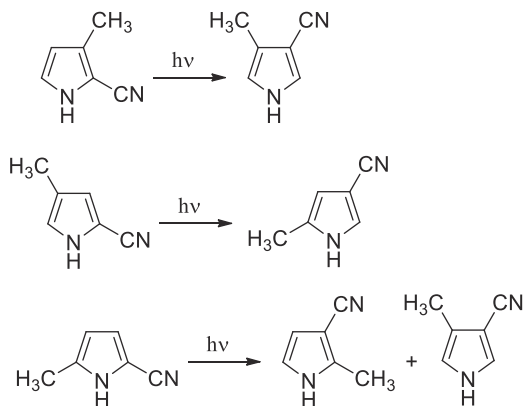
SCHEME 2.21 Isomerization of methyl susbstituted 2-cyanopyrroles.
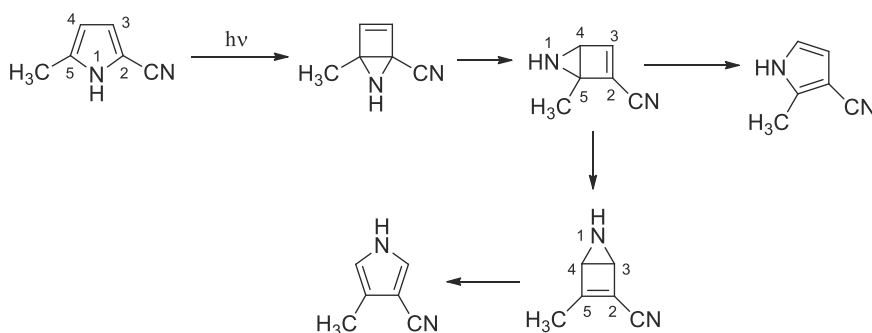
SCHEME 2.22 Isomerization of 2-cyano-5-methylpyrrole: Proposed mechanism.

The 1,3-sigmatropic shift in 2-cyanopyrrole was studied by using the SINDO1 semiempirical method.[97] This study showed that the reaction occurred via a π,π* transition and that some biradical intermediates are probably involved in the reaction (Scheme 2.23).

When pyrrole is irradiated, only decomposition products were obtained. Theoretical data fit this statement (Fig. 2.7). In fact, the direct irradiation populates the excited singlet state, which can be converted into the Dewar pyrrole or into the corresponding triplet state. Clearly, the intersystem crossing to the triplet state allows the system to reach the lowest energy state. The excited triplet state can give the biradical intermediate, and this
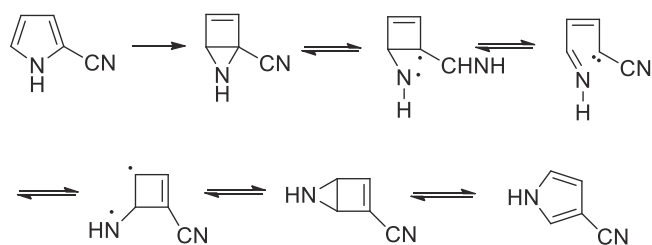
SCHEME 2.23 Proposed mechanism for 2-cyanopyrrole photo-chemical isomerization.
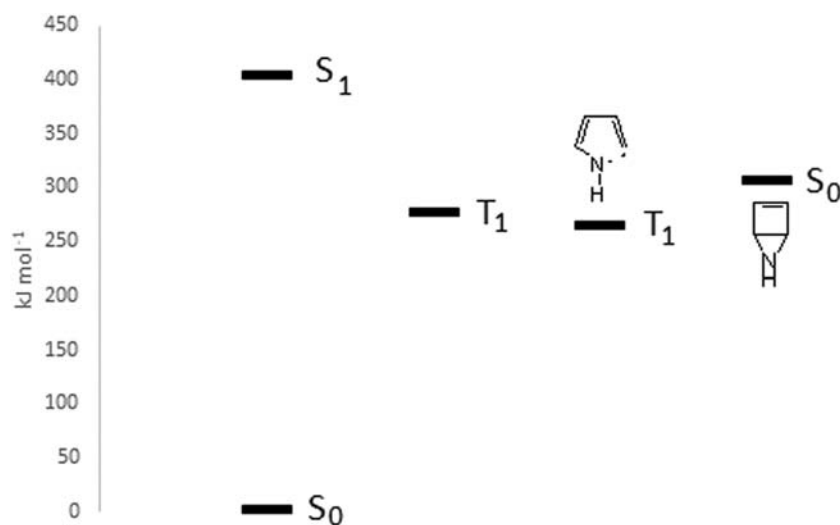
FIGURE 2.7 Relative energy of the excited states of pyrrole and of some reactive intermediates.
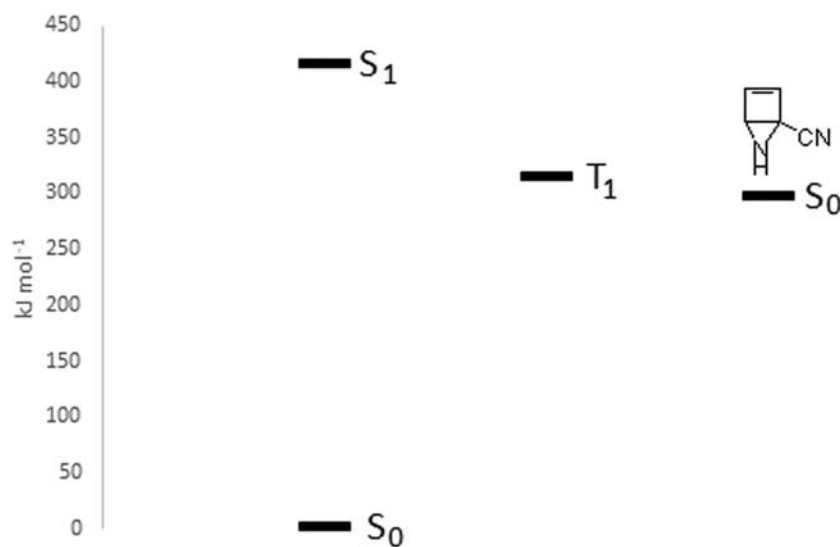
FIGURE 2.8 Relative energy of the excited states of 2-cyanopyrrole and of some reactive intermediates.

intermediate can give either the decomposition only or the cyclopropenyl derivatives that thermally evolves to give the decomposition products as reported above.[98]

In contrast, when the irradiation is performed on 2-cyanopyrrole, the isomeric products are observed. In fact, in this case, the corresponding Dewar pyrrole shows a lower energy than in the previous case, allowing the formation of the isomeric products (Fig. 2.8).[98] When 2-methylpyrrole is used as substrate, the formation of the triplet state is favored, but this triplet state cannot evolve through the formation of the biradical intermediate.[98]

The formation of Dewar pyrrole in the photoisomerization of 2-cyanopyrroles has been confirmed by a CASSCF and MP2-CAS study.[99]

2-Bromopyrrole derivatives gave an isomerization reaction. The irradiation in acetonitrile of 2-bromo-*N*-benzylpyrrole gave the 3-bromo substituted isomer in 59% yield (Scheme 2.24).[100] The reactivity is enhanced when the reaction is performed in the presence of trifluoroacetic acid.

SCHEME 2.24   Photochemical isomerization 2-bromopyrrole derivatives.
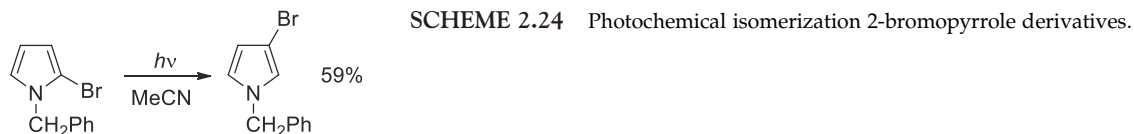
Finally, the irradiation of 2-trimethylsilyl-*N*-methylpyrrole gave the corresponding 3-trimethylsilyl derivative in 84% yield.[101]

The use of pyrrole derivatives bearing an alkene on the *N*-substituent can allow to obtain the [2 + 2] cycloadduct **45** that can give a retro [2 + 2] cycloaddition to give **46** (Scheme 2.25).[102] When the reaction is performed on **47** a different
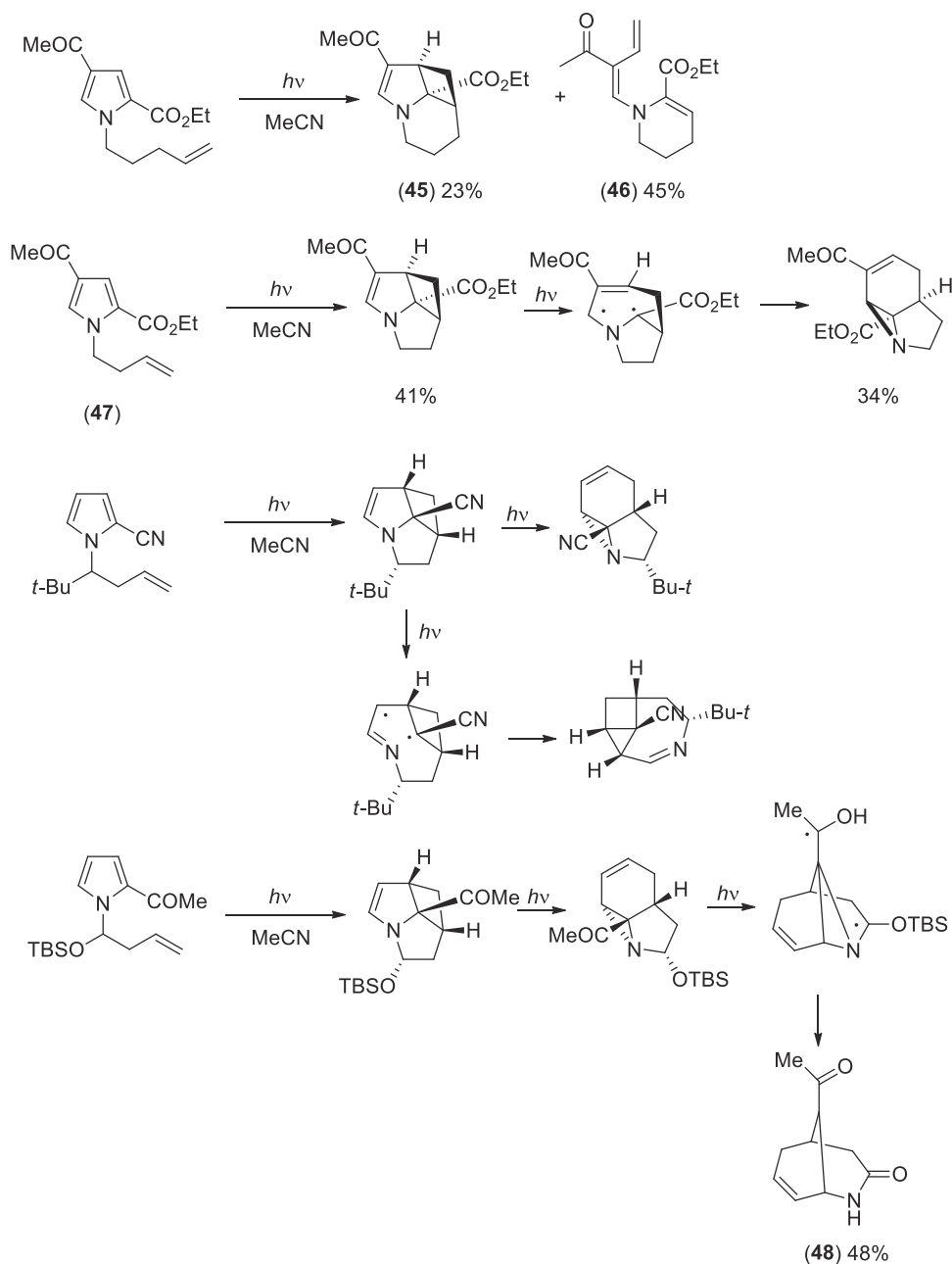
SCHEME 2.25   Other photochemical reactions of pyrroles.

reaction product was obtained (Scheme 2.25).[103] The reaction can be performed also by using a flow reactor giving ca. 22 g/day of the product. In the presence of bulky substituents, a conformational driven isomerization occurs (Scheme 2.25).[104] Furthermore, prolonged irradiation gave a further photochemical reaction to give **48** (Scheme 2.25).[104]

2.1.3 Isomerization of thiophene

The $2\ {}^1A_1$ character of the singlet excited state of thiophene has been investigated both computationally and by using femtosecond pump probe photoelectron spectroscopy. These studies show that ring opening could be a deactivation way for the excited singlet state of thiophene.[105,106] The irradiation of the thiophene in gas phase yields ethylene, allene, methylacetylene, carbon disulfide, and vinylacetylene. No Dewar thiophene or cyclopropane derivatives were isolated.[107] The irradiation in liquid phase gave the Dewar thiophene which can be trapped as a Diels−alder adduct with furan.[108] The Dewar thiophene and cyclopropane-3-thiocarbaldehyde can be obtained by irradiation in argon matrices at 10 K.[19]

Wynberg has discovered the most interesting reaction in the photochemical reactivity of thienyl derivatives. The irradiation of 2-substituted thiophenes gave the corresponding 3-substituted derivatives (Scheme 2.26).[109]
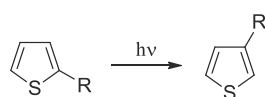
SCHEME 2.26 Photochemical isomerization of thiophene derivatives.

Several studies have been performed on the mechanism of this photoisomerization showing that the reaction takes place from the singlet excited state of the molecule,[110] that the interchange between C_2 and C_3 occurs without the concomitant interchange between C_4 and C_5, and that the bonds between ring carbons and the substituents are not broken.[111] For mechanisms have been proposed (Scheme 2.27). Wynberg preferred (iii)[112,113] more recently, however, several studies showed that mechanism (ii) is the most probalble.[114,115]
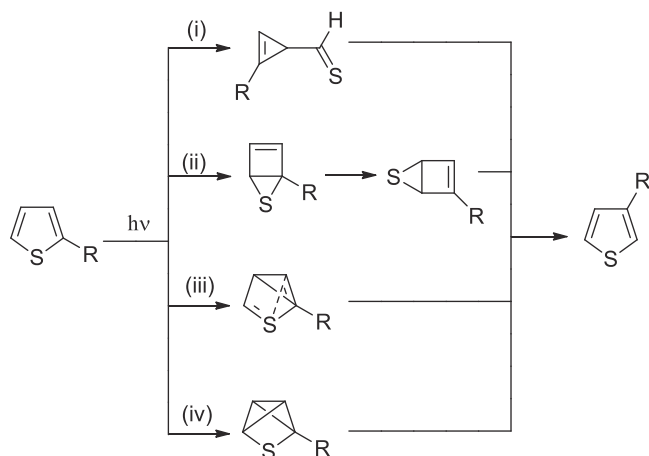
SCHEME 2.27 Proposed mechanims for the photochemical isomerization of thiophene derivatives.

Calculation results fit the experimental data (Fig. 2.9).[116] In fact, the singlet excited state can evolve, giving the Dewar thiophene (and then the isomeric thiophenes) or the corresponding excited triplet state. This triplet state cannot be converted into the biradical intermediate because this intermediate shows a higher energy than the triplet state, thus preventing the formation of the cyclopropenyl derivatives. Theoretical calculations described the dynamics of the rearrangement of Dewar thiphene.[117]

2.1.3.1 Alkylthiophenes

Alkylthiophenes reacted to give the corresponding transposition products, but they showed low reactivity.[118] Better results were obtained using perfluoroalkyl derivatives. The tetrakis(trifluoromethyl) Dewar thiophene, isolated in 1970 by vapor-phase irradiation of thiophene,[119] was the first Dewar isomer isolated in this series. The presence of trifluoromethyl groups induces fast formation and slow decomposition of strained systems. The slow decomposition may be partly due to the "siphoning" of vibrational energy into perfluoroalkyl
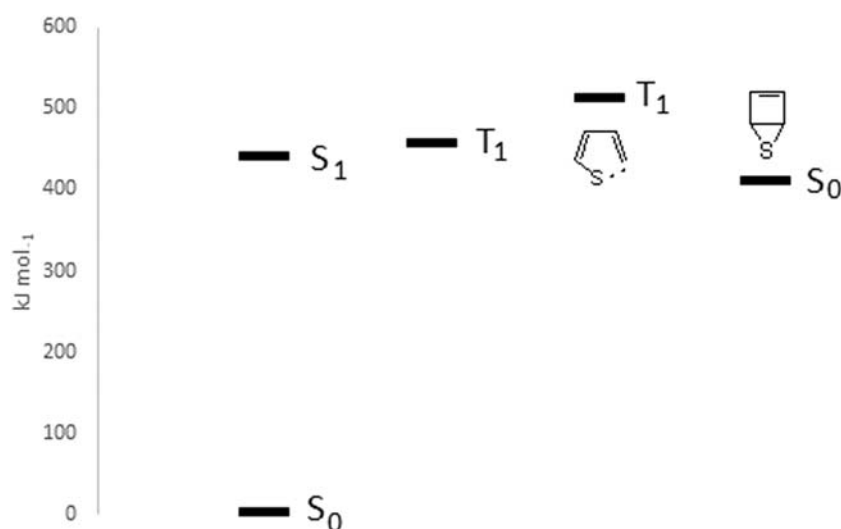
FIGURE 2.9　Relative energy of the excited states of thiophene and of some involved intermediates.

groups.[120] The Dewar structure was accepted with some equivocation[78] until confirmed by a ^{19}F NMR study[121] and an X-ray structure of the tetramethylfuran adduct.[122−124] The irradiation of 2,3-di(trifluoromethyl)thiophene (49) gave a mixture of products where the authors found both isomeric thiophenes and an 8:1 mixture of Dewar isomers 50 and 51 (Scheme 2.28).[125,126] The irradiation of the 2,5-di(trifluoromethyl)thiophene gave the corresponding 2,4 isomer, while 3,4-di(trifluoromethyl)thiophene gave the 2,4 isomer only in traces. 2,3,4-Tri (trifluoromethyl)thiophene gave the 2,3,5 isomer and a mixture of the corresponding Dewar isomers.[125]
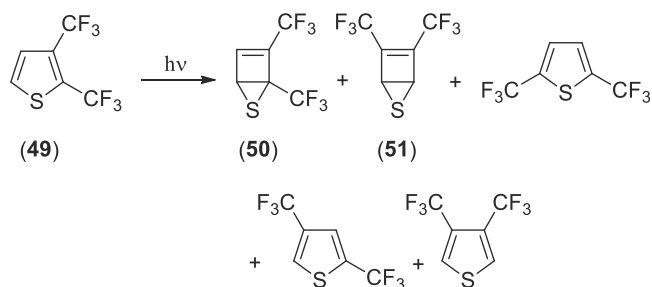
SCHEME 2.28　Photochemical isomerization of trifluoromethylthiophene derivatives.

As reported for the furan derivatives, thiophenes, when irradiated in the presence of an amine, gave the corresponding pyrroles.[41,42,127,128] The authors proposed the formation of a cyclopropenyl intermediate. Subsequently, however, a Dewar thiophene derivative, treated with aniline, gave the corresponding pyrrole, showing that it is probably the true intermediate in this reaction.[45]

Computational work confirmed the presence of Dewar thiophene derivative during the isomerization.[129]

2.1.3.2　Arylthiophenes

Arylthiophenes were used as substrates in the photoisomerization described in Scheme 2.26.[109,130−134] The dithienyls gave this reaction efficiently, while 2-(2-pyridyl)thiophene and 2-(2-furyl)thiophene did not give this reaction in a reasonable yield.[135,136] Carbonyl and olefinic substituents inhibit the rearrangement.[112,137−146]

The results of theoretical calculations on 2-phenylthiophene fit the experimental results (Fig. 2.10).[116,129,147] In fact, in this case, the formation of the triplet state of 2-phenylthiophene cannot allow the formation of the biradical intermediate allowing the formation of the Dewar thiophene.

2.1.3.3　Cyanothiophenes

The irradiation of 2- and 3-cyanothiophene gave interesting results in agreement with the scheme described earlier (Scheme 2.26). The photoisomerization reaction involved only the π,π^* excited singlet state and Dewar thiophenes were isolated when the reactions were carried out at −68°C and shown to be intermediates in the isomerization reaction (Scheme 2.29).[147,148]
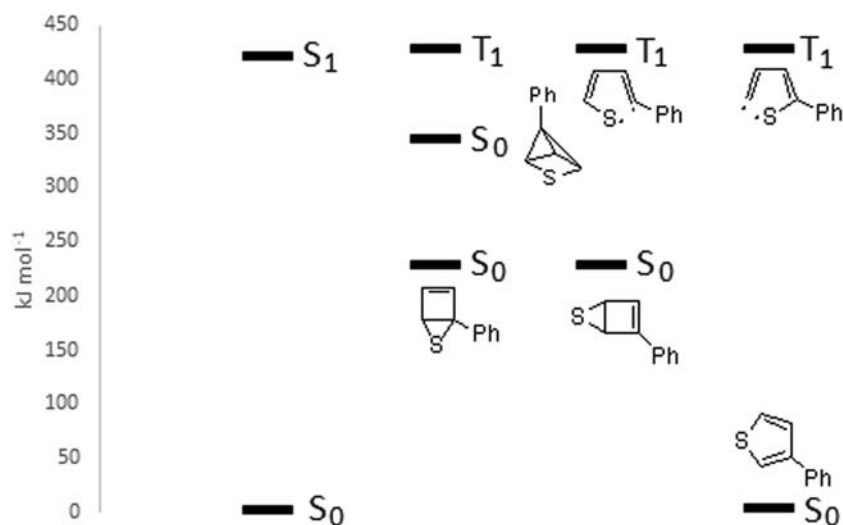
FIGURE 2.10 Relative energy of the excited states of 2-phenylthiophene and of some reactive intermediates.
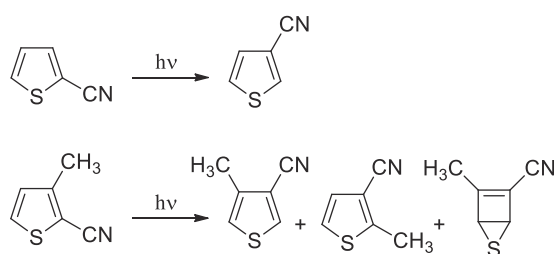
SCHEME 2.29 Photochemical isomerization of 2-cyanothiophene derivatives.
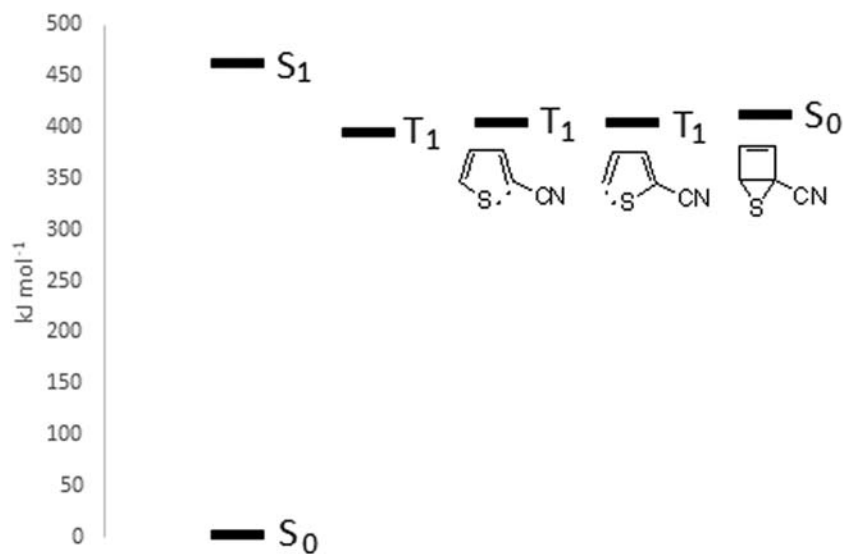
FIGURE 2.11 Relative energy of the excited states of 2-cyanothiophene and of some reactive intermediates.

When 2-cyanothiophene is used in calculations, the results fit the experimental results (Fig. 2.11). In fact, the formation of the triplet state of 2-cyanothiophene cannot allow the formation of the biradical intermediate allowing the formation of the Dewar thiophene.[116,128]

2.1.3.4 Other thiophenes

The irradiation of thiophene oxide derivatives can afford the deoxygenated product. This reaction is a well known one mainly on dibenzothiophene oxide.[149−152] However, in same cases, the reaction can allow the formation of the furan derivative (Scheme 2.30).[153,154]

SCHEME 2.30   Photochemical isomerization of a thiophene oxide derivative.
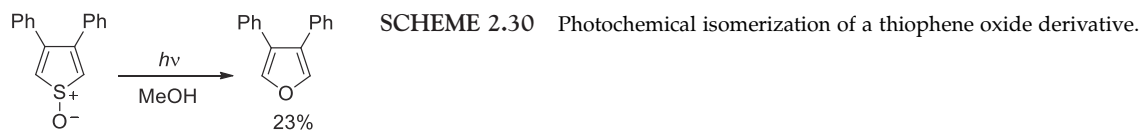
The isomerization has been described assuming the formation of an oxathiin intermediate (Scheme 2.31).

SCHEME 2.31   Proposed mechanism for thiophene oxide isomerization.
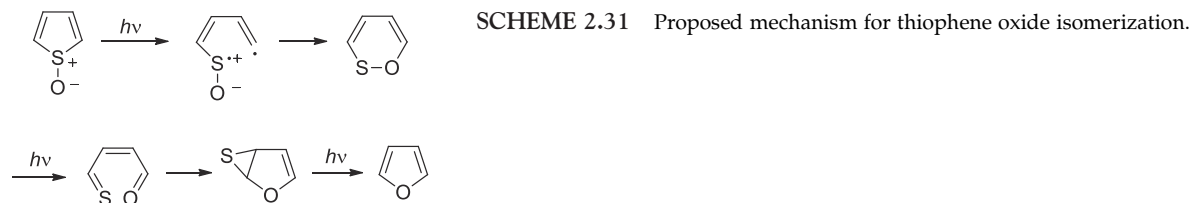
2.1.4 Isomerization of isoxazole

The photoisomerization of isoxazole to oxazole has been object of other reviews.[155] The photophysical properties of 4-chloro-5-phenylisoxazole has been studied showing that the first excited singlet state has a π,π^* character at 3.82 eV, while the first triplet state (π,π^*) is at 2.57 eV.[156] The photorearrangements of isoxazoles are well known reactions. Thus 3,5-diphenylisoxazole, when irradiated at 254 nm, gave 2,5-diphenyloxazole via the corresponding azirine **46** (Scheme 2.32).

SCHEME 2.32   Photochemical isomerization of isoxazoles.

(52)
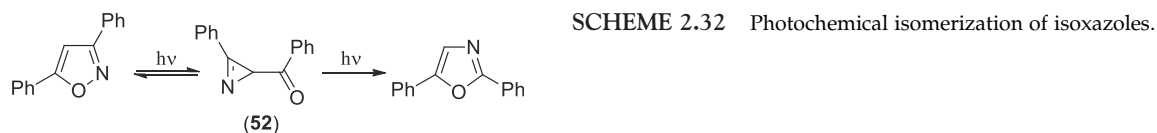
The azirine can be isolated; on irradiation at 254 nm, it gave the oxazole while irradiation at 334 nm gave the isoxazole.[157−162] It is noteworthy that in this case the formation of Dewar isoxazole cannot explain the obtained products.

The irradiation of 3,5-diphenylisoxazole in the presence of propylamine gave a mixture of 2,5-diphenyloxazole (20%) and N-propyl-2,5-diphenylimidazole (1%). The same distribution of the products was obtained starting from the azirine **52**.[42]

In the photochemical isomerization of isoxazoles, we have evidence for the presence of the azirine as the intermediate of this reaction. The azirine is stable and it is the actual first photoproduct of the reaction, as in the reaction of t-butylfuran derivatives. The fact that it is able to interconvert both photochemically and thermally into the oxazole could be an accident. In the case of 3,5-diphenyloxazole the cleavage of the O−N bond should be nearly concerted with N−C$_4$ bond formation;[162] nevertheless, the formation of the biradical intermediate cannot be excluded.

Irradiation at 221 nm of isoxazole in argon matrix at low temperature allowed the identification of several compounds (Scheme 2.33).[163]

SCHEME 2.33   Photochemical behavior of isoxazole in gas phase.
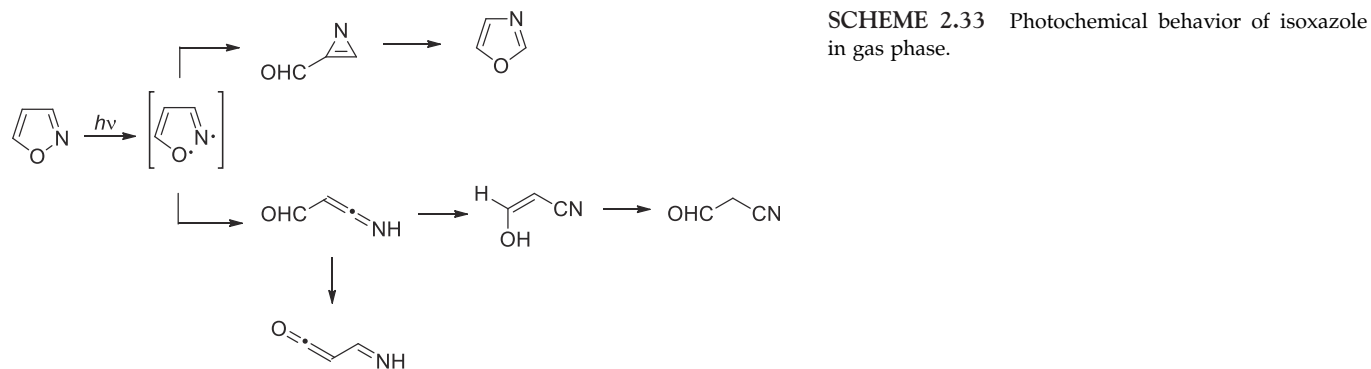
The photolysis of 3,5-dimethylisoxazole in acetonitrile gave as main product the corresponding azirine.[164,165] The same reaction, performed irradiating at 222 nm at low temperature (15 K) in argon matrix allowed the identification of several products (Scheme 2.34).[166]
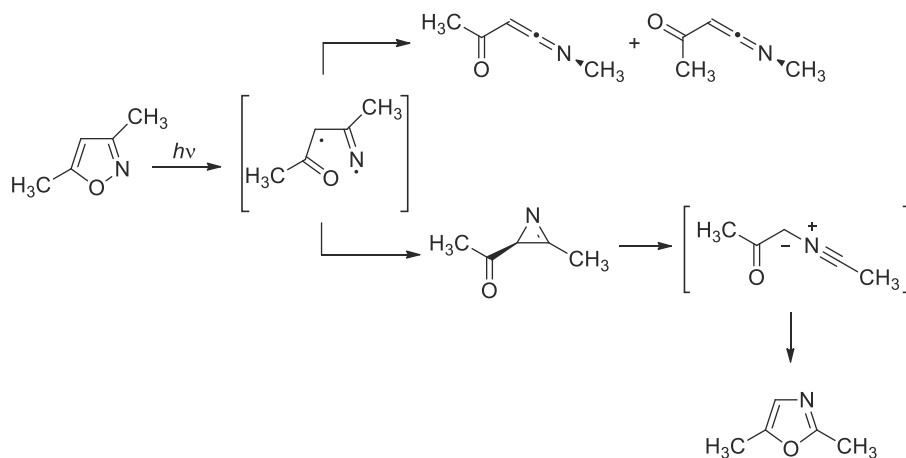
SCHEME 2.34 Photochemical behavior of 3,5-dimethylisoxazole.

The results of some calculations are in agreement with the formation of the azirine.[29] The excited singlet state can convert into a Dewar isomer or into the triplet state. The conversion into the triplet state is favored, allowing the formation of the biradical intermediate. The same results[29] were obtained using as substrate 3-phenyl-5-methylisoxazole[167] and 3,5-dimethylisoxazole.[168]

In the hypothesis described earlier, the reaction should occur through the triplet state of the molecules involved, as reported in the furan. In contrast, some experimental data[160] and theoretical calculations[162,169,170] are in agreement with a singlet state mechanism. The use of sensitizers does not solve the question, because they were used to invoke both singlet[160] and triplet sensitization.[159] However, the fact that 3,5-diphenyl-4-benzoylisoxazole, a compound with a high intersystem crossing quantum yield, does not react could support a singlet state process. However, calculations on this molecule showed that the triplet state can be formed, but it cannot evolve to the high-energy triplet biradical intermediate.[29] Furthermore, in the photochemical isomerization of 4-acyloxazoles, flash photolysis experiments showed the presence of a transient absorption due to the triplet state.[171]

2.1.4.1 Isoxazoles bearing electron-donating groups

The photolysis of 5-phenylisoxazole in methanol gave 5-phenyloxazole and benzoylacetonitrile. 4-Phenylisoxazole gave only 4-phenyloxazole (Scheme 2.35).[172] This behavior is compatible only with a mechanism involving the formation of the corresponding azirine.
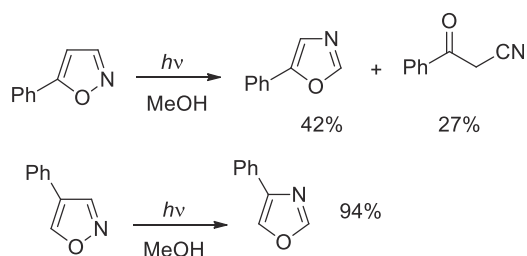
SCHEME 2.35 Photochemical isomerization of phenyl substituted isoxazole derivatives.

Spectroscopic study of the photochemical isomerization of methyl 4-bromo and 4-chloro-5-phenylisoxazole-5-carboxylate showed the presence of an azirine intermediate.[173] 3,5-Diphenylisoxazole gave under irradiation the corresponding azirine that can react with acetylacetone in the presence of Co(acac)$_2$ to give the

corresponding pyrrole (Scheme 2.36).[174] Furthermore, when a cyclohexenyl derivative is synthetized, it can give a further photochemical cyclization (Scheme 2.36).[175] Finally, the azirine obtained from 3,5-diphenyli-soxazole can react with the imine obtained from 2-cyclohexyl-2-aminoacetonitrile and *p*-nitrobenzaldehyde in the presence of a base, to give the corresponding imidazole (Scheme 2.36).[176] Pyrrole derivatives can be obtained also through the reaction of the azirine with another azirine molecule in the presence of Cu(II)-2-ethylhexanoate.[177]
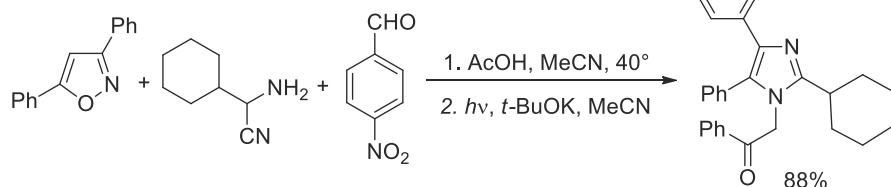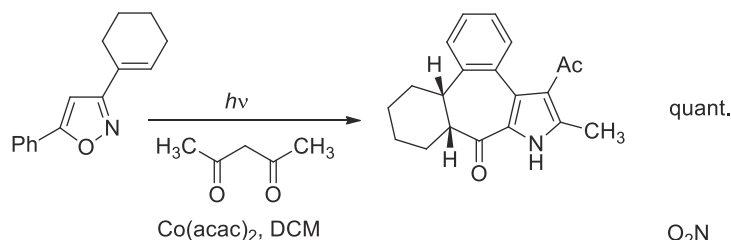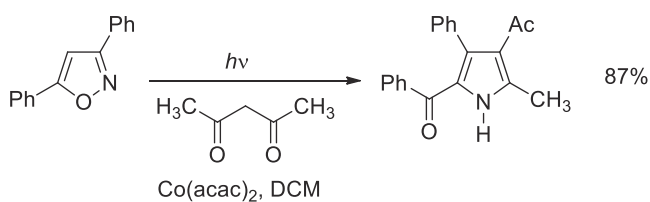
SCHEME 2.36   Reaction of 3,5-substituted isoxazoles with 1,3-dicarbonyl compounds.

It is noteworthy that, when there is a hydroxy group on the aromatic ring on C5 in the isoxazole ring the azirine intermediate can give a further cyclization reaction (Scheme 2.37).[178]
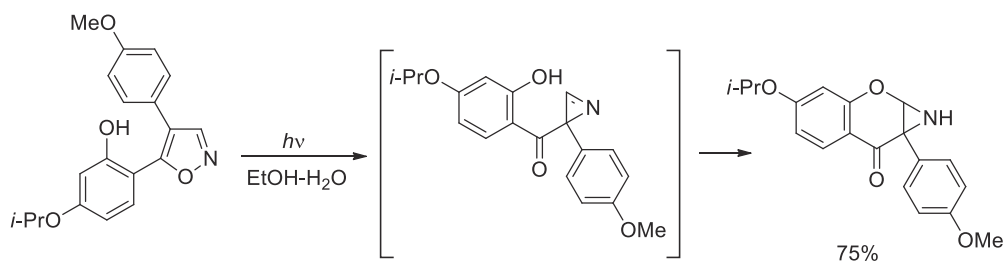
SCHEME 2.37   Participation of the hydroxy group in the photochemical isomerization of isoxazoles.

Some data were obtained from the photochemical isomerization of aminoisoxazoles. 5-Aminoisoxazoles gave the corresponding azirine (Scheme 2.38);[179] when a 4-carbethoxy-substituted derivative was used, no azirine was isolated and the oxazole was the only product obtained (Scheme 2.38).[180] The azirine intermediate was not observed upon irradiating 3-amino derivatives.[181]

Calculations are in agreement with the formation of the excited triplet state, and this intermediate can evolve to the formation of the azirine via the biradical intermediate.[29]

The photoisomerization of 3-hydroxyisoxazoles gave the corresponding 2-oxazolones without the isolation of the azirine (Scheme 2.38).[182] Also in this case calculations are in agreement with the experimental results.[29]
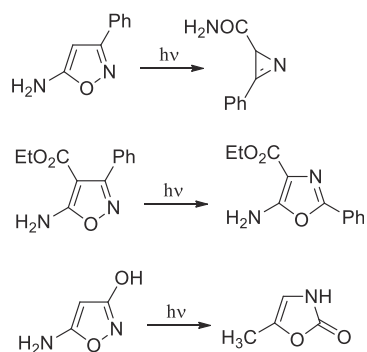
SCHEME 2.38 Photochemical behavior of amino substituted isoxazoles.

2.1.4.2 Isoxazoles bearing electron-withdrawing groups

The irradiation of 3-Carbomethoxyisoxazole (**53**) gave the corresponding oxazole (**54**) in very low yields (5%−8%) without the isolation of the corresponding azirine (Scheme 2.39).[183] Also in this case calculations show that the energy of the triplet state allows the formation of the biradical intermediate and then of the azirine. However, the low yields of the conversion can be explained considering that the transformation of the biradical intermediates into the azirine is an endothermic reaction (Fig. 2.12).[29]
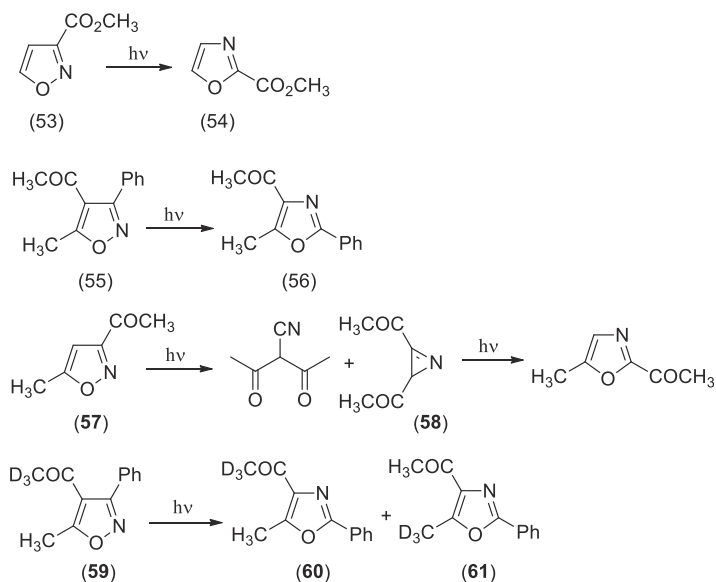
SCHEME 2.39 Photochemical behavior of carbonyl and carboxyl substituted isoxazoles.
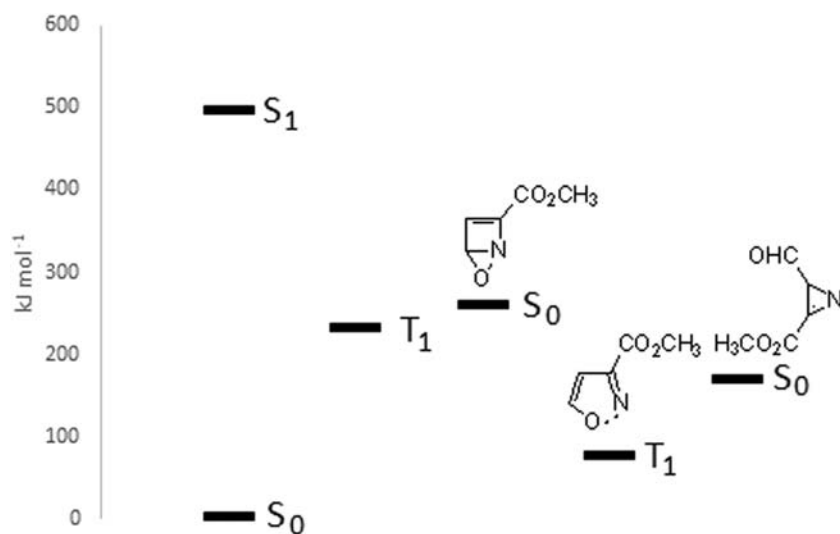
FIGURE 2.12 Relative energy of the excited states of 3-carbomethoxyisoxazole and of some reactive intermediates.

Photochemistry of Heterocycles

The irradiation of 3-phenyl-4-acetyl-5-methylisoxazole (**55**) gave the isomeric oxazole (**56**) (Scheme 2.39).[184,185] The reaction can involve the formation of the biradical intermediate starting from the triplet state, in agreement with the presence of the azirine derivative in the reaction mixture.[29] Using a very similar substrate, 3-acetyl-5-methylisoxazole (**57**), the formation of the azirine **58** was detected (Scheme 2.39).[171,186] When a deuterated substrate **59** was used a 1:1 mixture of oxazoles **60** and **61** were obtained (Scheme 2.39).[185]

This result was explained assuming the formation of the intermediate **62** after the cleavage of the azirine (Scheme 2.40).
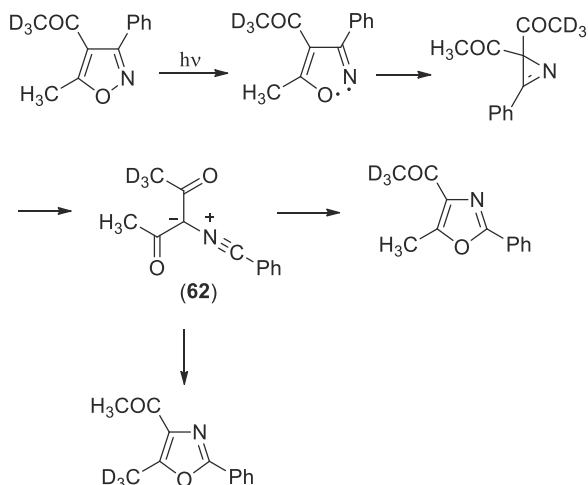
SCHEME 2.40   Proposed mechanism for the photochemical behavior of 4-carbonyl substituted isoxazole derivatives.

The same scheme can be rationalized the results of matrix-isolated low temperature photochemical isomerization of methyl 4-chloro-5-phenylisoxazole-3-carboxylate.[187]

The reaction of ethyl 5-(*p*-hydroxyphenyl)-isoxazole-3-carboxylate to give the corresponding oxazole (**63**) can be performed in a flow reactor (Scheme 2.41).[188]
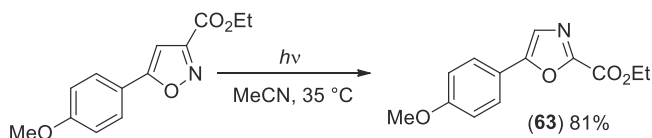
SCHEME 2.41   Photochemical isomerization of ethyl 5-(p-hydroxyphenyl)-isoxazole-3-carboxylate.

2.1.4.3 Benzisoxazoles

Benzisoxazole reacts with light giving an isomerization reaction. For example, benzisoxazole reacts when irradiating in acetic acid to give a mixture of benzoxazole and 2-cyanophenol (Scheme 2.42).[189,190] 3-methylbenzisoxazole react in methanol to give 2-methylbenzoxazole in high yields (Scheme 2.42),[190,191] while, when the reaction was performed in wet hexane to give the amide (**64**) (Scheme 2.42).[192]
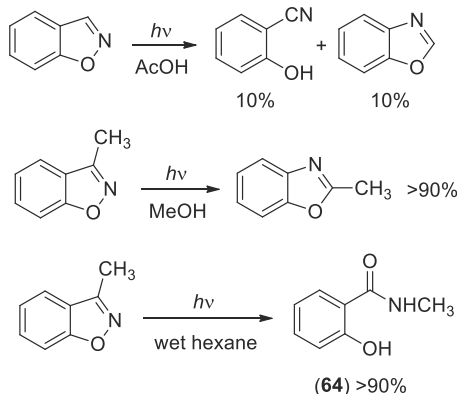
SCHEME 2.42   Photochemical isomerization of benzisoxazoles.

The mechanism of this reaction has been studied. Sensitization of the reaction allowed to consider that the reaction occurs through the first excited singlet state.[189] The mechanism of this reaction has been explained assuming the formation of an azirine intermediate (Scheme 2.43).[190,192,193] Only recently, a completely different approach, were very unusual Dewar isomers of benzisoxazole have been proposed, was presented.[194] Furthermore, the presence of the azirine derivative has been detected in a low temperature matrix isolation study.[195]
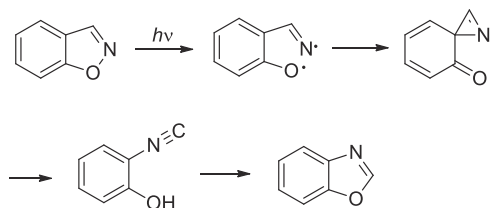
SCHEME 2.43   Proposed mechanism for benzisoxazole isomerization.

The azirine has been determined also in a similar study on 3-aminobenzisoxazole, while a ketenimine derivative has been detected in the reaction of 3-chlorobenzisoxazole (Scheme 2.44).[196]
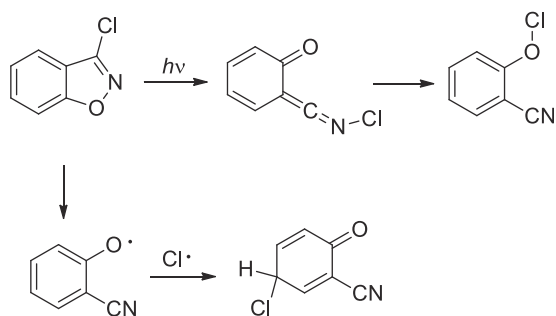
SCHEME 2.44   Photochemical isomerization of 3-chlorobenzisoxazole.

2.1.4.4 Isoxazolidones

The photochemical reaction of isoxalidone derivatives in acetonitrile can give some rearrangement products (Scheme 2.45).[197,198]
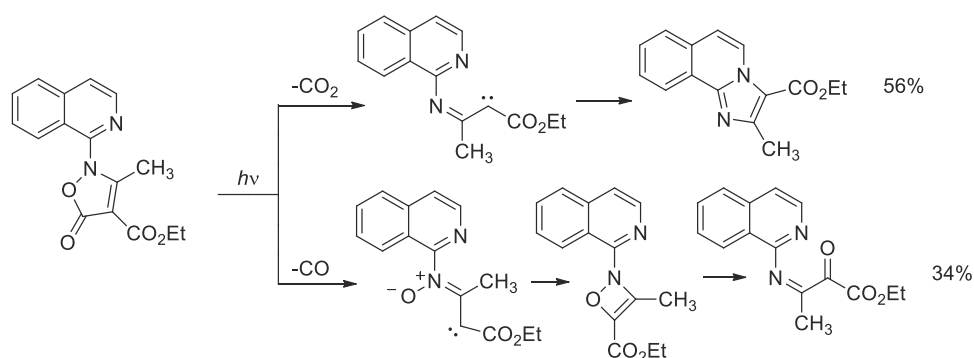
SCHEME 2.45   Photochemical behavior of isoxalidone derivatives in acetonitrile.

The formation of the carbenoid intermediate can be used also for the synthesis of oxazoles, thiazoles, and pyrroles (Scheme 2.46).[199−203]
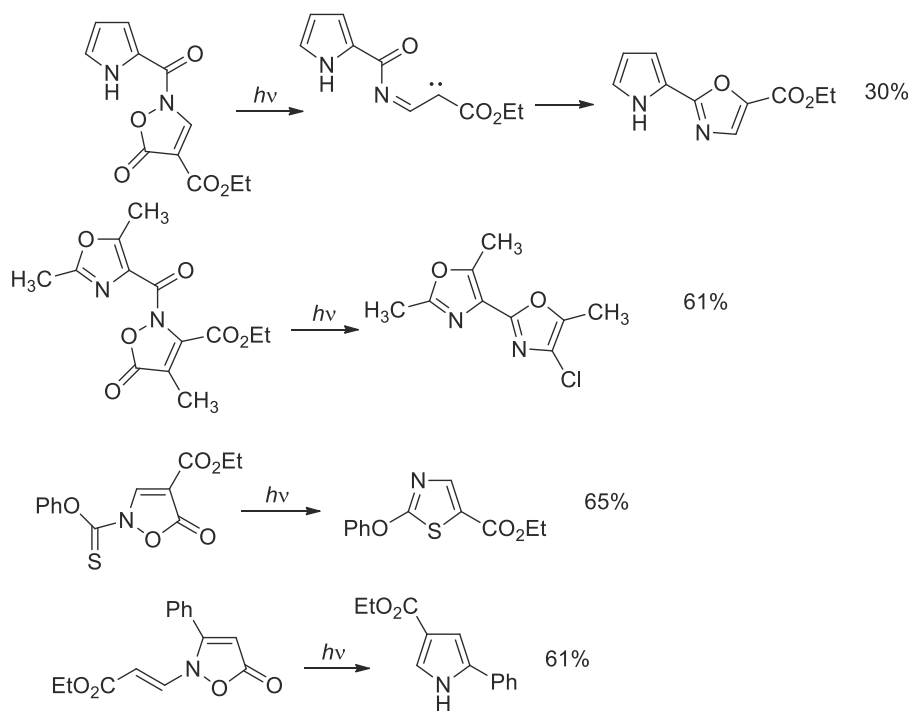
The photochemical synthesis of oxazoles can be obtained in 91% yield by irradiation of an isoxalidone with a blue LED in the presence *fac*-Ir(ppy)$_3$ as photocatalyst.[204]

2.1.5 Isomerization of oxazole

The photoisomerization of 2,5-diphenyloxazole (**65**) was first reported in 1969. 2,5-Diphenyloxazole, irradiated in ethanol at 80°C, gave three products, where the more important was 4,5-diphenyloxazole (**66**) (Scheme 2.47).[205,206] 4,5-Diphenyloxazole undergoes condensation to product **67**; in the presence of air, **67** was the only product obtained in good yields. In benzene, the overall yields are lower; however, the most noticeable change is the nature of the products. In fact, the main product was 3,5-diphenyloxazole in the presence of small amounts of 2,4-diphenyloxazole (**68**) (Scheme 2.47). The irradiation of **65** in the presence of propylamine gave **66** as the main product.[42]
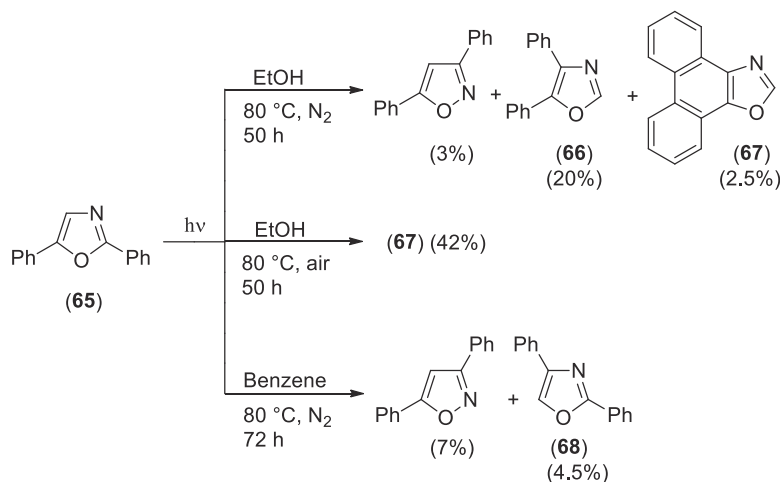
SCHEME 2.47 Photochemical isomerization of 2,5-diphenyloxazole.

All the products are compatible with both ring contraction-ring expansion mechanism and with a mechanism involving the formation of a Dewar intermediate.

2-Phenyloxazole, irradiated in benzene at 80°C, gave two products: **69**, derived from a ring contraction, and 4-phenyloxazole (**70**), obtained in very low yields (Scheme 2.48).[206,207] The authors thought that 4-phenyloxazole was ascribable to a Dewar intermediate.
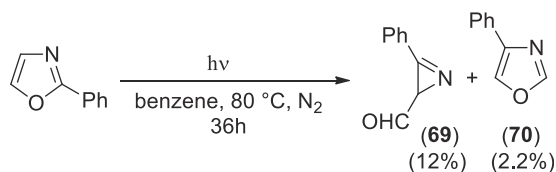
SCHEME 2.48   Photochemical isomerization of 2-phenyloxazole.
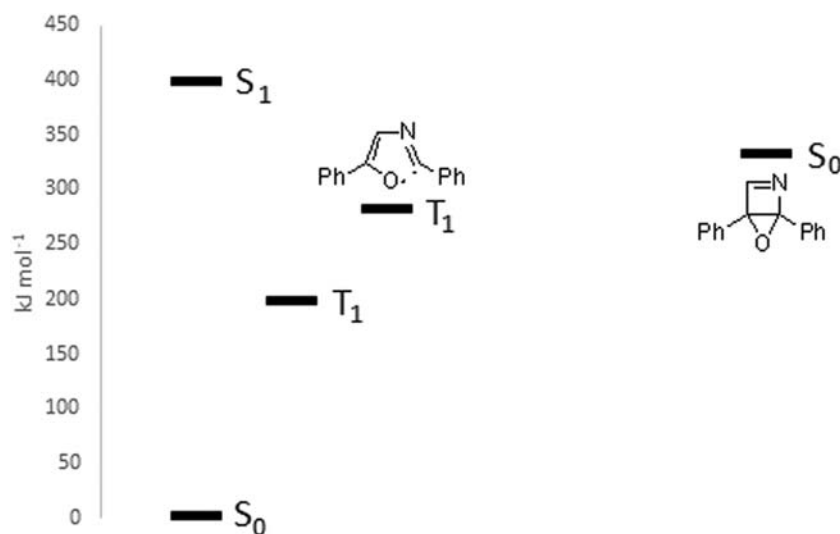
FIGURE 2.13   Relative energy of the excites states of 2,5-diphenyloxazole and of some reactive intermediates.

4,5-Diphenyloxazole gave only the product of the condensation between the aromatic rings without transposition, while 2,4-diphenyloxazole did not react appreciably.[206] However, some important information about the mechanism was obtained when 2-phenyloxazole and 2-phenyl-5-methyloxazole were irradiated with a monochromatic light at 294 nm at 24°C. In both cases, the only product observed was the corresponding azirine which did not convert into the corresponding isoxazole.

Concerning the mechanism of this reaction, calculations suggest that, in the presence of aromatic substituents on the oxazole ring, the mechanism involving the formation of a Dewar oxazole might be favored.[208] Probably, the observed formation of the azirine derives from a thermal isomerization of the first photoproduct, in line with that described in the case of furan and thiophene derivatives (Fig. 2.13). Another study on this type of reaction allowed the formation of both Dewar structure and the azirine as possible intermediates in the reaction occurring in the first excited singlet state.[209]

Finally, when the substrate is N'-benzyl-2-ethyl-benzimidazole-N-oxide the reaction product was N'-benzyl-N-ethyl-2-benzimidazolone (71%).[210]

2.1.6 Isomerization of pyrazole

Some review article have been published on the photoisomerization of these compounds.[211,212] The irradiation of 1-methylpyrazole (**71**) gave 1-methylimidazole (**72**) (Scheme 2.49).[182] Subsequently, a ring-opening product (**73**) was observed in the reaction mixture,[213] and, finally, **74** was detected in the residue after the reaction.[214] The
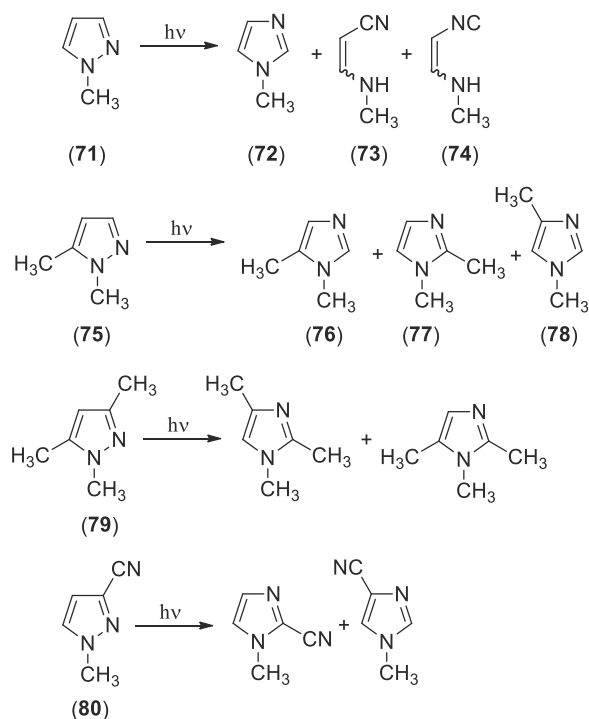
SCHEME 2.49   Photochemical isomerization of pyrazole derivatives.

irradiation of 1,5-dimethylpyrazole (**75**) gave a mixture of three products (**76**−**78**). While **77** and **78** can be obtained through both ring contraction − ring expansion and internal cyclization (Dewar) mechanisms, **76** can be obtained only via a the first mechanism (Scheme 2.49).[213,215] The formation of **78** is temperature-dependent: at 77 K it was not obtained.[215] Dewar pyrazole was invoked in the photoisomerization of 1,3,5-trimethylpyrazole (**79**), in the synthesis of **77** and **78** starting from **75**, and in the isomerization of cyanopyrazole (**80**) (Scheme 2.49).[216−219] A zwitterionic intermediate was also proposed.[220]

Ring-opening products were observed in the photoisomerization of 1-methyl-4-phenylpyrazole (**81**)[214,221] and in the reaction of 1-phenylpyrazole (**82**) (Scheme 2.50).[222] 1,4,5-Triphenylpyrazole gave in low yields (6%) the corresponding ring opening product.[223]
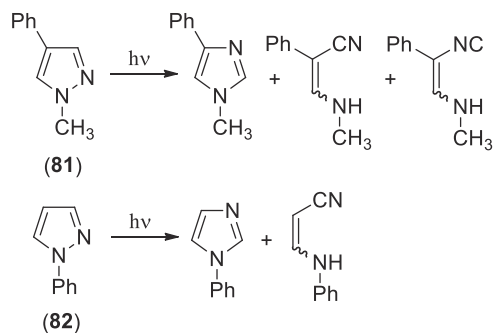
SCHEME 2.50   Photochemical isomerization of phenyl substituted pyrazole derivatives.

The mechanism depicted in the Scheme 2.51 accounts for the formation of the ring-opening products.[214] Compounds **84** and **85** can be obtained via an internal cyclization (Dewar) mechanism; in fact, the irradiation of **83** in the presence of furan gave the corresponding Diels−Alder adducts (**87** and **88**) formed from Dewar pyrazole derivative and furan (Scheme 2.52).[214]

There are several data in agreement with a mechanism involving an excited singlet state.[214,222] Theoretical calculations support this hypothesis. In fact, the singlet excited state can evolve to give the Dewar isomer and the corresponding triplet state. The latter shows a lower energy and probably can be obtained with higher efficiency. The triplet state can evolve to give the corresponding 1,2-biradical and, then, the isomerization product (Fig. 2.14).[224]
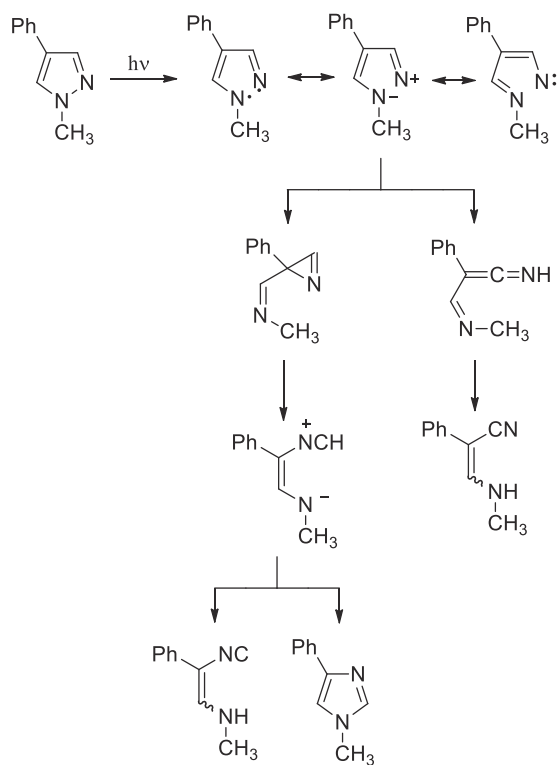
SCHEME 2.51 Proposed mechanism for phenyl substitute pyrazole isomerization.
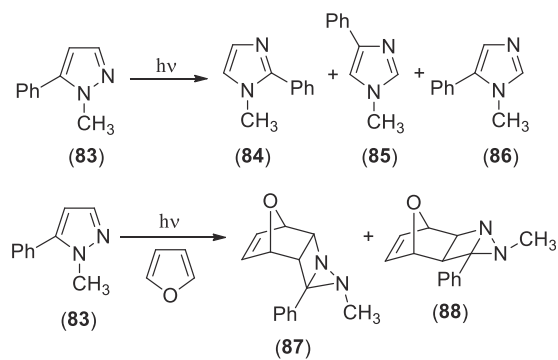
SCHEME 2.52 Photochemical isomerization of 5-phenyl pyrazole derivatives.
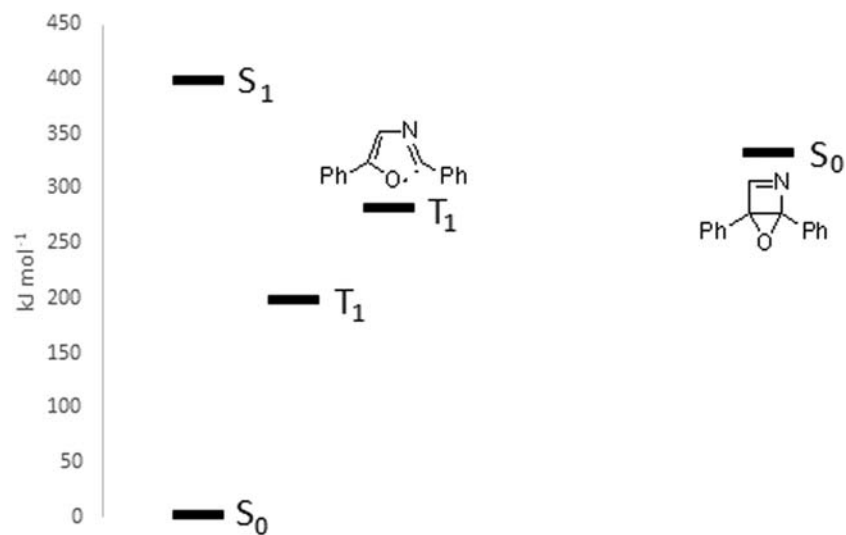
FIGURE 2.14 Relative energy of the excited states of 1-Methylpyrazole and of some reactive intermediates.

Photochemistry of Heterocycles
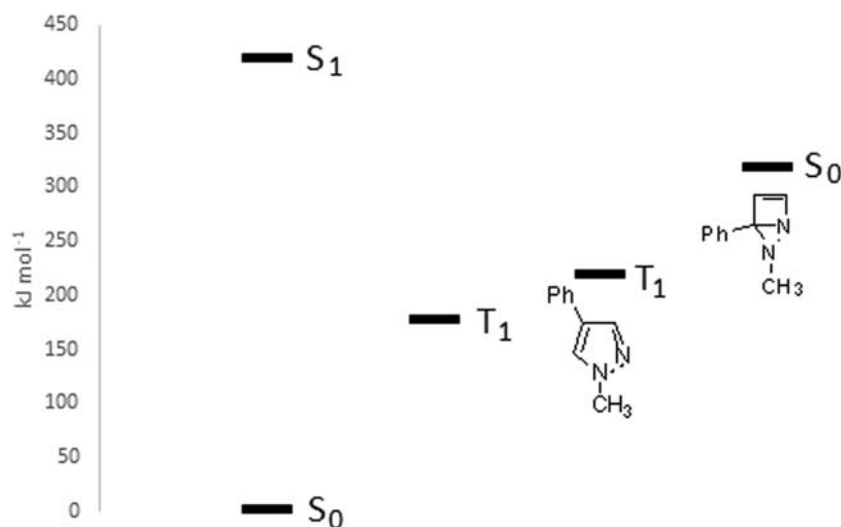
FIGURE 2.15 Relative energy of the excited states of 1-methyl-5-phenylpyrazole and of some reactive intermediates.

In the case of 1-methyl-5-phenylpyrazole, the singlet excited singlet state can evolve to give the Dewar isomer and the corresponding triplet state. However, the triplet state cannot evolve to give the corresponding biradical; in fact, it shows a higher energy than the triplet state. Then, the isomerization products can be obtained only from the Dewar isomer (Fig. 2.15).[224] A concerted mechanism, involving a conical intersection from the singlet state, has been proposed, although it is not in agreement with some experimental results.[225] 4-Dimethylamino-3-pyrazolin-5-one gave, under irradiation, ring opening products.[226]

The photoisomerization of indazole derivatives has been described.[227] This reaction occurred via the first excited singlet state through the formation of the corresponding Dewar isomer (Scheme 2.53).[228,229]
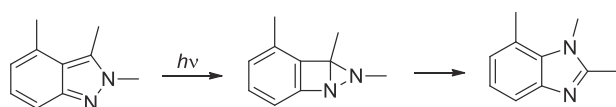
SCHEME 2.53 Photochemical isomerization of indazole derivative.

2.1.7 Isomerization of imidazole

The irradiation of imidazole derivatives such as **89** gave isomeric compounds **90** (Scheme 2.54).[216,217] Dewar isomer are invoked to justify the observed photochemical behavior.
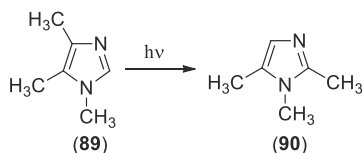
SCHEME 2.54 Photochemical isomerization of imidazole derivative.

Computational results are reported for the isomerization of 1,4,5-trimethylimidazole.[124] They show that the isomerization occurs through the Dewar isomer arising from the excited singlet state. The formation of the triplet state is energetically favored; however, the biradical intermediate cannot be produced because it had higher energy than the excited triplet state (Fig. 2.16).[230] Another study suggested that the isomerization occurred through a conical intersection in the first excited singlet state.[231]

2.1.8 Isomerization of thiazoles

The irradiation of thiazole did not give any interesting products.[232] However, 2-, 4-, and 5-methylthiazole gave the corresponding isothiazoles in low yields when irradiated in trifluoroacetic acid (Scheme 2.55).[233]
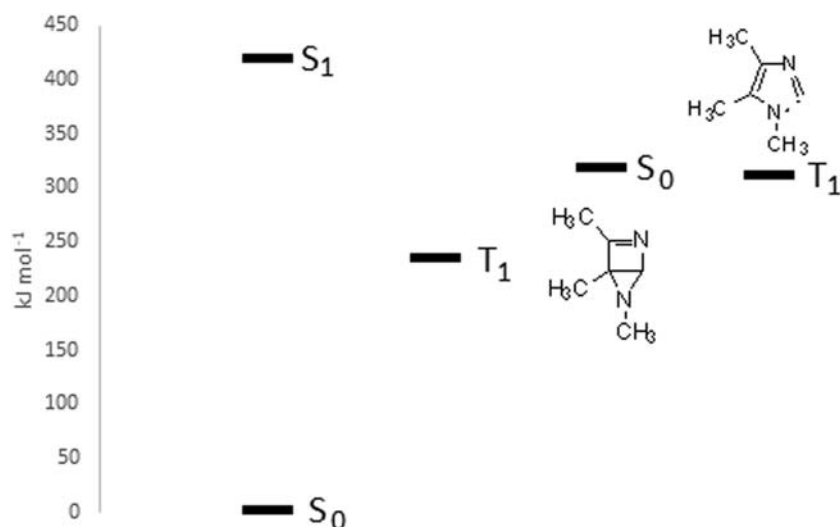
FIGURE 2.16 Relative energy of the excited states of 1,4,5-trimethylimidazole and of some reactive intermediates.
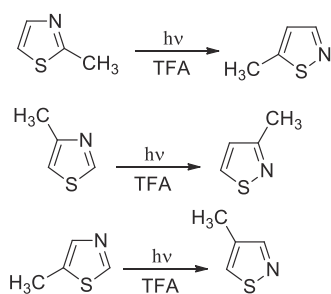
SCHEME 2.55 Photochemical isomerization of thiazole derivatives.

2.1.8.1 Aryl-substituted thiazoles

Many data have been reported on the reactivity of 2-phenylthiazole (**91**). In a pioneering work, the irradiation of this compound led to 4-phenylthiazole (**92**) and 3-phenylisothiazole (**93**); however, while the experimental conditions were provided (benzene, 12−24 h), the yields of the obtained products were not reported.[234] Subsequently, the same authors reported that the irradiation of a benzene solution of **91** (obtained through irradiation of 2-iodothiazole in benzene) in the presence of iodine leads to **93**, the major product, in addition, to small amounts of **92** (Scheme 2.56). When the reaction was carried out without iodine, the main product was 4-phenylthiazole (**92**) while 3-phenylisothiazole (**93**) was present in trace amount.[235,236]
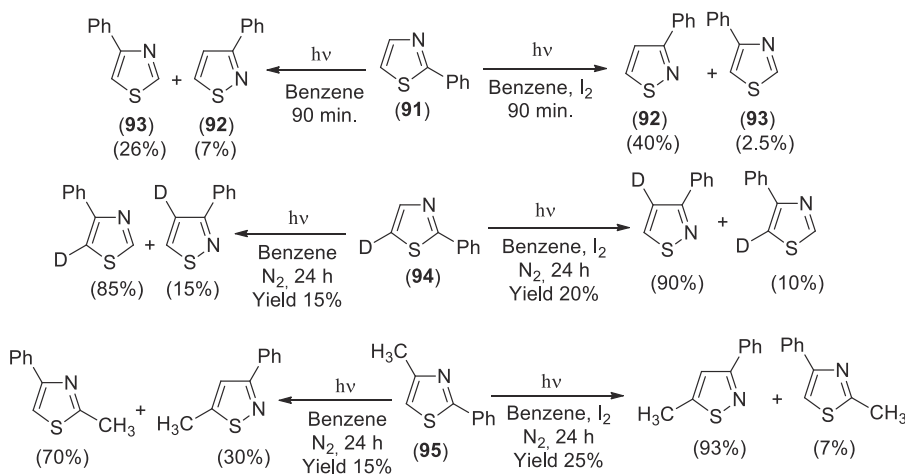
SCHEME 2.56 Photochemical isomerization of phenyl substitute thiazole derivatives.

2-Phenyl-5-deuterothiazole (**94**) and 2-phenyl-4-methylthiazole (**95**) showed the same behavior (Scheme 2.56).[236,237] By contrast, 4-phenylthiazole practically did not react, and 5-phenylthiazole gave 4-phenylisothiazole as the main product in very low yield.[236,238]

Other methyl derivatives were additionally studied. 2-Phenyl-5-methylthiazole furnishes mainly 3-phenyl-4-methylisothiazole; 2-methyl-5-phenylthiazole gives 3-methyl-5-phenylisothiazole; 4-methyl-5-phenylthiazole leads to the formation of 3-methyl-4-phenylisothiazole; 2-methyl-4-phenylthiazole gives 3-phenyl-5-methylisothiazole; and, finally, 4-phenyl-5-methylthiazole is converted into 3-phenyl-4-methylisothiazole.[239]

The authors generally considered the above results consistent with an internal cyclization (Dewar) mechanism. In this contest, iodine favors the intersystem crossing or the opening of the Dewar intermediate, as reported in Scheme 2.57.[237]
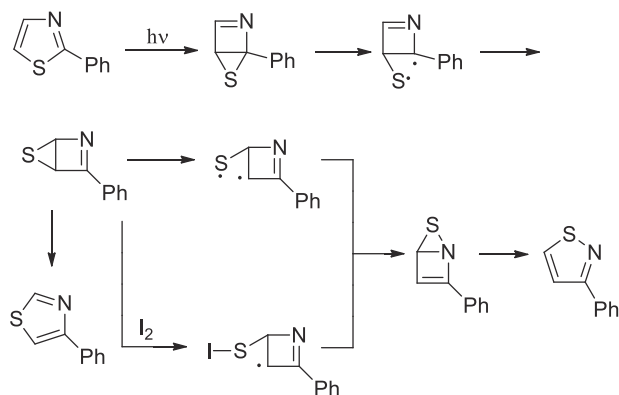
SCHEME 2.57   Proposed mechanism for 2-phenylthiazole isomerization.

However, such an explanation was not convincing for other authors. Maeda and Kojima found that the irradiation of 2-phenylthiazole in ethanol at 80°C led to the same products described before but in different ratio. Under the same reaction conditions, 5-phenylthiazole gave 4-phenylisothiazole, while 4-phenylthiazole was converted into 3-phenylisothiazole. The most important observation those authors made was that deuterated incorporation occurred when the reaction was carried out in benzene at 80°C in the presence of deuterium oxide. In fact, 2-phenylthiazole furnished deuterated 3-phenyl-4-deuteroisothiazole and 4-phenylthiazole without any deuterium incorporation. Likewise, 4-phenylthiazole was converted into 3-phenyl-4-deuteroisothiazole; however, 5-phenylthiazole did not undergo any deuterium incorporation.[240,241] On the basis of their results, the authors suggested a new mechanism hypothesis involving the participation of a polar intermediate (Scheme 2.58).[240,241] In fact, the formation of a polar intermediate could account for the deuterium incorporation. However, deuterium incorporation could also be explained by using the internal cyclization (Dewar) mechanism.[236]
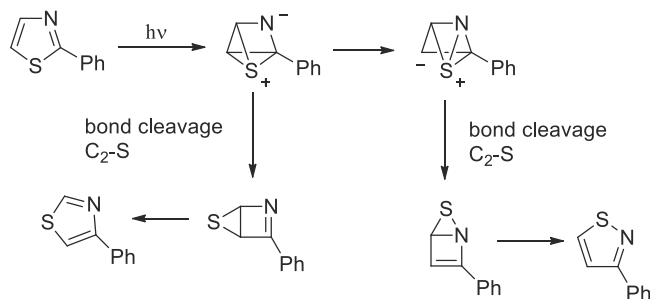
SCHEME 2.58   Alternative mechanism for 2-phenylthiazole isomerization.

The same authors discussed the reactivity of diphenylthiazoles. 2,5-Diphenylthiazole (**96**), irradiated in benzene at 80°C, gave 3,4-diphenylisothiazole (**97**) as the major product, together with minor amounts of 4,5-diphenylthiazole (**98**) and its cyclized derivative **99** (Scheme 2.59). 2,4-Diphenylthiazole (**100**) gave only a very low yield of 3,5-diphenylisothiazole (**101**), while 4,5-diphenylthiazole (**98**) was converted into the corresponding cyclized product **99** and 3,4-diphenylisothiazole (**97**) (Scheme 2.59).[241,242] All the data are in agreement with an internal cyclization mechanism.
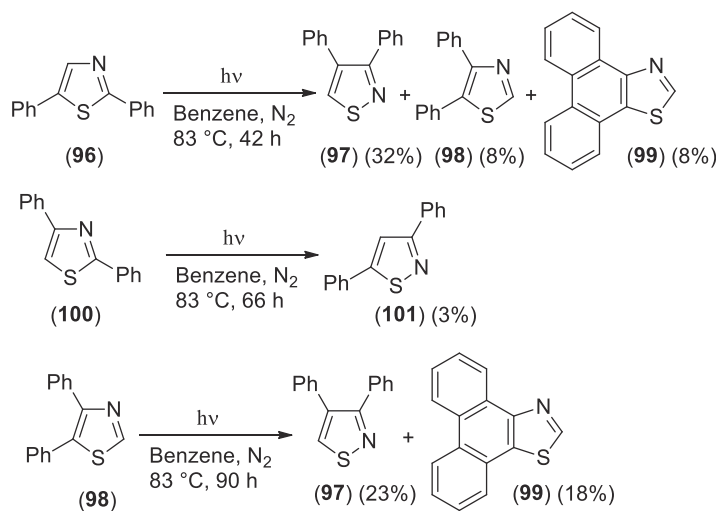
SCHEME 2.59 Photochemical behavior of diphenylthiazole derivatives.
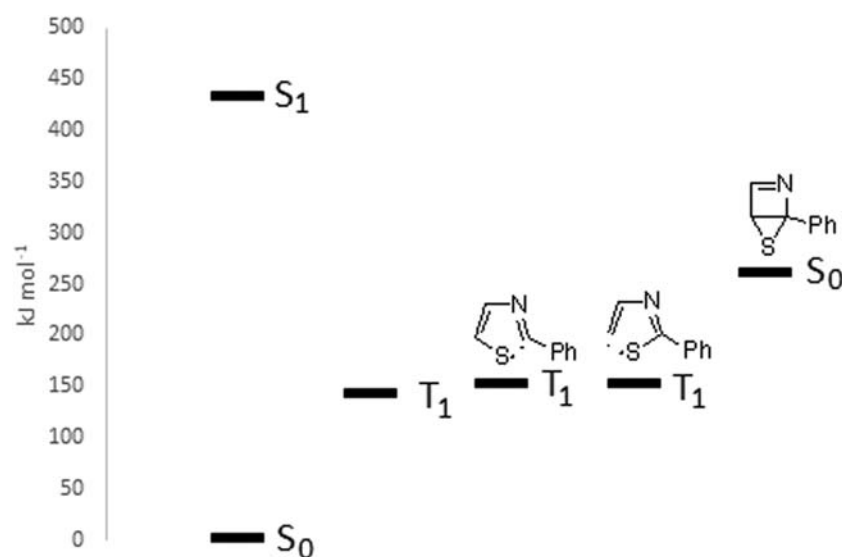
FIGURE 2.17 Relative energy of the excited states of 2-phenylthiazole and of some reactive intermediates.

Theoretical calculations explain the photochemical behavior of phenylthiazoles (Fig. 2.17).[243] The ring contraction − ring expansion mechanism cannot be invoked because the radical intermediates have higher energy than the corresponding triplet states. Furthermore, the formation of the Dewar isomer is favored in comparison with the formation of the zwitterionic intermediate.[29] Nevertheless, the reaction conditions used by Kojima and Maeda could allow for an endothermic reaction giving this type of intermediate.

These results were confirmed by the photochemical behavior of 1-acetylthiazole. The irradiation of this compound did not give any product. This behavior was in agreement with the corresponding theoretical calculations showing that, in this case, the biradical intermediates have a lower energy than that of the triplet state.[243]

Some years ago the irradiation of the iodothiazole 102 in the presence of aromatic and heteroaromatic compounds gave the arylation products where an isothiazole ring is present (Scheme 2.60).[244]
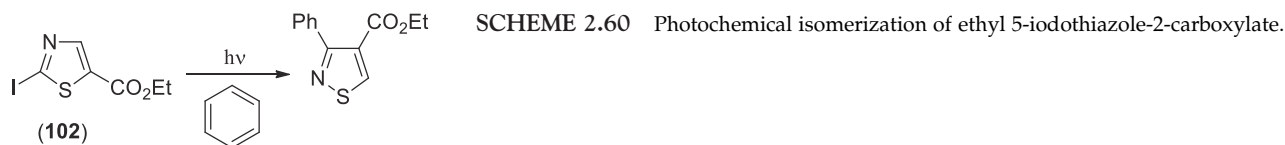
SCHEME 2.60 Photochemical isomerization of ethyl 5-iodothiazole-2-carboxylate.

In this case we can suppose the initial formation of ethyl 2-phenylthiazole-5-carboxylate followed by an isomerization reaction. Calculations have been performed on this reaction.[147] The results, in agreement with the formation of the Dewar isomer, are reported in Fig. 2.18. Furthermore, the study showed that the biradical intermediates proposed in Scheme 2.57 are transition states. Finally, the conversion from **104** to **105** requires a transition state energy of 71 kJ/mol while the direct conversion of **103** to **105** has a transition state at 53 kJ/mol, showing that this is the most probable process is the last one.

2.1.8.2 Bithiazoles

The irradiation of a 1:1 Cu-peplomycin complex, an antibiotic of bleomycin family (Fig. 2.19), leads to a product of an isomerization of a thiazole ring. In this case, the compound converted from a 2,4′-bithiazole derivative. When a 5:1 Cu-peplomycin complex was used, the product was a 3-isothiazolyl-4-thiazole derivative.[245,246]

This behavior has been verified with bithiazole derivative **106** (Scheme 2.61). Neither acetophenone nor benzophenone sensitized the reaction, in agreement with an internal cyclization mechanism via the excited singlet state.[246,247]
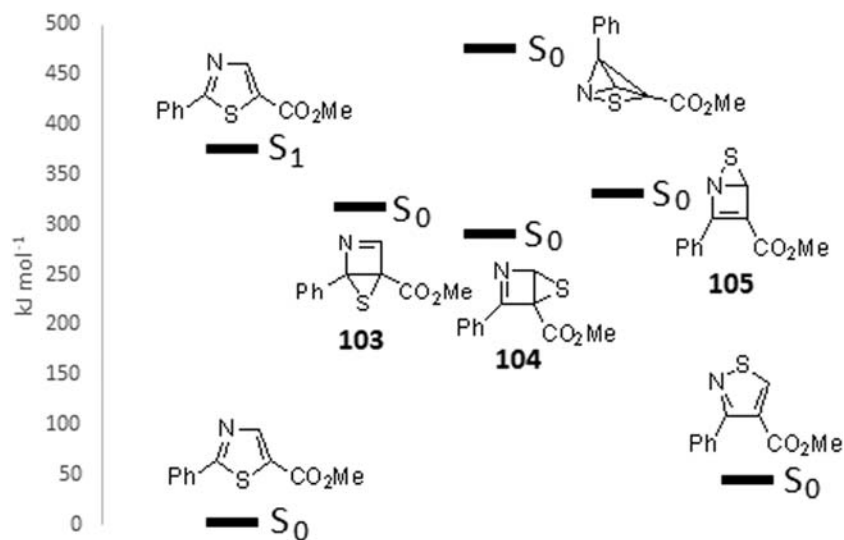
FIGURE 2.18   Relative energy of the excited states of methyl 2-phenylthiazole-2-carboxylate and of some reactive intermediates.
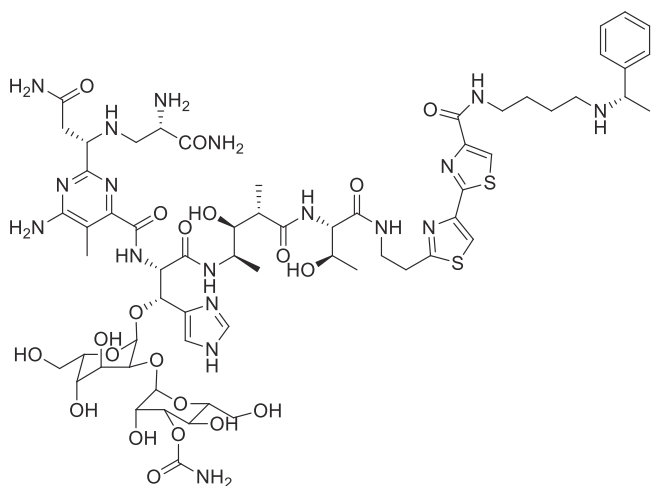
FIGURE 2.19   Peplomycin.
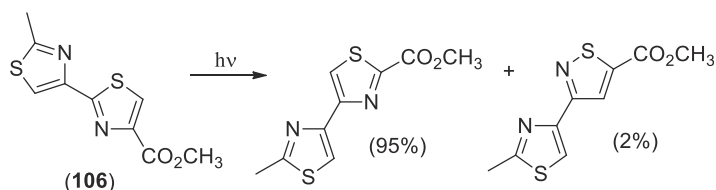
SCHEME 2.61   Photochemical isomerization of bithiazole derivatives.

Semiempirical calculation on **106** showed that it can isomerize only via the internal cyclization mechanism; in fact, the triplet state cannot evolve to give the corresponding biradical derivatives (Fig. 2.20).[29]

2.1.8.3 Trithiazoles

Trithiazole **107** gave the same type of the reaction described above. In this case, the isomerization occurred at the second ring (Scheme 2.62).[248]
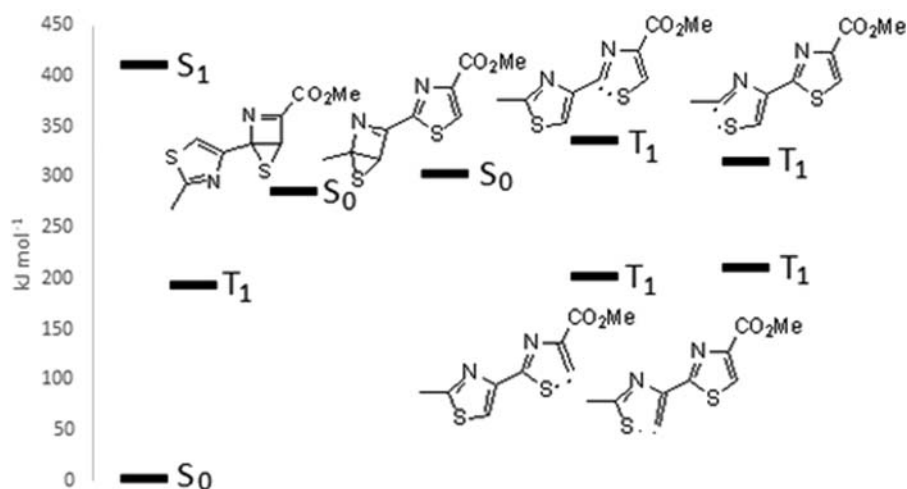
FIGURE 2.20 Relative energy of the excited states of bithiazole derivatives 106 and of some reactive intermediates.
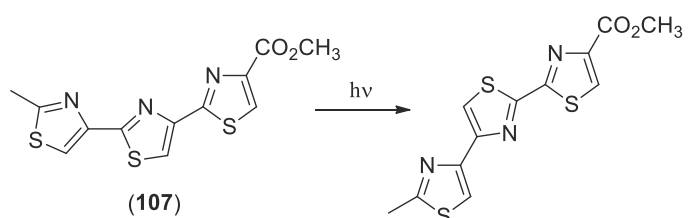
SCHEME 2.62 Photochemical isomerization of trithiazole derivatives.

The authors justified their result considering that the bond index $[B_{r,s} = (\text{coefficient } r \text{ LUMO})^2(\text{coefficient } s \text{ LUMO})^2]$ on the LUMO accounted for the formation of the Dewar isomer on the central ring of the trithiazole. By contrast, calculations show that the Dewar isomer should be formed on the third ring of the trithiazole.[29]

2.1.8.4 Benzothiazole

The irradiation of 2'-phenylthiazoloapocodeine (**108**) in acidic conditions at high temperature (90°C−95°C) gave the isothiazole derivative **109** in 38% yields (Scheme 2.63).[249] When the reaction is performed at room temperature, the extent of the isomerization is very low. DFT calculations are in agreement with a mechanism involving the triplet state and the formation of the azirine intermediate, where the isomerization of the azirine is a thermal step.
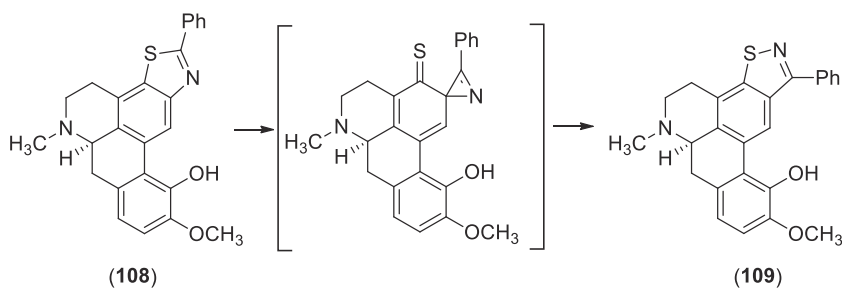
SCHEME 2.63 Photochemical isomerization of a benzothiazole derivative.

2.1.9 Isomerization of isothiazoles

The irradiation of isothiazole with a low-pressure mercury arc leads to the formation of thiazole.[232] The photochemical behavior of alkylisothiazoles has been studied. 3-Methylisothiazole gave 2-methylthiazole in a low yield. 4-Methylisothiazole was converted into 4-methylthiazole, and 5-methylisothiazole gave a mixture of 5-methylthiazole (55%) and 4-methylisothiazole (Scheme 2.64).[233,250] Either a zwitterionic involving mechanism[250] or an internal cyclization mechanism was invoked to justify these reactions.[233]
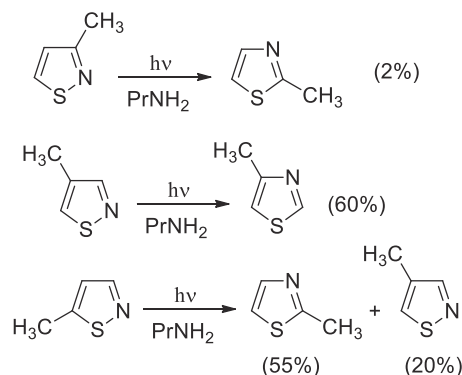
SCHEME 2.64   Photochemical isomerization of isothiazole derivatives.
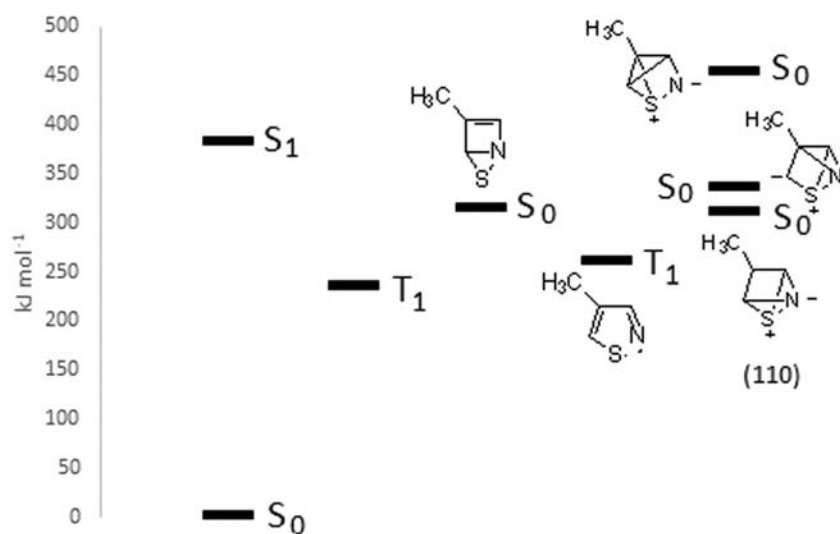
FIGURE 2.21   Relative energy of the excited states of 4-methylisothiazole and of some reactive intermediates.

Semiempirical calculations on 4-methylisothiazole showed that the reaction can occur through an internal cyclization mechanism with the formation of the Dewar isothiazole derivative (Fig. 2.21).[230] In fact, the triplet state of the isothiazole cannot evolve to the biradical. The zwitterionic mechanism can be excluded. Only the intermediate **110** showed an acceptable energy; however, it is a resonance structure of Dewar isothiazole. A CASSCF study on 3-methylisothiazole proposed a new route via a conical intersection.[251] This hypothesis is unable to explain the complexity of the observed reactivity.

3-Phenylisothiazole, irradiated in benzene, leads to 4-phenylthiazole, while 4-phenylisothiazole did not react. 5-Phenylisothiazole gave a variable mixture of 4-phenylthiazole and 3-phenylisothiazole (main product); however, in another work, the formation of 4-phenylthiazole (main product), 3-phenylisothiazole, 2-phenylthiazole, and 5-phenylthiazole has been described (Scheme 2.65).[234,236,238,252] Some other results were obtained using methylphenylisothiazole.[239,253]
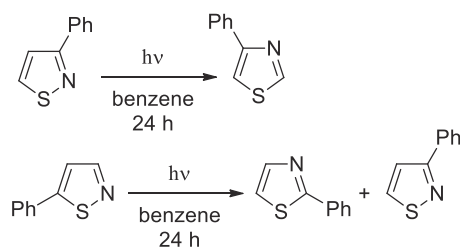
SCHEME 2.65 Photochemical isomerization of phenyl substituted isothiazole derivatives.

Different results have described in other articles. So, 5-phenylisothiazole gave 4-phenylthiazole (15%), 3-phenylisothiazole (5%), and 2-phenylthiazole (2%), when irradiated in benzene.[254] when the reaction was performed in methanol 5-phenylthiazole (23%), 4-phenylthiazole (6%), and 3-phenylisothiazole (2%) were obtained. When the reaction was performed in 2,2,2-trifluoroethanol only 5-phenylthiazole (32%) was obtained. If the irradiation is performed in benzene in the presence of triethyamine (TEA), 5-phenylthiazole was the main product (14%), together with 3-phenylthiazole (3%), and 4-phenylthiazole (4%).[254] Different product ratios were obtained when the irradiation was performed in methanol in the presence of TEA. The irradiation of 5-phenylisothiazole in ethyl ether allowed to isolate, after reaction with benzyl bromide, a ring opening product (Scheme 2.66).[254]
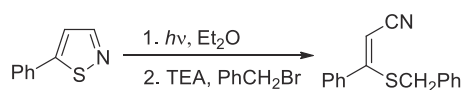
SCHEME 2.66 Isomerization of 5-phenylisothiazole.
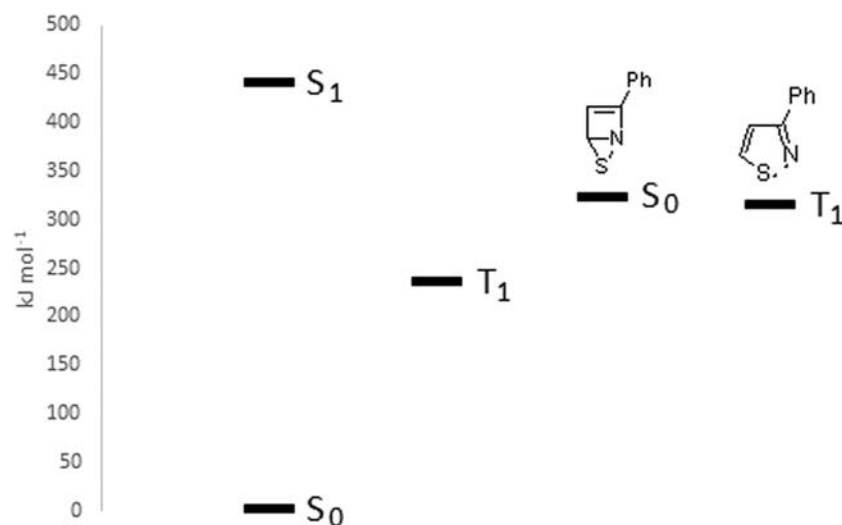
FIGURE 2.22 Relative excited states of 3-phenylisothiazole and of some reactive intermediates.

3-Phenylisothiazole gave 4-phenylthiazole (42%) and 2-phenylthiazole (3%). Similar results were obtained in the presence of TEA. In this case, the ring opening product cannot be detected.[254] The reaction occurred from the first excited π,π^* singlet state. The authors suggested that both ring opening-azirine formation and Dewar isomer formation were involved in the reaction.[254]

Calculations allow one to justify the observed behavior with some limitations (Fig. 2.22).[30] In the case of 3- and 5-phenylisothiazole, the reaction should implicate a Dewar isomer, because the excited triplet isothiazole derivative cannot be converted into the corresponding biradical. The above described hypothesis does not explain the mechanism in the case that both the mechanisms are involved in the first excited singlet state.

Some years ago the photochemical behavior of 4-phenylisothiazole has been reanalyzed.[255] This compound, on irradiation in ether, gave ring-opening products and 4-phenylthiazole (3% yield) (Scheme 2.67). The irradiation in methanol led to 4-phenylthiazole in 38% yield. Finally, in the presence of triethylamine, the yields of 4-phenylthiazole increased. All these data can be explained by assuming the formation of the ring-opening intermediate 111 displayed in Scheme 2.67.

SCHEME 2.67   Isomerization of 4-phenylisothiazole.
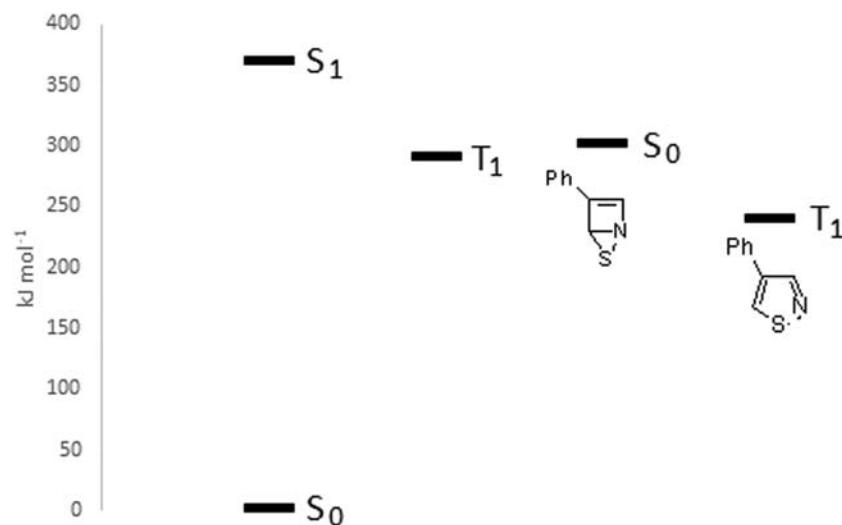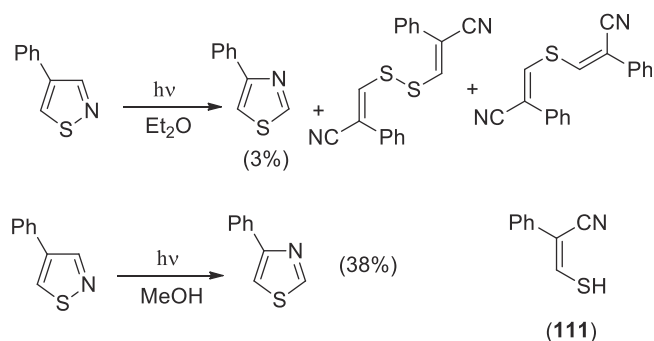
FIGURE 2.23   Relative energy of the excited states of 4-phenylisothiazole and of some reactive intermediates.

Calculations account for the experimental results with the limitations described earlier (Fig. 2.23).[29] The firs excited singlet state (which account for the absorption at 269 nm; calculated value 267 nm) was converted into the corresponding triplet state (289 kJ/mol; experimental 285 kJ/mol). The triplet state gives the cleavage of the S−N bond with the formation of the biradical intermediate. This intermediate leads to the product.

2.1.9.1 Benzoisothiazole

The first report on the photochemical reactivity of benzoisothiazole derivatives has been reported on a drug. Ziprasidone, an antipsychotic drug, gave, under irradiation, the corresponding benzothiazole (Scheme 2.68).[256]

SCHEME 2.68   Photochemical isomerization of a benzoisothiazole derivative.
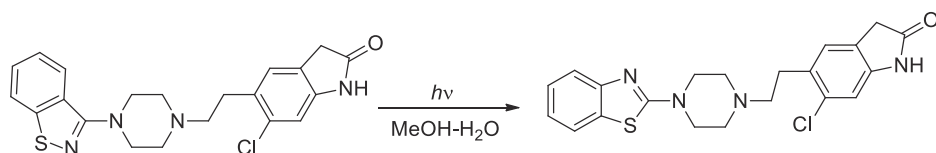
A mechanism involving the formation of the azirine has been proposed. More recently, the photochemical isomerization of the nitrobenzoisothiazole derivatives 112 through irradiation at λ >200 nm gave the corresponding thiazole in 88% yield (Scheme 2.69).[257] A possible mechanism involving both Dewar isothiazole and azirine has been proposed.

SCHEME 2.69   Photochemical isomerization of a benzoisothiazole derivative.
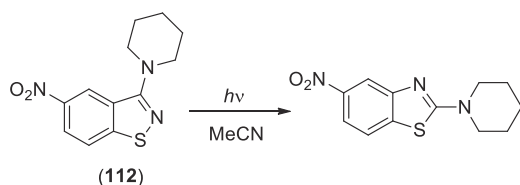
2.1.10 Isomerization of oxadiazoles

2.1.10.1 1,2,4-Oxadiazoles

The irradiation of 3-amino-5-phenyl-1,2,4-oxadiazole (**113**) gave the corresponding 1,3,4-oxadiazole (**114**) (Scheme 2.70).[258−261] The formation of **114** has been explained by assuming a ring contraction − ring expansion mechanism.
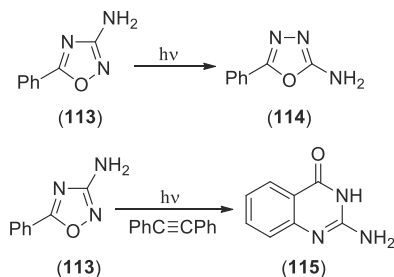
SCHEME 2.70   Photochemical isomerization of 1,2,4-oxadiazole derivatives.

1,3,4-Oxadiazole was obtained through the first excited singlet state. When the reaction was carried out in the presence of a triplet sensitizer, **114** was not detected but the quinazolinone **115** was obtained (Scheme 2.70).[262] Compound **114** cannot be obtained via the Dewar isomer. The authors supposed the formation of a zwitterionic intermediate through the heterolytic cleavage of the O−N bond.[262] The reaction of 3-methoxy-5-aryl-1,2,4-oxadiazole in the presence of diphenylacetylene to give the corresponding quinazolinones has been reinvestigated and an electron transfer mechanism was proposed.[263] Furthermore, the irradiation in methanol of **113** in the presence of an amine gave **114** in higher yields.[264] By contrast, the irradiation in methanol of 5-alkyl derivatives **116** gave the corresponding 1,3,4-oxadiazole derivatives, while the irradiation in methanol in the presence of triethylamine also the products deriving from the internal cyclization mechanism, 5-amino-3-alkyl-1,2,4-oxadiazole derivatives, was observed (Scheme 2.71).[265]
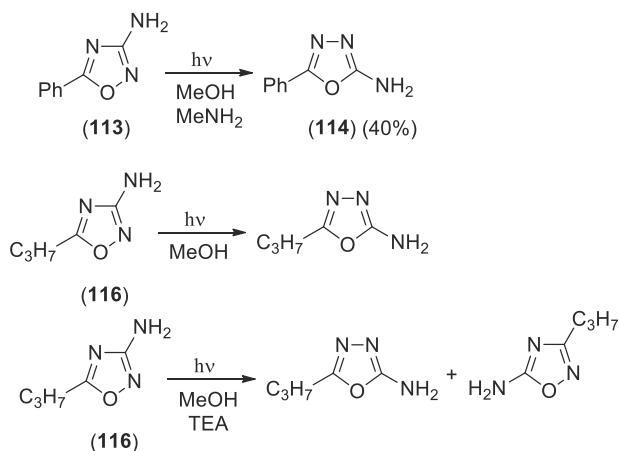
SCHEME 2.71   Photochemical isomerization of 3-amino-1,2,4-oxadiazole derivatives.

The above described behavior can be understood considering the results of calculations. Considering the 1,2,4-oxadiazole **113**, the formation of the 1,2-biradical intermediate after the formation of the corresponding excited triplet state is favored (Fig. 2.24).[266] The situation does not change when the conjugated base is considered. A CASSCF study on 3-amino-1,2,4-oxadiazole proposed a new route via a conical intersection mechanism on the excited singlet state; however, this hypothesis cannot explain the observed different behaviors and the presence of sensitized reactions.[267]

The same energy distribution has been observed in the case of 3-amino-5-methyl-1,2,4-oxadiazole.[266] By contrast, considering the conjugated base, the intersystem crossing to the first excited tripe state is not possible and the Dewar isomer can be obtained (Fig. 2.25).[266]
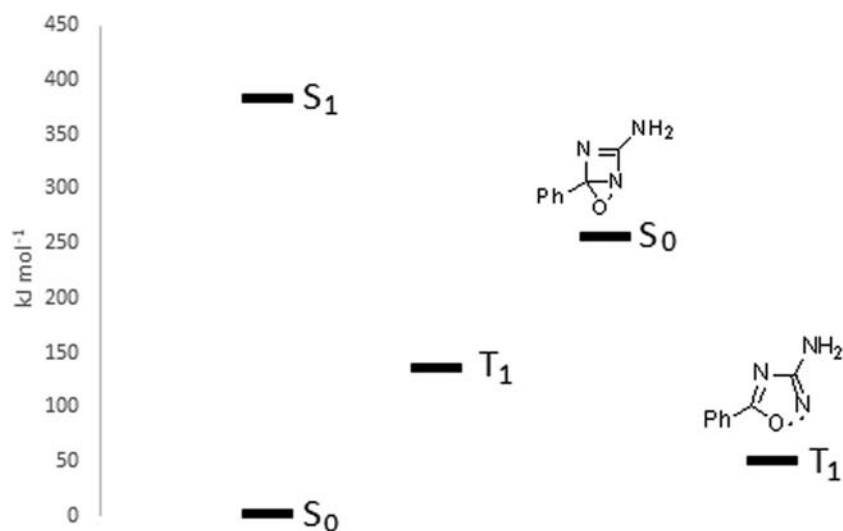
FIGURE 2.24 Relative energy of the excited states of 3-amino-5-phenyl-1,2,4-oxadiazole and of some reactive intermediates.
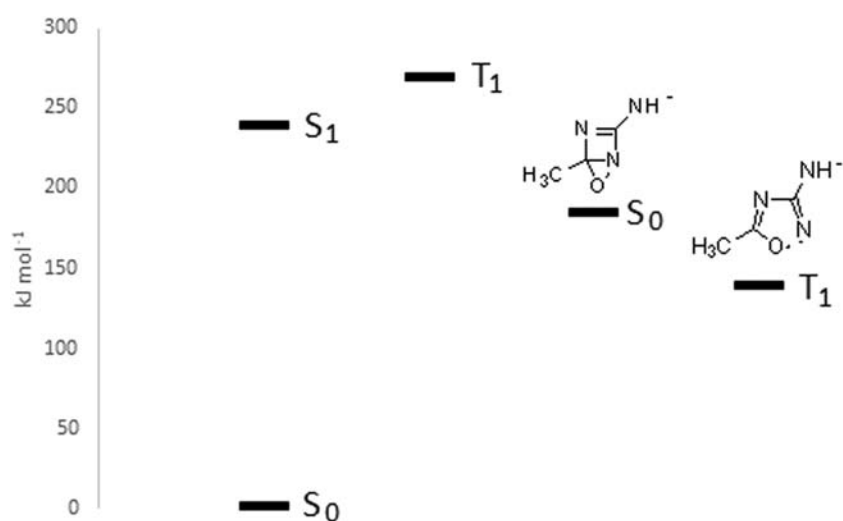
FIGURE 2.25 Relative energy of the excited states of the conjugated base of 3-methyl-5-methyl-1,2,4-oxadiazole and of some reactive intermediates.

On irradiation in ether at 254 nm 2,5-diphenyl-1,2,4-oxadiazole (**117**) did not give any interesting result. On the contrary, the irradiation in an immersion apparatus gave, with low conversion (33%), a mixture of three product (**118−120**) (Scheme 2.72).[261,268] When **117** was irradiated in the presence of NaY zeolite 2,5-diphenyl-1,3,4-oxadiazole was obtained in 60% yield.[269]

(117)   (118)   (119)   (120)
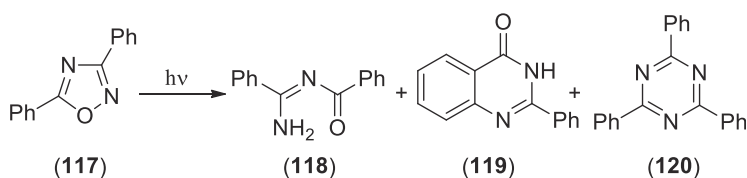
SCHEME 2.72 Photochemical behavior of 3,5-diphenyl-1,2,4-oxadiazole.

Compound **119** could not be obtained from **117**, and a hypothesis about its formation considered the (homolytic or heterolytic) cleavage of the O−N bond (Scheme 2.73).[268] The sensitized reaction did not give a different result; the author supposed that the reaction involved the excited triplet state of the molecule. When the reaction was carried out in methanol, **119** was obtained in ∼8% yield while the methoxy derivative of **117** was isolate as the main product (40%).[270]
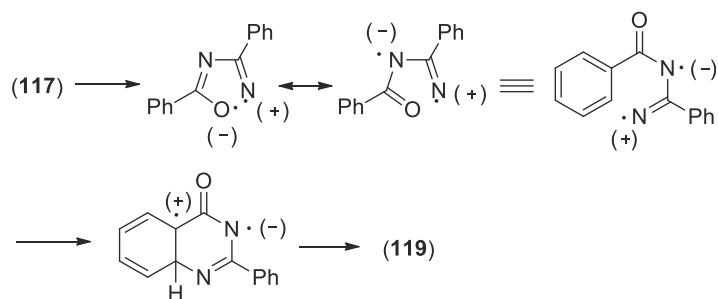
SCHEME 2.73 Proposed mechanism for 3,5-diphenyl-1,2,4-oxadiazole isomerization.
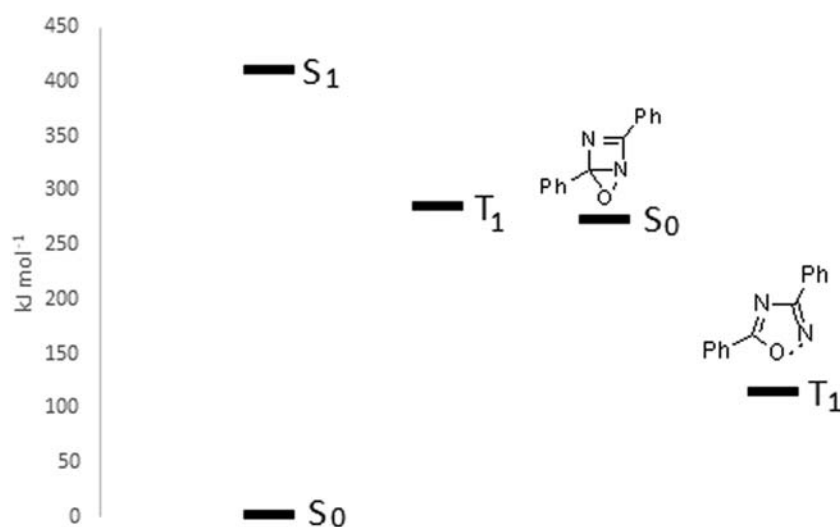
FIGURE 2.26 Relative energy of the excited states of 3,5-diphenyl-1,2,4-oxadiazole and of some reactive intermediates.

Semiempirical calculations on this compound showed that the excited triplet state can be obtained. This intermediate can evolve to the biradical (Fig. 2.26).[230]

When the reaction was carried out on the phenyl derivative **121**, only **122** was obtained (Scheme 2.74).[271] The formation of this product was rationalized assuming a heterolytic cleavage of the N-O bond followed by isomerization (Scheme 2.74). If the reaction occurs in the excited triplet state of the molecule, the biradical is the most probable intermediate.
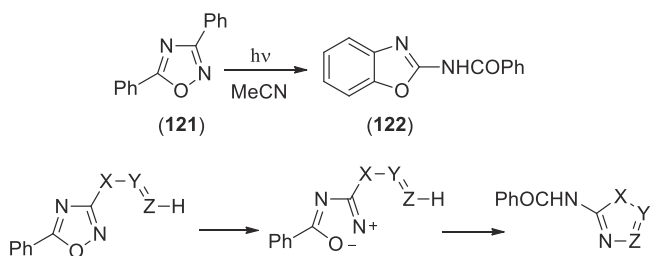
SCHEME 2.74 Photochemical behavior of 3,5-diphenyl-1,2,4-oxadiazole in acetonitrile.

The isomerization described in Scheme 2.74 could not be observed when the 5-methyl derivative **123** was used. The quinazolinone **124** was obtained in high yield, probably via **125** through the cleavage of the O−N bond in the triplet state (Scheme 2.75).[262,272,273] The same behavior (but in low yield) was observed with **126** (Scheme 2.75).[274]
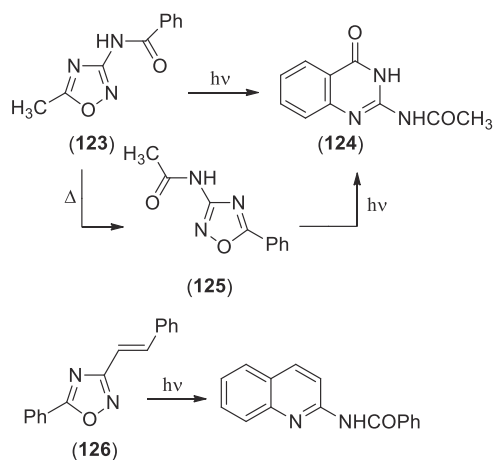
SCHEME 2.75   Synthesis of quinazoles from 1,2,4-oxadiazole derivatives.

The hydrazone derivative **127** can give a very similar isomerization reaction to give the corresponding 1,2,5-triazole (Scheme 2.76).[275] A different isomerization reaction were observed when Ru(bpy)$_2$Cl$_2$ was used as photocatalyst (Scheme 2.76).[276,277]
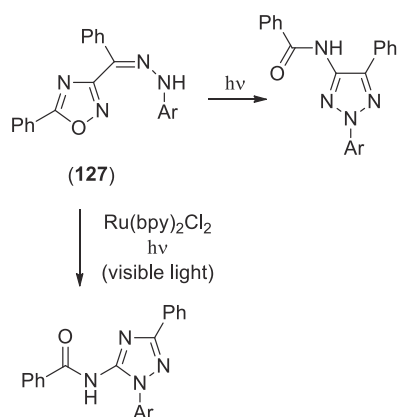
SCHEME 2.76   Photochemical isomerization of phenylhydrazones of 1,2,4-oxadiazole derivatives.

The irradiation of 5-amino-1,2,4-oxadiazole derivatives gave ring-opening products (**128**) (Scheme 2.77).[260] When external nucleophiles were added to the reaction mixture, products deriving from the attack of these nucleophiles to the ring-opening intermediate deriving from the O−N bond cleavage were observed. In the presence of amines, the triazole **129** was obtained (Scheme 2.77),[278] while, in the presence of thiourea, **130** was the main product (Scheme 2.77).[279] However, in the presence of sodium hydrogen sulfide, **131** was obtained without sulfur incorporation.[279]
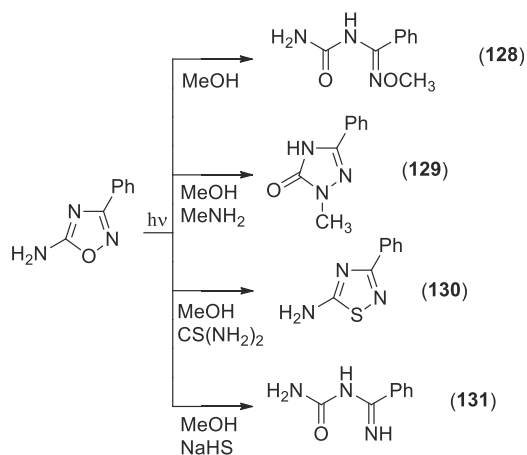
SCHEME 2.77   Photochemical isomerization of 5-amino-3-phenyl-1,2,4-oxadiazole.

Intensive research activity has been conducted on fluorine containing compounds. The reaction of a 5-perfluoroalkyl-3-amino-1,2,4-oxadiazole **132** with light in methanol gave a mixture of ring opening products (Scheme 2.78).[280] When the irradiation is performed in the presence of triethylamine, a different behavior has been observed: in this case, a 1,3,4-oxadiazole derivative **133** and 5-amino-1,2,4-oxadiazole **134** (Scheme 2.78).[280] Furthermore, the methylamino derivatives **135**, irradiated in methanol in the presence of methylamine, gave a mixture of a 1,3,4-oxadiazole and of 1,2,4-triazole (Scheme 2.78).[281]
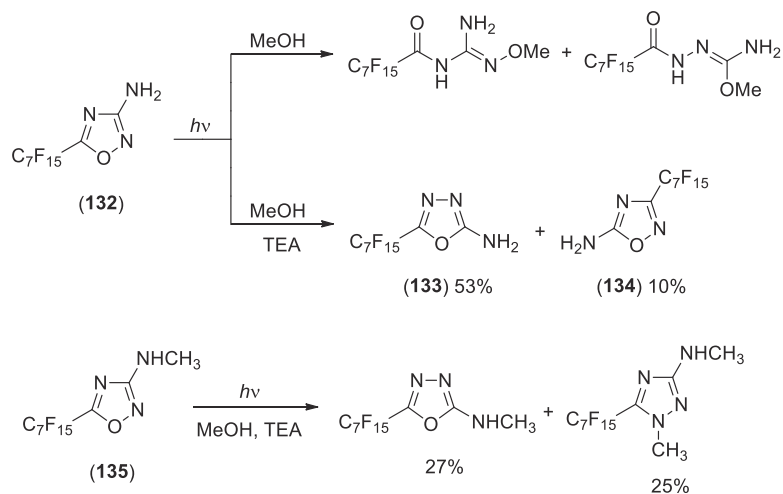
SCHEME 2.78 Photochemical behavior of 3-amino-5-perfluoroalkyl substituted 1,2,4-oxadiazoles.

All these results were explained in a DFT theoretical work on 3-amino-5-trifluoromethyl-1,2,4-oxadiazole, where, on the basis of a reactivity all occurring in the first excited singlet state, three possible pathways have been proposed, allowing to explain the observed reactivity (Scheme 2.79).[282]
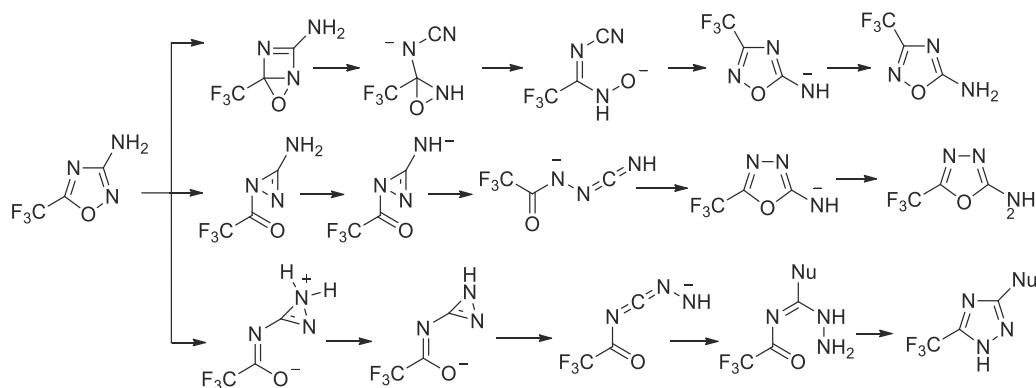
SCHEME 2.79 Proposed mechanism for 3-amino-5-trifluoromethyl-1,2,4-oxadiazole.

2.1.10.2 1,2,5-Oxadiazoles

The photolysis of 3,4-diphenyl-1,2,5-oxadiazole (**136**) in ether with a high-pressure mercury arc through Corex gave benzonitrile and phenyl isocyanate (Scheme 2.80).[283] When xanthone was used as triplet sensitizer, the
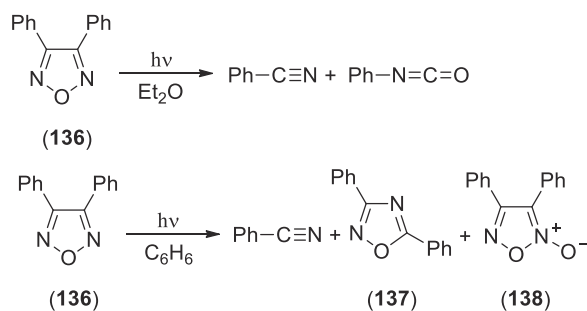
SCHEME 2.80 Photochemical behavior of 1,2,5-oxadiazole derivatives.

observed quenching of the reaction was in agreement with a reaction occurring on the excited singlet state. When the reaction was carried out in benzene through Pyrex, benzonitrile was the main product, but low yields of 3,5-diphenyl-1,2,4-oxadiazole (137) and diphenylfuroxan (138) were obtained (Scheme 2.80).[284] The authors considered that 137 was obtained by the coupling of benzonitrile and benzonitrile oxide while 138 was obtained by the recombination of two molecules of benzonitrile oxide.

The results described earlier represent the first example of the fragmentation-readdition route (Scheme 2.81).
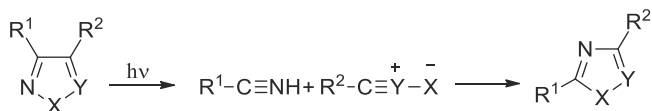
SCHEME 2.81 Proposed mechanism for 1,2,5-oxadiazole derivatives isomerization.
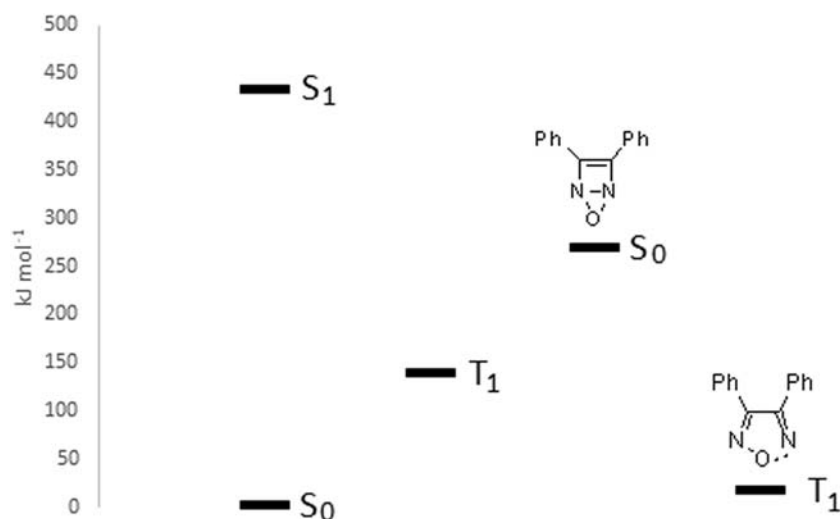
FIGURE 2.27 Relative energy of the excited states of 3,4-diphenyl-1,2,5-oxadiazole and of some reactive intermediates.

Semiempirical calculations on this molecule showed that the intersystem crossing to the excited triplet state is favored: the reaction can be sensitized by xanthone because the triplet state of 3,4-diphenyl-1,2,5-oxadiazole is lower than that of xanthone. The cleavage of the triplet state to the biradical is favored, considering the relative energy of this intermediate (Fig. 2.27).[230]

The irradiation of 3-acylamino derivative 139 in aqueous ammonia gave the corresponding 1,2,4-oxadiazoles (140) in 45%−50% yield (Scheme 2.82);[285,286] The observed reactivity can be explained by assuming a fragmentation reaction of the substrate to give a nitrile oxide intermediate that can react with ammonia and then with the acyl group. However, when 139 was irradiated in methanol, only benzonitrile, phenylcarbamate, and acetylcyanamide were detected in the reaction mixture.[287] The irradiation of 141 in methanol gave 1,2,4-oxadiazole derivatives 142 and 143 in 29 and 26% yield, respectively (Scheme 2.82).[287−289]
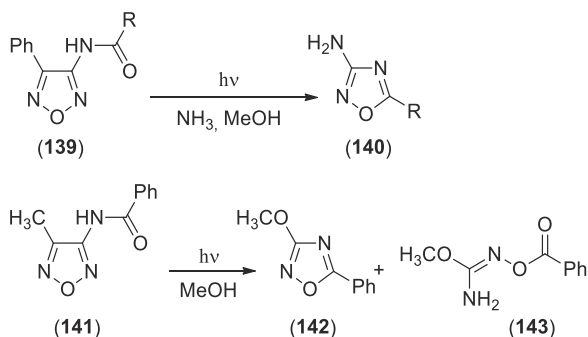
SCHEME 2.82 Photochemical behavior of 3-amino-1,2,5-oxadiazole derivatives.

2.1.11 Other pentaatomic heterocycles

Very few examples are available on the photoisomerization of other heterocycles. In the case of triazoles, the most common photochemical reaction is the formation of the biradical deriving from the loss of nitrogen from the parent molecule.[290,291] The same behavior has been observed on benzotriazole derivatives.[292–305] However, the irradiation of 1,4-diphenyl-5-amino-1,2,3-triazole in ethanol gave the corresponding rearrangement product in 35% yield (Scheme 2.83).[306] The reaction probably occurs through a ring contraction − ring expansion route.
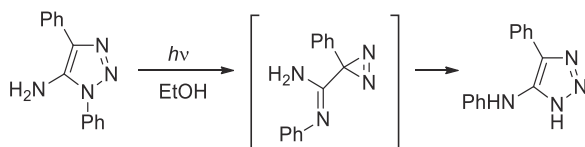
SCHEME 2.83 Photochemical isomerization of 1,4-diphenyl-5-amino-1,2,3-triazole.

The same behavior has been observed also in case of thiadiazoles. In this case, the main reaction is the loss of nitrogen from the starting material with the formation of a biradical species (or thiirene) that can undergo other chemical reactions.[307–327] Also in this case, a report on a photochemical isomerization is reported where a transposition of a benzylic group occurred (Scheme 2.84).[328]
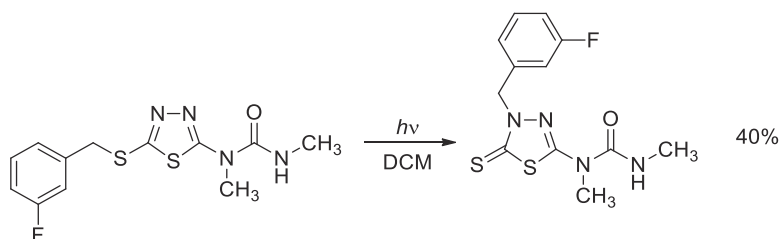
SCHEME 2.84 Photochemical isomerization of a thiadiazole derivative.

2.2 Photoisomerization of hexatomic heterocycles

2.2.1 Isomerization of pyridines

2.2.1.1 Pyridines

The electronic states of pyridine and the observed lack of phosphorescence in the presence of $\phi_{isc} = 0.3−0.5$, has been object of study in the 60 years of the last century.[329–334] The photochemical isomerization of pyridine in the excited state to form a Dewar structure has been postulated several years ago (Scheme 2.85).[335–345] Transient spectroscopy showed that the decay from S_1 and S_2 states had a fast component (2.2 ps) attributable to the motion on the $\pi\pi^*$ reaction path to form the isomer (an azaprefulvene isomer, see below).[346]
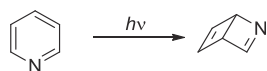
SCHEME 2.85 Dewar pyridine in the photoisomerization of pyridine.

The photochemical reactivity of pyridine it is known from the first steps of photochemistry studies. In 1932 Freytag described the reaction of pyridine with water when it is irradiated in aqueous solution.[347–349] The same reaction has been reconsidered several years ago (Scheme 2.86).[350,351]
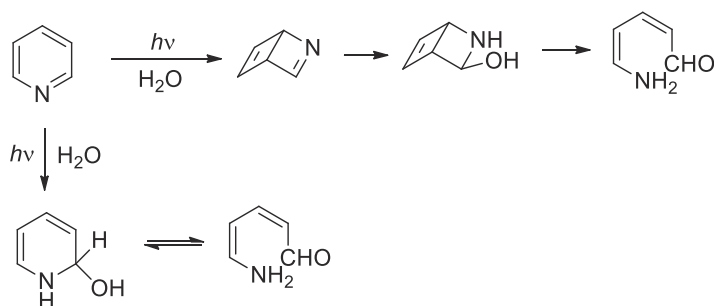
SCHEME 2.86 A Scheme explaining the observed products in the photoisomerization of pyridine.

Pyridine is able to form a complex in the presence of water and the spectroscopic properties of this complex has been studied.[352−356] Experiments performed in a cryogenic matrix, showed the presence of Dewar pyridine in the reaction of pyridine with water.[357]

A very similar reaction has been observed irradiation the pyridine derivative **144** in methanol (Scheme 2.87).[358,359]
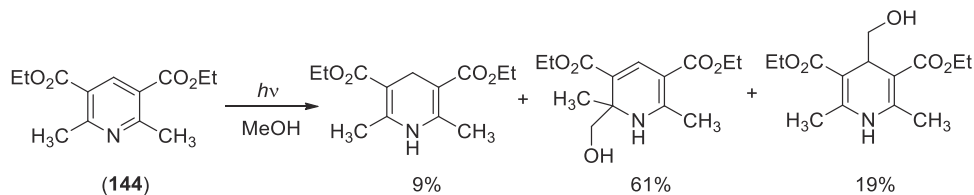
SCHEME 2.87   Reaction products in the reaction of 2,6-dimethyl-3,5-diethoxycarbonylpyridine.

The 2,4,6-trimethyl derivative **145** gave also a pyrrole derivative (Scheme 2.88).[359] The proposed mechanism is reported. The irradiation of pyridine in cyclohexane gave 2- and 4-cyclohexylpyridine in 10% yield.[360] Furthermore, pentakis(pentafluoroethyl)pyridine gave, if irradiated in perfluoropentane at λ >270 nm the Dewar isomer, that can be converted into the prismane derivative through irradiation at λ >200 nm in almost quantitative yields (Scheme 2.89).[361]
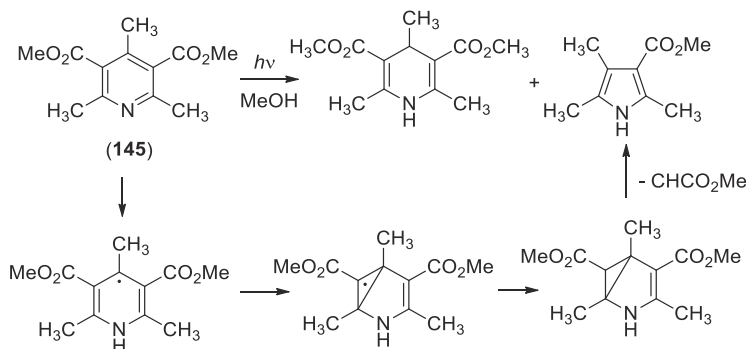
SCHEME 2.88   Possible reaction mechanism in the reaction of 2,4,6-trimethyl-3,5-diethoxycarbonylpyridine.
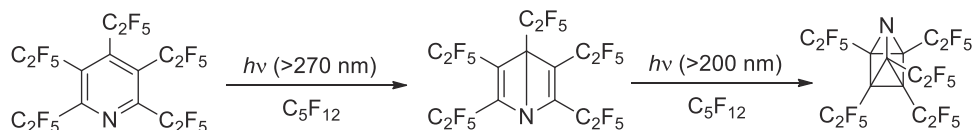
SCHEME 2.89   Dewar and prismane pyridine in the reaction of fluorinated pyridine.

The irradiation of pyridine in the gas phase gave only decomposition products (hydrogen, methane, ethene, acetylene, propylene, allene, methylacetylene, isobutylene).[362] Gas phase irradiation of 2-picoline gave conflicting results. An article claims as main product of the reaction 4-picoline (together with 2,5-ludidine and pyridine),[363] while another account showed that 2-picoline gave a mixture of 3- and 4-picoline with ϕ 5.1 $\times$ 10^{-4} and 4 $\times$ 10^{-5}, respectively.[364] Another study on gas phase photochemistry of dimethypyridine derivatives proposed a more complex scenario.[365] The irradiation at 254 nm of 2,3-dimethylpyridine (2,3-lutidine) results in the formation of 2,6-dimethylpyridine (5.7%), 3,4-dimethylpyridine (0.9%), and 2,5-dimethylpyridine (0.8%) (Scheme 2.90). However, when the reaction is performed in the presence of nitrogen, while the yields of 2,6-dimethylpyridine and 3,4-dimethylpyridine decreased, the yields of the third product increased. Furthermore, when the irradiation is performed at 290 nm, 2,5-dimethylpyridine was the only reaction product. The authors proposed that these reaction products derived from different pathways. The first two products derived from the S_2 state through a mechanism involving electrocyclic ring closure to form an azaprefulvene isomer and sigmatropic shifts (Scheme 2.91).
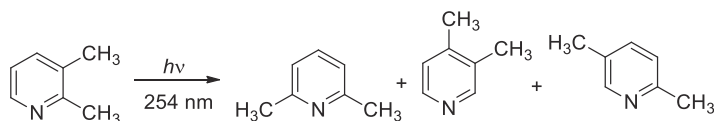
SCHEME   2.90   The   photoisomerization   of   2,3-dimethylpyridine.
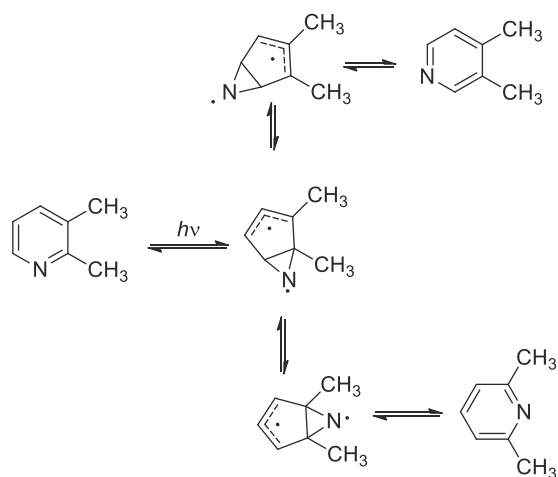
SCHEME 2.91 Proposed mechanism in the photoisomerization of 2,3-dimethylpyridine.

Furthermore, the formation of 2,5-dimethylpyridine occurred in the triplet state through the formation of a Dewar pyridine derivative followed by a sigmatropic shift of C−2 from C−3 to C−5 (Scheme 2.92).
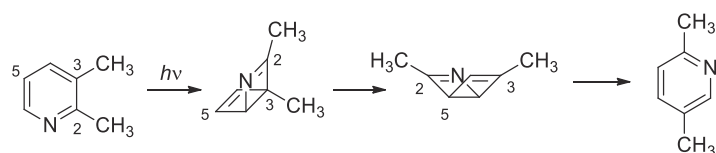
SCHEME 2.92 Proposed mechanism for the formation of 2,5-dimethylpyridine in the photoisomerization of 2,3-dimethylpyridine.

The photochemical reactivity of 3,4,5-trideuteriopyridine is compatible with the formation of an azaprefulvene isomer.[366] When the pyridine derivative **146** is irradiated in methanol some isomerization products have been observed (Scheme 2.93).[359] The mechanism proposed to justify these results involve the formation of Dewar pyridines and prismane (Scheme 2.94).[359]
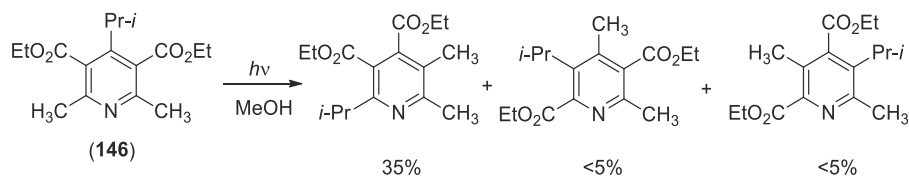
SCHEME 2.93 The photoisomerization of 2,6-dimethyl-4-i-propyl-3,5-diethoxycarbonylpyridine.
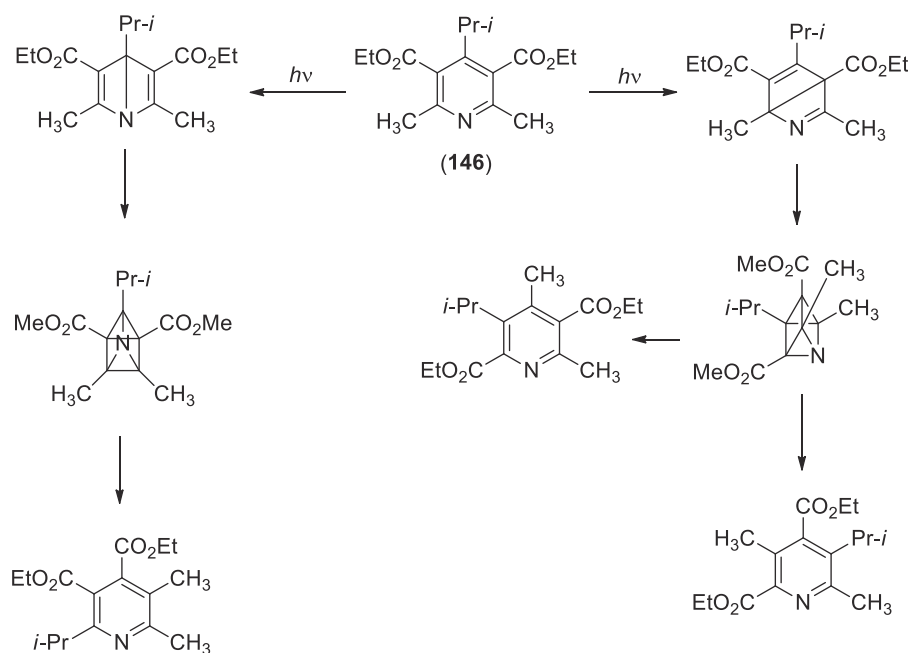
SCHEME 2.94 Proposed mechanism for the photoisomerization of 2,6-dimethyl-4-i-propyl-3,5-diethoxycarbonylpyridine.

The aniline derivative **148** was obtained as the main product after the irradiation of the nitrile **147** (Scheme 2.95).[367] Dewar pyridine was supposed to be involved in the reaction together with a [3,3] sigmatropic shift (Scheme 2.95).
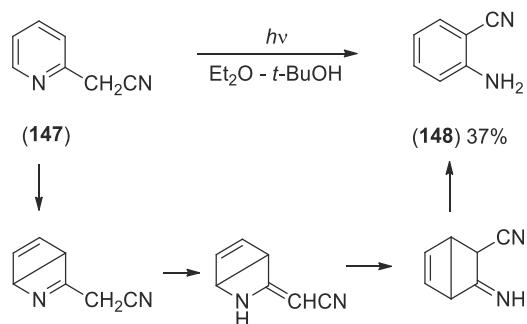
SCHEME 2.95   The photoisomerization of 2-cyanomethylpyridine.

2.2.1.2 Dihydropyridine

The dihydropyridine derivative **149** can give in very high yields the corresponding Dewar isomer (Scheme 2.96).[368] This reaction can be used in the synthesis of 1,4-oxazepines or 1,4-diazepines (Scheme 2.96).[369,370]
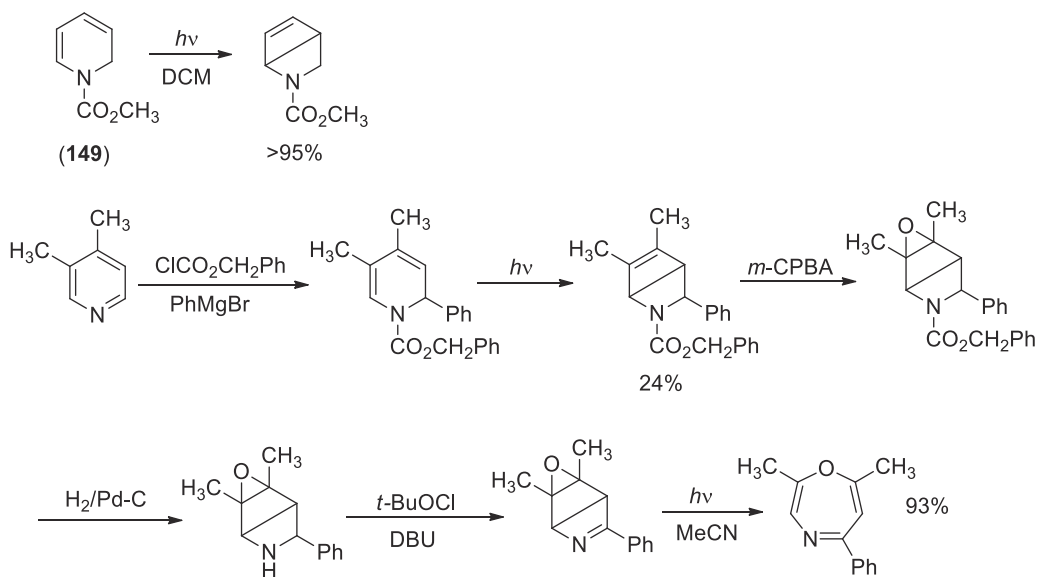
SCHEME 2.96   The photoisomerization of a dihydropyridine derivative.

The intervention of Dewar pyridine has been postulated also in the photochemical degradation of 2-halogenated pyridines in water.[371−373]

2.2.1.3 Pyridinium salts

The photochemical reaction of methylpyridium chloride in KOH yielded compound **150** with $\phi = 0.1$ (Scheme 2.97).[374] Recently, a very similar substrate (*N-n*-butyl bromide derivative) gave the analogs of **150** in 96% yield in a flow reactor able to give 3.7 g/L/h.[375] However, the methyl pyridinium salt **151** gave the corresponding dihydropyridine derivative in low yields (Scheme 2.97).[359]
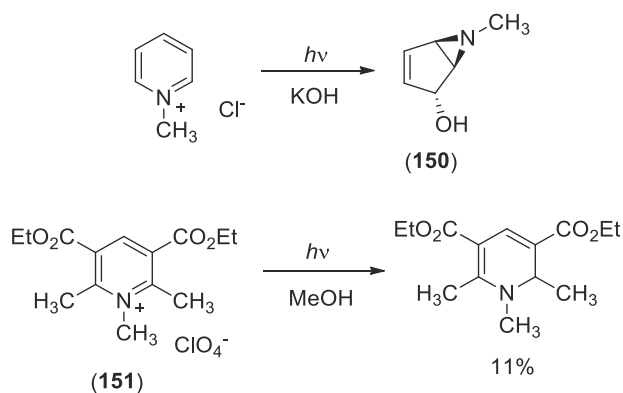
SCHEME 2.97   Photoisomerization of pyridinium salts.

The reaction of *N*-prenylpyridium perchlorate in methanol allowed the formation of the tetrahydropyridine derivatives **152** (Scheme 2.98), while the irradiation of *N*-allylpyridinium perchlorate in the same conditions gave the cyclopentene derivative **153** (Scheme 2.98).[376] Scheme 2.99 collects the proposed mechanism for the formation of **153**.[376]
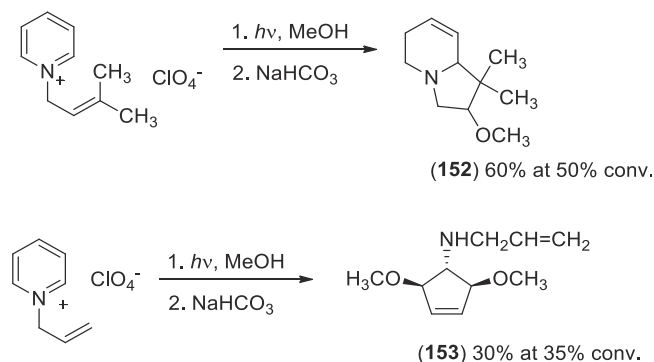
SCHEME 2.98   Photoisomerization of some pyridinium salts.
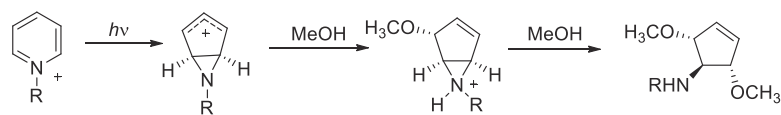
SCHEME 2.99   Proposed mechanism for the photoisomerization of pyridinium salts.

The reaction described in Scheme 2.98 allowing to obtain the compound **153** can be extended to other substrates. In some cases, the azirine deriving from the isomerization process can be isolated (Scheme 2.100).[377–379] The reaction showed a good stereoselectivity and an interesting regioselectivity.

Selection of the reaction conditions can allow to separate the formation of the azirine from its hydrolysis (Scheme 2.101).[380]

Finally, the reaction of **154** with light in aqueous KOH gave the corresponding azirine **155** in acceptable yields, and the azirine can be opened to give the spiro derivatives **156** (Scheme 2.102).[381]

The synthesis of aminocypentene derivatives through photochemical isomerization of pyridinium salts, coupled with a desymmetrization performed with electric eel acetylcholinesterase opened the possibility of the use of this reaction in organic synthesis.[382] This way, this type of compounds have been used in the synthesis of (+)-mannostatin A,[383,384] (−)-allosamizoline aminocyclopentitol,[385] 3-amino-3-deoxyaldopentoses,[386] polyhydroxylated indolizidines,[387,388] (+)-castanospermine,[388] trehazolin aminocyclitol,[389] and (+)-lactacystin.[390]

SCHEME 2.100   Some reactions of pyridinium salts.

SCHEME 2.101   Azirines in the photoisomeri-zation of pyridinium salts.

SCHEME 2.102   Spiro derivative in the reaction of the azirine obtained in the photoisomerization of pyridinium salts.
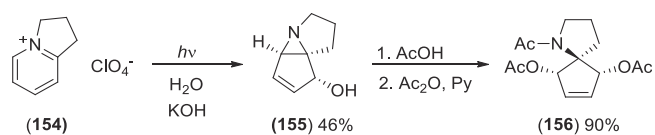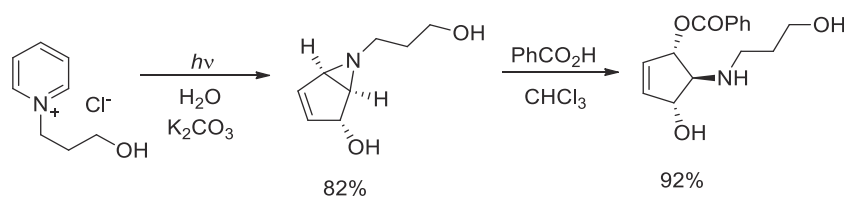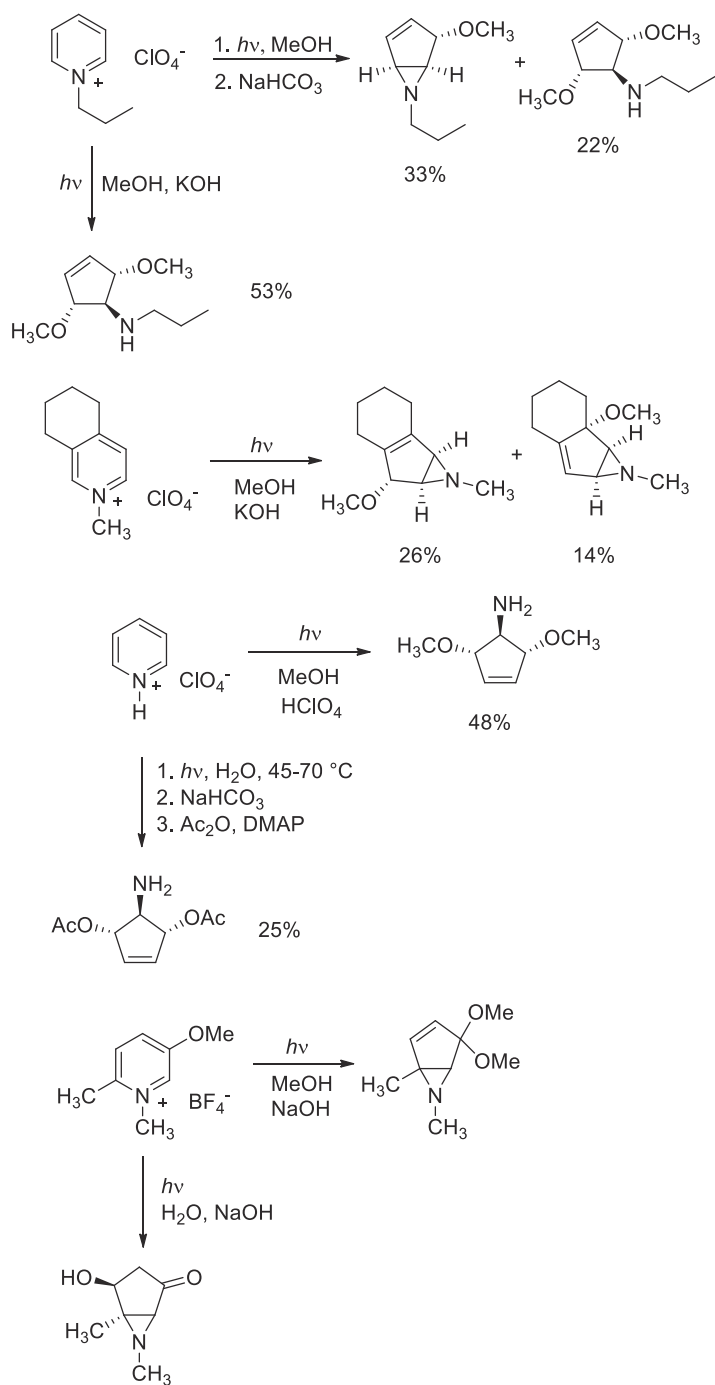
2.2.1.4 Pyridinium ylides

The photochemical reaction of the ylide **157** in benzene gave the corresponding pyrrole in 25% (Scheme 2.103).[391,392]

More interesting was the photochemical behavior of ethoxycarbonylimino-pyridinium ylide whose electronic states has been described showing the presence of two singlet excited states relative to π,π^* transitions.[393]
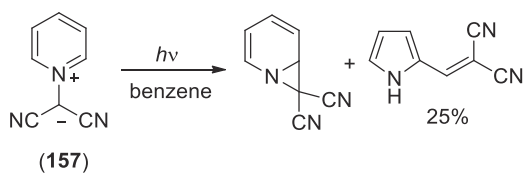
SCHEME 2.103   Photoisomerization of pyridinium ylides.

In this case, the irradiation of these compounds gave the corresponding diazepine, probably through the formation of a diazirine intermediate. It is noteworthy that the reaction is compatible with the presence of different electron withdrawing substituents on the nitrogen atom of the ylide; furthermore, the reaction is quite indifferent to the presence of electron donating or electron withdrawing substituents on the pyridine ring, with the exception of ethoxycarbonyl group in four position (Scheme 2.104).[394−404] Only in few cases, the reaction showed a
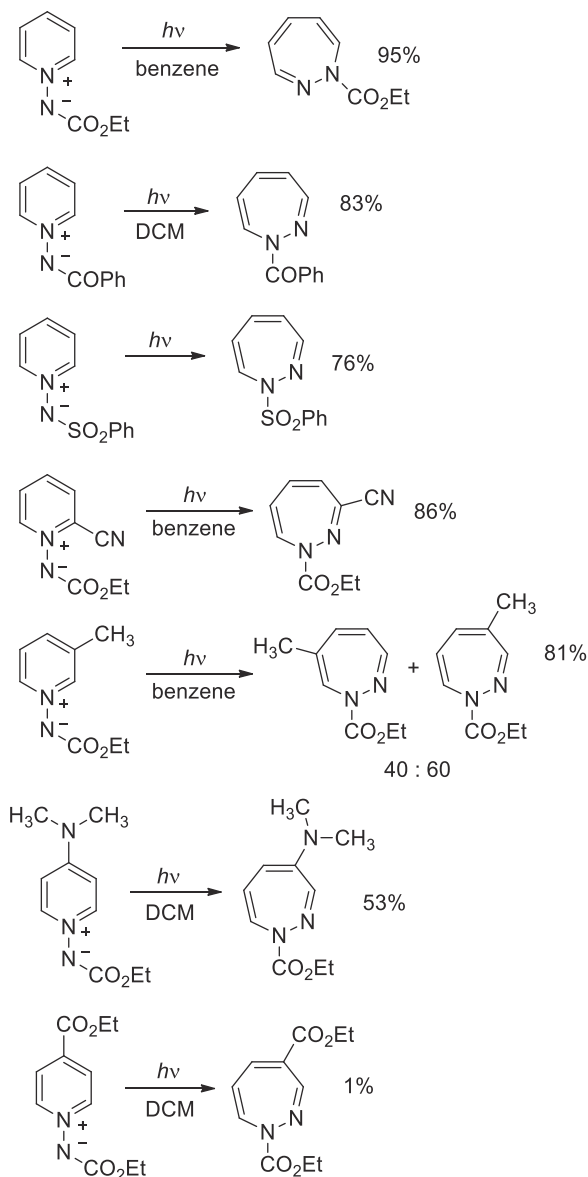
SCHEME 2.104   Synthesis of diazepines through the photoisomerization of pyridinium ylides.

different behavior. The use of pyridine derivatives bearing several phenyl groups inhibited the reaction and the pyridine was obtained as main product (Scheme 2.105); furthermore, the same result was obtained using an ylide with an ureic substituent on nitrogen ylide.[405-407] Furthermore, the diazepine is subject to a further photochemical reaction, giving the compound **158** (Scheme 2.105).[408]
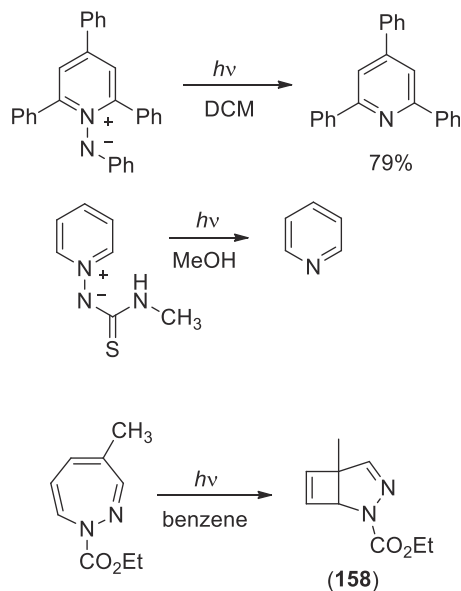
SCHEME 2.105   Synthesis of pyridine derivatives from pyridinium ylides and photochemical reaction of diazepines.

2.2.1.5 Pyridinium oxide

The photochemical reactivity of pyridinium oxide has been the object of a review.[409] The *N*-oxide of pyridine can be a source of reactive oxygen under photochemical conditions.[410] The excited singlet state ($^1A_1$) was found at 3.81 eV and has π,π^* character, while the triplet ($^3A_1$) was found at 1.66 eV (π,π^*).[411-413]

The irradiation pyridine *N*-oxide gave in low yields pyrrole-2-carbaldehyde (Scheme 2.106), probably through the formation of an oxaziriridine.[414] The same reaction can be performed in higher yields in the presence of $CuSO_4$ (Scheme 2.106).[415]
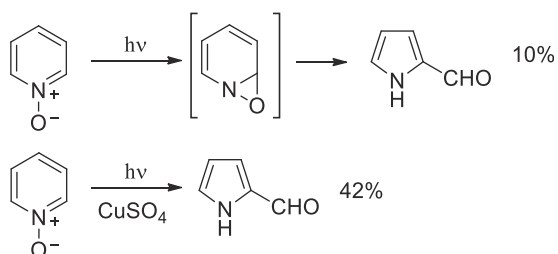
SCHEME 2.106   Photoisomerization of pyridinium oxide.

The use of alkyl substituted pyridine derivatives gave different results where the formation of the phenol is obtained in a complex reaction mixture (Scheme 2.107).[416,417]

In the complex mixture of products described in Scheme 2.107, it is possible to see the formation of the reduced pyridine derivatives. This reaction becomes important in the presence of an electron withdrawing substituent (Scheme 2.108).[418] However, the reaction of 2,6-dicyanopyridine *N*-oxide showed a different reactivity where the formation of an oxazepine is reported (Scheme 2.108).[419] The observed change in the reactivity can be due to a different solvent used in the reaction.

The oxazepine became a significant reaction product also when phenyl substituted pyridine derivatives were used as substrates (Scheme 2.109).[420,421]
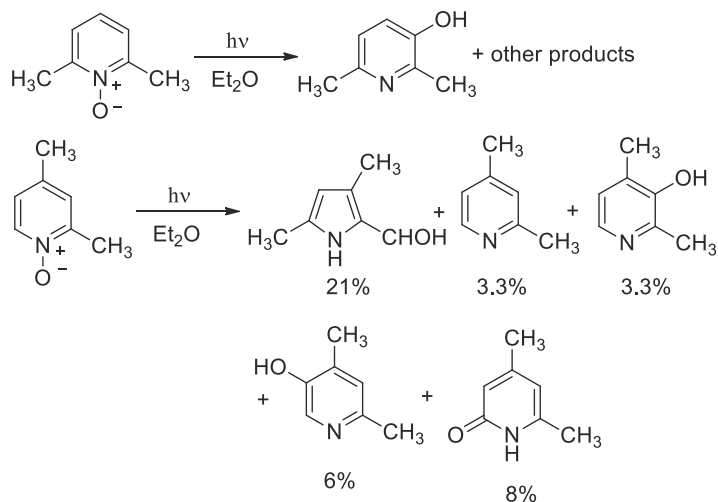
SCHEME 2.107 Photoisomerization of substituted pyridinium oxide derivatives.
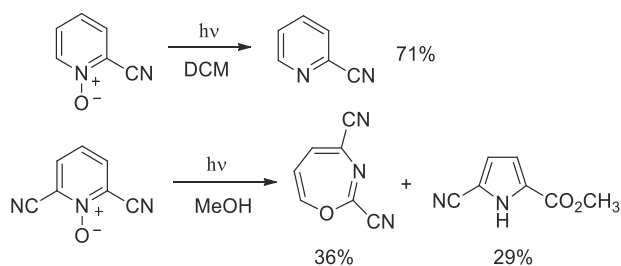
SCHEME 2.108 Photoisomerization of cyano substituted pyridinium oxide derivatives.
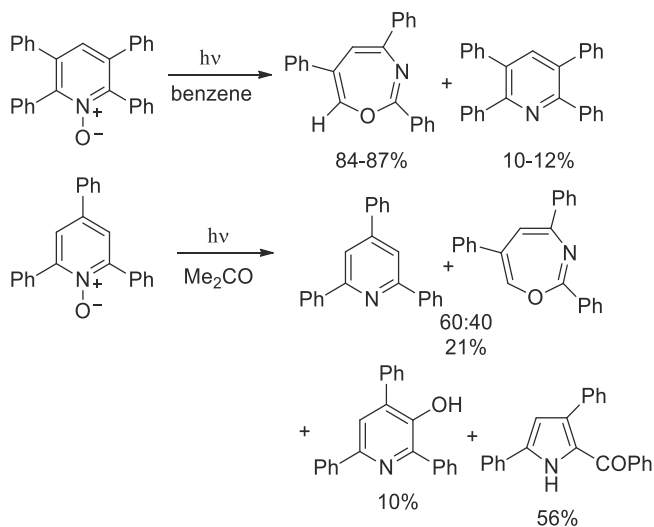
SCHEME 2.109 Photoisomerization of phenyl substituted pyridinium oxide derivatives.

2.2.1.6 Quinolines and isoquinolines

Most the results reported in literature on photochemical isomerization of quinolines and isoquinolines are relative to ylides and *N*-oxides. In fact, the photochemical reaction of pyridinium salts has been reported only in the case of a isoquinoline derivative **158** to give **159** (Scheme 2.110).[422,423] In the case of *N*-oxides, there are clear
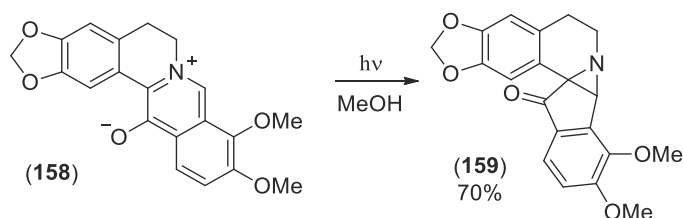
SCHEME 2.110 Photoisomerization of isoquinoline oxide derivative.

evidences about the role of the solvent but this evidence is not present in the case of ylides of quinoline and iso-quinoline derivatives. The reaction products were usually the native heterocycles, the amides and the diazepines. All the reactions can be explained assuming the formation of a diaziridine intermediate. The reaction usually occurred through the first excited singlet state.[424] In Scheme 2.111 we collected some results obtained using quin-oline ylides as starting materials.[424–428]
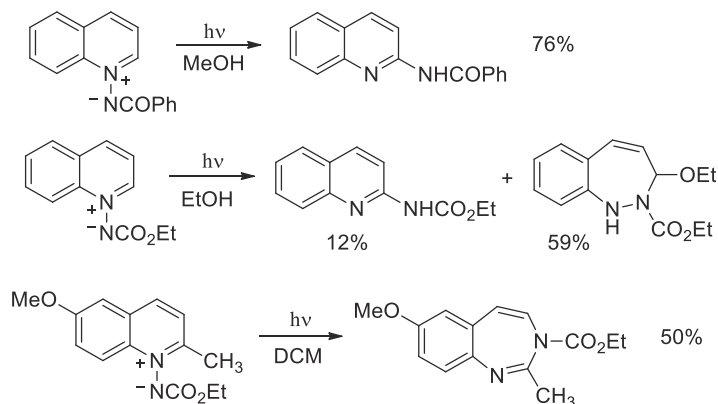
SCHEME 2.111 Photoisomerization of quinoline ylide derivative.

The same behavior was observed working on isoquinoline ylides. In this case, the yields seem to be lower (Scheme 2.112).[424,426,428–430]
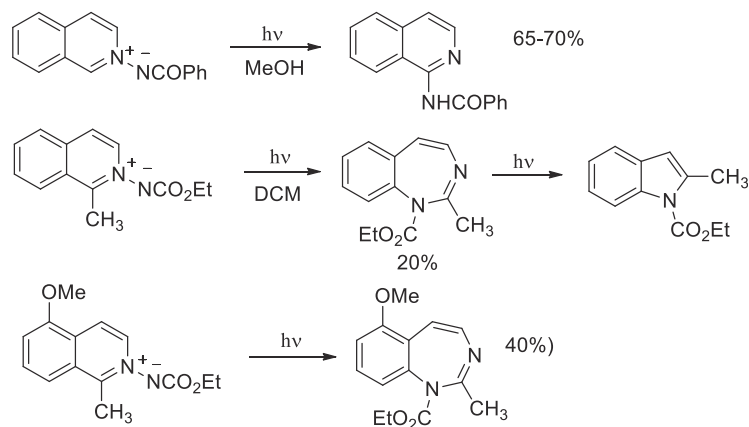
SCHEME 2.112 Photoisomerization of isoquinoline ylide derivatives.

It is noteworthy that the same type of reactivity can be observed also when other heterocycles rings were present in starting material instead of the benzenic ring (Scheme 2.113).[431]
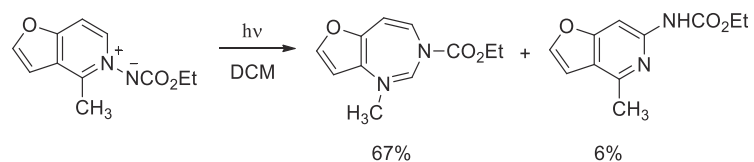
SCHEME 2.113 Photoisomerization of furo[3,2-c]pyridi-nium ylide derivative.

In the case of *N*-oxide of quinoline derivatives lactones, oxazepines, and pyrroles can be obtained. A general mechanism accounting for this type of reactivity has been proposed (Scheme 2.114).[432]
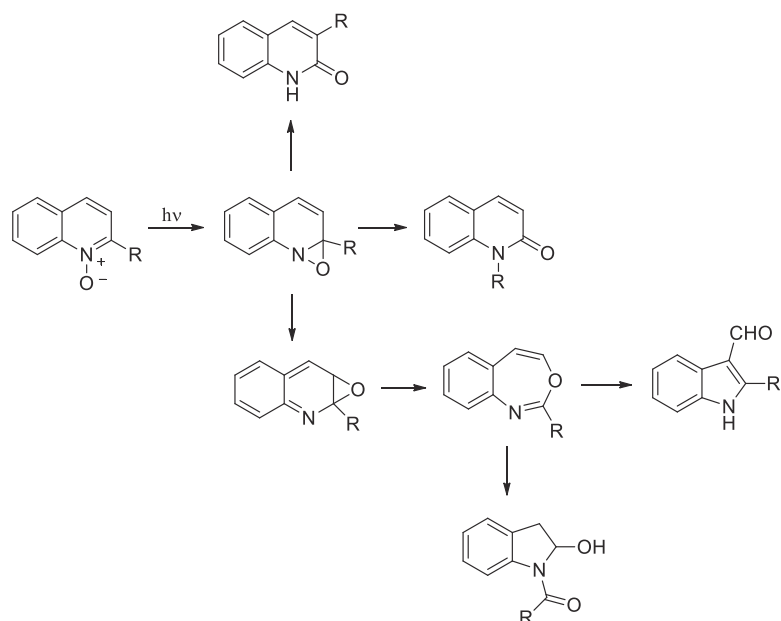
SCHEME 2.114 Proposed mechanism for the photoisomerization of quinoline oxide.

Furthermore, it is evident that polar solvent favored the formation of the lactones, while apolar solvent favored the formation of the oxazines.[433] However, the photochemical behavior is not clear. A study on the N-oxide of a isoquinoline has been reported where the transient absorption of the triplet state has been detected, and the authors supposed that the reactions occurred in the triplet state, while, in another work, the transient absorption of the triplet state has been detected, but its role in the reaction has not been considered important, showing that the reaction occurred in excited singlet state.[434,435] Furthermore, the second study did not find any evidence of the formation of an oxaziridine intermediate in the reaction.[435] However, in the case of N-oxide of quinoline, the intermediate has been isolated and expected from calculations(Scheme 2.115).[436,437]
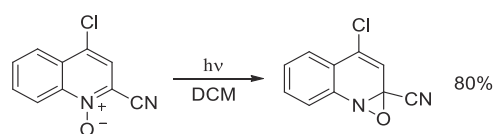
SCHEME 2.115 Photoisomerization of 2-cyano-3-chloroquinoline N-oxide.

Some examples of the observed reactivity on N-oxide of quinolines are reported in Scheme 2.116.[210,438−445]
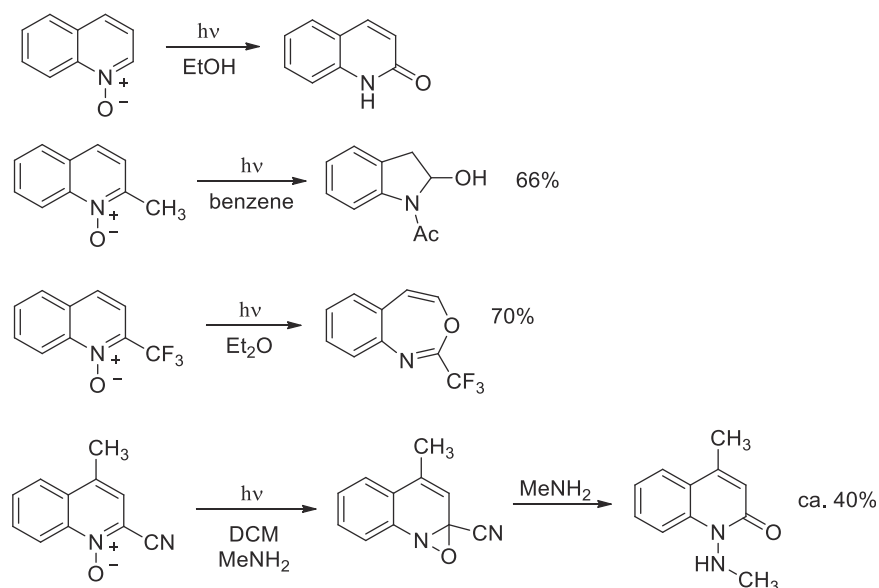
SCHEME 2.116 Photoisomerization of quinoline N-oxide derivatives.

Similar reactions have been described for acridine derivatives (Scheme 2.117)[446−449] and in the case isoquinoline derivatives (Scheme 2.118).[435,445]
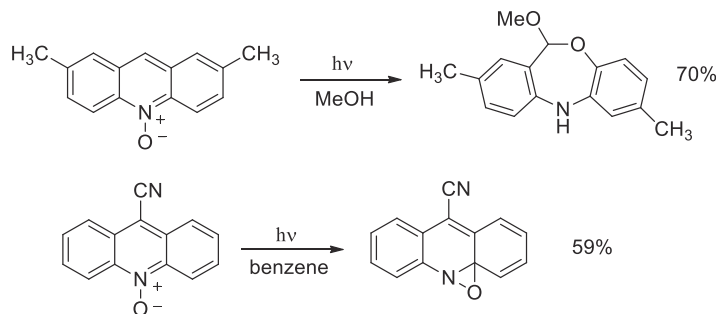
SCHEME 2.117   Photoisomerization of acridine *N*-oxide derivatives.
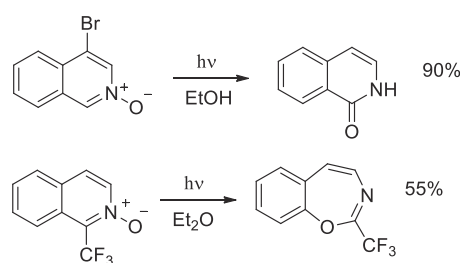
SCHEME 2.118   Photoisomerization of some isoquinoline *N*-oxide derivatives.

2.2.2 Isomerization of diazines

2.2.2.1 Pyrazine

The photoisomerization of pyrazine to pyrimidine has been described several years ago.[450] Furthermore, 2-methylpyrazine gave in gas phase a mixture of 4- and 5-methylpyrimidine, 2,6-dimethylpyrazine gave 4,5-dimethyl-pyrimidine, and 2,5-dimethylpyrazine gave a mixture of 4,6- and 2,5-dimethylpyrimidine (Scheme 2.119).[451] The reaction occurred through the first excited π,π^* singlet state.[451]
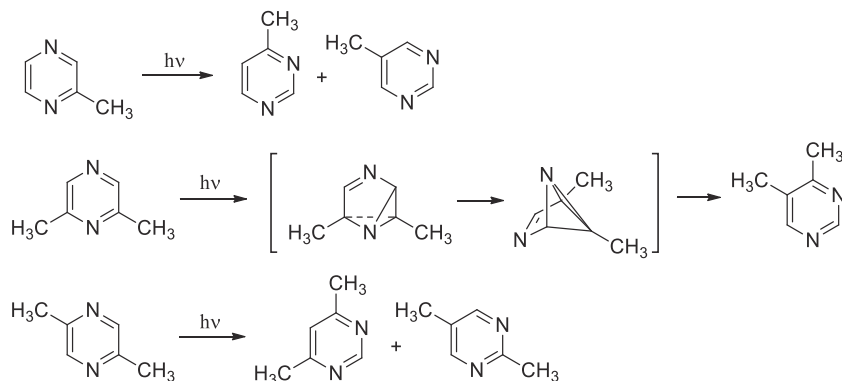
SCHEME 2.119   Photoisomerization of pyrazine derivatives.

The observed isomerization was explained assuming the formation of a benzvalene type structure (Scheme 2.119).[451] More recently a new hypothesis has been proposed where the radiationless decay from S_1 to S_0 of pyrazine occurs through a conical intersection, which results in a rapid $N = C$ bond rotation allowing to obtain the reaction products without the presence of any intermediate.[452]

Some other results on pyrazine derivatives were obtained on *N*-oxide derivatives. This way, the reaction the benzo[*a*]phenazine *N*-oxide (**160**) gave the corresponding oxodiazepine derivative (Scheme 2.120).[453] However, phenazine-5-oxide (**161**) gave a benzimidazole derivative when irradiated in benzene, and a benzoxazole when irradiated in acetonitrile (Scheme 2.120).[454,455] Furthermore, while quinoxaline *N*-oxide and dioxide are reported to give the corresponding 2-hydroxy derivative,[456] some other quinoxaline derivatives gave the corresponding benzimidazole reaction products (Scheme 2.120).[457,458] Finally, 2-aminoquinoxaline derivative can give the benzimidazole when irradiated in acetonitrile, while the reaction afforded a ring opening product if performed in dichloromethane.[459]
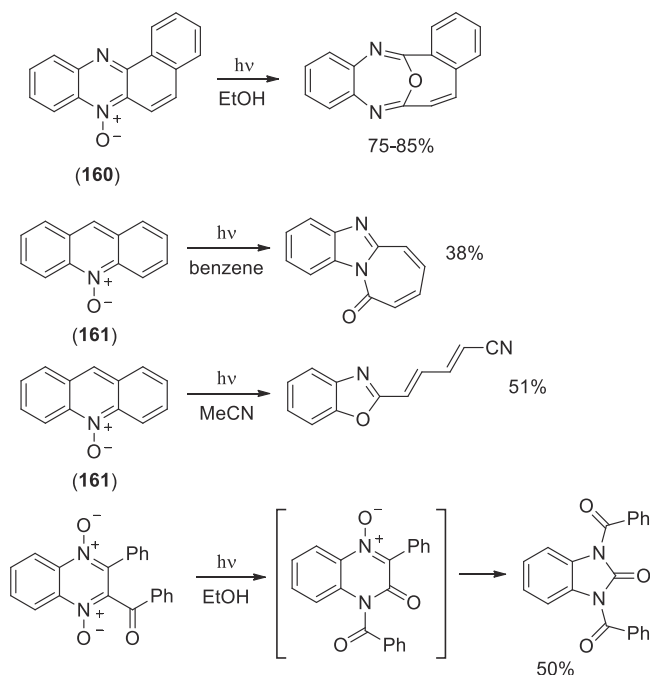
SCHEME 2.120 Photoisomerization of pyrazine *N*-oxide derivatives.

2.2.2.2 Pyridazine

Tetrafluoropyridazine via irradiation gave in almost quantitative yields tetrafluoropyrazine, probably from a singlet n,π* state.[460,461] The irradiation in gas phase of perfluoro-(4,5-bisisopropylpyridazine) allowed to isolate a valence isomers **162** and **163** (Scheme 2.121).[462−464] Compounds **161** and **163**, under the same conditions, can be transformed into the starting pyridazine and in the final pyrazine.
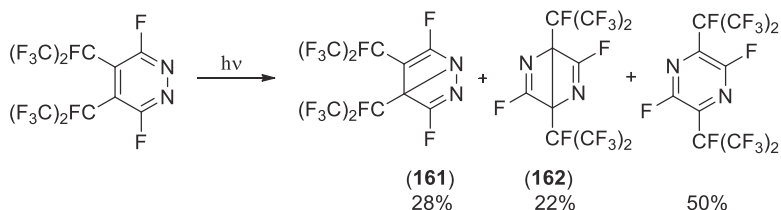
SCHEME 2.121 Photoisomerization of pyridazine derivatives.

On the contrary, the reaction of hexafluorocinnoline (a benzo[*c*]pyridazine) gave the corresponding quinazoline (benzopyrimidine) instead of a quinoxaline.[465] Furthermore, 3-hydroxymethyl-5-hydroxypyridazinium hydroxide, irradiated in ethanol, gave in 75% yield 6-hydroxymethyl-4-hydroxypyrimidine.[466]

The *N*-oxide of pyridazine can give very different reaction products. First of all, the parent reduced compound can be obtained,[467−471] and the *N*-oxide can be used as a source of reactive oxygen able to oxidize alkenes and aromatic compounds.[472,473] Thus the formation of cyclopropenyl derivative has been reported (Scheme 2.122).[468,470,474] Furthermore furan derivatives can be obtained (Scheme 2.122).[468,470,475,476] Finally, pyrazole derivatives can be
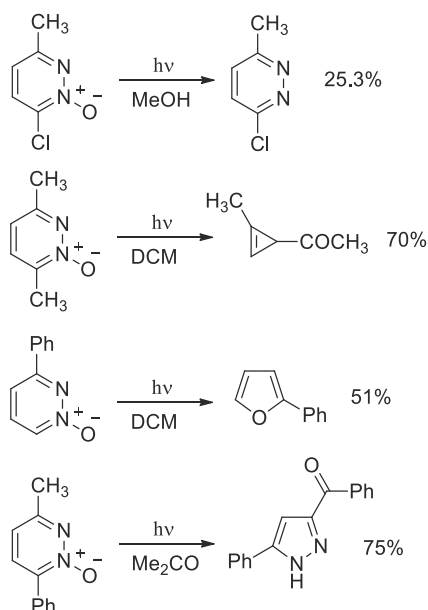
SCHEME 2.122 Photoisomerization of pyridazine *N*-oxide derivatives.

obtained (Scheme 2.122).[476–478] When the reaction gave the cyclopropenyl derivatives, if the reaction is performed in the presence of an amine, the corresponding pyrrole can be obtained, using a reaction just described in the case of furan photochemistry.[479]

This complex behavior can be explained considering several variants of the same photochemical process (Scheme 2.123). The most important unresolved problem is the fact that it not available a general criterion able to explain why a compound gave a furan and another one a pyrazole.
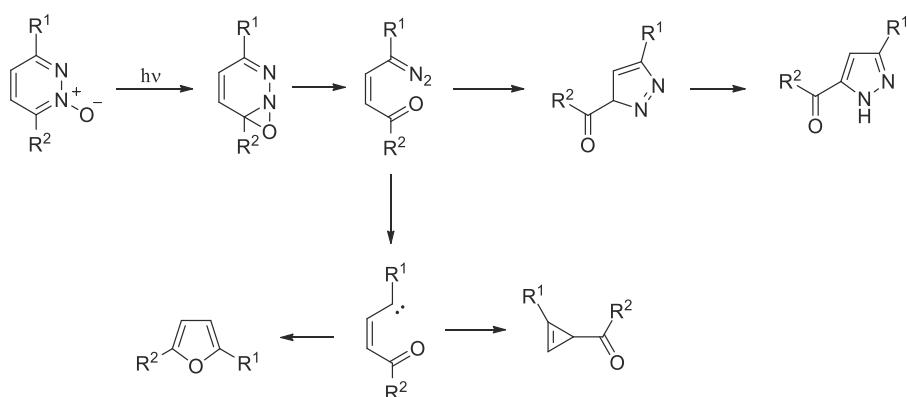
SCHEME 2.123 Proposed mechanism for the photoisomerization of pyridazine *N*-oxide derivatives.

It is noteworthy that the pyridazine **163** can be converted in very high yields into the corresponding pyrazole (Scheme 2.124).[478] The described reaction was applied to a multigram synthesis of hNK₃ antagonist **164** (Scheme 2.124).[478]
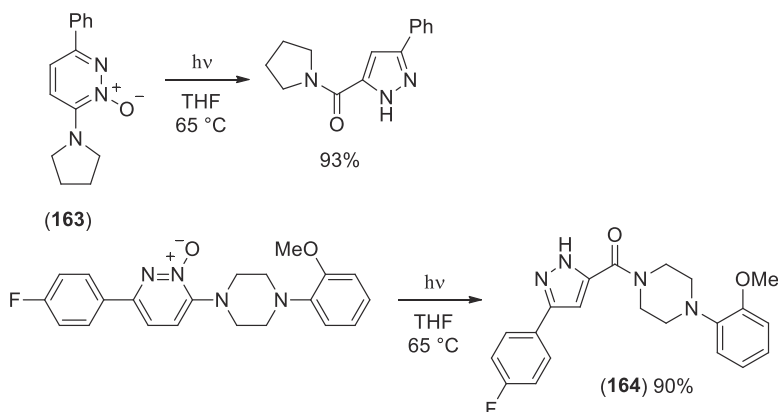
SCHEME 2.124 Photoisomerization of substituted pyridazine *N*-oxide derivatives.

(**163**)

(**164**) 90%

A completely different reactivity has been observed in the case of pyridazine 1,2-dioxides (Scheme 2.125). The authors supposed a mechanism involving the N-N bond fission.[480−482] The reaction of 2-methyl-3(2H)-pyridazinone 1 oxides gave low yields of some lactones (Scheme 2.126).[483]

SCHEME 2.125 Photoisomerization of pyridazine *N,N*-dioxide.

SCHEME 2.126 Photoisomerization of 2-methyl-3(2H)-pyridazinone 1-oxide.
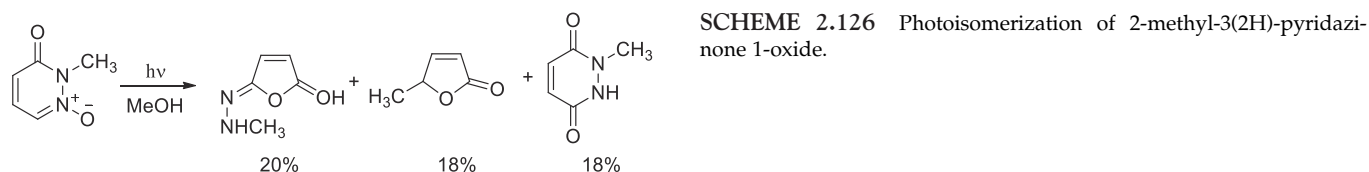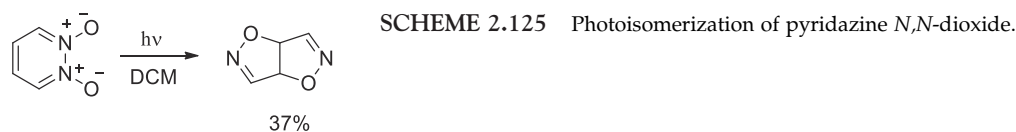
Pyridazine ylides showed a quite similar reactivity. Few examples are reported. In a case, the parent pyridazine was obtained,[484] while, in the second article, pyrazole and cyclopropenyl derivatives were obtained. (Scheme 2.127).[485]

SCHEME 2.127 Photoisomerization of pyridazine ylide derivatives.
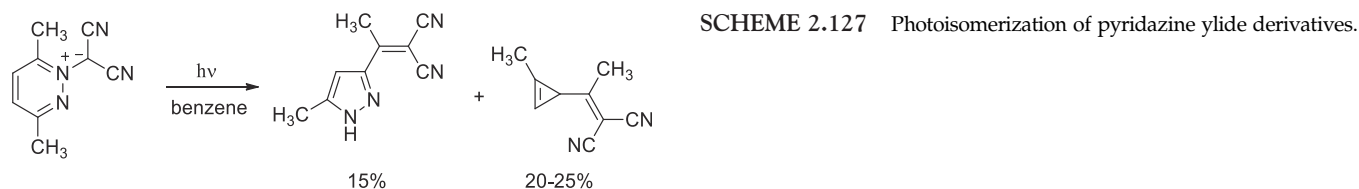
2.2.2.3 Pyrimidine

Mercury sensitized isomerization of pyrimidine gave the corresponding pyrazine, through a mechanism probably involving the formation of the triplet state.[486] The irradiation of 2,6-dimethyl-4-aminopyrimidine in alkaline medium gave in 50% or quantitative yields 2-amino-3-cyanopent-2-en-4-imine.[487,488] This behavior has been rationalized assuming the formation of a Dewar pyrimidine intermediate (Scheme 2.128).

SCHEME 2.128 Photoisomerization of pyrimidine derivatives.
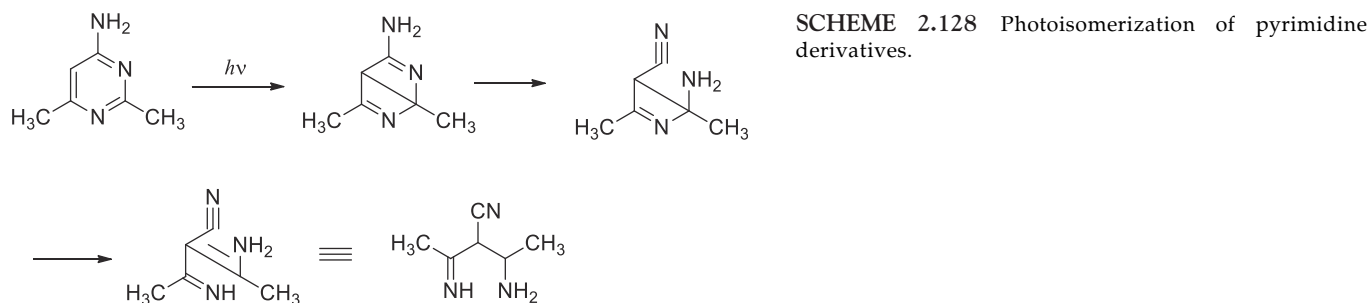
The Dewar isomer has been isolated in the irradiation of the nucleotide **165**. The irradiation of thymidyl-(3′-5′)-thymidine monophosphate can give the [2 + 2]-photoadducts and the (6−4)-photoadduct, that, under UV irradiation, gave the corresponding Dewar isomer (Scheme 2.129).[489,490] The same behavior was observed in the reaction of the involved heterocycles,[491] and in the reaction of the nucleosides, induced by UVA light.[492,493]
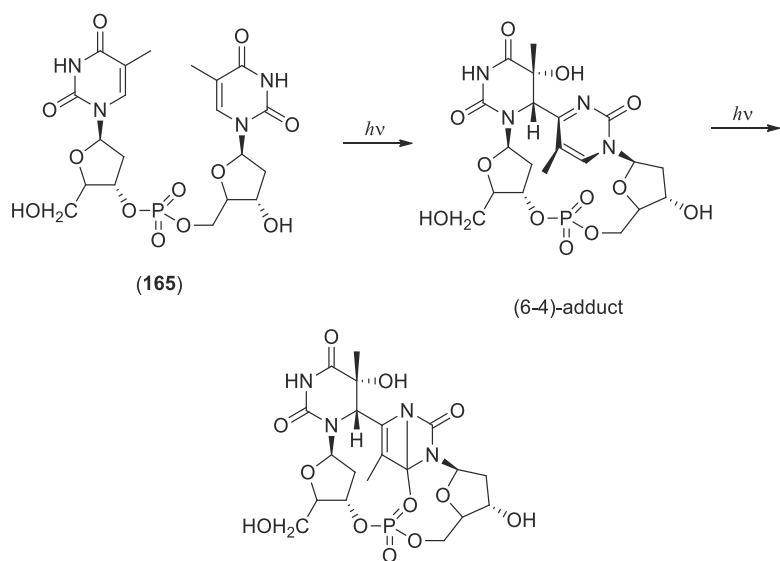
Pyrimidine *N*-oxide showed a photochemical reactivity. The irradiation in benzene of 5-methylpyrimidine *N*-oxide gave with 22% yield a ring opening product, probably deriving from the oxaziridine intermediate (Scheme 2.130).[494,495] The same behavior was observed by using 2-aminopyrimidine *N*-oxide (Scheme 2.130).[495]
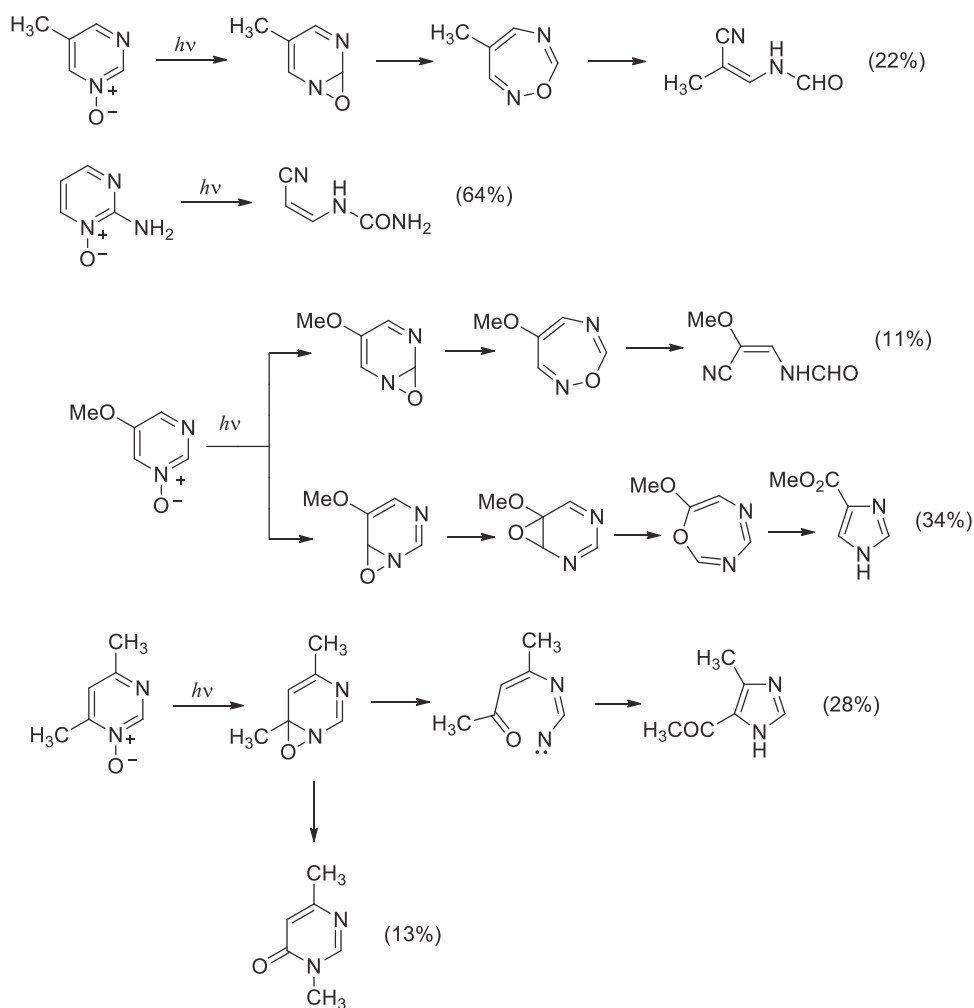
SCHEME 2.130   Photoisomerization of pyrimidine *N*-oxide derivatives.

Furthermore, 5-methoxypyrimidine *N*-oxide gave a ring opening product and an imidazole derivative, while 4,5-dimethylpyrimidine *N*-oxide allowed the formation of both a transposition product and an imidazole derivative (Scheme 2.130)[496,497]

In a study on the photochemistry of 1-hydroxypurines, 1-hydroxyxanthine gave 3-hydroxyxanthine that was reduced to xanthine.[498] The same result was obtained using 1-hydroxy and 1-methoxy-7-methyl-ipoxanthine.[499] It is interesting to note that, while 1-hydroxyipoxanthine was reduced from it first excited triplet state, a singlet state mechanism is invoked in the case of the other compound.

2.2.2.4 Other compounds

The irradiation of a solution of 2-pyrone in diethyl ether afforded in quantitative yields the Dewar isomer **166** (Scheme 2.131).[500] The same compound was obtained performing the reaction in an organized medium.[501]
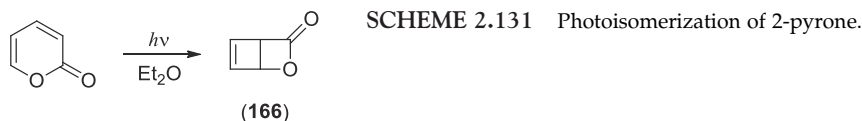
SCHEME 2.131   Photoisomerization of 2-pyrone.

This result is inserted in a complex frame of different results showing a complex and until now unclear rectivity. de Mayo reported that the irradiation of 4,6-dimethyl-2-pyrone in methanol gave methyl 4-acetonylcrotonate, probably deriving from an allene (O = C = CC(CH$_3$) = CHCOCH$_3$) originated by a ring opening reaction on the pyrone.[502] However, the same reaction in another study gave addition products of methanol to 4,6-dimethyl-2-pyrone.[503] The irradiation of a methanolic solution of 2-pyrone allowed to obtain methyl *trans*-4-formyl-3-butenoate, that can be a methanol adduct deriving from both **166** or the allene O = C = CHCH = CHCHO.[504]

In addition, to the problems associated with the different reactivity, another problem is connected with the primary photochemical processes. In studies performed in solid argon at 8 and 20 K, in laser flash photolysis with infrared detection and in matrix isolated FTIR determination on 2-pyrone, the absorptions of the ketene and that of the Dewar isomer have been detected.[505−508] However, a time resolved vibrational absorption spectroscopy study did not revealed the presence of the Dewar isomer.[509]

A completely different reactivity has been described in the case of 4-pyranones. The irradiation of this type of compounds in methylene chloride or in acetonitrile yielded the corresponding 2-pyrones (Scheme 2.132).[510,511]

A possible mechanism has been proposed involving the first excited singlet state (Scheme 2.133).[511]
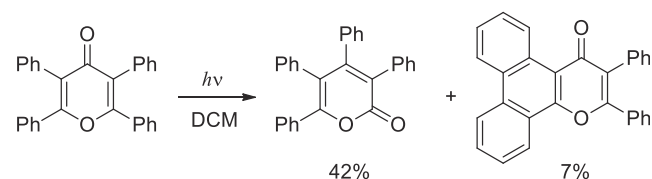
SCHEME 2.132   Photoisomerization of 4-pyrone derivatives.
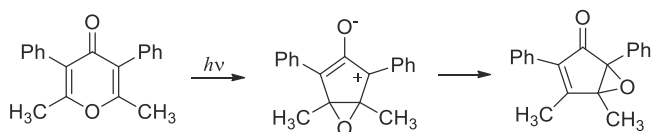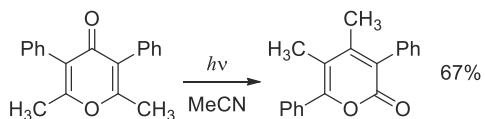
SCHEME 2.133   Proposed mechanism for 4-pyrone derivatives isomerization.
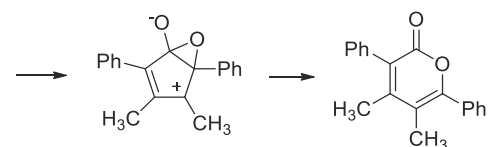
When the reaction is performed in 2,2,2-trifluoroethanol (TFE) cyclopentanone derivatives were obtained (Scheme 2.134).[512]
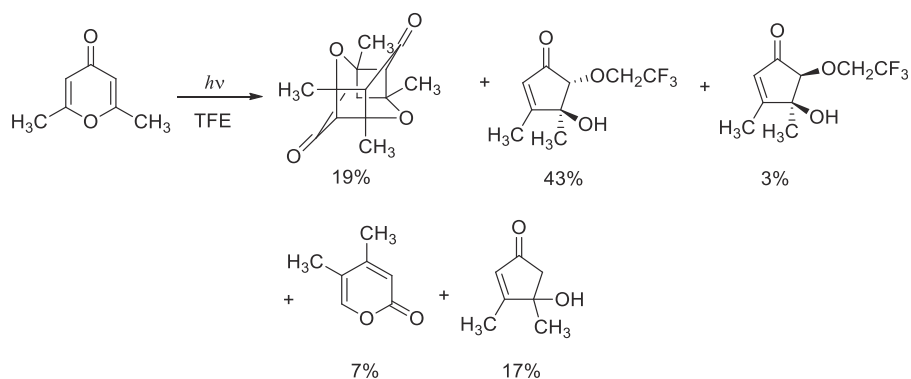
SCHEME 2.134 Photoisomerization of 4-pyrone derivatives in TFE.

The formation of the cyclopentanone derivatives was explained on the basis of the hypothesis reported in Scheme 2.135.
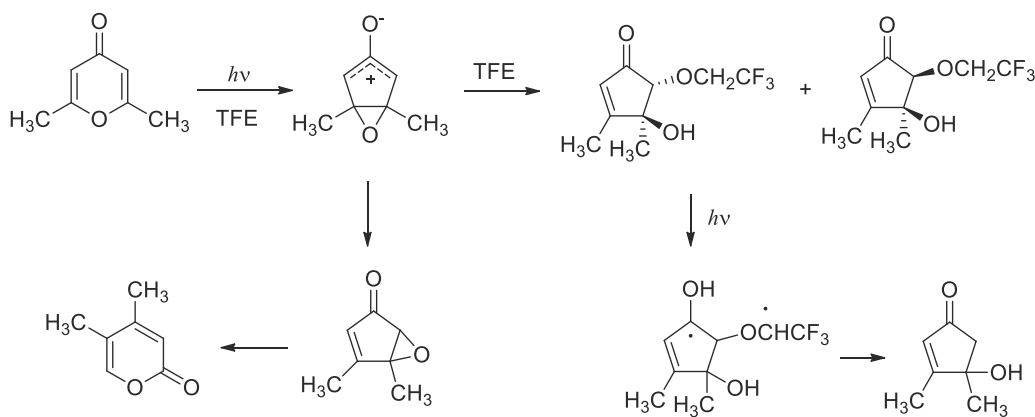
SCHEME 2.135 Proposed mechanism for the photoisomerization of 4-pyrone derivatives.

A quite similar behavior has been reported on some other 4-pyrones irradiated in methanol and in water.[513−516]

The same trends have been observed. The irradiation of 2-pyridones in methanol or in benzene gave the corresponding Dewar isomers.[517−520] 4-Pyridones can be converted into the corresponding 2-pyridinones through the π,π^* singlet state; however, in this case, a Dewar isomer can be involved in the reaction (Scheme 2.136).[521]
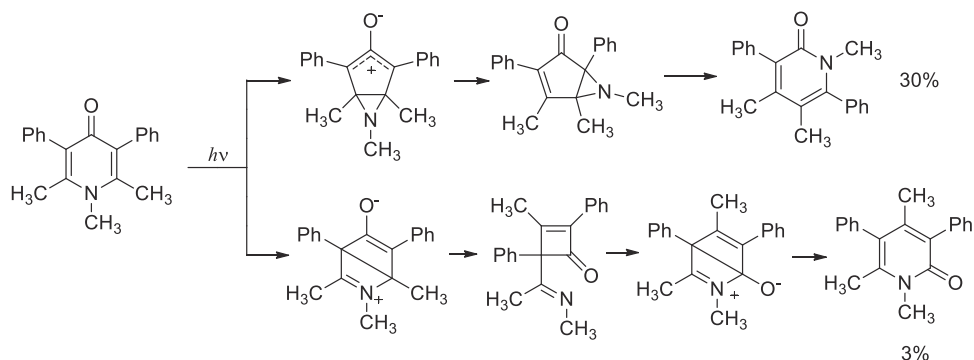
SCHEME 2.136 Photoisomerization of 4-pyridone derivatives.

If 4-pyrones were irradiated in a strong acidic medium (50%−96% H_2SO_4), 4-hydroxypyrilium cations are present and new isomerization reactions have been observed giving 2-hydropyrilium cation when the reaction is performed in concentrated sulfuric acid, and furan derivatives,[522,523] when the reaction is performed in 50% sulfuric acid.[524−526]

Usually, the reaction involved the formation of ring contraction products obtained through 2,6-bridging in the first excited singlet state;[527] however, this behavior is inhibited when bulky substituents are present on the starting materials favoring a mechanism involving a Dewar intermediate (Scheme 2.137).[528]
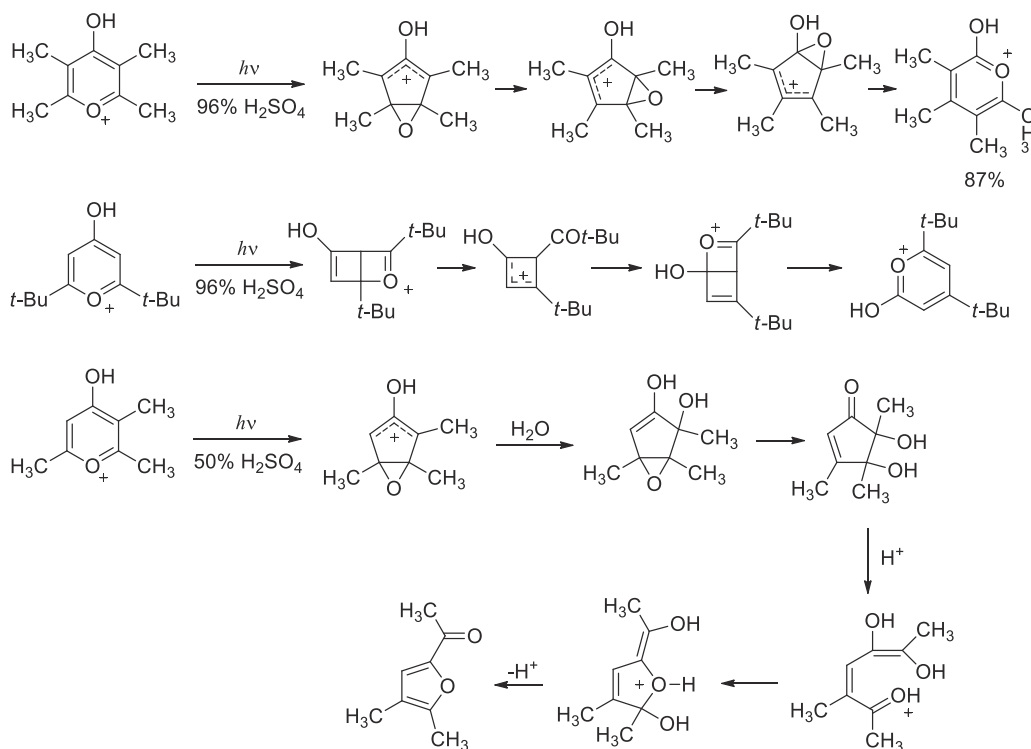
SCHEME 2.137   Photoisomerization of pyrilium cations.

The possible interaction of the 2,6-bridging product with nucleophiles (in the above reported examples, water) has been used in the reaction pyrilium perchlorate with acetic acid or acetonitrile (Scheme 2.138).[529]
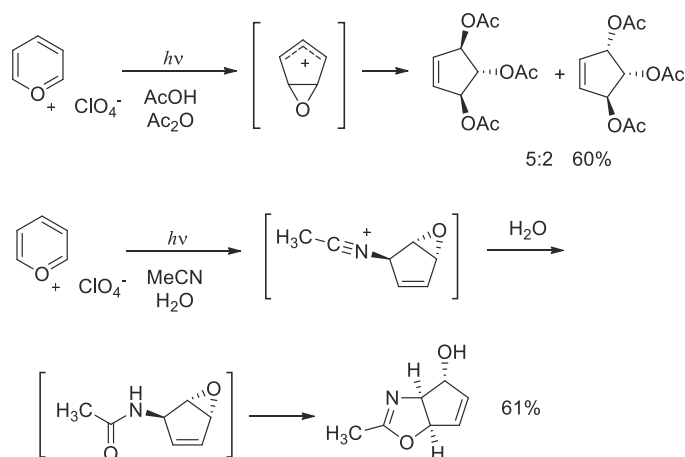
SCHEME 2.138   Photoiomerization of pyrilium perchlorate.

Finally, there are some sparse information on the photochemical behavior of other hexatomic hetero-cycles. Thus 1,2-benzothiazine 1,1-dioxide gave a transposition reaction to 1,2.benzothiazine derivatives (Scheme 2.139).[530] 1,2,3-Benzotriazine 3-*N*-oxides, irradiated in methanol, yielded 3-alkylanthranils.[531] Irradiation of *sym*-tetrazine at 1.6 K gave only HCN.[532] The irradiation of protected silabenzene allowed the formation of the corresponding silabenzvalene.[533] A theoretical study on this reaction showed that this reaction occurs via conical intersection in the singlet state without the formation of any intermediate.[534]
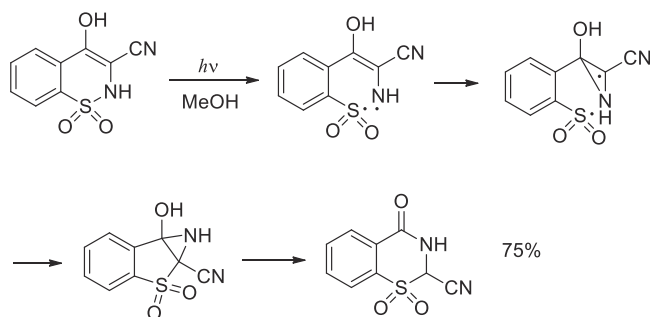
SCHEME 2.139   Photoisomerization of 1,2-benzothiazine 1,1-dioxide.

References

1. Nakatsuji, H.; Kitao, O.; Yonezawa, T. *J. Chem. Phys.* **1985,** *83,* 723−734.
2. Serrano-Andrés, L.; Merchán, M.; Nebot-Gil, I.; Roos, B. O.; Füischer, M. *J. Am. Chem. Soc.* **1993,** *113,* 6184−6197.
3. Palmer, M. H.; Walker, I. C.; Ballard, C. C.; Guest, M. F. *Chem. Phys.* **1995,** *192,* 111−125.
4. Nakano, H.; Tsuneda, T.; Hashimoto, T.; Hirao, K. *J. Chem. Phys.* **1996,** *104,* 2312−2320.
5. Trofimov, A. B.; Schirmer, J. *Chem. Phys.* **1997,** *224,* 175−190.
6. Christiansen, O.; Jørgensen, P. *J. Am. Chem. Soc.* **1998,** *120,* 3423−3430.
7. Wan, J.; Meller, J.; Hada, M.; Ehara, M.; Nakatsuji, H. *J. Chem. Phys.* **2000,** *113,* 7853−7866.
8. Hua, W.; Oesterling, S.; Biggs, J. D.; Zhang, Y.; Ando, H.; de Vivie-Riedle, R.; Fingerhut, B. P.; Mukamel, S. *Struct. Dyn.* **2016,** *3,* 023601.
9. Srinivasan, R. *J. Am. Chem. Soc.* **1967,** *89,* 1758.
10. Srinivasan, R. *J. Am. Chem. Soc.* **1967,** *89,* 4812−4813.
11. Srinivasan, R. *Pure Appl. Chem.* **1968,** *16,* 65−74.
12. Srinivasan, R. *Pure Appl. Chem.* **1969,** *20,* 263−270.
13. Wiberg, K. B.; Bartley, W. J. *J. Am. Chem. Soc.* **1960,** *82,* 6375−6380.
14. Salem, L. *J. Am. Chem. Soc.* **1974,** *96,* 3486−3501.
15. Poquet, E.; Dargelos, A.; Chaillet, M. *Tetrahedron* **1976,** *32,* 1729−1733.
16. Minaev, B. F.; Ågren, A. *EPA Newslett* **1999,** *65,* 7−38.
17. Hiraoka, H.; Srinivasan, R. *J. Chem. Phys.* **1968,** *48,* 2185−2187.
18. Price, D.; Ratajczak, E.; Sztuba, B.; Sarzynski, D. *J. Photochem.* **1987,** *37,* 273−279.
19. Rendall, W. A.; Clement, A.; Torres, M.; Strausz, O. P. *J. Am. Chem. Soc.* **1986,** *108,* 1691−1692.
20. Rendall, W. A.; Torres, M.; Strausz, O. P. *J. Org. Chem.* **1985,** *50,* 3034−3038.
21. Wirth, D.; Lemal, D. M. *J. Am. Chem. Soc.* **1982,** *104,* 847−848.
22. Warrener, R. N.; Pitt, I. G.; Russell, R. A. *J. Chem. Soc., Chem. Commun.* **1984,** 1464−1466.
23. Pitt, I. G.; Russell, R. A.; Warrener, R. N. *J. Chem. Soc., Chem. Commun.* **1984,** 1466−1467.
24. Pitt, I. G.; Russell, R. A.; Warrener, R. N. *J. Am. Chem. Soc.* **1985,** *107,* 7176−7178.
25. Warrener, R. N.; Pitt, I. G.; Russell, R. A. *Aust. J. Chem.* **1991,** *44,* 1275−1292.
26. Boriack, C. J.; Laganis, E. D.; Lemal, D. M. *Tetrahedron Lett.* **1978,** 1015−1018.
27. Kobayashi, Y.; Hanzawa, Y.; Nakanishi, Y.; Kashiwagi, T. *Tetrahedron Lett.* **1978,** 1019−1022.
28. Latajka, Z.; Ratajczak, H.; Orville-Thomas, W. J.; Ratajczak, E. *J. Mol. Struct. (Theochem)* **1981,** *85,* 303−309.
29. D'Auria, M. In *Targets in Heterocyclic Systems, Chemistry and Properties;* Attanasi, O. A., Spinelli, D., Eds.; 2; Italian Society of Chemistry: Rome, 1999; pp 233−279.
30. D'Auria, M. *J. Org. Chem.* **2000,** *65,* 2494−2498.
31. Gavrilov, N.; Salzmann, S.; Marian, C. M. *Chem. Phys.* **2008,** *349,* 269−277.
32. Gromov, E. V.; Trofimov, A. B.; Gatti, F.; Köppel, H. *J. Chem. Phys.* **2010,** *133,* 164309.
33. Fuji, T.; Suzuki, Y.-I.; Horio, T.; Suzuki, T.; Mitrić, R.; Werner, U.; Bonačić-Koutecký, V. *J. Chem. Phys.* **2010,** *133,* 234303.
34. Stenrup, M.; Larson, Å. *Chem. Phys.* **2011,** *379,* 6−12.
35. Gromov, E. V.; Lévéque, C.; Gatti, F.; Burghardt, I.; Köppel, H. *J. Chem. Phys.* **2011,** *135,* 164305.
36. Hiraoka, H.; Srinivasan, R. *J. Am. Chem. Soc.* **1968,** *90,* 2720−2721.
37. Hiraoka, H. *J. Chem. Phys.* **1970,** *74,* 574−581.
38. Buss, S.; Jug, K. *J. Am. Chem. Soc.* **1987,** *109,* 1044−1050.
39. Su, M.-D. *J. Phys. Chem. A* **2008,** *112,* 194−198.
40. Boué, S.; Srinivasan, R. *J. Am. Chem. Soc.* **1970,** *92,* 1824−1828.

41. Couture, A.; Lablache-Combier, A. *J. Chem. Soc. D.* **1971,** 891−892.
42. Couture, A.; Delavallee, A.; Lablache-Combier, A.; Párkányl, C. *Tetrahedron* **1975,** *31,* 785−796.
43. Tsuchiya, J.; Arai, H.; Igeta, M. *Chem. Pharm. Bull.* **1973,** *21,* 1516−1519.
44. Tsuchiya, J.; Aria, H.; Igeta, M. *Tetrahedron* **1973,** *29,* 2747−2751.
45. Kobayashi, Y.; Ando, A.; Kawada, K.; Kumadaki, I. *J. Org. Chem.* **1980,** *45,* 2968−2970.
46. van Tamelen, E. E.; Whitesides, T. H. *J. Am. Chem. Soc.* **1968,** *90,* 3894−3896.
47. van Tamelen, E. E.; Whitesides, T. H. *J. Am. Chem. Soc.* **1971,** *93,* 6129−6140.
48. Barton, T. J.; Hussmann, G. P. *J. Am. Chem. Soc.* **1983,** *105,* 6316−6318.
49. Srinivasan, R.; Hiraoka, H. *Tetrahedron Lett.* **1969,** 2767−2770.
50. Gandini, A.; Parsons, J. M.; Back, R. A. *Can. J. Chem.* **1976,** *54,* 3095−3101.
51. Kuş, N.; Reva, I.; Fausto, R. *J. Phys. Chem. A* **2010,** *114,* 12427−12436.
52. Samuel, C. J.; Rowlands, N. *J. Photochem. Photobiol., A: Chem.* **1994,** *78,* 15−17.
53. Hiraoka, H. *J. Chem. Soc. D.* **1971,** 1610−1611.
54. Hiraoka, H. *Tetrahedron* **1973,** *29,* 2955−2961.
55. Kemula, W.; Zawadowska, J. *Bull. Acad. Polon. Sci., Ser. Sci. Chim.* **1969,** *17,* 599−603.
56. Hunt, R.; Reid, S. T. *J. Chem. Soc., Perlin Trans.* **1972,** *1,* 2527−2528.
57. Mullen, P. A.; Orloff, M. K. *J. Chem. Phys.* **1969,** *51,* 2276−2279.
58. Dahl, J. P.; Hanson, A. E. *Theor. Chim. Acta* **1963,** *1,* 199−205.
59. Chiorboli, P.; Rastelli, A.; Momicchioli, F. *Theor. Chim. Acta* **1966,** *5,* 1−10.
60. Del Bene, J.; Jaffe, H. H. *J. Chem. Phys.* **1968,** *48,* 4050−4055.
61. Tanaka, K.; Nomura, T.; Nora, T.; Tatewaki, T. H.; Takada, T.; Kashiwagi, H.; Sasaki, F.; Ohno, K. *J. Chem. Phys.* **1977,** *67,* 5738−5741.
62. Butscher, W.; Thuneman, K. H. *Chem. Phys. Lett.* **1978,** *57,* 224−229.
63. Rawlings, D. C.; Davidson, E. R. *Chem. Phys. Lett.* **1983,** *98,* 424−427.
64. Rawlings, D. C.; Davidson, E. R. *Int. J. Quantum Chem.* **1984,** *26,* 237−250.
65. Trofimov, A. B.; Schirmer, J. *Chem. Phys.* **1997,** *214,* 153−170.
66. Pickett, L. W.; Corning, M. E.; Wieder, G. K. M.; Semenov, D. A.; Buckley, J. M. *J. Am. Chem. Soc.* **1953,** *75,* 1618−1622.
67. Horváth, G.; Kiss, A. I. *Spetrochim. Acta A* **1967,** *23,* 921−924.
68. Derrick, P. J.; Asbring, L.; Edqvist, O.; Jonsson, B. O.; Lindholm, E. *Int. J. Mass. Spectrom. Ion. Phys.* **1971,** *6,* 161−175.
69. Bavia, M.; Bertinelli, F.; Taliani, C.; Zauli, C. *Mol. Phys.* **1975,** *31,* 479−489.
70. Van Veen, E. H. *Chem. Phys. Lett.* **1976,** *41,* 535−539.
71. Flicker, W. M.; Mosher, O. A.; Kupperman, A. *Chem. Phys. Lett.* **1976,** *38,* 489−492.
72. Flicker, W. M.; Mosher, O. A.; Kupperman, A. *J. Chem. Phys.* **1976,** *64,* 1315−1321.
73. Sanche, L. *J. Chem. Phys.* **1979,** *71,* 4860−4882.
74. Cooper, C. D.; Williamson, A. D.; Miller, J. C.; Compton, R. N. *J. Chem. Phys.* **1980,** *73,* 1527−1537.
75. Roebber, J. L.; Gerrity, D. P.; Hemley, R.; Vaida, V. *Chem. Phys. Lett.* **1980,** *75,* 104−106.
76. Palmer, M. H.; Walker, I. C.; Guest, M. F. *Chem. Phys.* **1998,** *238,* 179−199.
77. Christiansen, O.; Gauss, J.; Stanton, J. F.; Jørgensen, P. *J. Chem. Phys.* **1999,** *111,* 525−537.
78. Wu, E. C.; Heicklen, J. *J. Am. Chem. Soc.* **1971,** *93,* 3432−3437.
79. Lippert, H.; Ritze, H.-H.; Hertel, I. V.; Radloff, W. *ChemPhysChem* **2004,** *5,* 1423−1427.
80. Wu, E. C.; Heicklen, J. *Can. J. Chem.* **1972,** *50,* 1678−1689.
81. Warrener, R. N.; Amaresekara, A. S.; Russell, R. A. *Chem. Commun.* **1996,** 1519−1520.
82. Vysotskii, Y. B.; Sivyakova, L. N. *Chem. Heterocycl. Comp.* **1986,** *22,* 133−140.
83. Patterson, J. M.; Burka, L. T. *Tetrahedron Lett.* **1969,** 2215−2217.
84. Shizuka, H.; Okutsu, E.; Mori, Y.; Tanaka, I. *Mol. Photochem.* **1969,** *1,* 135−141.
85. Patterson, J. M.; Bruser, D. M. *Tetrahedron Lett.* **1973,** 2959−2962.
86. Black, D. S. C.; Blackman, N. A. *Aust. J. Chem.* **1979,** *32,* 2035−2039.
87. Black, D. S. C.; Blackman, N. A.; Johnstone, L. M. *Aust. J. Chem.* **1979,** *32,* 2041−2048.
88. Santos, O.; Testa, A. C.; O'Sullivan, M. *J. Photochem.* **1983,** *23,* 257−263.
89. Patterson, J. M.; Ferry, J. D.; Boyd, M. R. *J. Am. Chem. Soc.* **1973,** *95,* 4356−4360.
90. Moody, C. I.; Ward, J. G. *J. Chem. Soc., Chem. Commun.* **1984,** 646−647.
91. Moody, C. I.; Ward, J. G. *J. Chem. Soc., Perkin Trans. 1* **1984,** 2903−2909.
92. Padwa, A.; Gruber, R.; Pashayan, D.; Bursey, M.; Dusold, L. *Tetrahedron Lett.* **1968,** 3659−3662.
93. Patjens, J.; Ghaffari-Tabrizi, R.; Margaretha, P. *Helv. Chim. Acta* **1986,** *69,* 905−907.
94. Hiraoka, H. *J. Chem. Soc. D.* **1970,** 1306.
95. Barltrop, J. A.; Day, A. C.; Ward, R. W. *J. Chem. Soc., Chem. Commun.* **1978,** 131−133.
96. Barltrop, J. A.; Day, A. C.; Moxon, P. D.; Ward, R. R. *J. Chem. Soc., Chem. Commun.* **1975,** 786−787.
97. Behrens, S.; Jug, K. *J. Org. Chem.* **1990,** *55,* 2288−2294.
98. D'Auria, M. *Heterocycles* **1999,** *50,* 1115−1136.
99. Su, M.-D. *J. Phys. Chem. A* **2006,** *116,* 12653−12661.
100. Park, S.-H.; Ha, H.-J.; Lim, C.; Lim, D.-K.; Lee, K.-H.; Park, Y.-T. *Bull. Korean Chem. Soc.* **2005,** *26,* 1190−1196.
101. Barton, T. J.; Hussmann, G. P. *J. Org. Chem.* **1985,** *50,* 5881−5882.
102. Elliott, L. D.; Berry, M.; Orr-Ewing, A. J.; Booker-Milburn, K. I. *J. Am. Chem. Soc.* **2007,** *129,* 3078−3079.
103. Maskill, K. G.; Knowles, J. P.; Elliott, L. D.; Alder, R. W.; Booker-Milburn, K. I. *Angew. Chem. Int. (Ed.)* **2013,** *52,* 1499−1502.
104. Koovits, P. J.; Knowles, J. P.; Booker-Milburn, K. I. *Org. Lett.* **2016,** *18,* 5608−5611.
105. Weinkauf, R.; Lehr, L.; Schlag, E. W.; Salzmann, S.; Marian, C. M. *Phys. Chem. Chem. Phys.* **2008,** *10,* 393−404.

106. Salznìmann, S.; Kleinschmidt, M.; Tatchen, J.; Weinkauf, R.; Marian, C. M. *Phys. Chem. Chem. Phys.* **2008,** *10,* 380−392.
107. Weibe, H. A.; Heicklen, J. *Can. J. Chem.* **1969,** *47,* 2965−2979.
108. Rendall, W. A.; Torres, M.; Strausz, O. P. *J. Am. Chem. Soc.* **1985,** *107,* 723−724.
109. Wynberg, H.; van Driel, H. *J. Am. Chem. Soc.* **1965,** *87,* 3998−4000.
110. Kellogg, R. M.; Wynberg, H. *Tetrahedron Lett.* **1968,** 5895−5898.
111. Wynberg, H.; Kellogg, R. M.; van Driel, H.; Beekhuis, G. E. *J. Am. Chem. Soc.* **1967,** *89,* 3501−3505.
112. Wynberg, H. *Acc. Chem. Res.* **1971,** *4,* 65−73.
113. Kellogg, R. M. *Tetrahedron Lett.* **1972,** 1429−1432.
114. Matsushita, T.; Tanaka, H.; Nishimoto, K.; Osamura, Y. *Theor. Chem. Acc.* **1983,** *63,* 55−68.
115. Jug, K.; Schluff, H.-P. *J. Org. Chem.* **1991,** *56,* 129−134.
116. D'Auria, M. *J. Photochem. Photobiol. A: Chem.* **2002,** *149,* 31−37.
117. Gómez, S.; Osorio, E.; Dzib, E.; Islas, R.; Restrepo, A.; Merino, G. *Molecules* **2020,** *25,* 284.
118. Kellogg, R. M.; Dik, J. K.; van Driel, H.; Wynberg, H. *J. Org. Chem.* **1970,** *35,* 2737−2741.
119. Braslavsky, S.; Wiebe, H. A.; Heicklen, J. *Centre for Air Environment Studies,* Publication No. 164-70, Pennsylvania State University, 1970.
120. Greenberg, A.; Liebman, J. F.; van Vechten, D. *Tetrahedron* **1980,** *36,* 1161−1166.
121. Wiebe, H. A.; Braslavsky, S.; Heicklen, J. *Can. J. Chem.* **1972,** *50,* 2721−2724.
122. Kobayashi, Y.; Kumadaki, I.; Ohsawa, A.; Sekine, Y. *Tetrahedron Lett.* **1974,** 2841−2844.
123. Kobayashi, Y.; Kumadaki, I.; Ohsawa, Y.; Sekine, Y.; Mochizuki, H. *Chem. Pharm. Bull.* **1975,** *25,* 2773−2778.
124. Kobayashi, Y.; Kumadaki, I.; Ohasawa, A.; Sekine, Y. *Tetrahedron Lett.* **1975,** 1639−1642.
125. Kobayashi, Y.; Kawada, K.; Ando, A.; Kumadaki, I. *Heterocycles* **1983,** *20,* 174.
126. Kobayashi, Y.; Kawada, K.; Ando, A.; Kumadaki, I. *Tetrahedron Lett.* **1984,** *25,* 1917−1920.
127. Couture, A.; Lablache-Combier, A. *J. Chem. Soc. D.* **1969,** 524−525.
128. Couture, A.; Lablache-Combier, A. *Tetrahedron* **1971,** *27,* 1059−1068.
129. Su, M.-D. *J. Comp. Chem.* **2010,** *31,* 43−56.
130. Wynberg, H.; Kellogg, R. M.; van Driel, H.; Beekhuis, G. E. *J. Am. Chem. Soc.* **1966,** *88,* 5047−5048.
131. Wynberg, H.; van Driel, H. *Chem. Comm. (Lond.)* **1966,** 203−204.
132. Wynberg, H.; van Driel, H.; Kellogg, R. M.; Buter, J. *J. Am. Chem. Soc.* **1976,** *89,* 3487−3494.
133. Kellogg, R. M.; Wynberg, H. *J. Am. Chem. Soc.* **1967,** *89,* 3495−3498.
134. Wynberg, H.; Beekhuis, G. E.; van Driel, H.; Kellogg, R. M. *J. Am. Chem. Soc.* **1967,** *89,* 3498−3500.
135. Wynberg, H.; van Bergen, T. J.; Kellogg, R. M. *J. Org. Chem.* **1969,** *34,* 3175−3178.
136. Wynberg, H.; Sinnige, H. J. M.; Creemers, H. M. J. C. *J. Org. Chem.* **1971,** *36,* 1011−1013.
137. Arnold, D. R.; Birtwell, R. J.; Clarke, B. M. *Can. J. Chem.* **1974,** *52,* 1681−1687.
138. Arnold, D. R.; Clarke, B. M. *Can. J. Chem.* **1975,** *53,* 1−11.
139. D'Auria, M.; De Mico, A.; D'Onofrio, F.; Piancatelli, G. *Gazz. Chim. Ital.* **1986,** *116,* 747−748.
140. Antonioletti, R.; D'Auria, M.; D'Onofrio, F.; Piancatelli, G.; Scettri, A. *J. Chem. Soc., Perkin Trans. 1* **1986,** 1755−1758.
141. D'Auria, M.; De Mico, A.; D'Onofrio, F.; Piancatelli, G. *J. Chem. Soc., Perkin Trans. 1* **1987,** 1777−1780.
142. D'Auria, M.; De Mico, A.; D'Onofrio, F.; Piancatelli, G. *J. Org. Chem.* **1987,** *52,* 5243−5247.
143. D'Auria, M.; De Mico, A.; D'Onofrio, F.; Piancatelli, G. *Gazz. Chim. Ital.* **1989,** *119,* 381−384.
144. D'Auria, M.; De Mico, A.; D'Onofrio, F.; Mendola, D.; Piancatelli, G. *J. Photochem. Photobiol. A: Chem.* **1989,** *47,* 191−201.
145. D'Auria, M. *Gazz. Chim. Ital.* **1994,** *124,* 195−197.
146. D'Agostini, A.; D'Auria, M. *J. Chem. Soc., Perkin Trans. 1* **1994,** 1245−1249.
147. D'Auria, M.; Racioppi, R. *Heterocycles* **2009,** *78,* 737−748.
148. Barltrop, J. A.; Day, A. C.; Irving, E. *J. Chem. Soc., Chem. Commun.* **1979,** 881−883.
149. Gurria, G. M.; Posner, G. H. *J. Org. Chem.* **1973,** *38,* 2419−2420.
150. Wan, Z.; Jenks, W. S. *J. Am. Chem. Soc.* **1995,** *117,* 2667−2668.
151. Gregory, D. D.; Wan, Z.; Jenks, W. S. *J. Am. Chem. Soc.* **1997,** *119,* 94−102.
152. Nag, M.; Jenks, W. S. *J. Org. Chem.* **2005,** *70,* 3458−3463.
153. Arima, K.; Ohira, D.; Watanabe, M.; Miura, A.; Mataka, S.; Thiemann, T.; Iniesta Valcarcel, J.; Walton, D. J. *Photochem. Photobiol. Sci.* **2005,** *4,* 808−816.
154. Heying, M. J.; Nag, M.; Jenks, W. S. *J. Phys. Org. Chem.* **2008,** *21,* 915−924.
155. Galenko, E. E.; Khlebnikov, A. F.; Novikov, M. S. *Khim. Geterotsik. Soedin.* **2016,** *52,* 637−650.
156. Fonseca, S. M.; Burrows, H. D.; Nunes, C. M.; Pinho e Melo, T. M. V. D.; D'Albuquerque Rocha Gonsalves, A. M. *Chem. Phys. Lett.* **2005,** *414,* 98−101.
157. Singh, B.; Ullman, E. F. *J. Am. Chem. Soc.* **1966,** *88,* 1844−1845.
158. Kurtz, D. W.; Schechter, H. S. *Chem. Commun. (Lond.)* **1966,** 689−690.
159. Singh, B.; Ullman, E. F. *J. Am. Chem. Soc.* **1967,** *89,* 6911−6916.
160. Singh, B.; Zweig, A.; Gallivan, J. B. *J. Am. Chem. Soc.* **1972,** *94,* 1199−1206.
161. Padwa, A.; Smolanoff, J.; Tremper, A. *J. Am. Chem. Soc.* **1975,** *97,* 4682−4691.
162. Tanaka, H.; Osamura, Y.; Matsushita, T.; Nishimoto, K. *Bull. Chem. Soc. Jpn.* **1981,** *54,* 1293−1298.
163. Nunes, C. M.; Reva, I.; Pinho e Melo, T. M. V. D.; Fausto, R. *J. Org. Chem.* **2012,** *77,* 8723−8732.
164. Sato, T.; Saito, K. *J. Chem. Soc., Chem. Commun.* **1974,** 781−782.
165. Sato, T.; Yamamoto, K.; Fukui, K.; Saito, K.; Hayakawa, K.; Yoshile, S. *J. Chem. Soc., Perkin Trans. 1* **1976,** 783−787.
166. Nunes, C. M.; Reva, I.; Fausto, R. *J. Org. Chem.* **2013,** *78,* 10657−10665.
167. Ullman, E. F. *Acc. Chem. Res.* **1968,** *1,* 353−359.
168. Murature, D. A.; Perez, J. D.; De Bertorello, M. M.; Bertorello, H. E. *Ann. Assoc. Quim. Argentina* **1976,** *64,* 337−340.

169. Su, M.-D. *J. Phys. Chem. A* **2015,** *119*, 9666−9669.
170. Cao, J. *J. Chem. Phys.* **2015,** *142*, 244302.
171. Sauers, R. R.; Hadel, L. M.; Scimone, A. A.; Stevenson, T. A. *J. Org. Chem.* **1990,** *55*, 4011−4019.
172. Pavlik, J. W.; Martin, H., St.; Lambert, K. A.; Lowell, J. A.; Tsefrikas, V. M.; Eddins, C. K.; Kebede, N. *J. Heterocycl. Chem.* **2005,** *42*, 273−281.
173. Fonseca, S. M.; Burrows, H. D.; Nunes, C. M.; Pinho e Melo, T. M. V. D. *Chem. Phys. Lett.* **2009,** *474*, 84−87.
174. Pusch, S.; Kowalczyk, D.; Opatz, T. *J. Org. Chem.* **2016,** *81*, 4170−4178.
175. Pusch, S.; Schollmeyer, D.; Opatz, T. *Org. Lett.* **2016,** *18*, 3043−3045.
176. Pusch, S.; Opatz, T. *Org. Lett.* **2014,** *16*, 5430−5433.
177. Paternoga, J.; Opatz, T. *Eur. J. Org. Chem.* **2019,** 7067−7078.
178. Wang, Q.; Zhang, Z.; Zhang, X.; Zhang, J.; Kang, Y.; Peng, J. *RSC Adv.* **2015,** *5*, 4788−4794.
179. Nishiwaki, T.; Nakano, A.; Matsuoka, H. *J. Chem. Soc. C.* **1970,** 1825−1829.
180. Wamhoff, H. *Chem. Ber.* **1972,** *105*, 748−752.
181. Buscemi, S.; Frenna, V.; Vivona, N. *Heterocycles* **1991,** *32*, 1765−1772.
182. Tiefenthaler, H.; Dörsheln, W.; Göth, H.; Schmid, H. *Helv. Chim. Acta* **1967,** *50*, 2244−2258.
183. Good, R. H.; Jones, G. *J. Chem. Soc. C.* **1971,** 1196−1198.
184. Padwa, A.; Chen, E.; Ku, A. *J. Am. Chem. Soc.* **1975,** *97*, 6484−6491.
185. Dietliker, K.; Gilgen, P.; Heimgartner, H.; Schmid, H. *Helv. Chim. Acta* **1976,** *59*, 2074−2099.
186. Sauers, R. R.; Van Arnum, S. D. *Tetrahedron Lett.* **1987,** *28*, 5797−5800.
187. Lopes, S.; Nunes, C. M.; Gómez-Zavaglia, A.; Pinho e Melo, T. M. V. D.; Fausto, R. *J. Phys. Chem. A* **2011,** *115*, 1199−1209.
188. Bracken, C.; Baumann, M. *J. Org. Chem.* **2020,** *85*, 2607−2617.
189. Ferris, J. P.; Antonucci, F. R.; Trimmer, R. W. *J. Am. Chem. Soc.* **1973,** *95*, 919−920.
190. Ferris, J. P.; Antonucci, F. R. *J. Am. Chem. Soc.* **1974,** *96*, 2014−2019.
191. Grellmann, K. H.; Tauer, E. *J. Photochem.* **1977,** *6*, 365−370.
192. Heinzelmann, W.; Märky, M. *Helv. Chim. Acta* **1974,** *57*, 376−382.
193. Ferris, J. P.; Trimmer, R. W. *J. Org. Chem.* **1976,** *41*, 13−19.
194. Su, M.-D. *J. Org. Chem.* **2009,** *74*, 6055−6063.
195. Nunes, C. M.; Pinto, S. M. V.; Reva, I.; Fausto, R. *Eur. J. Org. Chem.* **2016,** 4152−4158.
196. Nunes, C. M.; Pinto, S. M. V.; Reva, I.; Rosado, M. T. S.; Fausto, R. *J. Mol. Struct.* **2018,** *1172*, 33−41.
197. Singh, Y.; Prager, R. H. *Aust. J. Chem.* **1992,** *45*, 1811−1823.
198. Prager, R. H.; Singh, Y.; Weber, B. *Aust. J. Chem.* **1994,** *47*, 1249−1262.
199. Ang, K. H.; Prager, R. H.; Smith, J. A.; Weber, B.; Willimas, C. M. *Tetrahedron Lett.* **1996,** *37*, 675−678.
200. Prager, R. H.; Smith, J. A.; Weber, B.; Willimas, C. M. *J. Chem. Soc., Perkin Trans. 1* **1997,** 2665−2672.
201. Prager, R. H.; Taylor, M. R.; Williams, C. M. *J. Chem. Soc., Perkin Trans. 1* **1997,** 2673−2678.
202. Prager, R. H.; Willimas, C. M. *Aust. J. Chem.* **2000,** *53*, 665−671.
203. Cox, M.; Prager, R. H.; Riessen, D. M. *Arkivoc* **2001,** *7*, 88−103.
204. Mei, M.; Anand, D.; Zhou, L. *Org. Lett.* **2019,** *21*, 3548−3553.
205. Kojima, M.; Maeda, M. *Tetrahedron Lett.* **1969,** 2379−2381.
206. Maeda, M.; Kojima, M. *J. Chem. Soc., Perkin Trans. 1* **1977,** 239−247.
207. Maeda, M.; Kojima, M. *J. Chem. Soc., Chem. Commun.* **1973,** 539−540.
208. Tanaka, H.; Matsushita, T.; Nishimoto, K. *J. Am. Chem. Soc.* **1983,** *105*, 1753−1760.
209. Cao, J.; Xie, Z.-Z.; Yu, X. *Chem. Phys.* **2016,** *474*, 25−35.
210. Fielden, R.; Meth-Cohn, O.; Suschitzky, H. *J. Chem. Soc., Perkin Trans. 1* **1973,** 702−704.
211. Pavlik, J. W. *Int. Am. Photochem. Soc. Newslett* **2000,** *23* (2), 22−33.
212. Pavlik, J. W. *Progr. Heterocycl. Chem.* **2003,** *15*, 37−57.
213. Pavlik, J. W.; Kurzweil, E. M. *J. Org. Chem.* **1991,** *56*, 6313−6320.
214. Pavlik, J. W.; Kebede, N. *J. Org. Chem.* **1997,** *62*, 8325−8334.
215. Connors, R. E.; Burns, D. S.; Kurzweil, E. M.; Pavlik, J. W. *J. Org. Chem.* **1992,** *57*, 1937−1940.
216. Beak, P.; Mieser, J. L.; Messer, W. R. *Tetrahedron Lett.* **1967,** 5315−5318.
217. Beak, P.; Messer, W. *Tetrahedron* **1969,** *25*, 3287−3295.
218. Barltrop, J. A.; Day, A. C.; Mack, A. G.; Shahrisa, A.; Wakamatsu, S. *J. Chem. Soc., Chem. Commun.* **1981,** 604−606.
219. Connors, R. E.; Pavlik, J. W.; Burns, D. S.; Kurzweil, E. M. *J. Org. Chem.* **1991,** *56*, 6321−6326.
220. Labhart, H.; Heinzelmann, W.; Dubois, J. P. *Pure Appl. Chem.* **1970,** *24*, 495−507.
221. Pavlik, J. W.; Kebede, N.; Bird, N. P.; Day, A. C.; Barltrop, J. A. *J. Org. Chem.* **1995,** *60*, 8138−8139.
222. Pavlik, J. W.; Connors, R. E.; Burns, D. S.; Kurzweil, E. M. *J. Am. Chem. Soc.* **1993,** *115*, 7645−7652.
223. Grimshaw, J.; Mannus, D. *J. Chem, Soc. Perkin Trans. 1* **1977,** 2096−2099.
224. D'Auria, M.; Racioppi, R. *Lett. Org. Chem.* **2004,** *1*, 12−19.
225. Su, M.-R. *J. Phys. Chem. A* **2008,** *112*, 10420−10428.
226. Reisch, J.; Fitzek, A. *Tetrahedron Lett.* **1967,** 4515−4516.
227. Tiefenthaler, H.; Dörscheln, W.; Göth, H.; Schmid, H. *Tetrahedron Lett.* **1964,** 2999−3001.
228. Heinzelmann, W.; Märky, M.; Gilgen, P. *Helv. Chim. Acta* **1976,** *59*, 1512−1527.
229. Heinzelmann, W.; Märky, M.; Gilgen, P. *Helv. Chim. Acta* **1976,** *59*, 1528−1546.
230. D'Auria. *Adv. Heterocycl. Chem.* **2001,** *79*, 41−88.
231. Su, M.-D. *J. Phys. Chem.* **2007,** *111*, 1567−1574.
232. Catteau, J. P.; Lablache-Combier, A.; Pollet, A. *J. Chem. Soc., Chem. Commun.* **1969,** 1018.

233. Pavlik, J. W.; Pandit, C. R.; Samuel, C. J.; Day, A. C. *J. Org. Chem.* **1993,** *58*, 3407−3410.
234. Vernin, G.; Poite, J.-C.; Metzger, J.; Aune, J.-P.; Dou, H. J. M. *Bull. Soc. Chim. Fr.* **1971,** 1103−1104.
235. Vernin, G.; Jauffred, R.; Ricard, C.; Dou, H. J. M.; Metzger, J. *J. Chem. Soc., Perkin Trans. 2* **1972,** 1145−1150.
236. Pavlik, J. W., Tongcharoensirikul, P.; Bird, N. P.; Day, A. C.; Barltrop, J. A. *J. Am. Chem. Soc.* **1994,** *116*, 2292−2300.
237. Riou, C.; Vernin, G.; Doum, H. J. M.; Metzger, J. *Bull. Soc. Chim. Fr.* **1972,** 2673−2678.
238. Vernin, G.; Riou, C.; Dou, H. J. M.; Bouscasse, L.; Metzger, J.; Loridan, G. *Bull. Soc. Chim. Fr.* **1973,** 1743−1751.
239. Riou, C.; Poite, J. C.; Vernin, G.; Metzger, J. *Tetrahedron* **1974,** *30*, 879−898.
240. Maeda, M.; Kojima, M. *Tetrahedron Lett.* **1973,** 3523−3526.
241. Maeda, M.; Kojima, M. *J. Chem. Soc., Perkin Trans. 1* **1978,** 685−692.
242. Kojima, M.; Maeda, M. *J. Chem. Soc. D.* **1970,** 386−387.
243. D'Auria, M. *Tetrahedron* **2002,** *58*, 8037−8042.
244. Amati, M.; Belviso, S.; D'Auria, M.; Lelj, F.; Racioppi, R.; Viggiani, L. *Eur. J. Org. Chem.* **2010,** 3416−3427.
245. Morii, T.; Matsuura, T.; Saito, I.; Suzuki, T.; Kuwahara, J.; Sugiura, Y. *J. Am. Chem. Soc.* **1986,** *108*, 7089−7094.
246. Morii, T.; Matsuura, T.; Kuwahara, J.; Sugiura, Y. *J. Am. Chem. Soc.* **1987,** *109*, 938−939.
247. Saito, I.; Morii, T.; Okamura, Y.; Mori, S.; Yamaguchi, K.; Matsuura, T. *Tetrahedron Lett.* **1986,** *27*, 6385−6388.
248. Saito, I.; Morii, T.; Mori, S.; Yamaguchi, K.; Matsuura, T. *Tetrahedron Lett.* **1988,** *29*, 3963−3966.
249. Sipos, A.; Berényi, S. *Monatsh. Chem.* **2009,** *140*, 387−396.
250. Lablache-Combier, A.; Pollet, A. *Tetrahedron* **1972,** *28*, 3141−3151.
251. Su, M.-D. *Phys. Chem. Chem. Phys.* **2014,** *16*, 17030−17042.
252. Ohashi, M.; Iio, A.; Yonezawa, T. *J. Chem. Soc. D.* **1970,** 1148.
253. Vernin, G.; Poite, J.-C.; Dou, H. J. M.; Metzger, J. *Bull. Soc. Chim. Fr.* **1972,** 3157−3167.
254. Pavlick, J. W.; Tongcharoensirikul, P. *J. Org. Chem.* **2000,** *65*, 3626−3632.
255. Pavlick, J. W.; Tongcharoensirikul, P.; French, K. M. *J. Org. Chem.* **1998,** *63*, 5592−5603.
256. Sharp, T. R.; Leeman, K. R.; Bryant, D. E.; Horan, G. J. *Tetrahedron Lett.* **2003,** *44*, 1559−1561.
257. Tanikawa, H.; Ishii, K.; Kubota, S.; Yagai, S.; Kitamura, A.; Karatsu, T. *Tetrahedron Lett.* **2008,** *49*, 3444−3448.
258. Pace, A.; Pierro, P. *Org. Biomol. Chem.* **2009,** *7*, 4337−4348.
259. Buscemi, S.; Cicero, M. G.; Vivona, N.; Caronna, T. *J. Chem. Soc., Perkin Trans. 1* **1988,** 1313−1315.
260. Buscemi, S.; Cicero, M. G.; Vivona, N.; Caronn, T. *J. Heterocycl. Chem.* **1988,** *25*, 931−935.
261. Vivona, N.; Buscemi, S. *Heterocycles* **1995,** *41*, 2095−2116.
262. Buscemi, S.; Vivona, N. *J. Chem. Soc., Perkin Trans. 2* **1991,** 187−191.
263. Buscemi, S.; Pace, A.; Vivona, N.; Caronna, T.; Galia, A. *J. Org. Chem.* **1999,** *64*, 7028−7033.
264. Buscemi, S.; Pace, A.; Vivona, N.; Caronna, T. *J. Heterocycl. Chem.* **2001,** *38*, 777−780.
265. Buscemi, S.; Pace, A.; Pibiri, I.; Vivona, N. *J. Org. Chem.* **2002,** *67*, 6253−6255.
266. Buscemi, S.; D'Auria, M.; Pace, A.; Pibiri, I.; Vivona, N. *Tetrahedron* **2004,** *60*, 3243−3249.
267. Su, M.-D. *ChemPhysChem* **2014,** *15*, 2712−2722.
268. Newmann, H. *Tetrahedron Lett.* **1968,** 2417−2420.
269. Pace, A.; Buscemi, S.; Vivona, N. *J. Org. Chem.* **2005,** *70*, 2322−2324.
270. Newmann, H. *Tetrahedron Lett.* **1968,** 2421−2424.
271. Buscemi, S.; Vivona, N. *J. Heterocycl. Chem.* **1988,** *25*, 1551−1553.
272. Buscemi, S.; Vivona, N. *Heterocycles* **1989,** *29*, 737−744.
273. Buscemi, S.; Macaluso, G.; Vivona, N. *Heterocycles* **1989,** *29*, 1301−1308.
274. Buscemi, S.; Cusmano, G.; Gruttadauria, M. *J. Heterocycl. Chem.* **1990,** *27*, 861−863.
275. D'Auria, M.; Frenna, V.; Marullo, S.; Racioppi, R.; Spinelli, D.; Viggiani, L. *Photochem. Photobiol. Sci.* **2012,** *11*, 1383−1388.
276. D'Auria, M.; Frenna, V.; Monari, M.; Palumbo-Piccionello, A.; Racioppi, R.; Spinelli, D.; Viggiani, L. *Tetrahedron Lett.* **2015,** *56*, 6598−6601.
277. D'Auria, M. *Lett. Org. Chem.* **2018,** *15*, 1021−1024.
278. Buscemi, S.; Vivona, N.; Caronna, T. *J. Org. Chem.* **1996,** *61*, 8397−8401.
279. Vivona, N.; Buscemi, S.; Asta, S.; Caronna, T. *Tetrahedron* **1997,** *53*, 12629−12636.
280. Buscemi, S.; Pace, A.; Pibiri, I.; Vivona, N.; Caronna, T. *J. Fluor. Chem.* **2004,** *125*, 165−173.
281. Pace, A.; Pibiri, I.; Buscemi, S.; Vivona, N. *J. Org. Chem.* **2004,** *69*, 4108−4115.
282. Pace, A.; Buscemi, S.; Vivona, N.; Silvestri, A.; Barone, G. *J. Org. Chem.* **2006,** *71*, 2740−2749.
283. Cantrell, T. S.; Heller, W. S. *Chem. Commun. (Lond.)* **1968,** 977−978.
284. Mukai, T.; Oine, T.; Matsubara, A. *Bull. Chem. Soc. Jpn.* **1969,** *42*, 581.
285. Buscemi, S.; Frenna, V.; Caronna, T.; Vivona, N. *Heterocycles* **1992,** *34*, 2313−2322.
286. Buscemi, S.; Vivona, N.; Caronna, T. *Synthesis* **1995,** 917−919.
287. Buscemi, S.; Vivona, N.; Caronna, T. *J. Org. Chem.* **1995,** *60*, 4096−4101.
288. Buscemi, S.; Pace, A.; Vivona, N. *Tetrahedron Lett.* **2000,** *41*, 7977−7981.
289. Buscemi, S.; Pace, A.; Calabrese, R.; Vivona, N.; Metrangolo, P. *Tetrahedron* **2001,** *57*, 5865−5871.
290. Boyer, J. H.; Selvarajan, R. *Tetrahedron Lett.* **1969,** 47−50.
291. Mitchell, G.; Rees, C. W. *J. Chem. Soc., Perkin Trans. 1* **1987,** 413−422.
292. Burgess, E. M.; Carlthers, R.; McCullagh, L. *J. Am. Chem. Soc.* **1968,** *90*, 1923−1924.
293. Tsujimoto, K.; Ohashi, M.; Yonezawa, T. *Bull. Chem. Soc. Jpn.* **1972,** *45*, 515−519.
294. Märky, M.; Schmid, H.; Hansen, H.-J. *Helv. Chim. Acta* **1979,** *62*, 2129−2153.
295. Kulagowski, J. J.; Mitchell, G.; Moody, C. J.; Rees, C. W. *J. Chem. Soc., Chem. Commun.* **1985,** 650−651.
296. Kulagowski, J. J.; Moody, C. J.; Rees, C. W. *J. Chem. Soc., Perkin Trans. 1* **1985,** 2725−2732.
297. Kulagowski, J. J.; Moody, C. J.; Rees, C. W. *J. Chem. Soc., Perkin Trans. 1* **1985,** 2733−2739.

298. Wender, P. A.; Cooper, C. B. *Tetrahedron Lett.* **1987,** *28,* 6125−6128.
299. Mitchell, G.; Rees, C. W. *J. Chem. Soc., Perkin Trans. 1* **1987,** 403−412.
300. Döpp, D.; Orlewska, C.; Saczewski, F. *J. Heterocycl. Chem.* **1993,** *30,* 833−834.
301. Katritzky, A. R.; Lan, X.; Yang, J. Z.; Deniso, O. V. *Chem. Rev.* **1998,** *98,* 409−548.
302. Al-Awadi, H.; Ibrahim, M. R.; Al-Awadi, N. A.; Ibrahim, Y. A. *J. Heterocycl. Chem.* **2008,** *45,* 723−727.
303. Al-Jalal, N. A.; Ibrahim, M. R.; Al-Awadi, N. A.; Elnagdi, M. H. *Molecules* **2011,** *16,* 10256−10268.
304. Al-Jalal, N.; Al-Awadi, N. A.; Ibrahim, M. R.; Elnagdi, M. H. *Arkivoc* **2011,** *10,* 288−297.
305. Al-Jalal, N. A.; Al-Awadi, N. A.; Ibrahim, M. R.; Elnagdi, M. H. *Int. J. Chem.* **2013,** *5,* 80−89.
306. Ogata, Y.; Takagi, K.; Hayashi, E. *Bull. Chem. Soc. Jpn.* **1977,** *50,* 2505−2506.
307. Kirmse, W.; Horner, L. *Liebigs Ann. Chem.* **1958,** *614,* 4−18.
308. Strausz, O. P.; Font, J.; Dedio, E. L.; Kebarle, P.; Gunning, H. E. *J. Am. Chem. Soc.* **1967,** *89,* 4805−4807.
309. Zeller, K.-P.; Meier, H.; Müller, E. *Tetrahedron Lett.* **1971,** 537−540.
310. Zeller, K.-P.; Meier, H.; Müller, E. *Liebigs Ann. Chem.* **1972,** *766,* 32−44.
311. Krantz, A.; Laureni, J. *J. Am. Chem. Soc.* **1974,** *96,* 6768−6770.
312. Laureni, J.; Krantz, A.; Hajdu, R. A. *J. Am. Chem. Soc.* **1976,** *98,* 7872−7874.
313. Krantz, A.; Laureni, J. *J. Am. Chem. Soc.* **1977,** *99,* 4842−4844.
314. Krantz, A.; Laureni, J. *Ber. Bunsenges. Phys. Chem.* **1978,** *82,* 13−14.
315. Timm, U.; Bühl, H.; Meier, H. *J. Heterocycl. Chem.* **1978,** *15,* 697−698.
316. Font, J.; Torres, M.; Gunning, H. E.; Strausz, O. P. *J. Org. Chem.* **1978,** *43,* 2487−2490.
317. Krantz, A.; Laureni, J. *J. Org. Chem.* **1979,** *44,* 2730−2732.
318. Timm, U.; Meier, H. *J. Heterocycl. Chem.* **1979,** *16,* 1295−1296.
319. Mural, H.; Torres, M.; Strausz, O. P. *J. Am. Chem. Soc.* **1979,** *101,* 3976−3979.
320. Timm, U.; Merkle, U.; Meier, H. *Chem. Ber.* **1980,** *113,* 2519−2529.
321. Meier, H.; Kolshorn, H. *Z. Naturforsch.* **1980,** *35b,* 1040−1048.
322. Krantz, A.; Laureni, J. *J. Am. Chem. Soc.* **1981,** *103,* 486−496.
323. Torres, M.; Clement, A.; Strausz, O. P. *Z. Naturforsch.* **1983,** *38b,* 1208−1212.
324. Siegbahn, P. E. M.; Yoshimine, M.; Pacansky, J. *J. Chem. Phys.* **1983,** *78,* 1384−1389.
325. Meier, H.; Konnerth, U.; Graw, S.; Echter, T. *Chem. Ber.* **1984,** *117,* 107−126.
326. Larsen, B. D.; Eggert, H.; Harrit, N.; Holm, A. *Acta Chem. Scand.* **1992,** *46,* 482−486.
327. Su, M.-D. *ACS Omega* **2018,** *3,* 3482−3488.
328. Moorman, A. R.; Findak, D. C.; Ku, H. S. *J. Heterocycl. Chem.* **1985,** *22,* 915−920.
329. Innes, K. K.; Byrne, J. P.; Ross, I. G. *J. Mol. Spectrosc.* **1967,** *22,* 125−147.
330. Hoover, R. J.; Kasha, M. *J. Am. Chem. Soc.* **1969,** *91,* 6508−6510.
331. Fulscher, M. P.; Anderson, K.; Roos, B. O. *J. Phys. Chem.* **1992,** *96,* 9204−9212.
332. Bolovinos, A.; Tsekeris, P.; Philis, J.; Pantos, E.; Andritsopoulos, G. *J. Mol. Spectrosc.* **1984,** *103,* 240−256.
333. Villa, E.; Amirav, A.; Lim, E. C. *J. Phys. Chem.* **1988,** *92,* 5393−5397.
334. Mochizuki, Y.; Kaya, K.; Ito, M. *J. Phys. Chem.* **1976,** *65,* 4163−4169.
335. Wilzbach, K. E.; Rausch, D. J. *J. Am. Chem. Soc.* **1970,** *92,* 2178−2179.
336. Chapman, O. L.; McIntosh, C. L.; Pacansky, J. *J. Am. Chem. Soc.* **1973,** *95,* 614−617.
337. Ratajczak, E.; Sztuba, B. *J. Photochem.* **1980,** *13,* 233−242.
338. Yamazaki, I.; Murao, T.; Yamanaka, T.; Yoshihara, K. *Faraday Discuss. Chem. Soc.* **1983,** *75,* 395−405.
339. Vysotskii, Y. S.; Sivyakova, L. N. *Khim. Geterosikl. Soedin.* **1986,** *22,* 357−363.
340. Johnstone, D. E.; Sodeau, J. R. *J. Phys. Chem.* **1991,** *95,* 165−169.
341. Sobolewski, A. L.; Domcke, W. *Chem. Phys. Lett.* **1991,** *180,* 381−386.
342. Liu, R.; Zhou, X.; Pulay, P. *J. Phys. Chem.* **1992,** *96,* 3669−3674.
343. Kudoth, S.; Takayanagi, M.; Nakata, M. *J. Photochem. Photobiol. A: Chem.* **1999,** *123,* 25−30.
344. Wang, B.; Liu, B.; Wang, Y.; Wang, L. *Int. J. Mass. Spectrom.* **2010,** *289,* 91−97.
345. Su, M.-D. *J. Phys. Chem. A* **2007,** *111,* 971−975.
346. Chachisvilis, M.; Zewail, A. H. *J. Phys. Chem. A* **1999,** *103,* 7408−7418.
347. Freytag, H.; Neudert, W. *J. Prakt. Chem.* **1932,** *135,* 15−35.
348. Freytag, H.; Hlučka, F. *J. Prakt. Chem.* **1933,** *136,* 288−292.
349. Freytag, H. *J. Prakt. Chem.* **1934,** *139,* 44−62.
350. Joussot-Dubien, J.; Houdard, J. *Tetrahedron Lett.* **1967,** 4389−4391.
351. Joussot-Dubien, J.; Houdard-Pereyre, J. *Bull. Soc. Chim. Fr.* **1969,** 2619−2623.
352. Destexhe, A.; Smets, J.; Adamowicz, L.; Maes, G. *J. Phys. Chem.* **1994,** *98,* 1506−1514.
353. Dkhissi, A.; Adamowicz, L.; Maes, G. *J. Phys. Chem. A* **2000,** *104,* 2112−2119.
354. Reimers, J. R.; Cai, Z.-L. *Phys. Chem. Chem. Phys.* **2012,** *14,* 8791−8802.
355. Liu, X.; Sobolewski, A. L.; Borrelli, R.; Domcke, W. *Phys. Chem. Chem. Phys.* **2013,** *15,* 5957−5966.
356. Esteves-López, N.; Coussan, S.; Dedonder-Lardeux, C.; Jouvet, C. *Phys. Chem. Chem. Phys.* **2016,** *18,* 25637−25644.
357. Esteves-López, N.; Coussan, S. *J. Mol. Struct.* **2018,** *1172,* 65−73.
358. Kellogg, R. M.; van Bergen, T. J.; Wynberg, H. *Tetrahedron Lett.* **1969,** 5211−5214.
359. Van Bergen, T. J.; Kellogg, R. M. *J. Am. Chem. Soc.* **1972,** *94,* 8451−8471.
360. Caplain, S.; Catteau, J. P.; Lablache-Combier, A. *J. Chem. Soc. D.* **1970,** 1475−1476.
361. Barlow, M. G.; Dingwall, J. G.; Haszeldine, R. N. *J. Chem. Soc. D.* **1970,** 1580.
362. Mathias, E.; Heicklen, J. *Mol. Photochem.* **1972,** *4,* 483−500.

363. Caplain, S.; Lablache-Combier, A. *J. Chem. Soc. D.* **1970,** 1247−1248.
364. Roebke, W. *J. Phys. Chem.* **1970,** 74, 4198−4203.
365. Pavlik, J. W.; Kebede, N.; Thompson, M.; Colin Day, A.; Barltrop, J. A. *J. Am. Chem. Soc.* **1999,** 121, 5666−5673.
366. Pavlik, J. W.; Laohhasurayotin, S. *Tetrahedron Lett.* **2003,** 44, 8109−8111.
367. Ogata, Y.; Takagi, K. *J. Am. Chem. Soc.* **1974,** 96, 5933−5934.
368. Fowler, F. W. *J. Org. Chem.* **1972,** 37, 1321−1323.
369. Kurita, J.; Iwata, K.; Tsuchiya, T. *J. Chem. Soc., Chem. Commun.* **1986,** 1188−1189.
370. Kurita, J.; Iwata, K.; Tsuchiya, T. *Chem. Pharm. Bull.* **1987,** 35, 3166−3174.
371. Stapleton, D. R.; Mantzavinos, D.; Papadaki, M. *J. Hazard. Mat.* **2007,** 146, 640−645.
372. Stapleton, D. R.; Vlastos, D.; Skoutelis, C. G.; Papadaki, M. I. *J. Adv. Oxid. Technol.* **2008,** 11, 486−500.
373. Stapleton, D. R.; Kostantinou, I. K.; Hela, D. G.; Papadaki, M. *Water Res.* **2009,** 42, 3964−3973.
374. Kaplan, L.; Pavlik, J. W.; Wilzbach, K. E. *J. Am. Chem. Soc.* **1972,** 94, 3283−3284.
375. Siopa, F.; Antonio, J. P. M.; Afonso, C. A. *Org. Process. Res. Dev.* **2018,** 22, 551−556.
376. Yoon, U. C.; Quillen, S. L.; Mariano, P. S.; Swanson, R.; Stavinoha, J. L.; Bay, E. *J. Am. Chem. Soc.* **1983,** 105, 1204−1218.
377. Ling, R.; Yoshida, M.; Mariano, P. S. *J. Org. Chem.* **1996,** 61, 4439−4449.
378. Glarner, F.; Thornton, S. R.; Schärer, D.; Berardinelli, G.; Burger, U. *Helv. Chim. Acta* **1997,** 80, 121−127.
379. Penkett, C. S.; Simpson, I. D. *Tetrahedron* **1999,** 55, 6183−6204.
380. Acar, E. A.; Glarner, F.; Burger, U. *Helv. Chim. Acta* **1998,** 81, 1095−1104.
381. Zhao, Z.; Duesler, E.; Wang, C.; Guo, H.; Mariano, P. S. *J. Org. Chem.* **2005,** 70, 8508−8512.
382. Damiano, T.; Morton, D.; Nelson, A. *Org. Biomol. Chem.* **2007,** 5, 2735−2752.
383. Ling, R.; Mariano, P. S. *J. Org. Chem.* **1998,** 63, 6072−6076.
384. Cho, S. J.; Ling, R.; Kim, A.; Mariano, P. S. *J. Org. Chem.* **2000,** 65, 1574−1577.
385. Lu, H.; Mariano, P. S.; Lam, Y.-F. *Tetrahedron Lett.* **2001,** 42, 4755−4757.
386. Lu, H.; Su, Z.; Song, L.; Mariano, P. S. *J. Org. Chem.* **2002,** 67, 3525−3528.
387. Song, L.; Duesler, E. N.; Mariano, P. S. *J. Org. Chem.* **2004,** 69, 7284−7293.
388. Zhao, Z.; Song, L.; Mariano, P. S. *Tetrahedron* **2005,** 61, 8888−8894.
389. Feng, X.; Duesler, E. N.; Mariano, P. S. *J. Org. Chem.* **2005,** 70, 5618−5623.
390. Zhou, J.; Gong, M.; Mariano, P. S.; Yoon, U. C. *Bull. Korean Chem. Soc.* **2008,** 29, 89−93.
391. Streith, J.; Cassal, J.-M. *C. R. Acad. Sci. Paris.* **1967,** 264, 1307−1308.
392. Streith, J.; Blind, A.; Cassal, J.-M.; Sigwalt, C. *Bull. Soc. Chim. Fr.* **1969,** 948−952.
393. Gleiter, R.; Schmidt, D.; Streith, J. *Helv. Chim. Acta* **1971,** 54, 1645−1651.
394. Streith, J.; Cassal, J.-M. *Angew. Chem. Int. (Ed.)* **1968,** 7, 129.
395. Streith, J.; Cassal, J.-M. *Bull. Soc. Chim. Fr.* **1969,** 2175−2180.
396. Sasaki, T.; Kanematsu, K.; Kakehi, A. *J. Chem. Soc. D.* **1969,** 432−433.
397. Snieckus, V. *J. Chem. Soc. D.* **1969,** 831.
398. Sasaki, T.; Kanematsu, K.; Kakehi, A.; Ichikawa, I.; Hayakawa, K. *J. Org. Chem.* **1970,** 35, 426−433.
399. Balasubramanian, A.; McÌntosh, J. M.; Snieckus, V. *J. Org. Chem.* **1970,** 35, 433−438.
400. Streith, J.; Luttringer, J. P.; Nastasi, M. *J. Org. Chem.* **1971,** 36, 2962−2967.
401. Abramovitch, R. A.; Takaya, T. *J. Org. Chem.* **1973,** 38, 3311−3316.
402. Frankowski, A.; Streith, J. *C. R. Acad. Sci. Paris.* **1973,** 276, 959−962.
403. Nastasi, M.; Streith, J. *Bull. Soc. Chim. Fr.* **1973,** 630−634.
404. Tsuchiya, T.; Kurita, J.; Kojima, H. *J. Chem. Soc., Chem. Commun.* **1980,** 444−445.
405. Potts, K. T.; Dugas, R. *J. Chem. Soc. D.* **1970,** 732.
406. Snieckus, V.; Kan, G. *J. Chem. Soc. D.* **1970,** 172−173.
407. Bird, C. W.; Partridge, I.; Wonf, D. Y. *J. Chem. Soc., Perkin Trans. 1* **1972,** 1020−1022.
408. Kurita, J.; Kojima, H.; Tsuchiya, T. *Chem. Pharm. Bull.* **1981,** 29, 3688−3695.
409. Spence, G. G.; Taylor, E. C.; Buchardt, O. *Chem. Rev.* **1970,** 70, 231−265.
410. Jerina, D. M.; Boyd, D. R.; Daly, J. W. *Tetrahedron Lett.* **1970,** 457−460.
411. Leibovici, C.; Streith, J. *Tetrahedron Lett.* **1971,** 387−392.
412. Kubota, T.; Yamakawa, M.; Mizuno, Y. *Bull. Chem. Soc. Jpn.* **1972,** 45, 3282−3286.
413. Yanakawa, M.; Ezumi, E.; Mizuno, Y.; Kubota, T. *Bull. Chem. Soc. Jpn.* **1974,** 47, 2982−2985.
414. Streith, J.; Sigwalt, C. *Tetrahedron Lett.* **1966,** 1347−1350.
415. Bellamy, F.; Martz, P.; Streith, J. *Heterocycles* **1975,** 3, 395−400.
416. Streith, J.; Danner, B.; Sigwalt, C. *Chem. Commun. (Lond.)* **1967,** 979−980.
417. Streith, J.; Sigwalt, C. *Bull. Soc. Chim. Fr.* **1970,** 1157−1167.
418. Bellamy, F.; Barragan, L. G. R.; Streith, J. *J. Chem. Soc. D.* **1971,** 456.
419. Ishikawa, M.; Kaneko, C.; Yokoe, I.; Yamada, S. *Tetrahedron* **1969,** 25, 295−300.
420. Kumler, P. L.; Buchardt, O. *J. Chem. Soc. D.* **1968,** 1321−1323.
421. Buchardt, O.; Pedersen, C. L.; Harrit, N. *J. Org. Chem.* **1978,** 37, 3592−3595.
422. Hanaoka, M.; Iwasaki, M.; Mukai, C. *Tetrahedron Lett.* **1985,** 26, 917−920.
423. Hanoka, M.; Mukai, C.; Nagami, K.; Okajima, K.; Yasuda, S. *Chem. Pharm. Bull.* **1984,** 32, 2230−2240.
424. Becher, J.; Lohse, C. *Acta Chem. Scand.* **1972,** 26, 4041−4048.
425. Shiba, T.; Yamane, K.; Kato, H. *J. Chem. Soc. D.* **1970,** 1592−1593.
426. Tamura, Y.; Matsugashita, S.; Ishibashi, H.; Ikeda, M. *Tetrahedron* **1973,** 29, 2359−2364.
427. Tsuchiya, T.; Kurita, J.; Igeta, H. *J. Chem. Soc., Chem. Commun.* **1974,** 640−641.

428. Tsuchiya, T.; Okajima, S.; Enkaku, M.; Kurita, J. *J. Chem. Soc., Chem. Commun.* **1981,** 211−213.
429. Tsuchiya, T.; Enkaku, M.; Kurita, J.; Sawanishi, H. *J. Chem. Soc., Chem. Commun.* **1979,** 534−535.
430. Tamura, Y.; Ishibashi, H.; Tsujimoto, N.; Ikeda, M. *Chem. Pharm. Bull.* **1971,** *19,* 1285−1286.
431. Tsuchiya, T.; Sawanishi, H.; Enkaku, M.; Hirai, T. *Chem. Pharm. Bull.* **1981,** *29,* 1539−1547.
432. Buchardt, O.; Tomer, K. S.; Madsen, V. *Tetrahedron Lett.* **1971,** 1311−1314.
433. Lohse, C. *Angew. Chem.* **1972,** *84,* 220.
434. Ono, I.; Hata, N. *Bull. Chem. Soc. Jpn.* **1973,** *46,* 3658−3662.
435. Lohse, C. *J. Chem. Soc., Perkin Trans. 2* **1972,** 229−233.
436. Kaneko, C.; Yamada, S.; Ishikawa, M. *Tetrahedron Lett.* **1966,** 2145−2150.
437. Kaneko, C.; Yamada, S.; Yokoe, I. *Tetrahedron Lett.* **1970,** 2333−2336.
438. Buchardt, O. *Acta Chem. Scand.* **1963,** *17,* 1461−1462.
439. Ishikawa, M.; Yamada, S.; Kaneko, C. *Chem. Pharm. Bull.* **1965,** *13,* 747−749.
440. Buchardt, O.; Becher, J.; Lohse, C.; Møller, J. *Acta Chem. Scand.* **1966,** *20,* 262−263.
441. Streith, J.; Darrah, H. K.; Weil, M. *Tetrahedron Lett.* **1966,** 5555−5562.
442. Kaneko, C.; Yokoe, I.; Ishikawa, M. *Tetrahedron Lett.* **1967,** 5237−5240.
443. Kobayashi, Y.; Kumadaki, I.; Sato, H. *Tetrahedron Lett.* **1970,** 2337−2340.
444. Kaneko, C.; Hasegawa, H.; Tanaka, S.; Sunayashiki, K.; Yamada, S. *Chem. Lett.* **1974,** 133−136.
445. Kaneko, C.; Hayashi, S.; Kobayashi, Y. *Chem. Pharm. Bull.* **1974,** *22,* 2147−2154.
446. Kakeko, C.; Yamada, S.; Ishikawa, M. *Chem. Pharm. Bull.* **1969,** *17,* 1294−1297.
447. Yamada, S.; Ishikawa, M.; Kakeko, C. *Tetrahedron Lett.* **1972,** 971−976.
448. Yamada, S.; Ishikawa, M.; Kaneko, C. *Tetrahedron Lett.* **1972,** 977−980.
449. Yamada, S.; Ishikawa, M.; Kaneko, C. *J. Chem. Soc., Chem. Commun.* **1972,** 1093−1094.
450. Lahmani, F.; Magat, M. *C. R. Acad. Sci. Paris.* **1966,** *263,* 1005−1006.
451. Lahmani, F.; Ivanoff, N. *Tetrahedron Lett.* **1967,** 3913−3917.
452. Su, M.-D. *J. Phys. Chem. A* **2006,** *110,* 9420−9428.
453. Kaneko, C.; Yamada, S.; Ishikawa, M. *Tetrahedron Lett.* **1970,** 2329−2332.
454. Albini, A.; Bettinetti, G. F.; Pietra, S. *Tetrahedron Lett.* **1972,** 3657−3660.
455. Albini, A.; Bettinetti, G. F.; Pietra, S. *J. Chem. Soc., Perkin Trans. 2* **1974,** 342−344.
456. Landquist, J. K. *J. Chem. Soc.* **1953,** 2830−2833.
457. Haddadin, M.; Agopian, G.; Issidorides, C. H. *J. Org. Chem.* **1971,** *36,* 514−518.
458. Jarrar, A. A. *J. Chem. (Ed.)* **1974,** *51,* 755.
459. Burrell, R. A.; Cox, J. M.; Savins, E. G. *J. Chem. Soc., Perkin Trans. 1* **1973,** 2707−2713.
460. Allison, C. G.; Chambers, R. D.; Cheburkov, Y. A.; MacBride, J. A. H.; Musgrave, W. K. R. *J. Chem. Soc. D.* **1969,** 1200−1201.
461. Johnson, D. W.; Austel, V.; Feld, R. S.; Lemal, D. M. *J. Am. Chem. Soc.* **1970,** *92,* 7505−7506.
462. Chambers, R. D.; Musgrave, W. K. R.; Srivastava, K. C. *J. Chem. Soc. D.* **1971,** 264−265.
463. Chambers, R. D.; MacBride, J. A. H.; Maslakiewicz, J. R.; Srivastava, K. C. *J. Chem. Soc., Perkin Trans. 1* **1975,** 396−400.
464. Chambers, R. D.; Maslakiewicz, J. R.; Srivastava, K. C. *J. Chem. Soc. Perkin Trans. 1* **1975,** 1130−1134.
465. Chambers, R. D.; MacBride, J. A. H.; Musgrave, W. K. R. *J. Chem. Soc. D.* **1970,** 739−740.
466. Maki, Y.; Suzuki, M.; Furuta, T.; Hiramitsu, T.; Kuzuya, M. *Tetrahedron Lett.* **1974,** 4107−4110.
467. Ogata, M.; Kanǒ, K. *J. Chem. Soc. D.* **1967,** 1176−1177.
468. Tsuchiya, T.; Arai, H.; Igeta, H. *Tetrahedron Lett.* **1971,** 2579−2582.
469. Tsuchiya, T.; Arai, H.; Tonami, T.; Igeta, H. *Chem. Pharm. Bull.* **1972,** *20,* 300−303.
470. Tsuchiya, T.; Arai, H.; Igeta, H. *Tetrahedron* **1973,** *29,* 2747−2751.
471. Horspool, W. M.; Kershaw, J. R.; Murray, A. W. *J. Chem. Soc., Chem. Commun.* **1973,** 345−346.
472. Tsuchiya, T.; Arai, H.; Igeta, H. *Tetrahedron Lett.* **1969,** 2747−2750.
473. Tsuchiya, T.; Arai, H.; Igeta, H. *Tetrahedron Lett.* **1970,** 2213−2216.
474. Tsuchiya, T.; Arai, H.; Igeta, H. *J. Chem. Soc., Chem. Commun.* **1972,** 550−551.
475. Buchardt, O. *Tetrahedron Lett.* **1968,** 1911−1912.
476. Tomer, K. B.; Harrit, N.; Rosenthal, I.; Buchardt, O.; Kumler, P. L.; Creed, D. *J. Am. Chem. Soc.* **1973,** *95,* 7402−7406.
477. Kumler, P. L.; Buchardt, O. *J. Am. Chem. Soc.* **1968,** *90,* 5640−5641.
478. Portillo, M.; Maxwell, M. A.; Frederich, J. H. *Org. Lett.* **2016,** *18,* 5142−5145.
479. Tsuchiya, T.; Arai, H.; Igeta, H. *Chem. Pharm. Bull.* **1973,** *21,* 1516−1519.
480. Arai, H.; Ohsawa, A.; Saiki, K.; Igeta, H. *J. Chem. Soc., Chem. Commun.* **1977,** 153−154.
481. Arai, H.; Ohsawa, A.; Saiki, K.; Igeta, H.; Tsuji, A.; Akimoto, T.; Iitaka, Y. *J. Chem. Soc., Chem. Commun.* **1977,** 856−857.
482. Ohsawa.; Arai, H.; Igeta, H.; Akimoto, T.; Tsuji, A.; Iitaka, Y. *Tetrahedron* **1979,** *35,* 1267−1271.
483. Tsuchiya, T.; Arai, H.; Hasebe, M.; Igeta, H. *Chem. Pharm. Bull.* **1974,** *22,* 2301−2305.
484. Gait, S. F.; Rees, C. W.; Storr, R. C. *J. Chem. Soc. D.* **1971,** 1545−1546.
485. Arai, H.; Igeta, H.; Tsuchiya, T. *J. Chem. Soc., Chem. Commun.* **1973,** 521−522.
486. Lahmani, F.; Ivanoff, N. *J. Phys. Chem.* **1972,** *76,* 2245−2248.
487. Wierzchowski, K. L.; Shugar, D. *Photochem. Photobiol.* **1963,** *2,* 377−391.
488. Wierzchowski, K. L.; Shugar, D.; Katritsky, A. R. *J. Am. Chem. Soc.* **1963,** *85,* 827−828.
489. Taylor, J.-S.; Cohrs, M. P. *J. Am. Chem. Soc.* **1987,** *109,* 2834−2835.
490. Kan, L.-S.; Voituriez, L.; Cadet, J. *J. Photochem. Photobiol. B: Biol.* **1992,** *12,* 339−357.
491. Ai, Y.-J.; Liao, R.-Z.; Chen, S.-F.; Luo, Y.; Fang, W.-H. *J. Phys. Chem. B* **2010,** *114,* 14096−14102.
492. Douki, T.; Rebelo-Moreira, S.; Hamon, N.; Bayle, P.-A. *Org. Lett.* **2015,** *17,* 246−249.

493. Douki, T. *Photochem. Photobiol.* **2016,** *92,* 587−594.
494. Streith, J.; Martz, P. *Tetrahedron Lett.* **1969,** 4899−4900.
495. Streith, J.; Leibovici, C.; Martz, P. *Bull. Soc. Chim. Fr.* **1971,** 4152−4160.
496. Bellamy, F.; Martz, P.; Streith, J. *Tetrahedron Lett.* **1974,** 3189−3192.
497. Deeleman, R. A. F.; Van der Plas, H. C. *Rec. Trav. Chem. Pays-Bas* **1973,** *92,* 317−320.
498. Lam, F. L.; Brown, G. B.; Parham, J. C. *J. Org. Chem.* **1974,** *39,* 1391−1395.
499. Lam, F. L.; Parham, J. C. *J. Org. Chem.* **1973,** *38,* 2397−2403.
500. Corey, E. J.; Streith, J. *J. Am. Chem. Soc.* **1964,** *86,* 950−951.
501. Cram, D. J.; Tanner, M. E.; Thomas, R. *Angew. Chem. Int. (Ed.) Engl.* **1991,** *30,* 1024−1027.
502. De Mayo, P. *Adv. Org. Chem.* **1960,** *2,* 367−425.
503. McIntosh, C. L.; Chapman, O. L. *J. Am. Chem. Soc.* **1973,** *95,* 247−248.
504. Pirkle, W. H.; McKendry, L. H. *J. Am. Chem. Soc* **1969,** *91,* 1179−1186.
505. Chapman, O. L.; McIntosh, C. L.; Pacansky, J. *J. Am. Chem. Soc.* **1973,** *95,* 244−246.
506. Pong, R. G. S.; Shirk, J. S. *J. Am. Chem. Soc.* **1973,** *95,* 248−249.
507. Arnold, B. R.; Brown, C. E.; Lusztyk, J. *J. Am. Chem. Soc.* **1993,** *115* 1576-1571.
508. Breda, S.; Reva, I.; Lapinski, L.; Fausto, R. *Phys. Chem. Chem. Phys.* **2004,** *6,* 929−937.
509. Murdock, D.; Ingle, R. A.; Sazanovich, I. V.; Clark, I. P.; Harabuchi, Y.; Taketsugu, T.; Maeda, S.; Orr-Ewing, A. J.; Ashfold, M. N. R. *Phys. Chem. Chem. Phys.* **2016,** *18,* 2629−2638.
510. Ishibe, N.; Odani, M.; Sunami, M. *J. Chem. Soc. D.* **1971,** 1034−1035.
511. Ishibe, N.; Sunami, M.; Odani, M. *J. Am. Chem. Soc.* **1973,** *95,* 463−468.
512. Keil, E. B.; Pavlik, J. W. *J. Heterocycl. Chem.* **1976,** *13,* 1149−1151.
513. Pavlik, J. W.; Pauliukonis, L. T. *Tetrahedron Lett.* **1976,** 1939−1942.
514. Pavlik, J. W.; Snead, T. E.; Tata, J. R. *J. Heterocycl. Chem.* **1981,** *18,* 1481−1483.
515. Pavlik, J. W.; Kirincich, S. J.; Pires, R. M. *J. Heterocycl. Chem.* **1991,** *28,* 537−539.
516. Pavlik, J. W.; Keil, E. B.; Sullivan, E. L. *J. Heterocycl. Chem.* **1992,** *29,* 1829−1834.
517. Furer, H. *Chem. Ber.* **1972,** *105,* 2780−2790.
518. De Selms, R. C.; Schleigh, W. R. *Tetrahedron Lett.* **1972,** 3563−3566.
519. Sato, M.; Katagiri, N.; Muto, M.; Haneda, T.; Kaneko, C. *Tetrahedron Lett.* **1986,** *27,* 6091−6094.
520. Kurita, J.; Yoneda, T.; Kakusawa, N.; Tsuchiya, T. *Chem. Pharm. Bull.* **1990,** *38,* 2911−2918.
521. Ishibe, N.; Masui, J. *J. Am. Chem. Soc.* **1974,** *96,* 1152−1158.
522. Pavlik, J. W.; Kwong, J. *J. Am. Chem. Soc.* **1973,** *95,* 7914−7916.
523. Pavlik, J. W.; Clennan, E. L. *J. Am. Chem. Soc.* **1973,** *95,* 1697−1699.
524. Pavlik, J. W.; Bolin, D. R.; Bradford, K. C.; Anderson, W. G. *J. Am. Chem. Soc.* **1977,** *99,* 2816−2818.
525. Pavlik, J. W.; Spada, A. P. *Tetrahedron Lett.* **1979,** 4441−4444.
526. Pavlik, J. W.; Spada, A. P.; Snead, T. E. *J. Org. Chem.* **1985,** *50,* 3046−3050.
527. Pavlik, J. W.; Patten, A. D.; Bolin, D. R.; Bradford, K. C.; Clennan, E. L. *J. Org. Chem.* **1984,** *49,* 4523−4531.
528. Pavlik, J. W.; Dunn, R. M. *Tetrahedron Lett.* **1978,** 5071−5074.
529. Clark, M. A.; Schoenfeld, R. C.; Ganem, B. *J. Am. Chem. Soc.* **2001,** *123,* 10425−10426.
530. Elghamry, I.; Döpp, D.; Henkel, G. *J. Heterocycl. Chem.* **2007,** *44,* 849−852.
531. Horspool, W. M.; Kershaw, J. R.; Murray, A. W.; Stevenson, G. M. *J. Am. Chem. Soc.* **1973,** *95,* 2390−2391.
532. Hochstrasser, R. M.; King, D. S. *J. Am. Chem. Soc.* **1975,** *97,* 4760−4762.
533. Wakita, K.; Tokitoh, N.; Okazaki, R.; Takagi, N.; Nagase, S. *J. Am. Chem. Soc.* **2000,** *122,* 5648−5649.
534. Su, M.-D. *Organometallics* **2014,** *33,* 5231−5237.

3

Photochemical behavior of diheteroarylethenes and photochromism

3.1 Photochemistry of olefins: An overview

The chemical and physical behavior of organic compounds after interaction with visible and/or ultraviolet (UV) light is the object of molecular photochemistry of organic compounds.

When light interacts with a generic organic molecule (R), it can produce an electronically excited species (*R), which evolves to an isolated product P according to the whole process: $R + h\nu \rightarrow {*}R \rightarrow P$. A neat chemical change takes place in this case, and this is the major object of photochemistry of organic compounds.

Otherwise, if the produced *R does not undergo any chemical modification, the whole process $R + h\nu \rightarrow {*}R \rightarrow R$ only deals with the photophysics of the organic compound, in which *R relaxes to R by the means of light emission or internal conversion (IC).

Fig. 3.1 shows the boundary between photophysics and photochemistry. A generic reaction coordinate is plotted against the potential energy of the ground (solid line) and excited state (dashed line). The lines should be intended as simple generalizations of the multidimentional potential energy surfaces (PESs), which should be riguourously taken into account. However, it would be more difficult to represent. Furthermore, a singlet excited state is postulated for drawing Fig. 3.1 but the concepts exlained here can be extended to triplet surfaces, as well.

In the "zone" of photophysics, *R can emit light (-hν) (fluorescence or phosphorescence) or it can relax in nonradiative way because of the IC, which can take place when the two PESs are in closer in energy. If the excited state is a triplet, intersystem crossing (ISC) rather than IC is the nonradiative phenomenon.
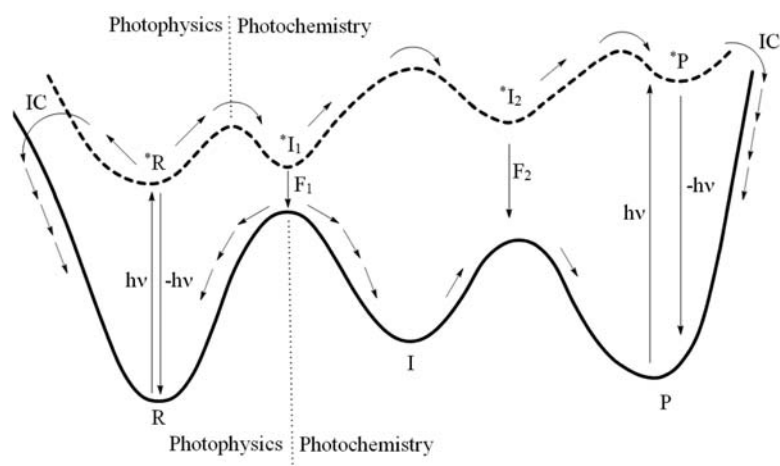
FIGURE 3.1 Schematic ground and excited potential energy surfaces showing the photophysical and photochemical processes in organic compounds.

The nature of *R is of basic importance for establishing if it will evolve toward a chemical change or not.

In addition to the photochemical processes shown in Fig. 3.1, *R can follow three different general pathways (called *primary photochemical processes*) leading to transformation in P. Which path is routed depends on the nature of *R.[1]

Along the first primary photochemical process, *R evolves into an intermediate in its ground state (I), which further reacts giving rise to the product P, according to the schematic mechanism: *R→I→P. The intermediate I can be a radical pair (RP), a biradical (BR) specie or a zwitterion (Z).

The jump from the excited to the ground state is performed at the "funnel" (F_1 in Fig. 3.1). Funnels are associated with a particular set of molecule internal coordinates at which a conical surface intersection is present between excited and ground states. Alternatively, F is a minimum in the excited state PES resulting from an avoided intersection between ground and excited states (as shown in Fig. 3.1).

In the second primary photochemical process, no ground-state intermediates are produced from *R evolution. At contrary, a "funnel" (F_2 in Fig. 3.1) between the excited and ground states takes to electronic relaxation from the excited state to the ground state PESs. After this "jump" toward the ground-state surface, the reaction path directly goes on toward P, without intermediates. This process can be represented as: *R→F→P, where "F" labels the funnel.

The last primary process consists in a chemical transformation taking place on the excited state PES. Two variants are possible: in the first one, the transformation leads to an excited state intermediate ($*I_2$ in Fig. 3.1), which gives rise to P after electronic relaxation to the ground state, according to the process: *R→*I→P. Alternatively, P is first produced in its excited state (*P) and successively, after relaxation (light emission or IC), it produces P according to the process: *R→*P→P.

The first primary photochemical process that leads to RP, BR, or Z is the most commonly observed one.

Modern organic photochemistry relates the structure, energetics, and dynamics of all the entities discussed earlier (R, hν, *R, I, F, *I, *P and P) with the characteristics of the studied reactions (like reaction yield and stereochemistry). Knowledge of these structures is extremely important to develop a deep understanding of the observed reactivity, going beyond a simple report of the obtained results.

This paragraph mainly focuses on the photochemistry of the olefin double bond. This basic knowledge will be extended to heteroatylethenes in the following paragraphs and to the photochromism of this class of compounds, as well.

As well known in organic chemistry, the concept of functional group is a useful guide to predict the physical and chemical properties of a certain compound, simply on the basis of the recognition of specific groups of atoms in the molecule under investigation. Here, we will couple the concept of functional group with a deeper characterization of it based on the molecular orbital (MO) theory. This will strongly aid to the comprehension of the photochemical processes we will be dealing with at least at a qualitative level.

In our case, the functional group of interest is the C=C double bond. Fortunately, the photochemical reactivity of R needs the relatively simple description of this bond in R itself, *R, I and P. In particular, the highest occupied molecular orbital (HOMO) and lowest unoccupied molecular orbital (LUMO) are often the only two MOs to be taken into account. Equally important is the spin multiplicity of the molecule associated with the HOMO and LUMO occupations (i.e., the spins that the electrons assume when occupy the two MOs).

Moreover, the MOs at lower energies respect to the HOMO are normally not significantly perturbed by changes of the HOMO and LUMO in their energies, shapes and/or electron occupations (HOMO and LUMO electron configuration). This allows assuming that all the lower MOs are unchanged during photochemical of photophysical processes.

Returning to the specific case of olefinic double bond, first, the nature of the HOMO and LUMO for R and *R has to be detailed as a first step in studying the relative photochemical or photophysical process.

In Scheme 3.1, an organic photochemical reaction of the type R + hν→ *R→I(D)→P is described with regard to the HOMO and LUMO occupations in the different situations, starting from R to reach P through an intermediate species (I) in its singlet/triplet state by means of a *R singlet state (^{1}*R) and/or *R triplet state (^{3}*R). It is possible to note several ISC processes between ^{3}*R and ^{1}*R and also between ^{3}I and ^{1}I and the electronic and spin configurations of all entities under exam.

As shown, R and P electronic configurations of the ground states are $(HOMO)^2(LUMO)^0$ and, according to the Pauli exclusion principle, the spin of the electrons in the same orbital have to be paired. This corresponds to a singlet (S) state (the lowest-in-energy electronic ground-state is always a singlet state and it is indicated with a subscript 0 namely S_0, whereas the first excited state is labeled with S_1, the second one with S_2 and so on).

After absorption of UV light, the singlet state of the electronically excited R (^{1}*R) could, by virtue of an ISC process, become a corresponding triplet (T) state (^{3}*R). The two electrons in nonbonding half-occupied orbitals $(NB_1)^1$ and $(NB_2)^1$ of the intermediate species I, are associated with very similar energies, differently from the HOMO and LUMO for all the remaining species (R, ^{1}*R, ^{3}*R, P). Consequently, they can generate similar-in-energy singlet (^{1}I) or triplet (^{3}I) states, according to their "antiparallel" ($\downarrow\uparrow$) or "parallel" ($\uparrow\uparrow$) dispositions into the two NB orbitals.

In the scheme, we use the symbol D (for diradical) for labeling the intermediate I; symbol D will be used for both RP (a species in which two radical centers are localized on two different molecular fragments) and BR (species in which the two radical centers are on a single molecular fragment). So, by using the script I(D), we indicate a diradical character in which the two half-filled orbitals show very similar energies, without specifying its RP or BR nature.

An additional possibility is the double occupation of only one of the two NB orbitals in the intermediate structure I, so to obtain an $I(NB)^2(NB)^0$ electron configuration. This particular state is a "zwitterion" in which one carbon atom assumes a negative partial charge (where the two electrons pair in the occupied NB orbital) and the second carbon atom assumes a positive charge. The label Z will be used for this state, so the Z intermediate will be labeled as I(Z). The Z intermediate I(Z) is involved in the ^{1}*R→^{1}I(Z) step of photoreactions.

Scheme 3.1 is a well known working reference for all photochemical reactions of organic molecules in which R, normally proceeding by a triplet state *R(T_1), can be, as a few examples, a carbonyl, an aromatic, an olefinic compound.

Knowledge of the HOMO and LUMO orbitals of each of these structures is necessary to infer information about the electronic configurations of the excited state *R; the shape and energies of the HOMO and LUMO (like all the MOs) are determined by the structure of the compound. Thus, it is necessary to gain information about the structures of the entities shown in Scheme 3.1, namely R(S_0), *R(S_1), *R(T_1), ^{3}I, ^{1}I and P(S_0), for predicting the pathways of the photochemical reactions and also the probabilities of the relative transitions.

Starting from the knowledge of the molecular structure (the nuclear structure, that is, the relative positions of the nuclei), a set of one electron orbitals (MOs) are computed and/or qualitatively predicted. Thereafter, electrons are assigned with spin up or down to each of the MOs so to build the electron configuration.
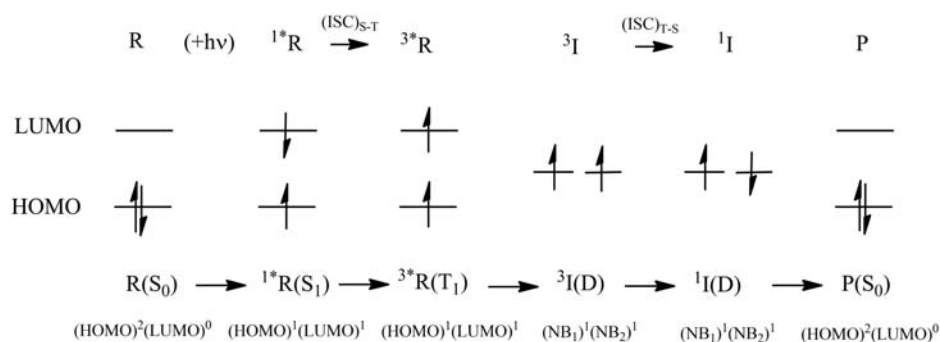
SCHEME 3.1 Changes in highest occupied molecular orbital and lowest unoccupied molecular orbital occupations along the generic reaction path: R + hν→*R→I(D)→P.

In most organic compounds, the ground state is a singlet state with all the electrons paired in the lowest in energy MOs (S_0). This will be the ground state always assumed in this chapter. The excited states of interest in photochemistry are normally the lowest excited state, as already anticipated. This means that, after light absorption, the produced *R states of interest are only the first and second excited states of singlet and triplet spin multiplicity (*R = S_1, S_2, T_1 and T_2).

As anticipated, organic compounds are relatively simple to be treated at a qualitative level. In fact, the relatively large energetic distance between occupied and unoccupied MOs allows to strongly reduce the number of MOs to be considered. It is a fortune that the excited states commonly involved in photochemical processes (also S_2 and T_2) can be qualitatively described by using the HOMO and LUMO alone. In other words, the nature of the four excited states listed earlier can greatly be related to changes in shape and occupations of only two MOs.

From the earlier discussion, the basic processes of absorption and emission of one photon (R + $h\nu \rightarrow$ *R and *R$\rightarrow$R + $h\nu$, respectively) can be associated with electron jumps between the HOMO and the LUMO.

Core MOs are normally not significantly affected by bond formation and can be considered identical to core atomic orbitals. A fortiori, their imperturbable character is also true when modifications are limited to the HOMO and LUMO shape and occupations. Valence MOs result from the mixing of valence rather than core electrons. They are affected, in general, by structure modification and/or changes in occupations of other MOs, like the HOMO and the LUMO. However, lower is the energy of valence MOs, smaller is the entity of the perturbation on them. In fact, lower is the energy of a MO, stronger is the nuclear attraction on them. This fact reduces the effect of changes in electron density associated with the HOMO and LUMO or other valence high energy MOs. This allows a further assumption: only the highest occupied MOs can be considered for interpreting the photochemistry of organic compounds, the lower occupied MOs can be considered unchanged.

As stated at the beginning of this paragraph, a brief overview is discussed about the photochemistry of olefins. Its comprehension is not possible without the fundamental notions exposed earlier.

Let's now consider an example of olefinic compound the easiest among all, ethylene (CH_2=CH_2).

The wave function representing an electronic ground-state Ψ_0 and corresponding to the electronic configuration of the ground-state (S_0) of ethylene can be represented as:

$$\Psi_0 = \ldots (\pi_{C=C})^2 \left(\pi_{C=C}^*\right)^0.$$

In this representation, the electrons in the σ orbitals (the lower-energy MOs) are not reported, because not important. The same is true for the unoccupied antibonding σ^* MOs which are much higher in energy than π^* and, consequently, not perturbed as the low energy σ.

As said, the $\pi_{C=C}$ orbital is the HOMO and the $\pi^*_{C=C}$ orbital is the LUMO (Scheme 3.2).

As sketched in Scheme 3.1, the lowest-energy electronic states in *R (namely S_1 and T_1) are associated with an electronic configuration in which one electron has been promoted from the HOMO of the ground-state configuration to the LUMO. These two states correspond to two half-occupied MOs of *R, in other words to a $(HOMO)^1(LUMO)^1$ electron configuration.

We can represent the wave function for an electronically excited state *Ψ of ethylene as:

$$*\Psi = \ldots (\pi_{C=C})^1 \left(\pi_{C=C}^*\right)^1.$$

In the following, the lowest-energy excited state will be labeled as a $(\pi,\pi)^*$ (Scheme 3.3). In summary, ethylene presents one only low-energy excited electron configuration labeled as *R(π,π^*), which is associated with the $S_1(\pi,\pi^*)$ and a $T_1(\pi,\pi^*)$ excited states, because the σ MOs are very low in energy and the σ^* MOs are very high in energy.

Electronic transitions are obviously described only in terms of the orbitals undergoing a change in electronic occupancy.

LUMO ($\pi^*_{C=C}$)^0 ———

HOMO ($\pi_{C=C}$)^2 ⥮
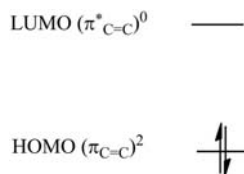
SCHEME 3.2   Electron configuration of ethylene in its ground state (S_0).

LUMO $(\pi^*_{C=C})^1$ LUMO $(\pi^*_{C=C})^1$

HOMO $(\pi_{C=C})^1$ HOMO $(\pi_{C=C})^1$

$^{1*}R(S_1)$ $^{3*}R(T_1)$
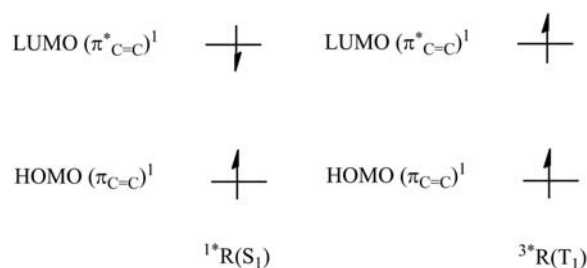
SCHEME 3.3   Excited singlet (S_1) and triplet (T_1) orbital occupations in ethylene.

Once one electron is excited from the HOMO and LUMO, chemical processes can start which can modify the C=C bond nature. The most common processes involving olefins after excitation are the twisting of the C=C bond and also the breaking of a same bond.

Continuing to use ethylene as a reference system for the π bond twisting or breaking of a generic olefin, the two carbon atoms in ethylene molecule assume a sp^2 hybridization in a trigonal planar geometry in which both the CH_2 groups are in the same plane.

As the ethylene molecule is twisted (the π bond twists), the energy of the π orbital increases whereas the energy of the π^* orbital decreases and two possible phenomena could happen. A first possibility is the perfect preservation of the carbon sp^2 hybridization. This occurs when the geometry around the carbon atoms continues to be trigonal planar. This situation is often assumed to take place during the twist, till the two methylene groups become mutually orthogonal (90° geometry). At this point, two orthogonal (non-overlapping) isoenergetic nonbonding orbitals are produced which corresponds to the carbon 2p orbitals (in ethylene), with each 2p orbital centered on each carbon atom. Furthermore, the π bond is completely broken and a "perfect" 1,2-diradical species is produced.

A second possibility is the partial loss of planarity of the structure surrounding one or both the carbon atoms during the twist. A partial pyramidalization of one carbon atom induces a different type of hybridization. As a result, the π and π^* MOs does not evolve in a couple of perfectly degenerate orbitals (for instance, the 2p atomic orbitals in ethylene), they rather give rise to not degenerate levels. Degeneration is removed because a different type of carbon hybridization is accomplished on the two carbon atoms (the 2p mixes itself with the 2s orbital differently on the two C atoms) and/or the existence of a significant overlap between the nonbonding hybrid orbitals on the two C atoms. In this case, a diradicaloid is produced rather than a perfect 1,2-diradical. The effect of a 90° twist on the π and π^* MOs of ethylene and also the effect of the twist on their occupations are showed in Schemes 3.4 and 3.5.

Scheme 3.4 regards the planar disposition of the two methylene groups, that is, before the twist starts. The occupations and spin of the two π electrons are sketched both in the ground (S_0) end in the excited states (singlet and triplet excited states); the different states are showed from left to right in order of increasing energy, that is:

$$S_0(\pi)^2 < T_1(\pi, \pi^*) < S_1(\pi, \pi^*) < S_2(\pi^*)^2.$$

Scheme 3.5 shows the situation when the twist angle reaches 90°, and carbon hybridization is maintained perfectly sp^2. The structural change associated with the twist leads to two perfectly degenerate nonbonding MOs (NB_1 and NB_2, 2p orbitals in ethylene) which can be occupied in four different ways. Also in this case the order in energies goes from the more stable situation on the left to increasingly higher energies ($^3D(p_1,p_2)$, $^1D(p_1,p_2)$, $Z_1(p_1)^2$, $Z_2(p_2)^2$).

Z_1 and Z_2 in Scheme 3.5 are degenerate if the olefin is symmetric (this is the obvious case of ethylene), the remaining singlet state ^1D is lower in energy, still lower is ^3D for the well known lower electron correlation in higher spin-multiplicity states.

It is interesting to correlate the singlet states in the completely twisted structure (Scheme 3.5) with the ones in the planar starting structure (Scheme 3.4), with particular interest on the lower in energy singlet state.

Fig. 3.2 shows the correlation in more detail and can be used as a reference in the following discussions.

Starting from the planar ground state $S_0(\pi^2)$, the effect of twisting is to destabilize the ground state. This is a consequence of the reduced overlap between the 2p carbon atoms and related destabilization of the π MO. The π^* MO lowers in energy but this is obviously immaterial in the ground state, being the π^* unoccupied. So, S_0 is continuously destabilized.

SCHEME 3.4   Orbital configurations of the planar and twisted at 90° geometries are shown.
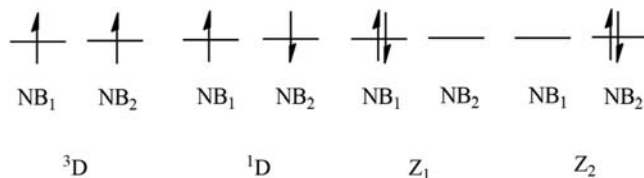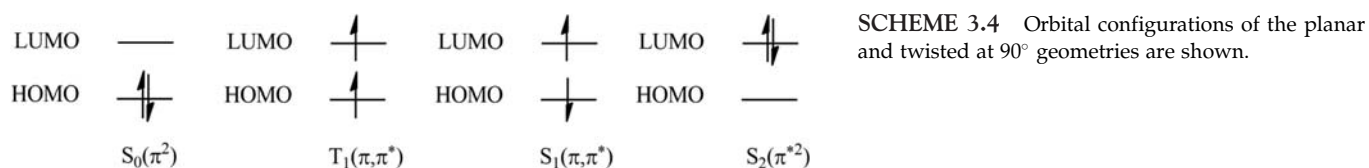
SCHEME 3.5   The possible orbital configurations of the twisted at 90° geometries are shown.
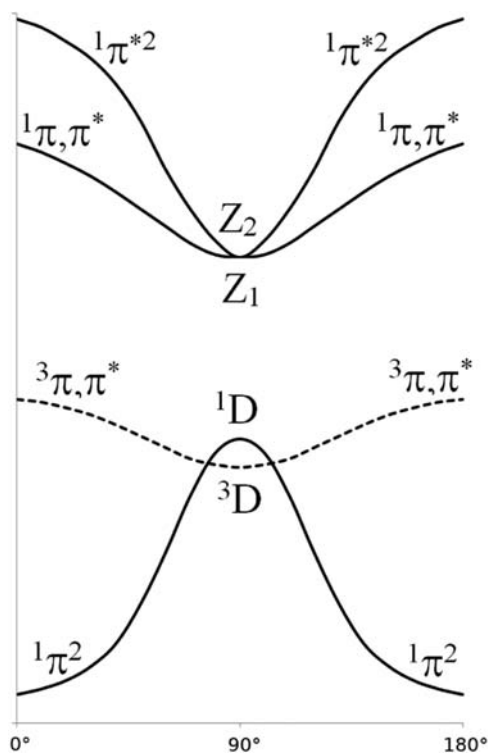
FIGURE 3.2   The potential energy surfaces associated with the twist around the C=C bond in ethylene. It is used as model for more complex olefins.

At the same time, S_1 and S_2 (and also T_1) are continuously stabilised along the twist.

In fact, in the planar ground-state structure, $S_1(\pi,\pi^*)$ is associated with the promotion of one electron from the bonding π MO to the antibonding π^* MO. This means that the π-bond results broken and, in this situation, the twist is stabilizing by virtue of the reduced steric repulsion of the two methylene groups. Furthermore, along the twist, a mixing of $S_1(\pi,\pi^*)$ and $S_2(\pi^{*2})$ occurs and, as consequence, S_1 and S_2 assume increasingly zwitterionic character.

When the full (90°) twist is reached, the lower singlet state, S_0 completes its transformation in the perfect BR ^{1}D (Scheme 3.5), whereas S_1 and S_2 complete their transformation in a couple of degenerate zwitterionic states at

higher energies (Z_1 and Z_2). Thus, the lowest in energy state in the twisted structure now is the triplet-state ^{3}D, the lowest in energy singlet state is the biradicalic ^{1}D and the lowest in energy excited states are the two zwitterionic states Z_1 and Z_2.

In summary, the correlations between singlet states are along the twist and starting from the planar ground structure:

$$S_0(\pi^2) \to {}^1D; \left(S_1\left(\pi^1\pi^{*1}\right)\right), S_2\left(\pi^{*2}\right) \to (Z_1, Z_2)$$
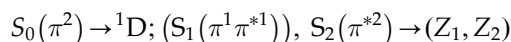
Now, we can consider what happens after light absorption: *R(π,π*) is obtained and, as said, twisting takes place to reduce the energy of the first singlet state.

Thus, an $S_1(\pi,\pi^*)$ excited state is expected to behave as a Z after structure relaxation (twist), thus it exhibits the typical reactivity of a carbonium ion or carbanion (see Scheme 3.6).

In more details, from $S_1(\pi,\pi^*)$ a Z can be produced, which could relax in a ground state Z which reacts according to its nature to give rise to proton or electron-transfer reactions, nucleophilic or elettrophilic additions and carbonium or carbanion rearrangements that proceed to isolated products, P; that is, $S_1(\pi,\pi^*) \to I(Z) \to P$. Another possibility even consists is the formation of Z_1 and Z_2 in the singlet excited states like before. Because they correspond to minima on the PES when a 90° twist is completed, they can act as funnels toward the ground state.

In this case, a $S_1(\pi,\pi^*) \to F \to P$ can be obtained and the product P is formed without passing through any ground state zwitterionic intermediate.

Also the triplet excited state, T_1, can be a funnel; also in this case a minimum on the triplet PES is reached when the twist is complete. ISC toward the ground state can take place and the product can be obtained without any intermediate according to the same scheme, apart from the necessity to populate the triplet state rather than the excited singlet state.

The presence of a planar or twisted C=C bond is very common in photochemical processes which originate from alkenes double bonds. The general description of the changes which can take place in terms of excited state nature and energies due to the twist can be easily transferred to all the compounds showing this functional group. However, more powerful interpretative tools are necessary if we want to explain or also predict the route of a photochemical reaction in depth, albeit we are limiting ourselves to a qualitative interpretation of the observed reactions. These tools allow the interpretation of the preferred direction followed by a photochemical process in the excited state of the substrate after light absorption.
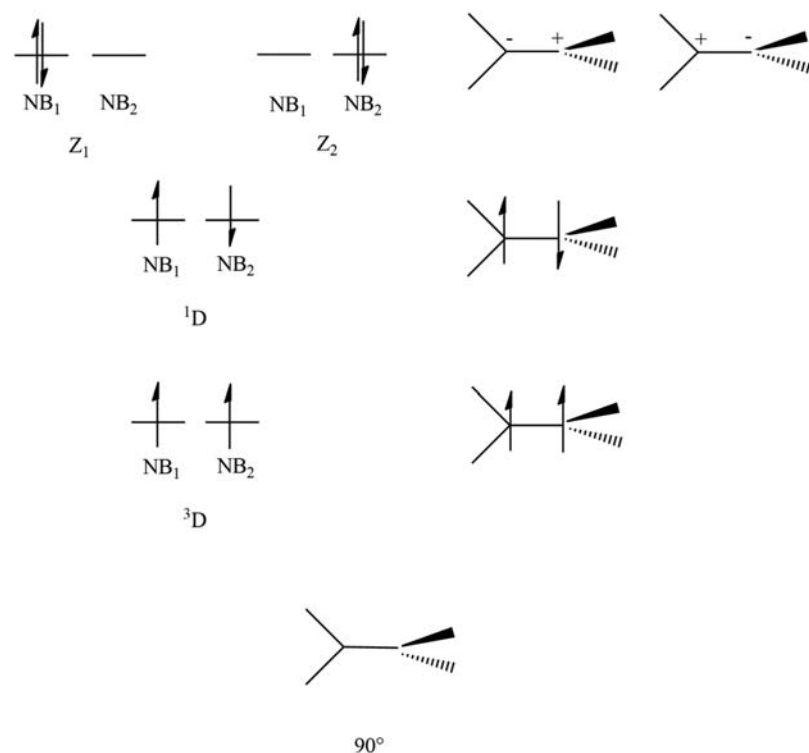
SCHEME 3.6 The possible different states which can be associated with the fully twisted geometry (90°) of the ethylene molecule.

The theory of the frontier molecular orbitals (FMOs) can be effectively used in this respect. The frontier orbitals of a molecule are the HOMO and LUMO and they often assume an extreme importance in establishing the reactivity of any organic compound (at least in first approximation). In any organic molecule, apart few particular cases, the electron configuration of R is $(HOMO)^2(LUMO)^0$, whereas a $(HOMO)^1(LUMO)^1$ configuration is associated with *R. Interactions between frontier orbitals of the same molecule or a couple of reacting molecules can be modeled as electron transfer (electron donation) from occupied to unoccupied MOs, or between occupied and half-occupied MOs.

Such interactions can be considered an extension of the Lewis acid-base concept to all the compounds. Such an extension is based on the idea that all the occupied MOs are able to donate electron charge, not only the compounds featuring lone pairs as predicted from their Lewis structure. The HOMO is the most suitable occupied MO in donating electron density, the LUMO is the most available to receive. The effectiveness of this HOMO/ LUMO interaction (donor/acceptor) is determined by the overlap integral between the donor and acceptor MOs and the energy gap between the same MOs ($\Delta E_{HOMO-LUMO}$). Small energy gaps and positive overlap integrals lead to good level of mixing [electron charge transfer (CT)] between the two MOs and a high level of stabilization is induced by this interaction. In case of comparable energy gaps between MOs, significant positive overlap of the interacting frontier orbitals of reagents implies higher stabilization.

These concepts find direct application in determining the reaction rate of simple reaction steps. In fact, if the electron CT takes place along a reaction pathway (or it is the only occurring chemical phenomenon), larger is the entity of the CT lower is energy barrier associated with this process. Lower activation barriers mean faster reactions. This is a well known idea in Chemistry but it could be less known that it can be applied to excited state reactions as well as ground state reactions. Hence, a negative or zero overlap of the frontier orbitals normally involves a large energy barrier in case of CT along the reaction path, because the favorable stabilization associated with the CT is not present and the reaction pathway crosses high energy zones of the PES.

From above, the degree of HOMO/LUMO interaction can discriminate a fast from a slow reaction pathway. If we have two possible reaction pathways (*R→I$_1$ or *R→I$_2$), the one associated with a lower energy barrier will be predominant or the only one which is actually followed.

The stereoelectronic control of a reaction pathway is the first application of the theory discussed earlier, as said, the FMO theory.

If the involved frontier orbitals are the same, the pathway of maximum overlap integral will be followed. If the overlap integral depends on the stereochemistry of the path, it will control the stereochemistry of the process. This idea is known as "principle of maximum positive overlap," albeit it is named "principle" it has a simple quantum-mechanical explanation that we have discussed earlier.

The HOMO is associated with the highest energy of all the occupied orbitals in the ground state. This means it is easily perturbed by external fields or interactions, it has the lowest ionization potential of any occupied orbital in the ground state R and it is the most suitable MO in releasing electron density to electrophylic sites (the LUMOs). Therefore, the HOMO is the most nucleofilic orbital and can be considered an electron donor (eD).

The LUMO is an unoccupied orbital in the ground state, as we already know, and it is electrophylic, being capable of accepting electron density.

If the reaction takes place in the first excited state, in a common organic compound it implies to be faced with a $(HOMO)^1(LUMO)^1$ electron configuration. Hence, half-filled HOMO and LUMO are present, and they are also referred to as singly-occupied MOs. Because *R has two singly occupied orbitals (a singly occupied HOMO and LUMO), a number of possible CT interactions are possible from or to the HOMO or LUMO of another molecule or some other groups in the same molecule. This is clearly true for singlet and triplet excited states.

Scheme 3.7 graphically describes how the charge transfer occurs from one orbital to another and how stereochemistry influences the plausibility of a reaction pathway.

Since we are concerned with CT interactions, we label the *R HOMO as an electron acceptor (eA) orbital because it is a half-filled bonding orbital at low energy and will be stabilised by accepting a second electron into the half-filled higher-in-energy HOMO.

We also label the LUMO of *R as an eD orbital because it is a half-filled antibonding orbital and will be stabilised by donating its electrons to a lower energy orbital that is accepting electron density.

Scheme 3.7 shows the possible interactions between the HOMO and LUMO of an excited state molecule (*R) and the HOMO and LUMO of a second molecule M. Two possible orbital interactions can occur when *R interacts with M in the hypothetical situation according to which the energies of the HOMOs of *R and M and the LUMOs of *R and M are similar: (a) M is an electron donor so that the HOMO of *R removes charge from the HOMO of M and (b) M is an electron acceptor so that the LUMO of *R transfer charge toward the LUMO of M.
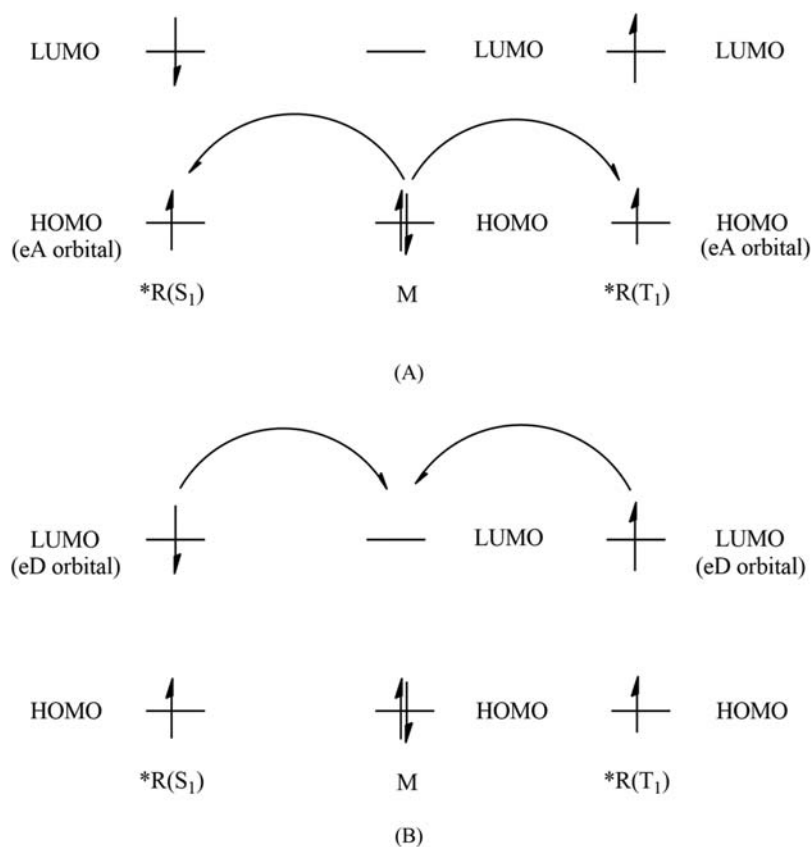
SCHEME 3.7 Interaction between frontier orbitals in an electronically excited molecule *R and a ground-state molecule M. (A) Electron transfer from the highest occupied molecular orbital of M to the half-filled highest occupied molecular orbital of *R (S_1) or *R(T_1); (B) Electron transfer from the lowest unoccupied molecular orbital of *R(S_1) or *R(T_1) to the lowest unoccupied molecular orbital of M.

Of the two possibilities sketched in Scheme 3.7, the one which is actually observed depends on the HOMO and LUMO shapes (propensity to produce large overlap integrals), the *R and M molecular structures around the interacting functional groups (phenomena like steric hindrance could limit the possibility of HOMO/LUMO approaching) and HOMO and LUMO energies (i.e., their energy separation).

If the first orbital interaction in Scheme 3.7 is associated with a larger energy stabilization than the second one, it will be the preferred (or plausible) process, which can give rise to a chemical modification specifically determined by the same interaction. Otherwise, the second process will be the favored.

Furthermore, the fact that *R can be an eA or an eD according to the nature of M allows to consider it as a strong oxidizing agent or a strong reducing agent, respectively.

Such redox attributes of *R will be of great importance when we will consider photoinduced electron transfer.

In conclusion, effective orbital interactions can be achieved in case of frontier orbitals with similar energies and able to produce large and positive overlap integrals. Thermodynamical aspects must be taken into account, as well, because they give further insights about the downhill direction which is reasonably followed by a reaction path.

The *R→F→P and *R→I→P processes are the most important primary photochemical reactions.

Among the *R→F →P reactions, we can consider the *cis-trans* isomerization about a C=C bond and the photochemically concerted pericyclic reactions initiated from $S_1(\pi,\pi^*)$ states of ethylene, conjugated polyenes and so on.

The photoinduced *cis-trans* isomerization of the C=C bond could take place on the $S_1(\pi,\pi^*)$ PES and $T_1(\pi,\pi^*)$ PES. It is a characteristic primary photochemical reaction of alkenes[2,3] but there could be structural, electronic or environmental barriers to *cis-trans* isomerization.

In case of alkyl-substituted ethenes and large-ring cycloalkenes undergo *cis-trans* isomerization upon direct excitation to $S_1(\pi,\pi^*)$ (Scheme 3.8).

Furthermore, the *cis-trans* isomerization in these class of compounds starts from $S_1(\pi,\pi^*)$ (after light absorption or other type of excitation) and proceeds with a twisting motion around the C=C bond. As already discussed in this paragraph, the singlet excited state is stabilised by the twist and it approaches the minimum on the excited singlet surface near the perpendicular geometry (close to 90° twist angle). This minimum possesses significant
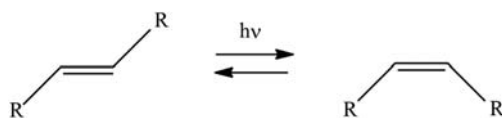
SCHEME 3.8   The *cis-trans* isomerization of a generic alkyl-substituted ethene.
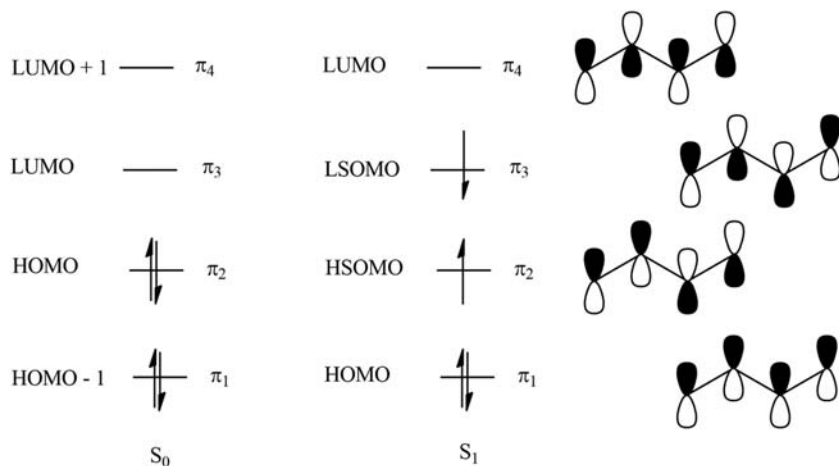
SCHEME 3.9   1,3-butadiene: schematic of the ground and excited S_1 states and their representation in terms of molecular orbitals.

zwitterionic character due to mixing between S_1 and S_2. It is an example of a $S_1(\pi,\pi^*) \rightarrow I(Z)$ path which could undergo one secondary thermal process or IC toward S_0.

The latter radiationless IC process consists in an almost vertical jump from the S_1 to S_0 PES and takes place near the maximum (almost complete twist). Some of the following trajectories on the S_0 PES are placed before of the maximum, thus they restore the original structure of the C=C bond and others proceed beyond the maximum (to the right of the maximum) and lead to a structural isomerization of the C=C bond.

The $S_1(\pi,\pi^*) \rightarrow T_1(\pi,\pi^*)$ ISC process is a low probability process in alkenes; hence, the use of sensitizers is necessary to promote the alkene in its ground state to $T_1(\pi,\pi^*)$ and induce *cis-trans* isomerization on this PES.

Although the triplet energies of simple alkenes are relatively high (~ 80 kcal/mol), it is possible to produce $T_1(\pi,\pi^*)$ efficiently with high-energy sensitizers such as benzene and alkyl benzenes (~ 80 kcal/mol).

There's no evidence that $S_1(\pi,\pi^*)$ or $T_1(\pi,\pi^*)$ are able to promote *cis→trans* photoisomerization in these small-ring cycloalkenes (cyclopropene, cyclobutene or cycloentene). The large ring strain in this cyclic structures strongly hinder any twisting motion around the C=C bond, forcing the molecules to maintain their *cis* conformation.

Cyclohexenes is the first in the series of cycloalkenes which shows photochemically induced *cis→trans* isomerization. It gives rise to a transient *trans*-cyclohexene which cannot be isolated as a stable species at room temperature. It quickly isomerizes back to the *cis* isomer but it can be chemically trapped. Cycloheptene behaves similar to cyclohexene in that *trans*-cycloheptene is a transient species that can only be chemically trapped. *Trans*-cyclooctene and larger ring *trans*-cycloalkenes behave as not-cyclic alkenes. They show a reltively good stability as *trans* isomers so that they can be isolated.

Scheme 3.9 is used to describe the *cis-trans* isomerization process in conjugated dienes. The case under study can be considered as a model for isomerization of 1,3-pentadiene and 2,4 hexadiene, as an example, because we consider the case of two conjugated double bonds.[4,5]

Upon $\pi_2 \rightarrow \pi_3$ photoexcitation, 1,3 dienes undergo an electronic transition which is associated with an increase of the π-bond order between the C_2 and C_3 atoms. This derives from the nature of the π_3 MO which shows a bonding character between these atoms (see Scheme 3.9).

At contrary, a decrease in bond order takes place between the C_1–C_2 atoms and between the C_3–C_4 atoms, because the π_3 orbital presents antibonding character between these atoms, whereas it is bonding in π_2.

As a result of these changes in bond orders, conformational changes on C=C bonds which are rapid in S_0 can be inhibited in both $S_1(\pi,\pi^*)$ and $T_1(\pi,\pi^*)$.

As a consequence, the *cis-trans* isomerization around the C_2-C_3 bond could be so slow in presence of excited states that the different rotamers cannot reach the chemical equilibrium among themselves. This results in the so-called nonequilibrating excited rotomers (NEERs). Thus, conformers of polyenes that are in rapid dynamic equilibrium in S_0, according to the NEER principle, do not necessarily possess lifetimes that allow them to equilibrated in $S_1(\pi,\pi^*)$ and $T_1(\pi,\pi^*)$.

Scheme 3.10 shows the NEER principle in a generic 1,3-diene.

In S_0, a single bond between C_2-C_3 and double bonds between C_1 and C_2 and between C_3 and C_4 are present. There is essentially free rotation around the C_2-C_3 bond.

In S_1 and T_1, there is some double-bond character between C_2-C_3 that inhibits rotation. Since the rates of deactivation for excited states of flexible alkenes are very high, *cis-trans* isomerization competes with conformational equilibration. As a result, the two conformers of 1,3-butadiene have different, noninterconverting structures in $S_1(\pi,\pi^*)$ and $T_1(\pi,\pi^*)$, as shown in Scheme 3.10.

When aromatic substituents bind the C=C double bond, π-conjugation can be able to change the nature of the excited states. It is possible that the electronic excitation continues to be localized on the C=C bond, as in the parent aliphatic olefin. Otherwise, it is possible that the excited states are localized on the aromatic ring or they are shared between the two functional groups.

Depending on several electronic and structural features, S_1 in aryl ethenes involves the double bond at different extends. The examination of the HOMO and LUMO (computed or characterized in other ways) provides some insights. Larger is the double bond character of S_1, stronger will be the opposition to the twist motion in the excited state and a slower *cis-trans* isomerization is expected.

As an example, in the specific case of 1-phenylethene, a substantial degree of double bond is found in S_1. At contrary in S_n ($n > 1$) such a double bond character is lower. As a consequence, we can easily predict a quicker twist in the higher excited states and a slower twist in S_1. As a consequence, a faster *cis-trans* isomerization is found in these higher states.

The photochemical *cis-trans* isomerization of stilbene (1,2-diphenylethene) (Scheme 3.11) has been studied in great detail.[6,7]

Several studies found out many details about the PES for the *trans→cis* and *cis→trans* geometric isomerization for excitations of both $S_1(\pi,\pi^*)$ and $T_1(\pi,\pi^*)$.
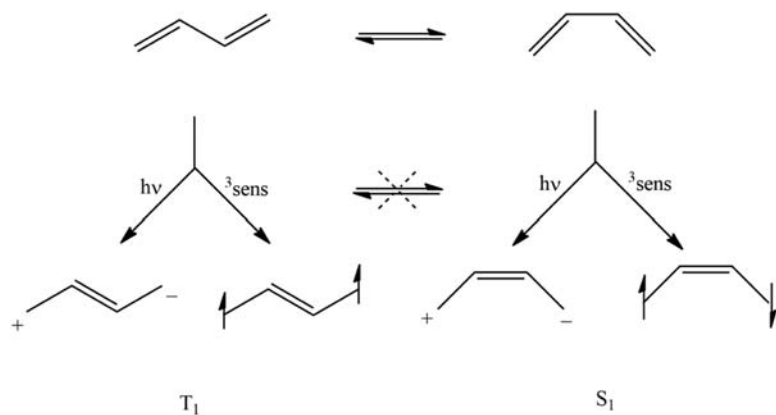
SCHEME 3.10 The NEER principle of noninterconverting excited-state rotomers applied on 1,3-butadiene. "Sens" is for sensitizers.
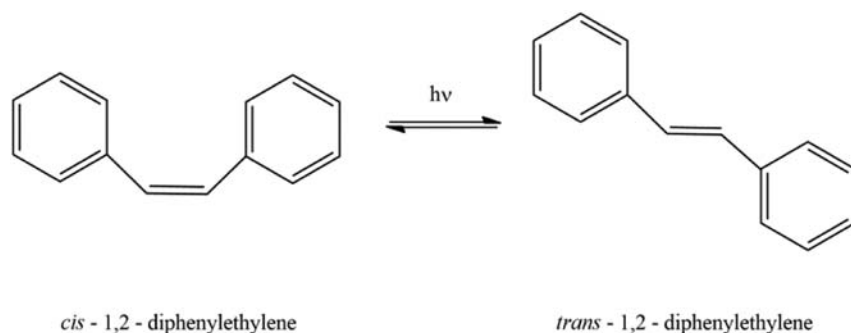
SCHEME 3.11 Photochemical cis-trans isomerization of stilbene.

cis - 1,2 - diphenylethylene

trans - 1,2 - diphenylethylene

Fig. 3.3 shows the PES involved in the process and the followed pathways.

Stilbene shows the particular spectroscopic feature which consists in emission from *trans*-stilbene after absorption of *cis*-stilbene. This is consistent with a photochemical process which converts *cis*-stilbene $S_1(\pi,\pi^*)$ directly into *trans*-stilbene $S_1(\pi,\pi^*)$.[8]

This result represents an example of an *R→*P primary photochemical process (a process occurring entirely on an excited-state surface). This direct conversion means that there cannot be a deep minimum for the twisted structure from the S_1 state of either geometric isomer.

The above observations and measured energies of the S_1 and T_1 states for stilbene allowed the construction of the energy surface diagram shown in Fig. 3.3 which depicts a more quantitative description of the geometric isomerization than Scheme 3.11.

A difference is expected passing from aliphatic alkenes to stilbene.

In stilbenes, the excited states are not completely localized on the C=C bond. As a consequence, a residual double bond character remains in $S_1(\pi,\pi^*)$, which opposes to the twist.

At the same time, steric hindrance favors the *trans* isomer respect to the *cis* one, also in the excited state. Such a different thermodynamical stability induces a lowering of the barrier in the direction of lower energies, that is, from the *trans* to the *cis* isomer. In the opposite direction, at contrary, a barrier is present.

Another important example of application of FMP theory for interpreting the observed photochemistry are pericyclic reactions consisting in electrocycling ring openings and ring closure, cycloaddition reactions and sigmatropic rearrangements.

In this respect, in the analysis of a photochemical reaction such as *R→F →P and *R→I, theoretically, one has to select the appropriate reaction coordinate or coordinates that describe the nuclear geometry changes accompanying the transformation of reactants to products. In principles, all the possible reaction coordinates should be analyzed.

In practice, we try to select only the lowest-energy reaction pathways by the use of orbital interactions and then analyze them by assuming that a certain symmetry is maintained along the reaction coordinate.

As an important example, the photochemical electrocyclic ring opening of cyclobutene and the related photochemical electrocyclic ring closure of 1,3-butadiene will be discussed here.

The general methods applied before on simple model compounds, can be readily extended to other photochemical electrocyclic reactions and other photochemical pericyclic reactions such as cycloadditions and sigmatropic reactions.

The guideline offered by the FMO theory lead to the stereochemical selection rules for pericyclic reactions. As an example, the Woodward-Hoffmann rules consist in theory used to predict the stereochemistry of pericyclic reactions based on the orbital symmetry. These rules are perfectly consistent with the FMO theory.
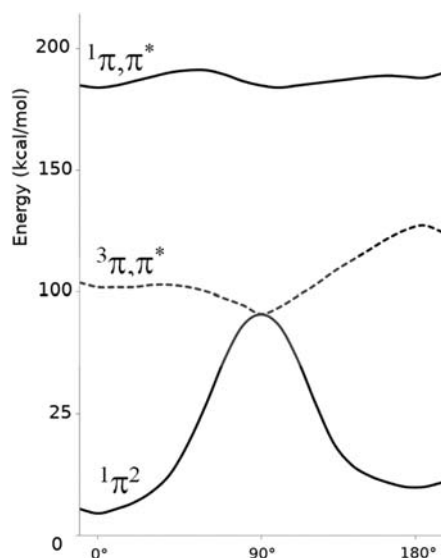
FIGURE 3.3   Stilbene potential energy surfaces of the ground ($^1\pi^2$), triplet excited state ($^3\pi,\pi^*$), and singlet excited state ($^1\pi,\pi^*$).

If the FMO theory is applied, the selection rules based on the best positive overlap and the smaller energy-gap are evaluated between the HOMO and LUMO. According to these guidelines, we are able to predict that, for reactions initiated from the $S_1(\pi,\pi^*)$ states of cyclobutene, both $\sigma(HOMO)\rightarrow\pi(HOMO)$ and $\pi^*(LUMO)\rightarrow\sigma^*$ (LUMO) are the best CTs because the $\sigma(HOMO)$ and $\pi(HOMO)$ are close in energy and this is true for the $\pi^*(LUMO)$ and $\sigma^*(LUMO)$. Therefore, lower energy barriers are expected for reaction paths which are able to enable those CTs.

Two possible reaction pathways can be predicted: in the conrotatory mode, both the end groups turn in the same direction rotating clockwise or counter-clockwise. As a consequence, the p atomic orbitals on the end carbon atoms rotate accordingly. In the disrotatory mode, the end groups turn in opposite directions and, consequently, one atomic orbital turns clockwise and the other counter-clockwise.

As sketched in Scheme 3.12, in *R, orbital symmetry for the disrotatory process is favored by the rule of maximum positive overlap. When the orbitals rotate in the disrotatory manner, the $\sigma(HOMO)\rightarrow\pi(HOMO)$ and $\pi^*(LUMO)\rightarrow\sigma^*(LUMO)$ CT correspond to positive overlap. At contrary, the conrotatory motion corresponds to negative overlap. So, simply from a consideration of frontier orbital interactions, we expect that for this four-electron system (for thermochemically feasible reactions) the disrotatory interconversion is photochemically allowed (favorable FMOs interactions) whereas the conrotatory interconversion is photochemically forbidden (unfavorable FMOs interactions).
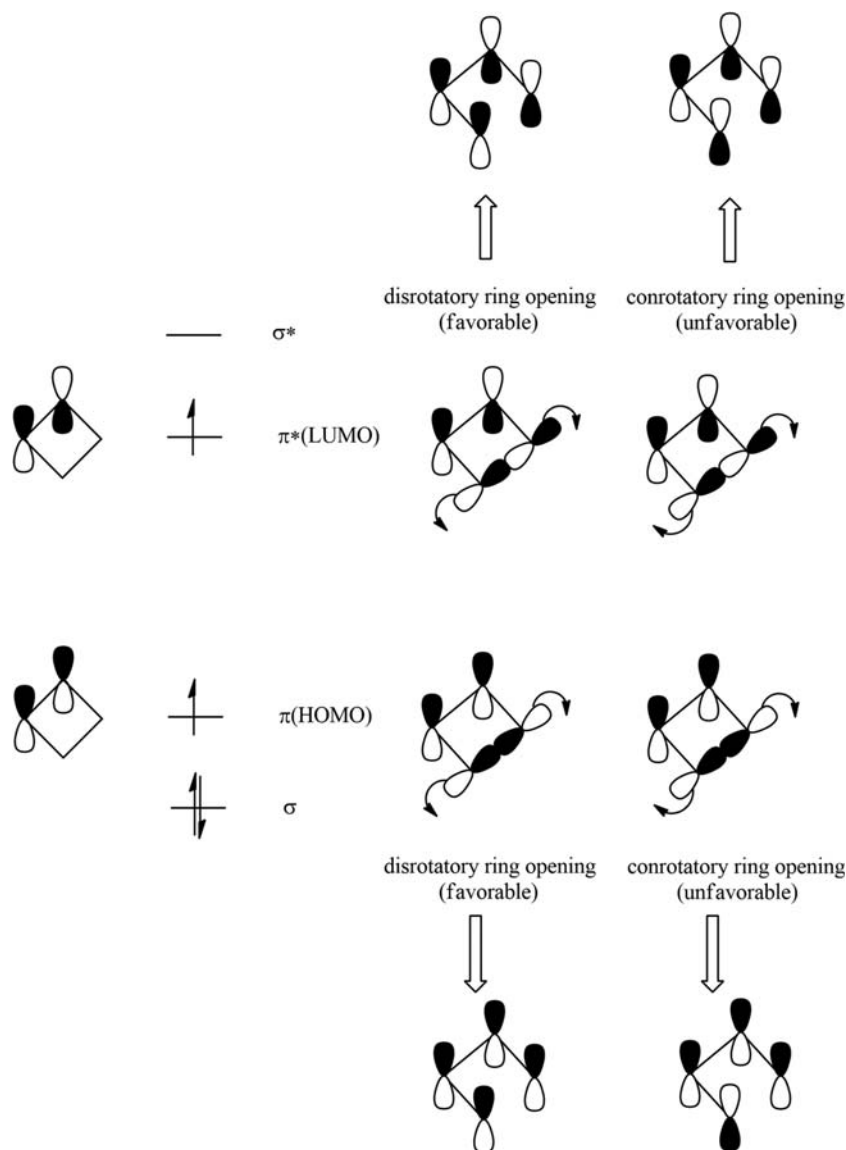
SCHEME 3.12 Conrotatory and disrotatory ring opening of the π,π^* state of cyclobutene to form 1,3-butadiene.

This conclusion is corroborated by the experiment and represents a success of the FMO theory in the prediction of the stereochemistry of photochemical reactions based on the knowledge of the π,π^* state electronic characteristics.

Concerted pericyclic reactions are not likely to occur in the $T_1(\pi,\pi^*)$ state. This is predicted by a general rule in photochemistry, according to which spin is maintained in an elementary step.

As concluding remarks, other primary photochemical reactions starting from the $S_1(\pi,\pi^*)$ state can be effectively described by the means of the FMO theory which have not be detailed in this paragraph. They mainly consists in reactions based on carbonium ions and of carbanions and electron transfer processes.

The actual rate of any of these reactions will depend on the details of the reactant structure and the reaction conditions; the probability of any reaction from $S_1(\pi,\pi^*)$ will depend on a competition between the rate of reaction and the rate of other photophysical or photochemical pathways from $S_1(\pi,\pi^*)$ states.

3.2 Photoinduced pericyclic reactions: Stilbene and its diheteroarylethenes derivatives

Oxidative photocyclization of stilbenes was reported before 1964[9,10] when Mallory settled experimental conditions which limited side-reactions and led to more quantitative yields.[11−13] Scheme 3.13 shows what happens after light absorption of a generic stilbene. Quick reversible reactions occur in excited state, which interconvert Z- and E stilbene and, at the same time, Z-stilbene with dihydrophenantrene (DHP). Such quick equilibria make immaterial the use of Z- or E-stilbene as starting substrate.

The Mallory major addition consisted in using iodine as oxidizing agent, so to trap DHP into phenantrene (P). In summary, the well known Mallory reaction is the iodine-catalyzed oxidatative photocyclization of stilbenes in presence of molecular oxygen.

It was proposed that iodine action is due to the following Scheme 3.14 photoreaction mechanism.[13]

The obtained hydrogen iodide is transformed back to iodine by reaction with molecular oxygen. Iodine concentration affects both reaction yields and selectivity (when present). Increasing iodine concentration beyond 5%−10% of stilbene normally leads to excessive side-reactions and consequent lower yields. As a result, the use of catalytic concentrations of iodine is usually recommended for higher yields.

In 1991 Katz and others[14] reported that the presence of iodide scavengers (typically metiloxirane)[15,16] strongly improves yields. This work demonstrated the fact the hydrogen iodide is the main responsible of side reactions and/or substrate degradation like stilbene double bond saturation. Furthermore, evidences were reported according to which it is not oxygen to restore iodine from iodide but substances formed from oxygen during the
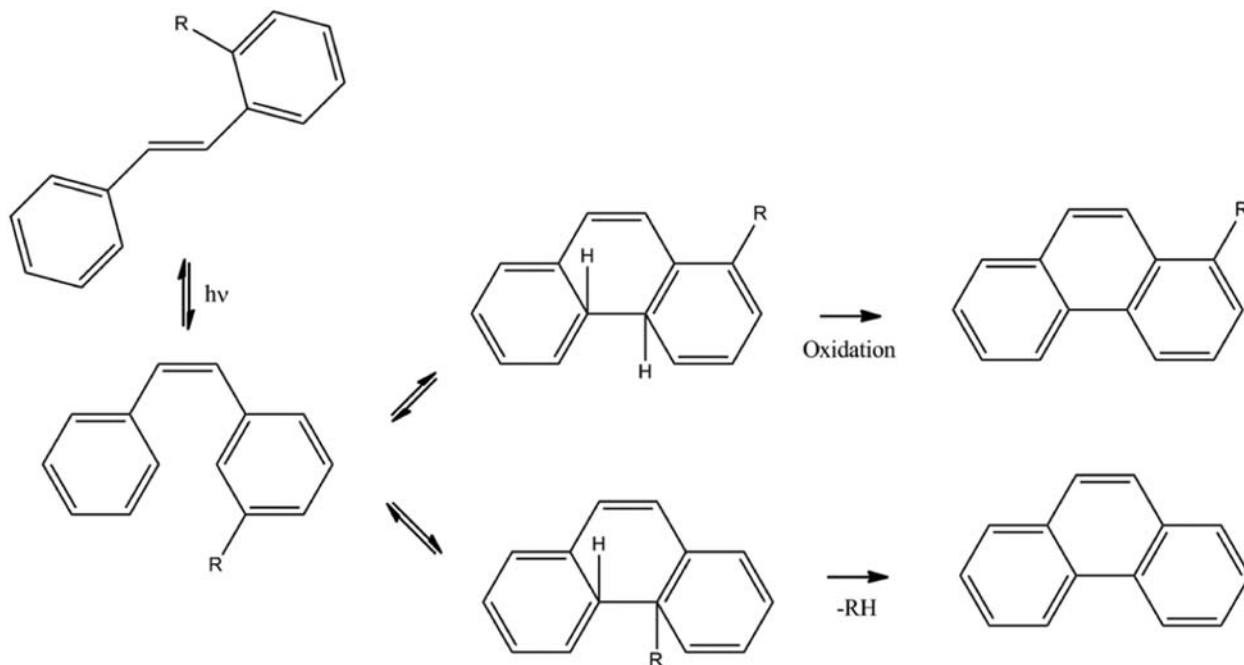
SCHEME 3.13   The excited state reaction paths of a generic stilbene occurring after ultraviolet absorption.
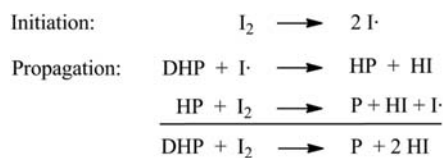
SCHEME 3.14   The photochemical oxidative action of diiodine. Dihydrophenantrene is dehydrogenated to hydrophenantrene (HP) and to phenantrene in the two steps of the chain propagation.

TABLE 3.1   Some examples of reaction yield gain due to the application of the Katz conditions in place of using catalytic amount of iodine.

Substrate	Product	Product yield (Catalytic I_2)	Product yield (Katz condition)
		51% (8 h)	95% (8 h)
		< 8% (3.5 h)	61% (13 h)
		< 4% (4.5 h)	71% (4.5 h)
		61% (4 h)	100% (1 h)
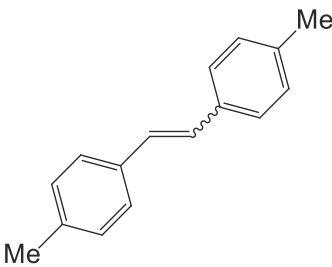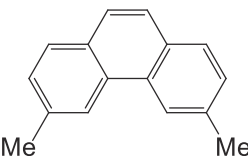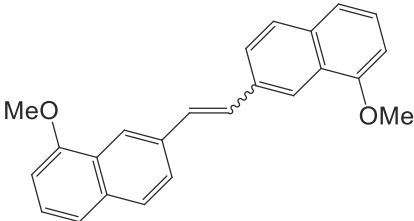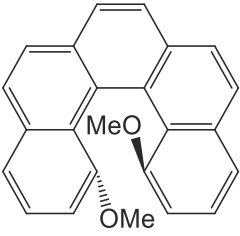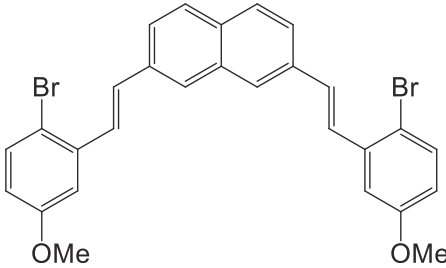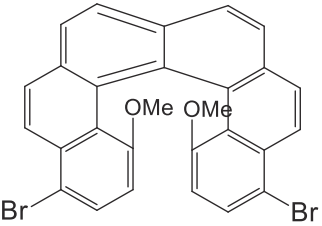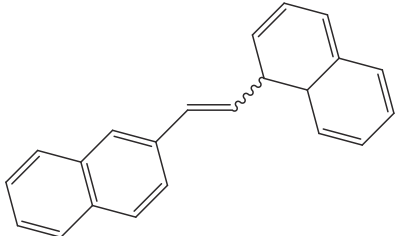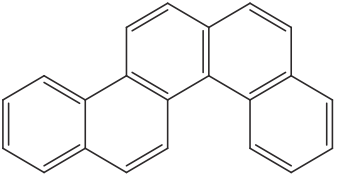
photocyclization.[14] Thus, oxygen removal from the reaction environment was a further step forwards a more quantitative reaction. In summary, the so-called Katz conditions of the Mallory reaction consist in using iodide scavengers, inert atmosphere and the presence of one equivalent of iodine rather than a catalytic amount (being iodine not reoxydated back by oxygen anymore).

Table 3.1 is intended to show only a few examples of the big improvement reported on going from the use of catalytic I_2 amount to the Katz conditions.[14]

Albeit the Mallory reaction allowed increasing the usable stilbene concentration and albeit the Karltz conditions sometimes helps in this respect, stilbene concentration remains limited to about 0.01 mol/L, at most, because higher concentrations lead to excessive [2 + 2] cycloaddition reactions between two stilbenes.[12] This drawback discourages the application of Mallory reaction for the production of phenantrene and other polyaromatic compounds (PACs) for biological and more in general technological applications, where quantitative and easy processes are desirable.

With the aim to circumvent the necessity of substrate low concentrations, alternatives to iodine as oxidizing agents are reported to be strongly encouraging like (2,2,6,6-tetramethylpiperidin-1-yl)oxyl, more concisely referred to as TEMPO.[17] It is interesting to note how the proposal of new oxidizing agents is strictly connected to the increasing knowledge about the excited state dynamics of stilbene.

Scheme 3.15 collects what is known about the stilbene photoreaction paths, more details can be found in reference 17.

It is assumed that the excited states reaction paths take place on the lowest singlet excited state (S$_1$). Though both Z- and E-stilbene can (in principle) be involved the [2 + 2] photocycloaddition process so produce tetraphenylcyclobutane (TPCB), only excited state Z-stilbene is assumed to undergo this side-reaction as shown in Scheme 3.15.[18,19]

This is due to the short lifetime of excited Z-stilbene (0.7−1.4ps) in comparison to the E-stilbene one (80−140ps).[20]

Thus E-stilbene very quickly evolves toward DHP and an intermediate pyramidalized species known as Phantom State. The Phantom State produces the ground state E- and Z-stilbene. Z-stilbene, at contrary, lives enough to produce TPCB.

Furthermore, the phantom state mostly produces the Phantom State and thus ground state stilbene.

The problem is that iodine is known to catalyze the formation of E-stilbene,[12] strongly limiting the amount of Z-stilbene available for reaction. Use of TEMPO as oxidizing agent allowed excellent reaction yields also at stilbene concentration of 0.1 mol/L.[17]

This is ascribed to its lower tendency to induce Z-stilbene. The easy availability and low cost of TEMPO is a further reason of choice, mostly for technological applications.
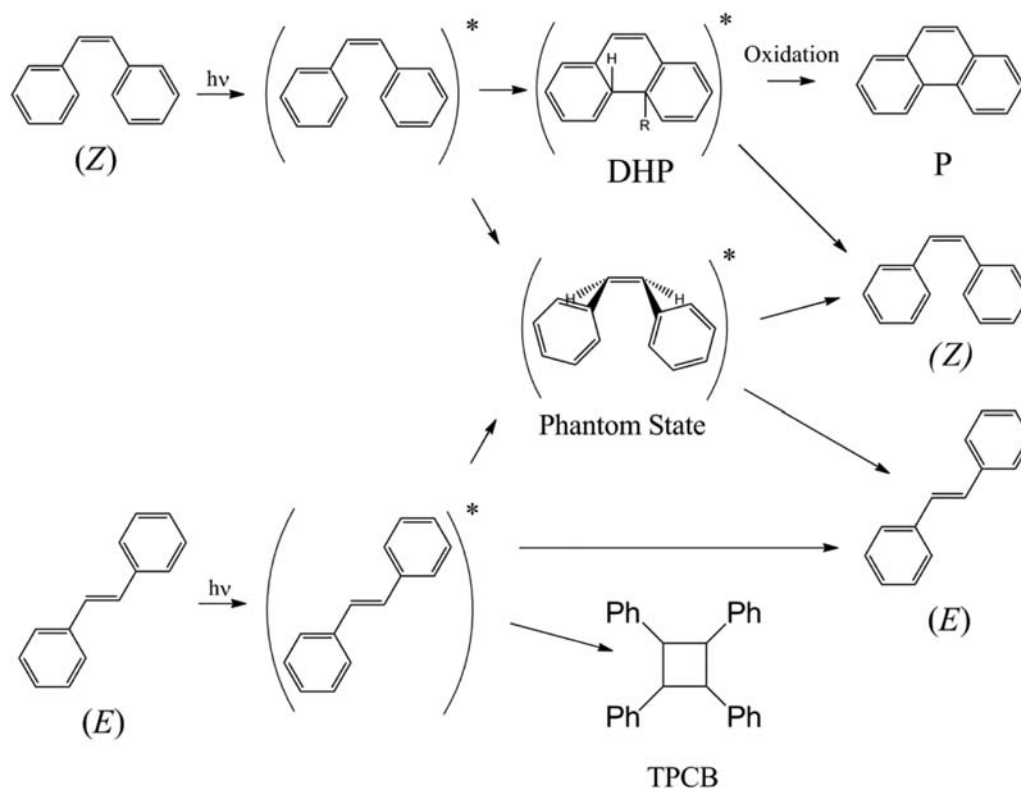
SCHEME 3.15   The supposed excited state pathways from E- and Z-stilbene to phenantrene though dihydrophenantrene and tetraphenylcyclobutane. Species in their excited states are labeled with an asterisk.
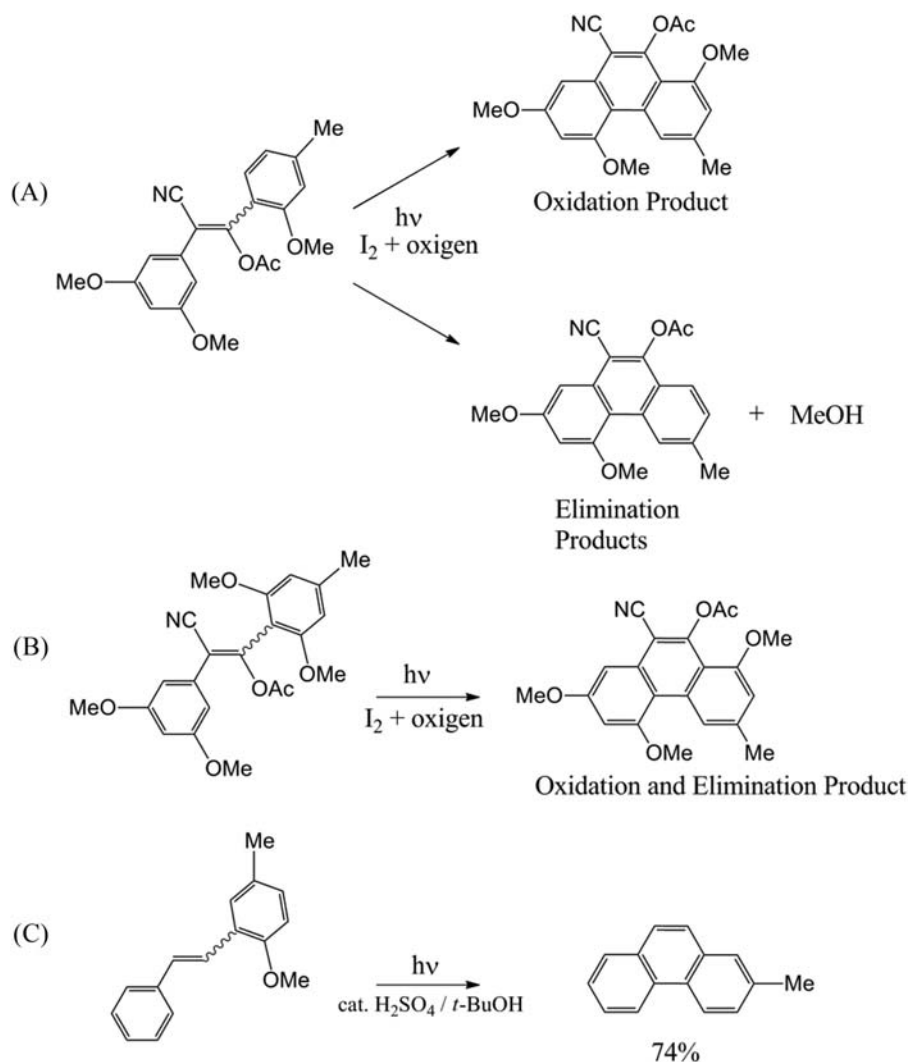
SCHEME 3.16 (A) Competition between oxidation and elimination mechanisms leads to different products in asymmetric cases; (B) the use of symmetric substrates easily overcomes the problem.

With reference to Scheme 3.13, elimination is the alternative trapping process of DHP.[21]

It is obviously possible when suitable substituents (R in the Scheme) are present in *orto* to the bridging double bond of stilbene. According to the goal of the synthesis, elimination can be desirable or not. The example of Scheme 3.16A shows how elimination can be deleterious if the oxidation product is the target.

The problem was easily circumvented in the specific example of Scheme 3.16 by using a symmetrically substituted stilbene[22] (Scheme 3.16B) but similar direct alternatives are not available in most cases and often difficult to isolate isomers are obtained.

With the aim to increase selectivity toward elimination, an acid environment has been proposed to improve in case of methanol elimination (Scheme 3.16C).[23]

Alternative approaches are based on better leaving groups like tosyl at the double bond bridge in combination with a basic environment.[24]

However, many observations allowed the conclusion that selectivity toward elimination can be improved in basic media but competition with oxidation cannot be considered completely overcome.[21,25]

3.2.1 Some applications of the Mallory reaction

In this subparagraph, a few examples are discussed of the many applications of the Mallory reaction and its variants exposed in the paragraph above.

Here, particular regard is addressed to the obtainment of polycyclic aromatic compounds useful in the field of material chemistry, like production of solvatochromic substances discussed in this chapter.

A family of thienoacene compounds with a fused pyrimidine ring **1(a-d)** (shown in Scheme 3.17) was prepared by irradiation of 4,5-dithienyl-substituted pyrimidines **1** using iodine as oxidant and propylene oxide to eliminate HI.[26] They find useful application in the field of organic semiconductors (OSCs) and show that the Mallory reaction can be directly applied to heteroaromatic stilbenes as well.

Corannulene is a polycyclic aromatic compound related with fullerene C_{60} that present optoelectronic properties and charge-transport characteristics with applications in material science.[26]

The corannulene nucleus **3** was obtained by irradiation of compound **2** with a medium pressure Hg lamp using iodine as oxidant and propylene oxide as hydrogen iodine scavenger (Scheme 3.17).[27]

Fluorinated phenanthrenoids **5(a-b)** (Scheme 3.17) were obtained by irradiation of derivatives **4(a-b)** with light at λ = 365 nm using iodide (0.5 equiv.) and excess of 1,2-epoxybutane.[28] Photoclycization by elimination in basic environment rather than oxidation found many applications in biological and material chemistry fields. HCl and HBr are the usual elimination products although tosyl is also many times proposed as leaving group.

Nanographene **6** was obtained by HCl elimination in basic environment with good yields (Scheme 3.18).[29]

Interestingly, in some cases the basic environment is not necessary.
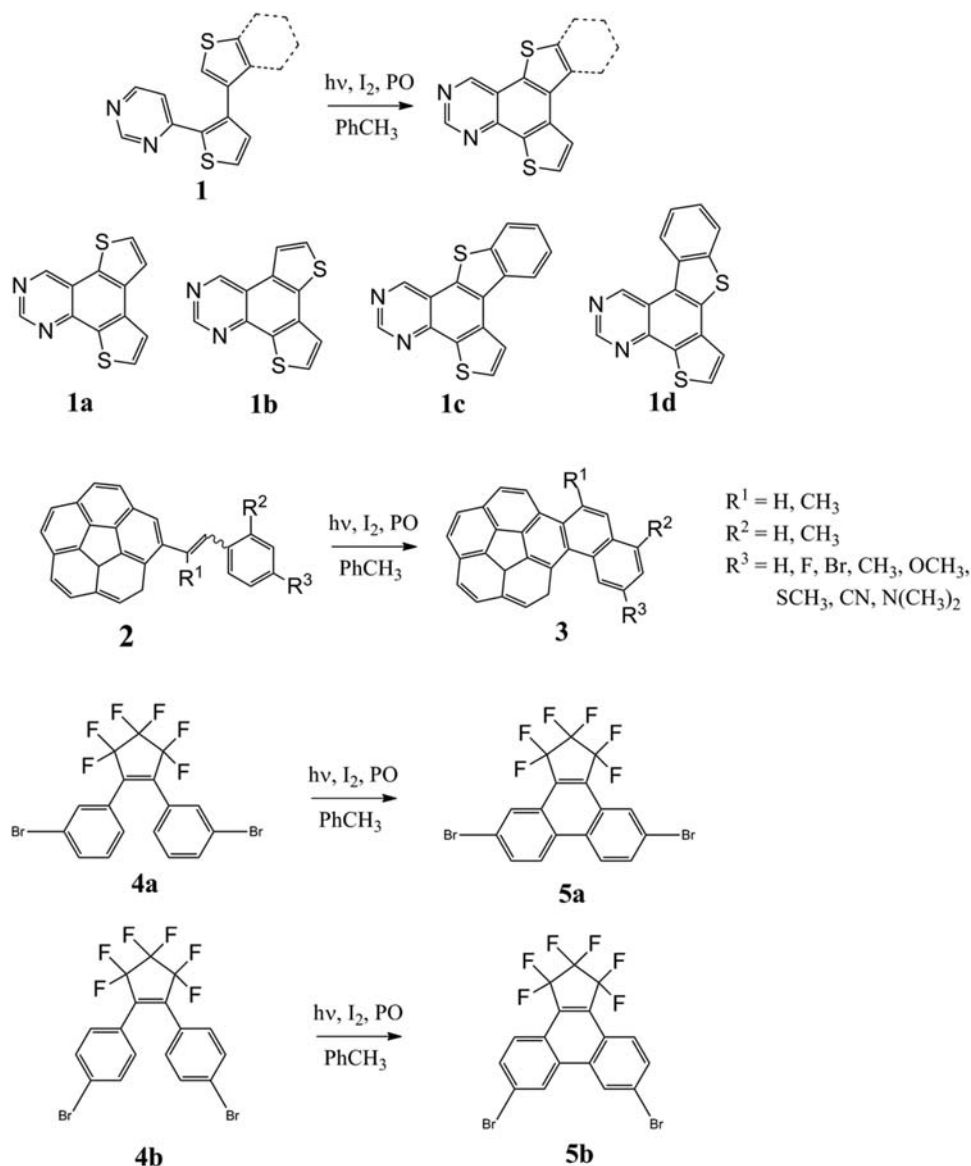
SCHEME 3.17   Some examples are reported about application of the Mallory reaction with Katz conditions for producing substances useful in material chemistry.
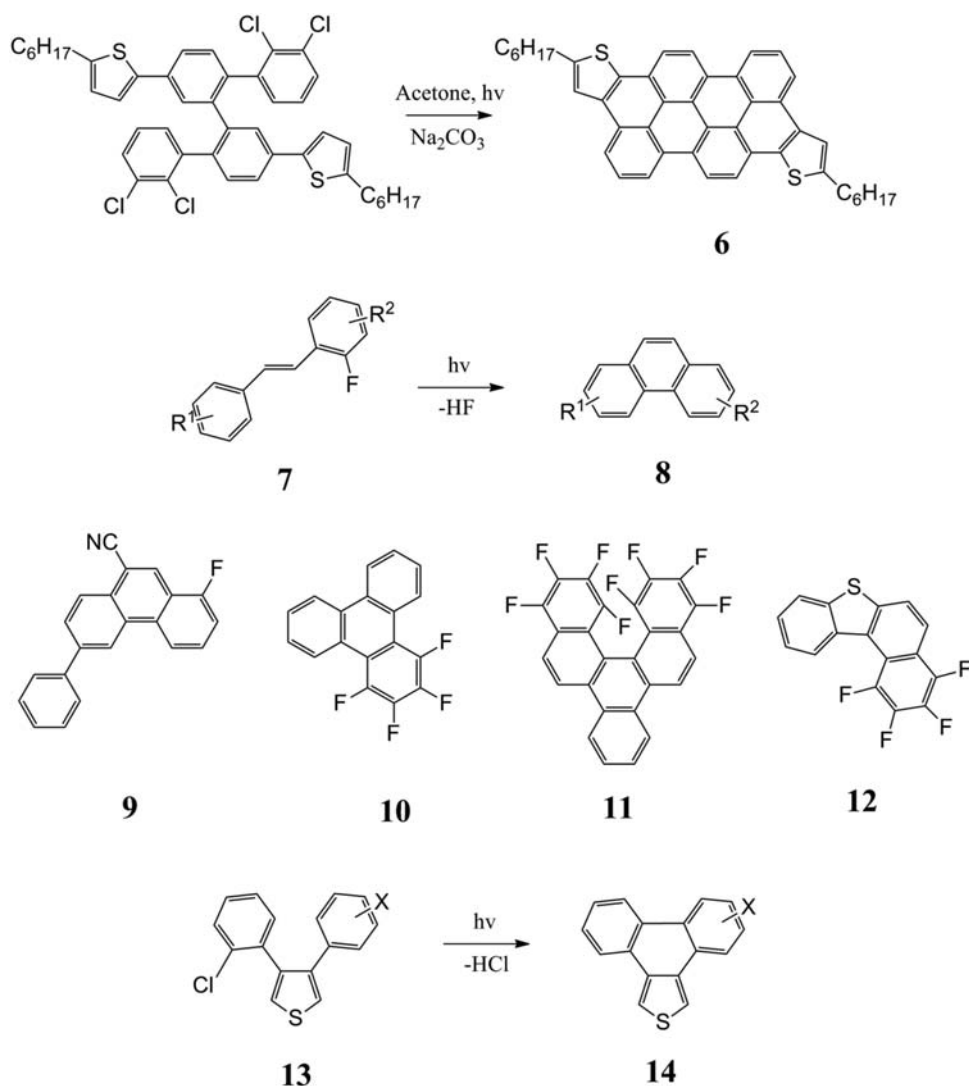
SCHEME 3.18 Some examples are reported about application of Mallory elimination process.

The leaving group is so effective that elimination takes place without any aid. Fluorinated aromatic compounds are clear examples of this type of Mallory elimination variant.

A wide variety of fluorinated stilbenes and stilbenoids possessing a fluorine atom at the ortho position 7 are irradiated in absence of oxidant and base to give the corresponding phenanthrenes and phenanthrenoids 8 with loss of HF (Scheme 3.18).

The photocyclodehidrofluorination (PCDHF) permitted the obtainment of selectively fluorinated polynuclear phenanthrenes with potential interest in material science (9−12 in Scheme 3.18).[30]

Thiophene derivatives 14 were synthesized by photocyclization of 3,4-diarylthiophenes 13, insolvent mixture of benzene and acetonitrile at $\lambda = 254$ nm (Scheme 3.18).[31]

3.3 The [2 + 2] photocycloaddition reactions on heteroarylethenes

Dimerization of stilbene to form (TPCB in Scheme 3.15, paragraph 3.2) has been already discussed in paragraph 2 as a side-reaction of photoinduced cyclization targeted to P-like structures. It was highlighted that dimerization occurs when relatively high concentration of stilbene are used. This fact forces the chemist interested to photocyclization to work at low stilbene (or stilbene analogs) concentrations.

Indeed, photoinduced stilbene dimerization is one of the milestones in organic photochemistry, being first observed by Ciamician and Silber in 1902[32]. In this light, this discovery anticipated the observation of the *E-Z* photoisomerization of stilbene in 1909 by Störmer[33] and the production of DHP in 1934 by Smakula.[9]

The possibility to accomplish this reaction at high concentration makes stilbene dimerization an useful synthetic route to substituted cyclobutanes commonly with high reaction yields. It is demonstrated that such reaction takes place from the encounter of a stilbene in its S_1 state (low energy singlet excited state) with a second stilbene in its ground state. Furthermore, Z-stilbene does not live enough in its excited state to react (see Paragraph 2). Hence, only *E*-stilbene has the time to diffuse in the solvent and meet a ground state counterpart to react.

Interestingly, exposing TPCB to UV light with wavelength shorter than 300 nm leads to cicloreversion. This allows reversing the reaction direction using different light wavelength as a switching method.

Stilbene isomerization is an example of [2 + 2] photocycloaddition.

In aliphatic alkenes, a fast excited state *cis-trans* isomerization competes with [2 + 2] cycloadditions, leading to very low reaction yields. In aromatic alkenes a small barrier is present which hampers the twist around the C=C bond at a certain extend. This is a consequence of a residual C=C double bond character in the excited state (see Paragraph 1) and makes possible the accomplishment of photoinduced cycloaddition in a more significant way. It is a general observation that higher *cis-trans* isomerization barriers are associated with higher photoaddition yields.[34,35]

If cycloaddition takes place on the S_1 PES, CT adducts are expected to be formed between one excited state molecule and one ground state molecule, they can be the same reactants or different ones. An exciplex (EX) can be formed as the precursor of the following C−C bond formation pointing toward the cyclobutane structure.

As said, this EX state can be formed by a BR *R state which is possible because twisting is not fully able to induce Z intermediates. In this light, two possible types of EX adducts are formed, according to the nature of the π and π* orbitals involved in the CT (Fig. 3.4).

Electron deficient ethenes feature low energy π and π*. This makes plausible a more favorable interaction between the half-filled π* MO of the excited ethene and the empty π* MO of the ground state counterpart. Electron rich double bonds present high energy frontier orbitals. This leads to more effective interaction between the occupied π MO of the ground state molecule with the half-filled π MO of the excited state reactant.

In other arylalkenes, the singlet excited state of stilbene evolves toward Z species. In this case, arylethene behaves as an eA through its empty orbital when an electron reach alkene is encountered. Otherwise, an electron deficient alkene will interact with the occupied orbital of the Z which acts as an eD.

The nature of the arylethene determines which pathway (BR and zwitterionic) is followed.

As shown in the top of Scheme 3.19, [2 + 2] photocycloaddition between excited state *trans*-stilbene and the electron reach 2,5-dimethyl-2,4-hexadiene leads to two isomeric products. Their structure clearly shows that the *trans* isomery of stilbene in maintained, as expected for a EX mechanism through a stilbene BR species.

As a further evidence, stilbene fluorescence is quenched by cycloaddition and quenching is more evident when the electron-rich character of the second alkene is higher (the ionization potential of the alkene is used for measuring the level of electron donation toward the C=C double bond). This confirms that a CT intermediate is formed.
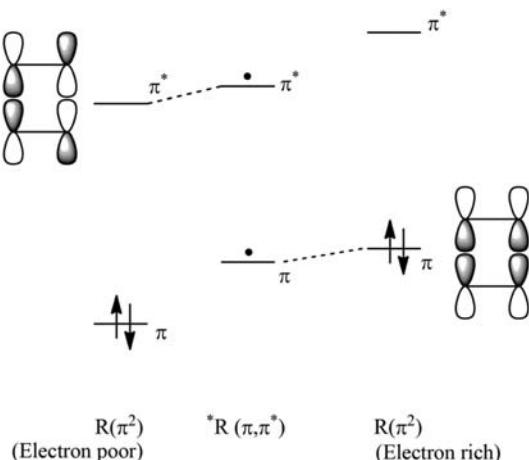
FIGURE 3.4   The most stabilizing molecular orbital interactions are represented in case of electron poor and electron rich alkenes with the excited state biradical (*R) frontier orbitals. The positive overlap associated with the charge transfer is sketched as well.
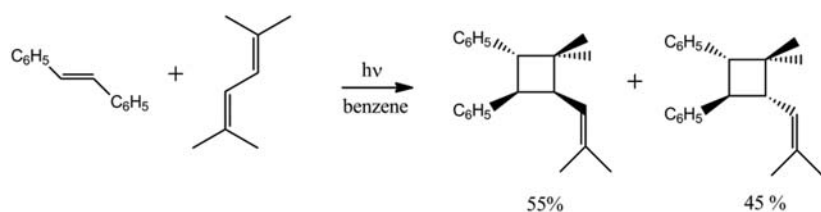
SCHEME 3.19 [2 + 2] photocycloaddition only occurs starting from *trans*-stilbene (top reaction) but not from the *cis* isomer; structurally constrained *cis* ethenes reacts both on the singlet and the triplet excited potential energy surface.
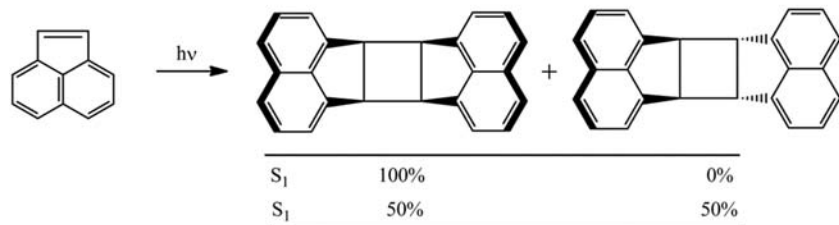
SCHEME 3.20 Dihenylvinylene carbonate undergoes significant [2 + 2] photocycloaddition in benzene and apolar solvents, whereas electron transfer processes in acetonitrile and polar solvents.
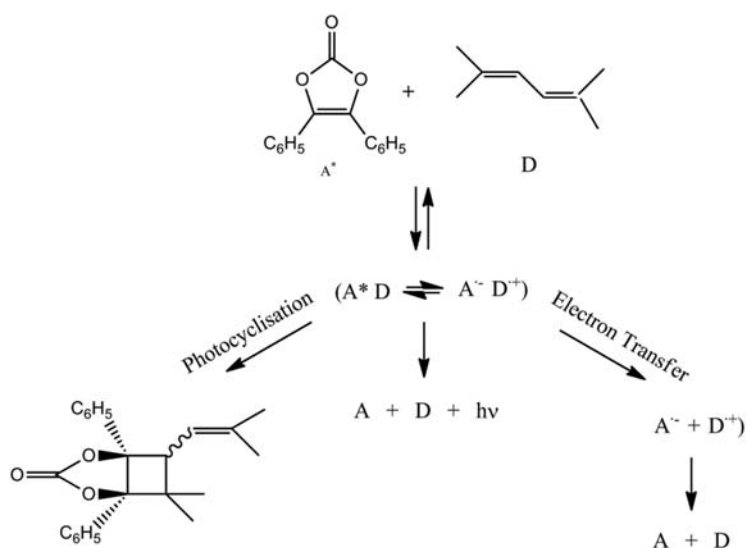
If the triplet excited state is populated by the means of a triplet sensitizer, usually only *cis-trans* isomerization is observed starting from both *cis* and *trans* diarylethenes and cycloaddition products are obtained in very low quantities.

On the singlet excited state PES, at contrary, a certain level of competition exists so that cycloaddition is possibly observed. This is particularly true starting from *trans*-diarylethenes; at contrary, *cis* isomers are much more prone to isomerization and less suitable to additions.

In *cis* diarylethenes with structurally hindered *cis-trans* isomerization (Scheme 3.19, bottom reaction), the deleterious effect of *cis-trans* isomerization is simply impossible, thus [2 + 2] cycloaddition is observed both with the singlet and the triplet excited states. Interestingly, a very different stereochemistry is reported in the two cases.[36]

The S_1 pathway leads to more hindered *cis* dimer; this is consistent with a CT pathway in which an efficient CT stabilization is obtained by facing the aromatic structures against each other, a fact which can be traced back to the delocalization of the frontier orbitals on the naphthalene structures.

Inducing ISC toward T_1 by a correct choice of the environment (presence of heavy atoms in solutions, like Xe or alkyl halides), similar amounts of *cis* and *trans* dimer are found, excluding the CT mechanism as the only relevant.

The structurally "blocked" dihenylvinylene carbonate in Scheme 3.20 shows a very different reactivity in polar and apolar solvents. In the formers, no reactivity is observed whereas cycloaddition is observed in apolar solvents. However, in all the solvents, the same rate of quenching of S_1 is measured. This means that different pathways are followed in the different environments. In apolar solvents, cycloaddition can be accomplished in a significant way (quantum yield equal to 0.6 in benzene), whereas in polar solvents, a much lower quantum yield is found (0.001 in acetonitrile).[34]

Polar solvents stabilize ions more effectively than apolar ones. This allows the hypothesis that, in polar solvents, CT is complete so that one radical cation and one radical anion are formed and, soon after, a quick reverse electron transfer takes place restoring the initial reactants. In apolar solvents, this route is thermodynamically less accessible and the less polar CT adduct is formed with consequent cycloaddition.

There are not substantial differences between arylic ethenes and heteroarylic ethenes in terms of general photochemical mechanism of dimerization. However, the use of substituents of the C=C carbon bond with extended π conjugation and/or heteroaryl groups offers the advantage to red shift the double bond π-π^* absorption band toward the visible spectrum, allowing dimerization though irradiation of visible light rather than irradiation in the UV-A and UV-B regime. This is very desirable in many biochemical and medical application, where UV-light is harmful for biological system.

Additionally, UV radiation has the drawbacks of short penetration in most media and also it can potentially induce degradation phenomena in materials in general. Use the visible spectrum could circumvent all these problems and can broaden the range of application of photoaddition also in switchable material.

A possible way to slightly bathochromically shift the excitation wavelengths and mostly improve photoaddition yield consists in forcing the process to take place on triplet excited state PES. In diaryl and heterodiarilethenes ISC is not an efficient process; hence, use of triplet sensitizers is a possibility.[37]

Use of Lewis acids is an alternative method in this respect[38] as it is the incorporation in a matrix.[39,40]

In spite of the effectiveness of the examples above, use of additional reactants and, even less, specific solid matrixes make problematic a direct application of them in material chemistry and also in biochemistry. Much more desirable would be shifting the photochemically-active absorption bands toward the visible spectrum by structural modifications of ethenes.

In this respect, use of diarylethenes with extended π-conjugation is a recent and promising possibility. Pyrene is one of the first proposed groups showing the ability to red-shift the photocycloaddition wavelength of diarylaethenes within the visible spectrum.

Scheme 3.21 shows the light-induced reversible process proposed for cross-linking polyethylen glicol (PEG)[41] which makes use of pyrilstyril functionalization. The extended π-conjugation of pyrene allows the use of light in the 400−500 nm range for accomplishing ethene [2 + 2] cycloaddition and not very harmful 340 nm UV light for reversing the process.

This is an example of photochromism which can be applied as a switching photochemical method which is demonstrated to be applicable to biological systems and to undergo to many reaction cycles with good reproducibility.

Although very promising, drawbacks have to be overcome yet. Pure styrilpyrene (i.e., not coupled to polymers) shows [2 + 2] photocycloaddition through irradiation at 460 nm,[42] but coupling of styrilpyrene with PEG for crosslinked hydrogel formation reduces the photoreactivity at the point that no useful reactivity was observed at wavelength higher than 420 nm.[41]
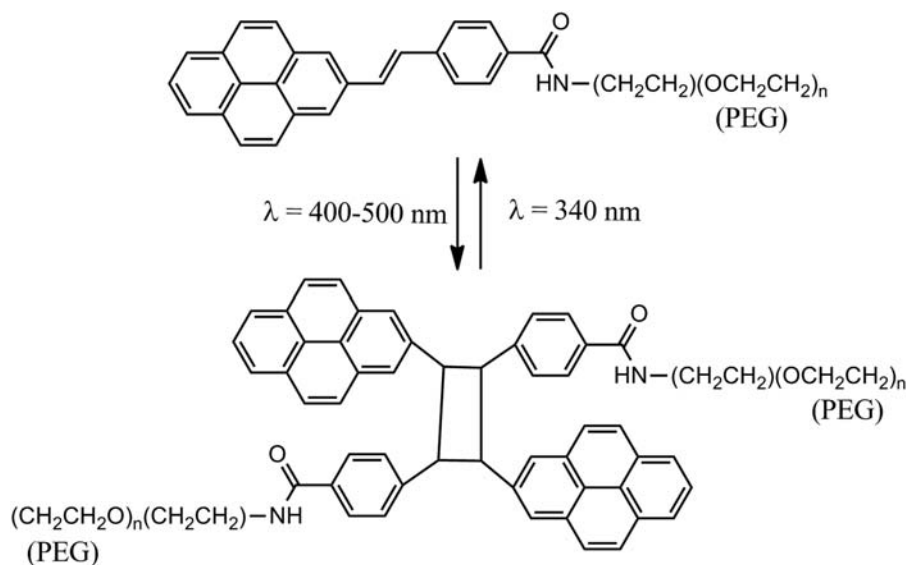
SCHEME 3.21 Polyethylen glycol functionalization with stirylpyrene allows visible-light driven [2 + 2] photoaddition.
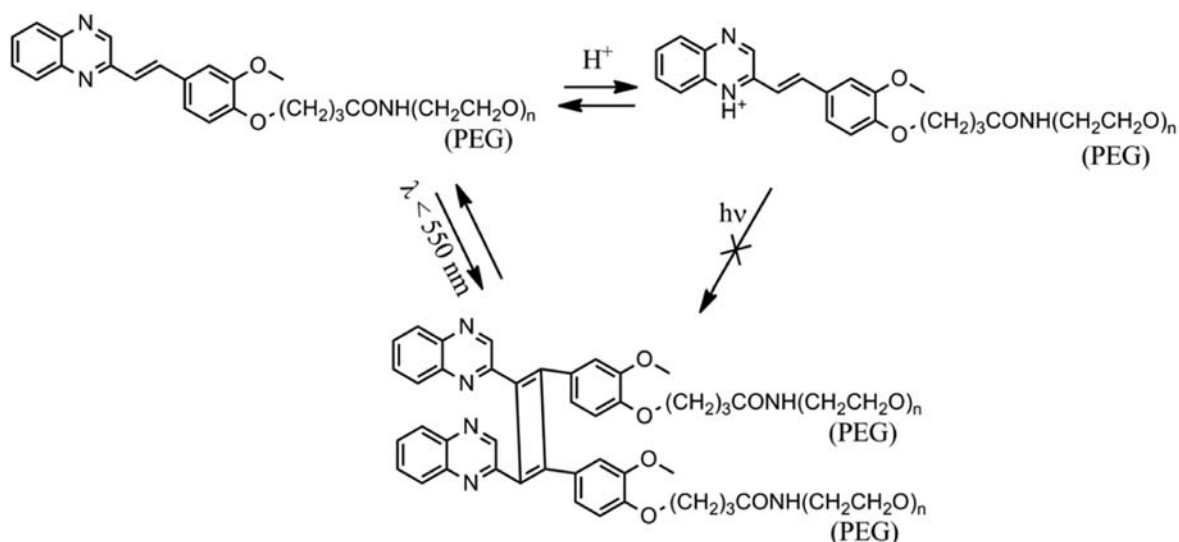
SCHEME 3.22 Quinoxaline allows a strong bathochromic shift of ethene [2 + 2] cycloadditions. Green light is sufficient for the cross-linking of polyethylen glycol. At acid pH, quinoxaline protonation disable cycloaddition.

Moreover, pyrilstirene is strongly hydrophobic, a big problem in biological applications in general and obviously not desirable is photoinduced cycloaddition is addressed to hydrogel formation.

The use of heteroaryl ethenes seems to go beyond these limits. Replacement of pyrene with quinoxaline led to the first reported green-light activated diarylethene photocycloaddition (Scheme 3.22).[43]

The halochromism of quinoxaline allows the switching of photocycloaddition, with acid environments (pH < 2) inactive. Interestingly, the use of the high penetrative green light allowed thicker hydrogel formation respect to UV light.

3.4 Photochromism of diheteroarylethenes

3.4.1 A brief historical overview and basic reaction mechanism

The term "photochromism" or "photochromic" comes from the Greek words φωτός (photos, light) and χρωμα (chroma, color) and it is (simply said) the property of some molecules to undergo a light-induced reversible change of color.

Dr. Yehuda Hirshberg coined the word photochromism in the 1950s while working on the synthesis of spiropyrans[44,45] and the first bianthrone,[46] while Dr. Willy Marckwald in the 1890s was the first to correctly describe the phenomenon of reversible color changes under light irradiation or photoisomerization[47−50] so, this phenomenon describes the photoreversible isomerization between two different states or isomers with distinct performances.

Since ancient times, photochromic compounds were empirically known. The king of Macedonia, Alexander the Great (356−323 BCE) equipped its armies with photochromic bracelets. It is unknown which photochromic compound was used at that age, but we know that the color change under sunlight was the agreed signal to attack enemies.[51,52]

In 1867 Dr. Fritzsche reported for the first time a peculiar behavior of tetracene solution: the initial orange color of the solution fades when the sample is irradiated by sunlight but can be recovered in a dark room.[53] Few years later (1899), as already written, Dr. Marckwald was the first scientist to describe in more details this phenomenon as a reversible process, studying the solid 2,3,4,4-tetrachloronaphthalen-1-(4H)-one named it "Phototropie." This German word translates into English as "Phototropy" and was in use until 1950s when Dr. Hirshberg proposed the currently used term photochromism.

In the 1930s, Dr. Harris and Dr. Gheorghiu performed mechanistic studies on this phenomenon on malachite green[54] and semicarbazones,[55] respectively.

In 1950s big advances were achieved in this field: many new photochromic compounds were discovered and synthesized and much progress was made in studying the mechanism underlying this phenomenon; many new organic and inorganic compounds were synthesized and their photochromic behavior was reported in more details.[51(b),56(g),57]

In the same period the work of Dr. Hirschberg was of great importance and gave a very strong impulse to the study of photochromism so that, from that moment on, all the scientists referred to this phenomenon as "photochromism."

The low photoresistance of organic photochromic molecules and their related fast degradation limited real developments of applications in the 1960s and the early 1970s. Only in the 1980s, spirooxazines,[58] particularly spironaphthoxazines, were developed for their high resistance to cycles of photoinduced transformation (high resistance to fatigue). Their applications to variable transmission glasses marked a turning point for photochromism applications. In the same period, well known compounds such as azobenzene derivatives (which were already known as photochromic dyes from half a century[59]) were investigated for their photoswitching properties.[60]

Applications of photochromic materials as molecular switches and data storage[61,62] started to appear in the 1990s. Although molecules such as fulgides have a century-long history, this period corresponds to the discovery of the diarylethene family (and also etheroarylethens). This domain certainly contributes to a tremendous increase in the number of publications since the 1990.

More recently, the developing digital age has tremendously expanded the fields of applications of photochromic materials. Optical properties can be effectively used to store binary data. CDs and DVDs are examples of light used to write and erase information because of the modifications in the optical properties of a material. Due to their reversible feature, photochromic species match the requirement of rewritable recording media, where memory bits have to commute between the two binary states ("0" and "1") upon request. In this domain, there is a race for high-capacity data storage media, where information can be written and erased at high speed.

Proposition of organic compound offers the big advantage of many possible chemical modifications of a basic structure addressed to improve the properties of interest. In this respect, scientific research plays a fundamental role. Collection of many experimental observations allows increasingly knowledge which can lead to useful rationalizations about the chemical requirements for a performing material; for example, good efficiency in the solid state can be achieved by following some established rules, such as intramolecular distances[63] or angles[64] and/or opportune bulky groups[44b] at the right positions.

Application in fluorescence microscopy imaging is one of the recent contributions of photochromism. Fluorescence microscopy is spreading in many scientific fields, such as biology, medicine, and material science. Recent technological progresses have led to faster microscopes with better resolution, along with the development of stable and bright fluorescent probes.

For having photochromism, a chemical transformation from molecule A to molecule B must take place after light absorption of A at a certain wavelength. A and B present different properties and, in particular, they must have a different absorption spectrum (and so a different color in the visible spectrum). Moreover, the chemical reaction from A to B must be reversible, so that the original color (spectrum of A) must be restored. The reverse reaction may be promoted by radiation of different wavelength or can proceed through thermally activated processes (which require that A is more stable thermodynamically). In the first case, the term "P-type" photochromism is used, when the reverse reaction is thermally activated, photochromism is called of "T-type." If only B is colored and light absorption induces coloration, photochromism is "positive" but this concept can be extended to all the cases with $\lambda_{abs}(B) > \lambda_{abs}(A)$. When $\lambda_{abs}(A) > \lambda_{abs}(B)$ the photochromism is called negative.

Fig. 3.5A is a schematic view of a the photochromic process involving 1,2-bis(2,5-dimethyl-3-thienyl)perfluorocyclopentene, which is a P-type photochromic substance.[65]

The photoinduced isomerization from the open form (A in Fig. 3.5) is promoted by UV light ($\lambda < 200$ nm in Fig. 3.5A, $\lambda < 400$ nm in common photochromic substances) and leads to an extension of the π-conjugation between the thiophenyl cycles and the alkene bridge. This reduces the HOMO-LUMO gap and shifts the low energy electronic transitions into the visible spectrum, hence the substance becomes colored (as an example of positive photochromism).

In the example of Fig. 3.5A, irradiation by visible light reverses back the process, leading to the open form.

In most cases, the chemical and photochemical processes are unimolecular so, isomerization occurs like in the example of Fig. 3.5, which is an example of photoinduced cyclization. In principle, all the photocyclization processes can be associated with photochromism. Photocyclizations can be associated or not to isomerization depending on the reaction evolution.

With reference to Scheme 3.13, photocyclization first leads to a cyclic compound which is an isomer of the reactant. The process is in theory reversible, so it is potentially a photochromic process. Known examples of photocyclization-originated photochromism are diaryl- and diheteroarylethenes forced in their *cis* conformation (like in Fig. 3.5).

Further evolution by the means of oxidation or elimination leads to a polycyclic aromatic compound. The whole chemical transformation from the reactant to the oxidation/elimination product can be considered photochromism without isomerization at the condition that the whole process can be reversed. This is usually not the case, photocyclizations are normally useful in photochromism only is they are stopped to the first not-aromatic cycle, which can react back in a T- and/or P-type photochromic process.

In other examples of photochromism, bimolecular processes are involved and we cannot consider the process an isomerization. This is the case of [2 + 2] photocycloadditions of arylalkenes (Paragraph 3.3). Light absorption induces cycloaddition in a bimolecular process and radiation of lower wavelength can be used to restore ethenes (the latter is a monomolecular process); cycloaddition cannot properly be considered an isomerization.
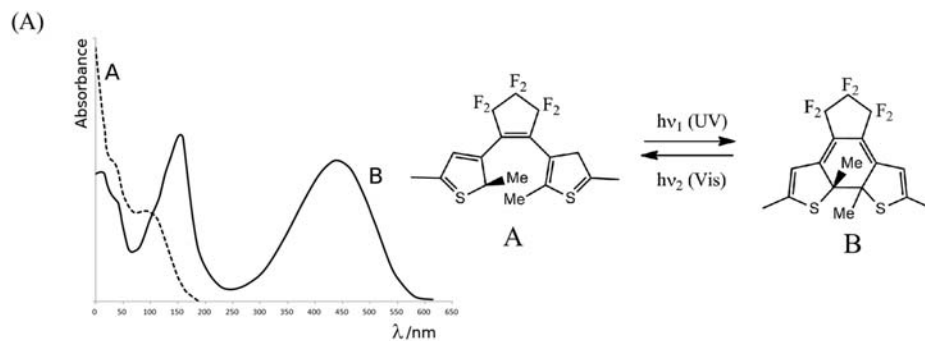
FIGURE 3.5 (A) Schematic of 1,2-bis(2,5-dimethyl-3-thienyl)perfluorocyclopentene in the open (A) and its closed forms (B). The related absorption spectra are reported, showing the origin of the color in the B form. Isomer A can be restored through irradiation of visible light, whereas UV induces photocyclization toward isomer B; (B) the (R,R) and (S,S) enantiomers obtained by photocyclization of the simple model compound 1,3,5-hexatriene; (C) the conrotatory ring closure pathways and related enantiomeric products.
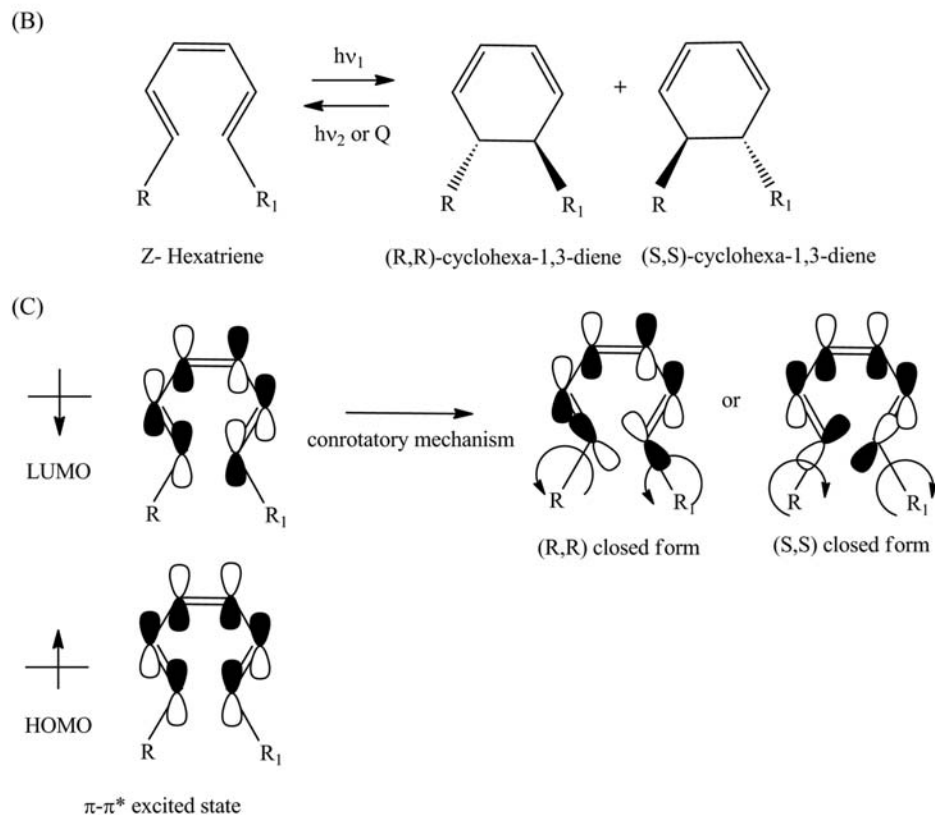
However, in almost all the used and studied photochromic diheteroarylethenes, the fundamental characteristics of the process can be traced back to the reversible photocyclization of Fig. 3.5A.

A model for it is the reversible photocyclization of 1,3,5-hexatriene (open form) to produce its closed form 1,3-cyclohexadiene. Because such a process will be the only one discussed in the remaining of chapter, a deeper description is required here.

Photocyclization reaction normally occurs in the singlet π-π* excited state, by the means of a conrotatory mechanism resulting in a stereospecific product (either S,S or R,R) as sketched in Fig. 3.5B and C.

The result is a racemic mixture of the two enantiomers if the reactant is 1,3,5-hexatriene. However, use of chiral substituents may favor one enantiomeric product over the other. Chiral control on the photocyclization will be discussed in Paragraph 3.4.5.

Indeed, the same process can in principle be observed on the first triplet excited state, following the same general pathway of Fig. 3.5. Normally used photochromic materials are not suitable to fast ISC, so that triplet population normally is not significant. However, use of triplet sensitizers allows useful triplet population with some beneficial consequences such as higher resistance against photoinduced degradation. We will discuss the use of triplet sensitizers in Paragraphs 3.4.2 and 3.4.6.

The cycled or closed form of a photochromic diheteroarylethene features an extended π-conjugation and is colored by virtue of the associated reduction of the HOMO-LUMO gap. The open form is normally colorless but recent developments are leading to colored open forms for visible light photochromism, as discussed in Paragraph 3.4.6. Another characteristic of the closed form is its lower structural flexibility respect to the open form, due to the fact that the heteroaryl rings are not free to rotate after photocyclization.

Inclusion of the ethene bridge double bond in a cycle (as the example in Fig. 3.5A) fixes its *cis* configuration and hinders the excited-state *cis-trans* isomerization which competes with photocyclization. This helps increasing the ring closure quantum yield. In this light, diheteroarylethenes based on cyclopentene and perfluorocyclopentene are the most studied. However, as long they are cyclic, ethene bridges of different structure have been effectively reported. In some of them, heteroarene structure is adopted as, for example, thiazole cycles for best photochromic performances.

Scheme 3.23 shows a few examples of photochromic molecules and it is intended to give a general view of the photochromic materials of interest in this chapter, apart from azobenzene (a in the scheme) which is reported as the typical example of T-type photochromic substances. Upon irradiation with UV radiations, azobenzene changes conformation from *trans* to *cis* and, at the same time, color from pale yellow to orange. Irradiating the orange *cis*-azobenzene with visible light it reverses back to the uncolored form. However, the latter is restored also by thermal conversion. This behavior is quite common in T-type substances, in which both spontaneous and light-induced restoration of the starting compound is possible.

Diheteroarylethenes based on symmetric indole or pyrrole rings (B and C in Scheme 3.23) normally give rise to thermally unstable closed forms (T-type photochromism).

By replacing one or both the cycles with thiophene, furane or benzothiophene groups (D-E), the asymmetric diheteroarylethene becomes thermally stable in the closed form and a T-type photochromism is achieved.

As the two compounds giving rise to photochromism are constitutionally different, all their properties (not only their color) are different.[47a] Hence, photoisomerization also alters properties like refractive index,[44] fluorescence,[66,67] nonlinear optical properties,[68] viscosity and dielectric constants. All these properties can be used to reveal the state of the photochromic material during the process.

Furthermore, by photochromism it is possible to alter, for example, the assumed phase, solubility, reactivity, stereochemistry, complexation or interaction between molecules or ions.[69]

In materials, photochromism can induce shape changes, and opens up a wide field of interest in photo-induced mechanics.[70]

Several examples of the huge number of applications of photochromic materials based on diheteroarylethenes will be presented in Paragraph 3.5. In the following of this paragraph, we will take into account some important topics regarding the design and mechanisms of photochromic materials. We will start from the effects of ethene bridge functionalization and we will proceed with the role of the heteroaryl rings, the effect of solvation, the stereochemical control of the cyclization process and, finally, the very desirable possibility offered by all-visible photochrimism.

Each of the topics above gave us the occasion for introducing the reader to the backgrounding Chemistry and Photochemistry regarding photochromic diheteroarylethenes.

3.4.2 Photochromism: Tuning with ethene bridges

A noticeable impulse toward the research of new photochromic materials derives from their technological applications in the fields of rewritable optical memories, photoswitches in general, actuators and molecular machines. One of the indispensable properties in this respect is the thermodynamic stability of both the forms of the used substance. P-type materials are mandatory because the digital information must be stored for an indefinite time; the lifetime of both the isomers should go beyond hundreds of years at room temperature.[65] If one of the forms (A or B) is significantly less stable, higher is the possibility that a ground state interconversion occurs in the direction of the most stable form with obvious loss of the stored information. The problem is kinetic, but similar thermodynamic stability of the two forms of the photochromic compound is normally a prerequisite for kinetic stability.

Appropriately selected diheteroarylethenes can satisfy this requirement. Fig. 3.5 and Scheme 3.23 shows the photochemical process behind photochromism in this class of compounds, which can be generally extended to all diarylethenes, indeed. A perycyclic photocyclization takes place which involves the two aryl cycles and the ethene bridge in a so-called 6-electrons 6π process; that is, six C-atoms forms a new cycle and their six 2p C orbitals overlap in an extended π system. The generic A and B forms of the photochromic material of Fig. 3.5 will be called "open" and "closed" forms from now on.

Taking into account diarylethenes and returning to the issue of the thermodynamic stability, the closed form is normally the problem, being usually less stable. In this respect, the level of aromaticity of the open and closed forms is one of the fundamental properties to accurately modulate; if the closed form features a relatively lower aromaticity, an unacceptable low lifetime can be expected for the closed form.

Aryl substituents of low aromaticity are the most used way to ensure similar stabilities of the open and closed forms. In this respect, the choice of thiophenyl or furanyl substituents is ideal and more effective than phenyl and other heteroaryl cycles. This topic will be the object of the following paragraph; here we discuss the role of the ethene bridge in this and other respects.

We are concerned with ethene bridges which must be included in a cyclic structure so to avoid *cis-trans* isomerization after light absorption. π-conjugation (and so also aromaticity) inside this cycle determines the level of double bond character of the bridge and, in turn, the level of aromaticity of the closed respect to the open forms. Compound **1** in Scheme 3.24 shows one application of fluorophore 1,8-naphthalimide as ethene bridge in a dithiophenylethene structure, proposed as photoswitch for technological applications in 2008.[71]

Albeit it can be considered a pioneer proposal for digital memories applications, this compound exhibits a relatively high level of aromaticity in the ethene bridge of the open form because it is part of the benzene cycle; therefore, passing to the closed form, there is a relatively big loss of aromaticity.

Starting from 2008, much effort was addressed to design new ethene bridges able to induce similar levels of aromaticity in the closed and open forms. **2** and **3** (Scheme 3.24) are two alternative proposals based on S,S-dioxide benzotiophene[72] and benxothiaole[73], respectively, with potential applications in many fields, like logic gates.[72]

The increasingly better performances in terms of stability of the closed form led to the benzobisthiadiazol bridged diarylethene reported in 2011 (**4** in Scheme 3.24) which showed the best stability of the closed isomer observed till that time and, furthermore, excellent resistance to degradation during many opening and closing cycles (good fatigue resistance).[74]

The reason of the big stability of the closed form can be referred to the higher degree of double bond character of the ethene bridge, which is a consequence of the reduced aromaticity due to the action of the benzobisthiadiazole structures. Thus, formation of the closed form is less deleterious in terms of π-structure stabilization.

The additional steric hindrance induced by the two benzobisthiadiazole groups in **4** was exploited for a net increase in the quantum yield of photocyclization from the open to the closed forms. The open form of a diheteroaryl ethene such as dithiophenylethene can lead to two stereoisomeries: the "parallel" and "antiparallel" ones.

Scheme 3.25 sketches the two isomers in case of **5**. Of the two, only the antiparallel form is photoactive and can therefore lead to the closed form through a conratotory process. If the two heterocycles rotate quickly, equilibrium is reached and the difference in thermodynamic stability between the two stereoisomers strongly determines the relative amount of antiparallel isomer and, consequently, the photocyclization quantum yield. In Table 3.2, the correlation between the steric hindrance on the thiophenyl groups (compound **5** in Scheme 3.25) and photocyclization quantum yield shows how quantum yield can be improved by favouring the antiparallel form with suitable structural modifications.

T-type Photochromic Examples
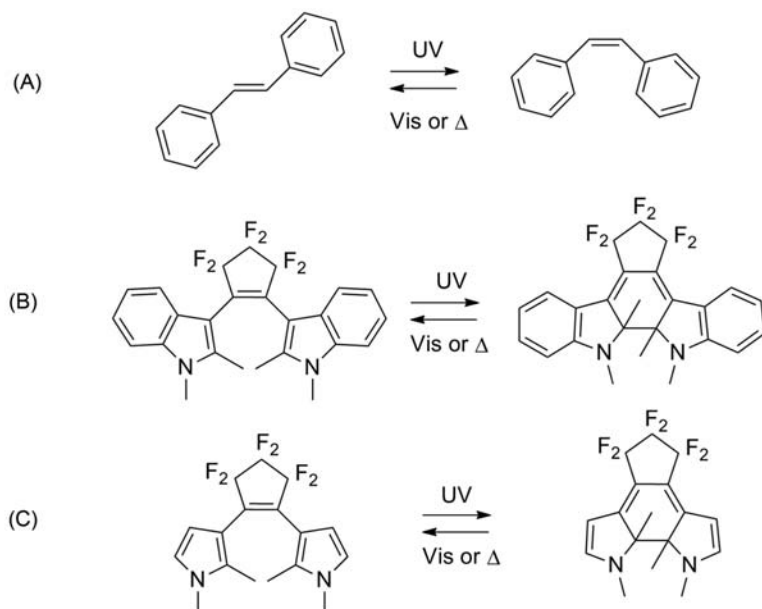
SCHEME 3.23 Some examples of typical photochromic substances.

P-type Photochromic Examples
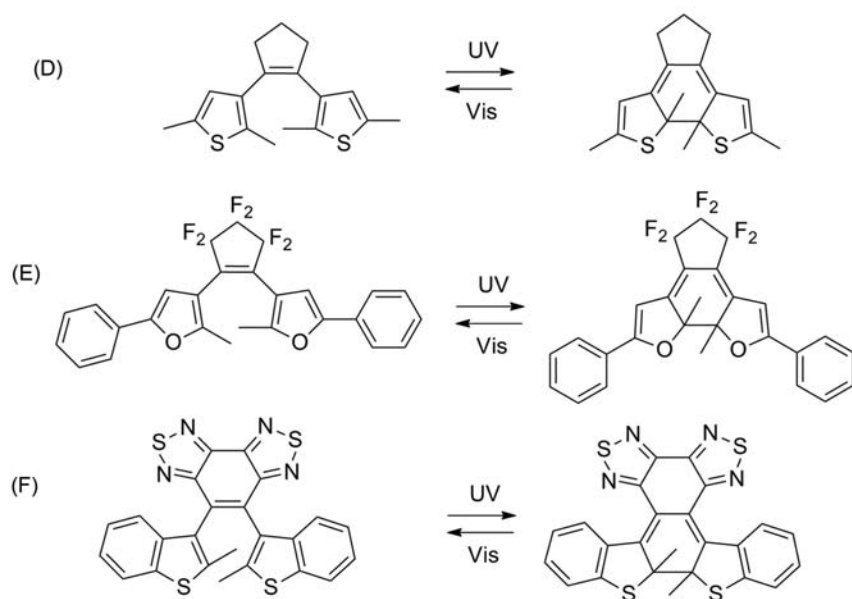
Table 3.2 focuses on the steric hindrance of the thiophenyl groups alone but, in **4**, this effect is potentially supported by the relatively extended ethene bridge. By replacing the thiophenyl groups of **4** with benzothiophenyl groups in **6** (Scheme 3.26), a quantum yield equal to 0.73 was obtained because of the cooperative steric hindrance of the ethene bridge and the benzothiophene cycles. Furthermore, the two enantiomers (**6a** and **6b**) do not interconvert with each other at room temperature, and this allows their separation even at room temperature by means of chromatography.[79,80]

This allows photocyclization to be performed starting from a single enatiomer rather than from a racemic mixture, with obtainment of specific cyclic enantiomers **7a** and **7b**. (Scheme 3.26). From above, **6** is an important example of chiroptical photochromic material.
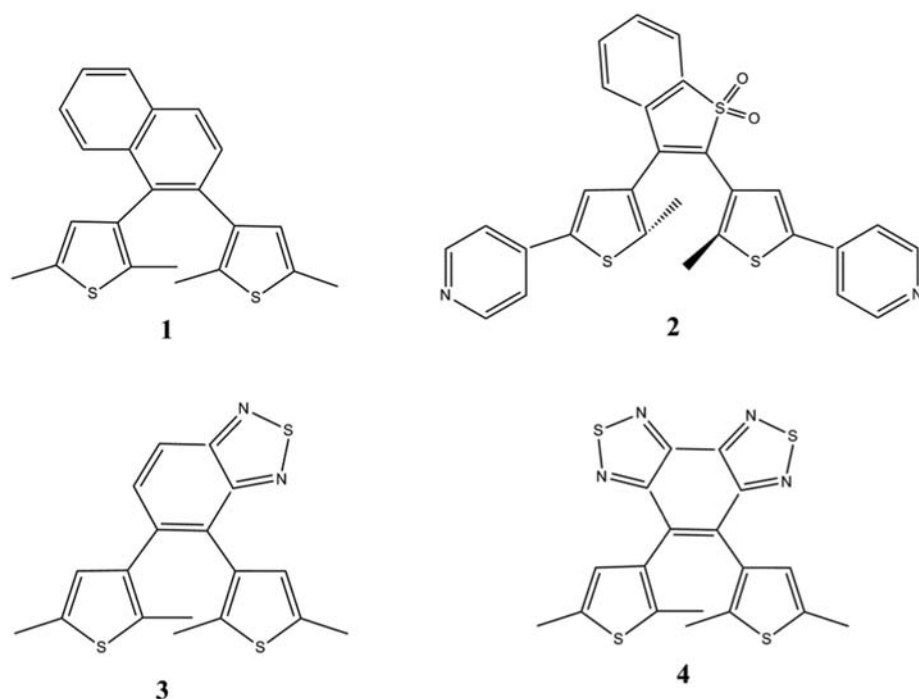
SCHEME 3.24 Some exemplar structures highlighting different ethene bridges.
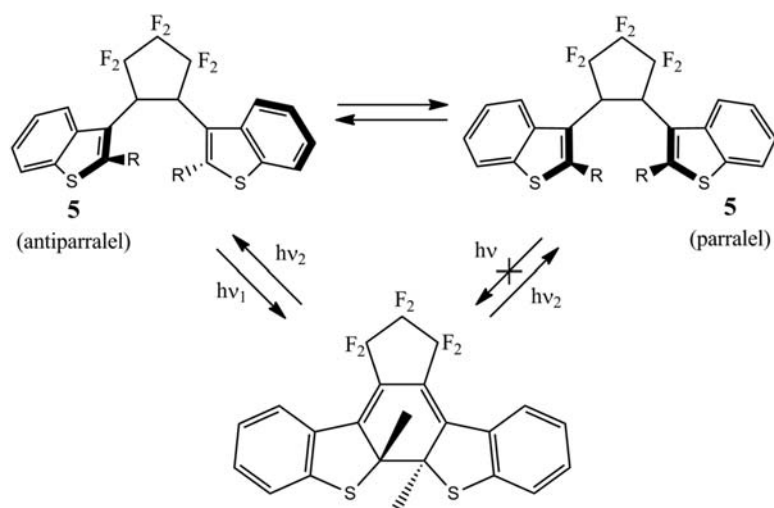
SCHEME 3.25 The parallel and antiparallel forms of **5**. Only the parallel form leads to photoreaction.

The ethene bridge can be functionalized to act as a ligand for the coordination of transition metals. Compound **8** (Scheme 3.27) is one of the first examples of this application.[81]

In it, we distinguish the structure responsible for photochromism, that is, for photocyclization (L in the scheme) and the coordination unit connected to it and based on a ruthenium complex (indicated coarsening with Ru but comprises a 1,10-phenanthroline ligand connected to L and two bipyridine chelants).

The Ru coordination unit performs the task of sensitizing in the triplet state; in this sense, the coordination unit initially absorbs light and, successively, gives rise to an efficient ISC toward the triplet state. In **8** the singlet excited state (S_1) consists of a CT from the central metal to the ligand (MLCT) which is localized on the coordination unit rather than on the photochromic structure (L). The same is true for the triplet excited state (T_1) which gives rise to an IC toward a lower energy triplet state. This is mainly localized on L and induces photocyclization in the triplet state.

In conclusion, the sensitizer allows the population of the triplet state of the photochromic unit to overcome the problem of the poor ISC in the organic structure and therefore the low population of the triplet states. Using triplet states, low energy radiation can be used to induce cyclization.

TABLE 3.2   Photocyclization quantum yields ($\Phi_{O \to C}$) of 5 derivatives with different steric hindrance of R (Scheme 3.25).

R	Antiparallel population (%)	$\Phi_{O \to C}$	Reference
CH$_3$	65	0.31	75,76
C$_3$H$_7$	74	0.41	77
C$_7$H$_{15}$	82	0.49	77
CH(CH$_3$)$_2$	94	0.52	78
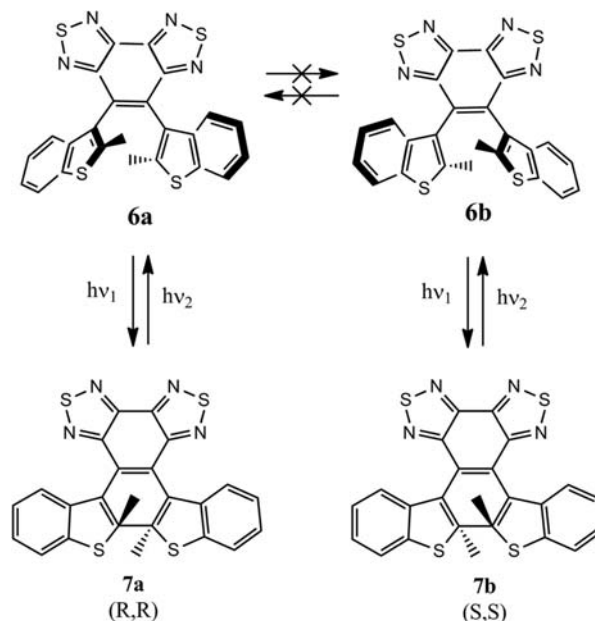
SCHEME 3.26   Steric hindrance of the ethene bridge prevents room-temperature isomerization between **6a** to **6b**. Thus, specific enantiomers **7a** and **7b** are photochemically obtained from pure **6a** and **6b**, respectively.

In compound **9** (Scheme 3.27), the ethene bridge is also the ligand of the transition metal.[82]

The goal in this case is a more direct connection between the ISC on the coordination unit and the photoactive excited state. Indeed, the triplet state on the coordination unit and the triplet state on the photoactive unit can be the same or they insist in the same part of the molecule. This should lead to a more efficient population of the photoactive triplet. A further favorable feature of **9** is the increased steric hindrance from the parallel structure which boosts the stability of the antiparallel conformation of the diarylethene structure with consequent higher cyclization quantum yield.

In compound **10** (Scheme 3.27), a noticeable red shift was observed in the first absorption band of the closed form of the photochromic unit in comparison to the not-coordinated ligand.[83]

The opening process of the free ligand is initiated by radiation of 580 nm wavelength. After Re complexation in **10**, the red shifted absorption band was measured at 710 nm. The proposed explanation of this spectroscopic change is attributed to the increased planarity between the pyridil ring and the bridging ring which is forced by Re complexation. The increased π-conjugation lowers the HOMO-LUMO gap of the ligand and shifts the first absorption band accordingly. The red shift of the open form is also evident (from 320 to 580 nm) but somewhat smaller. This is possibly connected to the less extended p-structure in the open form. Introducing main-group heteroatoms in the ethene bridge structure can be fruitfully used to impart unique properties. Boron offers the possibility to covalently bind three of four groups with big change in its electronic properties such as hybridisation. In compound **11** (Scheme 28), tetrahedral boron binds a thiophene b-diketonate ethene bridge. Thanks to
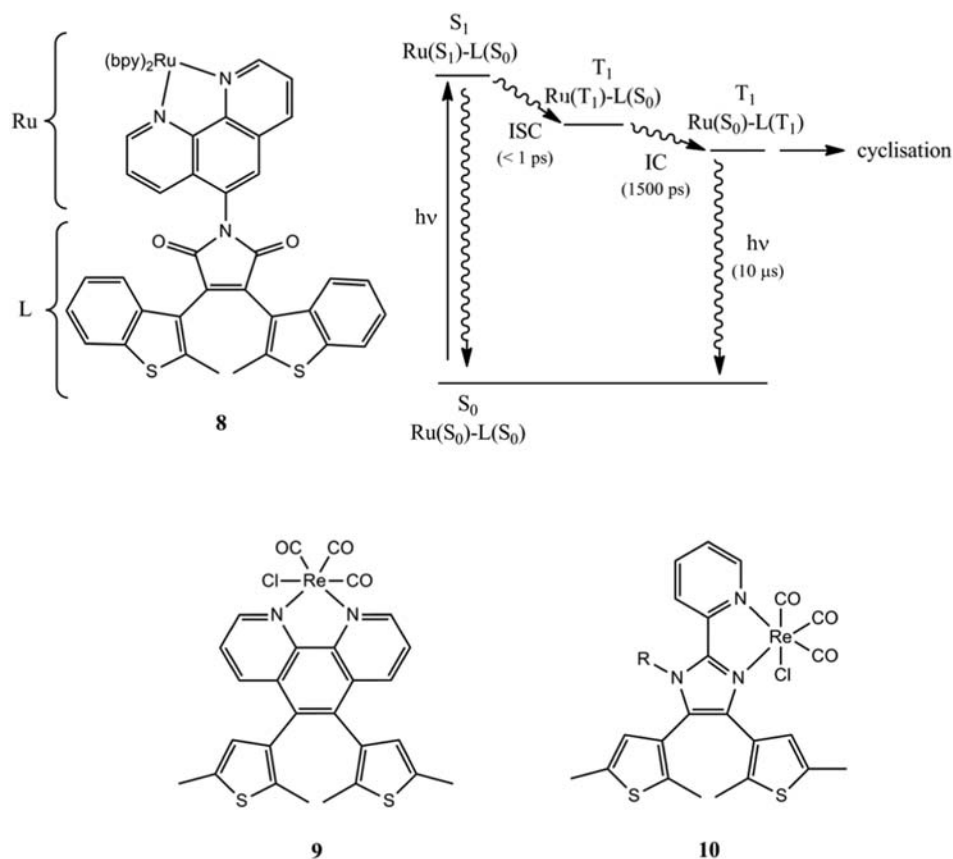
SCHEME 3.27 Examples of ethene bridges connected to a transition-metal coordination unit. Part of the triplet-sensitizing mechanism is showed in the top-right part for **8**. Wavy-arrows are used for nonradiative processes.

the electron-withdrawing action of the heteroatom, the photoactive absorption of the closed form can be extended till near-IR ($\lambda > 760$ nm).[84]

Trigonal planar Boron can offer strong p-conjugation effects due to its sp^2 hybridisation. When trigonal B binds the thiophenyl substituent of the bridge in **12**, photochromism is strongly prohibited because the strong electron-acceptor action of the dimesitylboron group leads to LUMO localisation of the external tiophenyl ring and consequent lower contribution of the ethene bridge on the same orbital. Reversible fluorine coordination of **12** cancels such a p-conjugation (sp^3 hybridisation of Boron) and, therefore, photochromism is restored in **13**.[85] Compound **13** is an example of chemically tuning of the photochromic reactivity. The possibility to change the photochromic reactivity by external stimuli is referred to as "gated" photochromism. The external stimuli can be chemicals like in this case, but also photons or heat. Compound **14** (Scheme 29) is an example of Silicon as heteroatom in the bridge structure.[86] The silole ring is characterised by an high level of double bond character in its diethene part, not dissimilar from cyclopentadiene. Such a low level of aromaticity induces great thermal stability of the closed form after photocyclisation and, more interestingly, makes the electronic structure of the closed form very similar to the open form. Similar aromaticity and energy levels in the open and closed forms allows a very efficient ring-opening process, with quantum yields of 0.42 where it is normally measured around 0.1.

Phosfole oxide and several its derivatives (**15** in Scheme 3.28) similarly show great thermal stability of the closed form which was assigned to the low level of aromaticity induced by the heteroatom. Cycloreverse reaction, however, did not show an equally good quantum yield.[87]

Compound **16** (Scheme 3.29) catalyzes transesterifications and amidations only in the open form, at contrary, its closed form is inactive. This opens the road for a photoswitchable catalyser based on a photochromic material.[88]

Compound **17** (Scheme 3.29) cannot undergo any photoinduced ring closing process because the thiophenyl rings are in the 3- and 4-positions of the furan cycle where no significant "ethene double bond" is present. But photocyclization and photochromism can be gated through a Diels-Alder reaction with maleimide with consequent appearance of the ethene bridge between the thiophenyl groups (**18** in Scheme 3.29).

After photocyclization, the closed form **19** cannot reverse back the Diels-Alder process anymore, because the ethene bridge evolves in the cyclohexadiene structure.[89]
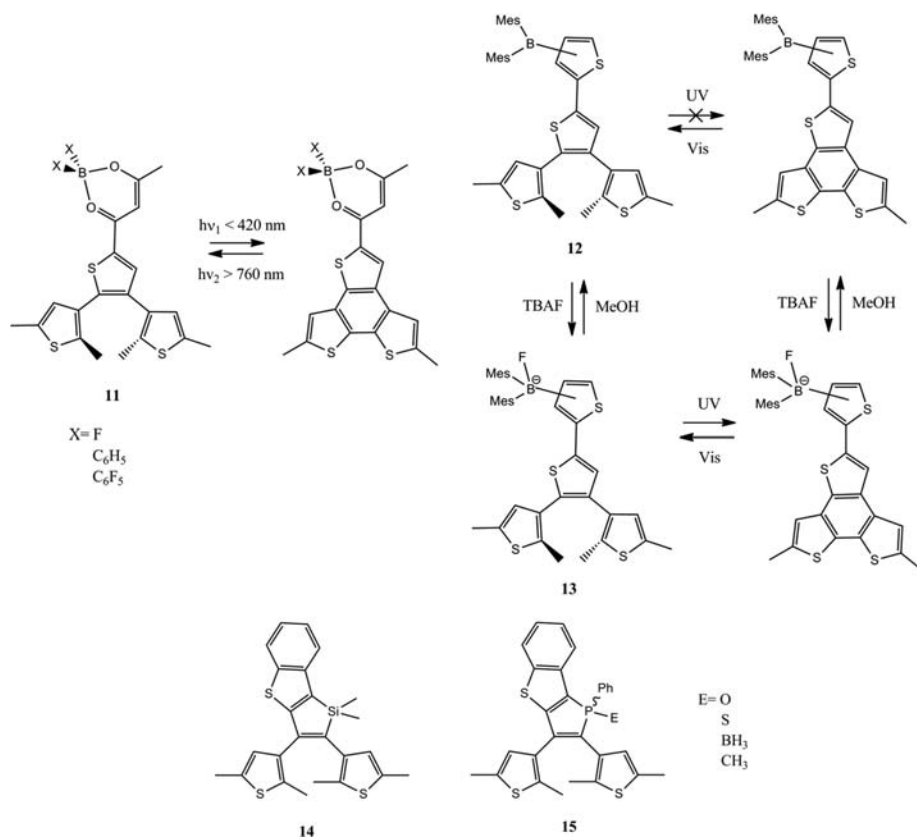
Thus, photochromism can be considered the switch of the Diels-Alder process, whereas the Diels-Alder process is the gate of photocyclization.

3.4.3 Photochromism: Tuning with funtionalised heteroaryl groups

It is no coincidence that all the examples of heteroarylethenes discussed in Paragraph 3.4.2 show thiophene or thiophene derivatives as constituents of aryl rings.

The reason has already been addressed in the previous paragraph: in almost all applications of photochromic diarylethenes, an essential request is the thermal stability of the closed form. To date, the best known way for satisfying this request consists in adopting low aromaticity cyclic structures both in the ethene bridge and, mostly, in the heteroaryl rings. In this way, the inevitable lowering of aromaticity passing from the open to the closed forms does not cause a large loss of thermodynamic stability, making the latter kinetically stable. Thiophene presents the lowest aromaticity level among the most used aryl rings and, consequently, it conveys most of the research efforts in the field of photochromism on its own.

Scheme 3.30 collects some of the very useful information from extensive studies about the thermal stability of the closed forms.[90] Three main factors are graphically exemplified in the scheme with regard to diarylethenes: the role of aromaticity, the effect of steric hindrance of substituents and, finally, the role of electron withdrawing groups.

From the half-life times shown in the scheme, it is possible to better evaluate the very high level of stability obtainable by using low aromaticity heterocycles such as furan and, above all, thiophene. The latter allows reaching very high levels of thermal stability even at temperatures exceeding 100°C.

The low-aromaticity advantage offered by furan and thiophene rings can be partially or neatly canceled by the use of bulky groups as substituents of the heterocycle which bind the two central carbon atoms (the reactive carbon atoms) in the closed form (Scheme 3.30B). It has been suggested that the loss of stability is mainly connected to the steric hindrance alone, because it does not seem dependent on the polarity of the substituents nor on the hyperconjugation of the α-hydrogens of the substituents.[91]
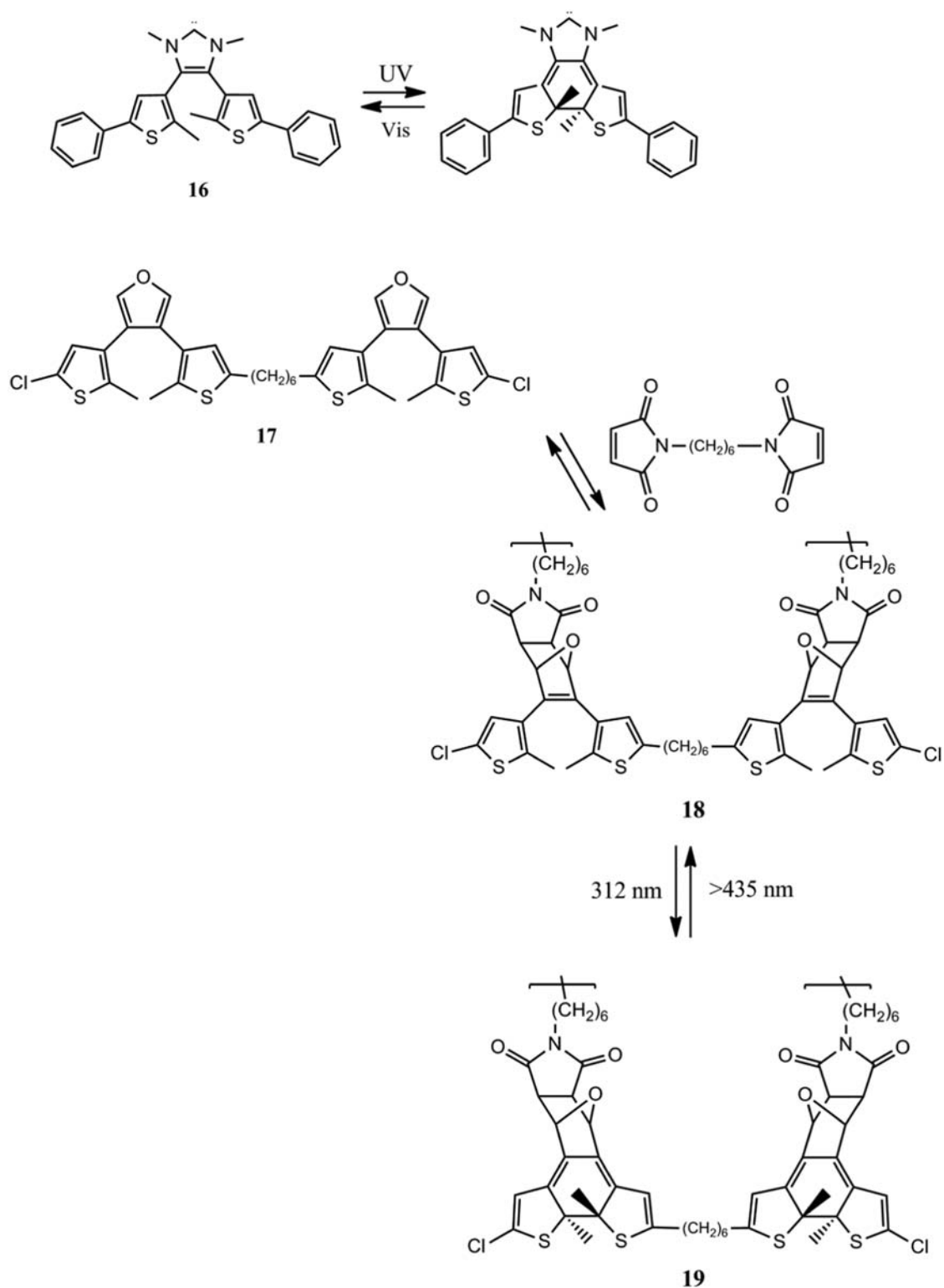
SCHEME 3.29 Two examples of application of ethene bridge functionalization for producing a photoswitchable catalyzer (**16**) and for gating photochromism through a Diels-Alder reaction (**17**).
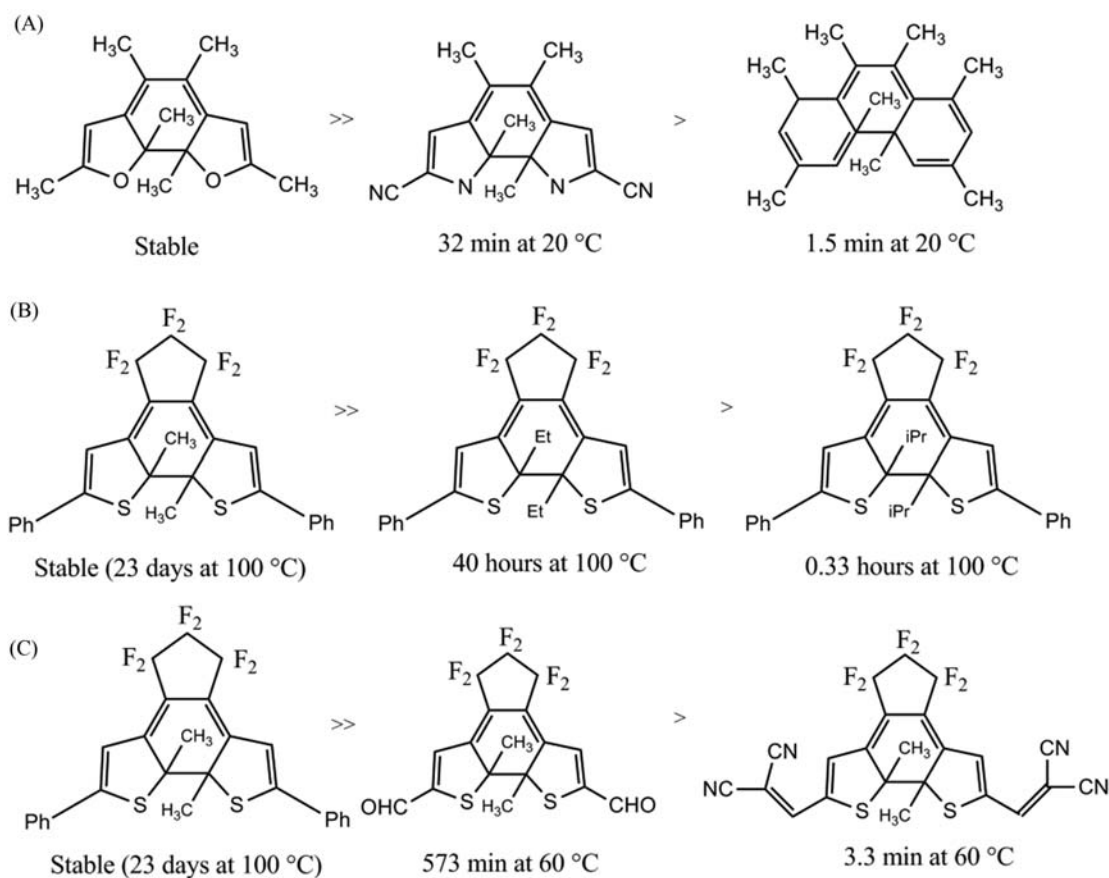
SCHEME 3.30   Trends in thermal stability of the closed forms of some diarylethenes measured by their half-life times observed at different temperatures and correlated to: (A) aromaticity of the aryl rings; (B) steric hindrance of ring substituents; (C) electron withdrawing ability of aryl substituents.

Furthermore, a good correlation has been reported between the observed stability of the closed forms and corrected Taft's steric substituent constants.[92,93]

The effect of electron-attracting groups can be equally strong (Scheme 3.30C) and is linked to the weakening they exert on the central carbon-carbon bond.[94]

The three factors contribute to determine the difference in enthalpy between the open and closed forms, which is in direct correlation with the opening kinetics of the closed form. The interesting aspect is that closed-forms thermal stability can be indirectly evaluated by the bond distance between the two central carbon atoms which can be easily evaluated by computational methods.[95]

A final note regarding this discussion about the thermal stability of the closed form is that no correlation exists between ground state stability and efficiency of photoinduced opening of the cycle. The latter runs on the excited state PES and, unfortunately, there is not any correlation with the ground state PES.

Compound **20** (Table 3.3) is one of the most used photochromic material and can be considered a reference in the following discussion about the ring opening process. Its photoinduced ring opening process shows a quantum yield ($\Phi_{C \to O}$) of 0.27 at 575 nm, which represents a good performance. Lowering the irradiation wavelength means directing more energy on the reactive closed form and this leads to the observation of an increased $\Phi_{C \to O}$.[75]

This is considered an evidence of the presence of an energy barrier between the closed and open forms in the excited state reaction pathway.

Computational investigations based on *post*-HF methods confirmed the presence of such a barrier which does not exist in the reverse direction (ring closure process).[103]

As reported in Table 3.3, replacement of benzothiophenyl rings with phenylthiophenyl leads to a large decrease of $\Phi_{C \to O}$; $\Phi_{C \to O}$ in **25** of one order of magnitude respect to **20**.

Moreover, the presence of electron releasing and electron withdrawing groups on the reactive carbon atoms has opposite and dramatic effects. eDs lead to a yield reduction of several order of magnitude (compounds **27**–**29**), whereas

TABLE 3.3 Ring closure and ring opening quantum yields ($\Phi_{O \to C}$ and $\Phi_{C \to O}$, respectively) and absorption peak wavelengths in selected photochromic diheteroaryl ethenes. Compounds 20–24 are based on benzophenone rings (top structure in this table). Compounds 25–29 are based on phenylthiophenyl rings (bottom structure).

Structure (Closed form)		Open form		Closed form		Ref.
		λ_{max}/nm	$\Phi_{O \to C}$	λ_{max}/nm	$\Phi_{C \to O}$	
	20: R = CH$_3$	258	0.31	575	0.27	[75]
				516	0.29	
				460	0.33	
	21: R = i-Pr	258	0.52	535	0.34	[78]
	22: R = OCH$_3$	270	0.34	547	0.030	[96]
	23: R = CN	273	0.28	496	0.59	[96]
	24: R = C≡CPh	309	0.13	520	0.55	[103]
	25: R = CH$_3$	280	0.59	575	0.013	[97]
	26: R = i-Pr	290	0.50	600	0.026	[98]
	27: R = OCH$_3$	309	0.44	625	$< 2 \cdot 10^{-5}$	[99]
	28: R = O-i-Pr	312	0.46	635	$6.6 \cdot 10^{-4}$	[100]
	29: R = O-t-But	306	0.48	656	0.031	[101]
	28: R = CN	284	0.42	545	0.41	[96]
	29: R = C≡CPh	309	0.17	575	0.32	[102]
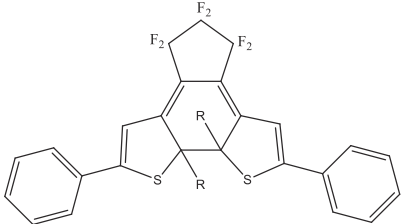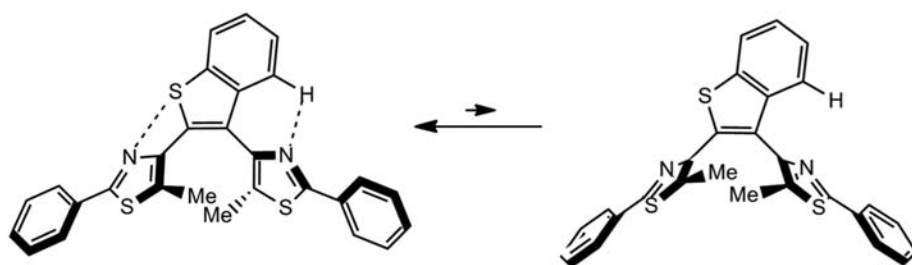
SCHEME 3.31 Intramolecular interactions between the ethene bridge and nitrogen atoms of the thiazole ring exist only in the antiparallel form.

electron attracting groups (**30**–**31**) clearly improve the quantum yield till excellent results. The observed trends from **25** to **26** and from **27** to **29** suggest an improvement of $\Phi_{C \to O}$ when steric hindrance of the alkoxy group is increased.

This is considered to be the result of the lowering of the energy barrier induced by steric hindrance. The same conclusion can be extended to the observed change in $\Phi_{C \to O}$ passing from **25** to **26**.

Returning to the case of benzothiophene rings, modification of **20** confirms the discussions earlier. Higher quantum yields are observed in this case for the closure process but, apart from this difference, similar trends in $\Phi_{C \to O}$ can be observed when steric hindrance is increased (from **20** to **21**) and also when eD or electron withdrawing substituents are present.

As discussed earlier, the ring opening process requires the overcome of an energy barrier. This means that, starting from the closed form on the excited state PES, an energy barrier is encountered along the reaction pathways and, beyond it, a funnel (energy minimum) is reached which allows the nonradiative relaxation on the ground state in the open form. Reversing the process, hence, starting from the open form in the ground state, absorption of an energetic UV photon leads to a point of the excited state PES which is higher in energy respect to both the funnel and the barrier. Hence, a fast overcome of the barrier is possible due to the downhill "acceleration" along the reaction path pointing to the funnel and also the barrier top.[103]

In this respect, the ring closure quantum yields are not expected to be dependent on structural features as in the open-ring process. A look to Table 3.3 clearly shows the relatively low dependence of $\Phi_{O \to C}$ on the nature of the thiophenyl ring and/or the substituents on the central carbon atoms.

The main factor affecting the ring closure quantum yield is the population of the antiparallel conformer before photocyclization is induced. We addressed this discussion in the previous paragraph. Table 3.2 shows the

correlation between the population of the antiparallel form and the quantum yield of the closure process in the case of compound **20** (sketched in Scheme 3.25 and repurposed in Table 3.3).

Compound **30** allowed reaching ring closure quantum yield of 0.98, because of the almost complete population of the antiparallel conformer.[104] This was achieved through intramolecular interactions between the thiophenyl cycles and specific sites on the ethene bridge (Scheme 3.31) which can be formed only in the antiparallel form.

3.4.4 Photocyclization reactions and solvent effect

Dithienylperfluorocyclopentene derivatives **31a-e** (open forms) and their closed forms in Scheme 3.32 have been chosen as starting point of this brief discussion about solvent effects on diheteroarylethenes photochromism. Table 3.4 collects some information about spectroscopic properties of the open and closed forms of the listed compounds, along with the measured quantum yields of the ring closure ($\Phi_{O \to C}$) and ring opening ($\Phi_{C \to O}$) processes.[105]

All the reported compounds show very small solvent effects, both in terms of solvatochromic shift of the absorption bands and in terms of quantum yields of the photoinduced processes. Solvent effects are not observed in the symmetric case **31a** and also in all the other asymmetric systems, nor it is related to the presence or not of fluorine substituents on the cyclopentene cycle.

Only in **31d**, solvent effects are strong and appear particularly effective on ring closure and quantum yield. Passing from hexane to acetonitrile $\Phi_{O \to C}$ decreases of about sixty times. At contrary, ring opening $\Phi_{C \to O}$ does not change in a significant way.

Interestingly, dissolving an acid in acetonitrile restores good level of quantum yield (0.66) in **31d**.[105]

Such behavior was ascribed to TICT in the excited state. Such a phenomenon is favoured in polar solvent as a consequence of the stabilization of a high energy charge-transfer excited state due to solvent polarity. CT excited states are more polar respect to non-CT states; hence, in polar solvents they can be stabilised at such a level to

SCHEME 3.32 Symmetric and non symmetric thiophenyl-based heteroarylethenes sketched for discussions about Table 3.4.
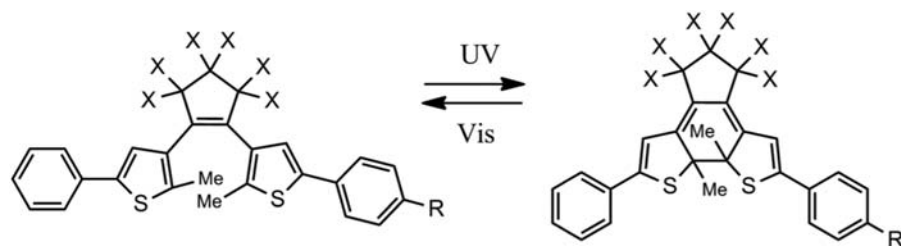
31a: X=F, R=H
31b: X=F, R=OMe
31c: X=F, R=OCOMe
31d: X=F, R=NEt$_2$
31e: X=H, R=NEt$_2$

TABLE 3.4 Some absorption properties and photoinduced quantum yields of the compounds in Scheme 3.32 in hexane and acetonitrile.

	Hexane solution				Acetonitrile solution			
	Open form		Closed form		Open form		Closed form	
	λ_{max}/nm	$\Phi_{O \to C}$	λ_{max}/nm	$\Phi_{C \to O}$	λ_{max}/nm	$\Phi_{O \to C}$	λ_{max}/nm	$\Phi_{C \to O}$
31a	280	0.59	575	–	285	0.56	587	–
31b	290	0.57	580	–	291	0.55	590	–
31c	284	0.53	575	–	286	0.50	585	–
31d	323	0.66	607	0.0053	335	0.011	630	0.0099
31e	321	0.51	538	–	329	0.70	540	–

become the lower excited states after geometry relaxation. In the TICT, structure relaxation consists in the twisting around a bond. Hence, in polar solvents, the populated excited state after UV absorption is the CT state, differently from apolar solvents where CT remains a higher state and is not populated. If the CT excited state is photochemically inactive, photocyclization does not occur, or it is strongly limited by the small residual population of the active excited state.

In dithienylcyclopentene systems, TICT is suggested to favor a perpendicular disposition of the thienyl rings respect to the cyclopentene cycle; this conformation is not suitable to photocyclization and low quantum yields are observed. This process was proposed in analogy to what already observed in dithienylmaleic anhydride (**32** in Fig. 3.6).[106] Also in this case ring closure quantum yield goes from 0.13 in hexane to 0.003 in acetonitrile. The proposed explanation of such a photocyclization quenching is shown in Fig. 3.6.

The TICT mechanism leads to twisted thienyl rings, unable to start the ring closure process. In apolar system, the usual co-planar conformation allows good quantum yields.

Returning to **31d** (Scheme 3.32), a similar phenomenon could be activated by the donor-acceptor CT excited state originated by the eD NEt$_2$ substituent and could be limited to only one thienyl ring, a sufficient condition to quench cyclization. Evidently, the OMe substituent (in **31b**) is not sufficient to induce the TICT and, due to the lack of evident TICT in **31e**, we can conclude that perfluoruration is equally important.

Whether or not a twisting takes place in the excited state, in both **31d** and **32** an excited state exists which becomes competitive with the active state and reduces cyclization only in solvent of relatively high dielectric constant (polarisability). When this competitive excited state does not exist, a relatively low dependence of cyclization and ring opening kinetics (and so quantum yields) is observed.

However, from the values in Table 3.4, passing from **31a** to **31c** a constant (also if small) reduction of $\Phi_{O \to C}$ is observed.

A recent investigation performed on **20** (Table 3.3) highlighted a more detailed trend of $\Phi_{O \to C}$ when solvent polarity is varied.[107]

The result is not a monotone trend.

Fig. 3.7A shows that $\Phi_{O \to C}$ reduces in relatively fast way passing from apolar solvents to moderately polar solvents ($\varepsilon < 10$), then it increases again by increasing polarity. This trend is not consistent with the change in population of the antiparallel conformation of the open form of the compound (Fig. 3.7B), which presents a monotone decreasing trend when polarity increases.
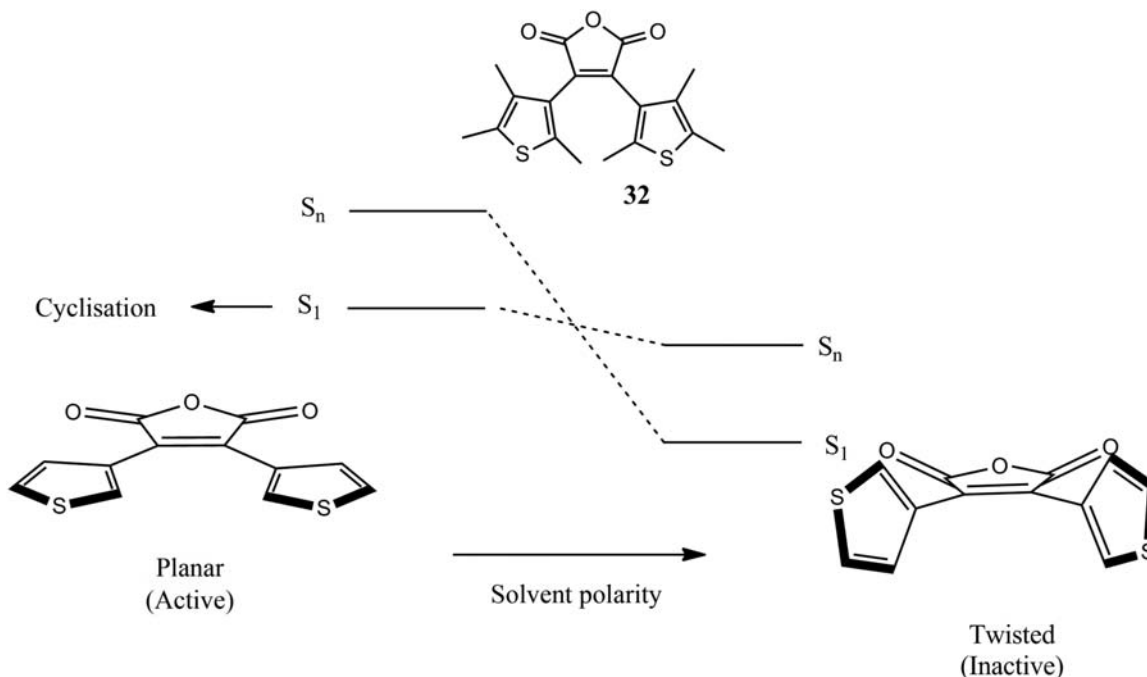
FIGURE 3.6 Twisted intramolecular charge transfer mechanism proposed in dithienylmaleic anhydride.
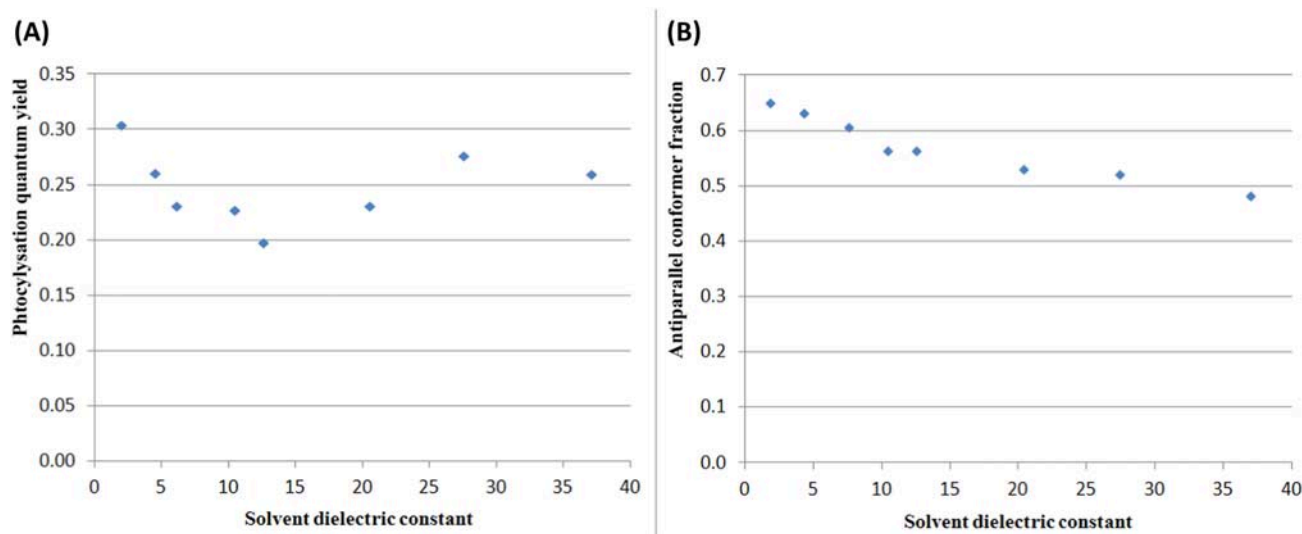
FIGURE 3.7   (A) The ring closure quantum yield of **20** changing the solvent polarity; (A) the fraction of antiparallel active conformer in the open form of **20**.

By application of transient spectroscopy it has been observed that the solvent polarity influences the rate of nonradiative deactivation of the excited states before cyclization but also increase the deactivation kinetics at the funnel.

More polar solvent shows higher deactivation rate of both the processes. At contrary, the position of the funnel respect to the energy barrier on the ground state is not dependent on solvent polarity.

Hence, a complex competition between the two nonradiative processes seems to be the only concurring phenomenon in setting the quantum yield which has to be added to the well-known population of the antiparallel form in the open ground state form.

3.4.5 Photochromism in chiral diheteroarylethenes

Chirality of diheteroarylethenes has been already introduced in Paragraph 3.4.2 regarding Scheme 3.26.

The interest was aimed at the possibility of separating the two antiparallel conformers of the open form of the diarylethene which normally quickly interconvert in a raceme, by making use of the steric hindrance of the ethene bridge. This is possible in some cases, as discussed there, a fact that open the way for the obtainment of specific enatiomers of the closed form after photocyclization.

In this paragraph we will deal more specifically with chirality and, more generally, with the stereochemistry of the ring closure process from the viewpoint of possible applications in photochromism. In this respect, we return on the origin of chirality in the open and closed forms of a typical diarylethene.

Scheme 3.33 shows the two enantiomers in the open forms of a generic diarylethene. Enantiomery originates from the different relative positions of the aryl rings, which induce helicity. Hence, the so-called P- and M-helical isomers can be distinguished, which are mirror images of one another.

The P-helix conformer (right hand helicity) can produce only one enantiomer through photocyclization that, just as an example in the scheme, we label as (R,R). The uniqueness of the obtained stereoisomer is a forced consequence of the conrotatory C−C bond formation in the excited state which follows a specific stereochemical pathway driving the bond formation between the central Carbon atoms. The M-helix isomer is the mirror image of the P-diarylethen and, starting from it, a mirror (chiral) conrotatory reaction pathway starts, taking to the enantiomeric product, which is the (S,S) enantiomer (if (R,R) was produced by the P open form).

Obviously, enantiomery in the products is a consequence of chiral carbon atoms, which are the reactive (central) ones.

Ring closure processes normally starts from a raceme because fast rotation of the aryl cycles leads to equilibration of the P- and M-isomers. In rare cases interconversion is sufficiently slow to allow separating the two helical enantiomers (chiral chromatography is a possible way) and potentially obtain a specific product, as discussed in Paragraph 3.4.2.
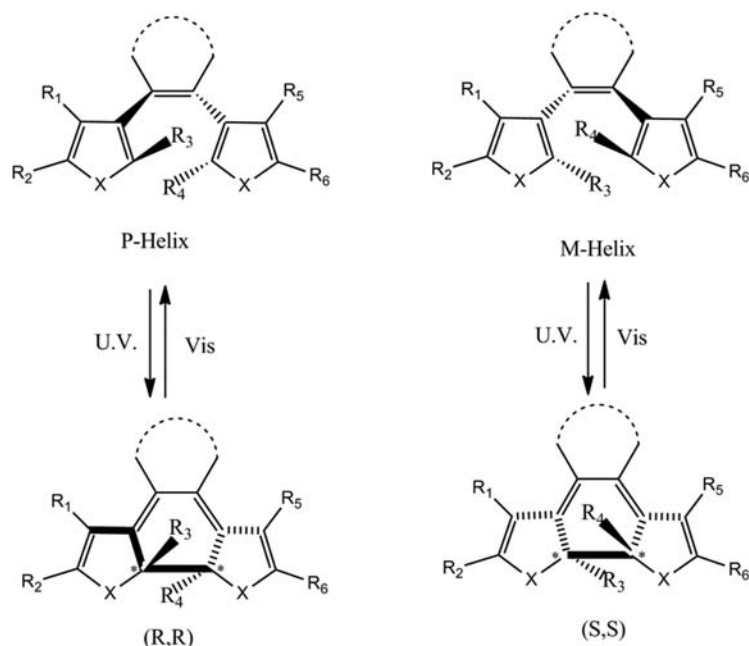
SCHEME 3.33 Helicity in the open forms of a generic diarylethene and corresponding chirality of the ring closure processes.
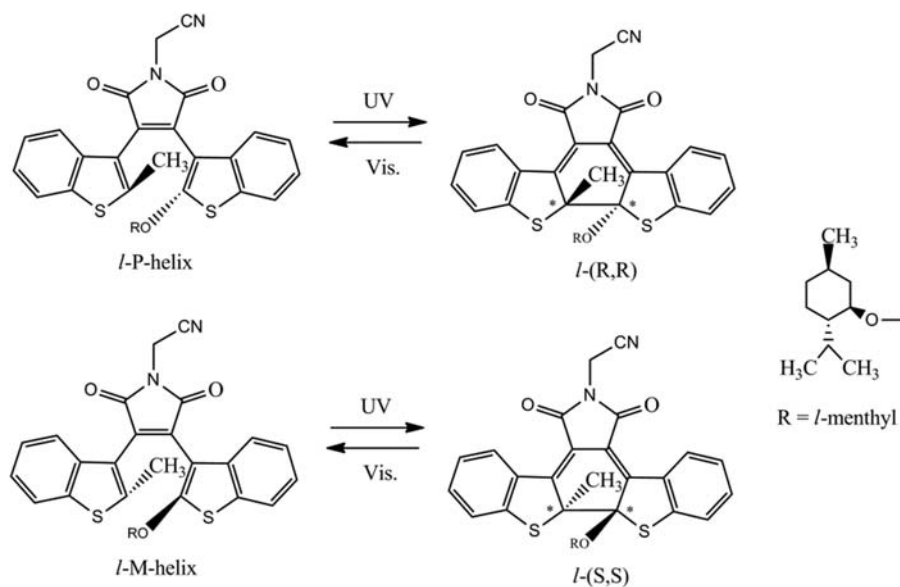
SCHEME 3.34 The different diastereoisomers obtained connecting a chiral group (*l*-menthyl) to the P- and M-isomers of the open forms and the (R,R) and (S,S) enantiomers of the closed forms.

However, the easiest way to obtain a specific enantiomer of the closed forms consists in breaking enantiomery between the M- and P-helical isomers and, at the same time, breaking the enantiomery between their pathways leading to the closed forms. Such a often-called "asymmetrization" of the PES means, more correctly, that the mirror symmetry plane which in origin characterizes the PES and which generates one half of the PES from the other half (each half of the PES comprises one helical open form and the chiral pathway toward its closed form as sketched in Scheme 3.33) is not present anymore. Structural changes in the open forms force the PES to change, featuring two different parts which are not mirror-related. One part is for the P- and the other for M-open forms.

This can be simply (in theory) achieved by connecting a chiral group taken in one specific enantiomeric form to the photochromic "core" structure, as close as possible to the reactive zones (the central reactive carbon atoms). In other words, diastereoisomery is induced, making different the energies of the helical enantiomers and also

the energies of the transient structures (and transition states) along the pathways starting from them. In this way, kinetically different pathways lead to two diastereoisomeric closed forms which are produced in different quantities.

Scheme 3.34 shows an example of this approach. *d*- or *l*-menthyl substituents[108] were connected to one of the benzotienyl reactive Carbon atoms.

If *l*-menthyl binds the open form, two diastereoisomers are possible which can be called *l*-P and *l*-M at different energies. Starting from them, photocyclization leads to *l*-(R,R) and *l*-(S,S) in a specific way (Scheme 3.34).

In toluene at −40°C, one of the two closed form diastereoisomers was obtained with a diastereoisomeric excess (*de*) of 86.6%. In *n*-hexane, photocyclization did not show any specificity but, adding a small quantity of THF, a *de* of 68% at 23°C was reported. Solvent effects are determinant and a deeper and interesting analysis is worth to be discussed here.

The observed stereochemical preference for one enantiomer of the closed form can derive from two phenomena. The first one is that the open form P- and M-isomers present different stabilities in different solvents so that the equilibrium favours one isomer in polar solvents and, consequently the (R,R) or (S,S) closed form prevails after ring closure. This hypothesis was rejected, because NMR of the open form did not distinguish the *l*-P and *l*-M isomers, a signal of fast interconversion and, moreover, the CD spectra did not show any change in different solvents, in contrast with the % *de* which is solvent dependent.

Hence, solvent effects are important in the excited state PES alone and a TICT phenomenon was taken into account.[108]

In Paragraph 3.4.4, TICT was described in a dithienylmaleic anhydride (see Fig. 3.6 and related discussions) which is structurally similar to the dibenzothienylmaleimide under study. Hence, the same process can be postulated, involving a CT excited state from the donor benzothiophene rings to the eA (methylcyano)-substituted maleimide moiety.

The effect of TICT is twisting the benzothienyl groups and their placement in the perpendicular direction respect to the ethene bridge plane. In this way, TICT quenches photocyclization and is favoured in polar solvents. In apolar solvents, instead, CT excited states are not populated and a planar and reactive position of the benzothienyl rings is possible. Hence, starting from a 1:1 mixture of *l*-P and *l*-M stereoisomers, each isomer completes its photocyclization leading to an equimolar mixture of the closed diastereoisomers. In strongly polar systems, both *l*-P and *l*-M isomers undergo the TICT process in their excited states, hence no (or very low) yields are observed.

In medium polarity solvents the things are more complex: following Fig. 3.8 as a schematic description of what is hypothesized, we label with A_C the most stable closed form and with A_O the open form which leads to it. A_O and B_O are at similar energies and in an equimolar equilibrium in the ground state. After light absorption, along the pathways from the S_1 of A_O, lower energies are expected respect to the pathway starting from S_1 of B_O, because the factors which make A_C more stable should influence the reaction path pointing to A_C in a similar way. Hence, the lower energy pathways has a higher probability to stay lower in energy respect to the TICT state.
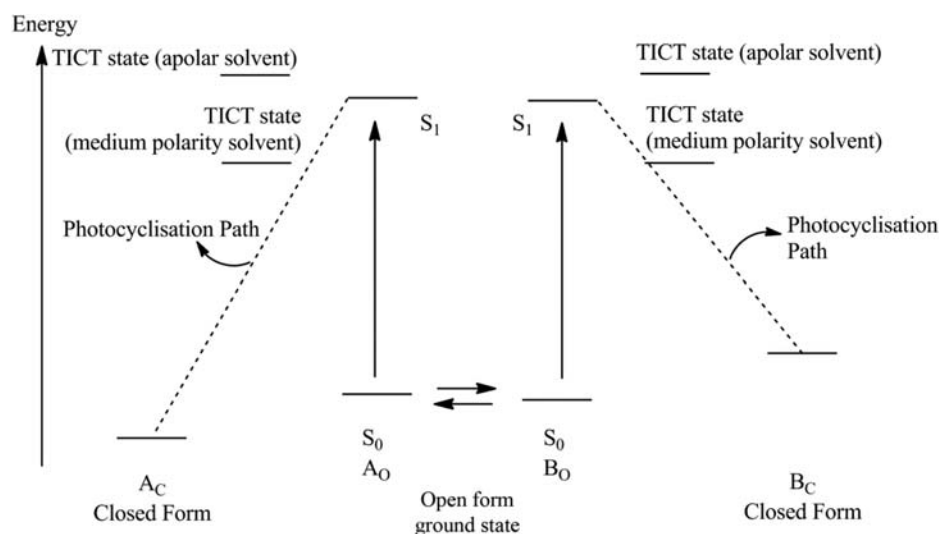
FIGURE 3.8 A schematic of the possible competition between the twisted intramolecular charge transfer excited state and the photoactive excited states.
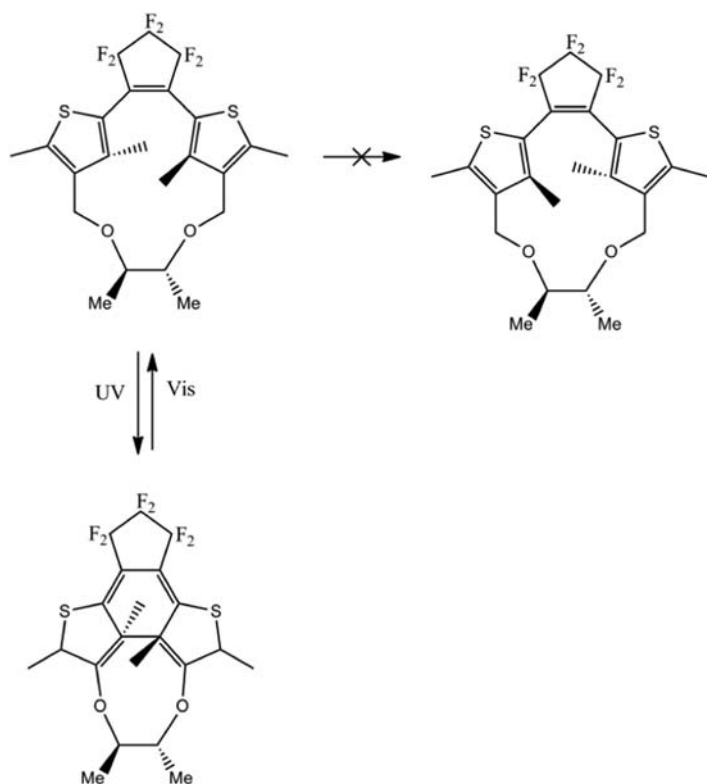
SCHEME 3.35 An example of external cyclic structure forcing a specific helical isomer of the open form.

At contrary, the less stable walk (toward B_C) incurs in an IC toward the TICT state with higher probability and consequently is less effective in completing the ring closure.

Scheme 3.35 shows a chemical way to force the open form of the photochromic core to a specific helical isomer. The cycle connecting the two thienyl rings induces diastereisomery and, at the same time, does not allow the thienyl rings to rotate respect to the ethene bridge. Thus, helicity inversion is impossible and only one diastereisomer of the closed form is formed by photocyclization of the P-helical isomer (showed in Scheme 3.35), that is, a 100% *de* is obtained.[109,110]

A similar result was obtained in a different way, as shown in Scheme 3.36.

A triethyleneglycol bridge induces a big steric hindrance on one face of the ring.[111]

In this way, only one antiparallel open form can be obtained and, consequently, only one closed form can be isolated. A *de* of 100% was obtained, moreover, also at 100°C no P-M isomerization is observed in the open form.

3.4.6 Ring closure processes induced by visible radiation and all-visible photochromism

Most of the photochromic substances described in this chapter as well as most of the photochromic substances commonly developed for application purposes are colorless or weakly colored in their open form. They take on color only in the closed form. The lack of visible absorption by the open form reflects the need to use UV radiation to trigger photocyclization.

As already mentioned elsewhere in this chapter, the use of UV radiation is problematic. First of all, this radiation can be harmful to biological tissues, hindering the field of application in the biochemical and biological fields. UV radiation can be harmful to some non-biological materials in certain cases by triggering photochemical degradation phenomena, including diarylethenes which are particularly sensible to UV radiation in their closed forms. Furthermore, UV rays do not have a high penetrative capacity in amorphous materials, polymers or gels, forcing photochromism applications to the external parts of materials.

These considerations push toward the research of new materials able to give both photocyclization and ring opening processes in the visible spectrum. Such all-visible photochromic compounds can be obtained by exploiting different chemical and/or physical processes.
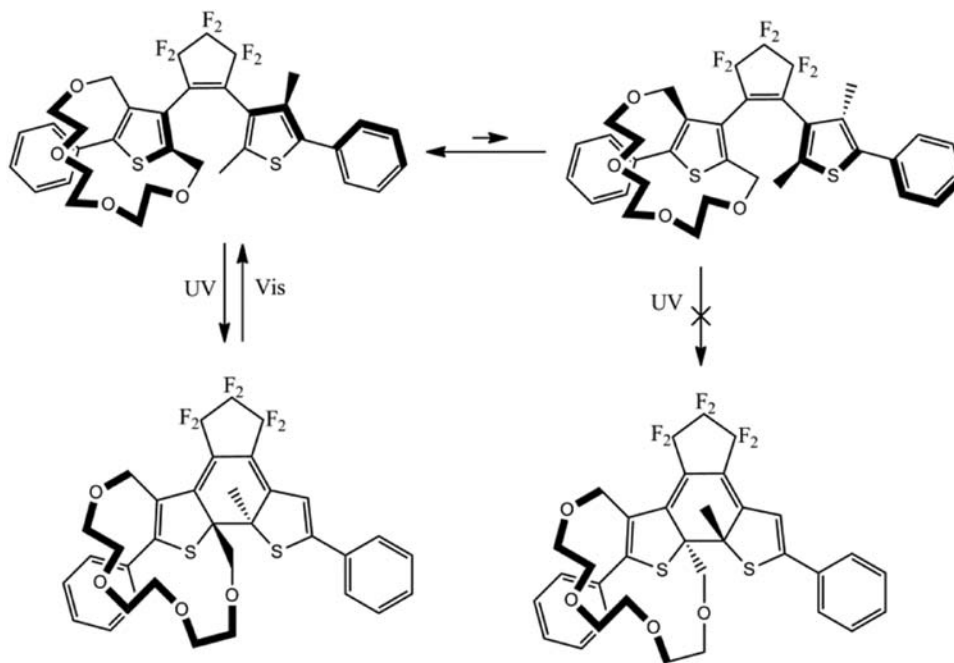
SCHEME 3.36 Facial steric hindrance shifts the equilibrium toward the P open form. Photocyclization is possible only from the P isomer to the (R,R) closed form.

In Paragraph 3.4.2 we have already described photochromic substances capable of giving rise to photocyclization in the triplet state through the use of chemically-connected sensitizers based on metal complexes. Efficient photocyclization in the triplet state is possible in common diheteroarylethenes but usually does not occur due to the poor efficiency of the ISC in this chromophores. The use of metal complexes based on heavy metals allows to have an efficient ISC and to transfer the energy of the excited state to the triplet of the photochromic unit.

Scheme 3.27 (Paragraph 3.4.2) and the related discussion describe in greater detail the photophysical processes that lead to the triplet state population of the diheteroarylethene core. The interesting aspect is that absorption of light is attributable to the metal complex which may be able to absorb in the visible or in near-UV. For example, compound **8** (Scheme 3.27) features an absorption maximum at about 450 nm, unlike the dithienylethene used as binder of Ru which, free from coordination, absorbs at 410 nm. Although the latter value is not particularly far from the boundaries of visible light, the coordination of Ru induces a significant red-shift, extending the photochemically active absorption up to about 500 nm.[81]

A much more evident bathochromic effect was observed in compound **9** (Scheme 3.27). The wavelength useful for triggering photocyclization passes from less than 340 nm for the free ligand to the visible spectrum at wavelength below 480 nm after Re complexation.[82]

Interestingly, Re complexation in **10** (Scheme 3.27) is less effective than **9** in the photocyclization process (λ_{max} passes from 350 to 380 nm) but it is evident in its closed form (λ_{max} from 580 to 710 nm).

An example of metal-free triplet sensitizers with photoactive absorption in the visible spectrum can is biacetyl. Scheme 3.37 shows possible applications of this chromophore in different forms.

The simplest use consists of intermolecular processes (Scheme 3.37, compound **33**).[112] The biacetyl has a good level of ISC after absorption of light, which can occur at 400 nm. Its triplet state is at high enough energies to sensitize the triplet state of common dithienylethenes. The problem is the poor biacetyl absorption at 400 nm due to the fact that it is associated with an n-π* transition with small absorbivity. The result is that, to have useful photocyclization kinetics, a large excess of biacetyl must be used, being 250 equivalents are needed.

With such a large excess of biacetyl, a quantum yield of 0.33 was obtained with 405 nm irradiation and triplet-state photocyclization.

With the aim to avoid the necessity of large acetyl concentrations, chemical connection of biacetyl to the photochromic unit was proposed with saturated (**34**) and unsaturated (**35**) linkers.[113] The behavior of **34** is very similar to **33** in terms of absorption spectra and photocyclization quantum yields when 333 nm radiation is used and
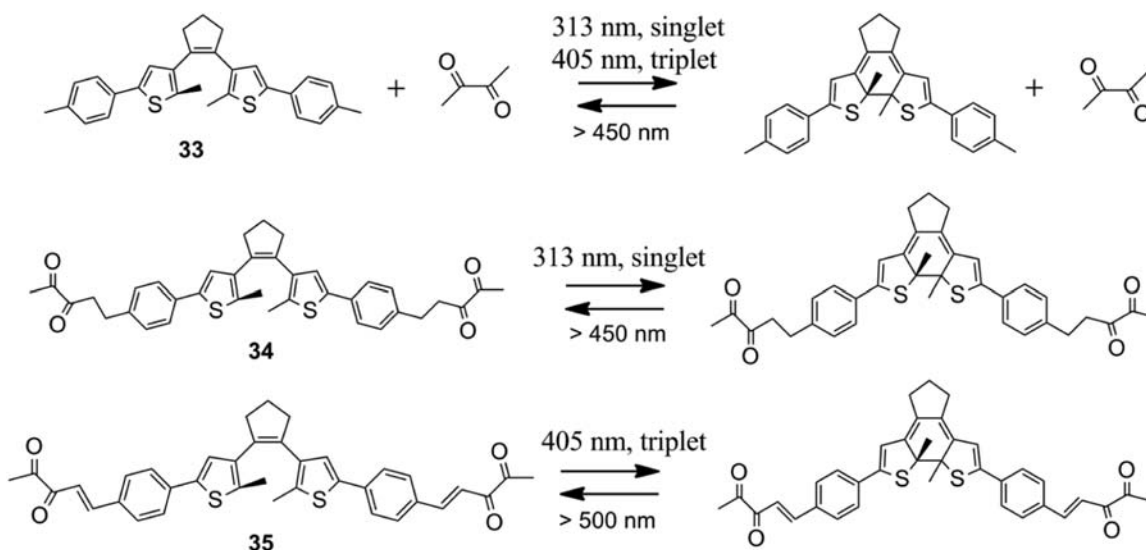
SCHEME 3.37 Different uses of biacetyl as triplet sensitizer.

singlet (UV induced) photocyclization takes place. Moreover, no cyclization is observed with 405 nm irradiation, possibly due to the low absorption of biacetyl.

The presence of the unsaturated linkage in **35** induces more evident changes. A strong bathochromical shift is observed in the first absorption band ($\lambda_{max} = 390$ nm) is observed as a consequence of the elongation of π conjugation. A photocyclization quantum yield of 0.30 was recorded by irradiating at 405 nm in deaerated solutions, similarly to **33** in concentrated biacetyl solutions. In presence of oxygen, photocyclization quantum yield strongly reduces. This proves that the triplet excited state is responsible of the ring closure process.

A final interesting aspect regarding **35** is the increased resistance to degradation after repeating cycles of ring closures and openings. This was observed when irradiating at 405 nm as a consequence of the lower photon energies and consequent less probable degradation processes, which are associated with the action of UV light mostly on the closed form. Still more interestingly, also irradiating **35** at 313 nm an excellent stability is observed. Possibly, easy ISC toward triplet states due to biacetyl makes the closed form more protected toward photoinduced degradation.

This discussion about photochromism of **35** highlights the importance of extending the π-conjugation to shift the absorption wavelength toward the visible spectrum. In reality, **35** absorbs intensely at 405 nm because of this phenomenon; the diacetyl intervenes by favouring the ISC and triggering the process in the excited triplet state.

Molecule **36** in Scheme 3.38 shows photocyclization at $\lambda > 402$ nm and strong absorption at 470 nm due to the long π conjugation from the thienyl to cyanine moieties. A photocyclization quantum yield of 0.12 is maintained almost constant from 402 nm to 500 nm and lowers to about 0.09 at longer wavelength up to 650 nm. After photocyclization, an absorption peak at 840 nm in the NIR is observed and associated with the closed form. However, this NIR band is not able to induce photoreversion to the open form; UV light is necessary for ring opening; hence, 36 is not a real all-visible option.

Finding efficient all-visible compounds is not easy; photocyclization quantum yield is prone to reduce when the π conjugation is extended because the weight of the double bond in the molecule HOMO and LUMO reduces accordingly.

Furthermore orbital interactions between the HOMO and LUMO of the photochromic unit and the frontier orbitals of the linked chromophores are often difficult to be predicted and can be different in the open and closed forms. Hence, good photochemical performances in the open form do not ensure equally good results for the closed form.

As an example of such complications, a brief discussion is presented here about compounds **37** and **38** (Scheme 3.38). In **37**, a perylene monoimide chromophore is linked to a photochromic unit by using a triple bond. The resulting π-conjugation is so extended that photocyclization can be achieved at 560 nm.[114,115]

In **38**, the perylene structure in liked at a different position. In both **37** and **38**, the perylene LUMO is close in energy to the diarylethene LUMO, good interaction takes place and a strong delocalization of the LUMO results on both the photochromic core and perylene chromophore. The HOMO remains localized on perylene.
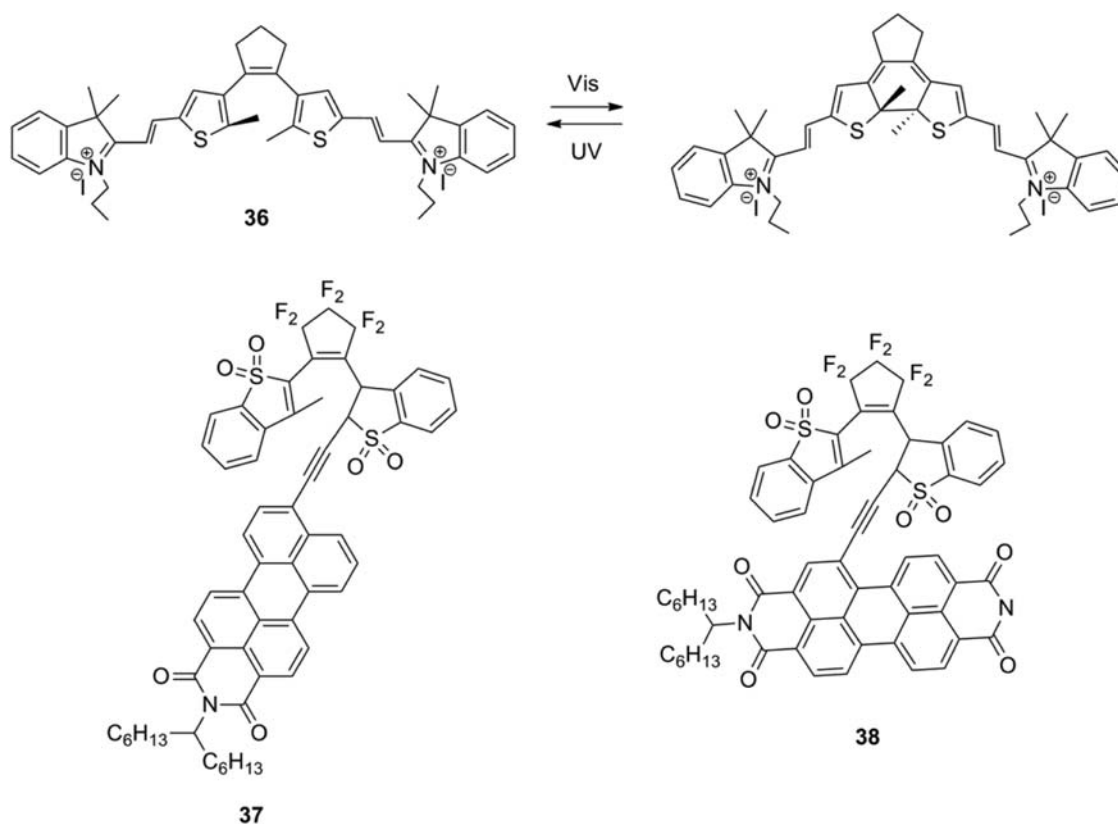
SCHEME 3.38 Examples of photocyclization induced by visible radiation achieved by elongation of the π conjugation. Only **37** is a real all-visible photochromic compound among the three reported here.

The resulting HOMO-LUMO electronic transition is enough to induce efficient photocyclization in both the compounds.

Photoinduced ring opening, at contrary, takes place only in the **37** closed form. In the **38** closed form, an excited state energy transfer from the diarylethene core to perylene takes place after light absorption. In fact, only in the closed form, a perylene-localized excited state is present at lower energies respect to the lowest diarylethene-localized excited state. This fact generates the energy transfer, which is efficient because an antiparallel orientation of the two transition dipoles is present in **38**, accordingly to the mutual orientation of perylene and the diarylethene.

In compound **37**, perylene is in a different orientation respect to the diarylethene. Hence, transition dipole moments are not antiparallel anymore, making much less probable the energy transfer. In conclusion, **37** shows photoinduced cycloreversion and real all-visible photochromism, the similar structure **38** is not equally performing.

In compound **39**, all-visible photochromism was achieved by using an intramolecular proton transfer (IPT). Scheme 3.39 graphically describes the involved processes.[116]

By increasing solvent polarity, a tautomerism is engaged in which the proton moves from the oxygen (**39a**) to the nitrogen atom (**39b**) in the salicylidene-propyl-amine group. The proton transfer induces big changes in the HOMO-LUMO gap, due to heavy electronic and/or electrostatic modifications associated with the proton transfer, giving rise to an all-visible compound with a noteworthy photocyclization quantum yield of 0.32 at 450 nm and photoreversion quantum yield of 0.07 at 600 nm.

From above, solvent polarity can be used to gate visible photochromism, otherwise a "normal" UV photochromism is present in apolar environments. Such a gating possibility allowed comparing the fatigue resistance of **39** under UV-driven photocyclization in **39a** and under Vis-driven photocyclization in **39b**.

A much higher resistance was observed in **39b**, confirming the importance in going on in the research of all-visible photochromic substances for better stability.
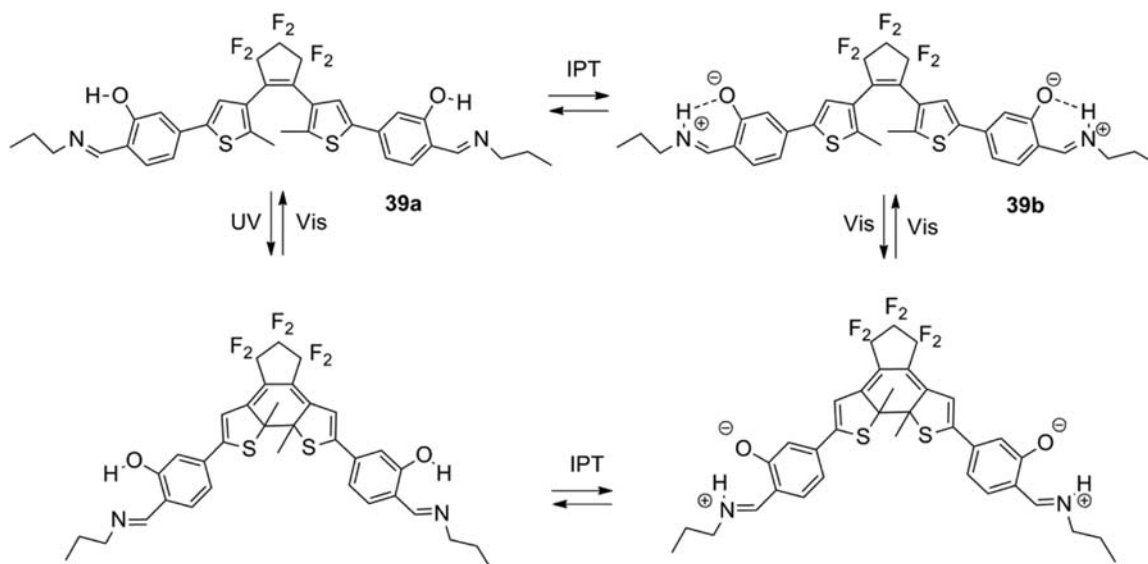
SCHEME 3.39 Intramolecular proton transfer in polar solvents induces all-visible photochromism.

3.5 Applications of photochromic molecules of diheteroarylethenes: Switches and optical memories

Photoinduced cyclization and its reverse ring opening process are easily feasible by many diheteroarylethenes. In many cases, high efficiency of the process allows a fast chemical transformation which can be easily obtained using light from an external source.

Such a transformation goes far beyond the change in color, making possible the tuning of other important properties of the material such as conduction and aggregation state but also chemical properties like catalytic action, acidity and biological activity among many others.

A huge number of diheteroarylethenes applications in many technological fields have been proposed. In this paragraph, we will present a few examples about how photocyclization can be used to tune or switch on and off desirable properties in materials and so in devices.

Paragraph 3.5.1 deals with the use of diarylethenes as a switch. In it, efforts have been made to connect the physical and chemical changes passing from the open to the closed form to the use that can derive in organic devices or condensed matter in general.

In this respect, according to us, it represents the starting point for understanding the second important applicative field of this class of compounds, that is, optical memories discussed in Paragraph 3.5.2.

3.5.1 Switches

Thermally-stable or P-type photochromic substances are desirable candidates for molecular switches. The use of light absorption is by far the easiest way for inducing the change of state ("on/off") in switches. In fact, it offers the possibility to induce switching from an external light source, hence in a direct and easy way and additionally offers a faster switch in comparison to other methods such as chemical or electric switches.

Selected diheteroarylethenes are able to change from their open to closed forms upon irradiation with UV light and reverse the change after absorption of visible light.

The two forms are different in several respects. From the structural viewpoint, the closed form presents a planar and rigid structure, differently to the more flexible open form.

Structural stiffness could be used to modify how molecules self-assemble in pure or composite systems, just as examples, the structure of a supramolecular aggregate can be changed with irradiation or a liquid crystal phase can be modified from a nematic to a cholesteric form. The change in the way molecules interact one another can be effective in other fields, for example the structure of a catalyst can be switched between two forms with different catalytic activities due to their differences in structure and/or chirality.

At the same time, the closed form of a diheteroarylethene shows an extended π-conjugation between the two bridged heteroaryl groups which cannot exist in the open form. Extending the π electron structure changes the energy and shape of frontier orbitals and normally reduces the HOMO-LUMO gap.

In these circumstances, electron and/or hole mobility is expected to be enhanced in molecular solid phases, which is the basis of good conductivity in this class of materials. The change in frontier orbitals energies modifies the hole or electron injection kinetics from electrodes to bulk material which, together with charge mobility, is another important process in determining the current-voltage response of molecular solids. Furthermore, a reduced HOMO-LUMO gap increases molecular polarizability and changes the optical properties of the material.

Extending the π conjugation from isolated to conjugated peripheral heteroaryl groups allows electronic coupling between them. This can be used to tune magnetic properties in case of peripheral radicalic systems connected by a diheteroarylethene bridge. It could also allow the obtainment of a conductive bridge between peripheral extended systems such as carbon nanotubes of fullerenes.

These are only a few examples of the many opportunities offered by these systems as molecular switches. In the following, several specific applications will be deepened; it will be evident from the discussion below that the core molecular system is commonly based on two thienyl groups bridged by different ethenes.

Functionalization of the thienyl and ethene groups is often intended to only chemically "connect" the system to other components of the device.

However, in many cases, functionalization is thought to tune the properties of the active closed form for best performances.

We will start the following overview from applications in molecular electronics.

3.5.2 Switchable electric conduction

Optoelectronic devices are commonly based on molecular solid phases in which electric conductance is guaranteed by hopping processes of hole and/or electrons between adjacent molecules in the solid-phase structure.

Frontier orbitals are strongly interested in this process and could favor high level of charge mobility in case of extended π-systems and reduced HOMO-LUMO gaps. The closed form of diheteroarylethenes can satisfy both these requirements, because of their π-structure extends from one heterocycle to the second one passing through the ethene bridge. The same cannot be said about the open form, of course. The orbital differences between closed and open forms allow the design of new materials which conductance can be switched by irradiation with UV light (closed form and switched-on conductance) or visible light (open form and switched-off conductance).

Π-conjugation opens the way for a large number of different functionalization addressed to tune the HOMO and LUMO levels by the choice of electron-donor or electron-withdrawal groups for best performances both in terms of conductance in bulk materials and in terms of charge injection from electrodes to the internal material.

A first example of applications in this field is offered by a polymeric organic light emitting diode (OLED) sketched in Fig. 3.9.

40
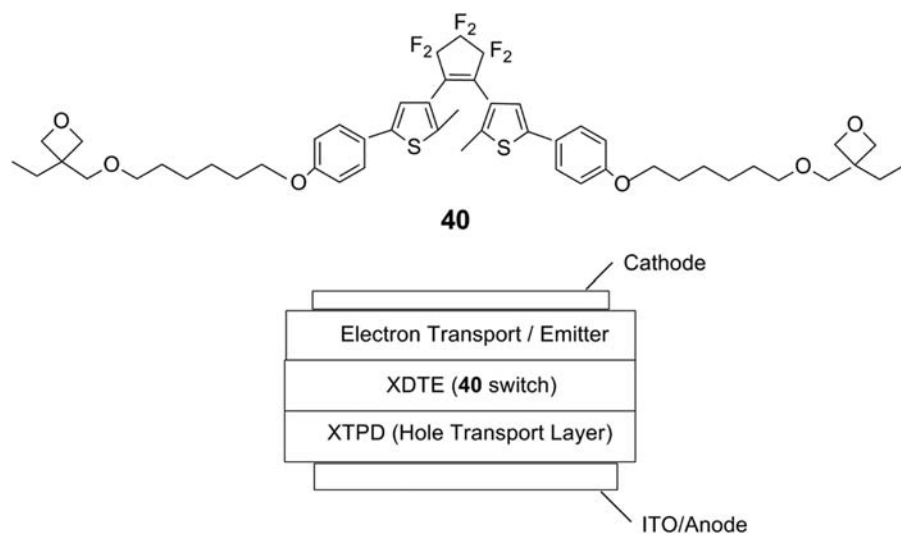
FIGURE 3.9 The shown dithienylethene **40**, upon polymerization, constitutes the switching layer XDTE in the sketched polymeric OLED. After irradiation at 312 nm, XDTE changes its color to orange, due to photocyclization, and good electrical connection is triggered between the hole transport layer (XTPD) and the electron/emitter layer. Visible orange light switches off the electric connection.

This figure describes some results from the work of Meerholz and co-workers[117].

An oxetane-functionalized dithienylperfluorocyclopentene **40** (Fig. 3.9) was prepared as the key component of an organic light-emitting device which can be photoswitched on and off. Polymerization of monomer **40** was accomplished by using a photoinitiated cationic ring-opening process.

In this way, a photochromic polymeric layer was prepared (XDTE in Fig. 3.9) and interposed between a hole-transport layer (XTPD and based on triphenylamine dimers) and the electron-transport/emitter layer ("blue-emitter).

Photochromism is used to change the HOMO level of **40** in the XDTE polymer. Higher HOMO energy in the closed form would favor hole injection from the XTPD to the XDTE layers, hence good overall device conductance. The open form causes a mismatch of the HOMO levels in the two layers and reduces conductance.

Additionally, the more extended π conjugation in the closed form can favor conduction in bulk material.

In conclusion, electrical conductivity was measured before and after photoisomerization toward the closed form and an increase of a factor 3000 was measured in terms of current density when UV light induces photocyclization.

More specific studies have been addressed to the injecting ability toward a diheteroarylethene in its closed and open forms and to charge transport in the bulk material, as well.

Again, the closed form is expected to present a higher-in-energy HOMO, with consequent easier charge injection. An evidence of this was reported by Tsujioka and Masuda[118], who prepared a device by depositing a diarylethene having diphenylamino groups (**41**) and a hole transport layer (N,N′-di(naphthalene-1-yl)-N,N′-diphenylbenzidine) (α-NPB) between magnesium cathode and ITO anode, as shown in Fig. 3.10. The authors performed various measurements addressed to the characteristics of carrier injection and transport in bulk material. The current was effectively controlled upon photoirradiation.

A different derivative of the dithienylperfluorocyclopentene (**42** in Scheme 3.40) was synthesized to achieve strong adsorption on carbon nanotubes[119]. The used "hook" was hexabenzocoronene shown in figure along with the used photochromic unit.

When the nanotube is covered by photoswitch **42** in its closed form (green color), good conduction is obtained whereas, when the nanotube coverage is in the switched-off open form (yellow color), the pendant switch hinders conduction.

Although the basic mechanism is the same of bulk materials, the obtainment of single-molecule switches for electric connection between two electrodes is a challenging and fascinating area of interest.

Fig. 3.11 collects two examples of a single dithienylethene fragment used as switchable connector between extended structures like gold[120] and nanotubes[121]. Nothing is new in terms of backgrounding phenomena: we newly find the same diheteroarylethene and π-conjugation in the closed form but the importance in terms of device design and potential technological perspective is clearly evident.
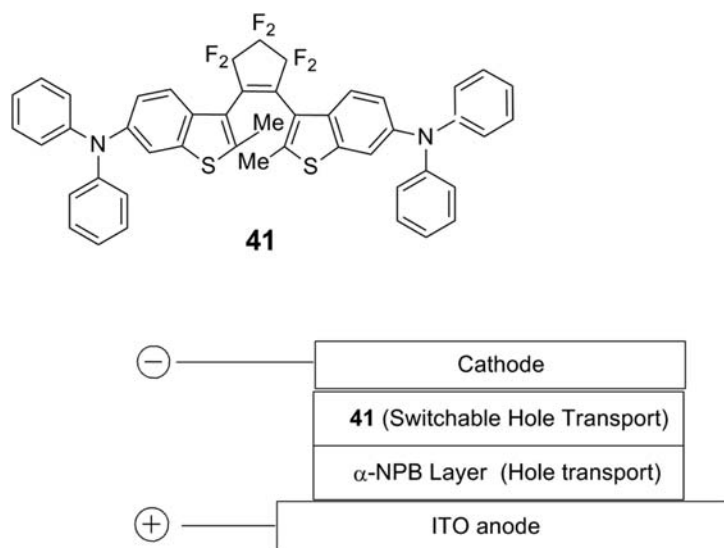

FIGURE 3.10   The modified dibenzothienylethene **41** used as switching conductive transport layer in the shown two-layer molecular device.
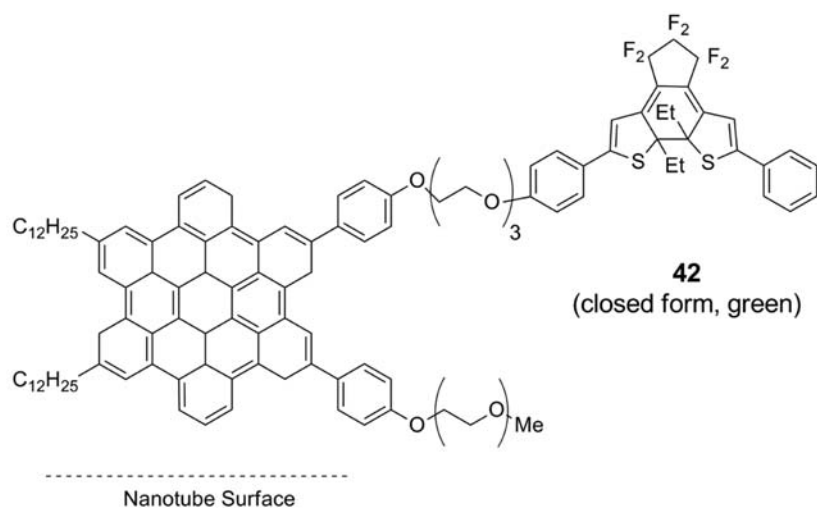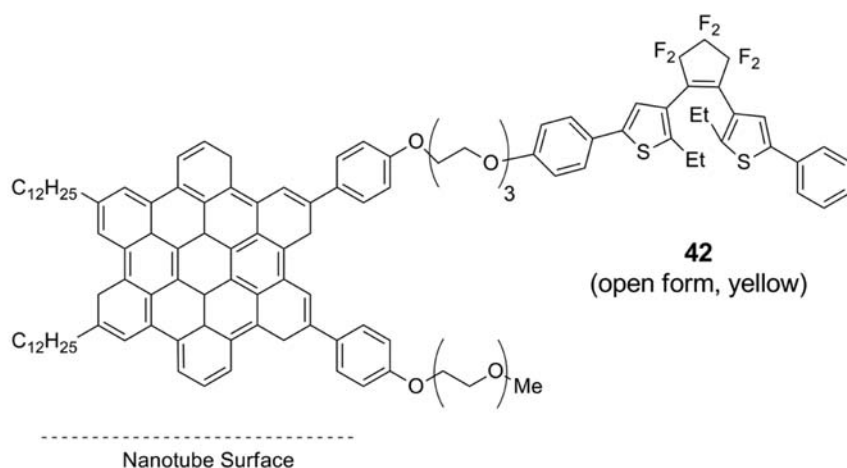
42
(open form, yellow)

42
(closed form, green)

Fig. 3.11A reports the dithienylethene functionalized with thiol groups which were used as bridging single molecule in a gold nanogap.[120] In the sketched UV-induced closed form, 3 orders of magnitude higher conduction was observed in comparison to the visible light-induced open form.

Fig. 3.11B shows the same successful schema applied to single-walled nanotubes.[121] Here an amide bridge was used for chemically binding the ending carboxylic groups of oxidated nanotube to the photoswitch periphery. An increase of five orders of magnitude was observed in conductivity passing from the open to the closed forms of the switching bridge.

The use of pyrrole heterocycles (R = NMe in Fig. 3.11B) in place of thiophene ones induced thermal relaxation to the open form, allowing a light-dark switching ability rather than the UV/Visible switch of thiophenyl-based photoswitches.

3.5.3 Switchable supramolecular systems

The structural changes from the flexible open form to the rigid closed form of a diheteroarylethene can be effectively used for changing the way in which intermolecular interactions take shape in condensed phase.

Supramolecular organizations can be changed accordingly, allowing a switchable structuration. Diheteroarylethenes were tethered to cyclodestrine (**43**) in Scheme 3.41.[122–124] The switch is the "usual" dithienylethene moiety.

In the open form, a much higher affinity was observed relative to *mesotetrakis*(4-sulfonatophenyl)porphyrin (TSPP), a fact attributed to the higher β-cyclodestrine cavity flexibility. In the closed form, a much lower affinity was observed.

(A)

(B)
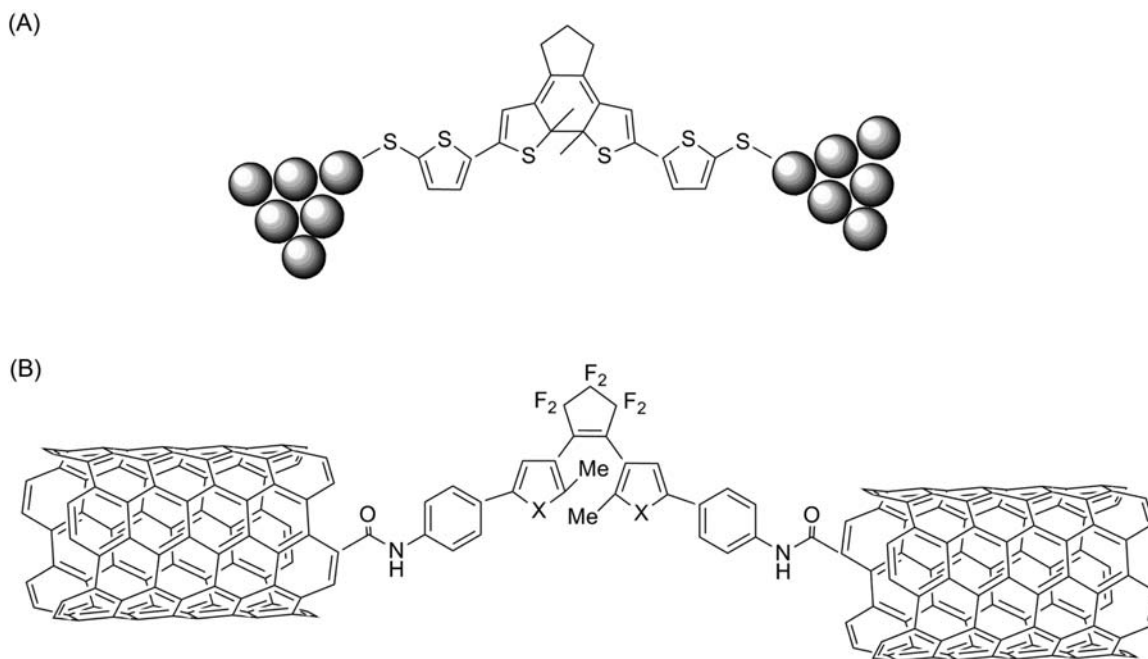
FIGURE 3.11   Two examples of electric conduction through a switchable single-molecule bridge. In (A) a dithienylethene bridge fills a gold nanogap acting as ligand toward the metal surfaces; in (B), carbon SW-nanotubes are chemically connected.

43

44

45
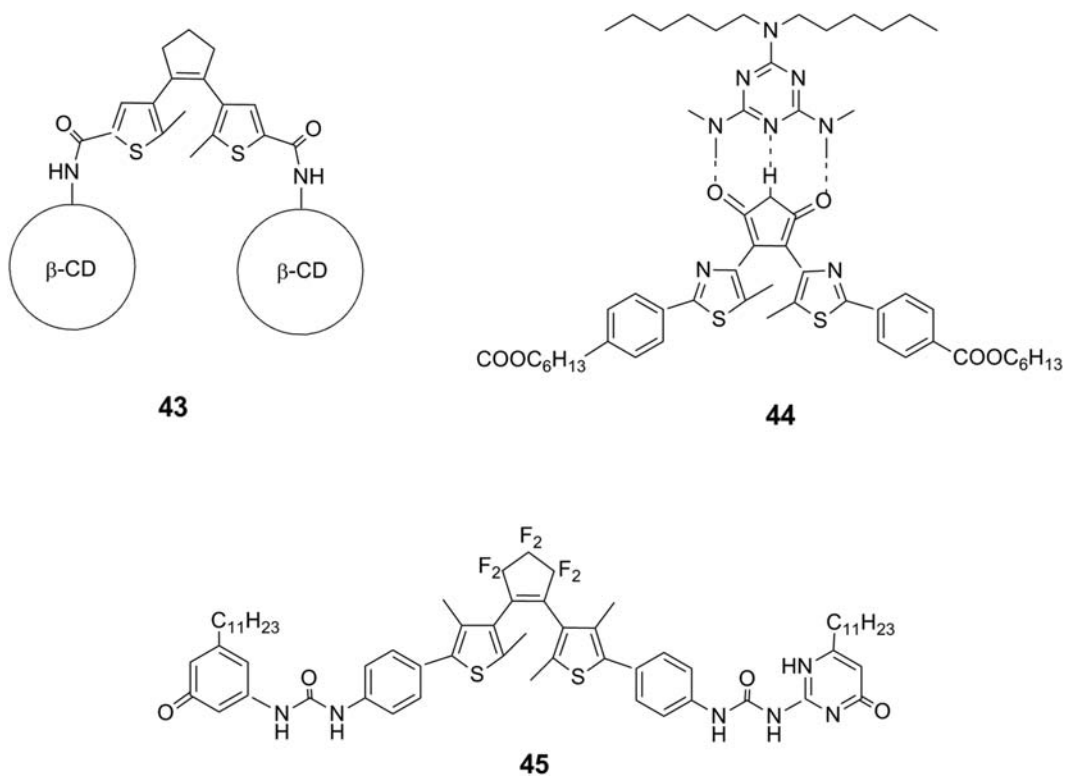
SCHEME 3.41   Examples of etheroaryl cycles functionalisation.

The change in TSPP-cyclodestrine binding ability is 35 times higher in the open form.

A different explanation is desirable in the case of system **44** in Scheme 3.41. Here we have a hydrogen-bonded system between the ethene-containing group of the switch and melamine. A higher affinity was observed in the case of the open form.

In this last case, electronic rather than structural factors are expected to change the melamine-switch interaction.[125]

Diarylethene **45** (Scheme 3.41) forms supramolecular polymers. Their particle size was found to increase when the diarylethenes undergo the photocyclization reaction.[126]

Diarylethene **46** (Scheme 3.42) is equipped with two melamine hydrogen-bonding sites.[127] Upon mixing its open form with oligothiophene-functionalized ditopic cyanurate (OTCA, **47**) in a nonpolar solvent, a supramolecular copolymers bearing photoswitchable moieties in their main chains and oligothiophene as side chains were formed. The flexibility of **46** open forms imparts the chains with sufficient conformational flexibility to fold into a helical nanofibers through interchain π−π stacking interactions between the pendent oligothiophene moieties.

The ring-closing reaction of **46** reduced the conformational flexibility of the chains, disabling them from organizing into higher-order structures.

Such results indicate that the hierarchical organization can be effectively controlled by photoirradiation.

3.5.4 Switchable liquid crystals

The same discussions about supramolecular systems can be directly extended to the structuration of liquid crystals.

Chiral diarylethene **48** (Scheme 3.43) is able to change the texture of the liquid crystal phase based of 4-cyano-4′-pentylbiphenyl **49**.[128] Compound **49** forms nematic texture liquid crystal phases which preserve the texture after a small add of the diarylethene. Upon UV irradiation, the nematic texture changes to a cholesteric finger-print texture. This is attributed to the larger helical twisting power of the closed-ring isomer.

Some diarylethene derivatives form liquid crystals themselves rather than been used as dopants.

The diheteroarylethene **50** (Scheme 3.43) features cyanobiphenyl groups as mesogens via oligomethylene chain spacers. The open-ring isomer showed smectic C phase between 33.3°C and 74.5°C and showed nematic phase between 74.5°C and 78.5 °C.
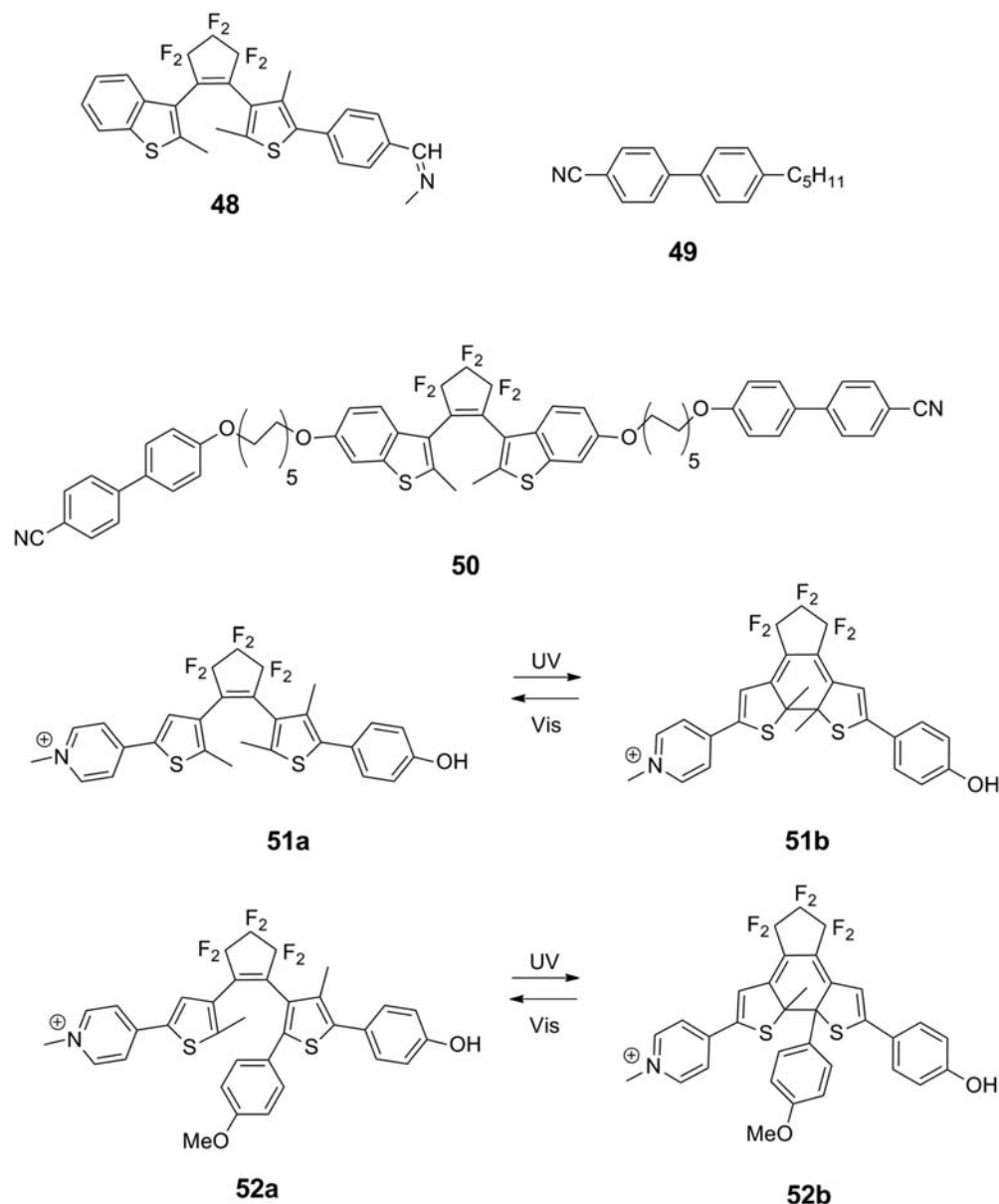
SCHEME 3.43   Some examples of photoswitchable diheteroarylethenes suitable to tune liquid crystal properties (**48-50**) and acid behaviour (**51-52**).

In presence of the closed-ring isomer after irradiation, smectic X phase appeared between 26.5°C and 54.6 °C and nematic phase between 54.6°C and 75.9 °C. Thus, the liquid crystalline properties can be modulated by photoirradiation.[129−133]

3.5.5 Switchable chemical properties and bioactivity

Extension of the π-conjugation can be used to change the acid behavior of diheteroarylethene derivatives.

In case of phenol-substituted diheteroarylethene **51** (Scheme 3.43), π-conjugation in the closed form **51b** allows the electron withdrawing action of the non-phenolic thiophenyl group, increasing the acidity of the open form **51a** (pK$_a$ equal to 10.5) to the closed form (pK$_a$ equal to 9.3).[134]

In the open-ring isomer **52a** (Scheme 3.43), the phenol unit interacts with the electron-donating methoxy group, but in the closed-ring isomer **52b** the phenol group interacts with the electron-withdrawing pyridinium
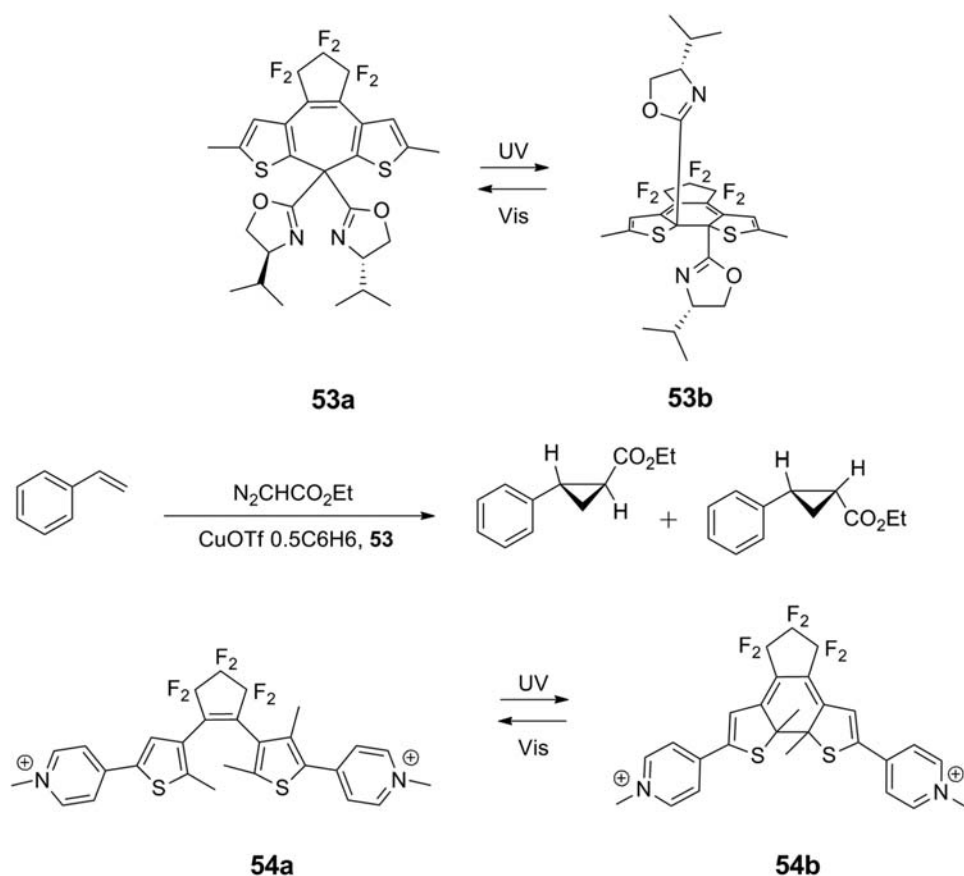
SCHEME 3.44 An example of catalytic switching (**53**) and switchable biological activity (**54**) provided by etheroarylethenes.

group. The pKa value decreased from 10.2 to 9.0 when the open-ring isomer undergoes photocyclization toward the closed-ring isomer.[135]

Catalytic activity can be switched by diheteroarylethenes, as well.

Control of coppercatalyzed cyclopropanation of olefins with diazoesters was reported.[136] When the copper complex comprises the open-ring isomer **53a** (Scheme 3.44), a significant enantioselectivity of the reaction is observed. At contrary, the presence of closed ring isomer **53b** in the complex did not lead to any enantioselectivity.

Photoswitching of bioactivity was reported in inducing paralysis of *Caenorhabditis elegans* (a nematode)[137]. *C. elegans* is ofted used in studies about neuroactivity due to its simple nervous system, consisting in 302 neurons.

When **54** (Scheme 3.44) is incorporated in *C. elegans*, paralysis is induced by cyclization by irradiation with UV light and canceled by cycloreversion reaction with visible light.

It is supposed that the best electron accepting ability of the closed form (lower LUMO, lower HOMO-LUMO gap) induces paralysis in *C. elegans* as a result of interruption of the metabolic electronic pathways.

3.5.6 Optical memories

P-type photochromic substances offer the possibility of storing binary type information if high thermal stability in the closed form is featured. This is obviously made possible by the open and closed forms that the molecule can assume, corresponding to 0 and 1 bits, capable of encoding any information. In a simple optical photochromic memory, radiation of different wavelengths is focused on a small portion of a layered material.

The active layer consists of a matrix in which the appropriate diheteroarylethene is introduced. In this way, this portion of the layer corresponds to bit 0 or 1 depending on whether the open or closed form has been induced by irradiation.

Compared to the optical memories currently used, which are based on heat induced by a laser beam and heat triggered changes in reflective properties of the medium, memories based on photochromic materials allow an increase of the amount of recordable data per surface unit.

Very noticeably, photochromic diheteroethens allowed going beyond the binary coding, accomplishing quaternary or octal coding for even higher data density capacities. Additionally, optical recording is potentially faster than thermal recording.

Diheteroarylethenes for optical memories should offer a high level of stability, called resistance to fatigue, the property to resist to degradation after many cycles of photocyclization and photoinduced ring opening. Furthermore, the photochemical processes should be fast, hence elevated quantum yields should be offered also in the more problematic (in this sense) closed form. Not surprisingly, the best current choice consists in dithienyl-perflurocyclopentene photochromic unit. This basic structural core will be the only encountered in the following of this paragraph, in which several examples of applications in optical memories will be presented.

Optically modifying the material (photon-mode) must be joined to a simple way to read the recorded information by a non destructive method. In other words, the reading process must use a property of the material other than the radiation used to induce photochromism.
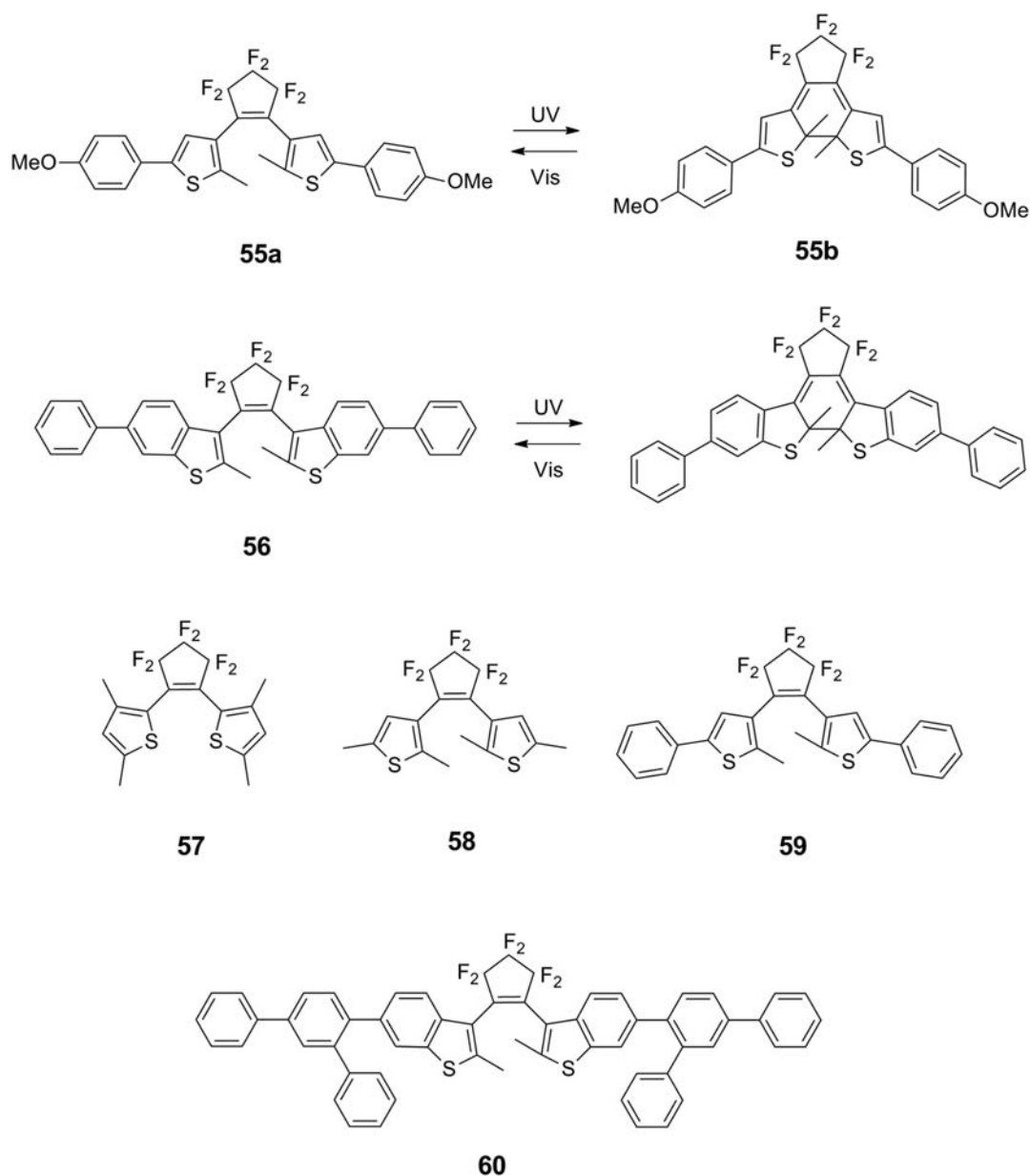
SCHEME 3.45   Some functionalised diheteroarylethenes for applications in optical memories.
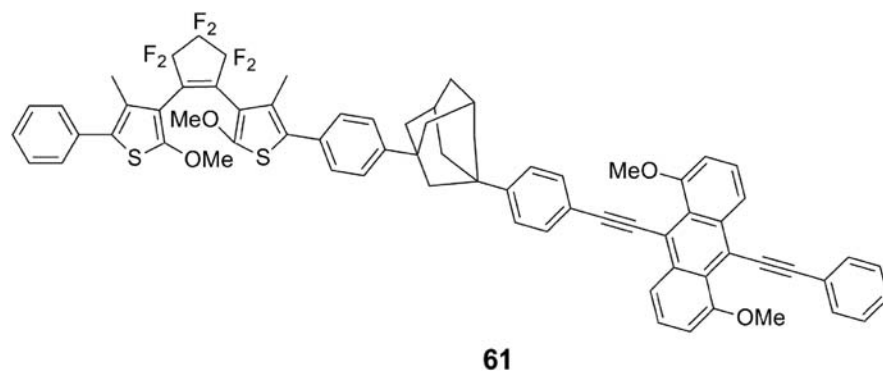
SCHEME 3.46 Compound **61** in this scheme represents an example of switchable fluorescence of the anthracene moiety induced by the dietheroarylethene core.

Fortunately, the passage from the open to the closed form is often associated with big changes in properties other than UV and visible electronic spectra.

The change in molecular structure between two constitutional isomers (as the open and closed forms) is obviously accompanied by changes in IR spectra. If IR absorption (or Raman scattering) changes are large at certain wavelengths, an easy read-out of the recorded data is feasible.

Compound **55** (Scheme 3.45) shows a strong IR absorption at 1465 cm^{-1} only in the closed form **55b**. It was reported that such a big change in IR absorption can be used for reading data.[138]

A similar change was observed in **56**. In this case, a big absorbivity change is found at 1590 cm^{-1} that can be potentially detected by IR imaging.[139]

Mixing three different diheroarylethenes in a matrix potentially allows an eight-states optical modification of the active layer. This was accomplished using compounds **57, 58** e **59**. After irradiation with UV light, the three compounds undergo photocyclization to the closed form. Using different visible wavelengths, photoreversion can be performed selectively for each component. As a consequence, a three-state system allows $2^3 = 8$ digits coding is possible in a single "optical" portion of the matrix.[140–142]

Using refractive index in place of IR absorption (IR imaging) is possible only measuring a large amount of photochromic material. This is caused by the small change in refractive index associated with the ring closure process of common photochromic substances.

Using compound **60** (Scheme 3.45) in a bulk amorphous layer allowed the detection of the closed of open forms on the basis of the refractive index of 817 nm radiation, which is not photoactive in photochromism.[143]

The possibility to undergo photocyclization through double-photon absorption opens the way to apply diheteroarylethenes in the so-called 3D optical memories. In them, the portion of the layer used for storing the information is not limited to the surface of the material but extends in the deep layers. In this way, higher data densities can be achieved.

For accomplishing double-photon absorption, a very strong laser beam should be focused in a small volume. Focusing the beat at different deep layers, photochemical changes can be induced in a 3D-matrix.

Several reports demonstrated that diheteroarylethenes are suitable to such a technique, after the first publication about it.[144]

A final impressive application in the field of optical data storage is the possibility to use a single diheteroarylethene molecule for storing a single bit. Compound **61** (Scheme 3.46) was used in this respect. In the open form, anthracene chromophore shows a very high level of fluorescence. In the close form, energy transfer from anthracene to the photochromic unit quenches emission.

On this basis, it was proved that fluorescence from a single molecule could be detected.[145,146]

Single molecule data storage can potentially lead to a huge increase of data density till the level of P bit/inch^2.

References

1. Turro, N. J.; Ramamurthy, V.; Scaiano, C. *Modern Molecular Photochemistry of Organic Molecules;* University Science Books: Sausalito, CA, 2010.
2. Saltiel, J.; Charlton, J. L.; De Mayo, P., Eds. *Rearrangements in Ground and Excited States*, Vol. 3; Academic Press: New York, 1980; p 25.
3. Saltiel, J.; D'Agostino, J.; Megarity, E. D.; Metts, L.; Neuberger, K. R.; Wrighton, M.; Zafiriou, O. C.; Chapman, O. L., Eds. *Organic Photochemistry*, Vol. 3; Marcel Dekker, Inc: New York, 1973; p 1.

4. Allen, M. T.; Whitten, D. G. *Chem.Rev.* **1989,** *89,* 1691.

5. Liu, R. S. H.; Horspool, W. M.; Song, P.-S., Eds. *CRC Handbook of Organic Photochemistry and Photobiology;* CRC Press: Boca Raton, FL, 1995; p 165.

6. Hammond, G. S.; Saltiel, J.; Lamola, A. A.; Turro, J. J.; Bradshaw, J. S.; Cowan, D. O.; Counsell, R. C.; Vogt, V.; Dalton, C. *J. Am. Chem. Soc.* **1964,** *86,* 3198.

7. Waldeck, D. H. *Chem.Rev.* **1991,** *91,* 415.

8. Saltiel, J.; Waller, A. S.; Sears, D. F., Jr. *J. Photochem. Photobiol., A: Chem* **1992,** *65,* 29.

9. Smakula, A. Z. *Physik. Chem* **1934,** *B25,* 90−98.

10. Buckles, R. E. *J. Am. Chem. Soc.* **1955,** *77,* 1040−1041.

11. Mallory, F. B.; Wood, C. S.; Gordon, J. T. *J. Am. Chem. Soc.* **1964,** *86,* 3094−3102.

12. Mallory, F. B.; Wood, C. S. *J. Org. Chem.* **1964,** *29,* 3374−3377.

13. Mallory, F. B.; Mallory, C. W. *Org. React.* **1984,** 30.

14. Liu, L.; Yang, B.; Katz, T. J.; Poindexter, M. K. *J. Org. Chem.* **1991,** *56,* 3769−3775.

15. Sudhakar, A.; Katz, T. J. *Tetrahedron Lett* **1986,** *27,* 2231−2234.

16. Sudhakar, A.; Katz, T. J.; Yang, B. *J. Am. Chem. Soc.* **1986,** *108,* 2790−2791.

17. Seylar, J.; Stasiouk, D.; Simone, D. L.; Varshney, V.; Heckler, J. E.; McKenzie, R. *RSC Adv.* **2021,** *11,* 6504−6508.

18. Lewis, F. D.; Wu, T.; Burch, E. L.; Bassani, D. M.; Yang, J.-S.; Schneider, S.; Jaeger, W.; Letsinger, R. L. *J. Am. Chem. Soc.* **1995,** *117,* 8785−8792.

19. Schraub, M.; Gray, H.; Hampp, N. *Macromolecules* **2011,** *44,* 8755−8762.

20. Meier, H. *Angew. Chem., Int. (Ed.) Engl.* **1992,** *31,* 1399−1420.

21. Jørgensen, K. B. *Molecules* **2010,** *15,* 4334−4358.

22. Finnie, A. A.; Hill, R. A. *J. Chem. Res., Synop.* **1987,** 78−79.

23. Mallory, F. B.; Rudolph, M. J.; Oh, S. M. *J. Org. Chem.* **1989,** *54,* 4619−4626.

24. Almeida, J. F.; Castedo, L.; Fernandez, D.; Neo, A. G.; Romero, V.; Tojo, G. *Org. Lett.* **2003,** *5,* 4939−4941.

25. Olsen, R. J.; Pruett, S. R. *J. Org. Chem.* **1985,** *50,* 5457−5460.

26. Verbitskiy, E. V.; Slepukhin, P. A.; Valova, M. S.; Cheprakova, E. M.; Schepochkin, A. V.; Rusinov, G. L.; Charushin, V. N. *Eur. J. Org. Chem.* **2014,** *79,* 8133−8141.

27. Rajeshkumar, V.; Stuparu, M. C. *Chem. Commun.* **2016,** *52,* 9957−9960.

28. Fukumoto, H.; Ando, M.; Shiota, T.; Izumiya, H.; Kubota, T. *Macromolecules* **2017,** *50,* 865−871.

29. Daigle, M.; Picard-Lafond, A.; Soligo, E.; Morin, J. F. *Angew. Chem.* **2016,** *55,* 2042−2047.

30. Li, Z.; Twieg, R. J. *Chem. Eur. J.* **2015,** *21,* 15534−15539.

31. Schnapperelle, I.; Bach, T. *Chem. Eur. J.* **2014,** *20,* 9725−9732.

32. Ciamician, G.; Silber, P. *Chem. Ber.* **1902,** *35,* 4128.

33. Störmer, R. *Ber. Dtsch. Chem. Ges.* **1909,** *42,* 4865.

34. Lewis, F. D.; Volman, D. H.; Hammond, G. S.; Gollnick, K. *Advances in Photochemistry*, Vol. 13. John Wiley & Sons, Inc: New York, 1986165.

35. Kaupp, G.; Horspool, W. M.; Song, P.-S. *CRC Handbook or Organic Photochemistry and Photobiology;* CRC Press: Boca Raton, FL, 199529.

36. Cowan, D. O.; Drisko, R. L. E. *J. Am. Chem. Soc.* **1980,** *102,* 4004.

37. Martinez-Haya, R.; Marzo, L.; König, B. *Chem. Commun.* **2018,** *54,* 11602−11605.

38. Lewis, F. D.; Barancyk, S. V. *J. Am. Chem. Soc.* **1989,** *111* (23), 8653−8661.

39. Pemberton, B. C. ;; Barooah, N.; Srivatsava, D. K.; Sivaguru, J. *Chem. Commun.* **2010,** *46* (2), 225−227.

40. Clements, A. R.; Pattabiraman, M. *J. Photochem. Photobiol., A* **2015,** *297* (15), 1−7.

41. Truong, V. X.; Li, F.; Ercole, F.; Forsythe, J. S. *ACS Macro Lett* **2018,** *7,* 464−469.

42. Marschner, D. E.; Frisch, H.; Offenloch, J. T.; Tuten, B. T.; Becer, C. R.; Walther, A.; Goldmann, A. S.; Tzvetkova, P.; Barner-Kowollik, C. *Macromolecules* **2018,** *51,* 3802.

43. Kalayci, K.; Frisch, H.; Truong, V. X.; Barner-Kowollik, C. *Nature Commun.* **2020,** *11,* 4193.

44. (a) Chauvin, J.; Kawai, T.; Irie, M. *Jpn. J. Appl. Phys.* **2001,** *Part 1, 40* (4A), 2518−2522.
   (b) Kawai, T.; Fukuda, N.; Groschl, D.; Kobatake, S.; Irie, M. *Jpn. J. Appl. Phys.* **1999,** *Part 2, 38* (10B), L1194−L1196.
   (c) Kim, E.; Choi, Y. K.; Lee, M. H. *Macromolecules* **1999,** *32* (15), 4855−4860.
   (d) Kim, M. S.; Maruyama, H.; Kawai, T.; Irie, M. *Chem. Mater.* **2003,** *15* (24), 4539−4543.
   (e) Bertarelli, C.; Bianco, A.; Castagna, R.; Pariani, G. *J. Photochem. Photobiol.* **2011,** *C, 12* (2), 106−125.

45. Fischer, E.; Hirshberg, Y. *J. Chem. Soc.* **1952,** 4522−4524.

46. Hirsberg, Y. *Compte Rendu.* **1950,** *7,* 116.

47. Stevenson, A.; Lindberg, C. A., Eds. *New Oxford American Dictionary;* 3rd edn Oxford University Press, 2010; p 2096.

48. Bouas-Laurent, H.; Durr, H. *Pure Appl. Chem.* **2001,** *73* (4), 639−665.

49. Higgins, S. *Chim. Oggi-Chem. Today* **2003,** *21* (1−2), 63−67.

50. <http://www.optiline.co.uk/index.php/information/common-knowledge/photochromic-sunglasses> <http://011101010.blogspot.fr> (**2015**).

51. (a) Wöhrle, D.; Tausch, M. W.; Stroher, W.-D. *Photochemie;* Wiley-VCH: Weinheim, 1998.
   (b) Dessauer, R.; Paris, J. P. *Adv. Photochem.* **1963,** *1,* 275−278.

52. Nakatani, K.; Piard, J.; Yu, P.; Métivier, R. In *Photochromic Materials: Preparation, Properties and Applications;* Tian, H., Zhang, J., Eds.; . 1st edn Wiley-VCH Verlag GmbH & Co. KGaA, 2016.

53. Fritzsche, J. Note sur les carbures d'hydrogène solides, tirés du goudron de houille. *C.R. Acad. Sci.* **1867,** *69,* 1035.

54. Harris, L.; Kaminsky, J.; Simard, R. G. *J. Am. Chem. Soc.* **1935,** *57,* 1151.

55. (a) Georghiu, C. V.; Arrventien, B. *Bull. Soc. Chim.* **1930,** *47,* 105.
   (b) Georghiu, C. V. *Bull. Soc. Chim.* **1934,** *1,* 97.
   (c) Georghiu, C. V.; Matei, V. *Bull. Soc. Chim* **1939,** *6,* 1324.

56. (a) Stobbe, H. *Verhandl*; Sachs Akademie: Leipzig, 1922161.
    (b) Stobbe, H. *Chem, Abstr.* **1923,** *17,* 3020.
    (c) Chakley, L. *Chem. Rev.* **1929,** *6,* 217.
    (d) Bhatanagar, S. S.; Kapur, P. L.; Hashmi, M. S. *J. Indian Chem. Soc.* **1938,** *15,* 573.
    (e) Overbeck, J. V. *Bot. Rev.* **1939,** *5,* 655.
    (f) Brown, G.H., Wright Air Development Center, **1959**;
    (g) Brown, G. H.; Shaw, W. G. *Rev. Pure Appl. Chem.* **1961,** *11,* 2.
57. (a) Douzou, P.; Wippler, C. *Science* **1961,** *28,* 70.
    (b) Schwab, H., Bertelson, R.C. Photochromism, state of the art review, Unconventional Photographic Systems Symposium, **1964**;
    (c) Luck, W.; Sand, H. *Angew. Chem.* **1964,** *3,* 570 Int. (Ed.).
    (d) Exelby, R.; Grinter, R. *Chem. Rev.* **1965,** *65,* 247.
    (e) Dorion, G.H., Weissbein, L. Discovery **1963**;
    (f) Inoue, E.; Kodado, H.; Shimizu, I.; Yoshida, K. *Photogr. Sci. Eng.* **1967,** *11,* 181.
    (g) Cohen, S. D.; Newman, G. H. *J. Photogr. Sci.* **1967,** *15,* 290.
58. (a) Chu, N. Y. C. *Can. J. Chem.* **1983,** *61* (2), 300−305.
    (b) Chu, N. Y. C. In Photochromism, *Molecules, and Systems*; Dürr, H., Bouas-Laurent, H., Eds.; Elsevier: Amsterdam, 1990; pp 493−509.
    (c) Maeda, S. In O*rganic Photochromic and Thermochromic Compounds*; Crano, J. C., Guglielmetti, R. J., Eds.; Kluwer Academic Publishers: New York, 2002; pp 85−109.
59. Hartley, G. S. *Nature* **1937,** *140* (3537). 281−281.
60. Rau, H. In *Photochemistry and Photophysics*; Rabek, J. F., Ed.; vol. 2; CRC Press: Boca Raton, FL, 1990.
61. Kawata, S.; Kawata, Y. *Chem. Rev.* **2000,** *100* (5), 1777−1788.
62. Irie, M. *Chem. Rev.* **2000,** *100* (5). 1683−1683.
63. Abe, J. In *New Frontiers in Photochromism*; Irie, M., Yokoyama, Y., Seki, T., Eds.; Springer: Tokyo, 2013; pp 161−181.
64. Hadjoudis, E.; Mavridis, I. M. *Chem. Soc. Rev.* **2004,** *33* (9), 579−588.
65. Irie, M.; Fukaminato, T.; Matsuda, K.; Kobatake, S. *Chem. Rev.* **2014,** *114,* 12174−12277.
66. Tian, Z.; Wu, W.; Li, A. D. *ChemPhysChem* **2009,** *10* (15), 2577−2591.
67. (a) Fukaminato, T. *J. Photochem. Photobiol., C* **2011,** *12* (3), 177−208.
    (b) Yun, C.; You, J.; Kim, J.; Huh, J.; Kim, E. *J. Photochem. Photobiol., C* **2009,** *10* (3), 111−129.
    (c) Cusido, J.; Deniz, E.; Raymo, F. M. *Eur. J. Org. Chem.* **2009,** *13,* 2031−2045.
    (d) Yildiz, I.; Deniz, E.; Raymo, F. M. *Chem. Soc. Rev.* **2009,** *38* (7), 1859−1867.
    (e) Raymo, F. M.; Tomasulo, M. *Chem. Soc. Rev.* **2005,** *34* (4), 327−336.
68. Delaire, J. A.; Nakatani, K. *Chem. Rev.* **2000,** *100* (5), 1817−1845.
69. (a) Patra, A.; Métivier, R.; Brisset, F.; Nakatani, K. *Chem. Commun.* **2012,** *48* (19), 2489−2491.
    (b) Takeshita, M.; Irie, M. *J. Org. Chem.* **1998,** *63* (19), 6643−6649.
    (c) Natali, M.; Giordani, S. *Chem. Soc. Rev.* **2012,** *41* (10), 4010−4029.
    (d) Yamamoto, S.; Matsuda, K.; Irie, M. *Angew. Chem. Int. (Ed.)* **2003,** *42* (14), 1636−1639.
    (e) Kodani, T.; Matsuda, K.; Yamada, T.; Kobatake, S.; Irie, M. *J. Am. Chem. Soc.* **2000,** *122* (40), 9631−9637.
    (f) Yamaguchi, T.; Uchida, K.; Irie, M. *J. Am. Chem. Soc.* **1997,** *119* (26), 6066−6071.
70. (a) Kobatake, S.; Takami, S.; Muto, H.; Ishikawa, T.; Irie, M. *Nature* **2007,** *446* (7137), 778−781.
    (b) Yu, Y. L.; Nakano, M.; Ikeda, T. *Nature* **2003,** *425* (6954). 145−145.
    (c) Kitagawa, D.; Nishi, H.; Kobatake, S. *Angew. Chem. Int. (Ed.)* **2013,** *52* (35), 9320−9322.
    (d) Koshima, H.; Ojima, N.; Uchimoto, H. *J. Am. Chem. Soc.* **2009,** *131* (20), 6890−6891.
71. Meng, X.; Zhu, W.; Zhang, Q.; Feng, Y.; Tan, W.; Tian, H. *J. Phys. Chem. B* **2008,** *112,* 15636.
72. Chen, S. J.; Yang, Y. H.; Wu, Y.; Tian, H.; Zhu, W. H. *J. Mater. Chem.* **2012,** *22,* 5486.
73. Zhu, W. H.; Meng, X. L.; Yang, Y. H.; Zhang, Q.; Xie, Y. S.; Tian, H. *Chem. - Eur. J* **2010,** *16,* 899.
74. Zhu, W.; Yang, Y.; Metivier, R.; Zhang, Q.; Guillot, R.; Xie, Y.; Tian, H.; Nakatanni, K. *Angew. Chem., Int. (Ed.)* **2011,** *50,* 10986.
75. Sumi, T.; Takagi, Y.; Yagi, A.; Morimoto, M.; Irie, M. *Chem. Commun.* **2014,** *50,* 3928.
76. Ern, J.; Bens, A. T.; Martin, H.-D.; Mukamel, S.; Schmid, D.; Tretiak, S.; Tsiper, E.; Kryschi, C. *Chem. Phys.* **1999,** *246,* 115.
77. Yamaguchi, T.; Irie, M. *J. Photochem. Photobiol., A* **2006,** *178,* 162.
78. Uchida, K.; Tsuchida, E.; Aoi, Y.; Nakamura, S.; Irie, M. *Chem. Lett.* **1999,** *28,* 63.
79. (a) Foster, J. A.; Steed, J. W. *Angew. Chem., Int. (Ed.)* **2010,** *49,* 6718.
    (b) Babu, S. S.; Praveen, V. K.; Ajayaghosh, A. *Chem. Rev.* **2014,** *114,* 1973.
    (c) Jones, C. D.; Steed, J. W. *Chem. Soc. Rev.* **2016,** *45,* 6546.
    (d) Segarra-Maset, M. D.; Nebot, V. J.; Miravet, J. F.; Escuder, B. *Chem. Soc. Rev.* **2013,** *42,* 7086.
80. Li, W.; Jiao, C.; Li, X.; Xie, Y.; Nakatani, K.; Tian, H.; Zhu, W. *Angew. Chem., Int. (Ed.)* **2014,** *53,* 4603.
81. Indelli, M. T.; Carli, S.; Ghirotti, M.; Chiorboli, C.; Ravaglia, M.; Garavelli, M.; Scandola, F. *J. Am. Chem. Soc.* **2008,** *130,* 7286.
82. (a) Yam, V. W. W.; Ko, C. C.; Zhu, N. *J. Am. Chem. Soc.* **2004,** *126,* 12734.
    (b) Lee, P. H. M.; Ko, C. C.; Zhu, N.; Yam, V. W. W. *J. Am. Chem. Soc.* **2007,** *129,* 6058.
83. Lee, P. H.-M.; Ko, C. C.; Zhu, N.; Yam, V. W. W. *J. Am. Chem. Soc.* **2007,** *129,* 6058.
84. Poon, C. T.; Lam, W. H.; Wong, H. L.; Yam, V. W. W. *J. Am. Chem. Soc.* **2010,** *132,* 13992.
85. Poon, C. T.; Lam, W. H.; Yam, V. W. W. *J. Am. Chem. Soc.* **2011,** *133,* 19622.
86. Chan, J. C. H.; Lam, W. H.; Yam, V. W. W. *J. Am. Chem. Soc.* **2014,** *136,* 16994.
87. (a) Chan, J. C. H.; Lam, W. H.; Wong, H. L.; Wong, W. T.; Yam, V. W. W. *Angew. Chem. Int. (Ed.)* **2013,** *52,* 11504.
    (b) Wu, N. M. W.; Wong, H. L.; Yam, V. W. W. *Chem. Sci.* **2017,** *8,* 1309.
    (c) Wu, N. M. W.; Ng, M.; Lam, W. H.; Wong, H. L.; Yam, V. W. W. *J. Am. Chem. Soc.* **2017,** *139,* 15142.

88. Neilson, B. M.; Bielawski, C. W. *J. Am. Chem. Soc.* **2012,** *134,* 12693.
89. (a) Asadirad, A. M.; Branda, N. R. *J. Am. Chem. Soc.* **2015,** *137,* 2824.
    (b) Asadirad, A. M.; Boutault, S.; Erno, Z.; Branda, N. R. *J. Am. Chem. Soc.* **2014,** *136,* 3024.
90. Yagi, K.; Irie, M. *Chem. Lett.* **2003,** *32,* 848.
91. Kitagawa, D.; Sasaki, K.; Kobatake, S. *Bull. Chem. Soc. Jpn.* **2011,** *84,* 141.
92. Taft, R. W., Jr. *J. Am. Chem. Soc.* **1952,** *74,* 3120.
93. Hancock, C. K.; Meyers, E. A.; Yager, B. J. *J. Am. Chem. Soc.* **1961,** *83,* 4211.
94. Gilat, S. L.; Kawai, S. H.; Lehn, J.-M. *Chem.-Eur. J.* **1995,** *1,* 275.
95. Chen, D.; Wang, Z.; Zhang, H. *J. Mol. Struct. (THEOCHEM)* **2008,** *859,* 11.
96. Morimitsu, K.; Kobatake, S.; Nakamura, S.; Irie, M. *Chem. Lett.* **2003,** *32,* 858.
97. Irie, M.; Lifka, T.; Kobatake, S.; Kato, N. *J. Am. Chem. Soc.* **2000,** *122,* 4871.
98. Kobatake, S.; Irie, M. *Chem. Lett.* **2003,** *32,* 1078.
99. Shibata, K.; Kobatake, S.; Irie, M. *Chem. Lett.* **2001,** *30,* 618.
100. Morimitsu, K.; Shibata, K.; Kobatake, S.; Irie, M. *J. Org. Chem.* **2002,** *67,* 4574.
101. Morimitsu, K.; Shibata, K.; Kobatake, S.; Irie, M. *Chem. Lett.* **2002,** *31,* 572.
102. Morimitsu, K.; Kobatake, S.; Irie, M. *Tetrahedron Lett* **2004,** *45,* 1155.
103. Guillaumont, D.; Kobayashi, T.; Kanda, K.; Miyasaka, H.; Uchida, K.; Kobatake, S.; Shibata, K.; Nakamura, S.; Irie, M. *J. Phys. Chem. A* **2002,** *106,* 7222.
104. Fukumoto, S.; Nakashima, T.; Kawai, T. *Angew. Chem., Int. (Ed.)* **2011,** *50,* 1565.
105. Kobatake, S.; Terakawa, Y.; Imagawa, H. *Tethahedron* **2009,** *65,* 6104−6108.
106. Irie, M.; Sayo, K. *J. Phys. Chem.* **1992,** *96,* 7671.
107. Ishibashi, Y.; Umesato, T.; Fujiwara, M.; Une, K.; Yoneda, Y.; Sotome, H.; Katayama, T.; Kobatake, S.; Asahi, T.; Irie, M., et al. *J. Phys. Chem. C* **2016,** *120,* 1170−1177.
108. Yamaguchi, T.; Uchida, K.; Irie, M. *J. Am. Chem. Soc.* **1997,** *119,* 6066.
109. Takeshita, M.; Jin-nouchi, H. *Chem. Commun.* **2010,** *46,* 3994.
110. Jin-nouchi, H.; Takeshita, M. *Chem.- Eur. J.* **2012,** *18,* 9638.
111. Shiozawa, T.; Hossain, M. K.; Ubukata, T.; Yokoyama, Y. *Chem.Commun.* **2010,** *46,* 4785.
112. Herder, M.; Schmidt, B.; Grubert, L.; Pätzel, M.; Schwarz, J.; Hecht, S. *J. Am. Chem. Soc.* **2015,** *137,* 2738−2747.
113. Fredrich, S.; Gostl, R.; Herder, M.; Grubert, L.; Hecht, S. *Angew. Chem., Int. (Ed.)* **2016,** *55,* 1208.
114. Kawai, T.; Sasaki, T.; Irie, M. *Chem. Commun.* **2001,** *8,* 711.
115. Osuka, A.; Fujikane, D.; Shinmori, H.; Kobatake, S.; Irie, M. *J. Org. Chem.* **2001,** *66,* 3913.
116. Xi, H.; Zhang, Z.; Zhang, W.; Li, M.; Lian, C.; Luo, Q.; Tian, H.; Zhu, W.-H. *J. Amer. Chem. Soc.* **2019,** *141,* 18467−18474.
117. Zacharias, P.; Gather, M. C.; Köhnen, A.; Rehmann, N.; Meerholz, K. *Angew. Chem., Int. (Ed.)* **2009,** *48,* 4038.
118. Tsujioka, T.; Masuda, K. *Appl. Phys. Lett.* **2003,** *83,* 4978.
119. He, Y.; Yamamoto, Y.; Jin, W.; Fukushima, T.; Saeki, A.; Seki, S.; Ishii, N.; Aida, T. *Adv. Mater.* **2010,** *22,* 829.
120. Dulić, D.; van der Molen, S. J.; Kudernac, T.; Jonkman, H. T.; de Jong, J. J. D.; Bowden, T. N.; van Esch, J.; Feringa, B. L.; van Wees, B. *J. Phys. Rev. Lett.* **2003,** *91,* 207402.
121. Whalley, A. C.; Steigerwald, M. L.; Guo, X.; Nuckolls, C. *J. Am. Chem. Soc.* **2007,** *129,* 12590.
122. Mulder, A.; Jukovic, A.; Lucas, L. N.; van Esch, J.; Feringa, B. L.; Huskens, J.; Reinhoudt, D. N. *Chem. Commun.* **2002,** 2734.
123. Mulder, A.; Juković, A.; Huskens, J.; Reinhoudt, D. N. *Org. Biomol. Chem.* **2004,** *2,* 1748.
124. Mulder, A. ;; Juković, A.; van Leeuwen, F. W. B.; Kooijman, H.; Spek, A. L.; Huskens, J.; Reinhoudt, D. N. *Chem-Eur. J.* **2004,** *10,* 1114.
125. Herder, M.; Pätzel, M.; Grubert, L.; Hecht, S. *Chem. Commun.* **2011,** *47,* 460.
126. Takeshita, M.; Hayashi, M.; Kadota, S.; Mohammed, K. H.; Yamato, T. *Chem. Commun.* **2005,** 761.
127. Yagai, S.; Ohta, K.; Gushiken, M.; Iwai, K.; Asano, A.; Seki, S.; Kikkawa, Y.; Morimoto, M.; Kitamura, A.; Karatsu, T. *Chem.-Eur. J.* **2012,** *18,* 2244.
128. Yamaguchi, T.; Inagawa, T.; Nakazumi, H.; Irie, S.; Irie, M. *Chem. Mater.* **2000,** *12,* 869.
129. Frigoli, M.; Mehl, G. H. *ChemPhysChem* **2003,** *4,* 101.
130. Frigoli, M.; Mehl, G. H. *Eur. J. Org. Chem.* **2004,** 636.
131. Frigoli, M.; Mehl, G. H. *Chem. Commun.* **2004,** 818.
132. Frigoli, M.; Mehl, G. H. *Chem.-Eur. J.* **2004,** *10,* 5243.
133. Frigoli, M.; Welch, C.; Mehl, G. H. *J. Am. Chem. Soc.* **2004,** *126,* 15382.
134. Kawai, S. H.; Gilat, S. L.; Lehn, J.-M. *Eur. J. Org. Chem.* **1999,** 2359.
135. Odo, Y.; Matsuda, K.; Irie, M. *Chem.-Eur. J.* **2006,** *12,* 4283.
136. Sud, D.; Norsten, T. B.; Branda, N. R. *Angew. Chem., Int. (Ed.)* **2005,** *44* 2019.
137. Al-Atar, U.; Fernandes, R.; Johnsen, B.; Baillie, D.; Branda, N. R. *J. Am. Chem. Soc.* **2009,** *131,* 15966.
138. Stellacci, F.; Bertarelli, C.; Toscano, F.; Gallazzi, M. C.; Zerbi, G. *Chem. Phys. Lett.* **1999,** *302,* 563.
139. Uchida, K.; Saito, M.; Murakami, A.; Nakamura, S.; Irie, M. *Adv. Mater.* **2003,** *15,* 121.
140. Uchida, K.; Saito, M.; Murakami, A.; Nakamura, S.; Irie, M. *ChemPhysChem* **2003,** *4,* 1124.
141. Uchida, K.; Saito, M.; Murakami, A.; Kobayashi, T.; Nakamura, S.; Irie, M. *Mol. Cryst. Liq. Cryst.* **2005,** *430,* 31.
142. Uchida, K.; Saito, M.; Murakami, A.; Kobayashi, T.; Nakamura, S.; Irie, M. *Chem.-Eur. J.* **2005,** *11,* 534.
143. Kim, M.-S.; Maruyama, H.; Kawai, T.; Irie, M. *Chem. Mater.* **2003,** *15,* 4539.
144. Toriumi, A.; Kawata, S. *Opt. Lett.* **1998,** *23,* 1924.
145. Irie, M.; Fukaminato, T.; Sasaki, T.; Tamai, N.; Kawai, T. *Nature* **2002,** *420,* 759.
146. Fukaminato, T.; Sasaki, T.; Kawai, T.; Tamai, N.; Irie, M. *J. Am. Chem. Soc.* **2004,** *126,* 14843.

This page intentionally left blank

4

Heterocyclic-based photoactive materials

4.1 Overview of photoactive materials

4.1.1 From natural to artificial photoactive systems

Photoactive compounds are materials that become active while interacting with light and modify their own properties and/or those of the interacting light electromagnetic field. The interaction between light and matter is the basis of life on Earth.[1] For example, photosynthesis is the fundamental process by which large amounts of sunlight's photons can be absorbed by plants' chlorophyll and, starting from atmospheric carbon dioxide and water, can be converted into carbohydrates and molecular oxygen available for life in our planet. For example, the information content of photons is at the base of vision-related processes in which retinal undergoes a *cis-trans* isomerization after absorbing light and triggers a cascade of physiological events that result in vision sensation.[2] Besides these natural processes occurring in nature, a variety of functions can also be obtained when light interacts with artificial photoactive systems[3,4] such as the photonic materials which employ the light to transfer information that were originally dedicated to the domain of electronics. During the late 1900s, the advent of laser technology changed the field of telecommunications because of glass fibers that transmit information using light rather than electrons such as in metal wires. In this context, several kind of effects of photoactivity have been investigated and the vast majority of them are related to: light emission (e.g., in LEDs and lasers), energy production by sunlight absorption and conversion (i.e., in photovoltaic devices of all generations), light signal

amplification (e.g., in photomultipliers), light detection and conversion into an electrical signal (i.e., in photo-diodes) and pollutants degradation by light absorption (e.g., in photocatalytic devices).

In this chapter, a particular attention has been given to the bottom-up synthesis of some heterocyclic photoactive organic systems deeply investigated in the last few decades, and most of the facilitate the development of efficient materials, which are part of the devices commonly used in our everyday life.

4.1.2 Explanation of photoactivity through the comprehension of the nature of light

The human research about the discovery of light's secrets has started from the 17th century when the sun spectrum has been extensively investigated by Isaac Newton. He was the first to demonstrate that white light is composed of the sum (in frequency) of all other colors by advancing the hypothesis that light is composed of particles.[5] This hypothesis gave life to the corpuscular theory of light, as opposed to the wave theory of light sponsored by Christiaan Huygens[6] and Thomas Young[7] corroborated later at the end of the 19th century by James Clerk Maxwell and Heinrich Hertz.[8] Maxwell, in the mid 1800s, postulated another paradigm by which was proposed that the light is composed of a force field of oscillating electric charges that have the characteristics of waves instead of particles.[9]

During the early 1800s, Joseph von Fraunhofer,[10] through the invention of the diffraction grating and the spectroscope, was the first to seriously investigate absorption lines in the spectrum of the sun. In this way, he transformed the spectroscopy into science, demonstrating how to exactly measure the wavelength of light.

In Newton's theory, the particles by which the light is composed were imagined to move at high speeds thorough empty space and transparent media. Through the help of a prism, Newton was able to demonstrate the decomposition of a white light beam into its particles possessing all the visible colors of the rainbow. Newton's thesis found confirmation, about two centuries later, with the introduction of the quantum of action by Max Planck (1900)[11] and with the article by Albert Einstein (1905)[12] on the interpretation of the photoelectric effect starting from the quantum of electromagnetic radiation, later called photon; these two interpretations will coexist in quantum mechanics, as predicted by the wave-particle dualism. For certain types of experiments the measurements of a property that describe light as a photon (i.e., absorption and emission) cause a lack of knowledge of all light's wave properties; while the measurement of a property related to the light considered as a wave (i.e., interferences) cause a lack of knowledge of all light's particle properties.

4.1.3 Explanation of molecular photoactivity through light—matter interaction models

As photoactivity is concerned with the absorption and emission of light by electrons of molecules, the most useful paradigm of light is represented by the photon model (already described in the 4.1.2. Section). Although, the initial interaction of light with the electrons of a molecule is better described by considering the light as an electromagnetic field that oscillates like a wave and interact with electrons that can be driven into oscillation by the absorption of light, as will be described in more details at the end of this section.

The possible pathways resulting from the interaction of light with photoactive organic molecules can be divided into: (1) photophysics allowing processes resulting in physical changes; (2) photochemistry allowing processes resulting in chemical changes.

As shown in Scheme 4.1, the photochemical process allows to produce the product P after the photon ($h\nu$) absorption of light whose frequency (ν) is the correct one to give the absorption by the reactant (R) and resulting in the electronic excited species (R*). Subsequently, R* can transform into the reactive intermediate molecule (I) which can be considered the precursor for the final product (P). On the contrary, after the photon light absorption by R and the formation of the electronically excited species R*, the photophysic can involve processes in which R* undergoes no chemical changes but (fast or slowly) will transform back into R. The transitions from R*
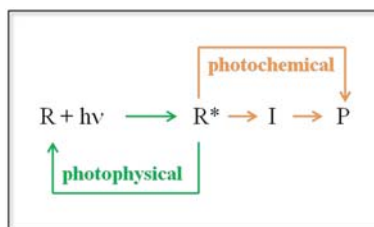
SCHEME 4.1   Overall photochemical and photophysical pathways after photon (hv) absorption by an organic photoactive molecule (R).

back to R can be mainly due to the: (a) emission of a photon ($-h\nu$); (b) radiationless transition to produce R and heat and both of them can involve excited singlet (S_n) or triplet (T_n) molecular states.

The Kasha's rule[13] states that within the photoreactions and photoemissions processes, the highest S_n and T_n electronic states are not involved because of their fast radiationless conversions (i.e., $S_n \rightarrow S_1$ and $T_n \rightarrow T_1$), so far the most useful candidates for the absorption and emission phenomena are the lowest excited singlet (S_1) and triplet (T_1) states. It follows that the spectroscopy of S_1 and T_1 states is of great interest since these two states are the starting points for photophysical and photochemical processes in organic photoactive compounds. Some selection rules anyway explain that among them only some transitions can be spin allowed (i.e., absorption $S_0 \rightarrow S_1$ and emission $S_1 \rightarrow S_0$) and some will be forbidden (i.e., absorption $S_0 \rightarrow T_1$ and emission $T_1 \rightarrow S_0$).

In this context, the electronic absorption and emission spectra provide important information about structure, energy levels, dynamics, lifetime, electron configuration, and quantum yields of electronically excited (R*) states populated after the absorption of light ($h\nu$) occurring from a photoactive organic molecule (R).

But how and why the light of certain wavelengths (frequencies) can be selectively absorbed by an organic photoactive molecule?

First of all, it is important to define that the relationship between the energy (E) of light absorbed and its frequency (ν) is the following:

$$E = h\nu \tag{4.1}$$

where h ($6.6260696 \times 10^{-34}$ J s) is the Planck's constant. From the Eq. (4.1) it follows that the higher the frequency, the higher the energy associated to the light. Furthermore, the relationship between the frequency (ν) and the wavelength (λ) is:

$$\lambda = c/\nu \tag{4.2}$$

where c is the speed of light. From the Eq. (4.2) it is clear that the higher the frequency is, the lower the wavelength is. Definitely, the larger the energy jump among the two electronic levels involved, the lower will be the wavelength of the light absorbed. To give a practical example, the functioning principle of a photovoltaic device is based on the generation of electrical current as a consequence of sunlight absorption by photoactive molecules due to the jump of electrons from the valence band (or Highest Occupied Molecular Orbital − HOMO) to the conduction band (or Lowest Unoccupied Molecular Orbital − LUMO) when the photoactive material is irradiated with light having energy equal or higher with respect to the HOMO-LUMO gap of the material (see the Fig. 4.1A).

Usually, the UV-vis absorption spectrometers work in a range from about 200 nm (near ultra-violet) to about 800 nm (near infra-red). Therefore, among all the plethora of the possible electron jumps (gray dashed arrows in Fig. 4.1B), only a limited number of them absorb light in the UV-vis region (black arrows in Fig. 4.1B) in a photoactive organic molecule. Instead, photons corresponding to wavelengths in the higher range of 800−10,000 nm
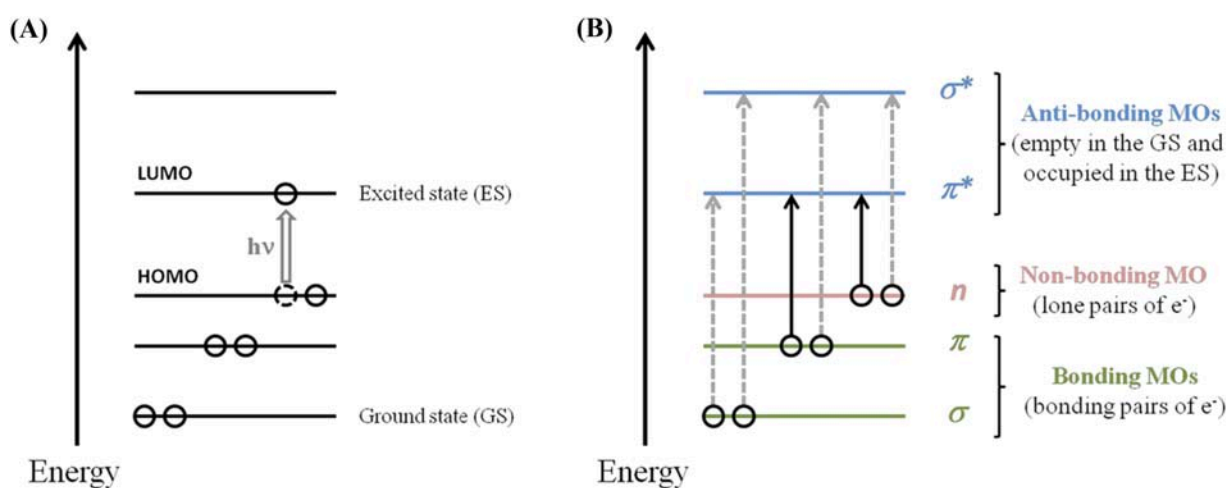

FIGURE 4.1 Diagrams showing (A) the HOMO (Highest Occupied Molecular Orbital) and the LUMO (Lowest Unoccupied Molecular Orbital) before and after the light ($h\nu$) absorption and in (B) a more detailed scheme about all the MO types: bonding σ and π MOs (in green), nonbonding n MOs (in pink) and anti-bonding σ^* and π^* MOs (in light blue). Among all the possible electron jumps (gray dashed arrows) only few of them can absorb light in the UV-vis range (black arrows).

(from near infrared to infrared) are able to excite fundamental molecular vibrations and are generally too small to excite electrons from HOMO to LUMO levels of organic photoactive molecules. The functional groups responsible for the light absorption are called chromophores, while the light emission units (by fluorescence and/or phosphorescence) are called lumophores within a photoactive molecule.

Although the classical wave theory provided by Maxwell's model of light is inadequate to explain the absorption and emission phenomena due to light−molecule interaction, it results to be useful in describing the interaction between the electromagnetic wave of light and the electrons in molecules.[14] The light−molecule interaction can be modeled as an interaction between two oscillating electromagnetic dipoles which, if a common frequency (ν) can be found, behave as a reciprocally interacting and oscillating donor and acceptor system. Indeed, a molecular system is made up of positive (nuclei) and negative (electrons) electric charges. These charges are not static, but can move relative to each other: for this reason, a molecule can be considered as an oscillating electric dipole. Moreover, also the electromagnetic field of light consists of an oscillating electric field. If the frequency of this electric field is equal to one of the frequencies with which the molecular electric dipole can oscillate, the energy carried by the radiation can be transmitted to the molecule to excite that particular oscillation of its own electric dipole.

The excitation is the process in which the electrons of the molecule R can absorb a photon and give rise to an electronically excited molecule R* by absorbing a precise resonance frequency (ν), corresponding to the transition $\Delta E = E_2\text{-}E_1 = h\nu$ of the electron from one molecular state (E_1) to another (E_2). In parallel, the emission is the reverse process in which an excited oscillating electron interacts by dipole-dipole coupling with the electromagnetic field which becomes excited by the photon emitted by the molecule R*.

The absorption and emission of energy are from the following: (i) the electric portion of the electromagnetic field by electrons are described by the electronic molecular spectroscopy; (ii) the electric portion of electromagnetic radiation by vibrating nuclei are at the base of vibrational molecular spectroscopy, and (iii) the magnetic portion of the electromagnetic field by the electrons concerning the field of magnetic resonance spectroscopy.

4.1.4 The molecular skeleton of photoactive molecules define the behavior of light absorption and emission in molecules

When light composed of many frequencies ($\nu_1,\nu_2,\nu_3\cdots\nu_n$) strikes a molecule, the molecular system will selectively absorb, reflect or transmit only certain frequencies of light. The way by which the light interacts with a molecule is jointly dependent on the frequency of the light and the nature of the chromophores inside the molecule.[15]

The alkane compounds, being saturated organic molecules, are transparent to light in the region 200−800 nm and its HOMO-LUMO electron jump is associated to a transition at wavelengths lower than 200 nm occurring among molecular orbitals (MOs) of σ→σ* type. While, unsaturated organic compounds (e.g., aromatic hydrocarbons, olefins, conjugated polyenes, etc.) show several absorption peaks in the range 250−700 nm corresponding to HOMO-LUMO π→π* transitions (for those compounds with π* electrons) as well to transitions n→π* (for those heterocyclic compounds with lone pairs electrons allocated in the n-type MOs).

Anyway, the most important finger print describing the behavior of the photoactive molecules are defined by their maximum of the longest wavelength (lowest energy) absorption band (λ_{max}) corresponding to the electronic HOMO-LUMO transition and the associated extinction coefficient at the same wavelength (ε_{max}) that represents its absorption strength. In the Table 4.1 it is shown a collection of the main classes of organic photoactive compounds with their typical λ_{max} and ε_{max} values associated to the HOMO-LUMO jump and the type of MOs involved in the transition.

The experimental measurement about the electronic absorption spectrum is ruled by the Lambert-Beer's law[16,17] which states that the quantity of the absorbed light (absorbance, A) from a molecule is proportional to the optical path length (l) of the incident light through the sample and the concentration of the absorbing species [R]; but it is completely independent by the initial intensity of the incident light (I_0) as follows:

$$A = \varepsilon l[R] \tag{4.3}$$

where ε is the molar extinction coefficient. An absorption spectrum is a graph of the absorption intensity (or absorbance − A) vs the wavelength (λ) of the absorbed light. The experimentally measured absorption intensity is rather called optical density (OD) and is defined as follows:

$$OD = log\left(I_0/I_t\right) \tag{4.4}$$

where I_0 is the intensity of the incident light interacting with the sample and I_t is the intensity of the transmitted light through a 1 cm path length of sample. In absorption plots, the molar extinction coefficient (ε) given by the following formula is usually employed:

TABLE 4.1 Typical HOMO-LUMO transitions of some organic chromophores with their associated λ_{max}, ε_{max}, and transition type.

Organic chromophore	HOMO-LUMO λ_{max}[nm]	ε_{max} [cm^{-1} M^{-1}]	MOs involved
Alkane (C—C)	<200	1000	$\sigma \to \sigma^*$
Alkane (C—H)	<200	1000	$\sigma \to \sigma^*$
Olefins (C=C)	180	10000	$\pi \to \pi^*$
Conjugated polyenes (C=C—C=C)	220	20000	$\pi \to \pi^*$
Benzene	260	200	$\pi \to \pi^*$
Condensed benezene rings (Napththalene)	310	200	$\pi \to \pi^*$
Condensed benezene rings (Anthracene)	380	10000	$\pi \to \pi^*$
Ketones (C=O)	280	20	$n \to \pi^*$
Diazo (N=N)	350	100	$n \to \pi^*$
Nitroso (N=O)	660	200	$n \to \pi^*$
Conjugated enones (C=C—C=O)	350	30	$n \to \pi^*$
	220	20000	$\pi \to \pi^*$
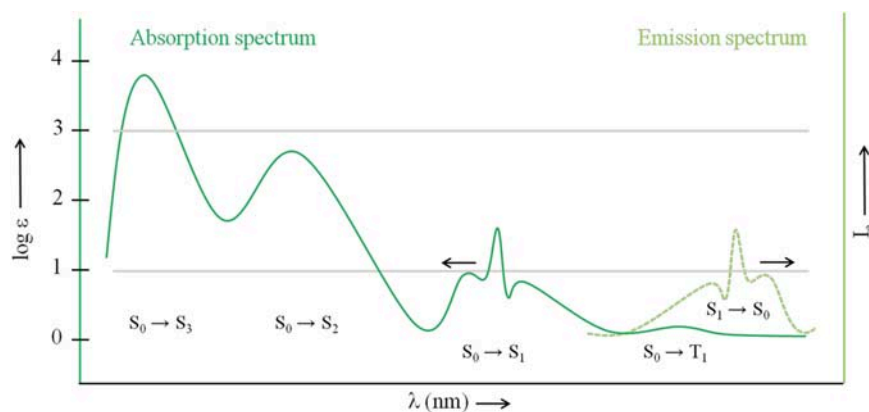
FIGURE 4.2 Schematic of the absorption (green line) and emission (light green dotted line) spectra of a simple photoactive molecule. The ordinate axis for the absorption spectrum is reported as log ε (left side), while the ordinate axis for the emission spectrum is reported as I_e. The abscissa axis is reported as wavelength (nm).

$$\varepsilon = \left[log\left(I_0/I_t\right) \right] l[R] \qquad (4.5)$$

Because of the wide variation of the ε values, absorption spectra are usually plotted as log ε (see the ordinate left axis in the plot of Fig. 4.2).

At a fixed excitation wavelength (λ_{exc}) and constant exciting intensity (I_0), an emission spectrum plots the emission intensity (I_e) as a function of the emitted wavelength. For weakly absorbing solutions (OD < 0.1) of a luminescent molecule R, the emission intensity is given by the following formula:

$$I_e = 2.3 I_0 \varepsilon_R l \phi_R [R] \qquad (4.6)$$

where ε_R is the extinction coefficient characteristic of the absorbing molecule; l is the optical path length; ϕ_R is the quantum yield of emission and [R] is the concentration of the emitting molecule R. Since from the Kasha's rule, ϕ_R is independent by the exciting wavelength (λ_{exc}) it follows that at fixed [R], I_0 and l, the intensity I_e is directly proportional to the extinction coefficient ε_R. Moreover, a plot of I_e vs λ has the same spectral shape and appearance as the absorption spectrum log ε vs λ (see the comparison among the absorption spectrum — green curve — and the emission — light green curve — spectra sketched in Fig. 4.2).[18]

Usually, the transition $S_0 \to S_1$ is relatively weak compared with the $S_0 \to S_2$ and the $S_0 \to S_3$ transitions located progressively at lower wavelengths. On the contrary, the transition $S_0 \to T_1$ appears usually at the highest wavelength in the absorption spectrum but is always too weak to be measured experimentally. Looking at the

emission spectrum (i.e., the shown transition $S_1 \rightarrow S_0$), it can be noticed that it resembles the shape of the related absorption $S_0 \rightarrow S_1$ band but it is a mirror image of it.

4.2 Main classes of heterocyclic photoactive compounds: synthesis and photochemical reactions

A heterocyclic compound is defined as any organic compound in which the molecules are characterized by rings containing at least one atom other than carbon. These compounds are structurally similar to cyclic organic hydrocarbons, but their properties can vary widely from those of their hydrocarbon counterparts and are largely governed by the identity, location, and number of heteroatoms present in the molecule.[19−21]

4.2.1 Three-membered heterocycles

4.2.1.1 Three-membered compounds with one heteroatom

4.2.1.1.1 Aziridines

Synthesis of aziridines

Thermal or photochemical reaction of azides with alkenes[22] Phenyl azides react thorough 1,3-dipolar cycloadditions with alkenes to give 4,5-dihydro-1,2,3-triazoles. These intermediate is finally converted into aziridine after nitrogen loss (Fig. 4.3):

Instead, the thermolysis of ethyl azidoformate produces ethylcarbonyl nitrene by a [2 + 1] cycloaddition reaction. This intermediate can react with alkenes to form aziridines (see Fig. 4.4):

Intramolecular cyclization of ß-amino alcohols Aziridines can be synthesized basically by the cyclization of ß-amino alcohols through three main strategies (see Fig. 4.5): **(A)** Gabriel method: reaction with thionyl chloride to give chloroamines intermediates which can be in turn cyclized to aziridines by alkali hydroxide and the leaving Cl group is substituted intramolecularly by the amino group on the $\beta-$C-atom[23]; **(B)** Wenker method: reaction with sulfuric acid giving amino sulfate esters as intermediates that produce aziridines when treated with alkali and the leaving OSO_3^- group is substituted by the amino group on the β-C-atom[24]; **(C)** direct cyclodehydration by using the Mitsunobu reagent: triphenylphosphine (Ph_3P) and azodicarboxylate such as diethyl azodicarboxylate (DEAD) or diisopropyl azodicarboxylate (DIAD)[25]:
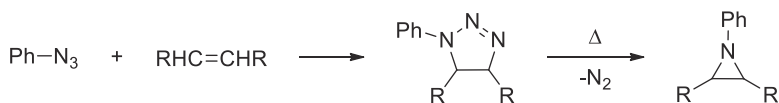
FIGURE 4.3   1,3-Dipolar cycloaddition of phenyl azides with alkenes.
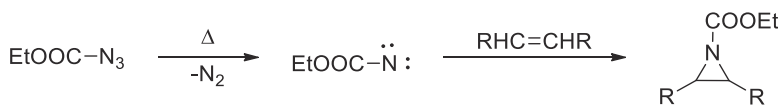
FIGURE 4.4   Thermolysis of ethyl azidoformate.
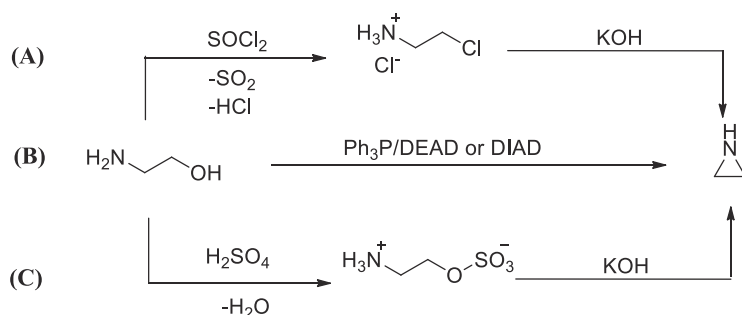
FIGURE 4.5   (A) Gabriel synthesis; (B) Wenker synthesis; (C) direct cyclodehydration.

Addition to imines (Johnson-Corey-Chaykovsky aziridation) The reaction of sulfur ylides with imines leads to the corresponding aziridines.[26] The ylides are generated in situ by the deprotonation of sulfonium halides with strong bases (Fig. 4.6).

From oxiranes Both direct conversion of chiral oxiranes[27] or oxiranes treated with substituted iminophosphorane[28] can be used as precursors for aziridines (Fig. 4.7):

Reactivity of aziridines

Photochemical reactions of aziridines Irradiation of 1,2,3-triarylaziridine in alcohol provides benzylideneaniline and alkylbenzyl ether as a final product because of trapping of phenylcarbene intermediate (see Fig. 4.8):

4.2.1.1.2 Azirines

Azirines are fowl-smelling liquids or low melting solids and irritant to the skin. 2H-Azirine is thermally unstable and has to be stored at very low temperatures. On the contrary, substituted 2H-azirines are more stable.

Synthesis of azirines The first synthesis of 2H-azirine was reported by Neber et al. in 1932,[29,30] through transformation of oxime p-toluenesulfonate to vinylnitrene in the presence of a base as a catalyst (Fig. 4.9).

FIGURE 4.6   Johnson-Corey-Chaykovsky aziridation.

FIGURE 4.7   Direct conversion of: (A) chiral oxiranes and (B) oxiranes.
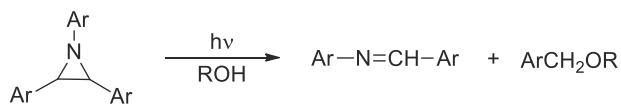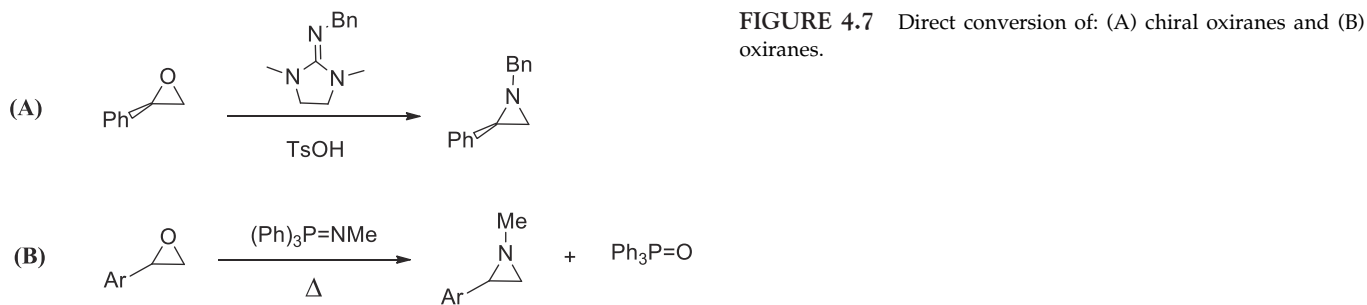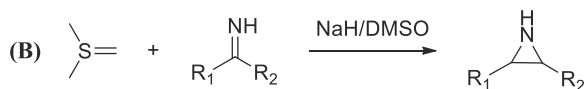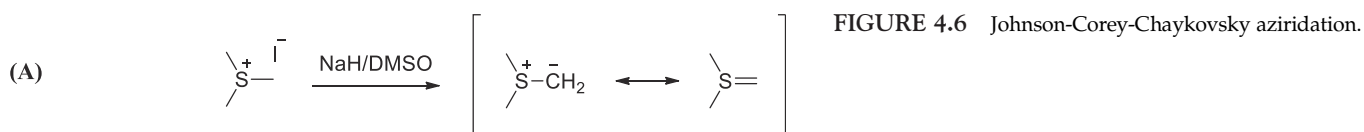
FIGURE 4.8   Photochemical reactions of aziridines.
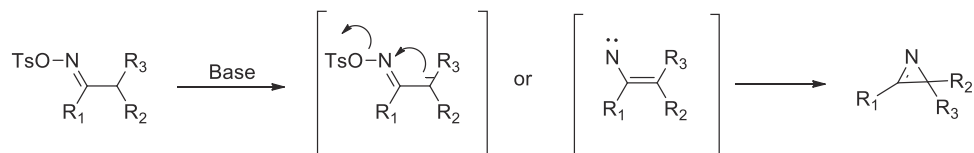
FIGURE 4.9   Neber synthesis of azirines.
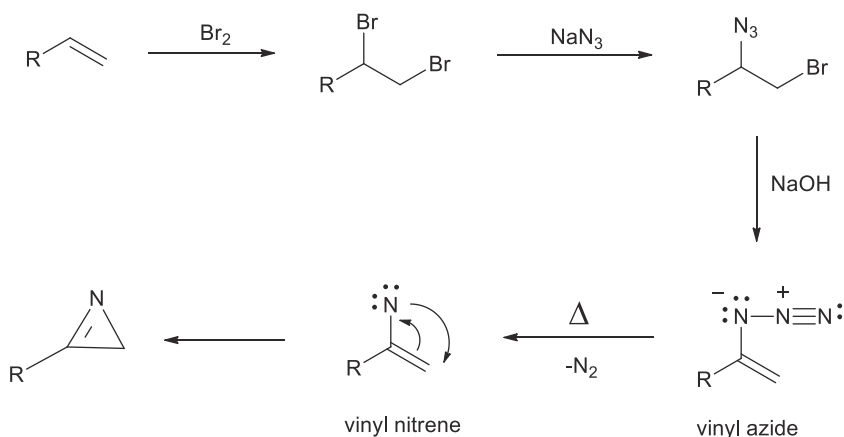
FIGURE 4.10   Thermolysis of vinyl azides.

vinyl nitrene   vinyl azide
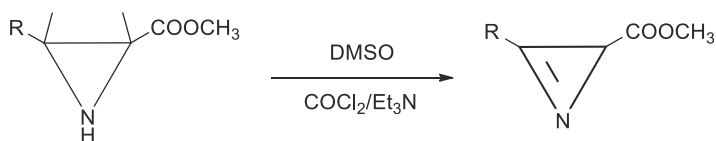
FIGURE 4.11   Elimination and oxidation reactions of aziridines.

Thermolysis of vinyl azides[31,32]   Vynyl azide are obtainable from alkenes in a three step pathway. Then a thermolysis provides the dediazoniation of the vinyl azide giving the vinyl nitrene. Finally, the cyclization of the vinyl nitrene gives the corresponding 2H-azirine (Fig. 4.10):

Elimination and oxidation reactions of aziridines   N- Sulfonyl, N-sulfinyl, and N-chloroaziridines undergo elimination when treated with base, providing 2H-azirines (Swern oxidation)[33] as reported in Fig. 4.11:

4.2.1.1.3 Oxirane

Oxirane $(CH_2)_2O$ is a colorless, water-soluble, extremely poisonous gas of bp 10.5°C. Instead, methyloxirane is a colorless, water-miscible liquid (bp 35°C). The viscosity of ethylene oxide at 0°C is 5.5 times less than water. It is readily soluble in water, ether, alcohol, and other organic solvents.

Oxiranes are of considerable importance as intermediates for multistep stereospecific syntheses of complex target molecules, because closing and opening reactions of the oxirane ring often occur without side reactions. Moreover, they proceed stereospecifically.

Because its high ring strain, oxiranes easily participate in a number of addition reactions that result in ring-opening. Moreover, another crucial property of oxiranes is their Brønsted-Lewis basicity due to two nonbonding electron pairs located on the O atom that makes oxiranes highly reactive with acids.

Reactivity of oxiranes   The photochemistry of 1,2-diaryl oxiranes proceeds through C−C bond cleavage to form carbonyl ylides (see Fig. 4.12(A)). On the contrary, the photochemistry of monoaryl oxiranes proceeds via cleavage of the benzyl C-O bond to generate 1,3-diradicals (see Fig. 4.12(B)).[34]

Intermediates such as ylides usually react by cycloaddition[35] or by fragmentation into the corresponding carbonyl compound and an aryl carbene.[36]

Intermediates such as 1,3-diradicals react preferentially through a 1,2-hydrogen shift to form carbonyl compounds.

4.2.1.1.4 Thiirane

With respect to oxirane, as a result of the greater atomic radius of the S atom compared to O atom, the thiirane form an acute-angled triangle. Thiirane is thermally less stable than oxirane and its properties are primarily due to ring strain. So far, even at room temperature, ring opening reactions can occur causing polymerization and formation of linear macromolecules. Substituted thiiranes are thermally more stable.

Synthesis of thiiranes
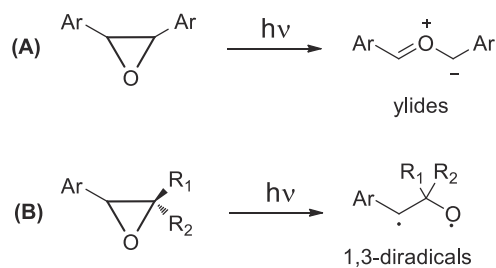
FIGURE 4.12   (A) C−C bond cleavage of 1,2-diaryl oxiranes; (B) photochemical cleavage of benzyl C-O bonds.
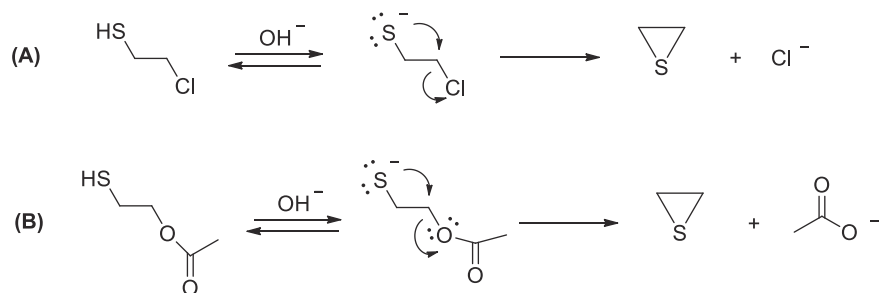
FIGURE 4.13   Cyclization of (A) β-Halo thiols and (B) β-acetoxy thiols.
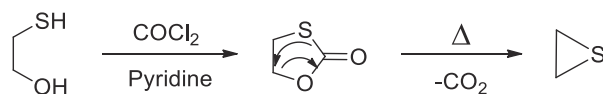
FIGURE 4.14   Cyclization of 2-mercaptoethanol.
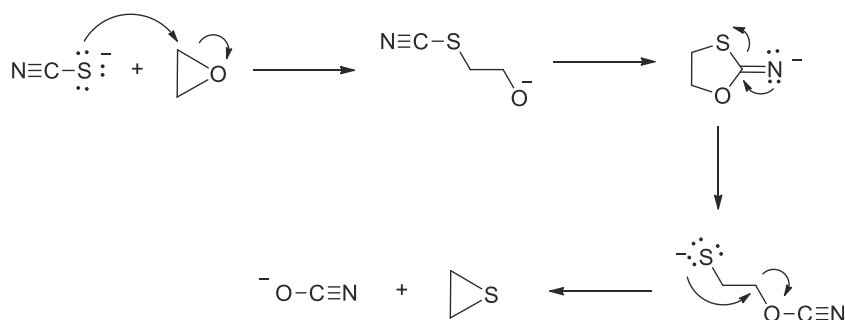
FIGURE 4.15   Ring transformation of oxiranes with thiocianate anion.
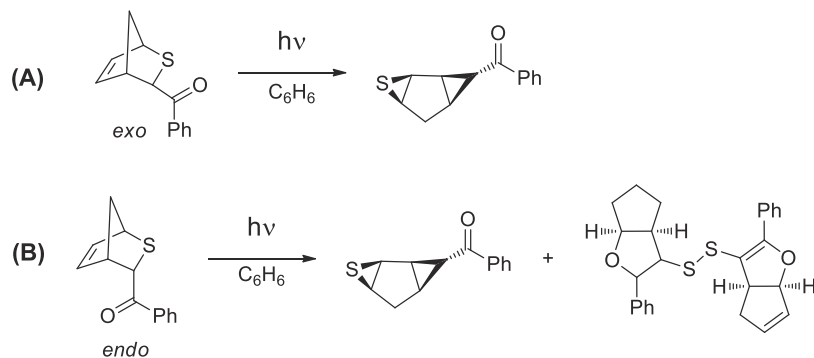
FIGURE 4.16   Ring transformation of (A) *exo* and (B) *endo* thianorbornenes.

Photochemistry of Heterocycles

Cyclization of β-substituted thiols β-Halo thiols (Fig. 4.13(A)) and β-acetoxy thiols (Fig. 4.13(B)) react with bases to give thiiranes in analogy with oxirane.

Furthermore, 2-mercaptoethanol reacts with phosgene (COCl$_2$) in the presence of pyridine to give l,3-oxathiolan-2-one, which on heating to 200°C decarboxylates to give thiirane as final product (see Fig. 4.14).

Ring transformation of oxiranes Oxiranes react with the thiocianate anion as source of sulfur to give thiiranes,[37] according to the following four steps mechanism sketched in Fig. 4.15:

Among the synthetic strategies of thiirane molecules, one of them involves *exo* and *endo* thianorbornenes[38] reported as starting molecular reactions of Fig. 4.16(A) and (B), respectively:

Since the sulfide bridgehead hydrogen is not accessible and the double bond is not neither accessible for the *exo*-benzoyl group, only one photoreactivity mode is available to the *exo*-thianorbornenes (i.e., the C−S bond fragmentation). The excited carbonyl group in the *endo*-isomers can also expel the sulfanyl radical to attack the double bond as in the Paternò-Büchi cycloaddition.

In detail, upon UV irradiation in benzene, the *exo*-photoprecursor yields nearly quantitatively the tricyclic thiirane. On the contrary, the *endo*-precursor exhibits dual photoreactivity, furnishing both thiirane and disulfide (see Fig. 4.16(B)).

From a mechanistic point of view, the formation of thiirane involves photoinduced benzyl-C-S homolytic bond fragmentation followed by radical addition to the *endo*-cyclic double bond (see Fig. 4.17), which probably occurs
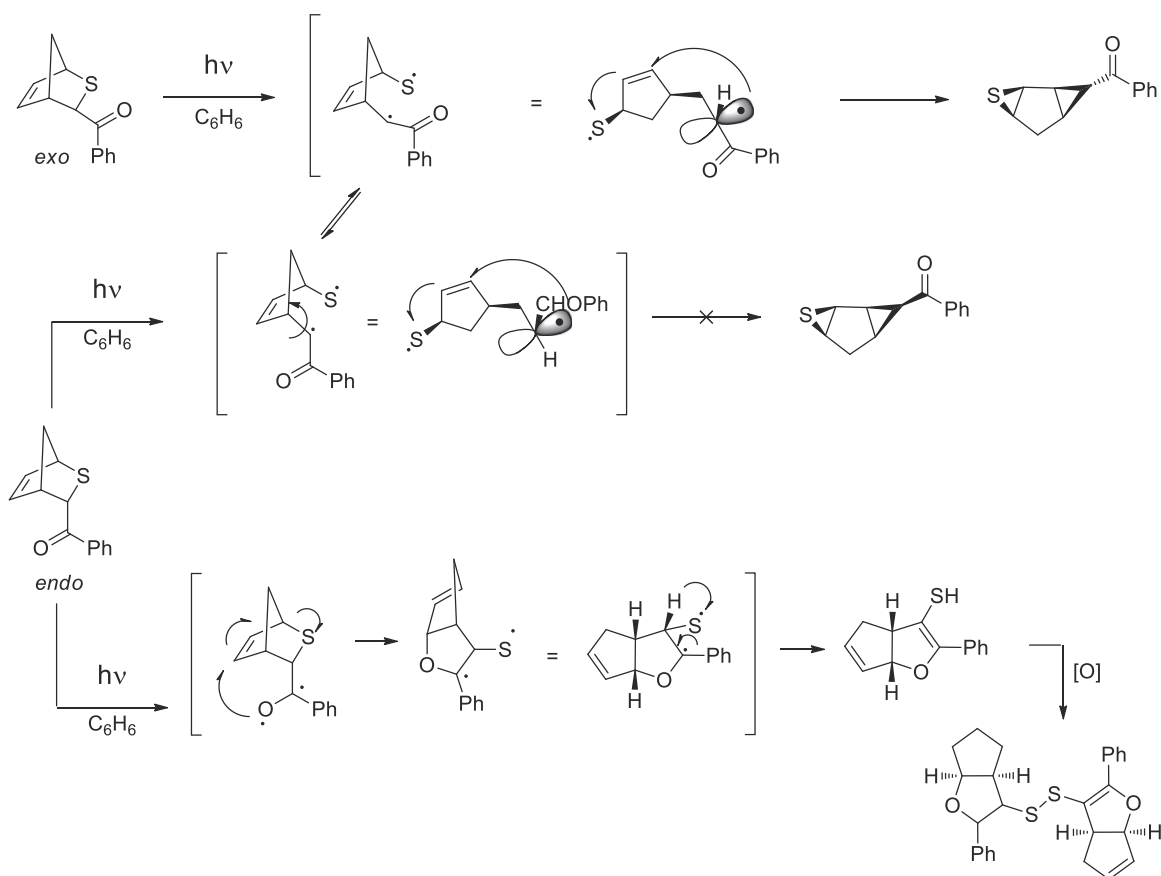
FIGURE 4.17   Photoreactivity mechanisms of *exo* and *endo*-photoprecursors.
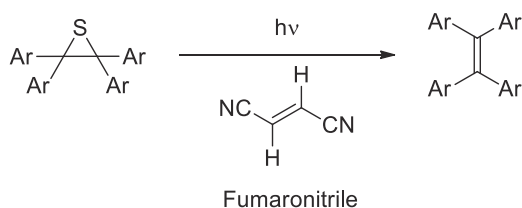
FIGURE 4.18   Desulfurization reaction of tetraarylthiirane.

stepwise or, at least, asynchronously. Before the phenacyl radical reacts it apparently has time to rotate, so both the *endo* and the *exo* isomers produce the same *exo*-benzylthiirane.

The oxapentalene channel starting from *endo*-isomer involves an interrupted Paternò-Büchi reaction, where the expulsion of the sulfanyl radical from the initially generated 1,4-diradical occurs faster than radical recombination forming the oxetane ring. Subsequent hydrogen migration, which amounts to disproportionation in the 1,3-diradical yields the thiol and the disulfide. The disulfide is formed in the presence of air, which is common for photochemical reactions of thiols.

Another typical reactivity of functionalized thiiranes is represented by the desulfurization reaction of tetraarylthiirane by UV irradiation in the presence of fumaronitrile that affords the corresponding alkenes (Fig. 4.18):

4.2.1.2 Three-membered compounds with two heteroatoms

4.2.1.2.1 Diaziridine

Diaziridines are crystalline and weakly basic compounds. Diaziridine are stable compounds and thus less prone to N−N cleavage. Furthermore, since the N atoms are configurationally stable stereoisomerism is possible.

Synthesis of diaziridines

Oxidative ring closure of aminals The most common method for the preparation of diaziridine is the oxidative ring closure of aminals[39] obtained by the reaction of ketones or formaldehyde with aliphatic amines in the presence of sodium hypochlorite as an oxidizing agent (see Fig. 4.19):

Condensation-cyclization reaction of ketones Furthermore, also the condensation-cyclization reaction between ketones and ammonia or primary amines and hydroxylamine-O-sulfonic acid also yields diaziridines[40] (Fig. 4.20):

In the same way, the amination of alkylimines with hydroxylamine-O-sulfonic acid yields diaziridines.[41]

Reactivity
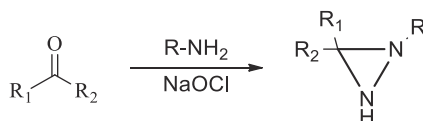
FIGURE 4.19   Oxidative ring closure of aminals.
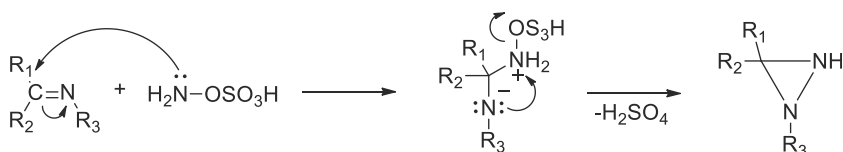
FIGURE 4.20   Condensation-cyclization reaction of ketones.
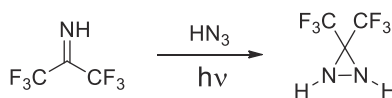
FIGURE 4.21   Photochemical reaction of ditrifluoromethyl ketone imine.
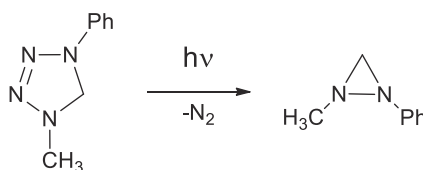
FIGURE 4.22   Photolysis of 1,4-disubstituted tetrazoline.

Photochemical reaction of ketone imines Ditrifluoromethyl ketone imine in the presence of hydrazoic acid (HN$_3$) undergoes a photochemical reaction that yields the 3-di(trifluoromethyl)diaziridine,[42] as sketched in Fig. 4.21:

Photolysis of 1,4-disubstituted tetrazoline A facile synthesis of diaziridines is developed through photolysis of 1,4-disubstituted tetrazoline to obtain unsymmetrical 1,2-disubstituted diaziridines[43] as reported in Fig. 4.22:

4.2.1.2.2 Oxaziridine

Trialkyl oxaziridines are color less liquids, sparingly soluble in water. It was first reported by Emmons in 1956.[44] It can be easily stored for indefinite periods at low temperature and reduced pressure.

The O−N bond is weakest compared to C−O and C−N because of the electronegativity and susceptibility of O and N atoms to cleavage by nucleophiles and electrophiles. Thus the oxiziridine ring is highly reactive due to its ring strain and relatively weakness of N-O bond, and results to be useful as aminating and oxygenating agents.[45−50] The following reactions are typical for oxaziridine.

Synthesis of oxaziridines The synthesis of *N*-H, *N*-alkyl, *N*-aryloxaziridines can be performed from imines, nitrones or carbonyl compounds.

Peroxidation of imines[51−53] As in the epoxidation of alkenes, the oxidation of imines in presence of peroxy acids proceeds as a stereospecific *cis*-addition giving the corresponding oxaziridine. For some oxaziridines, such as the 2-substituted oxaziridines, the activation enthalpy for the nitrogen inversion is so high that the configuration of the N atom results to be stable at room temperature due to an inversion barrier ($\Delta G^{\#}$) of 100−130 kJ/mol. Thus, the configuration of the starting material is preserved, and the racemate of one of the diastereoisomeric oxaziridines is formed. In the case of oxidation of chiral imines and oxidation of imines with chiral peracids enantiopure oxaziridines are reported (see Fig. 4.23):
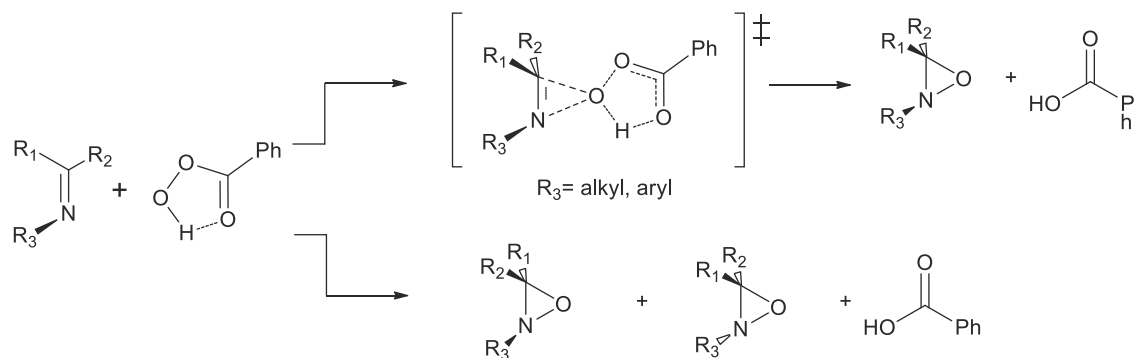
FIGURE 4.23 Stereospecific *cis*-addition for the peroxidation of imines in presence of peroxy acids.
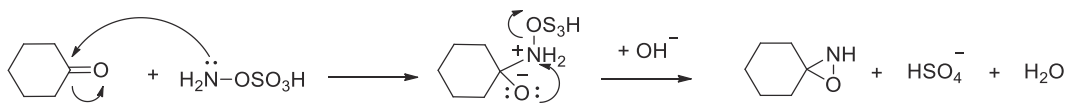
FIGURE 4.24 Amination of carbonyl compounds.
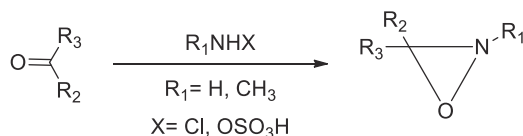
FIGURE 4.25 Intramolecular nucleophilic substitution on an N atom of carbonyl compounds.

Amination of carbonyl compounds   In addition to peracids, sodium hypochlorite has also been used as an oxidizing agent for the synthesis of N-unsubstituted oxaziridines due to incompatibility of imine toward peracids. Schmitz et al.[54] reported the synthesis of oxaziridine from the reaction of cyclohexanone with ammonia and sodium hypochlorite giving also a side product (see Fig. 4.24):

In presence of a base (such as hydroxylamine-*O*-sulfonic acid or chloramine aminate) carbonyl compounds give an intramolecular nucleophilic substitution on an N atom as shown in Fig. 4.25:

Reactivity of oxaziridine

Isomerization to nitrones   By thermolysis, oxaziridines can undergo the isomerization reaction for the conversion into nitrones (see the reversal photoisomerization of nitrones shown in Fig. 4.26).

The synthesis of *N*-H, *N*-alkyl, *N*-aryloxaziridines can be performed from imines, nitrones or carbonyl compounds.

Photoisomerization of nitrones   Oxaziridine formation by photoisomerization of nitrones was discovered almost simultaneously with the peracid procedure.[55,56] Oxaziridines are formed from the isomeric nitrone by visible light as shown in Fig. 4.26. The arrangement of substituents *cis* to the C=N double bond is retained during ring closure.

4.2.1.2.3 Dioxirane

Dioxiranes are known only since the mid-eighties.[57,58] The dioxirane is highly unstable and has never been observed at room temperature. When the hydrogens are replaced by other functional groups more stable derivatives can be obtained.

Dioxiranes are volatile organic peroxides and should be handled with care because of their toxicity and explosive nature. As a consequence, inflammable solvents (e.g., ethers and alcohols) should not be used as solvents in reactions occurring with dioxiranes. Difluorodioxirane is a pale yellow and stable gas (bp from $-80°C$ to $-90°C$), and it forms when equimolar mixture of FCO_2F and ClF pass over a CsF catalyst.[59,60] The dimethyldioxirane and the more stable methyl(trifluoromethyl)dioxirane, are used as oxidizing agents for the epoxidation of olefins[61] and for the oxidation: of enolates to α-hydroxycarbonyl compounds and of primary amines into nitro compounds.
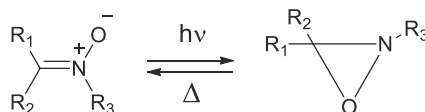
FIGURE 4.26   Photoisomerization of nitrones and thermolysis of oxaziridines.
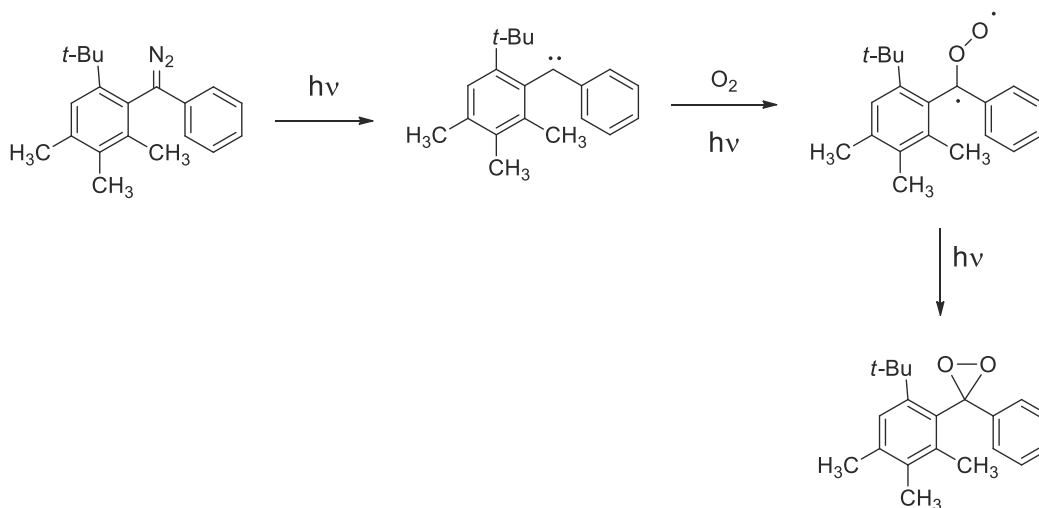
FIGURE 4.27   Photolytic oxidation of diaryl diazoalkanes.

Synthesis of dioxiranes

Photolytic oxidation of diaryl diazoalkanes Even if the photolytic oxidation of diaryl diazoalkanes is not commonly used in the synthetic laboratory, it represents a reaction leading to the synthesis of dioxiranes (Fig. 4.27).[62]

4.2.1.2.4 3H-Diazirine

3H-Diazirines are gases or colorless liquids with bp 21°C (i.e., 3,3-dimethyldiazirine). In 1960 3H-diazirine was first synthesized independently by Paulson and Schmitz. Liquid 3H-diazirines can decompose explosively and they are weakly basic in nature. They react slowly with acids and liberates nitrogen. Under UV light, three-substituted diazirines decompose smoothly to form carbenes.

Synthesis of 3H-diazirine

Oxidation reactions 3H-Diazirines are prepared by oxidation of *N*-unsubstituted diaziridines as already discussed for diazeridines. Moreover, 3-chloro-3H-diazirines are formed by oxidation of amidines with sodium hypochlorite as shown in Fig. 4.28:

Reactivity of 3H-diazirine

Dediazoniation The dediazoniation is a thermal or photochemical affected reaction involving the 3H-diazirines.[63,64] Without carbene acceptors, the initially formed carbenes isomerize to give olefins as sketched in the following Fig. 4.29:

4.2.2 Four-membered heterocycles

Four-membered heterocycles can be considered as the heterocyclic analogs of cyclobutane by replacing one or two methylene group(s) by one or two NH, O or S heteroatoms. Unlike the three-membered rings, four-membered heterocyclic rings are more stable since less strained (but their ring strain is approximately equal to that found in cyclobutane). This means that the ring cleavage is less likely even if the ring opening reactions forming acyclic products predominate, anyway.

Moreover, four-membered heterocycles are more difficult to synthesize by direct intramolecular cyclization than the three-membered heterocycles because ring forming ability falls off with the chain length.
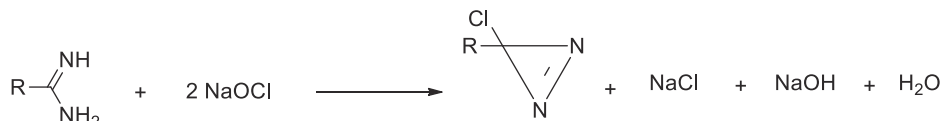
FIGURE 4.28   Oxidation of amidines.
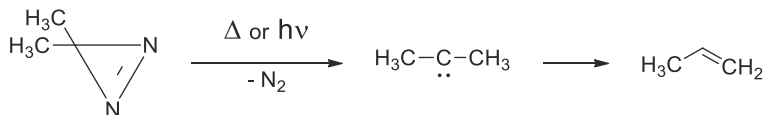
FIGURE 4.29   Thermal and/or photochemical dediazoniation of 3H-diazirines.
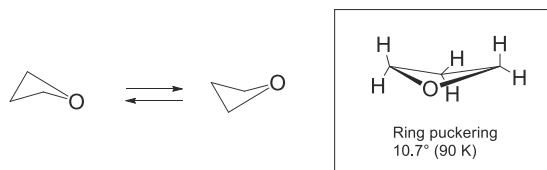
FIGURE 4.30   Pitzer strain of oxetane.

4.2.2.1 Four-membered compounds with one heteroatom

4.2.2.1.1 Oxetane

Oxetane, a colorless, water-miscible liquid (bp 48°C).[65] The planarity of the oxetane ring causes a considerable Pitzer strain due to the eclipsing interactions of the C−H bonds. As result, the total strain energy is minimized by a compromise between the bond angle strain and the Pitzer strain reached by ring-puckering between two nonplanar structures, which simultaneously leads to a reduction in the bond angles. The ring adopts an essentially planar structure with a puckering angle of only 8.7° at 140 K (10.7° at 90 K)[66,67] as shown in Fig. 4.30:

Since the activation energy of the ring inversion amounts only to 0.181 kJ/mol, the process occurs so fast that the molecule should be considered as planar.

Synthesis of oxetanes

Intramolecular cyclodehydrohalogenation of γ-substituted alcohols Oxetanes can be prepared by cyclization of alcohols containing a nucleophilic leaving group in the γ-position starting from a 1,3-diols reacting with monoarene sulfonates as follows from Fig. 4.31.

Another approach is the treatment with *n*-BuLi and tosyl chloride (TsCl) followed by the cyclization with *n*-BuLi (see Fig. 4.32):
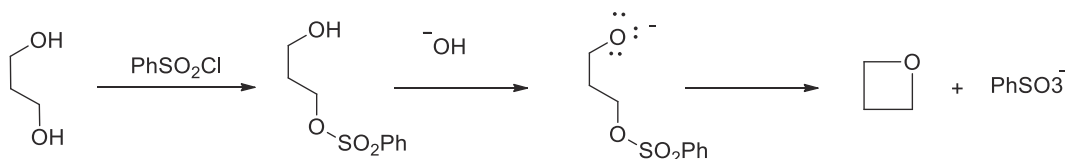
FIGURE 4.31   Intramolecular cyclodehydrohalogenation of γ-substituted alcohols containing a nucleophilic leaving group in the γ-position.
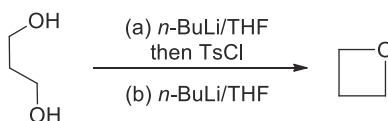
FIGURE 4.32   Intramolecular cyclodehydrohalogenation of γ-substituted alcohols with *n*-BuLi and tosyl chloride (TsCl) .
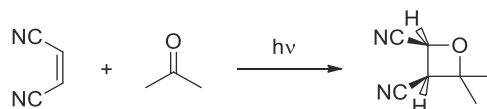
FIGURE 4.33   Photochemical [2 + 2] cycloaddition of carbonyl compounds (Paterno-Büchi reaction).
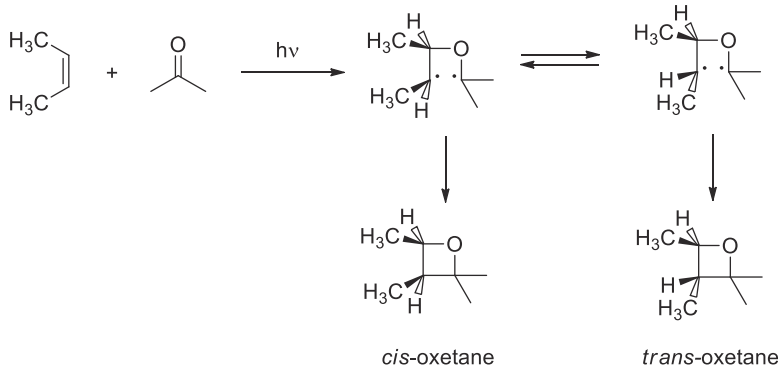
FIGURE 4.34   Paterno-Büchi reaction mechanism.

cis-oxetane   *trans*-oxetane

Photochemical cycloaddition (Paterno-Büchi reaction)[68] The Paterno-Büchi is the photochemical [2 + 2] cycloaddition of carbonyl compounds to alkenes yielding oxetanes.[69] In the first reaction step, the carbonyl compound absorbs a quantum of light and is converted first into an electronically excited singlet state (n → π* transition), and then into a lower energy triplet state. According to the Woodward-Hoffmann rules, the addition of the alkene should occur in a concerted and, therefore, in a stereospecific manner. This is indeed observed with alkenes possessing electron-withdrawing groups (EWGs) as sketched in Fig. 4.33:

Alkenes with electron-donor groups (EDG) react via radical intermediates as reported in Fig. 4.34:

4.2.2.1.2 Thietane

Thietane is a colorless and water-insoluble liquid (bp 94°C). Thietane undergoes facile polymerization with either Lewis acids or bases slowly at room temperature and faster on exposure to light. Thietanes display properties in between the highly reactive thiiranes and the more inert thiophanes.

Synthesis of thietanes

Cyclization of γ-halo thiols or their acetyl derivatives by bases Thietane can be synthesized under basic conditions by cyclization of *S*-acetyl-γ-chloropropane as shown in Fig. 4.35:

Action of sodium or potassium sulflde on 1,3-dihaloalkanes The best result to synthesize thietane are obtained from l-bromo-3-chloropropane by using thiourea and passing through the 2-(3-chloropropyl)isothiouronium chloride intermediate (see Fig. 4.36):

Reactivity of thietane Under proper acidic conditions thietane polymerize: slowly at room temperature and faster by exposure to light. Photolysis of thietane in the presence of catalytic amounts of diaryliodonium salts gives polymer with a 14% yield.[70]

4.2.2.1.3 Azete

Azete is the simplest antiaromatic heteroannulene. It is thermally unstable and extremely reactive, and until now has not been synthesized.

Synthesis and reactivityof azetes   In 1986 Regitz[71,72] succeeded in synthesizing tri-*tert*-butylazete by irradiation or thermolysis or flash vacuum pyrolysis of 3-azido-l,2,3-tri-*tert*- butylcyclopropene (Fig. 4.37):

Tri-*tert*-butylazete crystallizes as reddish needles (mp 37°C). Tri-*tert*-butyl azete result to be kinetically stabilized in two ways since the *tert*-butyl groups act as space fillers preventing therefore that the ring undergoes both polymerization and decomposition of the compound into an alkyne and a nitrile as a consequence of a
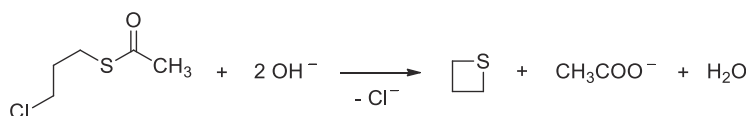
FIGURE 4.35   Cyclization of γ-halo thiols or their acetyl derivatives.

FIGURE 4.36   Action of sodium or potassium sulflde on 1,3-dihaloalkanes.
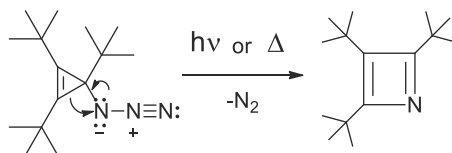
FIGURE 4.37   Regitz synthesis of azetes.

concerted [2 + 2] cycloreversion. Both reaction proceeds extremely slowly because their ΔG* is high even at elevated temperatures, while the second reaction is not allowed also according to the Woodward-Hoffmann rules.

Later on, in 1973 also the tris(dimethylamino)azete was described for the first time.

4.2.2.1.4 Azetidine

Azetidine is a water-miscible, colorless liquid (bp 61.5°C) at room temperature. It possesses a strong odor of ammonia and fumes in air. Azetidines are thermally stable and less reactive than aziridines.

Synthesis of azetidines

Cyclization of γ-substituted amines γ-Halogen substituted amines are dehydrohalogenated by bases giving the resulting cyclization N-substituted aziridine products as follows from Fig. 4.38:

Also γ-amino alcohols are suitable of cyclodehydration by the Mitsunobu reagent (triphenylphosphine (Ph$_3$P) plus azodicarboxylate such as diethyl azodicarboxylate (DEAD) or diisopropyl azodicarboxylate (DIAD))[73] to provide N-substituted aziridine derivatives as reported in Fig. 4.39:

*Action of **p**-toluenesulfonamide and bases on 1,3-dihaloalkanes* 1,3-Dihalopropane and *p*-toluenesulfonamide react under basic conditions to produced 1-tosylazetidine, which on reductive elimination of the tosyl group offers azetidine (see Fig. 4.40):
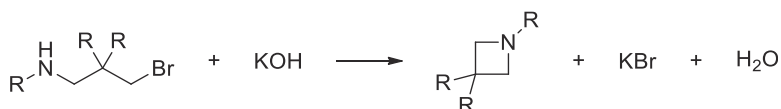
FIGURE 4.38   Cyclization of γ-halo amines.
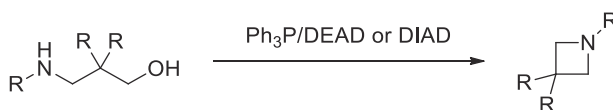
FIGURE 4.39   Cyclization of γ-amino alcohols.
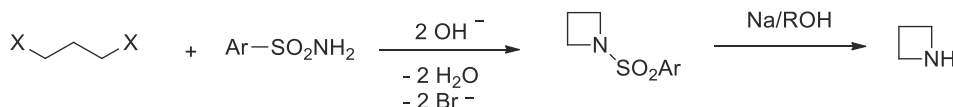
FIGURE 4.40   Reaction of 1,3-dihaloalkanes with *p*-toluenesulfonamide and bases.
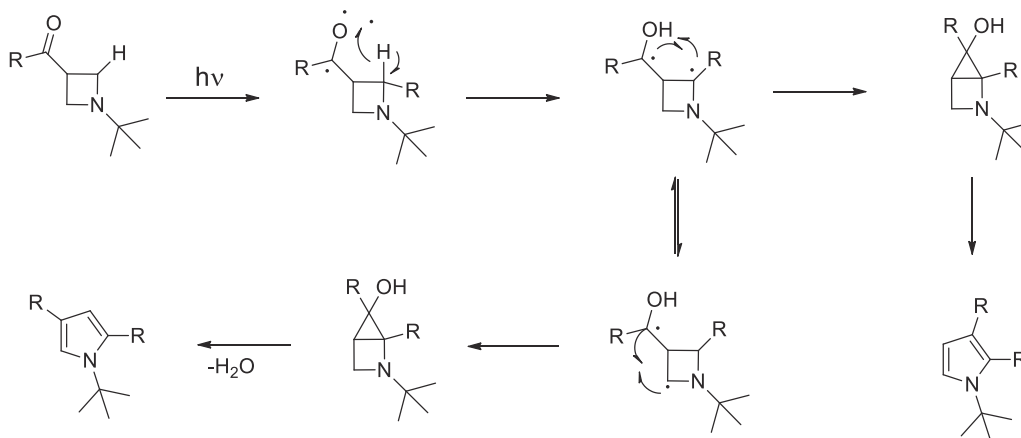
FIGURE 4.41   Photo-induced ring expansion reaction of 3-acetylazetidine.

Reactivity of azetidines

Rearrangement reaction 3-Acetylazetidine undergoes rearrangement in the presence of light and provides functionalized pyrroles via ring expansion reaction.[74−76] This ring expansion probably occurs through a free radical cyclization reaction as illustrated in Fig. 4.41:

4.2.2.2 Four-membered compounds with two heteroatoms

4.2.2.2.1 1,2-Dioxetane

1,2-Dioxetanes are highly endothermic compounds. This is due both to ring strain, but it is especially due to the low bond energy of the peroxide bond. The tetramethyl-1,2-dioxetane has been isolated in the form of yellow crystals (mp 76°C−77°C), and a few degrees above its melting point it emits blue light (i.e., chemiluminescence[77,78]) because it undergoes thermal decomposition. This phenomenon is explained by a thermal process and according to the principle of conservation of orbital symmetry, during the thermal decomposition two moles of acetone are eliminated, one of which is an electronically excited molecule. Then, with emission of light ($h\nu$), the ground state is restored (see Fig. 4.42):

4.2.2.2.2 Synthesis of 1,2-dioxetane

Dehydrohalogenation of β-halo hydroperoxides The dehydrohalogenation of β-halo hydroperoxides was first introduced by Kopecky and co-workers in 1973.[79] The electrophilic bromination of alkenes in the presence of hydrogen peroxide leads to β-bromo hydroperoxides intermediates which are cyclized with bases or with silver acetate to give 1,2-dioxetanes (Fig. 4.43):

FIGURE 4.42 Thermal decomposition of 1,2-dioxetanes.

FIGURE 4.43 Dehydrohalogenation of β-halo hydroperoxides.
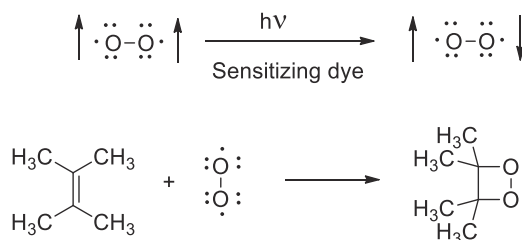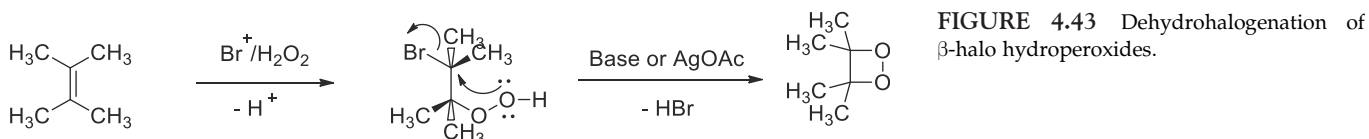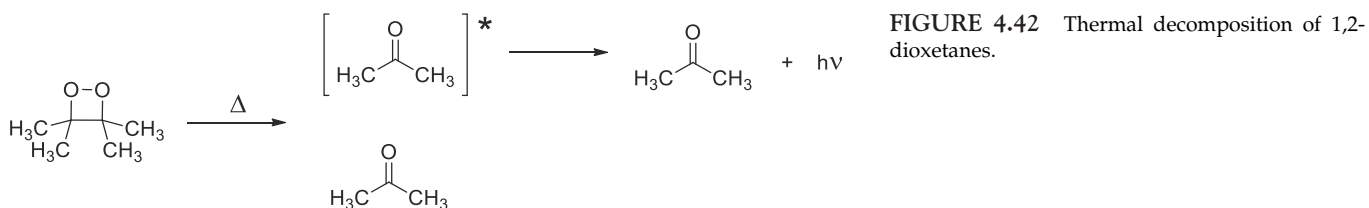
FIGURE 4.44 Photooxygenation of alkenes.

FIGURE 4.45 Intramolecular photodimerization of dithiocarbonyl compounds.
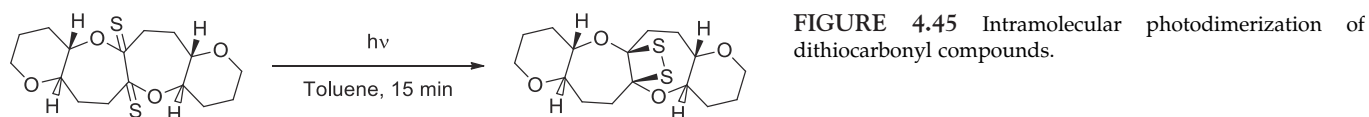
Photooxygenation of alkenes   Alkenes substituted with EDGs react by a [2 + 2] cycloaddition with singlet oxygen to yield 1,2-dioxetanes. By passing oxygen through a solution of the alkene, the singlet oxygen is generated under irradiation in the presence of a sensitized (e.g., methylene blue) as sketched in Fig. 4.44:

4.2.2.2.3 1,2-Dithietane

Dithietanes are promising molecules from the theoretically, chemically, and biologically point of view.[80,81] Unfortunately, the repulsion between the lone pair on adjacent sulfur atoms and the strain of the four-membered ring seems to be responsible for the high instability of this class of molecules.[82,83] Anyway, the first isolated 1,2-dithietane derivative has been the *trans*-3,4-diethyl-1,2-dithietane-1,1-dioxide formed by spontaneous dimerization of propanethiol-S-oxide. The stability of this molecule is attributable to the replacement of the lone pair of sulfur with oxygen.[84]

Synthesis of 1,2-dithietanes   The first stable 1,2-dithietane derivative reported was dithiatopazine formed by intramolecular photodimerization of a dithiocarbonyl compound in 65% of yield by using toluene as solvent and a UV lamp irradiating the mixture for 15 min at ambient temperature (see Fig. 4.45):

4.2.2.2.4 1,2-Dithiete

1,2-Dithiete is iso-π-electronic with benzene. The calculations predicted a delocalization energy of 92 kJ/mol, which overcompensates for the strain enthalpy of 43 kJ/mol and results in stabilization of the molecule. However, 1,2-dithiete has not yet been prepared. Instead, the 3,4-Bis(trifluoromethyl)-l,2-dithiete is a yellow liquid (bp 95°C) which has been prepared by heating hexafluorobut-2-yne with molecular sulfur (S_8) as sketched in the first reaction of Fig. 4.46.

Synthesis and reactivity of 1,2-dithietes

Valence isomerization of disubstituted 1,2-dithietes   A typical transformation to which disubstituted 1,2-dithietes undergo is their valence isomerization resulting in the 1,2-dithiones formation. The equilibrium favors the
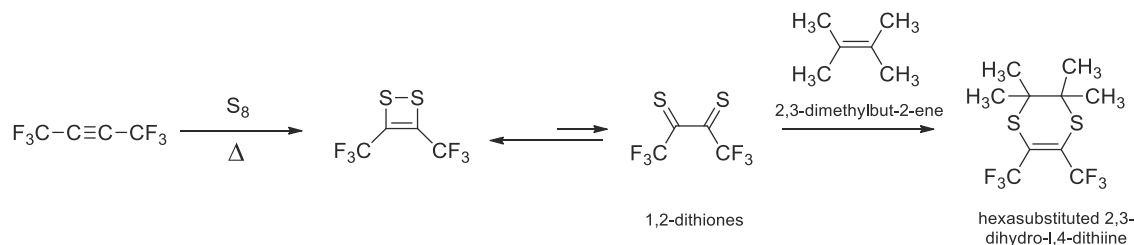
FIGURE 4.46   Synthesis of 3,4-bis(trifluoromethyl)-l,2-dithiete.
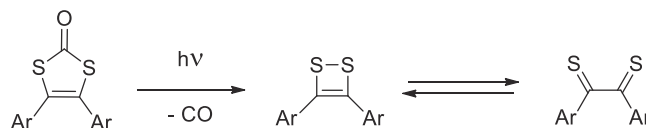
**FIGURE 4.47**   Valence isomerization of disubstituted 1,2-dithietes.
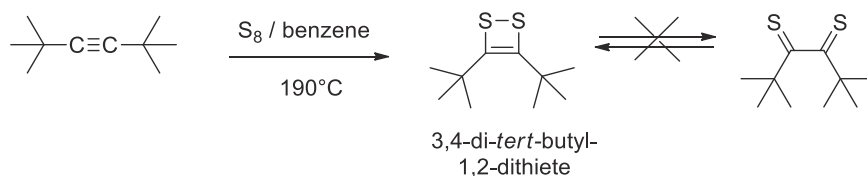
**FIGURE 4.48** Synthesis of 3,4-di-*tert*-butyl-l,2-dithiete.
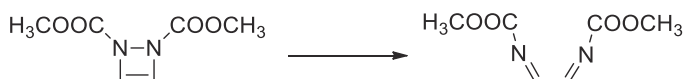
FIGURE 4.49   Synthesis of l,2-dihydro-l,2-diazete.

**FIGURE 4.50**   Photolysis of dihydropyridazine.
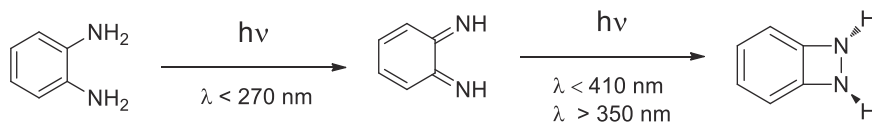


FIGURE 4.51   Photolysis of benzene-1,2-diamine.
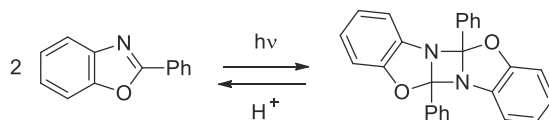
FIGURE 4.52   Photodimerization reaction of 2-phenylbenzo[*d*]oxazole.

1,2-dithiete with EWGs such as CF$_3$. The reaction with 2,3-dimethylbut-2-ene to give a hexasubstituted 2,3-dihydro-1,4-dithiine proceeds, however, as a [4 + 2] cycloaddition via the 1,2-dithione (see last reaction path of Fig. 4.46):

Due to valence isomerization the 3,4-Bis(4-dimethylaminophenyl)-1,2-dithiete exists in solution in equilibrium with the corresponding 1,2-dithione (Fig. 4.47)[85−87]:

One thermally stable 1,2-dithiete is represented by 3,4-di-*tert*-butyl-1,2-dithiete. It does not exist in equilibrium with its corresponding 1,2-dithione since its valence isomerization into the dithione form would enhance the steric strain and thus is unfavorable. 3,4-di-*tert*-butyl-1,2-dithiete is obtained by heating di-*tert*-butyl acetylene with sulfur in benzene in an autoclave at 190°C[88,89] as illustrated in Fig. 4.48:

4.2.2.2.5 1,2-Dihydro-1,2-diazete

As 1,2-dithiete, also this system is iso-π-electronic with benzene.

Synthesis of 1,2-dihydro-1,2-diazete   Within this class of compound, only the 1,2-bis(methoxycarbonyl)-1,2-dihydro-1,2-diazete has been prepared until now since it undergoes a slow valence isomerism to the corresponding 1,2-diimine[90] at room temperature as shown in Fig. 4.49:

Moreover, it was shown that fused diazetidine is, despite the low yield, expediently provided by photolysis of dihydropyridazine, as follows in Fig. 4.50:

The formation of the benzo-fused 1,2-dihydro-1,2-diazete structures was observed on irradiation of diimines generated by photolysis of benzene-1,2-diamine (Fig. 4.51)[91,92]:

Instead, diimines with methyl substituents at the benzene ring could not be induced to cyclize.[93]

4.2.2.2.6 1,2-Diazetidine and 1,3-diazetidine

Synthesis of 1,2-diazetidine and 1,3-diazetidine   Even if the preparation of the diazetidine compounds, in general, has not been achieved numerous functionalized 1,2- and 1,3-diazetidines are already known.

Such an example, the 1,3-diazetines derivatives can be prepared by [2 + 2] cycloadditions of benzoxazoles. As an example, the 2-phenylbenzo[*d*]oxazole undergoes the photodimerization reaction hereafter reported (Fig. 4.52):

Reactivity of 1,2-diazetidine and 1,3-diazetidine   The interesting behavior is that, in the dark and in solution, the 1,3-diazetidine photodimer undergoes an acid-catalyzed fission in an exothermic reaction ($\Delta H° = -116$ kJ/mol). This energy is only a small part of the liberated resonance energy. The strain enthalpy of the doubly condensed diazetidine system makes the major contribution.
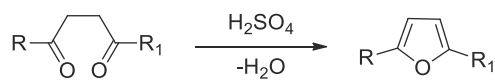
**FIGURE 4.53** Paal-Knorr synthesis.
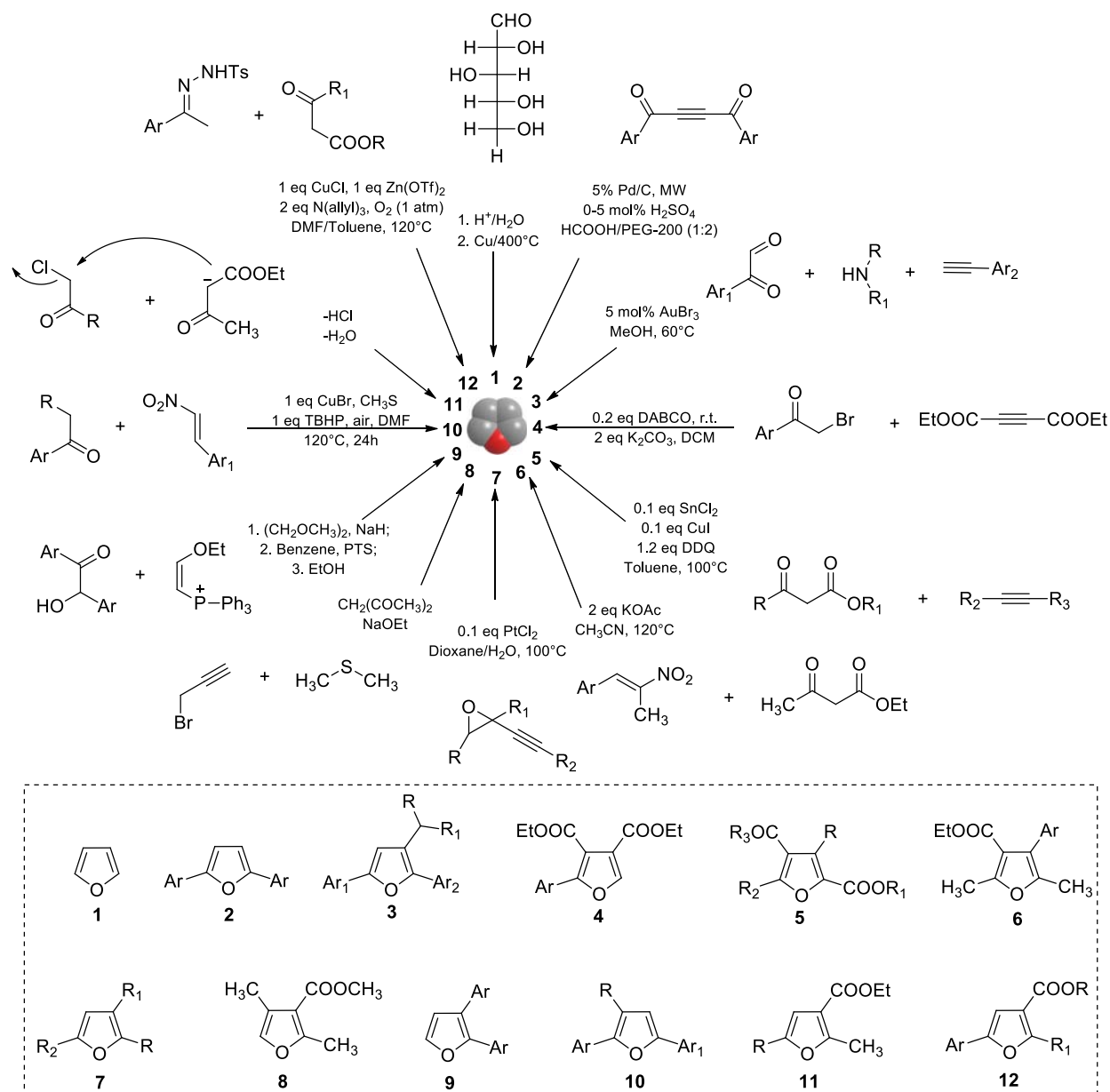
FIGURE 4.54 Summary of some main strategies for the synthesis of furan and furan substituted molecules.

4.2.3 Five-membered heterocycles

4.2.3.1 Five-membered compounds with one heteroatom

4.2.3.1.1 Furan

Furan is a five-membered planar heterocycle containing one oxygen and four conjugated carbon atoms. To the 6π electron system delocalized over the ring and responsible for the aromatic character of furan participate one

lone pair of electrons of the oxygen. While, the other oxygen' lone pair remains flat in the plane of the ring and occupies the sp^2 hybrid orbital.

Synthesis of furans   The most important method for furan's synthesis is represented by the Paal-Knorr synthesis.[94] It is an acid-catalyzed intramolecular cyclization of not sterically hindered 1,4-diketones (see Fig. 4.53).

Besides the classic Paal-Knorr synthesis, there are a wide range of synthetic methods allowing the synthesis of furan and furan substituted molecules. Some of them are summarized in Fig. 4.54 including: **1**. the acidic-catalyzed dehydration of carbohydrates; **2**. the microwave-assisted transormations of butyne-1,4-diones[95]; **3**. the gold catalyzed coupling of phenyl glyoxal, secondary amines and terminal alkynes[96] to give trisubstituted furans; **4**. trisubstituted furans can be prepared aldo by the palladium-catalyzed cyclization of 1-aryl-2-bromomethanone and dimethyl acetylenedicarboxylate in DCM using DABCO under mild reaction conditions[97]; **5**. the Sn(II) and Cu (II)-promoted addition and oxidative cyclization of alkynoates and 1,3-dicarbonyl compounds in the presence of 2,3-dichloro-5,6-dicyanobenzoquinone (DDQ)[98] represents a valid method to synthesize polysubstituted furan compounds; **6**. the FeCl$_3$-catalyzed addition-cyclization using KOAc as a base of ethyl acetoacetate with nitro olefins[99] represents a direct route for the synthesis of tetra-substituted furans; **7**. the Pt-catalyzed reaction of propargylic oxiranes[100] allows to obtain trisubstituted furans; **8**. successive addition of dimethyl sulfide and acetyl acetone to propargyl bromide in the presence sodium ethoxide in acetonitrile[101,102] produced 2,3,4-trisubstituted furan in good yields; **9**. the nucleophilic addition of benzoin to β-ethoxyvinylphosphonium bromide followed by intramolecular cyclization[103] allows to prepare 2,3-disubstituted furans; **10**. the copper-mediated addition of enolate derived from ketone to nitrostyrene followed by cyclization produced trisubstituted furans[104]; **11**. the Feist-Benary reaction[105] is an aldol condensation between α-haloketone and β-ketoester initiated with a substitution reaction accompanied by liberation of HCl. This step is between followed by subsequent cyclization with elimination of water to form a trisubstituted furan derivative; **12**. the copper-mediated [3 + 2] oxidative cyclization of N-tosylhydrazones allows to obtain furan derivatives in good yields.[106]

Reactivity of furan   2-Hydroxymethylfuran with benzophenone undergoes photochemical reaction giving, after 96 hours, a mixture of the two [2 + 2] cycloadducts: the (6,6-diphenyl-2,7-dioxabicyclo[3.2.0]hept-3-en-3-yl) methanol in 20% and the (6,6-diphenyl-2,7-dioxabicyclo[3.2.0] hept-3-en-1-yl)methanol in 65% yields (see Fig. 4.55).[107]

Furthermore, the photochemical reaction of furan with aldehydes (aliphatic, aromatic and heteroaromatic) gives oxetanodihydrofurans. Such an example, furan reacts photochemically with *n*-butyl-2-oxoacetate providing the (5R)-*n*-butyl2,7-dioxabicyclo[3.2.0]-hept-3-ene-6-carboxylate, which on further proton-catalyzed acetal cleavage produces the *n*-butyl-2-(furon-3-yl)acetate (Fig. 4.56):

4.2.3.1.2 Benzo[b]furan, benzo[c]furan, dibenzofuran

Within the class of benzofurans, benzo[*b*]furan obtained by the fusion of benzene at the 2,3-positions of the furan ring is one of the most useful heterocyclic cyclic systems. If the fusion of a benzene ring concerns the 3,4-positions of the furan ring, the obtained compound is the benzo[*c*]furan. Comparing the properties of these two heterocyclic systems, it results that the resonance energy of benzo[*c*]furan is lower than that of benzo[*b*] furan. It follows that benzo[*c*]furan, beeing highly unstable, polymerize rapidly already at low temperature
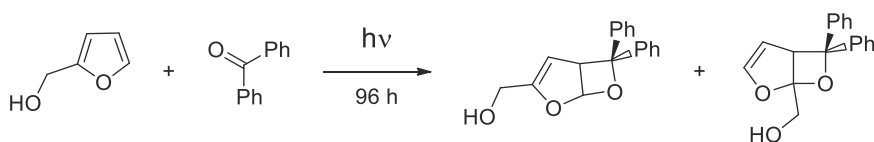

FIGURE 4.55   Photochemical reaction of 2-hydroxymethylfuran with benzophenone.
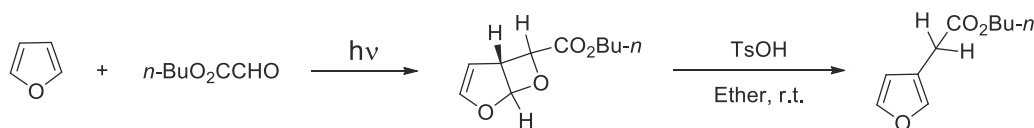

FIGURE 4.56   Photochemical reaction of furan with aldehydes.
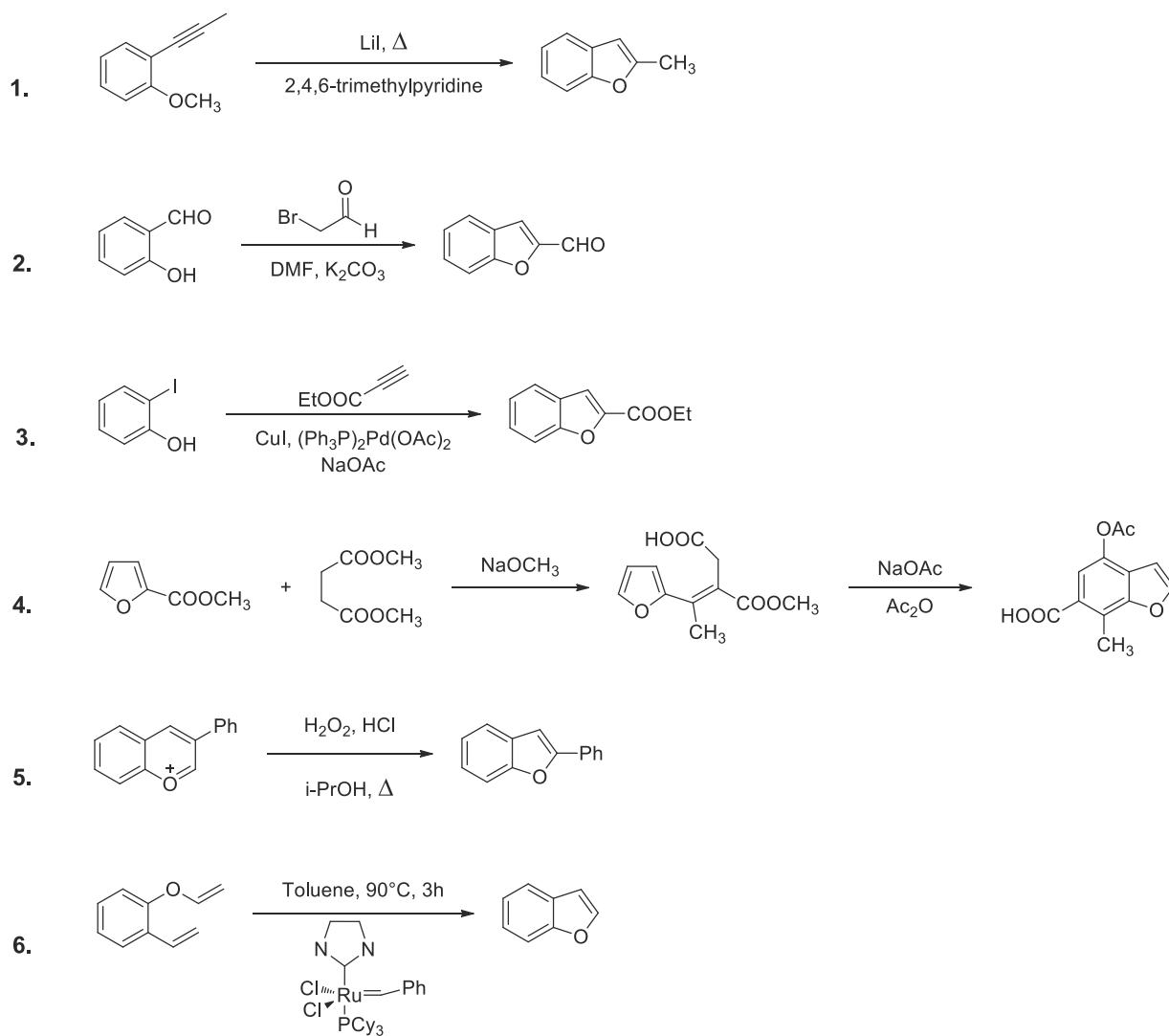
FIGURE 4.57 Synthetic strategies toward benzo[*b*]furans.
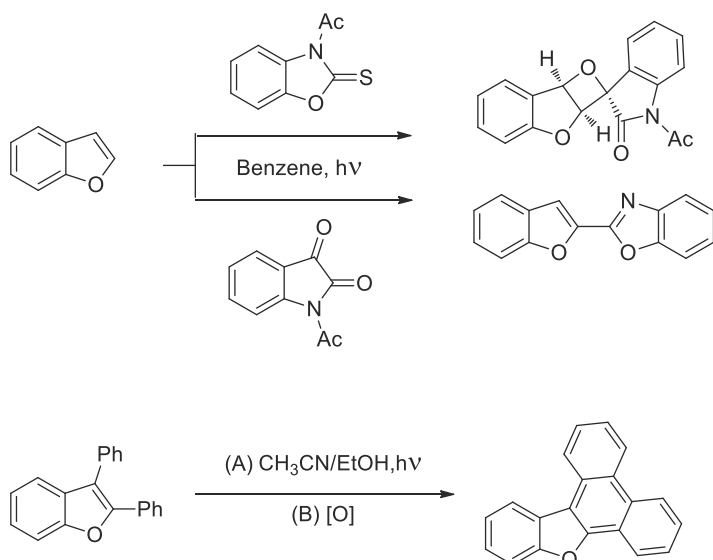
FIGURE 4.58 Photochemical reactions of benzo[*b*]furan in presence of benzoxazole-2-thione or 1-acetylisatin in benzene.

FIGURE 4.59 Photolysis of 2,3-diphenylbenzo[*b*]furan.

Photochemistry of Heterocycles

thus preventing the isolation of the parent benzo[c]furan. Functionalizing benzo[c]furans by introducing electron-withdrawing substituents at the 1- and 3-positions of the ring, the stability can be remarkably increased. In general, benzo[c]furan derivatives show luminescent and electroluminescent properties very important for their technological exploitation for organic light-emitting diode devices. Dibenzofuran is a tricyclic heterocyclic compound isolated for the first time from coal tar and made by two benzene rings fused at 2,3- and 4,5-positions of the furan ring.

Synthesis of benzo[b]furans There are several approaches useful to synthesize benzo[b]furans. Among them the most synthetically viable and important synthesis have been sketched in Fig. 4.57 and take advantages from: **1**. aryl ethers[108]; **2**. 2-hydroxybenzaldehyde[109]; **3**. 2-substituted phenol[110]; **4**. furan derivatives[111,112]; **5**. ring contraction reactions[113]; **6**. olefin metathesis approach.[114]
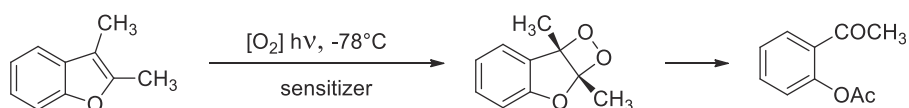
FIGURE 4.60   Photooxygenation of 2,3-dimethylbenzo[b]furan.
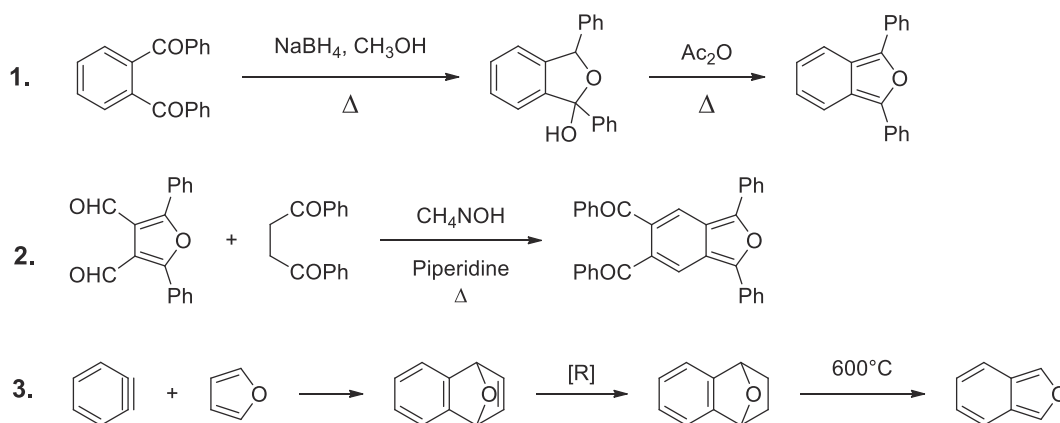
FIGURE 4.61   Synthesis of parent and substituted benzo[c]furans.
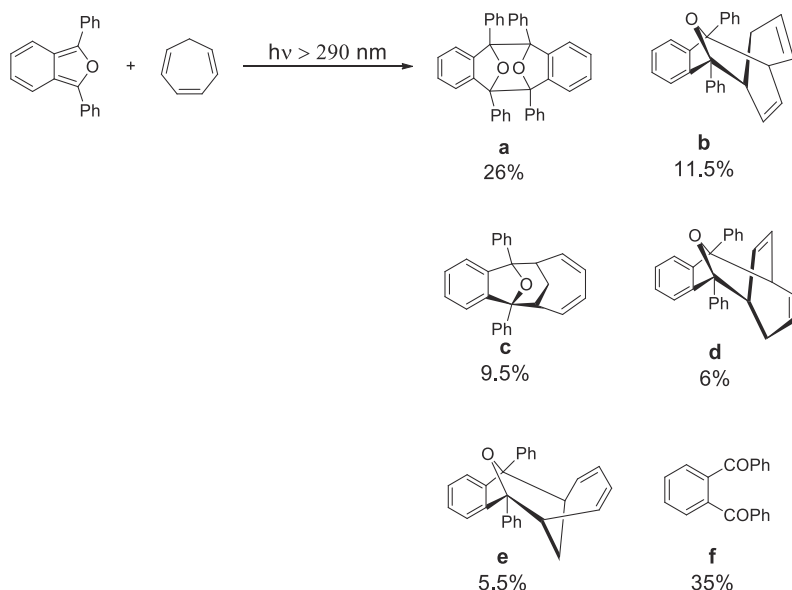
FIGURE 4.62   Photochemical [6 + 4] and [4 + 4] cycloaddition reaction of 1,3-diphenylbenzo[c]furan in presence of cycloheptatriene.

a
26%

b
11.5%

c
9.5%

d
6%

e
5.5%

f
35%

Reactivity of benzo[b]furans Irradiation of a solution of benzo[*b*]furan in benzene affords in presence of benzoxazole-2-thione the 2-benzofuryl-benzoxazole[115] (see upper part of Fig. 4.58) with 35% yield; while the photochemical reaction of benzo[*b*]furan with 1-acetylisatin in benzene represents a way to obtain in good yields the spiro-type molecule[116] sketched in the lower part of Fig. 4.58:

Photolysis of 2,3-diphenylbenzo[*b*]furan in a mixture of acetonitrile and ethanol gives the benzo[*b*]phenanthro [9,10-*d*]furan[117] (see Fig. 4.59):

Photooxygenation of 2,3-dimethylbenzo[*b*]furan[118] produces the intermediate dioxetane (see Fig. 4.60), which finally isomerizes at room temperature giving the 2-acetoxyacetophenone product:

Synthesis of benzo[c]furans The synthesis of parent and substituted benzo[*c*]furans can be designed following mainly three synthetic strategies (see reactions' schemes in Fig. 4.61): **1**. annulations to arenes[119]; **2**. annulations to furan[120−122]; **3**. flash-vacuum pyrolysis of benzyne-furan cycloadducts:

Reactivity of benzo[c]furans Photochemical [6 + 4] and [4 + 4] cycloaddition reactions occur when a solution of 1,3-diphenylbenzo[*c*]furan in presence of a large excess of cycloheptatriene in benzene is irradiated at room temperature by using a Hg high-pressure lamp emitting at >290 nm.[123] The reaction's products sketched in Fig. 4.62 are a mixture of [6 + 4] and [4 + 4] cycloadducts with *exo*- and *endo*-configurations (**b**, **c**, **d**, and **e**) together with the corresponding photodimer **a**. However, irradiation in solvent saturated with air gave 1,2-dibenzoylbenzene **f** as a photooxidized:

Synthesis of dibenzofurans The two main reaction strategies useful to synthesize dibenzofurans plan to start from: **1**. Diphenyl ether; **2**. Benzo[*b*]furan as better shown in Fig. 4.63.

The former one, represents the intramolecular cyclization of *ortho*-diazonium salts of diaryl ether in presence of palladium acetate as a catalyst in ethanol.[124] An alternative efficient strategy consists in the synthesis of dibenzofurans through Pd/C-catalyzed intramolecular cyclization of *o*-iododiaryl ethers in DMA under ligand-free conditions.[125] An example of the latter synthetic strategy represents the acid-catalyzed condensation of 2-methylbenzo[*b*]furan-3-carboxaldehyde that with Meldrum's acid gives a condensed product that under flash vacuum pyrolysis undergoes [1,5]-proton shift and cyclization to the final 3-hydroxydibenzofuran product.[126]

Reactivity of dibenzofurans Dibenzofuran absorbs UV light above 300nm, but UV absorption rises sharply below 300 nm, which indicates the potential for direct photolysis in the environment. Indeed, vapor-phase
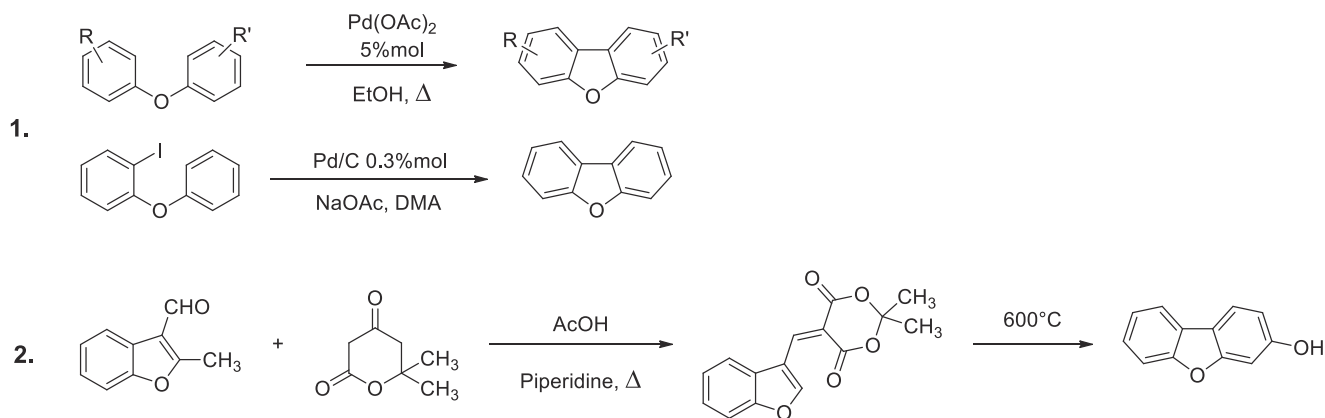

FIGURE 4.63 Synthesis of dibenzofurans.
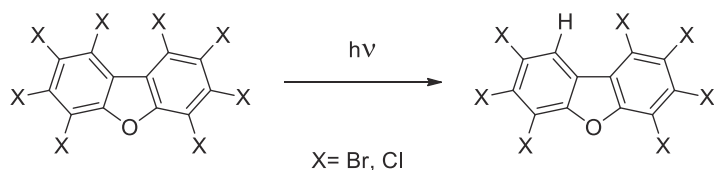
FIGURE 4.64 Photodehalogenation reaction of polychlorinated and polybrominated dibenzofurans.
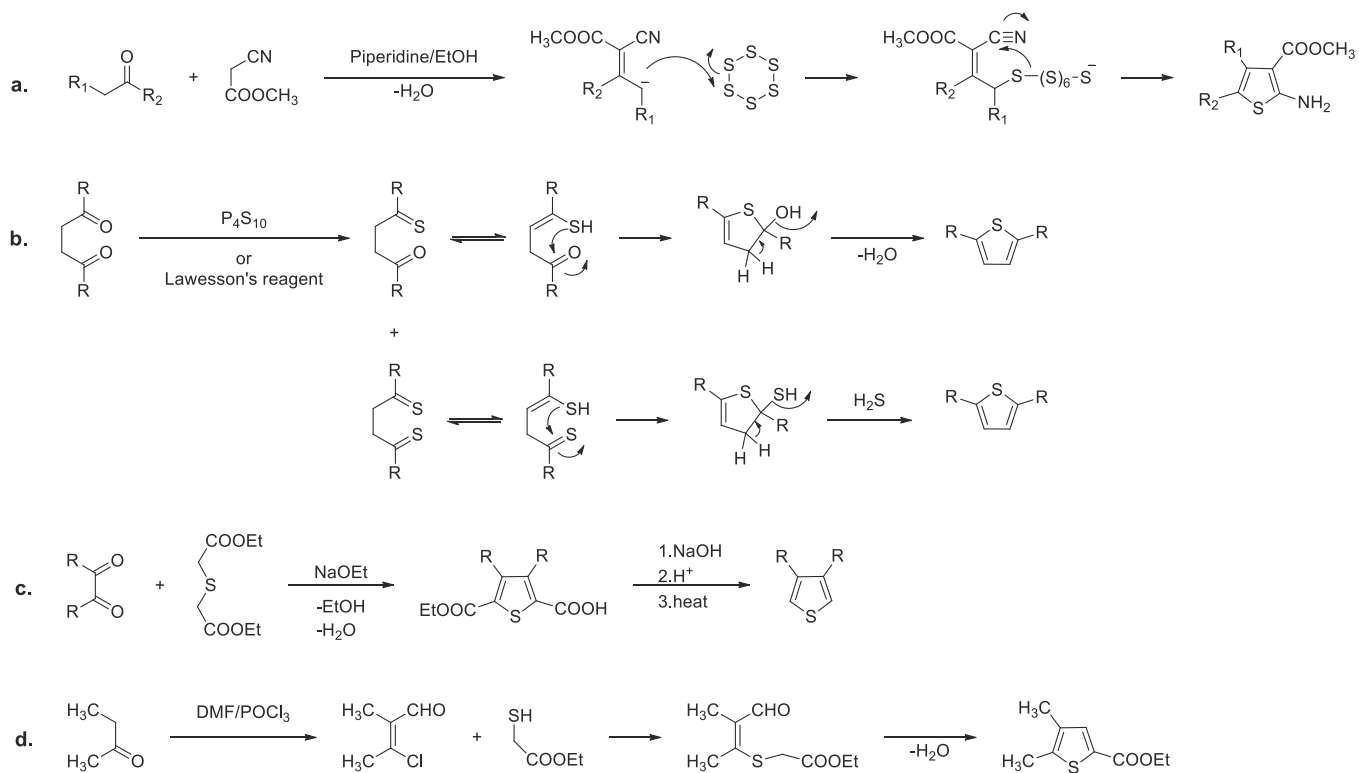
FIGURE 4.65 Common synthetic approaches (a-d) for the synthesis of thiophene ring and derivatives.
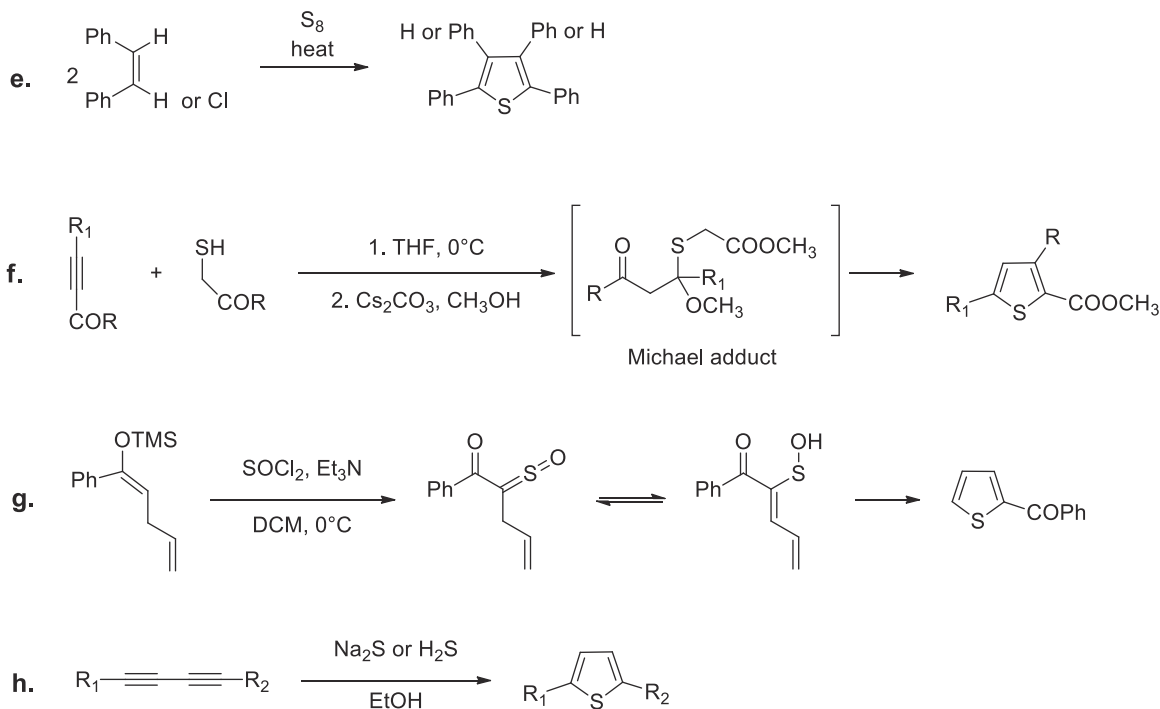

FIGURE 4.66 Common synthetic approaches (e-h) for the synthesis of thiophene ring and derivatives.
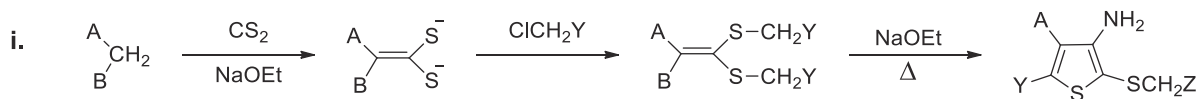

FIGURE 4.67 Common synthetic approaches for the synthesis of thiophene ring and derivatives form ketene dithioacetals.

dibenzofuran deminstrated the tendency to be degraded in the atmosphere by reaction with photochemically-produced hydroxyl radicals within 4 days. Quantum chemical calculations studies have been performed to investigate the photodehalogenation mechanisms of polychlorinated (PCDFs) and polybrominated dibenzofurans (PBDFs).[127] From their results the photodehalogenation reactivity of PCDFs and PBDFs increases with an increase of halogenation degree. In particular, the photodehalogenation reaction of PCDFs and PBDFs results in the dissociation of C-X bond at 1 or 9 position (see Fig. 4.64):

4.2.3.1.3 Thiophene

Thiophene has been discovered in 1882 by Victor Meyer as a contaminant of commercial benzene. It is a five-membered heterocycle comprised of four carbon atoms and one sulfur atom.

Synthesis of thiophene Numerous synthetic strategies for the preparation of a thiophene ring and derivatives are known form literature which differ for the starting precursors. The most common synthetic approaches require the following classes of precursors: **1**. carbonyl compounds by: **a**. Gewald,[128] **b**. Paal-Knorr,[129] **c**. Hinsberg[130] and **d**. Fliessman[131] synthesis (Fig. 4.65):
  2. **e**. Alkenes,[132] **f**. Alkynes,[133] **g**. Dienes,[134,135] and **h**. Diynes[135,136] (Fig. 4.66):
  3. **i**. Ketene dithioacetals[137] (Fig. 4.67):
  4. **l**. ring contraction.[138,139] (Fig. 4.68) and **m**. expansion reactions (Figs. 4.68 and Fig. 4.69, respectively):

Reactivity of thiophene
Photochemical oxidation and substitution The first step in the oxidative ring opening of 2,5-dimethylthiophene is the cycloaddition of singlet oxygen to thiophene to yield endoperoxide, which under thermal decomposition produced cis-enedione by the following mechanism[140] (Fig. 4.70):

In presence of electron-withdrawing substituents on thiophene the reaction with phenylacetylene proceed by a photochemical substitution yielding 2-substituted biphenyls as follows[141] (Fig. 4.71):

4.2.3.1.4 Benzo[b]thiophene, benzo[c]thiophene, dibenzo[b,d]Thiophene

Benzo[b]thiophene and benzo[c]thiophene are heteroaromatic bicyclic ring systems with 10π electrons in which the benzene ring is, respectively, fused with the 2,3- or 4,5-positions of the thiophene ring. Since both benzene
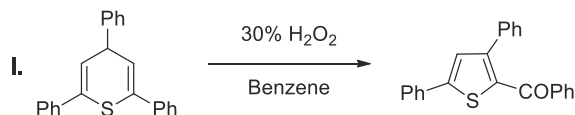

FIGURE 4.68   Common synthetic approach by ring contraction for the synthesis of thiophene ring and derivatives.
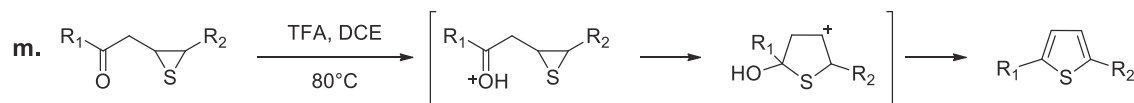

FIGURE 4.69   Common synthetic approach by ring expansion for the synthesis of thiophene ring and derivatives.
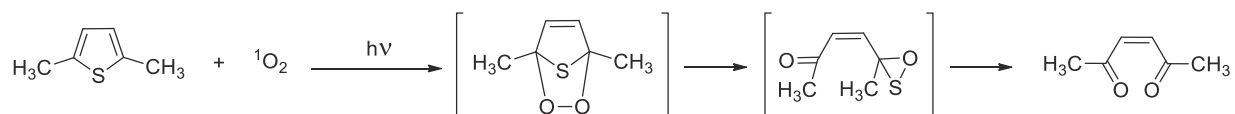

**FIGURE 4.70**   Oxidative ring opening of 2,5-dimethylthiophene.
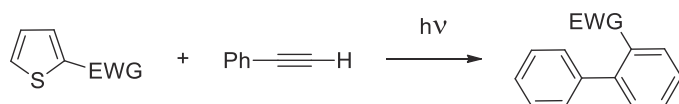
FIGURE 4.71 Photochemical substitution occurring with electron-withdrawing (EWG) substituents on thiophene in presence of phenylacetylene.
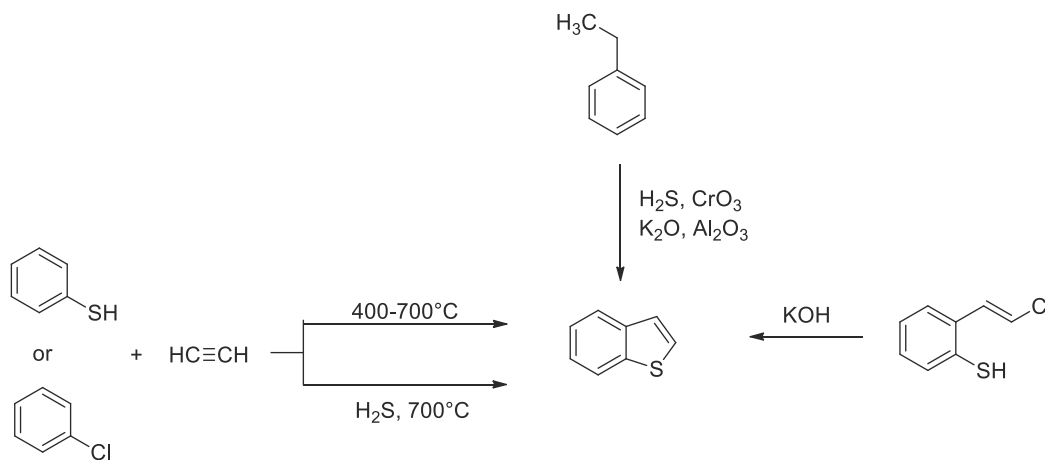
FIGURE 4.72   Intramolecular cyclization of α-mercapto-β-chlorostyrene.
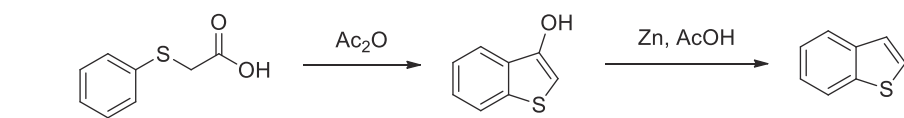
**FIGURE 4.73**   Intramolecular cyclization of aryl sulfides.
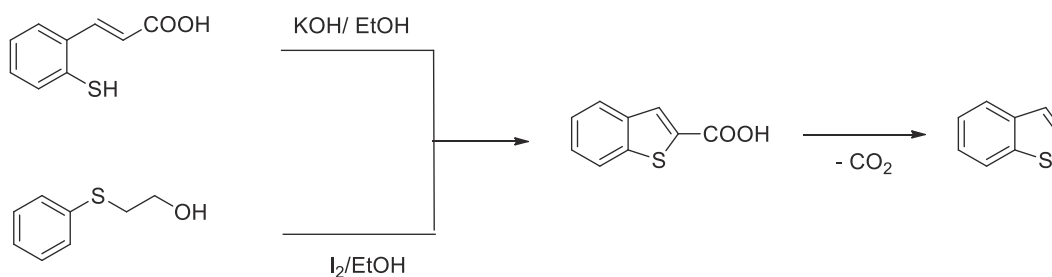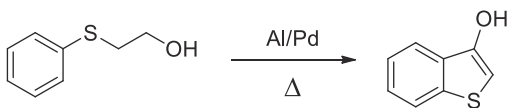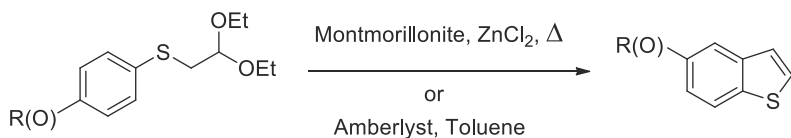
FIGURE 4.74   Oxidative cyclization of 2-mercaptocinnamic acid or of α-mercaptocinnamic acid.
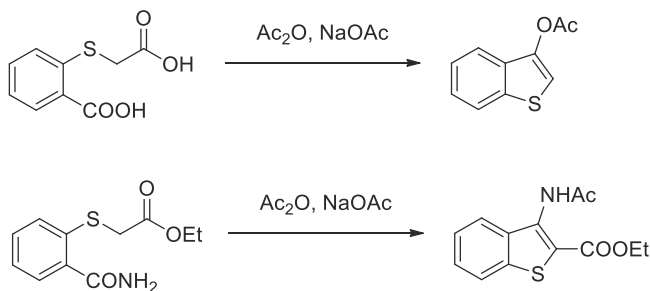
FIGURE 4.75   Dieckman-like condensation reactions.

and thiophene rings are planar, in benzothiophenes, all the carbon atoms are sp^2 hybridized. Dibenzo[*b,d*]thiophene was first synthesized in 1870 by Stemhouse by heating biphenyl with iron scrap. Depending on the nature of the oxidizing agent, it can be easily oxidized to corresponding sulfoxide and sulfone. As an example, the 3,7-diaminodibenzothiophene-5,5-dioxide is used as a dye and fluorescent whitener.

Synthesis of benzo[b]thiophene Benzo[*b*]thiophenes can be synthesized by a huge variety of strategies. Hereafter, have been reported just the main class of precursors and kind of cyclization strategies: (**a**) intramolecular cyclization of α-mercapto-β-chlorostyrene in alkaline medium (Fig. 4.72):
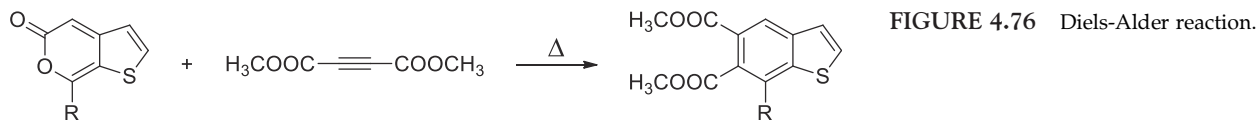

FIGURE 4.76   Diels-Alder reaction.
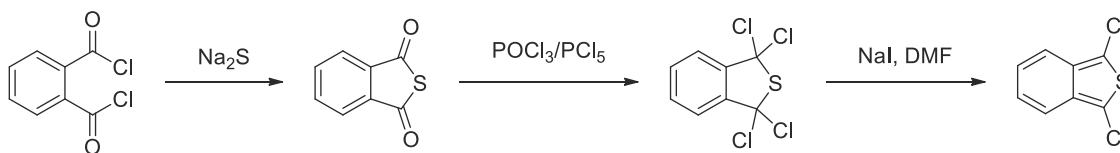
FIGURE 4.77   Three-steps synthethic pathway for the synthesis of benzo[c]thiophene.
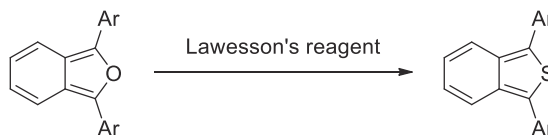
FIGURE 4.78   Synthesis of 1,3-diarylbenzo[*c*]thiophenes.
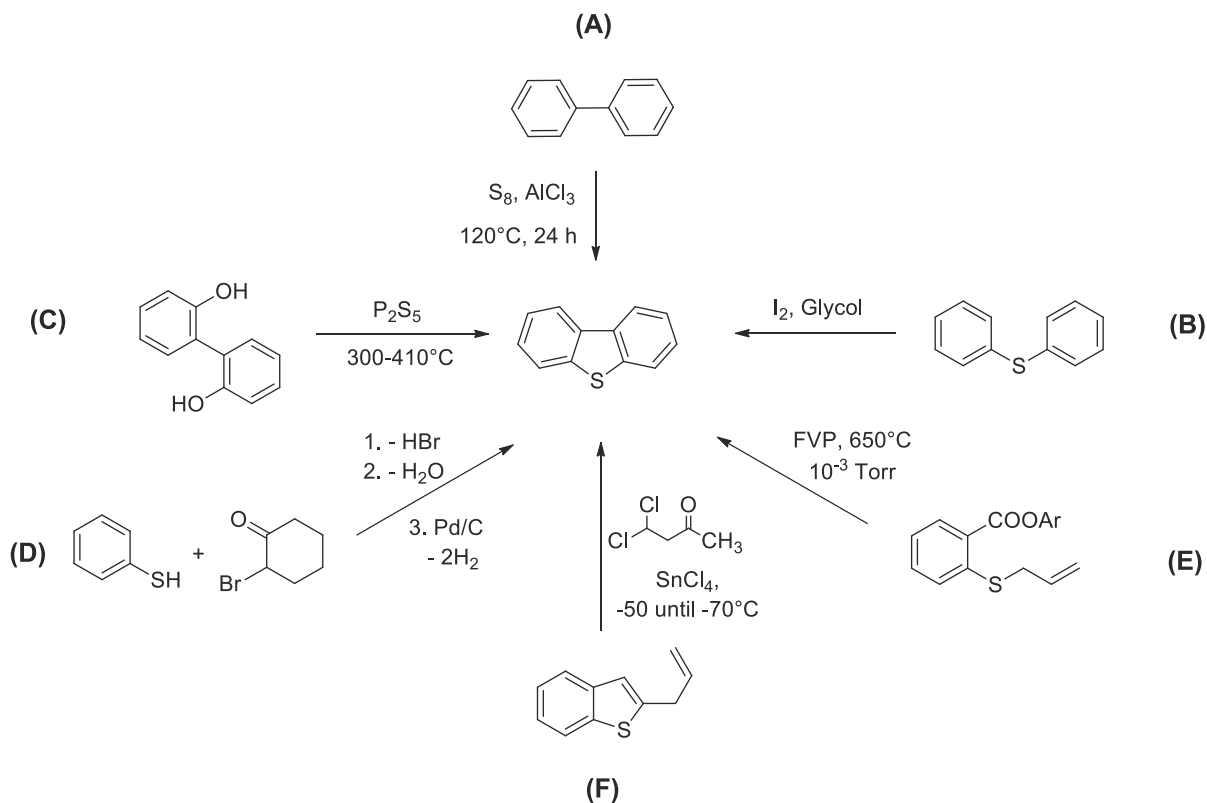
FIGURE 4.79   Synthetic stategies for unsubstituted dibenzo[*b,d*]thiophenes.

(b) intramolecular cyclization of aryl sulfides by different catalysts and reaction conditions (Fig. 4.73):

(c) oxidative cyclization of 2-mercaptocinnamic acid in alkaline solutions or of α-mercaptocinnamic acid in presence of iodine[142,143] (Fig. 4.74):

Dieckman-like condensation   Dieckman-like condensation of functionalized benzoic acids represents one of the synthetic strategies for the construction of 3-substituted benzo[*b*]thiophenes. As starting molecules, the 2-(carbox-ymethylthio)benzoic acid or, alternatively, the ethyl 2-(2-carbamoylphenyl)thioacetate by heating in presence of acetic anhydride and sodium acetate afford benzo[*b*]thiophen-3-yl acetate and ethyl 3-acetamidobenzo[*b*]thio-phene-2-carboxylate, respectively[144−146] (Fig. 4.75):

Diels-Alder reaction   The reaction of 2-alkylthieno[2,3-*c*]pyran-5-one with diethyl acetylenedicarboxylate in bromobenzene under reflux produces dimethyl 7-alkylbenzo[*b*]thiophene-5,6-dicarboxylate[147] (Fig. 4.76):

Synthesis of benzo[c]thiophene   One of the most useful reaction pathways to synthesize the benzo[c]thiophene con-sists of 3 steps. The first step is the formation of benzo[*c*]thiophene-1,3-dione from phthaloyl followed by a chlorination to 1,3-tetrachlorobenzo[*c*]thiophene finally treated with NaI in DMF to give the 1,3-dichlorobenzo[*c*]thiophene[148] (Fig. 4.77):

Another useful strategy to prepare 1,3-diarylbenzo[*c*]thiophenes is by replacing oxygen by sulfur in 1,3-diaryl-benzo[*c*]furan because of the Lawesson's reagent (Fig. 4.78):

Synthesis of dibenzo[b,d]thiophene   The unsubstituted dibenzothiophene can be synthesized following different methods as summarized in Fig. 4.79: **(A)** by heating a mixture of biphenyl with sulfur in presence of anhydrous AlCl₃[149]; **(B)** by oxidative cyclization of biphenyl sulfide in ethyleneglycol using iodine as catalyst[150]; **(C)** by heating a mixture of biaryl-2,2′-diol and P₂S₅ at 300°C−410°C[151]; **(D)** by condensation of thiophenol with 2-bromocyclohexanone afforded a substitution product which undergoes cyclization and the subsequent dehy-drogenation over Pd/C at 350°C[152] **(E)** by flash vacuum pyrolysis of aryl 2-(allylsulfanyl)benzoate at 650°C under reduced pressure[153]; **(F)** by intramolecular cyclization of 2-allylbenzo[b]thiophene in presence of dichloroacetone and SnCl₄ at low temperature.[154]
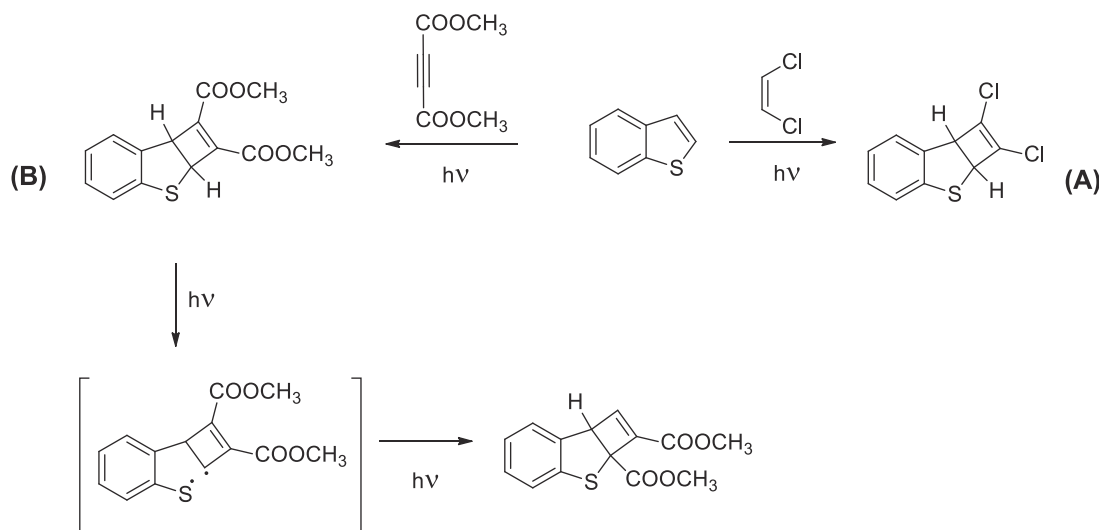

FIGURE 4.80 Photochemical cycloaddition of benzo[b]thiophene in presence of (A) dichloroethene and (B) dimethyl acetylenedicarboxylate.
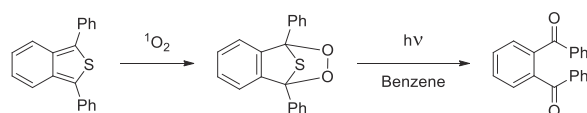

FIGURE 4.81   Photo-oxidation of 1,3-diphenylbenzo[c]thiophene.

Reactivity of benzo[b]thiophene Benzo[b]thiophenes tipically undergo photochemical cycloaddition with alkenes and alkynes bearing EWGs to give different cycloadducts. For example, by reaction of benzo[b]thiophene with the dichloroethene dienophile a mixture of cis- and trans-1,2-dichloro-1,2,2a,7b-tetrahydrobenzo[b]cyclobuta [d]thiophene (see Fig. 4.80(A)) is produced:

Similarly, the photochemical cycloaddition in presence of dimethyl acetylenedicarboxylate, at hν 300 nm, gives the same kind of product (i.e., dimethyl 2a,7b-dihydrobenzo[b]cyclobuta[d]thiophene-1,2-dicarboxylate) that, after subsequent irradiation by using the 366 nm light, undergoes a photochemical rearrangement yielding dimethyl 2,2a,7b-dihydrobenzo[b]cyclobuta[d]thiophene-2,2a-dicarboxylate (see Fig. 4.80(B)).

Reactivity of benzo[c]thiophene Photogenerated singlet oxygen provokes the photo-oxidation of 1,3-diphenyl-benzo[c]thiophene affording the dibenzoylbenzene as final product generated after the decomposition by sulfur elimination of an intermediate cycloadduct (Fig. 4.81):

FIGURE 4.82 Ru-catalyzed ring-closing metathesis of diallylated amines.

FIGURE 4.83 Copper and/or Rhodium catalyzed ring-closure reaction of terminal alkynes with tosyl azides and alkenyl alkyl ethers.

FIGURE 4.84 Insertion reaction of terminal-conjugated alkynes, primary amines and aldehydes.

FIGURE 4.85 Ring expansion reactions: (A) Paal-Knorr; (B) Van Leusen synthesis; (C) Barton-Zard reaction; (D) Piloty-Robinson synthesis.

4.2.3.1.5 Pyrrole

Pyrrole is a five-membered nitrogen containing heterocycle isolated from the distillation of coal tar, in 1834, for the first time by F.F. Runge. The nitrogen' lone pair of electrons participates to the delocalized 6π electron system contributing to its aromatic character.

Synthesis of pyrrole   Among the enormous number of synthetic strategies to prepare the pyrrole systems a selection of them is hereafter reported.

1. Catalytic and non-catalytic cyclization reactions

One general catalytic route to synthesize 3-substituted pyrroles proceeds by Ru-catalyzed ring-closing metathesis of diallylated amines yielding pyrrolines. The selective aromatization of these intermediates by FeCl$_3$ gives the corresponding final 3-substituted pyrrole product[155] (Fig. 4.82):

For the construction of polysubstituted pyrroles a general route starts from terminal alkynes reacting with tosyl azides and alkenyl alkyl ethers providing, in presence of Copper and/or Rhodium catalysts, α-imino rhodium carbene complexes, affording substituted pyrroles[156] (Fig. 4.83):

Instead, tetrasubstituted pyrroles can be easily prepared by a microwave assisted reaction of terminal-conjugated alkynes, primary amines and aldehydes[157] (Fig. 4.84):

2. Insertion reactions

Substituted pyrroles are commonly prepared by the Paal-Knorr reaction. It is a condensation of 1,4-dicarbonyl compounds with ammonia or primary amine[158] (see Fig. 4.85(A)). The Van Leusen synthesis is a reaction of tosyl-methyl isocyanide with an enone in presence of base provides a substituted pyrrole ring[159] (see Fig. 4.85(B)). Another way to prepare substituted pyrroles is the Barton-Zard reaction that is a 1,4-addition of nitroalkene to an isocyanoacetate followed by 5-*endo*-dig cyclization with elimination of the nitro group and tautomerisation[160] (see Fig. 4.85(C)). Furthermore, the Piloty-Robinson synthesis is a reaction between an aldehyde and hydrazine,
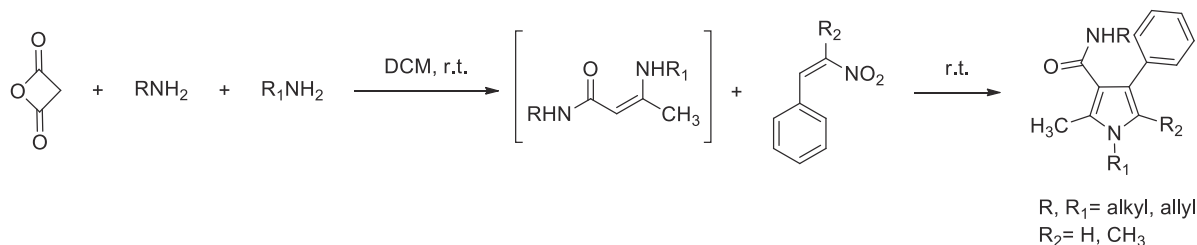

**FIGURE 4.86**   Ring expansion reaction of two primary amines and oxetane-2,4-dione.
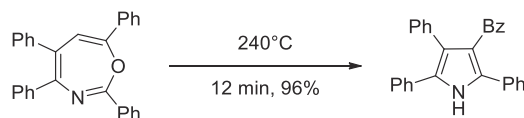
FIGURE 4.87   Thermal ring contraction of 1,3-oxazepines.
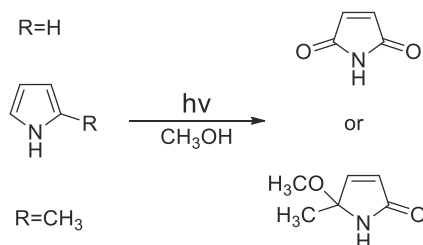

FIGURE 4.88   Photo-oxygenation reaction of functionalized pyrrole (upper side) and of 2-methylpyrrole (lower side).
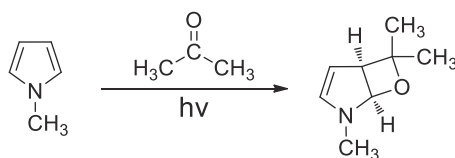
**FIGURE 4.89** Photo-induced reaction of 1-methylpyrrole in presence of aldehyde or ketones.
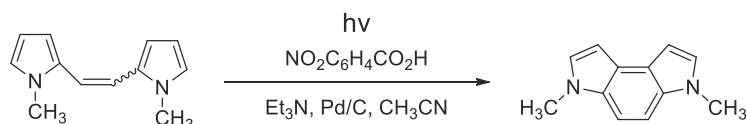
FIGURE 4.90 Photochemical annulation of pyrrole-based stilbenes analogs.
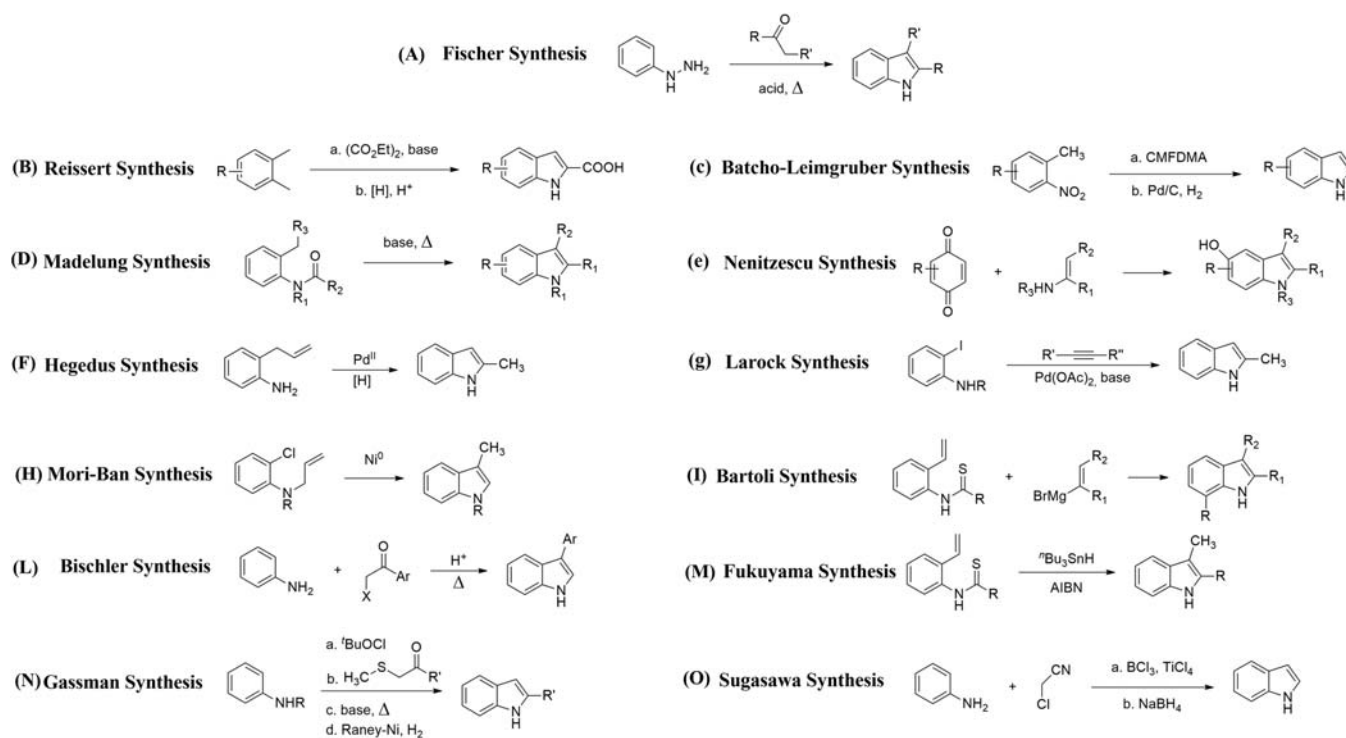

FIGURE 4.91 Summary of the main synthetic procedures for indole synthesis.

which forms diimine. After[3,3]-sigmatropic rearrangement this intermediate diimine provides a pyrrole deriva-tive[161] (see Fig. 4.85(D)).

3. Ring expansion reactions

Among the ring expansion strategies to prepare substituted pyrroles in good yields, there is the reaction of two primary amines and oxetane-2,4-dione. This reaction gives an intermediate enaminone which, in the pres-ence of nitrostyrene, provides pyrrole derivatives[162] (Fig. 4.86).

4. Ring contraction reactions

Tetrasubstituted aryl pyrroles can be obtained by thermal ring contraction of 1,3-oxazepines at 240°C[163] (Fig. 4.87):

Reactivity of pyrrole Functionalized pyrrole in presence of triplet oxygen undergoes photooxygenation reac-tion forming maleimide (upper side of Fig. 4.88). Instead, the photo-oxygenation of 2-methylpyrrole in methanol yields as a main product the 5-methoxy-5-methyl-Δ3-pyrrolin-2-one (lower side of Fig. 4.88).

On the contrary, the 1-methylpyrrole undergoes photo-induced reaction in presence of aldehyde or ketones forming as product the fused oxetane shown in Fig. 4.89:

Pyrrole-based stilbenes analogs undergo photochemical annulation in presence of dehydrogenating catalysts such as the Pd/C yielding the 3,6-dimethyl-3,6-dihydropyrrolo[3,2e]indole (Fig. 4.90):

4.2.3.1.6 Indole, isoindole, indolizine

Indole is a heterocyclic aromatic compound consisting of a pyrrole ring fused with a benzene ring. This compound is highly stable and is one of the most used building blocks for the synthesis of novel organic compounds. On the other hand, its isomers isoindole and indolizine are much less stable and are normally isolated when bonded to other stable compounds.

Fischer indole synthesis[164,165] was first discovered in 1883 by Emil Fischer, and represents the most general strategy for indole synthesis. It is an acid-catalyzed cyclization of aryl hydrazones obtainable from the condensation of aryl hydrazine and ketones with loss of water (see Fig. 4.91(A)).

Most of the synthetic strategies for indole preparation can be classified as condensation reactions: Reissert,[166] Leimgruber-Batcho,[167,168] Madelung,[169] Nenitzescu,[170] respectively sketched in Fig. 4.91(B−E). Among them, should be cited the metal catalyzed condensation reactions (i.e., Hegedus, Larock, Mori-Ban Synthesis, respectively sketched in Fig. 4.91(F−H)).

More synthetic strategies take advantages from vinyl Grignard reagents (Bartoli synthesis in Fig. 4.91I).[171]

The cyclization of 2-Arylaminoketones, obtained from the reaction of aryl amine with 2-haloketone, in presence of strong acid gives 2-aryl indoles (Bischler synthesis sketched in Fig. 4.91(L)).[172,173]
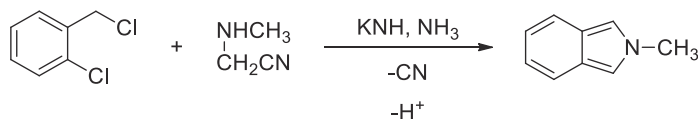

FIGURE 4.92 Aryne cyclization strategy for isoindoles synthesis.
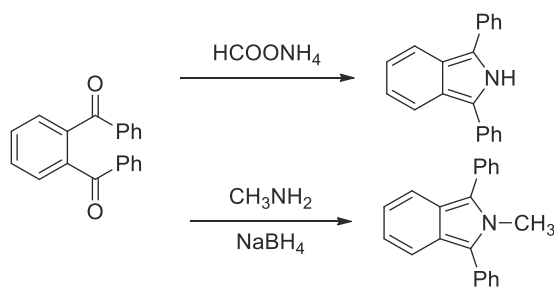
FIGURE 4.93 Condensations strategies of 1,3-dibenzoylbenzene for 1,3-diphenylisoindole synthesis.
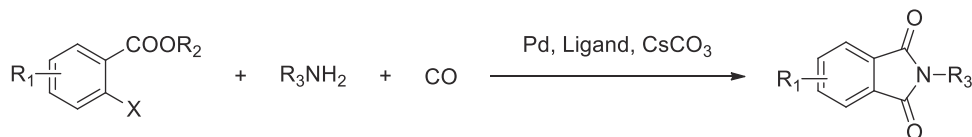

FIGURE 4.94 One-pot palladium-catalyzed aminocarbonylation of *o*-halobenzoates for the isoindole-1,3-diones synthesis.
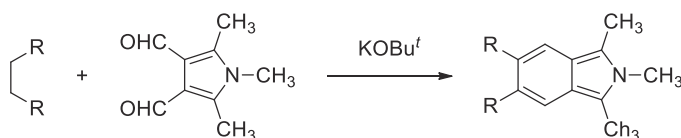
FIGURE 4.95 Condensation of 3,4-diformylpyrrole for the synthesis of the corresponding isoindole.

R= CN, COPh

Also a radical cyclization route of 2-alkenylthioanilides in presence of tributyltin hydride and a radical initiator is available for the construction of 2,3-disubstituted indoles (Fukuyama synthesis in Fig. 4.91(M)).[174]

The Gassman synthesis (Fig. 4.91(N)),[175] is the reaction of aniline and *tert*-butyl hypochlorite in dichloromethane (DCM) at −70°C giving the N-chloroaniline. This on reaction with β-ketosulfide in the presence of a base formed ylide, which on [3,2]-sigmatropic rearrangement followed by aromatization provides 2,3-disubstituted indole. The final hydrogenation of 2,3-disubstituted indole allows to remove the methylthio group to yield 2-methylindole.

The Sugasawa synthesis (Fig. 4.91(O)),[176] instead, starts from an *o*-chloroacetylated aniline, obtained by Friedel-Crafts reaction of aniline and chloroacetonitrile in presence of anhydrous BCl_3 and $TiCl_4$. Reductive cyclization of this intermediate by $NaBH_4$ delivered indoles.

Synthesis of isoindole Isoindoles can be synthesized by aryne cyclization strategy. Such an example, *N*-(2-chlorobenzyl)-N-methylacetonitrile reacts with potassium amide in liquid ammonia to give *N*-functionalized isoindole in high yields as shown in Fig. 4.92.[177]

1,3-Diphenylisoindole can be, instead, synthesized through condensation of 1,3-dibenzoylbenzene with ammonium formate. Similarly, when aryldiketones react with methylamine and sodium borohydride ($NaBH_4$) provide a reduction reaction which gives 1,3-diphenyl-N-methylisoindole as product (Fig. 4.93).[178]

A one-pot approach to the synthesis of isoindole-1,3-diones consists into the palladium-catalyzed aminocarbonylation of *o*-halobenzoates in very good yields.[179] Due to the high compatibility related to various common
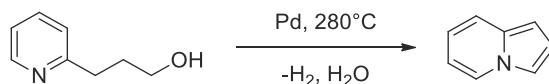

FIGURE 4.96   Intramolecular cyclization of functionalized pyridine.
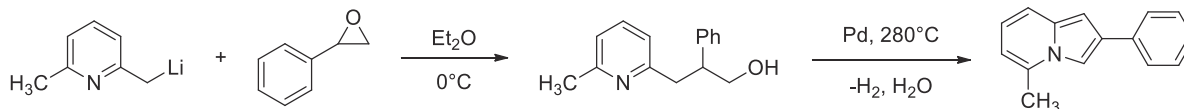

FIGURE 4.97   Oxidative cyclization of functionalized pyrrole.
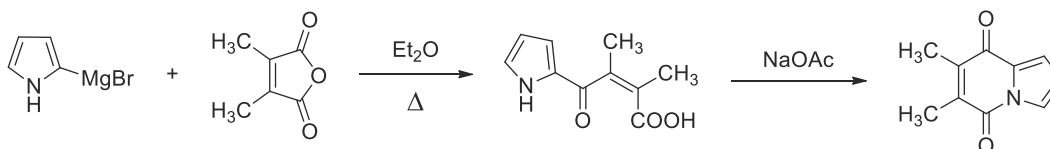

FIGURE 4.98   Reaction of pyrrole magnesium bromide with dimethylmaleic anhydride followed by the cyclization of the (Z)-2,3-dimethyl-4-oxo-4-(1H-pyrrol-2-yl)but-2-enoic acid intermiadate.
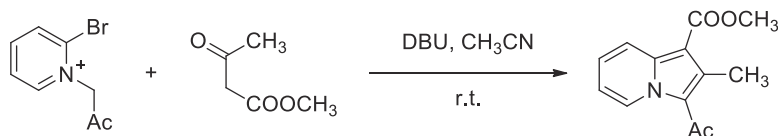

FIGURE 4.99   Reaction of 2-halopyridinium salts with β-ketoesters or α,β-diketones.
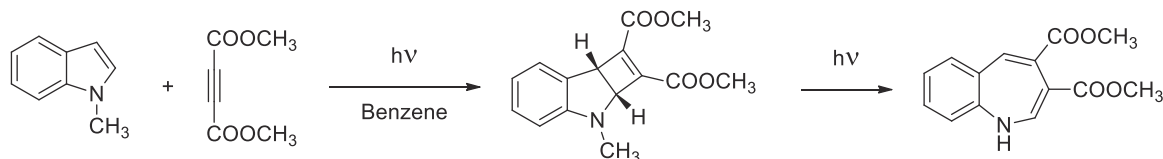

FIGURE 4.100   Photocyclization reactions of *N*-protected indoles.

functional groups, such as: methoxy, hydroxy, nitro and carbonyl groups, this strategy results to be more advantageous than other procedures (Fig. 4.94).

Furthermore, the condensation of 3,4-diformylpyrrole with succinonitrile or dibenzoylethane under basic conditions results in the formation of the corresponding isoindole as shown in Fig. 4.95.[180]

Synthesis of indolizine Indolizines can be synthesized by taking advantages from two main strategies hereafter described.

1. Intramolecular cyclization of functionalized pyridine

Among this strategy, one of the most efficient methods giving indolizines in 50% yields is represented by the intramolecular thermal oxidative cyclization of 3-(2-pyridyl)propan-1-ol in presence of palladium (Fig. 4.96).[181]

Instead, the oxidative cyclization, in ether at 0°C, of monolithiated 2,6-dimethylpyridine in presence of styrene oxide provides substituted indolizines (Fig. 4.97).

**2. Building a pyridene ring from functionalized pyrrole**
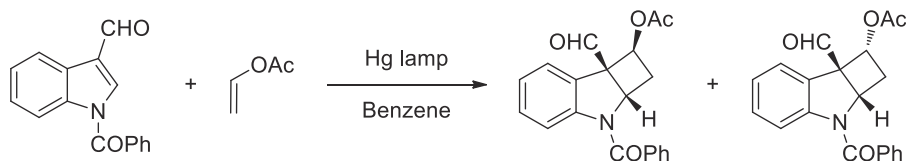
FIGURE 4.101 Photocyclization reaction of N-benzoyl-3-formylindole and vinylacetate.
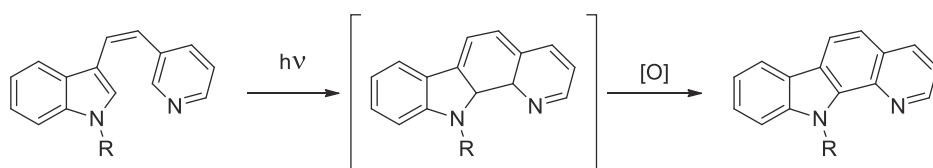
FIGURE 4.102 Photochemical [4 + 2] cycloaddition of indoles functionalized with an electron-rich diene.
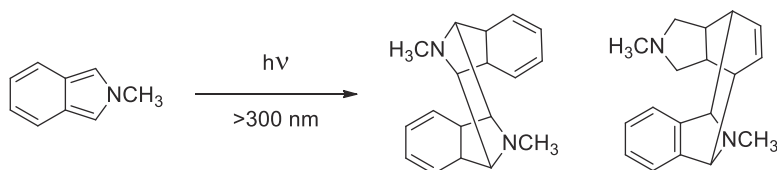
FIGURE 4.103 Photodimerization of 2-methylisoindole.

(A) Graebe-Ullmann Synthesis
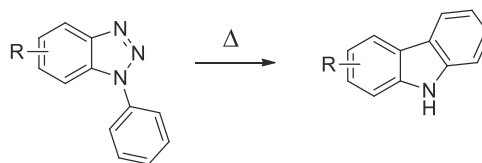
(B) Bucherer Synthesis


X= OH, NH$_2$
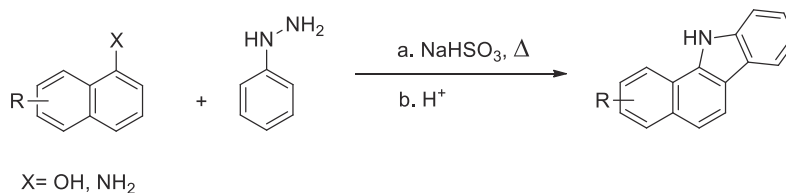
FIGURE 4.104 Graebe-Ullmann synthesis.

The reaction of pyrrole magnesium bromide with dimethylmaleic anhydride provides a (Z)-2,3-dimethyl-4-oxo-4-(1H-pyrrol-2-yl)but-2-enoic acid intermiadate that by cyclization with sodium acetate under reflux provides the indolizine ring system (Fig. 4.98).[182]

Another helpful method for the synthesis of indolizines consists into the reaction of 2-halopyridinium salts with β-ketoesters or α,β-diketones in presence of 1,8-diazabicyclo[5.4.0]undec-7-ene (DBU) (Fig. 4.99).[183]

Reactivity of indole Typically, N-protected indoles, under UV irradiation, undergo photocyclization reactions in presence of DMAD to give dimethyl 3-methyl-3,7b-dihydro-2aH-cyclobuta[b]indole-1,2-dicarboxylate. This intermediate under further irradiation gives dimethyl 1H-benzo[b]azepine-3,4-dicarboxylate as final product (Fig. 4.100).

N-Benzoyl-3-formylindole together with vinylacetate undergoes a photocyclization reaction that presumably proceed through biradical intermediate. As final product, this reaction gives the mixture of the two isomeric cyclobutylindoles shown in Fig. 4.101.[184]

The reaction of indoles functionalized with an electron-rich diene results into a photochemical [4 + 2] cycloaddition yielding a polycyclic heterocycle. As an extension, carbazole derivatives can be conveniently prepared by intramolecular photocyclization of indole-based stilbenes (Fig. 4.102).[185]

Reactivity of isoindole By irradiation with a high-pressure mercury lamp (>300 nm) of 2-methylisoindole in hexane the two dimeric products reported in Fig. 4.103 can be obtained.[186]

4.2.3.1.7 Carbazole

Synthesis of carbazoles Functionalized carbazoles can be prepared by Graebe-Ullmann synthesis[187]: the thermal decomposition of benzotriazole obtained from the diazotization of 2-aminodiphenylamine (Fig. 4.104(A)).
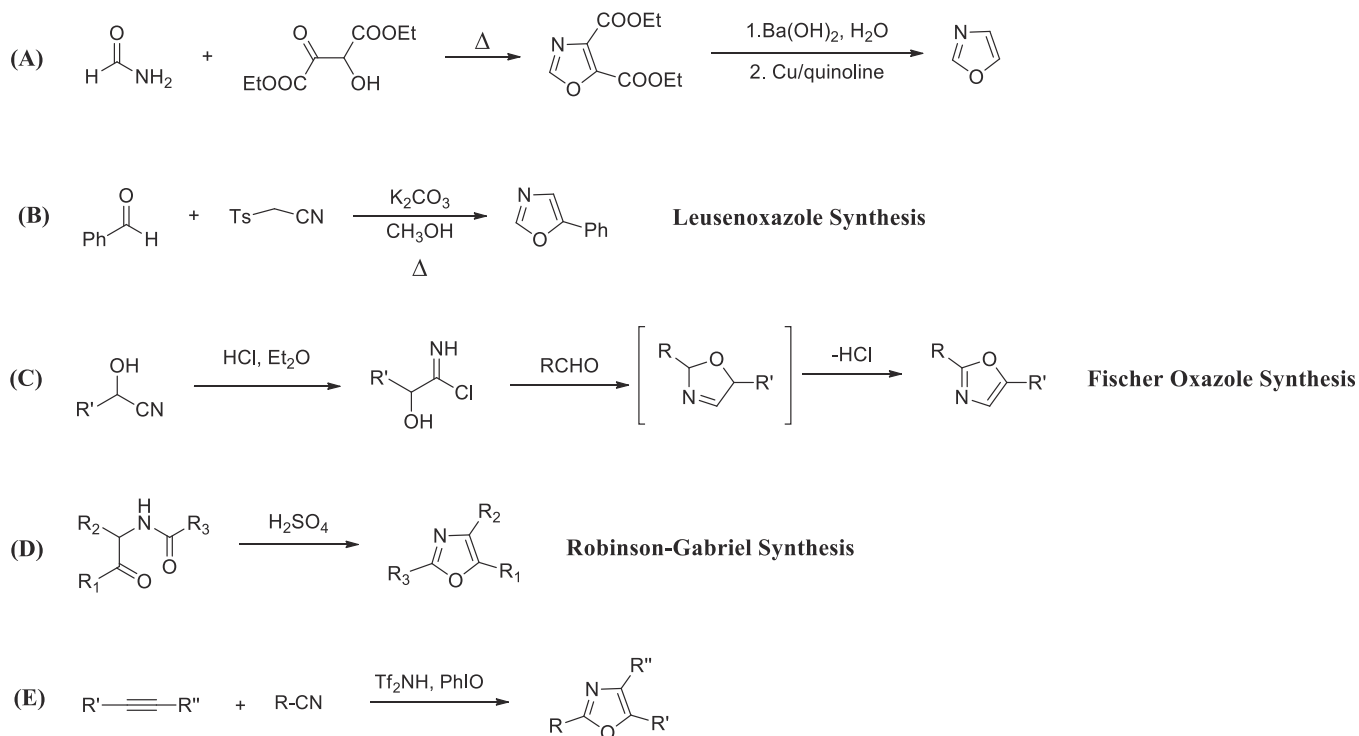

FIGURE 4.105 Intramolecular condensation reactions occurring in presence of dehydrating agents for the synthesis of oxazoles.
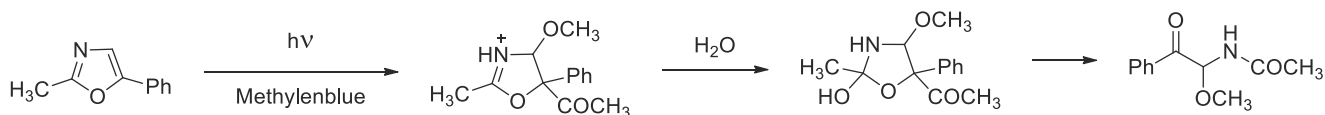

FIGURE 4.106 Photoinduced oxazol ring cleavage.

The strategy used to synthesize carbazoles from naphthols and aryl hydrazines by using sodium bisulfite is known as Bucherer synthesis (Fig. 4.104(B)).

4.2.3.2 Five-membered compounds with two heteroatoms

4.2.3.2.1 1,3-oxazole (oxazole)

Oxazole is a five-membered heteroaromatic system with one pyridine-like nitrogen and one oxygen atom, respectively, localized in correspondence of the 1,3-positions of the ring.

Synthesis of oxazole Many improvements have been reported for the synthesis of these molecules due to their large applications in different fields. As sketched in Fig. 4.105, the most used protocols yielding to the oxazole scaffold are typically based on intramolecular condensation reactions occurring in presence of dehydrating agents, starting from: **(A)** primary amides; **(B)** isocyanides (van Leusenoxazole synthesis); **(C)** cyanohydrins (Fischer Oxazole synthesis); **(D)** α-acylaminoketones (Robinson-Gabriel synthesis); **(E)** internal alkynes.
Furthermore, many other methodologies are also useful to synthesize these pharmaceutically important oxazole molecule.[188−190]

Oxazole reactivity Oxazole is a five-membered 6π delocalized electrons heteroaromatic system containing one nitrogen (behaving as a pyridine) and one oxygen (behaving as a furan) separated by methine (=CH).

Reaction with singlet oxygen The singlet oxygen generated in situ in presence of light plus a sensitizier, such as the methylene blue, is able to cleave the oxazole ring to obtain acyclic molecules (Fig. 4.106).[189]
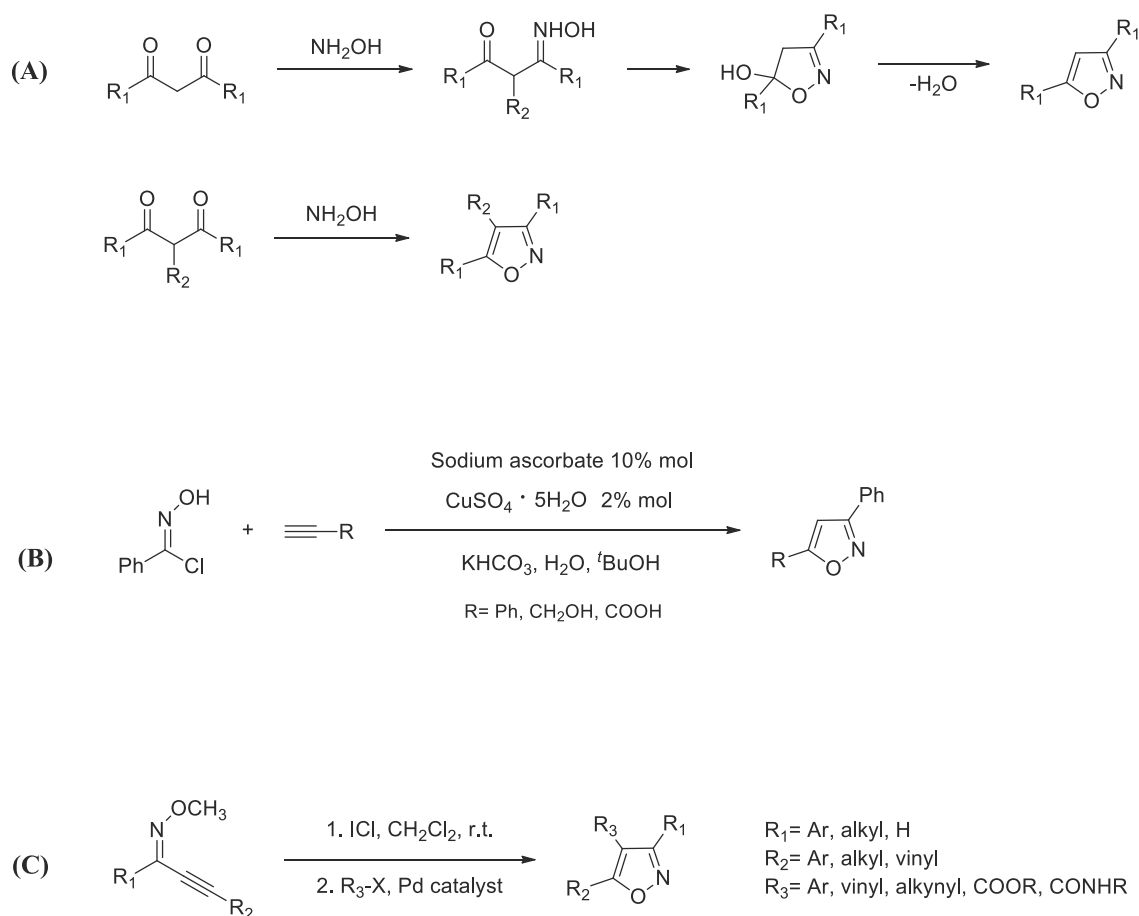

FIGURE 4.107 Main strategies for the synthesis of isoxazoles involving (A) 1,3 diketones with hydroxylamine; (B) nitrile oxides and terminal alkynes; (C) 2-alkynone O-methyl oximes.
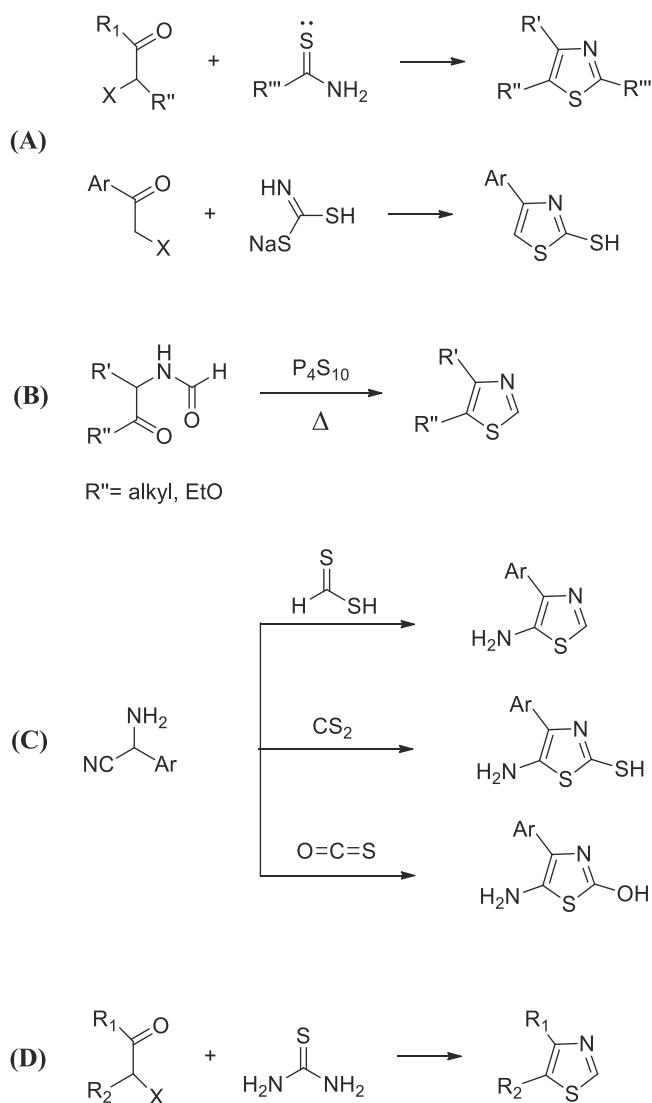
FIGURE 4.108   Main strategies for thiazole ring construction.
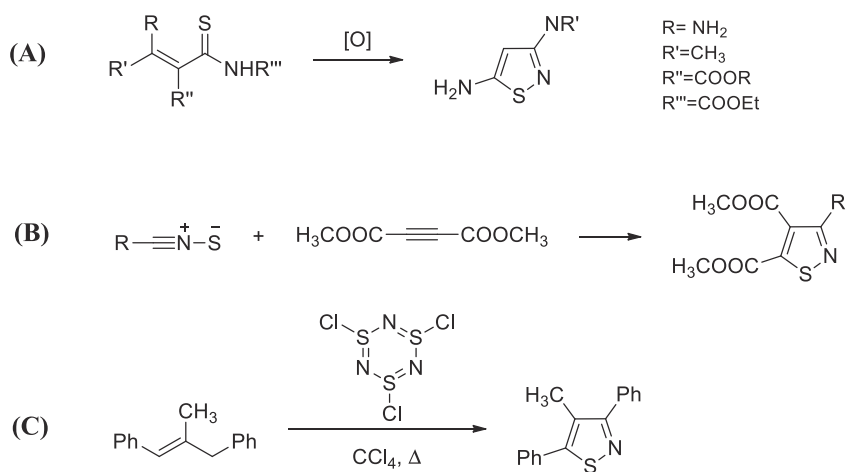
FIGURE 4.109   Main strategies for the synthesis of parent and substituted isothiazoles.

Photochemistry of Heterocycles

4.2.3.2.2 1,2-oxazole (isoxazole)

Isoxazoles are five-membered aromatic heterocycles containing three regular sp^2 carbon atoms and two heteroatoms: one nitrogen and one oxygen in a relative 1- and 2-position.

Synthesis of isoxazoles   These five-membered two heteroatoms ring systems can be easily prepared by using different methods. The main strategies are summarized in the following Fig. 4.107 involving: **(A)** 1,3 diketones with hydroxylamine; **(B)** dipolar [3 + 2] cycloadditions reactions of nitrile oxides and terminal alkynes[191,192]; **(C)** cycloisomerizations of adjacent heteroatoms such as 2-alkynone O-methyl oximes with a substrate such as ICl, I$_2$, Br$_2$, PhSeBr, etc.[193−196]

4.2.3.2.3 1,3-Thiazole (thiazole) and 1,2-thiazole (isothiazole)

Thiazole and isothaizole are five-membered, heteroaromatic systems containing one sulfur atom and one pyridine-type nitrogen atom, respectively, at 1,3- and 1,2-positions of the cyclic ring system.

Synthesis of thiazoles   There are numerous protocols for construction of the thiazole ring system. The most used synthetic routes are summarized in Fig. 4.108: **(A)** the first synthesis of thiazole derivatives has been reported by Hantzsch in 1887. It precedes by the reaction of α-haloketone or aldehyde with thioamide or alternatively with ammonium dithiocarbonate; **(B)** the Gabriel reaction of α-acylamino ketones or amino acetal with
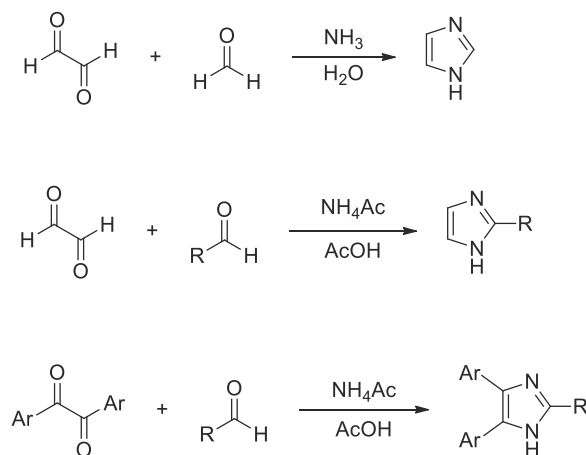


FIGURE 4.110   Radziszewski synthesis.
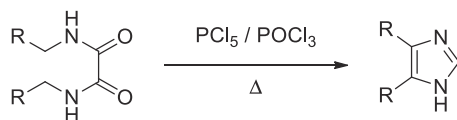

FIGURE 4.111   Wallach synthesis.
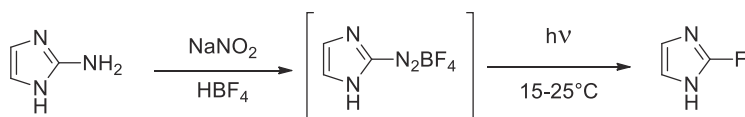
FIGURE 4.112   Diazotization of 2-aminoimidazole.
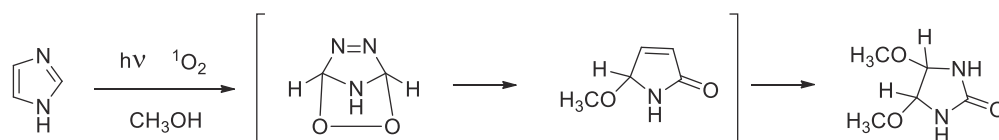
FIGURE 4.113   Photosensitized oxidation of imidazole.

P$_4$S$_{10}$ provides 2,5-disusbstituted thiazoles in good yields; **(C)** 5-amino thiazole can be prepared by Cook-Heilborn's synthesis starting from α-aminonitriles in presence, alternatively, of dithioacid or esters, CS$_2$ and carbonyl sulfide; **(D)** 2-aminothiazole can be synthesized by condensation of thiourea and α-haloketones or aldehyde.

A huge number of strategies are available for the synthesis of parent and substituted isothiazoles. Some important synthetic protocols are those reported in Fig. 4.109: **(A)** oxidative cyclization of acrylic acid amides; **(B)** 1,3-dipolar cycloaddition reaction; **(C)** condensation cyclization of propene derivatives.

FIGURE 4.114 Synthetic approaches for the synthesis of parent and substituted pyrazoles.

4.2.3.2.4 Imidazole

Imidazole is a five-membered, 6π electron ring system consisting of two nitrogen atoms at 1- and 3-ring positions. The nitrogen atom attached to hydrogen is a pyrrole type, participates in the π sextet and is less basic than the other one which is a pyridine-type nitrogen. It contributes only with one electron to the imidazole aromaticity leaving a lone pair in the sp^2 hybrid orbital which is responsible for its basic characteristic.

Synthesis of imidazoles Radziszewski synthesis[197] is the classical method for the synthesis of imidazole and mono-, di-, and trisubstituted imidazoles that consists into the condensation of 1,2-dicarbonyl compounds (i.e., α-ketoaldehyde, α-ketoketone) with aldehyde in the presence of NH_3/H_2O or $NH_4Ac/AcOH$ mixtures (Fig. 4.110).

Wallach synthesis represents another classical method for the preparation of imidazoles. It precedes through cyclization of *N,N'*-disubstituted oxamides obtaining 1-substituted 5-chloroimidazoles (Fig. 4.111).[198,199]

Reactivity of imidazoles

Fluorination 2-Aminoimidazole undergoes diazotization reaction with $NaNO_2$ and HBF_4 at $-5°C$ to $-10°C$ and the resulting imidazole diazonium fluoroborate intermediate after irradiation by a 450 W mercury lamp affords 2-fluoroimidazole as final product (Fig. 4.112):

Photooxidation Imidazole undergoes photosensitized oxidation in presence of singlet oxygen to deliver, passing through the cyclic peroxide as intermediate, the imidazolidin-2-one (Fig. 4.113):

4.2.3.2.5 Pyrazole

Pyrazole is a sp^2 hybridized five-membered heterocyclic system with 6π delocalized electrons and two adjacent nitrogen atoms having one lone pair of electrons each. One lone pair delocalized on the ring nitrogen connected with hydrogen participates in the aromatic sextet showing therefore nonbasic properties. Instead, the lone pair of electrons belonging to the nitrogen atom which is not part of the aromatic system extends in the plane of the ring and is responsible for the basicity of the molecule resembling amines.

Synthesis of pyrazoles Due to their wide therapeutic importance, a large variety of synthetic approaches have been developed for the preparation of parent and substituted pyrazoles which have been summarized in Fig. 4.114: **(A)** condensation of 1,3-diketones with hydrazine hydrate and aryl hydrazines yielding, respectively, 3,5-disubstituted and 1,3,5-trisubstituted pyrazoles[200]; **(B)** reaction of α-enones with substituted hydrazines
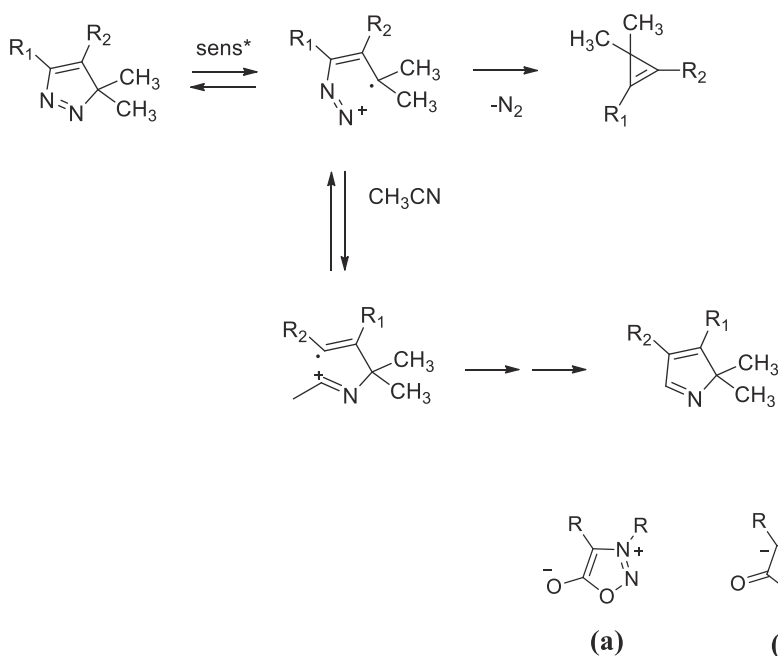

FIGURE 4.115   Photolysis reaction of dimethyl-3H-pyrazoles .

(a)   (b)

FIGURE 4.116   Sydnone (a) and sydnonimine (b) molecules.

and by condensation–cyclization of α-ynones with hydrazine hydrate[201,202]; **(C)** terminal alkyne reacts with N-alkylated tosylhydrazone affording 1,3,5-pyrazoles in very good yields, complete regioselectivity and compatibility of functional groups[203]; **(D)** ring transformation reactions starting from 3-Benzoyl-2-substituted 5-phenylfurans affording 4-benzoylmethyl-3(5)-phenylpyrazoles in moderate yields,[204] or from 3-acyl-2H-pyran-2,4-diones with phenylhydrazine give corresponding hydrazines, which on refluxing in acetic acid afford 5-pyrazolone derivatives[205]:

Reactivity of pyrazoles Dimethyl-3H-pyrazoles can be photolyzed in acetonitrile (see Fig. 4.115) in the presence of sensitizers such as 2,4,6-triphenylpyrylium tetrafluoroborate or 9,10-dicyanoanthracene. A 1,3-radical cation is obtained as intermediate forming cyclopropenes and 2H-pyrroles as solvent adducts after N_2 expulsion by cyclization and/or back electron transfer reactions.[206]
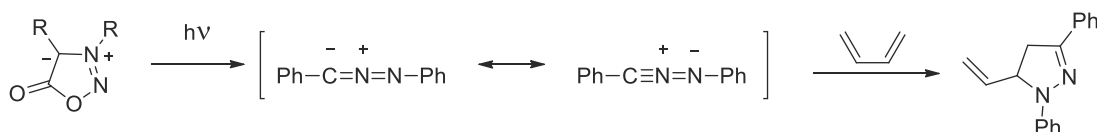

**FIGURE 4.117** Photochemically induced reaction of 1,3-dipolarophiles.
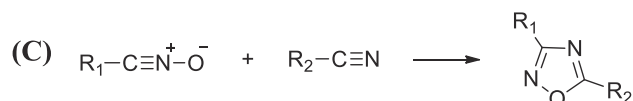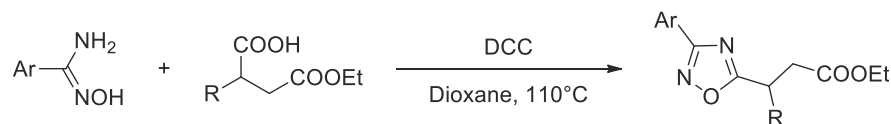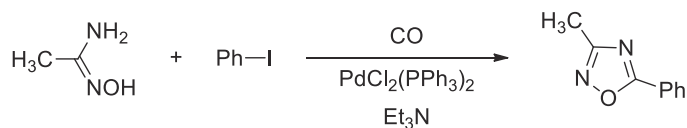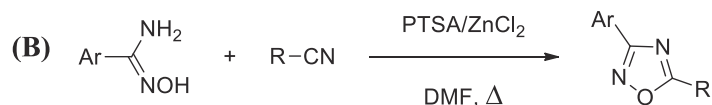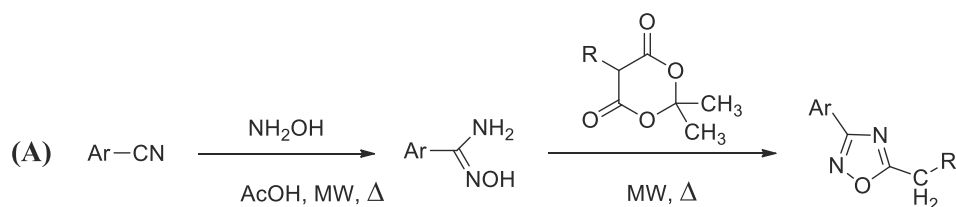
FIGURE 4.118 Main strategies to synthesize 3,5-disubstituted 1,2,4-oxadiazoles.

4.2.3.3 Five-membered compounds with three heteroatoms

There are numerous five-membered heterocycles characterized by three heteroatoms. Hereafter, the discussion will be focused on oxadiazoles (one oxygen and two pyridine type nitrogen atoms), and thiadiazoles (one sulfur and two pyridine type nitrogen atoms) systems. Depending on the position of nitrogen atoms in the ring, four possible regioisomeric structures can be derived for oxadiazoles and thiadiazoles. Anyway, the stability of the ring depends not only on the position of heteroatoms but also on the properties of the substituents functionalizing the ring.
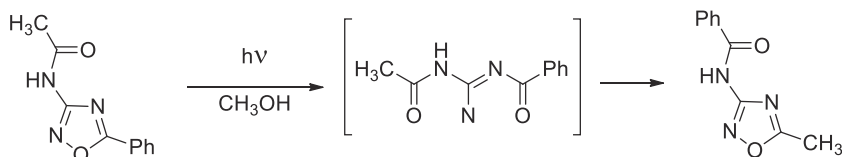
FIGURE 4.119 Photochemical reaction of 1,2,4-oxadiazoles.
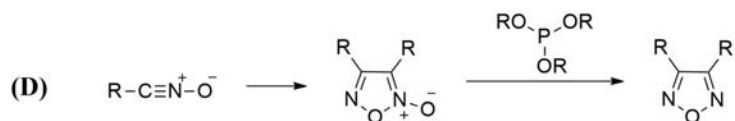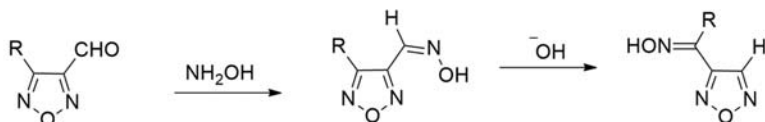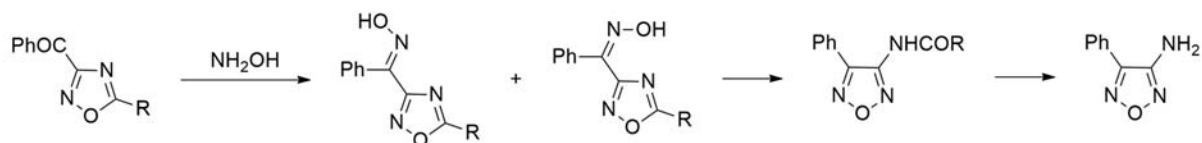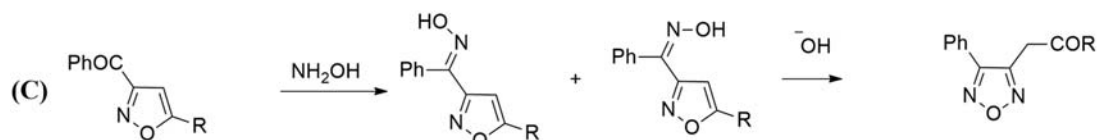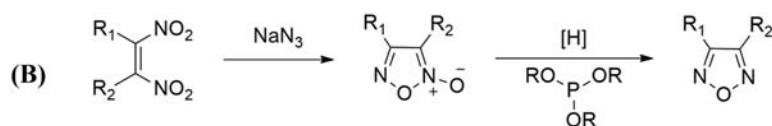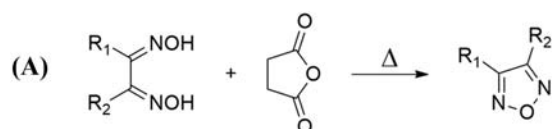
FIGURE 4.120 Summary of the main strategies to synthesize 1,2,5-oxadiazoles.

4.2.3.3.1 1,2,3-Oxadiazole

1,2,3-Oxadiazole is a cyclic unstable five-membered heteroaromatic system with one oxygen atom and two pyridine-type nitrogen atoms linked consecutively (i.e., O-N-N). 1,2,3-Oxadiazole quickly isomerizes to give the open chain structure (i.e., α-diazoketone).[207]

Anyway, two stable 1,2,3-oxadiazole ring systems have been isolated: sydnone (Fig. 4.116(A)) and sydnonimine (Fig. 4.116(B)).

Photochemistry of 1,2,3-oxadiazoles   3,4-Diphenylsydnone can be involved in photochemically induced reactions giving the 1,3-diphenyl-5-vinylpyrazole as final product in presence of 1,3-dipolarophiles such as 1,3-butadiene (Fig. 4.117).[208]

4.2.3.3.2 1,2,4-Oxadiazole

1,2,4-Oxadiazole is a five-membered, conjugated aromatic heterocyclic system comprised of one oxygen atom and two pyridine-like nitrogen atoms at positions 2 and 4 of the oxadiazole ring. Due to the instability of the parent 1,2,4-oxadiazole molecule, its synthesis has been reported only in 1962; while, the preparation of substituted 1,2,4-oxadiazole ring systems has been first reported in 1880.

Synthesis of 1,2,4-oxadiazole   The main strategies to synthesize 3,5-disubstituted 1,2,4-oxadiazoles foresee, as summarized in Fig. 4.118, to take advantage from: **(A)** nitriles through a one-pot synthesis occurring in presence of hydroxylamine and Meldrum's acid under microwaves[209]; **(B)** amidoximes in presence, for example, of organic nitriles,[210] succinic anhydride,[211] or 4-ethoxy-2-alkyl-4-oxobutanoic acid[212]; **(C)** 1,3-dipolar cycloadditions between organic nitrile oxide and nitrile.[213]

Reactivity of 1,2,4-oxadiazole

Photochemical reactions of 1,2,4-oxadiazoles   Photochemical intramolecular rearrangement through the cleavage of N−O bond can occur on 1,2,4-oxadiazoles with NCO substituent (Fig. 4.119)[214,215]:

4.2.3.3.3 1,2,5-Oxadiazole

1,2,5-Oxadiazole is a heteroaromatic five-membered heterocycle containing two nitrogen atoms and one oxygen atom in the between (N−O−N).
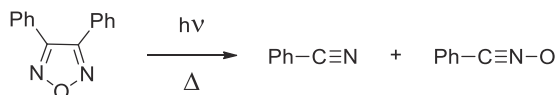

**FIGURE 4.121**   Photochemical bonds cleavage in 1,2,5-oxadiazoles.
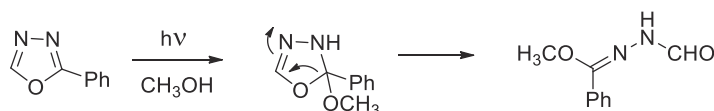
**FIGURE 4.122**   Photolysis of 1,3,4-oxadiazoles.
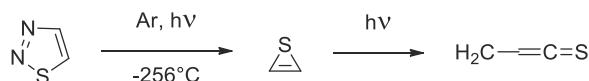
FIGURE 4.123   Photolysis of parent and substituted 1,2,3-thiadiazoles.
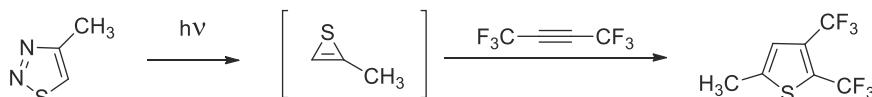

FIGURE 4.124   Photolysis of 4-methyl-1,2,3-thiadiazole.

Synthesis of 1,2,5-oxadiazole The principal way to prepare 1,2,5-oxadiazole are sketched in the following Fig. 4.120 and can be rationalized as follows: **(A)** dehydration of glyoxaldioxime by heating with $SOCl_2$ as a dehydrating agent; **(B)** deoxygenation of 1,2,5-oxadiazol-5-oxide followed by reduction of 1,2,5-oxadiazole-2N-oxide with trialkylphosphite providing alky, aryl, acyl, cyano, and amino groups containing 1,2,5-oxadiazoles, and **(C)** Boulton-Katritzky rearrangement[216,217] that is a ring transformation reaction involving oximes deriving from oxazoles (i.e., 3-acylisoxazoles) or oxadiazoles (i.e., 3-acyl-1,2,4-oxadiazoles and 3-acyl-1,2,5-oxadiazoles) occurring in thermal or base-catalyzed conditions; **(D)** dimerization of nitrile oxide and the subsequent deoxygenation with trialkylphosphite affords 3,4-disubstituted 1,2,5-oxadiazoles.[218]

Photochemical ring cleavage of 1,2,5-oxadiazole 1,2,5-Oxadiazoles undergo photochemical reaction providing mixtures of nitrile and nitrile oxide reaction products by the cleavage of O_1-N_2 and C_3-C_4 bonds. For example, as shown in Fig. 4.121 the photolysis of 3,4-diphenyl-1,2,5-oxadiazole provides benzonitrile and benzonitrile oxide as products:

4.2.3.3.4 1,3,4-Oxadiazole

Photolysis of 1,3,4-oxadiazoles 2-Phenyl-1,3,5-oxadiazole undergoes photolysis at 300 nm in methanol. This reaction proceeds through a regioselective addition of the methoxy group to the C_2-position of the ring. The resulting intermediate provides the 1-(α-methoxybenzylidene)-2-formylhydrazine as final product obtained through a ring opening reaction (Fig. 4.122)[219]:
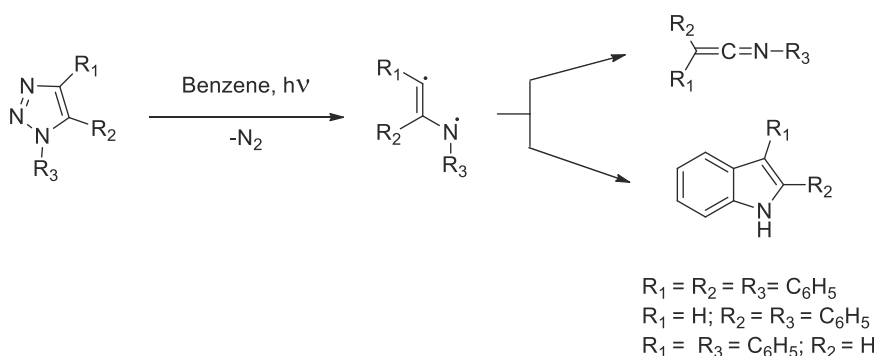
FIGURE 4.125 Potochemical decomposition of 1H-1,2,3-triazole derivatives.

$R_1 = R_2 = R_3 = C_6H_5$
$R_1 = H; R_2 = R_3 = C_6H_5$
$R_1 = R_3 = C_6H_5; R_2 = H$
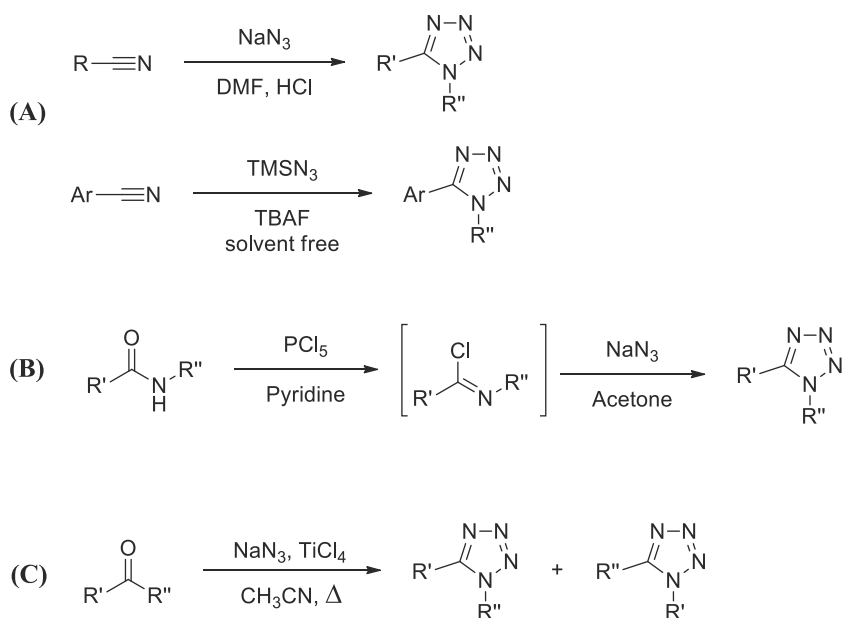
FIGURE 4.126 Synthetic protocols for the synthesis of tretrazole substituted rings.

4.2.3.3.5 1,2,3-Thiadiazole

1,2,3-Thiadiazole is a five-membered conjugated heteroaromatic, containing one sulfur atom and two nitrogen atoms. There are four possible regioisomeric structures depending on the relative position of heteroatoms, but in the following discussion we will focus on the regioisomer characterized by the following relative heteroatoms position: S−N−N.

Thermal and Photochemical Reactions Photolysis of parent and substituted 1,2,3-thiadiazoles provides thiirene which, after a photo-assisted rearrangement yields the final thioketene (Fig. 4.123).[220]

Photolysis of 4-methyl-1,2,3-thiadiazole allow the formation of 2-methyl thiirene as an intermediate. The trapping of this intermediate with hexafluoro-2-butyne allows to form the reaction product shown in Fig. 4.124.[221]

4.2.3.3.6 1H-1,2,3-triazole

1,2,3-Triazole is an aromatic five-membered heterocycle with 6π available electrons delocalized on the ring. It is comprised of three nitrogen atoms: one pyrrole type and two pyridine types.

FIGURE 4.127 Photochemical reaction of 5-phenyl-2H-tetrazole.

52%   21%   8%

FIGURE 4.128 Main synthetic strategies for the synthesis of pyridines.

Reactivity of 1H-1,2,3-triazole   The photochemical decomposition of 1H-1,2,3-triazole derivatives[222] provides two products in different ratios depending on the substituents: a ketenimine and a substituted indole passing through a common radical intermediate shown in Fig. 4.125:

4.2.3.4 Five-membered compounds with four heteroatoms

4.2.3.4.1 Tetrazole

Tetrazole is a five-membered heterocycle characterized by 6π electrons delocalized over the ring. Tetrazole presents four nitrogen atoms (three pyridine-like, one pyrrole-like) and one carbon atom at the 5-position of the ring.

Synthesis of tetrazole   There are several synthetic protocols useful to build tretrazole substituted rings, most of them are summarized in Fig. 4.126. The most used strategy for the synthesis of tetrazole derivatives is reported in Fig. 4.126(A). It can be conducted by following two different reaction conditions: the reaction of NaN_3 (sodium azide) with nitriles or, alternatively, the reaction of aryl nitrile with trimethylsilyl azide ($TMSN_3$) providing the 5-phenyl-1H-tetrazole product.[223] Another useful synthetic strategy for 5-substituted tetrazoles is shown in Fig. 4.126(B) and consists in the two steps reaction of secondary amides. The first step, is the reaction with PCl_5 or $SOCl_2$, providing the imidoyl chloride intermediate, and the second step is a treatment with NaN_3 allowing the cyclization to give the final product.[224,225] Furthermore, mixture of positional isomers of 1,5-disubstituted 1H-tetrazoles can be prepared by reaction of ketones with NaN_3 in the presence of $TiCl_4$ as shown in Fig. 4.126(C)[226]:

Reactivity of Tetrazole   5-Phenyl-2H-tetrazole by irradiation at 254 nm in THF undergoes a photochemical reaction producing the products shown in Fig. 4.127: 3,6-diphenyl-1,2-dihydro-1,2,4,5-tetrazine (52%), 3,6-diphenyl-1,2,4,5-tetrazine (21%), 3,5-diphenyl-1,2,4-triazole (8%), and benzonitrile.[227,228]

4.2.4 Six-membered heterocycles

4.2.4.1 Six-membered compounds with one heteroatom

4.2.4.1.1 Pyridine

Pyridine is a six-membered heterocycle consisting of one nitrogen and five carbon atoms isolated in 1849 by Thomas Anderson within the constituents of bone oil.

Synthesis of pyridine   Many different synthetic methods giving pyridines are known, some of these are discussed hereafter and shown in detail in Fig. 4.128(A−E): **(A)** Ciamician-Dennstedt rearrangement represents a [2 + 1] cycloaddition reaction starting from pyrrole in presence of dichlorocarbene and sodium chloroacetate


FIGURE 4.129   Photolysis of pyridine.

FIGURE 4.130   Thermal and photochemical reaction of pyridine.

(basic environment) yielding a bicyclic intermediate that after elimination of hydrogen chloride produces 3-chloropyridine as final product[229−231]; **(B)** Krohnke synthesis of pyridine derivatives is a reaction occurring typically between α-pyridinium methyl ketone salts and α,β-unsaturated carbonyl compounds[232]; **(C)** Bohlmann-Rahtz allows the synthesis of trisubstituted pyridine derivatives through a cycloaddition reaction reported for the first time by H. Bohlmann and D. Rahtz[233] involving a Michael addition of ethynyl ketone with enamine; **(D)** Guareschi synthesis of pyridine derivatives proceed by a condensation reaction of a primary amide with acetoacetic ester in presence of ammonia[234,235]; **(E)** Chichibabin pyridine synthesis[236−238] relates with an under pressure condensation of a aldehyde, ketone or α,β-unsaturated carbonyl compound with ammonia.

Reactivity of pyridine

Photolysis of pyridine   Photochemical reaction of pyridine at 254 nm in butane solution led to the formation of Dewar pyridine sketched in Fig. 4.129. If the irradiation of this product is prolonged in aqueous sodium borohydride solution it undergoes a reduction of one double bond yielding the stable 2-azabicyclo[2.2.0]hex-5-ene bicyclic compound. On the contrary, hydration (addition of water across the imine double bond) takes place if the Dewar pyridine is irradiated in water only. Subsequently, the hydrated Dewar pyridine intermediate, being unstable, undergoes a ring-opening process giving the 5-amino-2,4-pentadienal final product.

4.2.4.2 Six-membered compounds with two heteroatoms

4.2.4.2.1 Pyridazine, pyrimidine, pyrazine

Pyridazine, pyrimidine and pyrazine are two nitrogen atoms containing six-membered heterocycles that can be considered, respectively, isomeric 1,2-, 1,3- and 1,4-diazines. Unsubstituted pyridazine has been first synthesized by Tauber.[239] Pyrimidine is also known as 1,3-diazabenzene since it contains two nitrogen atoms at the 1,3-positions of the six-membered aromatic heterocycle. Among the three isomers, pyrazine is the symmetrical compound containing two nitrogen atoms at the 1,4-positions.

Thermal and photochemical reaction   Pyridazine can be converted both to pyrimidine or pyrazine depending on the treatment of which it is affected. In fact, by heating at high temperature (300°C), pyridazine is converted to pyrimidine via a diazabenzvalene intermediate. On the other hand, photolysis of pyridazine converts this molecule to pyrazine passing through a transient Dewar benzene-like intermediate as shown in Fig. 4.130:

4.2.4.3 Six-membered compounds with three heteroatoms

4.2.4.3.1 Triazines: 1,2,3-triazine, 1,2,4-triazine, 1,3,5-triazine

Triazines are three nitrogen atoms containing six-membered heterocycles that can be considered, analogous of benzene in which three carbon atoms are replaced by three consecutive nitrogen atoms. Depending on the relative positions of these three nitrogen over the six-membered ring, three isomeric compounds can be distinguished by using the following systematic names: 1,2,3-triazine, 1,2,4-triazine, and 1,3,5-triazine.
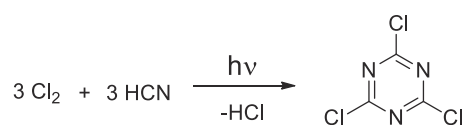

FIGURE 4.131   Photochemical synthesis of 2,4,6-trichloro-1,3,5-triazine.
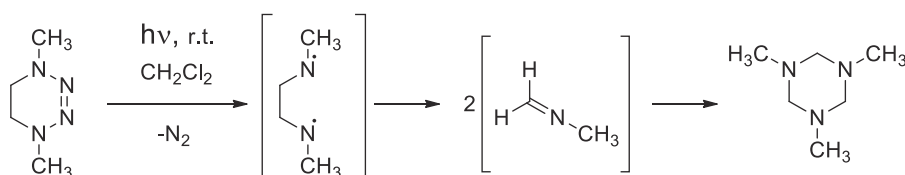

FIGURE 4.132   Photochemical reaction of 1,4-dimethyl-1,4,5,6-tetrahydro-1,2,3,4-tetrazine.

2,4,6-Trichloro-1,3,5-triazine can be prepared by treatment with cyanuric chloride (starting from chlorine and hydrocyanic acid) exposed to the direct sunlight (Fig. 4.131).[240]

4.2.4.4 Six-membered compounds with four heteroatoms

4.2.4.4.1 Tetrazines: 1,2,3,4-tetrazine, 1,2,3,5-tetrazine, 1,2,4,5-tetrazine

Tetrazines are six-membered heterocycles in which the four C-H units of benzene are replaced by four nitrogen atoms. The three main possible isomers of tetrazines are the following: 1,2,3,5-tetrazine, 1,2,3,4-tetrazine, and 1,2,4,5-tetrazine.

Photochemical reaction 1,4-Dimethyl-1,4,5,6-tetrahydro-1,2,3,4-tetrazine undergoes photochemical reaction yielding to the final 1,3,5-trimethyl-1,3,5-triazinane product. This photochemical reaction passes through the two intermediates shown in Fig. 4.132: the first one is the biradical intermediate and then trough the formaldehyde N-methylimine which, probably due to trimerization, produces the corresponding triazinane product.[241]

4.3 Applications and technology of the main classes of heterocyclic photoactive compounds

4.3.1 Heterocyclic conjugated backbones for efficient emerging organic photovoltaics

Organic solar cells (OSCs) based on organic semiconducting materials have been introduced since 1958 by Calvin[242] and co-workers and have attracted significant attention in the last 30 years. Today, the third-generation of solar cells represents the most concrete possibility for converting solar light into electricity, maintaining a satisfactory compromise between low manufacturing costs, low weight, flexibility, solution processability, printability, and high efficiency of the resulting panels.[243−249]

Polymer- and small-molecules-based OSCs are currently the most widely studied systems by the scientific community. These devices are substantially based on hybrid or polymeric/small-molecule materials acting as semiconductors and exciton carriers.

Furthermore, among all kinds of solar cells architectures, bulk heterojunction (BHJ) devices have showed to improve the power conversion efficiencies (PCE) of both polymer and small-molecule OSCs due to the increase of the interface between electron-donor (D) and electron-acceptor (A) by the mixing of properly designed molecules.

However, the device performance depends on many other factors in addition to the nature of the donor and acceptor components, including their D:A ratio, the processing and annealing conditions, the choice of electrode and interlayer materials and the device architecture, for example, whether conventional or inverted. Furthermore, the control of the distribution of the D and A components onto the substrate has been revealed to be fundamental since their random spread might lead to charge trapping in the pathways to the electrodes.

4.3.1.1 Organic solar cell device' major architectures: planar heterojunction (PHJ) vs bulk heterojunction

An OSC device can be fundamentally made by two different kind of architectures depending on the type of interaction occurring between the organic photoactive semiconductors involved in the device. In the beginning, the Planar Heterojunction (PHJ) architecture has been much used for OSCs. The main drawback of this PHJ architecture is the exciton length diffusion so short that only the exciton near the D/A interface can have chance to reach it.
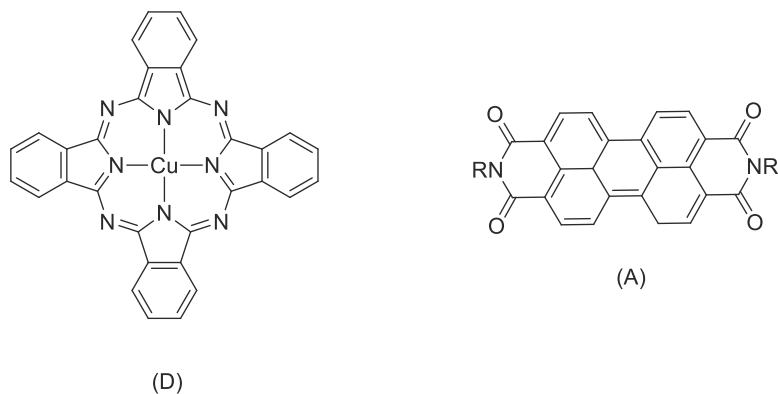

FIGURE 4.133 Phthalocyanine (D) and perylene moiety (A) structures.

(A)

(D)
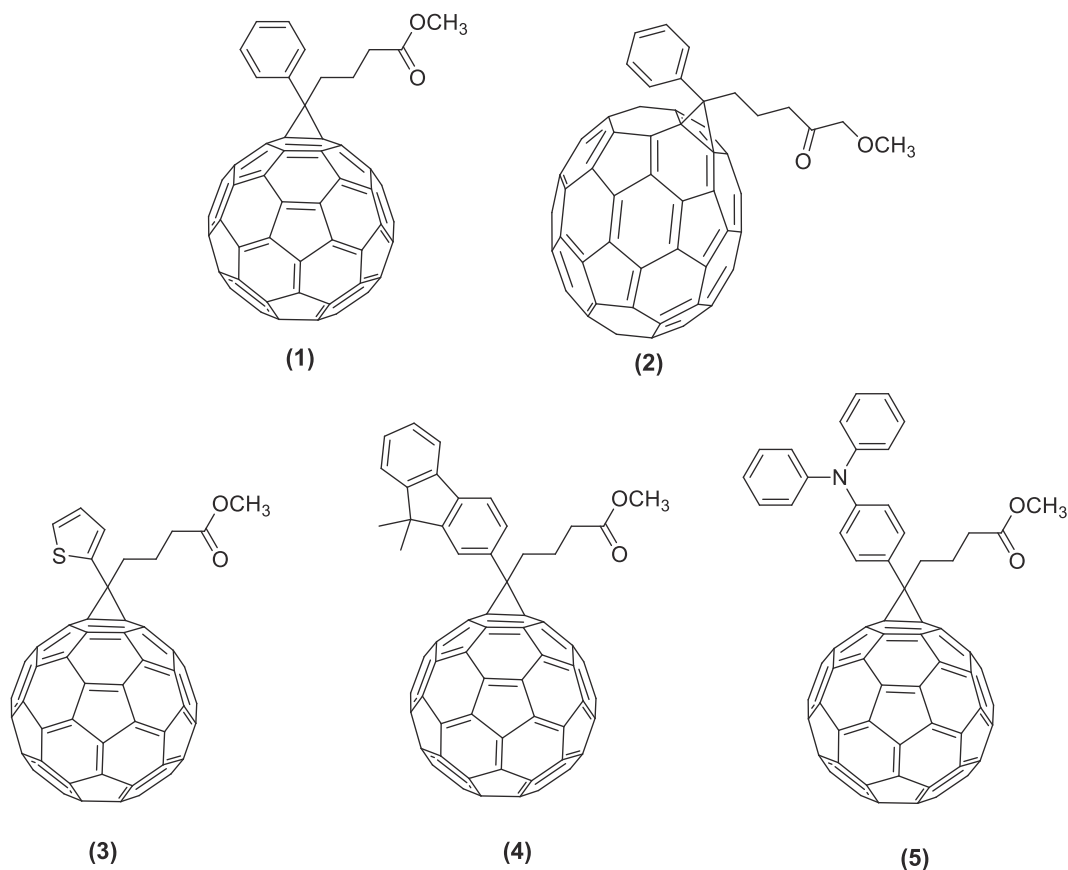
FIGURE 4.134 $PC_{61}BM$ (1) and $PC_{70}BM$ (2) structures shown together with some PCBM derivatives containing different functional moieties such as: thiophene (3); fluorene (4); or triphenylamine (5) substituents.
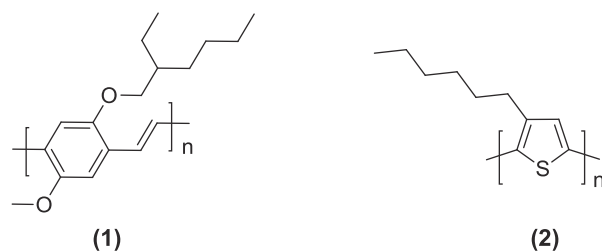

FIGURE 4.135 MEH-PPV (1) and P3HT (2) polymers.

Instead, the BHJ architecture for OSCs allows to overcome the problem because of the different way in which the active layer is made[243,250,251]: the donor and the acceptor are blended together by a co-deposition. This blending produces two main effects: (i) a large increase in the interfacial area compared to the PHJ and (ii) from any point within the active D-A layer the exciton experiences a relatively short distance to reach charge-separation at the interface.[252]

The first useful PHJ, reaching a PCE of 1%, was composed of an active layer represented by a donor (i.e., a phthalocyanine) and an acceptor layer (i.e., a perylene moiety) shown respectively in Fig. 4.133(D and A).

On the other hand, first attempts to build a BHJ made by a mixture of a D and an A were discussed in the 1990s. This architecture, by increasing the area of the heterojunction between the donor and the acceptor, allows to extend the effective charge separation throughout the active layer, enhancing the device PCE until 3%.[253]

Fullerenes C_{60} and C_{70} together with their more soluble derivatives have been used as acceptors in OSCs showing the best efficiency due to the following peculiar advantages: (i) ability to mix with donor molecules
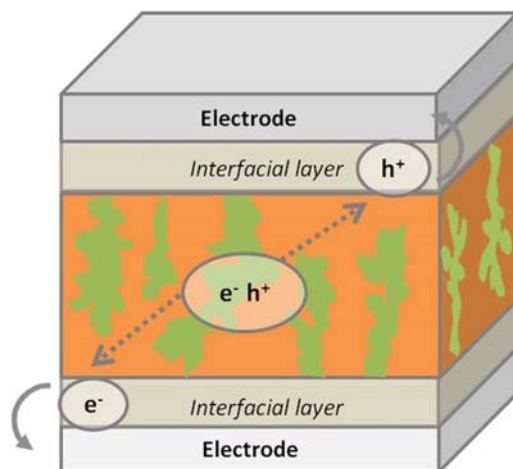
FIGURE 4.136 The structure of a BHJ structure of an ideal OSC. The donor (orange) and acceptor (green) materials undergo nanoscale phase separation forming a bicontinuous interpenetrating network useful to generate large D-A interfacial areas. The interfacial layers, forming ohmic contacts between the electrode and active layer, can work as: charge-blocking and charge-transport layers and as optical spacers, too.

forming a nanoscale morphology in the resulting BHJ; (ii) high electron mobility; (iii) high electron affinity (EA) needed for high efficiencies into the catching of electrons from the donor moiety.[254,255] The most widely used fullerenes in OSCs are methanofullerenes, such as: [6,6]-phenyl-C61-butyric acid methyl ester (PC$_{61}$BM) and their analogs compounds based on C$_{70}$, for example, phenyl-C71- butyric acid methyl ester (PC$_{70}$BM). The latter one shows a slightly higher optical absorption than the former. Their chemical structures are sketched respectively in Fig. 4.134(1, 2):

In the last years, a deep research toward the design and synthesis of new optimized fullerene derivatives for OSCs has been addressed finding some new PCBM derivatives containing, instead of a phenyl group, different functional moieties such as: thiophene (Fig. 4.134(3))[256]; fluorene (Fig. 4.134(4)); or triphenylamine substituents (Fig. 4.134(5)).[257]

Beside these acceptor compounds, a wider increase in OSCs efficiency became possible by taking advantages from polymers and oligomers as donor organic semiconductors. These new organic donors having broader band of spectral absorption and a high charge-carrier mobility allowed to reach enhanced properties.[258]

In particular, in 1995 an OSC device made by a blend of the electron donor MEH-PPV polymer (shown in Fig. 4.135(1)) and the electron acceptor PC$_{61}$BM, has been tested and showed a wide increase in the interfacial area inducing both a reduction of the distance from the polymer area with respect to the charge-separation interface and an improvement of the efficiency of charge collection.[243]

Later on, the use of poly (3-hexylthiophene) (P3HT, shown in Fig. 4.135(2)) has been introduced as electron donor polymer since it shows high thermal and chemical stability and desirable optical/electrical properties. Owing to these characteristics, P3HT results to be one of the most spread polymers in OSCs until now, allowing an even more increase of PCE until 5%. Furthermore, due to its high processability and scalability, P3HT represents also a valuable candidate for OSCs' mass fabrication.[259−263]

In an ideal BHJ device the donor and the acceptor materials undergo a nanoscopically phase separation forming interpenetrating bicontinuous networks enhancing the donor−acceptor interfacial areas (see Fig. 4.136):

The green and the orange regions represent the acceptor and donor domains, respectively. The interfacial materials have different fundamental roles: (i) charge-transport; (ii); charge-blocking; (iii) optical spacers; and (iv) ohmic contacts between the electrode and active layer. The most useful interfacial layers within all categories such as: metals and metal oxides, salts, organic acids, π-conjugated compounds, small molecules and polymers.

Excitons (e$^-$h$^+$) diffuse toward the D-A interface (in Fig. 4.136, the boundaries among the green and the orange regions), where they form charge-transfer (CT) states that can then dissociate into free holes (h$^+$) and free electrons (e$^-$). Holes and electrons are then transported through the interfacial layers (i.e., respectively the donor-rich and acceptor-rich phases), to the respective electrodes where they are finally collected.

Attention needs to be paid to the exciton diffusion lengths that, for the vast majority of organic materials useful for OSCs, are shorter than the film thicknesses required usually for an efficient light absorption.
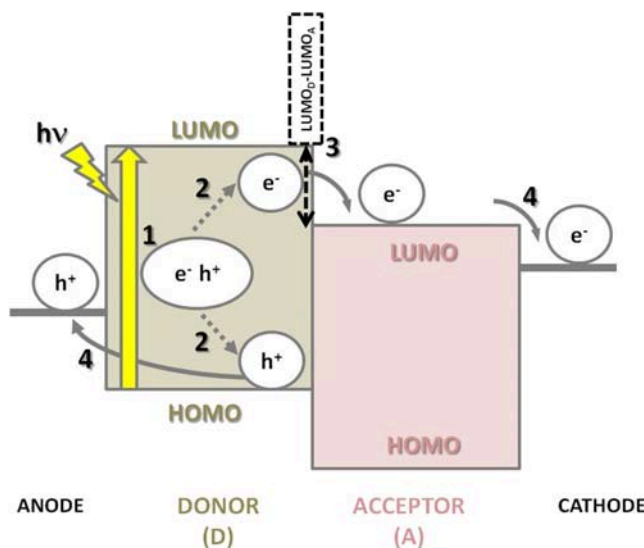
FIGURE 4.137 Main processes occurring in OSCs explained through the donor's and acceptor's band diagram: 1. Photon absorption and exciton formation (e⁻h⁺); 2. Exciton dissociation into free e⁻ and h⁺ species; 3. Charge diffusion; 4. Charge extraction at electrodes.

On the contrary of the PHJs, in which the D and the A materials are usually deposited using an evaporation method, the introduction for the first time of the solution processing method, has favored the use of BHJs (Fig. 4.136). In fact, in BHJs devices the D and A are co-deposited from solution forming an ideal bicontinuous interpenetrating D and A networks opening, respectively, hole and electron channels. In this way, BHJs architectures allow good exciton diffusion lengths because all excitons are formed close to a D-A interface also in the case of thick organic films.[243]

4.3.1.2 Principles of organic solar cells operation

A photovoltaic device absorbs the sunlight converting it into electricity. This process consists into three main steps: (a) formation of light induced charge generation; (b) transport of the generated charges and (c) charges collection by the electrodes.[264,265]

So far, a typical OSC device is composed by electrodes and active and charge transporting layers. The light harvesting part of an OSC device is represented by the active layer, made by organic p- (donor) and n-type (acceptor) materials blended together and ensuring the charge separation process.

An efficient sunlight conversion into electricity can be guaranteed through a wide range of harvest within the solar radiation spectrum. The degree of sunlight absorption depends on the absorption coefficient (a) which is an intrinsic characteristic of the active material.

From one side, thin layers (i.e., 100−200 nm) of organic photoactive materials are characterized, in general, by high absorption coefficients at specific wavelengths providing efficient light harvesting.[265] On the other side, since organic photoactive molecules are usually characterized by narrow absorption spectra, they have the drawback to cover only a small part of the near infrared region. For this reason, it is of primary importance to fine tune the molecular structure of organic photoactive molecules in terms of their energy gaps (i.e., the HOMO-LUMO energy separation) and absorption spectra broadening to increase the sunlight spectrum matching. Usually, the donor absorption shifting toward lower energies is provided by increasing the degree of delocalization obtained so far by using organic large π-conjugated systems. The most used donor active materials are usually represented by dyes and low band gap polymers; on the contrary, the most used electron acceptor materials are fullerene and derivatives (i.e., perylenediimide or other *n*-type materials).[259]

In Fig. 4.137 the main processes occurring in a OSC device are sketched in detail. From a practical point of view, when a photoactive molecule absorbs light an electron is promoted from the Highest Occupied Molecular Orbital (HOMO) to the Lowest Unoccupied Molecular Orbital (LUMO) (see process 1).

As a consequence, a exciton (i.e., an excited states characterized by a tightly bound electron-hole pair having a large binding energy comprised in the 0.3−1 eV range)[266] is formed (in Fig. 4.137 it is represented by the e⁻h⁺ notation at the end of step 1). Only by overcoming this binding energy value, the exciton can dissociate (see step 2) into free charges (electrons e⁻ and holes h⁺) and produce the corresponding photocurrent because of two

more steps indicated in Fig. 4.137 as step 3 (diffusion of e$^-$ to the acceptor's LUMO) and step 4 which is the final captures at electrodes (e$^-$ by the cathode and h$^+$ by the anode). The just described dissociation needs first the exciton migration toward the D/A interface (the junction where p- and n-type semiconductors are in contact)[267] through a diffusive process from high to low exciton concentration regions.[268] Of course, the efficiency of exciton diffusion is strictly correlated both to the exciton diffusion length (L$_D$) and to the film thickness[265] (as reported in the following Eq. (4.7)):

$$L_D = (D\tau)^{1/2} \tag{4.7}$$

where, D represents the diffusion coefficient and τ the exciton lifetime.

Typically, the L_D value varies in the 1$-$10 nm range, limiting drastically the possible absorbing layer thickness in organic semiconductors. Indeed, for layers thicker than 10 nm, the efficiency of sunlight conversion into electricity is seriously limited since the excitons generated at a distance larger than L_D from the D/A interface, decay to ground state before having the possibility to dissociate.

The electron transfer from the exciton (e$^-$h$^+$) to the acceptor's LUMO results in a positively charged donor and a negatively charged acceptor (D$^+$/A$^-$) at the interface (i.e., the charge transfer state, CT). The offset between the donor's LUMO and the acceptor's HOMO (shown in Fig. 4.137 through the LUMO$_D$-LUMO$_A$ notation) corresponds to the driving force for this process. The electron and the hole into the CT state of adjacent molecules are located at the D/A interface and are maintained close by coulombic attraction.[259] Finally, the CT state can be converted into a charge separated (CS) state, characterized by free electron and hole charge, only if the distance between the electron and hole becomes greater than the Coulomb capture radius.

Taking advantages from the working principles of OSCs, it can be concluded that an efficient device requires the presence of a heterojunction.[269] The heterojunction represents the practical way to establish a contact between the two different organic semiconductors on which an OSC is based on: an electron donor and an electron acceptor counterpart.

4.3.1.3 Evaluate the performances of a bulk heterojunction organic solar cells

As already discussed in detail in the previous section, solar cells by absorbing light give rise to excitons which then separate into holes and electrons non-Coulombically bound among them. The exciton's ability to dissociate depends on its binding energy (E_b), defined according to the following Eq. (4.8):

$$E_b = IE - EA - E_{op} \tag{4.8}$$

The solid-state ionization energy (*IE*) and electron affinity (*EA*) within the *IE-EA* term express the energy needed from the ground state to form a pair of free charges. Instead, E_{op} is the energy related to the relaxed exciton with respect to the ground state. In the solid state, for any organic electronic material the electron affinity, being the energy released during the capture of an electron, results to be positive.

Typically, in the most part of inorganic materials E_b is small (e.g., $E_b \approx$ 15 meV, for silicon) and is easily overcome by thermal energy. On the other side, organic materials exhibit larger E_b values. Just to make an example, for the P3HT polymer $E_b \approx$ 0.7 eV.[270] Unfortunately, in single-component OSCs this value translates into a very ineffective charge separation process. That's why, to reach a efficient charge separation process an useful active layer should be, instead, composed of both electron-rich (i.e., electron-donor) and electron-poor (i.e., electron-acceptor) materials. In general, these materials should be chosen so that the exciton dissociation process results to be exergonic ($-\Delta G_{CS}$) as expressed by the following Eq. (4.9):

$$\Delta G_{CS} = IE_D - EA_A - E_{op} - T\Delta S_{CS} < 0 \tag{4.9}$$

where E_{op} refers to the material with the lowest-energy absorption and the usually negligible ΔS_{CS} term defines the entropy of charge separation. So far, neglecting the term $T\Delta S_{CS}$ and if $E_{op}(D) < E_{op}(A)$, the previous Eqs. (4.8) and (4.9), translate into the following Eq. (4.10):

$$EA_A - EA_D > E_{b(D)} \tag{4.10}$$

This corresponds to the requirement for an offset in the energy range of the LUMOs of the donor and acceptor materials.

Similarly, for many donor $-$ NFA acceptor blends, it results that $E_{op}(A) < E_{op}(D)$, so that:

$$IE_A - IE_D > E_{b(A)} \tag{4.11}$$

Evaluating the performance of an OSCs, the most important index is the power conversion efficiency (PCE). It is based on the following parameters: the short circuit current density (J_{sc}); the open circuit voltage (V_{oc}); the fill factor (*FF*) and the power density of the incident solar radiation (P_{in}). The PCE is defined as reported in Eq. (4.12):

$$PCE = J_{SC} V_{OC} \, FF / P_{in} \tag{4.12}$$

where $FF = P_{max}/(J_{SC} V_{OC})$, with P_{max} = the maximum power density, J_{sc} is limited by: (i) the rate at which the donor and acceptor materials absorb photons; (ii) the efficiency of exciton dissociation and (iii) the efficiencies with which the resultant charges are transported to and collected at the electrodes. The V_{oc} is instead reduced by: (i) the radiative and non-radiative recombination processes via the charge-transfer state and (ii) the energy of the interfacial donor−acceptor charge-transfer excited state (E_{CT}) which is equal to:

$$E_{CT} = IE_{(D)} - EA_{(A)} - E_{bCT} \tag{4.13}$$

where $E_{b(CT)}$ represents the exciton binding energy for the charge-transfer state[271] and is much smaller than $E_{b(D)}$ or $E_{b(A)}$ and corresponds to the Coulombic attraction between D^+ and A^-.

Thus, to reach the highest PCE value for an OSC, a compromise must be found between the J_{SC} and the V_{OC}. The former is maximized by absorbing the largest part of the visible and near-infrared (NIR) solar radiation. The latter increases with an increase in $IE_{(D)} - EA_{(A)}$ part of the Eq. (4.13).

In the case of an ideal single-junction OSC in the Shockley−Queisser limit, absorbing only photons characterized by $E > E_{op}$, the optimum E_{op} is $\sim 1.1-1.4$ eV and, therefore, PCE results to be about 34%.[272] Trough the Shockley−Queisser limit we are considering that: (i) no driving force is required for charge separation so that the materials should be chosen by according to $E_{op} = IE_{(D)} - EA_{(A)}$ and (ii) there are no voltage losses from non-radiative recombinations.

In reality, higher optimum values of E_{op} should be considered since a driving force is often needed for OSCs, and non-radiative recombinations are unavoidable. As a consequence, higher is the deviation from Shockley−Queisser limit, higher will be the energy losses (i.e., elementary charge) shown in Eq. (4.14):

$$E_{loss} = E_{op} - eV_{oc} \tag{4.14}$$

In the discussion here presented, *IE*, *EA* and E_{op} values are referred to solid films. Anyway, taking in consideration the thin film absorption spectrum, E_{op} can be evaluated also from the long-wavelength onset of absorption (λ_{onset} [nm]), by using the following relation: $E_{op}[eV] = \frac{1240}{\lambda_{onset}}$.

Instead, especially for solution-based systems which show a high tendency to aggregate, their *IE* and *EA* values differ from the typical films' values. However, *IE* and *EA* are often related to $-E_{HOMO}$ and $-E_{LUMO}$, respectively. Electrochemical measurements represent usually the more direct techniques to estimate these
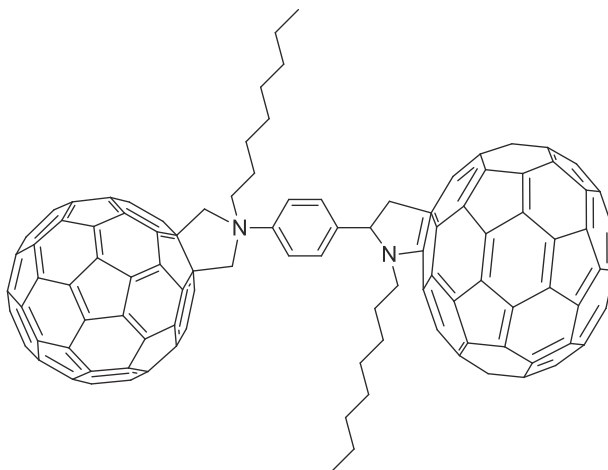

FIGURE 4.138   Example of heterodimer made by two covalently linked fullerene units.

values. Instead, the less widely available techniques are the UV Photoelectron Spectroscopy (UPS) for the ionization energy and Inverse Photoelectron Spectroscopy (IPES), for the electron affinity.

It is important to specify that even though different relationships between redox potential and *IE* or *EA* have been proposed and used, there isn't a direct relationship because solvation energies and solid-state polarization energies are critically dependent on: size, shape and charge distribution of the molecules.[273]

Furthermore, in some cases, the *EA* is estimated from an electrochemical ionization energy or the *IE* estimated from an electrochemical electron affinity assuming, so far, that $IE - EA = E_{op}$ by neglecting E_b.

4.3.1.4 In principle the most widely used photoactive acceptors: fullerene acceptors (FA)

Historically, fullerenes represent the most widely employed electron acceptors materials in OSCs due to their ability to transport charges together with high electron affinity and high electron mobility. As already discussed in the previous section, usually C_{60} fullerene and C_{70} fullerene derivatives are commonly blended with the donor material, such as polymers or small molecules electron-donor systems, to form the BHJ active layer. It is important to evidence that the pristine fullerenes have been less considered because of some major drawbacks: (i) the shortage of the visible light absorption limiting the PCE of the corresponding OSC devices; (ii) the scarce solubility in organic solvents reducing the possibility of pristine fullerenes to be deposited by spin coating.

For these reasons, the molecular structure of pristine fullerenes have been properly modified primarily to improve their solubility in organic solvents. Therefore, instead of pristine C_{60} fullerene and C_{70} fullerene, improved derivatives have been designed and synthesized: $PC_{61}BM$ (see Fig. 4.134(1)) and $PC_{71}BM$ (see Fig. 4.134(2)), for which the absorption of light in the visible region results to be improved and thus the photogeneration current is increased.[274,275]

Another efficient strategy to improve the absorption capability of the fullerene derivatives is to bridge two fullerene units (equal or different, e.g., C_{60} and C_{70} fullerene derivatives) via covalent linking forming an heterodimer (see the molecular sketch in Fig. 4.138) in which an electron coupling among the two fragments is established. Compared to the $PC_{61}BM$ derivative, an heterodimer shows an increase in its absorption coefficient.[276−278] Furthermore, the resulting electronic properties of the heterodimer acceptors can be finely tuned also by the proper chose of the bridge structure: single or multiple bridges to freeze the resulting acceptor system in the desired conformation influencing the efficiency of the charge carrier generation in OSC devices.[279,280]

Over the last decades, the fullerene-based systems have occupied the most important positions in defining the devices' photophysics and electro-optics comprehension. Furthermore, in 2017 they highly improved the PCEs reaching the maximum value of 12.1% by using a ternary blends made by two polymeric donors and one fullerene acceptor (i.e., $PC_{70}BM$).[281]
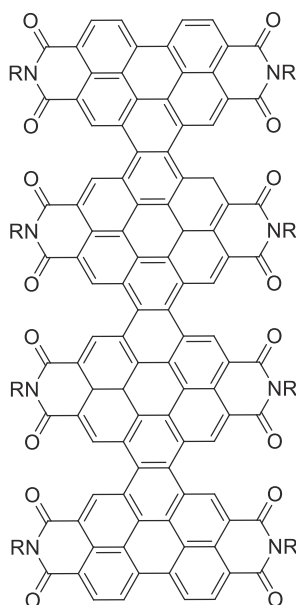

FIGURE 4.139 Structure of an helical molecule made by four PDI units linked by a two-carbon bridges.
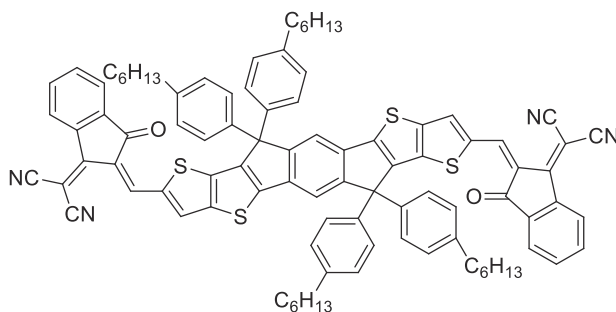
FIGURE 4.140   Molecular structure of the ITIC molecule.

In the field of organic PV, the level of efficiency, reached by the electron-acceptor fullerenes and fullerene derivatives in combination with adequate electron-donors, is poorly comparable with the most valuable commercial devices based, for example, on silicon or other inorganic semiconductors. Furthermore, the challenging scaling up strategies, the development of proper devices' manufacturing processes and the achieving of required solar cell lifetimes have relegated the organic PV technology only to a limited number of specific applications.

4.3.1.5 A novel concept of photoactive electron-acceptors: non fullerene acceptors (NFAs)

Even though conventional OSCs are typically based on BHJs device architectures consisting of mixtures of electron-donor and fullerene-acceptor (FAs) materials, the actual research in this field has shifted toward the design and the synthesis of organic non-fullerene acceptors (NFAs) characterized by several encouraging properties to avoid the main issues related to their fullerene-based predecessors.

NFAs have been developed specifically pursuing the goal of increasing absorption and solubility with respect to their fullerene-acceptor counterparts. To give an example, PDI derivatives (see structure in Fig. 4.133(A)) offer the possibility to replace fullerene acceptors in BHJ solar cells used as n-type organic acceptor materials. The most promising trend in designing new NFAs is represented by bulky and/or twisted PDI structures with a decreased aggregation tendency that suppress the formation of undesired excimers by avoiding large charge traps domains.[282]

For example, Nuckolls et al.[283] developed an helical molecule designed by fusing four PDI units linked by a two-carbon bridges (see molecular structure in Fig. 4.139).

Due to nonplanar molecular structures induced by the steric congestion in the junction point among the PDI units, these molecules show strong photon absorptions and scarce aggregation tendency. On the contrary of C_{60} and its derivatives, the helical PDI electron donor molecules are characterized by enhanced cross-section for the absorption in the visible region of the solar spectrum and tunable bandgaps. Through these improved characteristics these novel helical PDI materials allowed the fabrication of OSCs characterized by conversion efficiencies of about 8.3%, therefore similar to the PCE of FA-based devices.

4.3.2 Light stability of non-fullerene acceptors: photo-oxidation and photophysical degradations

Light stability is a well-liked characteristic for organic semiconductors. Unfortunately, it is often an unreached characteristic due to the major tendency of organic molecules to degrade under exposure of light. Two are the main routes by which an organic molecule can undergo light degradation: photochemical and photophysical. The photochemical degradation of NFAs can be mainly described by two different kind of reactions: (i) photo-oxidation by oxygen and (ii) photocatalytic reaction with interfacial materials. On the contrary, no chemical reactions are responsible for the photophysical degradation which induces, instead, only to morphological induced changes under the effect of light irradiation.

It is well-known that in absence of light NFAs are quite stable but a degradation due to photo-oxidation can occur instead under exposure of light, already in ambient conditions.

Recently, Guo et al.[284] have studied the photon-oxidation process occurring in a wide number of NFA systems. Such as an example, the ITIC (3,9-bis(2-methylene-(3-(1,1-dicyanomethylene)-indanone))-5,5,11,11-tetrakis(4-hexylphenyl)-dithieno[2,3-d:2′,3′-d′]-s-indaceno[1,2-b:5,6-b′]dithiophene), represents the first example of a new generation of small NFAs molecules for OSCs applications (structure shown in Fig. 4.140).
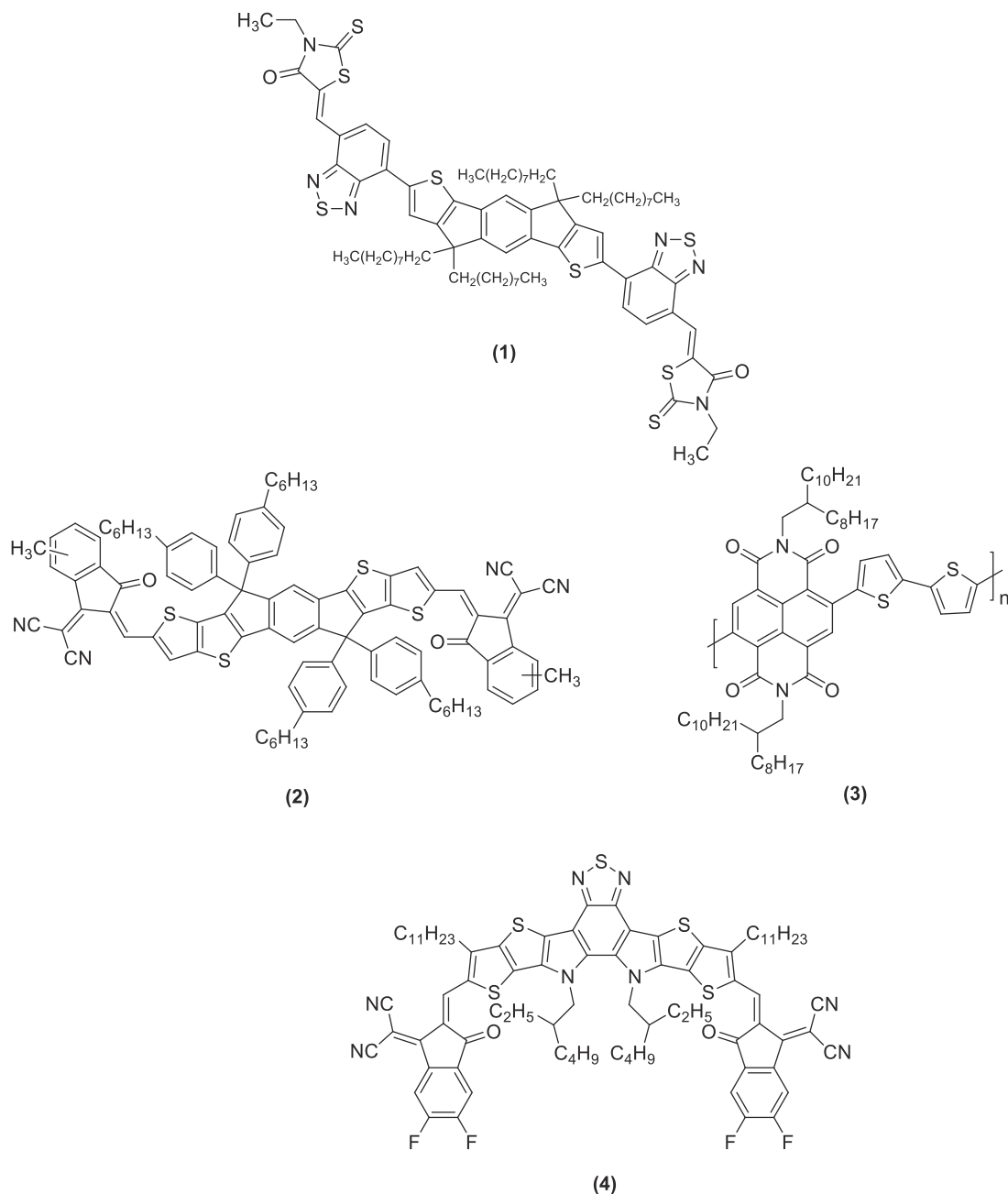
FIGURE 4.141   Molecular structure of: O-IDTBR (1), ITIC-M (2), N2200 (3) and Y6 (4) molecules.

The energy levels of ITIC allow good alignment with low band-gap polymers, giving the possibility to enhanced charge separation efficiency and reduced energy loss. ITIC also shows strong and broad (from visible to near infrared) absorption bands increasing the total absorption for a device.

Guo et al. discovered that under light O_2 molecules can attach to the ITIC molecule inducing an irreversible structural modification. Differently to what happens with fullerene acceptors, for which the photon-oxidation only affects the absorption of the fullerene moiety, the NFAs' planar structure provide many active sites capable to induce photon-oxidation, for example: (i) the linkage between the donors and the acceptors units, inducing, as total effect, a marked reduction in the absorption spectra; (ii) the thiophene, bithiophene and side chains rings' C=C bonds.

On the contrary, under inert environmental conditions the light irradiation of NFAs is not able to induce any chemical degradation but only photophysical degradation processes may occur. These degradation processes are mainly associated to: morphological, optical, and electronic changes induced by the light adsorbed by the

molecules. Xiao et al.,[285] for example, for the blend film made by PTB7-Th (Poly[4,8-bis(5-(2-ethylhexyl)thiophen-2-yl)benzo[1,2-*b*;4,5-*b*′]dithiophene-2,6-diyl-alt-(4-(2-ethylhexyl)-3-fluorothieno[3,4-*b*]thiophene-)-2-carboxylate-2—6-diyl)] used as donor polymer and the ITIC molecule as NFA. Under inert conditions, they observed an increased phase separation between the D-A interface upon prolonged photon irradiation (250 h). This experimental evidence is attributable to the ITIC molecules' aggregation occurring in the PTB7-Th polymeric matrix and resulting both in reduced photoluminescence quenching and exciton dissociation efficiency.

4.3.2.1 Chemical stability: water and oxygen resistance

Mostly oxygen and water molecules are both responsible for the degradation of organic semiconducting materials because of their diffusion from surrounding toward the interfacial and electrode layers of material.[274,286,287]

In presence of water, the fullerene acceptors, for example, exhibit irreversible degradation affecting both the electronic structure and the charge mobility of the resulting FA film.[275,288] In contraposition, even if their oxygen resistance is still challenging, NFAs have shown a high resistance to water. By UP Spectroscopy and without extra illumination, Wang et al.[289] have highlighted the effect of the oxygen and water on the energetics of the most useful NFAs molecules. For example, for the NFA such as the O-IDTBR ((5Z,5′Z)-5,5′-((7,7′-(4,4,9,9-tetraoctyl-4,9-dihydro-s-indaceno[1,2-*b*:5,6-*b*′]dithiophene-2,7-diyl)bis(benzo[*c*][1,2,5]thiadiazole-7,4-diyl))bis(methanylylidene))bis(3-ethyl-2-thioxothiazolidin-4-one), shown in Fig. 4.141(1), only a negligible change in the electronic structure was found by prolonged exposition (more than 25 h) of this film to water vapor. This evidence indicates a good tolerance to water molecules in contraposition to what happens typically with FAs.

Upon oxygen exposure, instead, the electronic structure related to the HOMO and LUMO orbitals of NFAs undergo important variations. It is interesting to underline that the oxygen induced degradation of NFAs is in part reversible and can be decreased in ambient environment since water molecules available in air play a beneficial oxygen-passivating role by decreasing the chemical interaction among oxygen and NFAs. Recently, many studies[276−278] have conformed these evidences demonstrating that, under ambient and dark conditions, the optical and electronic properties of NFAs are stable. At this regard, many NFAs based OSCs: ITIC (Fig. 4.140), ITIC-M (3,9-bis(2-methylene-((3-(1,1-dicyanomethylene)-6/7-methyl)-indanone))-5,5,11,11-tetrakis(4-hexylphenyl)-dithieno[2,3-*d*:2′,3′-*d*′]-s-indaceno[1,2-*b*:5,6-*b*′]dithiophene), (Fig. 4.141(2)), N2200 (Fig. 4.141(3)) and Y6 (Fig. 4.141(4)), can achieve similar device performance by processing in air.[279,280,282,290]

Anyway, upon illumination and oxygen exposures, extended degradation processes could still occur.

4.3.2.2 Chemical resistance

In general, the molecular structure and the morphology of organic semiconductors can be easily damaged by external factors, such as: photon illumination, chemical environment and thermal treatment and, usually, these changes lead to variations in optical, electronic and optoelectronic properties.[291−294]

It follows that also the FAs result to be therefore instable, which means that their electronic structure could be easily modified simply by exposure to environmental oxygen and water and leading, as a consequence, to issues like: crystallization, clustering, dimerization and/or diffusion.[288,295−297] On the contrary, NFAs due to their versatility in molecular design, exhibit more flexible physical and chemical properties.[298−301] Anyway, due to their
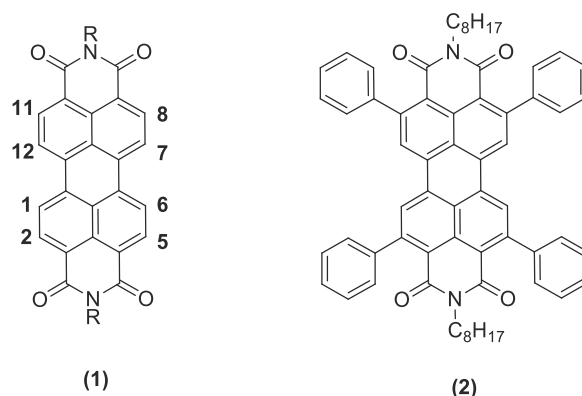

FIGURE 4.142 *Ortho*-functionalized PDIs structure (1): positions 2, 5, 8 and 11 correspond to the "ortho" positions. Positions 1, 6, 7, 12 correspond to the "bay" positions. Example of NFA molecule (2).

complex structures, NFAs provide many reactive sites that enable complex morphological evolution and/or degradation during the applicative use of these molecules. This represents both a big challenge because the study of
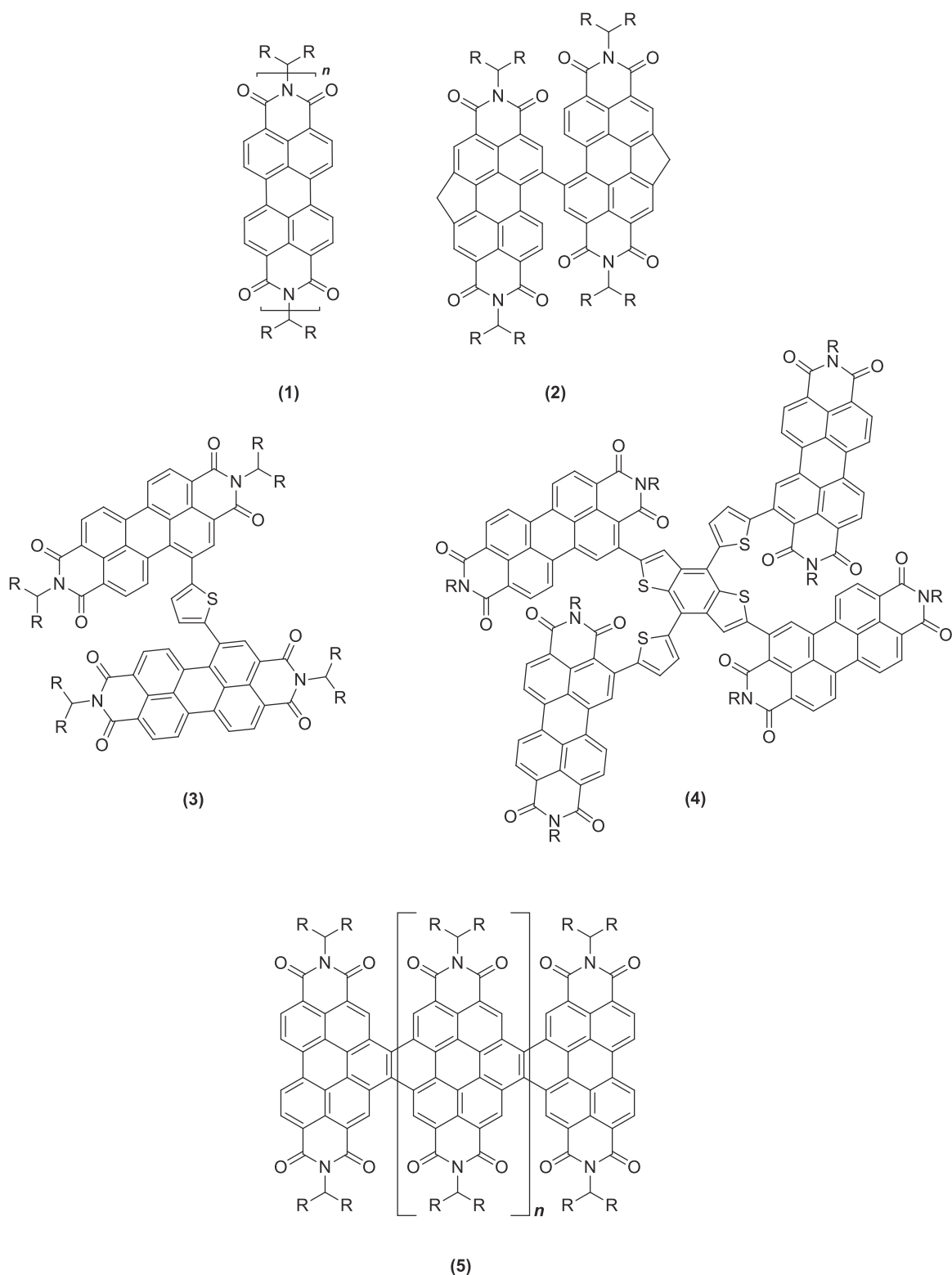

FIGURE 4.143   Examples of molecular structures obtained by: linking directly two or more monomeric PDI simple units (1, 2); the introduction of a planar or non-planar core unit (3, 4); fusing together PDI units (5).

their degradation mechanisms become quite complicated but, on the other side, also an opportunity to improve their stability through a fine structural design.[302−305]

4.3.3 Major classes of non-fullerene acceptors: rylene diimides

The most used NFAs are rylene diimides (i.e., perylene diimides − PDIs and naphthalene diimides − NDIs)[306−309] and their derivatives containing other π-conjugated cores.[310−313] This class of NFA have some interesting peculiarities, such as: (i) strong photon absorptions, (ii) intermolecular π-stacking tendency, (iii) high thermal and oxidative stability, and (iii) electron affinities similar to those of FAs.[308,314]

Unfortunately, BHJ OSCs based on unfunctionalized monomeric PDIs show generally low PCEs. Many simple PDIs show the tendency to form monodimensional π-π stacks in their crystal structures but it has been demonstrated that the electron transport within a monodimensional (1D) π-π stack is much more efficient than intermolecular electron transport among stacks.[315] So far, a theoretical study about amorphous PDIs revealed only a limited charge transport attitude if compared with the PC$_{61}$BM electron acceptor system.[316] On the other side, also large crystalline domains in PDIs revealed a limited electron transport ability from crystal domains to the electrodes.[315]

Furthermore, excitons in some 1D π-π stacked PDI aggregates are quickly deactivated due to excimer formation.[317]

Due to these relevant issues experienced by PDIs, worldwide researchers have joined common efforts to design and develop new complex systems made by the combination of proper donors with newest NFAs resulting in optimized systems for BHJ in OSCs. The best PCEs obtained ranged from 3% to 5%.[318] Among them, some simple *ortho*-functionalized PDIs (see general structure in Fig. 4.142(1)) have resulted to be able to suppress the excimer formation due to their ability to arrange in a twisted-stacking mode (i.e., the angle between the π-stacking direction and the plane of the molecules is < 90°) but keeping their ability to provide intramolecular electron-transport. For example, the NFA of Fig. 4.142(2) for which the before mentioned angle is of 47° giving a an almost homogeneous morphology and small PDIs crystal domains, provided the good PCE of 3.67%.[319]

Anyway, from the point of view of OSCs performances, the most promising rylene diimide-based NFAs have resulted to be the ones with more complex structures as hereafter discussed.

4.3.4 Major classes of non-fullerene acceptors: perylene diimide small molecules

Since monodimensional π-π stacking in PDIs shows unwanted properties, the most of NFAs research have been oriented toward the avoiding of π stacks and keeping the intermolecular LUMO-LUMO overlap ensuring the needed electron transport within the system. The most useful strategies to reach these aims and affording PCEs of up to 9.5%[320] have been the followings obtained by: (i) linking directly two or more monomeric PDI simple units (such an example, respectively see Fig. 4.143(1, 2)); (ii) the introduction of a planar or non-planar core unit (see some examples in Fig. 4.143(3, 4)); or (iii) fusing together PDI units (see examples in Fig. 4.143(5)).

Among the examples of PDI family classes before shown it has been highlighted that those systems like the one in Fig. 4.143(1) in which the PDI units are bonded through the nitrogen atoms belonging to the imide groups, each PDI unit arrange in an orthogonal orientation due to (steric and electrostatic) repulsion between the oxygen atoms of the imide group.[321−327] For example, these molecular arrangements are more keen to provide higher PCEs (2.78%) in BHJ solar cells than a monomeric PDIs itself (0.13%).[328] The corresponding trimeric PDIs molecule, sketched in Fig. 4.143(1), shows only little higher PCEs (5.81%) if compared with the corresponding dimeric PDI compound (5.58%) in combination with the same donor counterpart.


FREAs general architecture

X = C or S
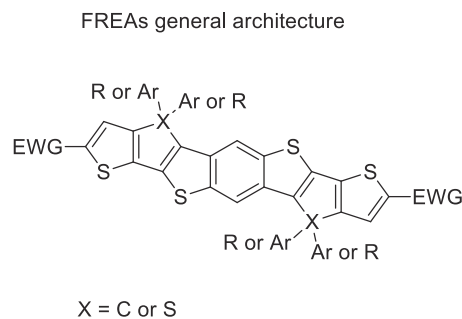
FIGURE 4.144   Fused-ring electron acceptors general architecture.

On the other side, also the PDI dimers bonded through C—C bonds show the tendency to adopt twisted orientations and the monomeric units can be linked both through the *ortho*[329] and the "bay" positions[330−335] (see Fig. 4.142(1)) for which the evaluated PCE is about 5.90%.

Molecules composed of three or more PDI units linked through the "bay" positions to a different core (Fig. 4.143(4)) have been deeply studied as well.[336−339] Among them, the NFA of Fig. 4.143(5) represents an example of a four-membered PDI system in which the units are linked through their *ortho* positions to the core.[340]

If compared with the bay-linked molecular systems, usually, the *ortho*-linked counterparts result to be more planar facilitating, so far, a closer packing of the π-conjugated backbone. On the contrary, fused oligomers, as the example shown in Fig. 4.143(5), have the tendency to arrange in helical structures avoiding the interactions among C—H groups in the *ortho* positions of adjacent units.[283,341]

It is interesting to discuss the electro-optical properties of the PDI derivatives previously described. It has been demonstrated that for the vast majority of the oligomers here discussed, their properties match those of monomeric PDIs. It is only when fused PDI derivatives (Fig. 4.143(5)) are taken into account that their electro-optical properties change drastically evidencing important red-shift absorptions as long as their electron affinities increase with the increase of oligomer length: a clear evidence of substantial inter-PDI coupling.

4.3.5 Major classes of non-fullerene acceptors: fused-ring electron acceptors

Fused-ring electron acceptors (FREAs) are molecular systems containing the following moieties: (i) fused-ring core; (ii) EWGs and (iii) side chains. FREAs architecture consist mainly of two π-electron-withdrawing moieties strongly bonded by a planar π-conjugated bridge made by a fused-ring core generally functionalized with aryl (Ar) or alkyl (R) side chains (Fig. 4.144).[342] Therefore, the molecular design of new promising FREA systems characterized by improved ranges of absorption wavelengths, ionization energies and electron affinities passes through the variation of the main moieties constituting the FREAs, that is, fused-ring core, EWGs. While, side
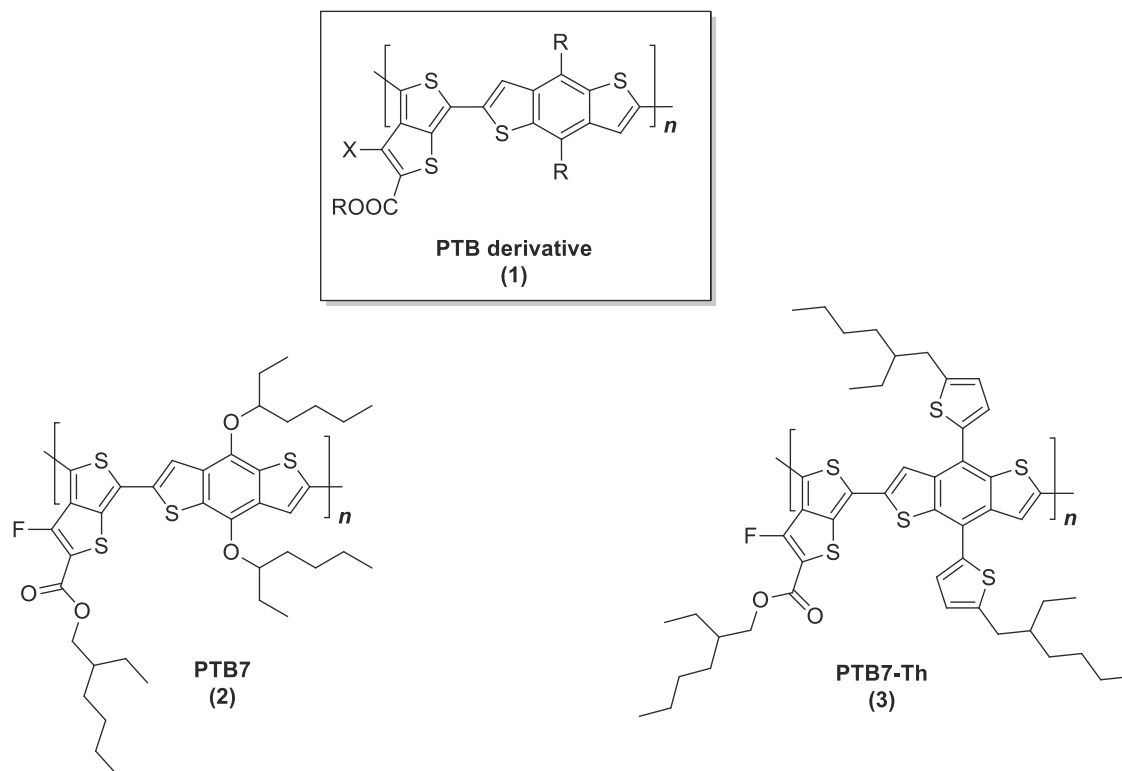
FIGURE 4.145　General structure of polymeric PTB derivatives (1) shown together with two examples of PTB derivatives: PTB7 (2) and PTB7-Th (3).
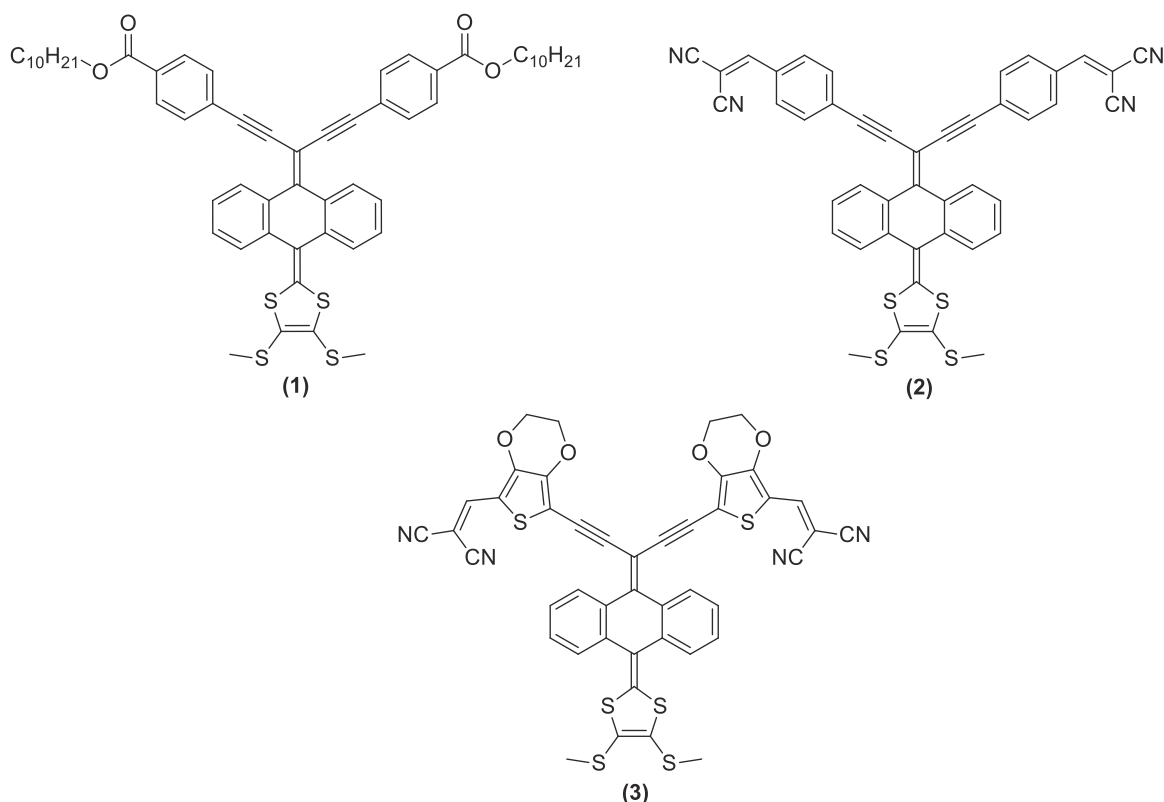
FIGURE 4.146 Examples of push-pull dyes based on the 10-(1,3-dithiol-2-ylidene)-anthracene electron donor core unit, a conjugated π-bridge plus two electron accepting units.

chains affect solution processability, miscibility with donors and intermolecular arrangement. Furthermore, the presence of side chains avoid the formation of both monodimensional π stacks and π-π stacking in favor of the intermolecular π interactions occurring between the electron-rich core of one molecule and the electron-poor end group of slipped neighbors.

For example, the widely known FREA compound, the ITIC, previously shown in Fig. 4.140 has been demonstrated to arrange forming strong interpenetrating networks by the π interactions between the end chain groups of adjacent molecular units. These 3D networks allow to form films exhibiting highly isotropic electron transport properties than the corresponding isolated crystals.[343]

4.3.6 Polymers and small-molecule donors

The most spread donor materials for OSCs are represented by conjugated polymers characterized by narrow band-gap and deep-lying HOMO level. Such an example, the polymeric PTB derivatives are often the most used materials.[344] The PTB derivatives consist of two heterocyclic co-monomers, for example, the fused-ring benzodithiophene and thieno[3,4-b]thiophene, shown schematically in Fig. 4.145(1).

Among them, PTB7 (see Fig. 4.145(2)) is the most widely used material[345−347] but, to improve the co-planarity of the main backbone and to obtain a bathochromic shifts of its absorption wavelengths, 2-ethylhexyl-thienyl group has been incorporated in the benzodithiophene core of the PTB7-Th molecule[348] (Fig. 4.145(3)), reaching a PCE of 11.3% in the PTB7-Th:PC71BM tandem architecture.[349]

Unfortunately, besides these advantages the conjugated polymers show some drawbacks such as the synthesis' reproducibility, their subsequent purification and, therefore, their electronic properties.[350] A valuable alternative to polymers has been found in small molecule semiconductors, which are characterized by well-defined molecular structures, the possibility to fine tune their electronic properties and lower charge motilities than their polymeric counterparts.

The classical example of the most widely used small molecule donors in OSCs are the phthalocyanines (Fig. 4.133(D)): mostly planar p-type molecules chelating a single metal or metalloid ion within their internal cavity and showing high molar absorptivity especially in the low-energy region and good thermal stability.[351−353]

Among small molecule donors, now the push-pull systems represent the most promising materials for highly efficient OSCs. Some recent examples of push-pull dyes absorbing in an extended region of the visible spectrum and based on the 10-(1,3-dithiol-2-ylidene)-anthracene electron donor core unit, a conjugated π-bridge plus two electron accepting units have been published. Some examples are shown in Fig. 4.146(1−3).

As the push-pull effect is reinforced by an efficient electronic communication between the donor and acceptor moieties, more intense charge-transfer bands and a decrease of the optical band gap can be observed.[354−356]

4.3.7 Nonlinear optical materials

Nonlinear optic (NLO) describes the behavior of light in materials in which the polarization density (P) responds non-linearly to the electric field (E) of the light. The research about NLO materials has boosted by the potentiality of their applications in many different fields, such as: photonics, biology, medicine (photodynamic therapy), material processing (optical engineering), and so on. As a consequence of their nonlinear response to the light, these materials exhibit nonlinear optical properties such as: conversion of light wavelength, light amplification, conversion of the refractive index depending on optical intensity.[357,358] Starting from the 1960s, when a laser oscillation was reported for the first time by Maiman T. through the construction of the first laser and the Second Harmonic Generation (SHG) was discovered by Franken et al. in 1961,[359,360] the development of inorganic nonlinear optical materials has started.[361] Soon after, also organic NLO materials have shown efficient nonlinear optical properties due to their highly delocalized π-electrons translating in a rapid responsiveness of these class of materials.[362−364]

In general, the light−matter interaction at high intensities influences microscopic properties such as: polarizability, absorption cross-section and lifetime that, as a consequence, induce changes to the materials' macroscopic properties (e.g., polarization, absorption, and susceptibility) as a function of the intensity of the interacting light.[365,366]

When a material is invested with light, photons interact with the material and can be absorbed by electrons reaching a specific excited state. The reverse transition may consist into the emission of photons through radiative channels usually characterized by a different energy than the excitation energy. Anyway, the light−matter interaction may also lead to other types of excitation (e.g., rotational and vibronic), or to a change in the medium polarization.

To evaluate the specific applicative implications of light−matter interaction, it is of fundamental importance to evaluate how the microscopic and macroscopic properties change with the light intensity and therefore, it is

D	A
-N(CH$_3$)$_2$	-NO
-NH$_2$	-NO$_2$
-OCH$_3$	-CHO
-OH	-CN
-CH$_3$	-SO$_2$CH$_3$
-SCH$_3$	-SO$_2$CF$_3$
-N(CH$_3$)$_2$	=C(CN)$_2$
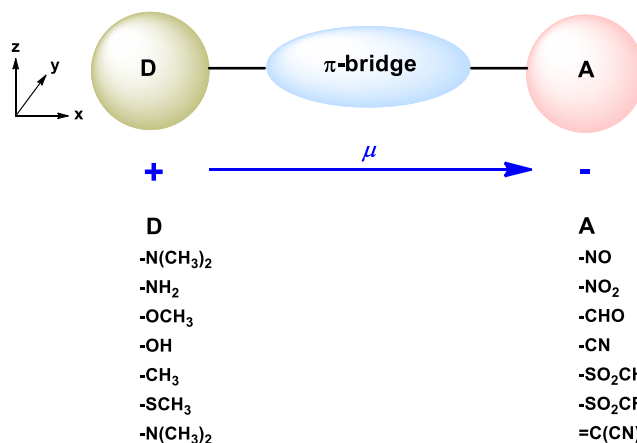
FIGURE 4.147　The schematic architecture of charge transfer molecules: D (donor), A (acceptor) and π-bridge; the χ_{xxx} tensor component and the typical electron donating (D) and electron accepting (A) groups.
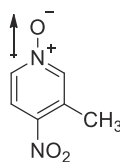
FIGURE 4.148   3-Methyl-4-nitropyridine-1-oxide (POM).
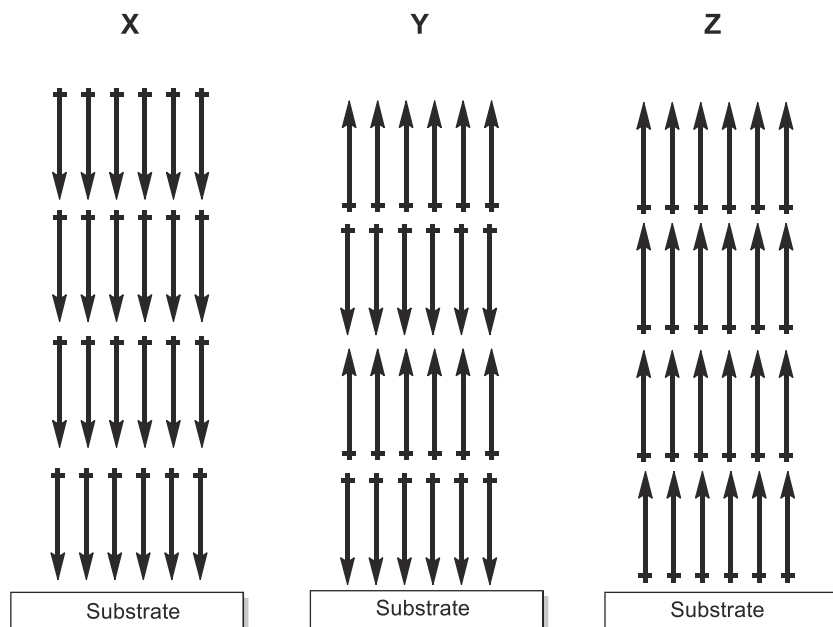
FIGURE 4.149   Schematic of X, Y, Z type Langmuir– Blodgett films. The arrows indicate the direction of dipole moments with respect to the normal to film surface.

important to be able to measure these changes by different nonlinear techniques.[367–370] A non-linear behavior, in fact, can be observed in the presence of high intensity of the electric field, as in the case of high intensity pulsed laser beams, in which the highest order terms come into play in the series development of the dielectric constant of the material, as will be better discussed in the following section. As an example, the susceptibility (χ), which describes the material behavior as a function of both wavelength and pulse width of the laser light used, can be estimated from the intensity-dependent macroscopic parameters.[371]

4.3.7.1 Second-order nonlinear optical materials: molecules, bulk materials and poled polymers

Depending on the specific application aimed, many advanced materials showing enhanced second-, third-, and higher-order NLO properties have been designed both on molecular (e.g., molecule's individual hyper-polarizability) and macroscopic (e.g., molecules' assembling in the bulk) level.

The second-order NLO response may be shown only in non-centrosymmetric materials. Therefore, the most promising molecules for second-order NLO devices' applications are the intramolecular charge transfer compounds made by electron donating (D) and electron accepting (A) counterparts, linked together by a π-conjugated bridge as sketched in Fig. 4.147.

In nonlinear optic materials the relation between P and E become the following:

$$P_{NL} = \varepsilon_0\left(x^{(1)}E^1 + x^{(2)}E^2 + x^{(3)}E^3 + \ldots\right) \tag{4.15}$$

where χ is the susceptibility and ε is the material refractive index.

In particular, the second-order effects become important when the intensity of the incident field modifies the natural elastic-type response to the perturbation that the atom would have if the incident intensity were much smaller than that of the atomic field. In general, the perturbing field, for example the one created by a laser beam, generates a decentralization in a single atom between the barycentres of the electron cloud ($-$) and of the nucleus ($+$).
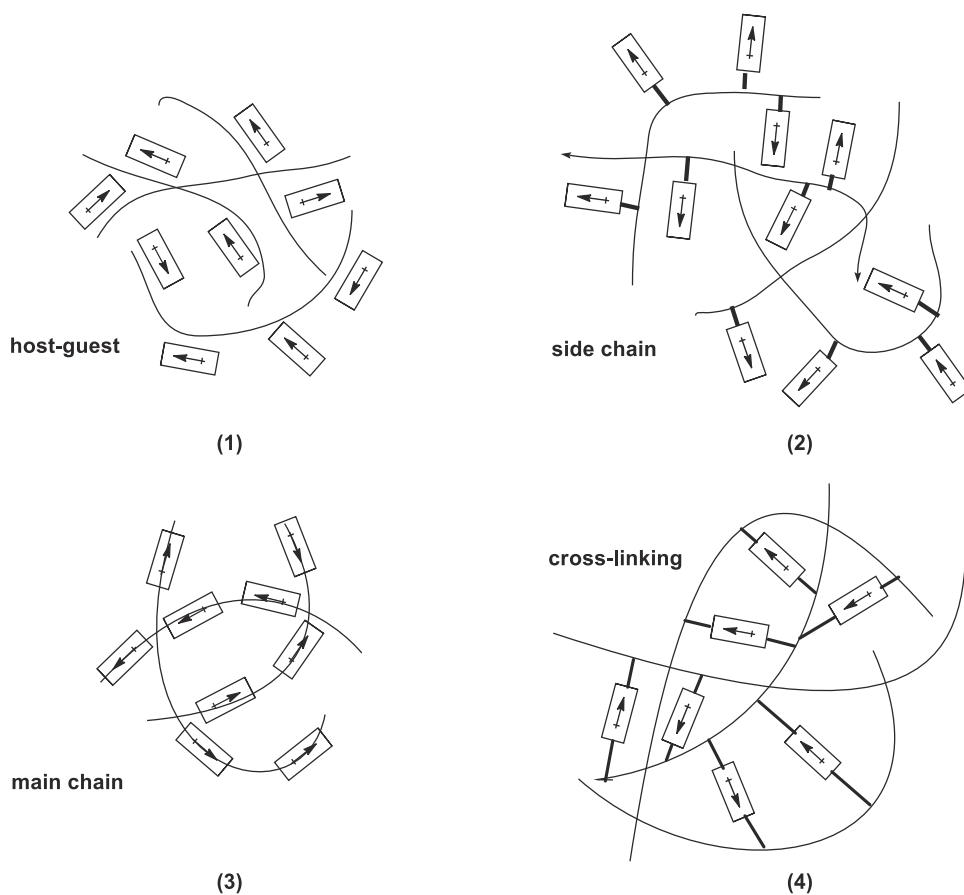
FIGURE 4.150   Schematic of four main functionalized polymers' arrangements showing second-order NLO effects: (1) guest−host systems, (2) side chain polymers, (3) main chain polymers, (4) cross-linking polymers. The arrows indicate the NLO chromophores linked to the polymer.
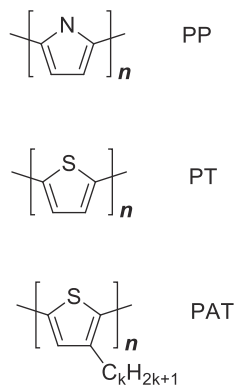
FIGURE 4.151   Polypirrole (PP), Polythiophene (PT) and Poly(3-alkyl-thiophene) (PAT).

The charge transfer molecules, for example, exhibit a large susceptibility tensor component enhanced in the charge transfer x direction (χ_{xxx}). The χ_{xxx} value depends: (i) on the strength of electron donating and electron accepting groups, and (ii) on the conjugation length (L) of the bridge through the following dependence:

$$x_{xxx} \propto L^{a_S} \tag{4.16}$$

where $\alpha_s > 1$. Since the conjugated backbone is composed of a definite number of alternate single/double or single/triple bonds, the scaling law is function of the number of double (or triple) bonds N, as follows from Eq. (4.17):

$$x_{xxx} \propto N^{a_b} \tag{4.17}$$

Usually, $\alpha_\beta \sim 2.5$ for charge transfer molecules having the same electron donating and electron accepting groups but differing only in the length of their conjugated bridge. Anyway, in the case of phenyl oligomers used as bridge, if the number of double bonds is greater than 4 (i.e., $N > 4$), the χ_{xxx} value tends to saturate.

Different strategies can be used to design non-centrosymmetric materials, and one of these is represented by the single crystals growth. The main disadvantage of the single crystals growth is that not so many molecules are able to crystallize in a non-centrosymmetric good-quality optical single crystals. Indeed, for example, charge transfer molecules exhibit generally a large ground state dipole moment and their strong dipole–dipole interaction leads to antiparallel alignments, and as a consequence, to a centrosymmetric bulk structure. Therefore, it is necessary to design and synthesize molecules with a negligible ground state dipole moment such as POM (3-methyl-4-nitropyridine-1-oxide), whose molecular structure is shown in Fig. 4.148.

Many other strategies to grow non-centrosymmetric materials have been exploited and are represented by: (i) the use of chiral molecules which usually form spontaneously non-centrosymmetric films, (ii) application of an external electric field, especially to produce poled polymers, (iii) the use of an adequate substrate favoring epitaxy, pseudoepitaxy, or self-assembly growths, (iv) ordered layered structures inducing intramolecular charge transfer, and (v) Langmuir–Blodgett (i.e., interaction between molecules and molecules–substrate) films.

By following the Langmuir–Blodgett strategy it is possible to obtain three main types of ordered structures characterized by tunable thickness (i.e., X; Y; Z shown in Fig. 4.149). Among them only the X and Z type structures are able to provide non-centrosymmetric thin films exhibiting second-order NLO properties.

In designing materials exhibiting excellent second-order NLO properties the best results are, usually, obtained by taking advantages from poled polymers: a polymer matrix functionalized with active NLO charge transfer

Photoconducting polymer
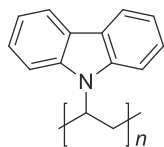
PVK

2nd order NLO chromophore

DHD

Photosensitizers

TNFDM

C60

Plasticizer

ECZ
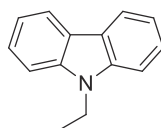
FIGURE 4.152 Polyvinylcarbazole (PVK), 4-(*N*,*N*-bis(ß-dihydroxyethyl)amino)-4′-nitrostilbene (DHD), (2,4,7-trinitro-9-fluorenylidene)malononitrile (TNFDM), fullerene C$_{60}$ and *N*-ethylcarbazole (ECZ).
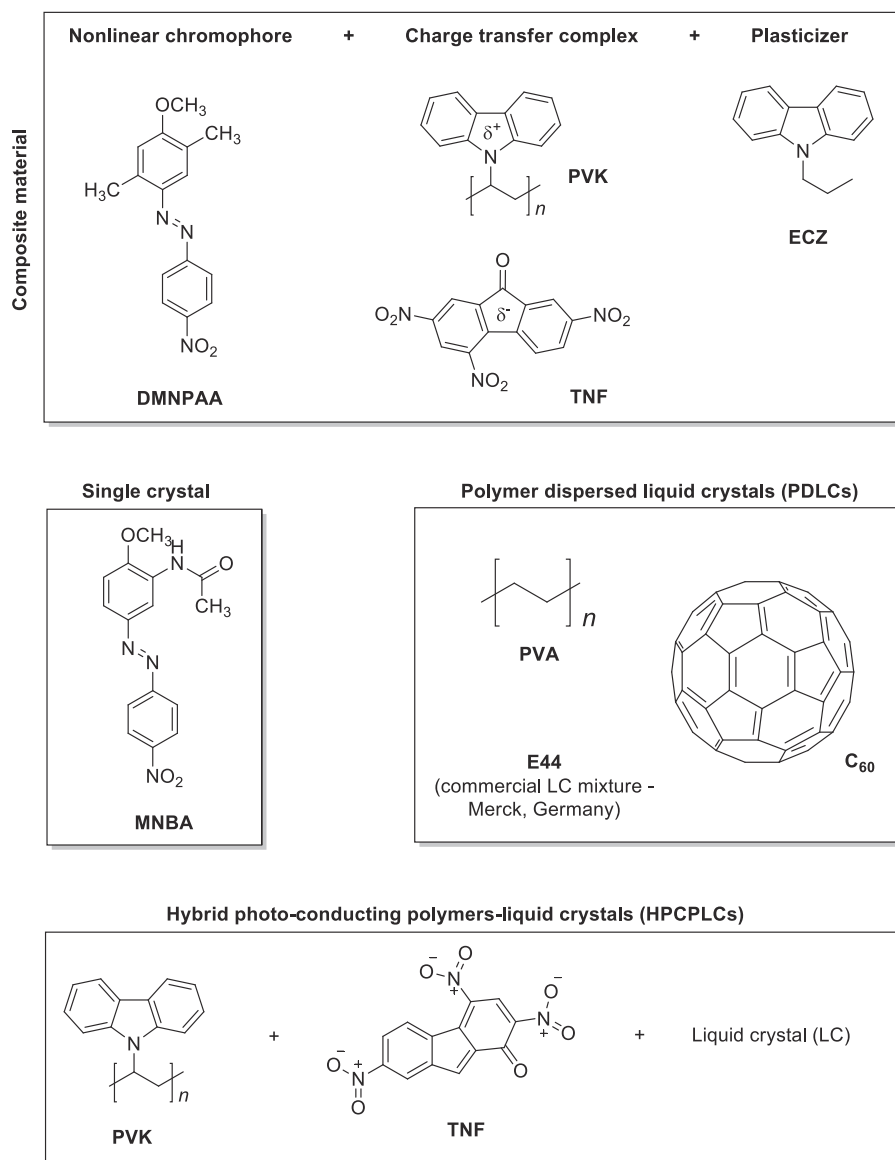
FIGURE 4.153 Examples of some representative organic photorefractive structures.

molecules as chromophores. Schematically, the four kinds of structures shown in Fig. 4.150 can be designed: (i) guest−host polymers; (ii) side chain polymers; (iii) main chain polymers; and (iv) thermally or photo-crosslinked polymers.

On the contrary to materials for second-order NLO effects, third- and higher-odd-order NLO materials are useful in many more fields of applications, such as third-harmonic generation, optical bistability, optical switching, and so on.

Moreover, for third- or higher-odd-order NLO materials, there are no symmetry restrictions to show nonlinear optical effects. Regarding organic heterocyclic materials, conjugated quasi 1D π electron systems exhibit an enhanced third-order NLO response. Among these systems, the semiconducting heterocyclic polymers shown in Fig. 4.151 can be taken into account.

4.3.7.2 Photorefractive heterocyclic materials: composite materials, liquid crystals and polymers

The basic condition to provide a photorefractive effect into a material is the Pockels effect which is a refractive index modulation created by the photoinduced space charge field combined with an applied external field. As a results, it determines the generation of a refractive index grating in an NLO material by its inhomogeneous illumination.

It follows that the refractive index grating will result in phase mismatch with respect to the intensity grating thus leading to the transfer of photons from one beam to another and thus providing light amplification.

There are four main processes involved in the photorefractive effect: (i) photo-charge generation by photon absorption, (ii) transportation of the generated charge carriers, (iii) trapping of the charge carriers in specific centers leading to charge separation and formation of the space charge field, and (iv) phase grating formation as a result of the space-charge field modulation of the refractive index via the linear electro-optical effect.

Ferroelectric single crystals have been the first systems showing a photorefractive effect. Anyway, in 1990, the photorefractive effect has been observed for the first time also in an organic doped molecular crystal.[372] In organic compounds is mainly the rotational mobility of NLO chromophores under the applied external electric field to contribute to photorefractive effect. Furthermore, in addition to rotational mobility, the organic material has to possess also: charge generation and separation capacity, charge mobility and linear electro-optic (Pockels) effect.

The common strategy used to satisfy the four different requirements needed for photorefractive effect consist into mixing together four types of molecules, ensuring that each of which satisfy at least one characteristic. The major examples of these class of molecules consisting in composite materials and/or polymers are shown in Fig. 4.152 and include: photo-conducting polymers (e.g., PVK, Polyvinylcarbazole), highly second-order nonlinear charge transfer molecules (e.g., DHD, 4-(N,N-bis(ß-dihydroxyethyl)amino)-4'-nitrostilbene), photosensitizer for charge generation under illumination (e.g., TNFDM, (2,4,7-trinitro-9-fluorenylidene)malononitrile and fullerene C_{60}) and plasticizer (e.g., ECZ, N-ethylcarbazole), lowering the glass transition temperature, thus increasing the rotational mobility.

Even if these molecules show high diffraction efficiencies and large exponential gain coefficients, they are characterized by two disadvantages consisting in: slow response times (in the order of seconds), and large external operation electric fields (about 100 V/μm) needed to show photorefractive effect.

TPID   **TPIR**
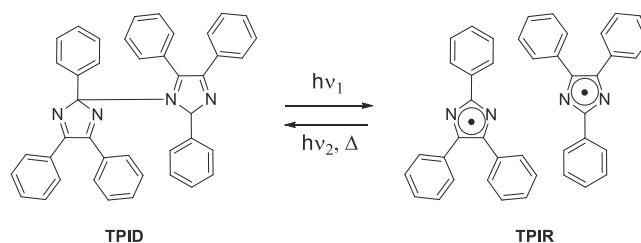
FIGURE 4.154   Photoinduced cleavage of the C−N bond in the triphenylimidazolyl dimer (TPID) leads to the production of two radicals triphenylimidazolyl radicals (TPIR).

closed form
N form

cis open form

trans open form
(MC form)

N=C Spiropyran
X=N Spirooxazines

zwitterionic form

quinoic form
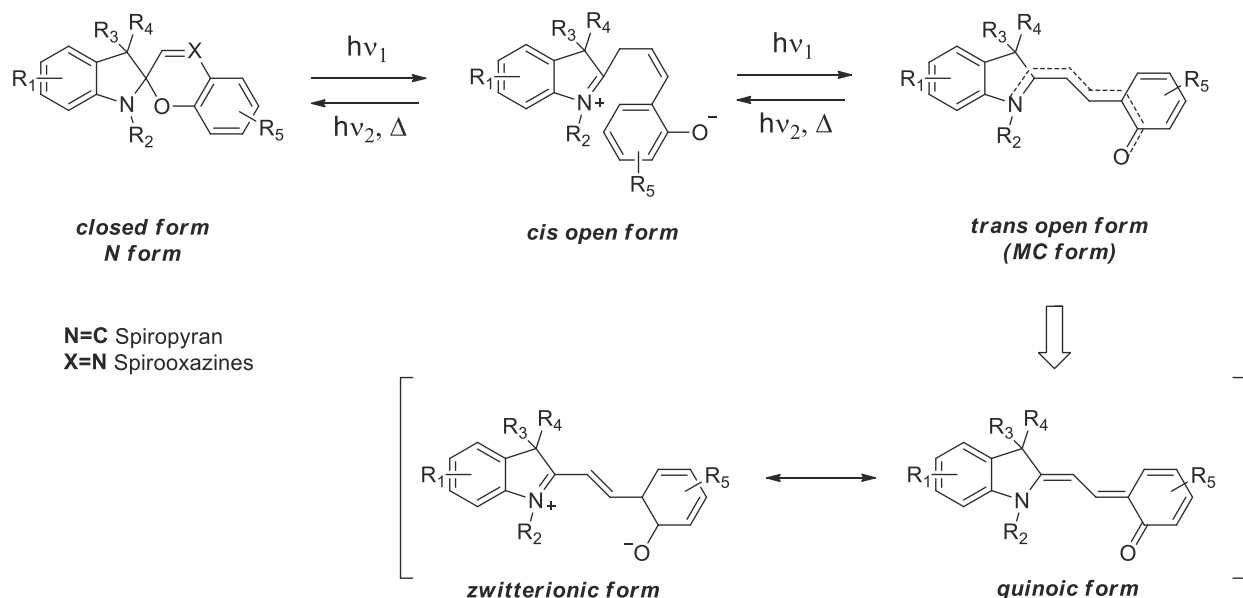
FIGURE 4.155   Example of cyclization reaction induced by UV light occurring in heterocyclic spiropyrans compounds.

Taking into account these drawbacks and with the aim to improve the response of organic photorefractive materials, liquid crystals have been used. They provide large rotational mobilities thus requiring an applied relatively small electric field and providing response time in the milliseconds range. In contrast with the composite materials for which the reorientation of individual molecules should take place to provide a photorefractive effect, the reorientation of small domains requires lower electric fields. Several types of photorefractive liquid crystal-based structures have been realized: (i) composite materials in which the NLO chromophores are represented by liquid crystals or mesogens (compounds displaying liquid crystal properties); (ii) polymer dispersed liquid crystals (PDLCs); (iii) hybrid photo-conducting polymers—liquid crystals (HPCPLCs). Furthermore, it has to be considered that the employing of photo-conducting polymer enhances the photorefractive effect by promoting the modulation of the electric field on the liquid crystal layer. Some representative organic photorefractive structures belonging to: mesogens (MNBA, 4'-nitrobenzylidene-3-acetamino-4-methoxyaniline), composite materials (e.g., DMNPAA:PVK:ECZ:TNF, 2,5-dimethyl-4-(p-nitrophenylazo)anisole, poly(N-vinylcarbazole), 2,4,7-
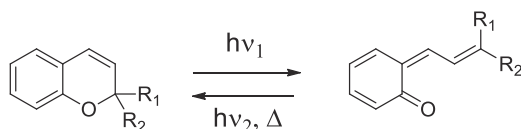
FIGURE 4.156   Example of an heterocyclic photochromic chromene compound undergoing cyclization reaction.

X=O Fulgides
X=NR Fulgimides

Aberchrome 540
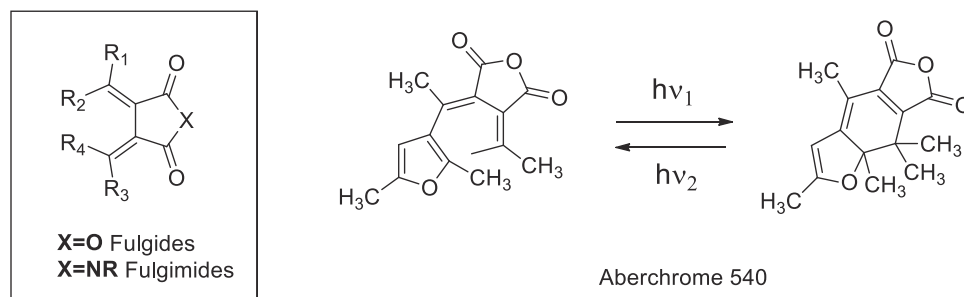
FIGURE 4.157   Cyclization reaction in fulgides and fulgimides occurs as a conversion among π and σ bonds and leads to an electrocyclization.
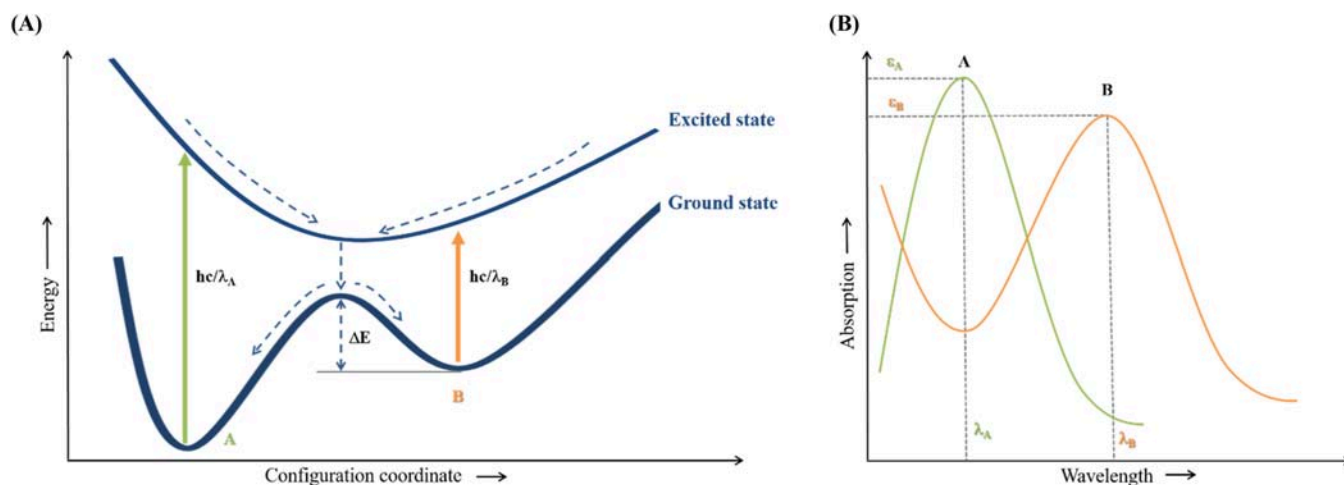
FIGURE 4.158   Left side (A): accepted model to describe the photochromism as a two-way unimolecular reaction occurring between two molecular species indicated as A (green) and B (orange) and separated by the potential barrier ΔE. Right side (B): the spectral absorption window in which the absorption bands of the species A and B are located.

trinitro-9-fluorenone, N-ethylcarbazole), PDLCs (e.g., PVA:E44:C60), and HPCPLCs (e.g., PVK/TNF/LC, Polyvinylcarbazole, 2,4,7-trinitrofluorenone, liquid crystal) are shown in Fig. 4.153.

4.3.7.3 Photochromic heterocyclic materials

The photochromism phenomenon is a color change due to the reversible conversion of a chemical species between two isomeric forms caused by electromagnetic radiation absorption.

Materials exhibiting photochromic properties are generally transparent but, when exposed to light, show increased light absorption and can be included into the families of optical glasses or plastic materials. From a practical point of view, the photochromic properties usually are originated by the addition of a photochromic substance to a transparent material.

Starting from the 2000s, most studies about organic heterocyclic photochromism deal with a group of less than 10 classes of compounds, and the vast majority concern diarylethene,[373−376] spiropyran,[377,378] spiroxazine,[379,380] chromene[381,382] and azobenzene[383,384] derivatives. Only few other classes of organic photochromic molecules have been studied until now and they include salicylideneanilines (anils), fulgides, and hexaarylbiimidazoles (HABIs).

The chemical reaction involved during the photochromic process can be grouped as follows: (i) proton transfer (e.g., salicylideneanilines or anils); (ii) *trans−cis* photoisomerization (e.g., azobenzene); (iii) homolytic cleavage (e.g., TPID); (iv) cyclization reaction (e.g., spiropyrans, spirooxazines, and chromenes, fulgides and fulgimides, diarylethenes). Among all the photochromic process just cited, only few examples related to some heterocyclic compounds are hereafter discussed.

The homolytic cleavage plays an essential role in the hexaarylbiimidazoles (HABIs) compounds.[385] In particular, the cleavage of the C−N bond linking the two imidazole moieties in the triphenylimidazolyl dimer (TPID) leads to the production of two radicals: the triphenylimidazolyl radicals (TPIR) shown in Fig. 4.154:

Heating the TPIR radical is a way to allow the recombination reaction occurring within few minutes at room temperature and reverting back to the starting TPID dimer. While TPID absorbs only in the UV range (less than 100 fs) and is colorless, TPIR has a large absorption band in the visible light.[386]

The cyclization reaction represents the way by which the majority of the studied photochromic systems react. It involves six p electrons delocalized over six different atoms, for example, in spiropyran, fulgides, diarylethenes and some related classes of compounds such as spirooxazine, chromene, and fulgimides. Just to make some examples, in Fig. 4.155, have been reported the heterocyclic spiropyrans compounds for which UV light irradiation of the colorless closed form (spiro or normal form, *N*) leads firstly to an open pyran ring reaction involving the cleavage of the C−O bond, and secondly to a *cis−trans* isomerization to finally give the colored merocyanine (MC) form.[387−389] This MC form is highly conjugated and exists as two mesomeric: zwitterionic and quinonic forms (sketched in Fig. 4.155) responsible for the intense absorption band in the visible range and therefore colored. In the closed form, owing to the broken conjugation at the spiro carbon atom, the molecule appears, instead, colorless as it absorbs only in the ultraviolet spectral region.

Another example of heterocyclic photochromic compounds based on a cyclization reaction is represented by the family chromenes[377,381,382] as sketched in Fig. 4.156:

Similar to spiropyrans and chromenes, photochromism in fulgides and fulgimides (Fig. 4.157) is based on a cyclization reaction occurring as a conversion among π and σ bonds and leading to an electrocyclization. On the contrary of spiropyrans, the open form of fulgides and fulgimides is colorless while their cyclized form is colored.

The widely accepted model useful to describe the photochromism is a simple two-way unimolecular reaction occurring between two molecular species indicated, in Fig. 4.158(A), as A and B and separated by the potential barrier ΔE.

Metastable systems for which the barrier ΔE is low are called T-type (thermally induced reaction from B to A), and B reverts back spontaneously to A. On the other hand, in bistable systems the ΔE barrier is high and only photons are able to cause the reaction (i.e., P-type systems) which means that in the dark conditions nothing changes. Typically, in photochromic bistable systems, such as ferroelectric or (ferro)magnetic systems, the conversion between the two states does not follow the same route, and they show the well-known hysteresis behavior, by plotting the polarization or the magnetization vs the electric or the magnetic field.

Usually, A absorbs in the (near) UV wavelengths region, and its peculiar absorption band and absorption coefficient are indicated, respectively, as λ_A and ε_A. When a photon matching the wavelength λ_A is absorbed, A is promoted from the ground to an upper energy state (excited state). The quantum yield quantifies the probability ($\phi_{A \rightarrow B}$) of the excited A* to yield B. A similar pattern is followed from B reverting back to A after that B is excited by absorbing at wavelength λ_B. The spectral window in which the absorption bands are located (see Fig. 4.158(B)), provides not only an indication about the color of light needed to induce the photochromism but also the molecule's color aspect after the reaction.

References

1. Björn, L. O., Ed. *Photobiology — The Science of Life and Light;* Springer: New York, 2008.
2. Clayton, R. K. *Light and Living Matter, The physical Part;* McGraw-Hill: New York, 1970.
3. Ceroni, P.; Credi, A.; Venturi, M. Light to investigate (read) and operate (write) molecular devices and machines. *Chem. Soc. Rev.* **2014,** *43,* 4068.
4. Venturi, M.; Iorga, M. I.; Putz, M. V. Molecular devices and machines: Hybrid organic-inorganic structures. *Curr. Org. Chem.* **2017,** *21* (27), 2731−2759.
5. I. Newton, Light Optics: Or a Treatise of the Reflections, Refractions, Inflections and Colors of Light — Fourth Edition London, 1730.
6. Huygens, C. *Traité de la Lumière;* Pieter van der Aa: Leiden, 1690.
7. Philosophical Transactions of the Royal Society. 94 (1804) 1−2.
8. Hertz, H. (Sifzungsber. D. Berl. Akad. D. Wiss., February 2, 1888, Wiedemann S Ann., 34, pp. SI), in H. Hertz In *On the Finite Velocity of Propagation of Electromagnetic Action;* Jones, D. E., Ed.; Dover Publications Inc.: Electric Waves, New York, 1962.
9. J. C. Maxwell, A Dynamical Theory of the Electromagnetic Field, Phil. Trans., 166, 1865, pp. 459−512; reprinted in The Scientific Papers of James Clerk Marwell, Volume I, New York, Dover, 1952, pp. 528−597.
10. Fraunhofer, J. Bestimmung des Brechungs- und des Farbenzerstreuungs-Vermögens verschiedener Glasarten, in Bezug auf die Vervollkommnung achromatischer Fernröhre. *Annalen der Phys.* **1817,** *56* (7), 264−313.
11. Planck, M. Zur Theorie des Gesetzes des Energieverteilung in Normalspektrum. *Verhandlungen der Deutschen Physikalischen Ges.* **1900,** *2,* 237−245.
12. Einstein, A. Über einen die Erzeugung und Verwandlung des Lichtes betreffenden heuristischen Gesichtspunkt. *Annalen der Phys.* **1905,** *332,* 132−148.
13. Kasha, M. *Disc. Faraday Soc.* **1950,** *9,* 14.
14. Kauzman, W. *Quantum Chemistry;* Academic Press: New York, 1957546ff.
15. Suzuki, H. *Electronic Absorption Spectra and Geometry of Organic Molecules. An Application of Molecular Orbital Theory,* 1st Edition; Academic Press: New York, 1967.
16. J.H. Lambert, Photometria sive de mensura et gradibus luminis, colorum et umbrae [Photometry, or, On the measure and gradations of light intensity, colors, and shade] (in Latin). Augsburg, (Germany) (1760): Eberhardt Klett.
17. Beer, A. Bestimmung der Absorption des rothen Lichts in farbigen Flüssigkeiten [Determination of the absorption of red light in colored liquids]. *Annalen der Phys. und Chem. (Ger.)* **1852,** *86* (5), 78−88.
18. Lakowicz, J. R. *Principles of Fluorescence Spectroscopy;* Plenum: New York, 1999.
19. T. Eicher, S. Hauptmann, A. Speicher, The Chemistry of Heterocycles: Structures, Reactions, Synthesis, and Applications, 3rd, Completely Revised and Enlarged Edition.
20. V. J. Ram, A. Sethi, M. Nath, R. Pratap, The Chemistry of Heterocycles Nomenclature and Chemistry of Three-to-Five Membered Heterocycles (2019).
21. Gupta, R. R.; Kumar, M.; Gupta, V. *Four-Membered Heterocycles. Heterocyclic Chemistry;* Springer: Berlin, Heidelberg, 1998357−410.
22. Mahoney, C.; Smith, R.; Johnston, J. N. *J. Am. Chem. Soc.* **2005,** *127,* 1354.
23. Gabriel, S.; Weiner, J. *Chem. Ber.* **1888,** *21,* 2669.
24. Wenker, H. *J. Am. Chem. Soc.* **1935,** *57,* 2328.
25. Pfister, J. R. *Synthesis* **1984,** 969.
26. Corey, E. J.; Chaikovsky, M. *J. Am. Chem. Soc.* **1965,** *87,* 1353.
27. Tsuchiya, Y.; Kumamoto, T.; Ishikawa, T. *J. Org. Chem.* **2004,** *69,* 8504.
28. Appel, R.; Halstenberg, M. *Chem. Ber.* **1976,** *109,* 814.
29. Neber, P. W.; Huh, G. *Liebigs Ann. Chem.* **1935,** 283.
30. Neber, P. W.; Burgard, A. *Liebigs Ann. Chem.* **1932,** *281,* 75.
31. Padwa, A.; Ku, H. *J. Org. Chem.* **1979,** *44,* 255.
32. Wip, P.; Heimgartner, H. *Helv. Chim. Acta* **1988,** *7,* 140.
33. Gentilucci, L.; Grijzen, Y.; Thijs, L.; Zwanenburg, B. *Tetrahedron Lett.* **1995,** *36,* 4665.
34. Kristinnson, H.; Griffin, G. W. *J. Am. Chem. Soc.* **1966,** *88,* 1579.
35. Brokatzky-Geiger, J.; Eberbach, W. *Tetrahedron Lett.* **1984,** *25,* 1137.
36. Kristinnson, H.; Griffin, G. W. *Angew. Chem., Int. (Ed.) Engl.* **1965,** *4,* 868.
37. Azizi, N.; Yadollahy, Z.; Rahimzadeh-oskooee, A. *Synlett* **2014,** *25,* 1085.
38. Valiulin, R. A.; Bhuvan Kumar, N. N.; Kuznetsov, D. M.; Kutateladze, A. G. *J. Sulfur. Chem.* **2013,** *34,* 209−221.
39. Schmitz, E.; Habisch, D. *Chem. Ber.* **1962,** *95,* 680−687.
40. Hwang, K.; Yu, C.; Lee, I. Y. *Bull. Korean Chem. Soc.* **1994,** 523.
41. Denisenko, S. N. *Mendelev Commun.* **1998,** *8,* 54.
42. Middleton, W. J.; Krespan, C. G. *J. Org. Chem.* **1965,** *30,* 1398.
43. Abendroth, H. J.; Henrich, G. *Angew. Chem.* **1962,** *95,* 2714.
44. Emmons, W. D. *J. Am. Chem. Soc.* **1956,** *78,* 6208.
45. Davis, F. A.; Jenkins, R.; Yocklovich, S. G. *Tetrahedron Lett.* **1978,** *5171,* 272.
46. Arnone, A.; Novo, B.; Regnolato, P. M.; Resnati, G.; Terreni, M. *J. Org. Chem.* **1997,** *62,* 6401.
47. Davis, F. A.; Tringer, S. O. D.; Billmers, J. M. *Tetrahedron Lett.* **1983,** *24,* 1213.
48. Zajac, W. W., Jr; Walters, T. R.; Darcy, M. G. *J. Org. Chem.* **1988,** *53,* 5856.
49. Davis, F. A.; Vishwakarma, L. C.; Billmers, J. G.; Finn, J. *J. Org. Chem.* **1984,** *49,* 3241.
50. Davis, F. A.; Sheppard, A. C. *J. Org. Chem.* **1987,** *52,* 954.
51. Boyd, D. R.; Jennings, W. B.; Spratt, R.; Jerina, D. M. *Chem. Commun.* **1970,** 745.

52. Emmons, W. D. *J. Am. Chem. Soc.* **1957,** *79*, 5739.
53. Ogata, Y.; Sawaki, Y. *J. Am. Chem. Soc.* **1973,** *95*, 4687.
54. Schimtz, E.; Ohme, R.; Schramm, S.; Striegler, H.; Heyne, H. U.; Rusche, J. *J. Prakt. Chem.* **1977,** *319*, 195.
55. King, R. Y.; Douvan, I.; Sternbach, L. H. *J. Org. Chem.* **1970,** *35*, 2243.
56. Splitter, J. S.; Calvin, M. *J. Org. Chem.* **1958,** *23*, 651.
57. Gilbert, M.; Ferrer, M.; Sanchez-Baeza, F.; Messeguer, A. *Tetrahedron* **1997,** *53*, 8643.
58. Denmark, S. E.; Wu, Z. *J. Org. Chem.* **1997,** *62*, 8964.
59. Reiser, O. *Angew. Chem. Int. (Ed.) Engl.* **1994,** *33*, 69.
60. Adam, W.; Smerz, A. K.; Zhao, C.-G. *J. Prakt. Chem.* **1997,** *339*, 298.
61. Murray, R. W.; Shiang, D. L. *J. Chem. Soc., Perkin Trans.* **1990,** *2*, 349.
62. Schroeder, K. W. S. *Eur. J. Org. Chem.* **2005,** 496.
63. Liu, M. T. H. *Chem. Soc. Rev.* **1982,** *11*, 127.
64. Likhotvorik, I. R.; Tae, E. L.; Ventre, C.; Platz, M. S. *Tetrahedron Lett.* **2000,** *41*, 795.
65. Dale, J. *Tetrahedron* **1993,** *49*, 8707.
66. Chan, S. I.; Zinn, J.; Gwinn, W. D. *J. Chem. Phys.* **1961,** *34*, 1319−1329.
67. Luger, P.; Buschmann, J. *J. Am. Chem. Soc.* **1984,** *106*, 7118−7121.
68. Bull, J. A.; Croft, R. A.; Davis, O. A.; Doran, R.; Morgan, K. F. *Chem. Rev.* **2016,** *116* (19), 12150−12233.
69. Braun, M. *Nachr. Chem. Techn. Lab.* **1985,** *33*, 213.
70. Part 3 Hassner, A., Ed. *The Chemistry of Heterocyclic Compounds*, Volume 42; Small Ring Heterocycles, 1982.
71. Vogelbacher, U.-J.; Regitz, M.; Mynott, R. *Angew. Chem. Int. (Ed.) Engl.* **1986,** *25*, 842.
72. Regitz, M. *Nachr. Chem. Techn. Lab.* **1991,** *39*, 9.
73. Sammes, P. G.; Smith, S. *J. Chem. Soc., Chem. Commun.* **1983,** 682.
74. Ogier, L.; Turpin, F.; Baldwin, R. M.; Riche, F.; Law, H.; Innis, R. B.; Tamagnan, G. *J. Org. Chem.* **2002,** *67*, 3637.
75. Marinetti, A.; Hubert, P.; Genet, J.-P. *Eur. J. Org. Chem.* **2000,** 1815.
76. Padwa, A.; Gruber, R.; Hamilton, L. *J. Am. Chem. Soc.* **1967,** *89*, 3077.
77. Adam, W.; Cilento, G. *Angew. Chem. Int. (Ed.) Engl.* **1983,** *22*, 529.
78. Adam, W.; Baader, W. J. *Angew. Chem. Int. (Ed.) Engl.* **1984,** *23*, 166.
79. Kopecky, K. R.; Lockwood, P. A.; Filby, J. E.; Reid, R. W. *ibid* **1973,** *57*, 468.
80. Guttenberger, H. G.; Bestmann, H. J.; Dickert, F. L.; Jorgensen, F. S.; Snyder, J. P. *J. Am. Chem. Soc.* **1980,** *103*, 159.
81. Block, E. In *Reactions of Organosulfur Compounds;* Blomquist, A. T., Wasserman, H. H., Eds.; Academic: New York, 1978.
82. Bartlett, P. D.; Landis, M. E. In *In Singlet Oxygen;* Wasserman, H. H., Murray, R. W., Eds.; Academic: New York, 1979.
83. Lown, J. W.; Koganty, R. R. *J. Am. Chem. Soc.* **1986,** *108*, 3811.
84. Block, E.; Bazzi, A. A.; Rsvelle, L. K. *J. Am. Chem. Soc.* **1980,** *102*, 2490.
85. Küsters, W.; De Mayo, P. *J. Am. Chem. Soc.* **1973,** *P5*, 2383.
86. Nielsen, S. B.; Senning, A. *Sulfur. Rep.* **1995,** *16*, 371.
87. Nakayama, J.; Mizumura, A.; Yokomori, Y.; Krebs, A. *Tetrahedron Lett.* **1995,** *36*, 8583.
88. Nakayama, J.; Choi, K. S.; Akiyama, I.; Hoshino, M. *Tetrahedron Lett.* **1993,** *34*, 115.
89. Choi, K. S.; Akiyama, I.; Hoshino, M.; Nakayama, J. *Bull. Chem. Soc. Jpn.* **1993,** *66*, 623.
90. Nunn, E. E.; Warrener, R. N. *J. Chem. Soc., Chem. Commun.* **1972,** 818.
91. Ujike, K.; Kudoh, S.; Nakata, M. *Chem. Phys. Lett.* **2004,** *396*, 288.
92. Ujike, K.; Akai, N.; Kudoh, S.; Nakata, M. *J. Mol. Struct.* **2005,** *735−736*, 335.
93. Moderhack, D. *Chem. Heterocycl. Comp.* **2019,** *55*, 3−24.
94. Inomata, K.; Sumita, M.; Kotake, H. *Chem. Lett.* **1979,** 709.
95. Rao, H. S. P.; Jothilingam, S. *J. Org. Chem.* **2003,** *68*, 5392−5394.
96. Liu, J. L. L.; Ding, D.; Sun, J.; Ji, Y.; Dong, J. *Org. Lett.* **2013,** *15*, 2858−2861.
97. Duan, X.-H.; Liu, X.-Y.; Guo, L.-N.; Liao, M.-C.; Liu, W.-M.; Liang, Y.-M. *J. Org. Chem.* **2005,** *70*, 6980.
98. Liu, W.; Jiang, H.; Zhang, M.; Qi, C. *J. Org. Chem.* **2010,** *75*, 966−968.
99. Li, L.; Zhao, M.-N.; Ren, Z.-H.; Li, J.; Guan, Z.-H. *Synthesis* **2012,** *44*, 532−540.
100. Yoshida, M.; Al-Amin, M.; Shishido, K. *Synthesis* **2009,** 2454−2466.
101. Howes, P. D.; Sterling, C. J. M. *Org. Synth.* **1973,** *1*, 53.
102. Batty, J. W.; Howes, P. D., et al. *J. Chem. Soc. Perkin Trans.* **1973,** *1*, 65.
103. Garst, E.; Spencer, T. A. *J. Org. Chem.* **1974,** *39*, 584.
104. Ghosh, M.; Mishra, S.; Hajra, A. *J. Org. Chem.* **2015,** *80*, 5364.
105. Dann, O.; Distler, H. *Merkel Chem, H. Ber.* **1952,** *85*, 457.
106. Huang, Y.; Li, X.; Yu, Y.; Zhu, C.; Wu, W.; Jiang, H. *J. Org. Chem.* **2016,** *81*, 5014.
107. D'Auria, M.; Racioppi, R.; Romaniello, G. *Eur. J. Org. Chem.* **2000,** *3265*.
108. Buckle, D. R.; Rockell, C. J. M. *J. Chem. Soc. Perkin Trans.* **1985,** *1*, 2443.
109. Brewer, J. D.; Elix, J. A. *Tetrahedron Lett.* **1969,** 4139.
110. Arcadi, A.; Marinelli, F.; Cacchi, S. *Synthesis* **1986,** 749.
111. Abdel-Wahhab, S. M.; El-Rayyes, N. R. *J. Prakt. Chem.* **1972,** *314*, 213.
112. El-Abbady, A. M.; El-Assal, L. S. *J. Chem. Soc.* **1959,** *1024*, 311.
113. Deschamps-Vallet, C.; Ilotse, J.-B.; Meyer-Dayan, M.; Molho, D. *Tetrahedron Lett.* **1979,** 1109.
114. van Otterlo, W. A. L.; Morgans, G. L.; Madeley, L. G.; Kuzvidza, S.; Moleele, S. S.; Thornton, N.; de Koning, C. B. *Tetrahedron* **2005,** *61*, 7746−7755.
115. Nishio, T.; Shiwa, K.; Sakamoto, M. *Helv. Chim. Acta* **2003,** *86*, 3255.

116. Jhang, Y.; Xue, J.; Gao, Y.; Fun, H.-K.; Xu, J.-H. *J. Chem. Soc. Perkin Trans. I* **2002,** 345.
117. Ashraf, M. A.; Jones, M. A.; Kelly, N. E., et al. *Tetrahedron Lett.* **2003,** *44,* 3151.
118. Sauter, M.; Adam, W. *Acc. Chem. Res.* **1995,** *28,* 289.
119. Potts, K. I. T.; Elliott, J. *Org. Prep. Proced. Int.* **1972,** *4,* 269.
120. Lepage, L.; Lepage, Y. *J. Heterocycl. Chem.* **1978,** *15,* 793.
121. Serpaud, B.; Lepage, Y. *Bull. Soc. Chim. Fr.* **1977,** 539.
122. Christopfel, W. C.; Miller, L. L. *Tetrahedron* **1987,** *43,* 3681.
123. Sasaki, T.; Kanematsu, K.; Hayakawa, K.; Sugiura, M. *J. Am. Chem. Soc.* **1975,** *97,* 355.
124. Du, Z.; Zhou, J.; Si, C.; Ma, W. *Synlett* **2011,** 3023−3025.
125. Panda, N.; Mattan, I.; Nayak, D. K. *J. Org. Chem.* **2015,** *80,* 6590−6597.
126. Brown, R. F. C.; Jones, C. M. *Aust. J. Chem.* **1817,** *1980,* 33.
127. Wang, S. X.; Hao, S. C.; Gao, Z.; Chen, J.; Qiu, J. *Computational Theor. Chem.* **2014,** *1042,* 49−56.
128. Gewald, K.; Schinke, E.; Bottcher, H. *Chem. Ber.* **1966,** *94,* 99.
129. Steliou, K.; Mrani, M. *J. Am. Chem. Soc.* **1982,** *104,* 3104.
130. Hinsberg, O. *Ber.* **1910,** *43,* 901.
131. Fiesselmann, H., et al. *Chem. Ber.* **1954,** *87* (837), 841.
132. Voronkov, M. G.; Udre, V. E.; Popova Khim, E. P. *Geterotsikl. Soedin.* **1967,** 1003.
133. Obrecht, D.; Gerber, F.; Sprenger, D.; Masquelin, T. *Helv. Chim. Acta* **1997,** *80,* 531.
134. Schulte, K. E.; Reisch, J.; Horner, L. *Angew. Chem.* **1960,** *920,* 72.
135. Schulte, K. E.; Reisch, J.; Horner, L. *Chem. Ber.* **1943,** *1962,* 95.
136. Freeman, F.; Lu, H.; Rodriguez, E. *Tetrahedron Lett.* **1753,** *1993,* 34.
137. Ram, V. J.; Haque, N.; Shoeb, A. *Sulfur. Lett.* **1993,** *16,* 165.
138. Drevko B. I., Smushkin M. I., Kharchenko V. G., *Khim. Geterotsikl. Soedin* 1996, 32, 913. *Chem. Heterocycl. Compd.* (Engl. Transl.) 1996, 32, 777.
139. Lie Ken Jie, M. S. F.; Zheng, Y. F. *Synthesis* **1988,** 467.
140. Rajappa, S.; Natekar, M. V. In *In Comprehensive Heterocyclic Chemistry, II;* Katritzky, A. R., Rees, C. W., Scriven, E. F. V., Eds.; vol. 2; Pergamon: Oxford, 1996; p. 491.
141. D'Auria, M. *Tetrahedron Lett.* **1995,** *36,* 6567.
142. Neidlein, R.; Gehringer, C. *Tetrahedron* **1977,** *33,* 3233.
143. Campaigne, E.; Clong, R. E. *J. Org. Chem.* **1956,** *21,* 39.
144. Campaigne, E.; Abe, Y. *J. Heterocycl. Chem.* **1975,** *12,* 889.
145. Iddon, B.; Scrowston, R. M. *Adv. Hetercycl. Chem.* **1970,** *11,* 177.
146. Hansch, C.; Lindwall, H. G. *J. Org. Chem.* **1945,** *10,* 381.
147. Abarca, B.; Ballesteros, R.; Enriquez, E.; Jones, G. *Tetrahedron* **1985,** *41,* 2435.
148. Okuda, Y.; Lakshikantham, M. V.; Cava, M. P. *J. Org. Chem.* **1991,** *56,* 6024.
149. Voronkov, M. G.; Faitel'son, F. D. *Khim Geterotsikl Soedin.* **1970,** *2,* 245.
150. Klemm, L. H.; McCoy, D. R.; Olsen, D. R. *J. Heterocycl. Chem.* **1970,** *7,* 1347.
151. Carruthers, W.; Douglas, A. G. *J. Chem. Soc.* **1959,** 2813.
152. McCall, E. B. *Br. Pat.* **1953,** *701,* 267.
153. Black, M.; Cadogan, J. I. G.; McNab, H. *Tetrahedron* **1992,** *48,* 7747.
154. Ashby, J.; Ayad, M.; Meth-Cohn, O. *J. Chem. Soc. Perkin Trans. 1* **1973,** 1099.
155. Bunrit, A.; Sawadjoon, S.; Tšupova, S.; Sjöberg, P. J. R.; Samec, J. S. M. *J. Org. Chem.* **2016,** *81,* 1450−1460.
156. Kim, C.-E.; Park, S.; Eom, D.; Seo, B.; Lee, P. H. *Org. Lett.* **2014,** *16,* 1900−1903.
157. Tejedor, D.; González-Cruz, D.; García-Tellado, F.; Marrero-Tellado, J. J.; Rodríguez, M. L. *J. Am. Chem. Soc.* **2004,** *126,* 8390−8391.
158. Yan, R.; Kang, X.; Zhou, X.; Li, X.; Liu, X.; Xiang, L.; Li, Y.; Huang, G. *J. Org. Chem.* **2014,** *79,* 465.
159. Possel, O.; van Leusen, A. M. *Heterocycles* **1977,** *7,* 77.
160. Li, J. K. *Heterocyclic Chemistry in Drug Discovery;* Wiley: New York, 2013. ISBN: 9781118354421.
161. Piloty, O. *Chem. Ber.* **1910,** *489,* 43.
162. Alizadeh, A.; Rezvanian, A.; Bijanzadeh, H. R. *Synthesis* **2008,** 725−728.
163. Pedersen, C. L.; Buchardt, O. *Acta. Chem. Scand.* **1973,** *27* (271).
164. Robinson, B. *Chem. Rev.* **1963,** *63,* 373.
165. Robinson, B. *Fischer Indole Synth.* **1969,** *69,* 273.
166. Noland, W. E.; Baude, F. *J. Org. Synth. Coll.* **1973,** *V,* 567.
167. Clark, R. D.; Repke, D. B. *Heterocycles* **1984,** *22,* 15.
168. Cournoyer, R.; Evan, D. H., et al. *J. Org. Chem.* **1991,** *56,* 4576.
169. Madelung, W. *Chem. Ber.* **1912,** *45,* 1128.
170. Nenitzesch, C. D. *Bull. Soc. Chim. Rom.* **1929,** *11,* 37−43.
171. Bartoli, G.; Palonieri, G., et al. *Tetrahedron Lett.* **1984,** *30,* 2129.
172. Bischler, A.; Brion, H. *Chem. Ber.* **1892,** *25,* 2860.
173. Bischler, A.; Firemann, P. *Chem. Ber.* **1893,** *26,* 1336.
174. Kobayashi, Y.; Fukuyama, T. *J. Heterocycl. Chem.* **1998,** *35,* 1043.
175. Gassman, P. G.; Van Bergin, T. J., et al. *J. Am. Chem. Soc.* **1974,** *96,* 5495.
176. Sugasawa, T.; Adachi, M., et al. *J. Org. Chem.* **1979,** *578,* 44.
177. Jaques, B.; Wallace, R. G. *Tetrahedron* **1977,** *33,* 581−588.
178. Haddadin, M. J.; Chelhot, N. C. *Tetrahedron Lett.* **1973,** 5185.

179. Worlikar, S. A.; Larock, R. C. *J. Org. Chem.* **2008,** *73,* 7175.

180. Kreher, R.; Vogt, G. *Angew. Chem. Int. (Ed.) Engl.* **1970,** *9,* 955.

181. Boekelheide, V.; Windgassen, R. J., Jr. *J. Am. Chem. Soc.* **1959,** *81,* 1456.

182. Cornforth, J.; Ming-Hui, D. *J. Chem. Soc. Perkin Trans.* **1990,** *1,* 1463.

183. Nugent, R. A.; Murphy, M. *J. Org. Chem.* **1987,** *52,* 2206.

184. Ikeda, M.; Ohno, K.; Mohri, S.-I.; Takahashi, M.; Tamura, Y. *J. Chem. Soc. Perkin Trans. 1* **1984,** *405,* 122.

185. Rawal, V. H.; Jones, R. J.; Cava, M. P. *Tetrahedron Lett.* **1985,** *26,* 2423.

186. Rettig, W.; Wirz, J. *Helv. Chim. Acta* **1978,** *61,* 444.

187. Miller, R. B.; Stowell, J. G. *J. Org. Chem.* **1983,** *48,* 886.

188. Kotani, E.; Kobayashi, S.; Adachi, M.; Tsujioka, T.; Nakamura, K.; Tobinaga, S. *Chem. Pharm. Bull.* **1989,** *37,* 606−609.

189. Kohda, A.; Nagayoshi, K.; Maemoto, K.; Sato, T. *J. Org. Chem.* **1983,** *48,* 425−432.

190. Lee, J. C.; Song, I. G. *Tetrahedron Lett.* **2000,** *41,* 5891−5894.

191. Himo, F.; Lovell, T.; Himgraf, R.; Rostovtsev, V. V.; Noddleman, L.; Sharpless, A. B.; Fokin, V. V. *J. Am. Chem. Soc.* **2005,** *210,* 127.

192. Hansen, T. V.; Wu, T.; Fokin, V. V. *J. Org. Chem.* **2005,** *7761,* 70.

193. Waldo, J. P.; Larock, R. C. *Org. Lett.* **2005,** *7,* 5203−5205.

194. Waldo, J. P.; Larock, R. C. *J. Org. Chem.* **2007,** *72,* 9643−9647.

195. Jeong, Y.; Kim, B. I.; Lee, J. K.; Ryu, J. S. *J. Org. Chem.* **2014,** *79,* 6444−6455.

196. She, Z.; Niu, D.; Chem, L.; Gunawan, M. A.; Shanja, X.; Hersh, W. H.; Chen, Y. *J. Org. Chem.* **2012,** *77,* 3627−3633.

197. Bredereck, H., et al. *Chem. Ber.* **1959,** *92,* 338.

198. Wallach, O. *Annalen* **1882,** *214,* 257.

199. Wallach, O.; Boehringer, A. *Annalen* **1887,** *184,* 50.

200. Knorr, L. *Chem. Ber.* **1883,** 2597−2599.

201. Hutter, R., et al. *Ann* **1956,** *598,* 186.

202. Von Auwers, K.; Stuhlmann, H. *Chem. Ber.* **1926,** *59,* 1043.

203. Tang, M.; Wang, Y.; Wang, H.; Kong, Y. *Synthesis* **2016,** *48,* 3065.

204. Okuro, K.; Furuune, M.; Miura, M.; Nomura, M. *J. Org. Chem.* **1992,** *57,* 4754.

205. Gelin, S.; Chantegrel, B.; Nadi, A. I. *J. Org. Chem.* **1983,** *48,* 4078.

206. Miyagawa, N.; Karatsu, T.; Kitamura, A. *Chem. Lett.* **1997,** 1005.

207. Clapp, L. B. In *In Comprehensive Heterocyclic Chemistry;* Katritzky, A. R., Rees, C. W., Eds.; vol. 6; Oxford: Pergman, 1984; p 365.

208. Eber, G.; Schneider, S.; Ber, F. D. *der Bunsen-Gesellschaft-Physical Chem. Chem. Phys.* **1980,** *84,* 281.

209. Adib, M.; Mahdavi, M.; Mahmoodi, N.; Pirelahi, H.; Bijanzadeh, H. R. *Synlett* **2006,** 1765−1767.

210. Augustine, J. K.; Akabote, V.; Hegde, S. G.; Alagarsamy, P. *J. Org. Chem.* **2009,** *74,* 5640−5643.

211. Leite, A. C. L.; Viera, R. F.; Wanderley, A. G., et al. *Il Farmaco* **2000,** *55,* 719.

212. Braga, A. L.; Lüdtke, D. S.; Alberto, E. E.; Dornelles, L.; Severo Filho, W. A.; Corbellini, V. A.; Rosa, D. M.; Schwab, R. S. *Synthesis* **2004,** 1589−1594.

213. Jochims, J. C.; Thomas, E. W. In *In Comprehensive Heterocyclic Chemistry;* Potts, K. T., Ed.; vol. 4; Pergamon Press: Oxford, 1996; p. 179.

214. Buscemi, S.; Vivona, N. *Heterocycles* **1989,** *29,* 737.

215. Buscemi, S.; Macaluso, G.; Vivona, N. *Heterocycles* **1989,** *29,* 1301.

216. Andrianov, V. G.; Semenikhina, V. G.; Eremeev, A. V. *Zhurnal Organicheskoi Khimii* **1993,** *29,* 1062.

217. Andrianov, V. G.; Eremeev, A. V. *Khimiya Geterotsiklicheskikh Soedinenii* **1990,** 1443.

218. Bianchi G., De Micheli C., et al. Wiley, London 1977, 369.

219. Sherman, W. R.; Von Esch, A. *J. Org. Chem.* **1961,** *27,* 3472.

220. Torres, M.; Clement, A.; Bertie, J. E., et al. *J. Org. Chem.* **1978,** *43,* 2490.

221. Font, J.; Torres, M.; Gunning, H. E.; Strausz, O. P. *J. Org. Chem.* **1978,** *43,* 2487.

222. Burgess, E. M.; Carithers, R.; McCullagh, L. *J. Am. Chem. Soc.* **1968,** *90* (7), 1923−1924.

223. Koguro, K.; Oga, T.; Mitsui, S.; Orita, R. *Synthesis* **1998,** 910−914.

224. Li, J.; Chen, S. Y.; Tao, S., et al. *Bioorg. Med. Chem. Lett.* **1825,** *2008,* 18.

225. Prasad, V. S. R.; Sambaiah, T.; Reddy, K. K. *Synth. Commun.* **1983,** *1990,* 20.

226. Suzuki, H.; Hwang, Y. S.; Nakaya, C.; Matano, Y. *Synthesis* **1993,** 1218−1220.

227. Scheiner, P. *J. Org. Chem.* **1969,** *34,* 199.

228. Chae, Y. B.; Chang, K. S.; Kim, S. S. *Daehan Hwuhak Hwoejee* **1967,** *11,* 85 *Chem. Abst.* 1969, 70, 20031.

229. Skell, P. S.; Sandler, R. S. *J. Am. Chem. Soc.* **1958,** *88,* 2024.

230. Jones, R. L.; Rees, C. W. *J. Chem. Soc. C. (Org.)* **1969,** *18,* 2249.

231. Gambacorta, A.; Nicoletti, R.; Cerrini, S.; Fedeli, W.; Gavuzzo, E. *Tetrahedron Lett.* **1978,** *19,* 2439.

232. Zecher, W.; Krohnke, F. *Chem. Ber.* **1961,** *94,* 690.

233. Bohlmann, F. *Rahtz Chem. Ber.* **1957,** *90,* 2265.

234. Guareschi, I. *Real. Mem. Accad. Sci. Torino.* **1896,** *46,* 1.

235. Baron, H.; Rernfry, F. G.; Thorpe, J. F. *J. Chem. Soc.* **1726,** *1904,* 85.

236. Chichibabin, A. E. *J. Russ. Phys. Chem. Soc.* **1906,** *37,* 1229.

237. Chichibabin, A. E. *J. Prakt. Chem.* **1924,** *107,* 122.

238. Frank, R. L.; Seven, R. P. *J. Am. Chem. Soc.* **1949,** *71,* 2629.

239. Tauber, E. *Chem. Ber.* **1895,** *28,* 451.

240. Serullas, A. *Ann. Chim. Phys.* **1828,** *38,* 379.

241. Nelsen, S. F.; Fibiger, R. *J. Am. Chem. Soc.* **1972,** *94,* 8497.

242. Kearns, D.; Calvin, M. *J. Chem. Phys.* **1958,** *29,* 950.

243. Yu, G.; Gao, J.; Hummelen, J. C.; Wudl, F.; Heeger, A. J. *Science* **1995,** *270*, 1789.
244. Krebs, F. C.; Nielsen, T. D.; Fyenbo, J.; Wadstrøm, M.; Pedersen, M. S. *Energy Environ. Sci.* **2010,** *3*, 512.
245. Yun, J.-M.; Yeo, J.-S.; Kim, J.; Jeong, H.-G.; Kim, D.-Y.; Noh, Y.-J.; Kim, S.-S.; Ku, B.-C.; Na, S.-I. *Adv. Mater.* **2011,** *23*, 4923.
246. Armin, A.; Li, W.; Sandberg, O. J.; Xiao, Z.; Ding, L.; Nelson, J.; Neher, D.; Vandewal, K.; Shoaee, S.; Wang, H. A. T.; Heumueller, T.; Brabec, C.; Meredith, P. *Adv. Energy Mater.* **2021,** *11*, 2003570.
247. Wöhrle, D.; Meissner, D. *Adv. Mater.* **1991,** *3*, 129.
248. Lu, L.; Zheng, T.; Wu, Q.; Schneider, A. M.; Zhao, D.; Yu, L. *Chem. Rev.* **2015,** *115*, 12666.
249. Servaites, J. D.; Ratner, M. A.; Marks, T. J. *Energy Environ. Sci.* **2011,** *4*, 4410.
250. Hiramoto, M.; Fujiwara, H.; Yokoyama, M. *Appl. Phys. Lett.* **1991,** *58*, 1062.
251. Halls, J. J. M.; Walsh, C. A.; Greenham, N. C.; Marseglia, E. A.; Friend, R. H.; Moratti, S. C.; Holmes, A. B. *Lett. Nat.* **1995,** *376*, 498.
252. Spanggaard, H.; Krebs, F. C. *Sol. Energy Mater. Sol. Cell* **2004,** *83*, 125.
253. Brabec, C. J.; Sariciftci, N. S.; Hummelen, J. C. *Adv. Funct. Mater.* **2001,** *11*, 15.
254. Mihailetchi, V. D.; Xie, H. X.; De Boer, B.; Koster, L. J. A.; Blom, P. W. M. *Adv. Funct. Mater.* **2006,** *16*, 699.
255. Huang, J. S.; Li, G.; Yang, Y. *Appl. Phys. Lett.* **2005,** *87*, 112105.
256. Choi, J. H.; Son, K.-I.; Kim, T.; Kim, K.; Ohkubo, K.; Fukuzumi, S. *J. Mater. Chem.* **2010,** *20*, 475.
257. Zhang, Y.; Yip, H.-L.; Acton, O.; Hau, S. K.; Huang, F.; Jen, A. K. Y. *Chem. Mater.* **2009,** *21*, 2598.
258. Cheng, Y.-J.; Yang, S.-H.; Hsu, C.-S. *Chem. Rev.* **2009,** *109*, 5868.
259. Etxebarria, I.; Ajuria, J.; Pacios, R. *Org. Electron.* **2015,** *19*, 34.
260. Schilinsky, P.; Waldauf, C.; Brabec, C. J. *Appl. Phys. Lett.* **2002,** *81*, 3885.
261. Reyes-Reyes, M.; Kim, K.; Carroll, D. L. *Appl. Phys. Lett.* **2005,** *87*, 83506.
262. Li, G.; Shrotriya, V.; Huang, J.; Yao, Y.; Moriarty, T.; Emery, K.; Yang, Y. *Nat. Mater.* **2005,** *4*, 864.
263. Ma, W.; Yang, C.; Gong, X.; Lee, K.; Heeger, A. J. *Adv. Funct. Mater.* **1617,** *2005*, 15.
264. Brédas, J. L.; Norton, J. E.; Cornil, J.; Coropceanu, V. *Acc. Chem. Res.* **1691,** *2009*, 42.
265. Mazzio, K. A.; Luscombe, C. K. *Chem. Soc. Rev.* **2015,** *44*, 78.
266. Sauvé, G.; Fernando, R. *J. Phys. Chem. Lett.* **2015,** *6*, 3770.
267. Sariciftci, N. S.; Smilowitz, L.; Heeger, A. J.; Wudl, F. *Science* **1992,** *258*, 1474.
268. Feron, K.; Belcher, W. J.; Fell, C. J.; Dastoor, P. C. *Int. J. Mol. Sci.* **2012,** *13*, 17019.
269. Darling, S. B.; You, F. *RSC Adv.* **2013,** *3*, 17633.
270. Deibel, C., et al. *Phys. Rev. B* **2010,** *81*, 085202.
271. Vandewal, K.; Tvingstedt, K.; Gadisa, A.; Inganas, O.; Manca, J. V. *Nat. Mater.* **2009,** *8*, 904.
272. Shockley, W.; Queisser, H. J. *J. Appl. Phys.* **1961,** *32*, 510.
273. Sworakowski, J.; Lipinski, J.; Janus, K. *Org. Electron.* **2016,** *33*, 300.
274. Glen, T. S.; Scarratt, N. W.; Yi, H.; Iraqi, A.; Wang, T.; Kingsley, J.; Buckley, A. R.; Lidzey, D. G.; Donald, A. M. *J. Polym. Sci. Part B: Polym. Phys.* **2016,** *54*, 216.
275. Bao, Q.; Liu, X.; Braun, S.; Fahlman, M. *Adv. Energy Mater.* **2014,** *4*, 1301272.
276. Ko, E. Y.; Park, G. E.; Lee, J. H.; Kim, H. J.; Lee, D. H.; Ahn, H.; Uddin, M. A.; Woo, H. Y.; Cho, M. J.; Choi, D. H. *ACS Appl. Mater. Interfaces* **2017,** *9*, 8838.
277. Holliday, S.; Ashraf, R. S.; Wadsworth, A.; Baran, D.; Yousaf, S. A.; Nielsen, C. B.; Tan, C. H.; Dimtrov, S. D.; Shang, Z.; Gasparini, N., et al. *Nat. Commun.* **2016,** *7*, 11585.
278. An, Q.; Zhang, F.; Gao, W.; Sun, Q.; Zhang, M.; Yang, C.; Zhang, J. *Nano Energy* **2018,** *45*, 177.
279. Xu, Y.; Yuan, J.; Zhou, S.; Seifrid, M.; Ying, L.; Li, B.; Huang, F.; Bazan, G. C.; Ma, W. *Adv. Funct. Mater.* **2019,** *29*, 1806747.
280. Fan, X.; Wen, R.; Xia, Y.; Wang, J.; Liu, X.; Huang, H.; Li, Y.; Zhu, W.; Cheng, Y.; Ma, L., et al. *Sol. RRL* **2020,** *4*, 1900543.
281. Lin, Y.; Wang, J.; Zhang, Z.-G.; Bai, H.; Li, Y.; Zhu, D.; Zhan, X. *Adv. Mater.* **2015,** *27*, 1170.
282. Zhang, L.; Lin, B.; Hu, B.; Xu, X.; Ma, W. *Adv. Mater.* **2018,** *30*, 1800343.
283. Zhong, Y.; Trinh, M. T.; Chen, R.; Purdum, G. E.; Khlyabich, P. P.; Sezen, M.; Oh, S.; Zhu, H.; Fowler, B.; Zhang, B., et al. *Nat. Commun.* **2015,** *6*, 8242.
284. Guo, J.; Wu, Y.; Sun, R.; Wang, W.; Guo, J.; Wu, Q.; Tang, X.; Sun, C.; Luo, Z.; Chang, K., et al. *J. Mater. Chem. A* **2019,** *7*, 25088.
285. Xiao, J.; Ren, M.; Zhang, G.; Wang, J.; Zhang, D.; Liu, L.; Li, N.; Brabec, C. J.; Yip, H. L.; Cao, Y. *Sol. RRL* **2019,** *3*, 1900077.
286. Norrman, K.; Krebs, F. C. *Sol. Energy Mater. Sol. Cell* **2006,** *90*, 213.
287. Cao, H.; He, W.; Mao, Y.; Lin, X.; Ishikawa, K.; Dickerson, J. H.; Hess, W. P. *J. Power Sources* **2014,** *264*, 168.
288. Speller, E. M.; Clarke, A. J.; Aristidou, N.; Wyatt, M. F.; Francàs, L.; Fish, G.; Cha, H.; Lee, H. K. H.; Luke, J.; Wadsworth, A., et al. *ACS Energy Lett.*, 4. ; 2019846.
289. Wang, C.; Ni, S.; Braun, S.; Fahlman, M.; Liu, X. *J. Mater. Chem. C* **2019,** *7*, 879.
290. Li, H.; Huang, K.; Dong, Y.; Guo, X.; Yang, Y.; Luo, Q.; Yang, Y.; Gao, X.; Yang, J. *Appl. Phys. Lett.* **2020,** *117*, 133301.
291. Bertho, S.; Janssen, G.; Cleij, T. J.; Conings, B.; Moons, W.; Gadisa, A.; D'Haen, J.; Goovaerts, E.; Lutsen, L.; Manca, J., et al. *Sol. Energy Mater. Sol. Cell* **2008,** *92*, 753.
292. Kawano, K.; Pacios, R.; Poplavskyy, D.; Nelson, J.; Bradley, D. D.; Durrant, J. R. *Sol. Energy Mater. Sol. Cell* **2006,** *90*, 3520.
293. Norrman, K.; Gevorgyan, S. A.; Krebs, F. C. *ACS Appl. Mater. Interfaces* **2009,** *1*, 102.
294. Kumar, A.; Devine, R.; Mayberry, C.; Lei, B.; Li, G.; Yang, Y. *Adv. Funct. Mater.* **2010,** *20*, 2729.
295. Heumueller, T.; Mateker, W. R.; Distler, A.; Fritze, U. F.; Cheacharoen, R.; Nguyen, W. H.; Biele, M.; Salvador, M.; Egelhaaf, H. J.; McGehee, M. D., et al. *Energy Environ. Sci.* **2016,** *9*, 247.
296. Distler, A.; Sauermann, T.; Egelhaaf, H. J.; Rodman, S.; Waller, D.; Cheon, K. S.; Lee, M.; Guldi, D. M. *Adv. Energy Mater.* **2014,** *4*, 1300693.
297. Mateker, W. R.; Sachs-Quintana, I. T.; Burkhard, G. F.; Cheacharoen, R.; McGehee, M. D. *Chem. Mater.* **2015,** *27*, 404.
298. Yan, C.; Barlow, S.; Wang, Z.; Yan, H.; Jen, A. K. Y.; Marder, S. R.; Zhan, X. *Nat. Rev. Mater.* **2018,** *3*, 18003.
299. Gurney, R. S.; Lidzey, D. G.; Wang, T. *Rep. Prog. Phys.* **2019,** *82*, 036601.

300. Hou, J.; Inganäs, O.; Friend, R. H.; Gao, F. *Nat. Mater.* **2018,** *17,* 119.
301. Zhang, J.; Tan, H. S.; Guo, X.; Facchetti, A.; Yan, H. *Nat. Energy* **2018,** *3,* 720.
302. Cheng, P.; Zhan, X. *Chem. Soc. Rev.* **2016,** *45,* 2544.
303. Li, Y.; Li, T.; Lin, Y. *Mater. Chem. Front.* **2021,** *5,* 2907.
304. Wadsworth, A.; Moser, M.; Marks, A.; Little, M. S.; Gasparini, N.; Brabec, C. J.; Baran, D.; McCulloch, I. *Chem. Soc. Rev.* **2019,** *48,* 1596.
305. Yang, W.; Wang, W.; Wang, Y.; Sun, R.; Guo, J.; Li, H.; Shi, M.; Guo, J.; Wu, Y.; Wang, T., et al. *Joule* **2021,** *5,* 1209.
306. Li, C.; Wonneberger, H. *Adv. Mater.* **2012,** *24,* 613.
307. Guo, X.; Facchetti, A.; Marks, T. J. *Chem. Rev.* **2014,** *114,* 8943.
308. Zhan, X., et al. *Adv. Mater.* **2011,** *23,* 268.
309. Suraru, S. L.; Wurthner, F. *Angew. Chem. Int. (Ed.)* **2014,** *53,* 7428.
310. Li, H., et al. *J. Am. Chem. Soc.* **2014,** *136,* 14589.
311. Pho, T. V.; Toma, F. M.; Chabinyc, M. L.; Wudl, F. *Angew. Chem. Int. (Ed.)* **2013,** *52,* 1446.
312. Li, H., et al. *Angew. Chem. Int. (Ed.)* **2013,** *52,* 5513.
313. Li, H., et al. *Adv. Mater.* **2015,** *27,* 3266.
314. Kang, H., et al. *Acc. Chem. Res.* **2016,** *49,* 2424.
315. Shoaee, S., et al. *J. Am. Chem. Soc.* **2010,** *132,* 12919.
316. Savoie, B. M., et al. *Proc. Natl Acad. Sci. USA* **2014,** *111,* 10055.
317. Schubert, A., et al. *J. Phys. Chem. Lett.* **2013,** *4,* 792.
318. Sharenko, A., et al. *Adv. Mater.* **2013,** *25,* 4403.
319. Hartnett, P. E., et al. *J. Am. Chem. Soc.* **2014,** *136,* 16345.
320. Liu, J., et al. *Nat. Energy* **2016,** *1,* 16089.
321. Langhals, H.; Jona, W. *Angew. Chem. Int. (Ed.)* **1998,** *37,* 952.
322. Langhals, H.; Saulich, S. *Chem. Eur. J.* **2002,** *8,* 5630.
323. Holman, M. W.; Yan, P.; Adams, D. M.; Westenhoff, S.; Silva, C. *J. Phys. Chem. A* **2005,** *109,* 8548.
324. Wilson, T. M.; Tauber, M. J.; Wasielewski, M. R. *J. Am. Chem. Soc.* **2009,** *131,* 8952.
325. Shivanna, R., et al. *Energy Environ. Sci.* **2014,** *7,* 435.
326. Ye, L., et al. *ACS Appl. Mater. Interfaces* **2015,** *7,* 9274.
327. Liang, N., et al. *Adv. Energy Mater.* **2016,** *6,* 1600060.
328. Rajaram, S.; Shivanna, R.; Kandappa, S. K.; Narayan, K. S. *J. Phys. Chem. Lett.* **2012,** *3,* 2405.
329. Fan, Y., et al. *ACS Omega* **2017,** *2,* 377.
330. Jiang, W., et al. *Chem. Commun.* **2014,** *50,* 1024.
331. Zang, Y., et al. *Adv. Mater.* **2014,** *26,* 5708.
332. Ye, L., et al. *Org. Electron.* **2015,** *17,* 295.
333. Wu, C., et al. *Adv. Funct. Mater.* **2015,** *25,* 5326.
334. Sun, D., et al. *J. Am. Chem. Soc.* **2015,** *137,* 11156.
335. Meng, D., et al. *J. Am. Chem. Soc.* **2016,** *138,* 375.
336. Lin, Y., et al. *Adv. Mater.* **2014,** *26,* 5137.
337. Duan, Y., et al. *Adv. Mater.* **2017,** *29,* 1605115.
338. Lin, H., et al. *Adv. Mater.* **2016,** *28,* 8546.
339. Chen, W., et al. *J. Mater. Chem. C.* **2015,** *3,* 4698.
340. Wu, Q.; Zhao, D.; Schneider, A. M.; Chen, W.; Yu, L. *J. Am. Chem. Soc.* **2016,** *138,* 7248.
341. Zhong, Y., et al. *J. Am. Chem. Soc.* **2014,** *136,* 15215.
342. Lin, Y.; Zhan, X. *Adv. Energy Mater.* **2015,** *5,* 1501063.
343. Han, G.; Guo, Y.; Song, X.; Wang, Y.; Yi, Y. *J. Mater. Chem. C.* **2017,** *5,* 4852.
344. Liang, Y.; Feng, D.; Wu, Y.; Tsai, S.-T.; Li, G.; Ray, C.; Yu, L. *J. Am. Chem. Soc.* **2009,** *131,* 7792.
345. Das, S.; Keum, J. K.; Browning, J. F.; Gu, G.; Yang, B.; Dyck, O.; Do, C.; Chen, W.; Chen, J.; Ivanov, I. N., et al. *Nanoscale* **2015,** *7,* 15576.
346. Lu, L.; Yu, L. *Adv. Mater.* **2014,** *26,* 4413.
347. Liang, Y.; Xu, Z.; Xia, J.; Tsai, S. T.; Wu, Y.; Li, G.; Ray, C.; Yu, L. *Adv. Mater.* **2010,** *22,* E135.
348. Liao, S. H.; Jhuo, H. J.; Cheng, Y. S.; Chen, S. A. *Adv. Mater.* **2013,** *25,* 4766.
349. Zhou, H.; Zhang, Y.; Mai, C. K.; Collins, S. D.; Bazan, G. C.; Nguyen, T. Q.; Heeger, A. J. *Adv. Mater.* **1767,** *2015,* 27.
350. Roncali, J.; Leriche, P.; Blanchard, P. *Adv. Mater.* **2014,** *26,* 3821.
351. Walter, M. G.; Rudine, A. B.; Wamser, C. C. *J. Porphyr. Phthalocyanines* **2010,** *14,* 759.
352. Lessard, B. H.; Grant, T. M.; White, R.; Thibau, E.; Lu, Z.-H.; Bender, T. P. *J. Mater. Chem. A* **2015,** *3,* 24512.
353. Izaki, M.; Chizaki, R.; Saito, T.; Murata, K.; Sasano, J.; Shinagawa, T. *ACS Appl. Mater. Interfaces* **2013,** *5,* 9386.
354. Bouit, P.-A.; Infantes, L.; Calbo, J.; Viruela, R.; Ortí, E.; Delgado, J. L.; Martín, N. *Org. Lett.* **2013,** *15,* 4166.
355. Bouit, P. A.; Villegas, C.; Delgado, J. L.; Viruela, P. M.; Pou-Amérigo, R.; Ortí, E.; Martín, N. *Org. Lett.* **2011,** *13,* 604.
356. Bouit, P.-A.; Rauh, D.; Neugebauer, S.; Delgado, J. L.; Di Piazza, E.; Rigaut, S.; Maury, O.; Andraud, C.; Dyakonov, V.; Martin, N. *Org. Lett.* **2009,** *11,* 4806.
357. Flytzanis, C.; Oudar, J. L. *Nonlinear Optics: Materials and Devices;* Springer: Berlin, 1986.
358. Hayden, L. M.; Kowel, S. T.; Srinivasan, M. P. *Opt. Comm.* **1987,** *61,* 351.
359. Franken, E. P.; Hill, A. E.; Peters, C. E.; Weinreich, G. *Phys. Rev. Let.* **1961,** *7,* 118.
360. Franken, P. A.; Ward, J. F. *Rev. Mod. Phys.* **1963,** *35,* 23.
361. Armstrong, J. A.; Bloembergen, N.; Ducuing, J.; Pershan, P. S. *Phys. Rev.* **1918,** *1962,* 127.
362. Chemla, D. S.; Zyss, J. *Nonlinear Optical Properties of Organic Molecules and Crystals;* Academic Press: New York, 1987.
363. Prasad, P. N.; Ulrich, D. R. *Nonlinear Optical and Electroactive Polymers;* Plenum: New York, 1988.

364. Ulrich, D. R.; Orenstein, J.; Heeger, A. J. *Nonlinear Optical Properties of Polymers;* Material Research Society: Pittsbourgh, 1988.
365. Fiorentini, V.; Bernardini, F.; Ambacher, O. *Appl. Phys. Let.* **2002,** *80*, 1204.
366. Marder, S. R.; Gorman, C. B.; Meyers, F.; Perry, J. W.; Bourhill, G.; Brédas, J. L.; Pierce, B. M. *Science* **1994,** *265*, 632.
367. Sutherland, R. L.; McLean, D. G.; Kirkpatrick, S. *Handbook of Nonlinear Optics*, 2 nd edn.; Marcel Dekker Inc, 2003.
368. Sipe, J. E.; Boyd, R. W. *Phys. Rev. A* **1614,** *1992*, 46.
369. Yin, Y.; Li, W.; Chen, Y.; Wang, Y. *Optik* **2018,** *154*, 372.
370. Li, Y.; Zhang, H.; Jiang, Z.; Li, Z.; Hu, C. *Optik* **2014,** *125*, 2851.
371. Dmitriev, V. G.; Gurzadyan, G. G.; Nikogosyan, D. N. *Handbook of nonlinear optical crystals*, 64. Springer, 2013.
372. Sutter, K.; Günter, P. *J. Opt. Soc. Am. B* **1990,** *7*, 2274.
373. Kim, E.; Choi, Y. K.; Lee, M. H. *Macromolecules* **1999,** *32*, 4855.
374. Kim, M. S.; Maruyama, H.; Kawai, T.; Irie, M. *Chem. Mater.* **2003,** *15*, 4539.
375. Kitagawa, D.; Nishi, H.; Kobatake, S. *Angew. Chem. Int. (Ed.)* **2013,** *52*, 9320.
376. Matsuda, K.; Irie, M. *J. Am. Chem. Soc.* **2000,** *122*, 7195.
377. Berkovic, G.; Krongauz, V.; Weiss, V. *Chem. Rev.* **1741,** *2000*, 100.
378. Benard, S.; Yu, P. *Adv. Mater.* **2000,** *12*, 48.
379. Chu, N. Y. C. In *Photochromism, Molecules, and Systems;* Dürr, H., Bouas-Laurent, H., Eds.; Elsevier: Amster- dam, 1990; pp 493−509.
380. Maeda, S. In *in Organic Photochromic and Thermochromic Compounds;* Crano, J. C., Guglielmetti, R. J., Eds.; Kluwer Academic Publishers: New York, 2002; pp 85−109.
381. Van Gemert, B. In *Organic Photochromic and Thermochromic Compounds;* Crano, J. C., Guglielmetti, R. J., Eds.; Kluwer Academic Publishers: New York, 2002; pp 111−140.
382. Becker, R. S.; Michl, J. *J. Am. Chem. Soc.* **1966,** *88*, 5931.
383. Hartley, G. S. *Nature* **1937,** *140*, 281.
384. Rau, H. In *Photochemistry and Photophysics;* Rabek, J. F., Ed.; vol. 2; CRC Press: Boca Raton, FL, 1990.
385. Hayashi, T.; Maeda, K. *Bull. Chem. Soc. Jpn.* **1960,** *33*, 565.
386. Satoh, Y.; Ishibashi, Y.; Ito, S.; Nagasawa, Y.; Miyasaka, H.; Chosrowian, H.; Taniguchi, S.; Mataga, N.; Kato, D.; Kikuchi, A., et al. *Chem. Phys. Lett.* **2007,** *448*, 228.
387. Fischer, E.; Hirshberg, Y. *J. Chem. Soc.* **1952,** 4522.
388. Guglielmetti, R. In *Photochromism, Molecules, and Systems;* Dürr, H., Bouas-Laurent, H., Eds.; Elsevier: Amsterdam, 1990; pp 314−466.
389. Bertelson, R. C. In *Organic Photochromic and Thermochromic Compounds;* Crano, J. C., Guglielmetti, R. J., Eds.; Kluwer Academic Publishers: New York, 2002; pp. 11−83.

Photodegradation of drugs and crop protection products

5.1 Introduction

It happened to each of us, reading the leaflet of a drug or the safety data sheet of a crop protection product, to find that some drugs or some agricultural products need to be protected from light.

It should be emphasized that heterocycles are common fragments of the vast majority of marketed drugs for improved pharmacological, pharmacokinetic, toxicological, and physicochemical properties of drug candidates and ultimately drugs.[1] Likewise, more than two-thirds of all agrochemicals launched to the market within the last several years belong to the heterocyclic group of chemicals.[2]

This chapter deals with the photodegradation of drugs and crop protection products that contain heterocycles.

This chapter describes the general mechanism of the photodegradation of drugs and crop protection products as well the analysis of specific groups of drugs and xenobiotics.

5.2 General mechanisms of photodegradation of drugs

Photodegradation is the result of photophysical process of absorption and dissipation of light energy.

Because of the absorption of a photon, molecule A_0 is promoted to the singlet excited state with antiparallel electron spins.

$$A_0 \text{(single ground state)} \xrightarrow{h\nu} {}^1A \text{(single excited state)}$$
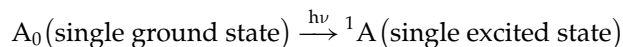
The molecule in the single excited state may suddenly dissipate its energy by internal conversion, fluorescence, or photoionization. In the first two cases, the molecule comes back to the ground state.

$$^1A \text{(single excited state)} \rightarrow A_0 \text{(single ground state)}$$

$$^1A \text{(single excited state)} \rightarrow A_0 \text{(single ground state)} + h\nu$$
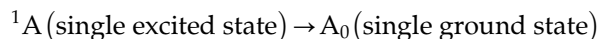
On contrary, photoionization occurs in the presence of an electron acceptor results in the remotion of an electron from ^1A to give an anionic state.

$$^1A \text{(single excited state)} \rightarrow A^{\bullet +} \text{(anionic state)}$$
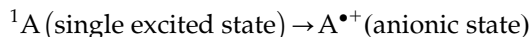
When the energy does not suddenly dissipate, the intersystem crossing is possible and the result is a metastable triplet excited state ^3A.

$$^1A \text{(single excited state)} \rightarrow {}^3A \text{(triplet excited state)}$$
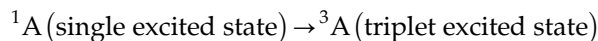
The molecule in the triplet excited state may again suddenly dissipate its energy by internal conversion or phosphorescence.

$$^3A \text{(triplet excited state)} \rightarrow A_0 \text{(single ground state)}$$

$$^3A \text{(triplet excited state)} \rightarrow A_0 \text{(single ground state)} + h\nu$$
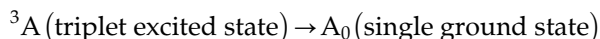
A photochemical process leading to the formation of ionic radicals (cationic and anionic) or neutral ones (oxidized or reduced) is possible.

$$^3A + A_0 \rightarrow A^{\bullet +} + A^{\bullet -} \text{(ionic radicals)}$$

$$A^{\bullet +} \xrightarrow{-H} A^{\bullet} \text{(oxidized radical)}$$

$$A^{\bullet -} \xrightarrow{+H} AH^{\bullet} \text{(reduced radical)}$$
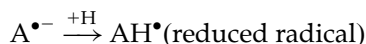
The obtained reduced radical may react to give the final product of degradation.

$$AH^{\bullet} \rightarrow AH_2 + A_0$$

The main chemical functions that can produce photoreactivity are[3]:

1. The carbonyl group because of an electrophilic radical in the $n\pi^*$ excited state. Typical reactions are reduction via intermolecular hydrogen abstraction and fragmentation either via α-cleavage ("Norrish Type I") or via intramolecular y-hydrogen abstraction followed by $C_\alpha - C_\beta$ cleavage ("Norrish Type II").
2. The nitroaromatic group, which behaves as a radical, undergoes intermolecular hydrogen abstraction or rearrangement to a nitrite ester.
3. The N-oxide function. This rearranges easily to an oxaziridine, and the final products often result from the further reaction of this intermediate.
4. The C=C double bond is liable to EIZ isomerization and oxidation.
5. The aryl chloride is liable to homolytic and/or to heterolytic dichlorination.

6. Products containing a weak C−H bond, for example, at a benzylic position or to amine nitrogen. These compounds often undergo photoinduced fragmentations via hydrogen transfer or electron-proton transfer.
7. Sulfides, alkenes, polyenes, and phenols. These are highly reactive with singlet oxygen, formed through photosensitization from the relatively harmless ground state oxygen.

The main reactions involved in the pathway of drug degradation are as follows:

1. Photoaddition
2. Photoaquation
3. Photocyclization
4. Photodealkylation
5. Photodecarboxylation
6. Photodehalogenation
7. Photodehydrogenation
8. Photodimerization
9. Photoelimination
10. Photoinduced hydrolysis
11. Photoisomerization
12. Photooxidation
13. Photoinduced rearrangement
14. Photoreduction
15. Photoinduced ring cleavage.

Often more than one pathway may be involved. Some of the reactions listed through specific examples are described in the following sections.

5.3 Anti-inflammatory, analgesic, and immunosuppressant drugs

The drugs with photosensitivity response have specific characteristics. They usually have a low molecular weight. These are planar, tricyclic, or polycyclic structures with often heteroatoms. Specific examples related to the degradation of different classes of drugs containing heterocycles are reported in the following section.

5.3.1 Nonsteroidal anti-inflammatory drugs

Several nonsteroidal anti-inflammatory drugs (NSAIDs) have been investigated.

Among them, 2-aryl propionic acid derivatives (Fig. 5.1) are the most photoreactive ones. The most photoactive member of this group is benoxaprofen (λ_{max} 315 nm, ε_{max} 23,000 M^{-1}/cm). This drug, which is no longer in use because of the serious damage due to photosensitivity, started the study of photochemistry of the NSAID group.

FIGURE 5.1 Chemical structure of NSAIDs containing the 2-aryl propionic acid group.
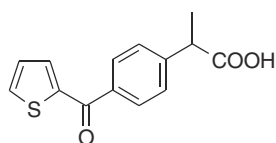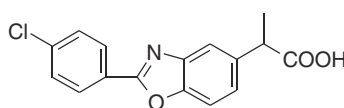
SUPROFEN

BENOXAPROFEN
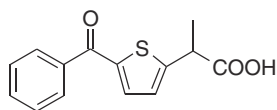
TIAPROFENIC ACID
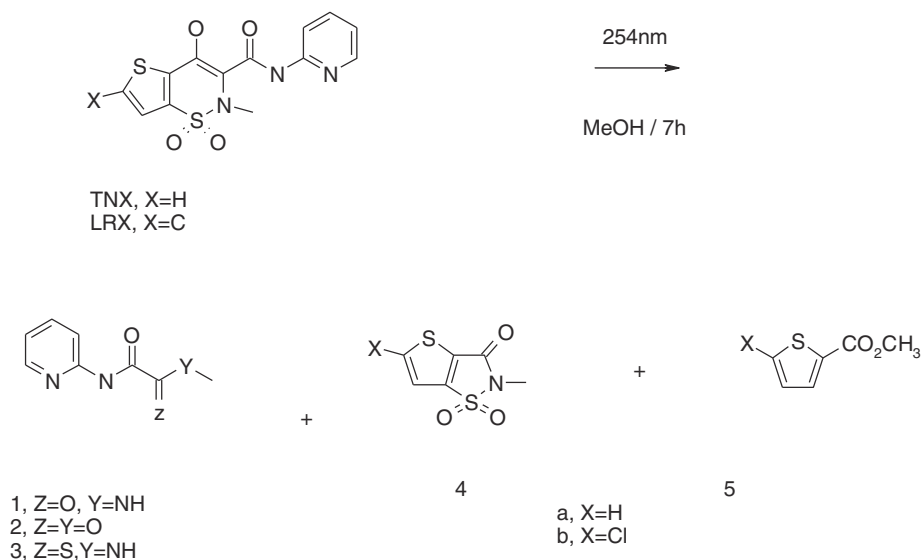
FIGURE 5.2   Photodegradation of tenoxicam and lornoximax.

The photochemistry of 2-aryl propionic acid is dominated by an efficient photodecarboxylation process, although the specific aryl chromophore influences the nature of the primary photo process.[4] The 2-aryl propionic acid can produce significant yields of singlet oxygen and free radical species upon irradiation with sunlight-simulating radiation. The effect of singlet oxygen or free radical on biological substrates can lead to cell disruption.

Photo-induced binding of tiaprofenic acid and suprofen to proteins and cells occurs in an oxygen-free system, thereby providing a mechanism for the initiation of photoallergic response.

Of course, drugs that do not contain 2-aryl propionic acid were also investigated.

Recently, a study of photodegradation of tenoxicam (TNX) and lornoximax (LRX) has been reported.[5]

TNX and LRX are two examples of oxicams and nonsteroidal anti-inflammatory drugs used for the treatment of rheumatic arthritis and osteoarthritis.

TNX and LRX undergo photodegradation when photo-irradiated with 254 nm irradiation in methanol for 7 h, giving five main products. The photodegradation products were identified using different spectroscopic tools as N-methyl-N'-(pyridin-2-yl)oxalamide (**1**), methyl(pyridin-2-ylcarbamoyl)formate (**2**), N-methyl-N'-(pyridin-2-yl carbamoyl)methanethioamide (**3**), N-methyl-3-oxothieno[3,2-d]-1,2-thiazole-1,1-dioxides **4a**, **4b** and methyl thiophene-2-carboxylates **5a**, **5b** (Fig. 5.2).

Photoexcited oxicam reacts with singlet oxygen at $C_3 = C_4$ in the thiazine ring to form dioxetane intermediate **6**. Subsequent dioxetane ring-opening leads to intermediate **7** (Fig. 5.3). The later intermediate undergoes either nucleophilic attack by the solvent lone pair to form methyl (pyridin-2-ylcarbamoyl)formate (**2**), and N-methyl-3-oxothieno[3,2-d]-1,2-thiazole-1,1-dioxides **4a**, **4b** or extrusion of sulfur dioxide and methylation to yield N-methyl-N'-(pyridin-2-yl)oxalamide (**3**) and methyl thiophene-2-carboxylates **5a**, **5b**.[5]

However, the formation of photoproduct **3** as one of the aerobic photolysis products of tenoxicam and lornoxicam is quite abnormal and unexpected for such photodegradation. In addition, it was not detected or reported as one of the photolysis, oxidation, or metabolites of such oxicams.[6]

The isolated photodegradation products and the pharmaceutical agents were examined for DNA binding and degradation: the products **1**, **2**, and **3** in DMSO were added independently to 1 µg of calf thymus DNA (life technologies) and incubated at 37°C for 60 min and a powerful degradation effect on calf thymus DNA at 8 µM concentration was noticed.[7]

5.3.2 Pyrazolone analgesic and antipyretic drugs

Pyrazolones are among the oldest synthetic drugs. Knorr first prepared antipyrine in 1883. The most important drugs are derived by substitution of the C−4 atom on the basic group to give propyphenazone (Fig. 5.4).[8,9] This has improved antipyretic and analgesic properties and exhibits anti-inflammatory activity.[8]
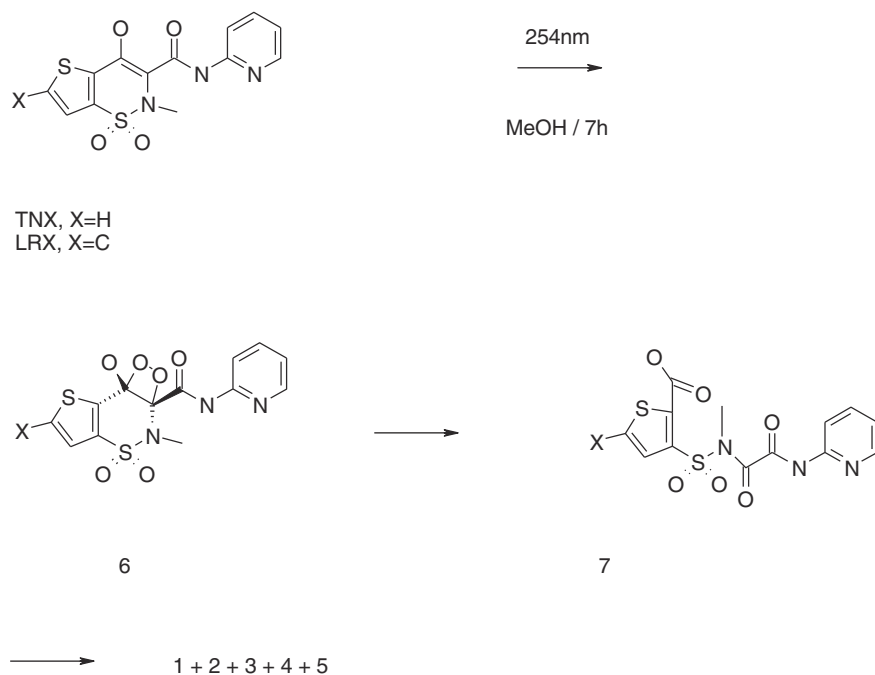
FIGURE 5.3   Reaction with singlet oxygen at $C_3 = C_4$ in the thiazine ring.

254nm

MeOH / 7h

TNX, X=H
LRX, X=C

6

7

1 + 2 + 3 + 4 + 5

—H   Antipyrine
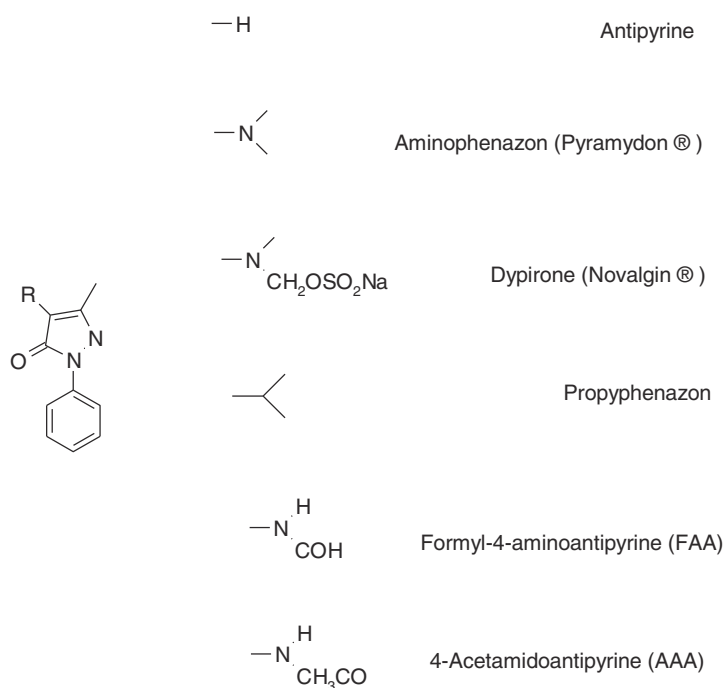
FIGURE 5.4   Pyrazolones derivates.

Aminophenazon (Pyramydon ®)

Dypirone (Novalgin ®)

Propyphenazon

Formyl-4-aminoantipyrine (FAA)

4-Acetamidoantipyrine (AAA)

Recently, the degradation of pyrazolones by UV was investigated.[9] UV degradation experiments were conducted in a 1-L glass vessel equipped with a double-layer plunging recipient hosting a generic 15-W low-pressure mercury UV (254 nm) lamp. The vessel was filled with 800 mL of a 100 mg/L solution of each of the four pyrazolone compounds: FAA, AAA, propyphenazone, and phenazone. A magnetic stirrer was used and aluminum foil was wrapped around the vessel. The experiment was started as the lamp was ignited and samples were taken at 0 s, 10 s, 20 s, 30 s, 40 s, 50 s, 60 s, 90 s, 2 min, 5 min, 10 min, and 20 min. The samples were transferred in vials and analyzed by LC/Ms. Experiments were conducted at pH 7. All 11 degradation products have been identified by high-resolution mass spectrometry. The structures of the transformation products are given in Fig. 5.5.
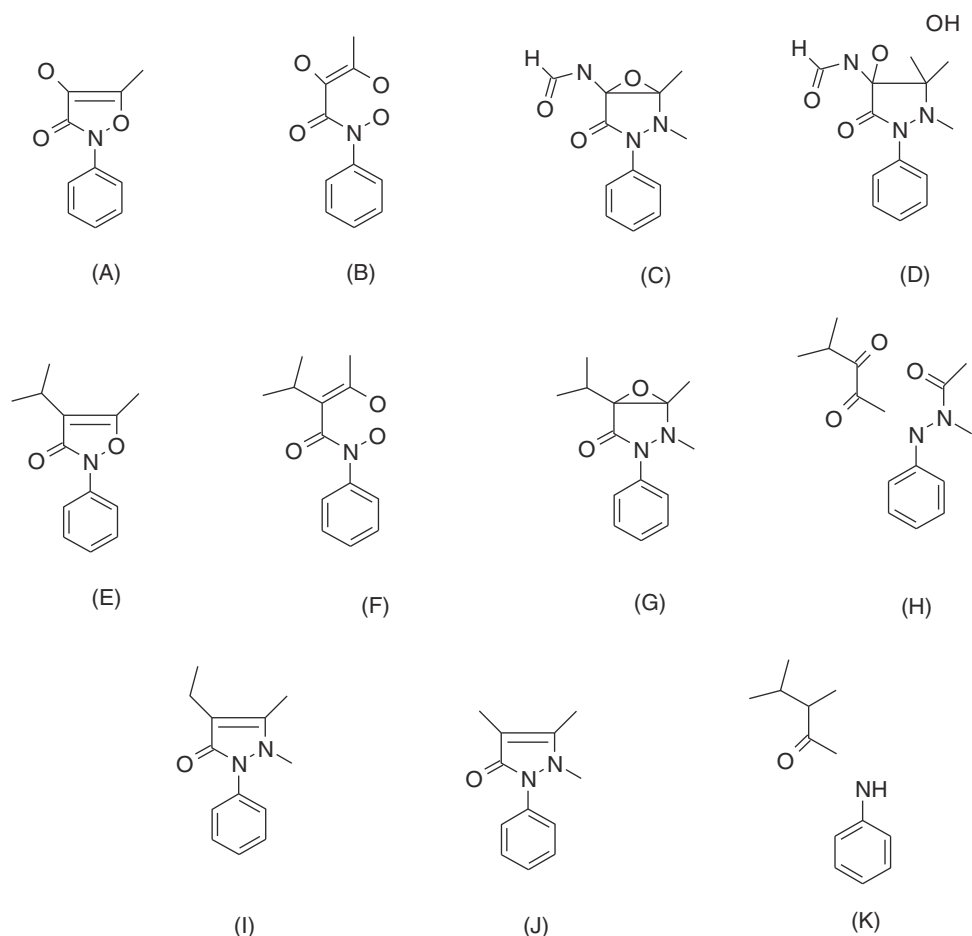
FIGURE 5.5   The degradation products of pyrazolones.

For these products and their four parents, ecotoxicity was evaluated and it showed that the degradation is, in this case, a transformation into compounds showing higher ecotoxicological potential. The toxicity of products was valued using QSAR modeling and reported in Table 5.1.[9]

Differences in toxicity between products (**a-k**) and their parent compounds showed that when the C=C bond is partially oxidized to an epoxy (**c** i **g**), the toxicity is increased with the respect to the parent compounds.

5.3.3 Immunosuppressant and anti-histamic drugs

Immunosuppressant drugs are a class of drugs that suppress the strength of the body's immune system. They can be used in postoperative treatment to prevent transplanted organ such as kidney, liver, or heart from any damage, and also for the treatment of autoimmune disorders such as lupus, psoriasis, Crohn's disease, and rheumatoid arthritis.

Azathioprine (AZA) (Fig. 5.6) is an immunosuppressive drug that was synthesized for the first time in 1957 by George Herbert Hitching and Gertude Elion[10] and from then to today it is among the most frequently prescribed drugs.

Unfortunately, AZA as well as other thiopurine drugs can cause life-threatening toxicity[11] that has been extensively investigated. This investigation has been particularly directed to the influence of UV light, and recently it has been demonstrated the ability of photoluminescence and the UV-VIS and IR absorption spectroscopy for the assessment of AZA photodegradation under UV light.[12]

The photodegradation process of AZA is observed by the gradual increase in the intensity of the photoluminescence (PL) spectrum recorded under an excitation wavelength of 300 nm.

TABLE 5.1 Toxicity evaluation for pyrazolone compounds and their degradation products after UV degradation using QSAR modelling.

	Fish LC50[a] 96 h (ppm)	Daphind LC50 48 h	Green Algae EC50[b] 144 h
G	0.1	1.1	0.6
C	0.4	2.2	0.8
Propyphenazone	0.9	3.5	1.0
A	1.0	–	–
F	1.1	–	–
B	1.2	–	–
I	1.2	4.2	1.0
J	1.9	5.2	1.0
Phenazone	3.1	6.8	1.1
FAA	4.1	8.8	1.4
AAA	8.3	13.5	1.7
K	19.4	22.1	14.9
E	26.1	29.7	19.5

[a]*LC50 (Lethal Concentration 50%) is the estimated air concentration of a substance administered via the inhalation route. A lower LC50 value indicates higher acute toxicity.*
[b]*EC50 (median effective concentration) is the concentration of the test substance, which results in a 50 percent reduction in either algae growth or daphina immobilization.*
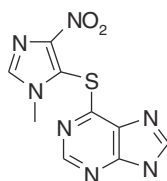
FIGURE 5.6   Azathioprine (AZA).

Regardless of whether the immunosuppressive compound is in the state of powder, tablet, or solution, the PL and UV-VIS absorption spectroscopy studies have demonstrated that a photodegradation process under UV light takes place. According to the PL studies carried out under ambient as well as vacuum conditions, the photodegradation process of AZA is influenced by the oxygen from air.

After UV-irradiation of AZA for 9 h and 18 min., the disappearance of the PL bands with maxima at 2.54, 2.73, and 3.1 eV confirms the formation of the two products reported in Fig. 5.7.

Because of these results, AZA manipulation in the absence of UV light is important regardless of whether the compound will be used as an immunosuppressive drug in medical treatments or in analysis for its electrochemical/optical detection using different sensitive platforms.

Antihistamines are drugs that inhibit histamine receptors (H receptors), that is, they block the effect of enhancing the inflammatory and immune responses of the body.

They are categorized as either H1 or H2 according to the type of targeted H receptor. H1 is usually used to treat allergic reactions. A recent study has reported the photodegradation of the H1 antihistaminic topical drugs to estimate their potential toxicity.[13]

Different H1 antihistaminic drugs (Fig. 5.8), emedastine (EME), epinastine (EPI), and ketotifen (KET), were irradiated using a solar simulator irradiating with UV/Vis light (300–800 nm) in solutions of different pH values.

Next, HPLC experiments were performed for quantitative determinations. As a result, EME was observed to be photolabile in a wide pH range, with a degradation value of 32.38%–41.52% after the maximal irradiation. As far as EPI is concerned, the photodegradation was lower, achieving 8.10%–19.10% with the pH decreasing from 10 to 3 after the highest irradiation. Finally, when KET was irradiated with the maximal dose od of light
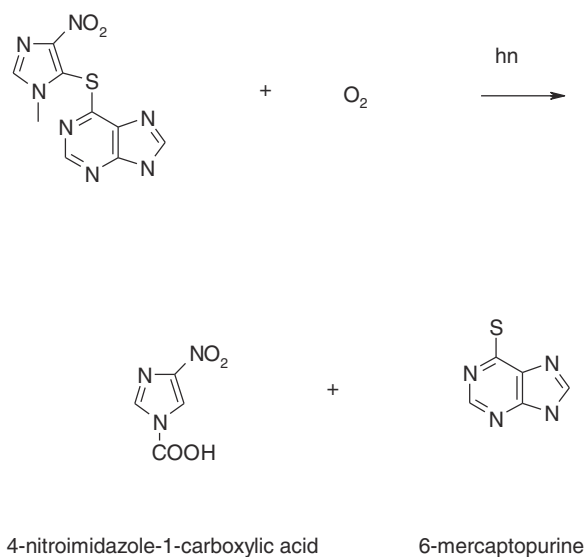
FIGURE 5.7　The degradation products of AZA.
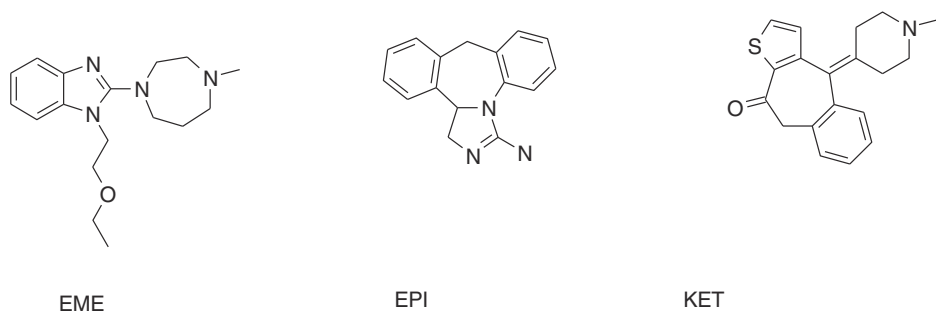
FIGURE 5.8　H1 antihistaminic drugs used.

(94,510 kJ/m^2), it degraded to 14.64% at pH 3.0 and to 19.28% at pH 7.0. However, almost 100% degradation of KET was observed at pH 10.0 after a much lower dose of energy of 37,804 kJ/m^2.

UPLC-Ms/Ms experiments are used for the separation and identification of respective photodegradation products.

From the full scan mass spectra of EME, EPI, and KET, it is possible to speculate all the steps in the fragmentation pathway shown in Figs. 5.9–5.11, respectively.

According to the official guidelines, the phototoxic potential of drugs can be elucidated by monitoring ROS generation under exposure to UV/Vis radiation, as SO (type 2 photochemical reaction) and SA (type 1 photochemical reaction) generation.

5.4　Drugs acting on the central nervous system

The central nervous system consists of the brain and the spinal cord, the two parts of the body that contain majority of the nerves.

Drugs can alter the function of the CNS to provide anticonvulsant effects, sedation, and analgesia.

The photochemical stability of drugs was extensively reviewed. In the following sections, we report some specific examples related to the degradation of different classes of drugs that act on CNS-containing heterocycles.

5.4.1 Barbituric acid derivatives

The photochemical degradation of barbituric acid derivatives has been extensively investigated in both solution and solid states.
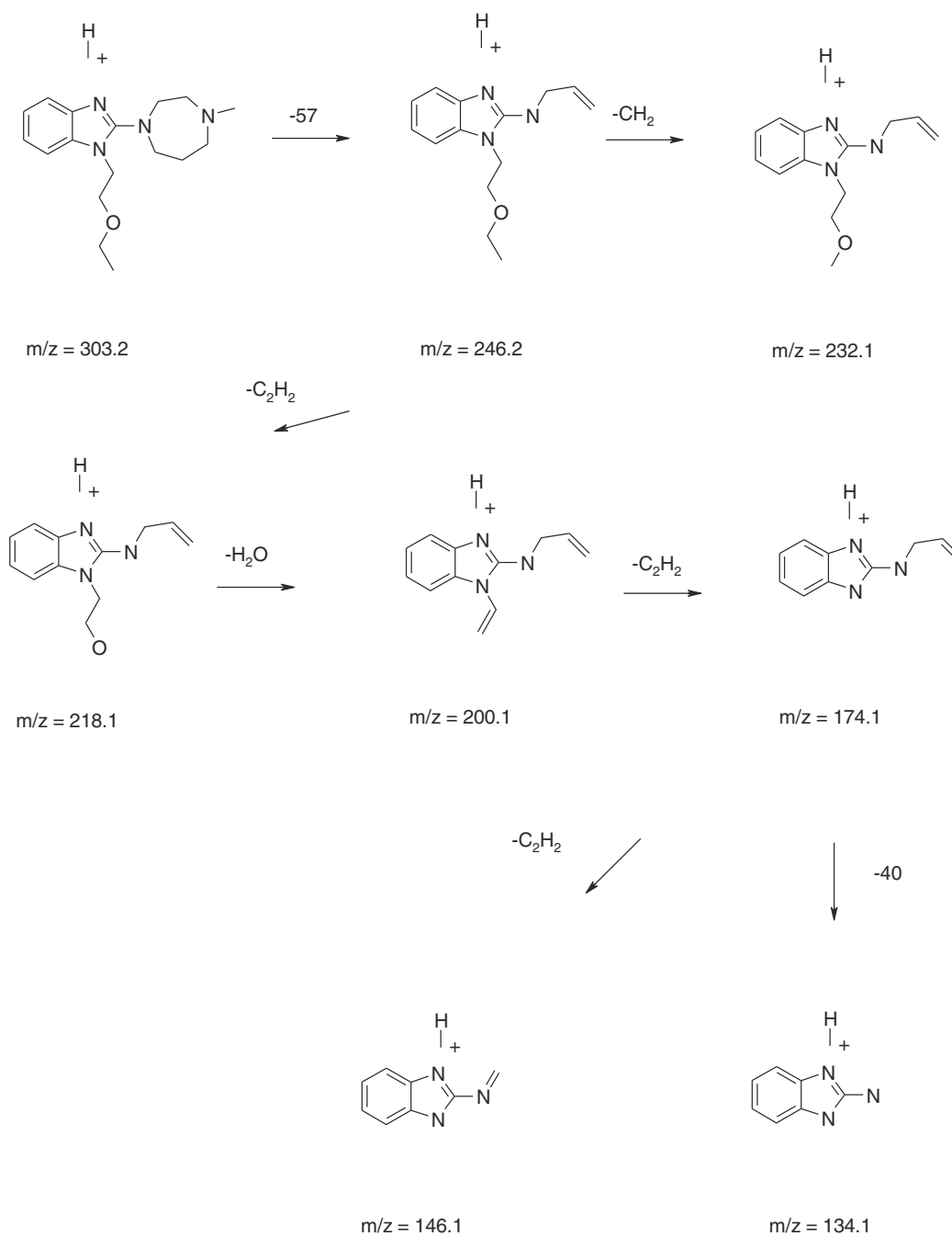
FIGURE 5.9   The fragmentation pathway of EME.

In particular, the course of photolysis and hydrolysis of one of barbituric acid derivatives used in therapy was investigated. Several photodegradation products were isolated and identified.

The photolysis of 5-ethyl-5-(1-methylbutyl) barbituric acid (pentobarbital) **1** (Fig. 5.12) in alkaline solution was irradiated with a low-pressure mercury lamp with the maximum intensity at 253.7 nm, and the course of reaction was monitored by UV and TLC.

The following products were detected: 5-ethyl barbituric acid (**2**), 2-ethyl-3-methylhexanoic acid ureide (**3**) and 2-ethyl-3-methylhexanoic acid amide (**4**). When the reaction was prolonged other products were also identified (Fig. 5.12).

The hydrolytic degradation of pentobarbital in an alkaline medium was carried out at 80 °C for 15 days with an equimolar amount of sodium hydroxide. Malonuric acid (**7**) and ureide (**3**) were detected as products (Fig. 5.11). Also, in this case, the prolongation of the time caused the formation of other products: amide (**4**) and acid (**9**).
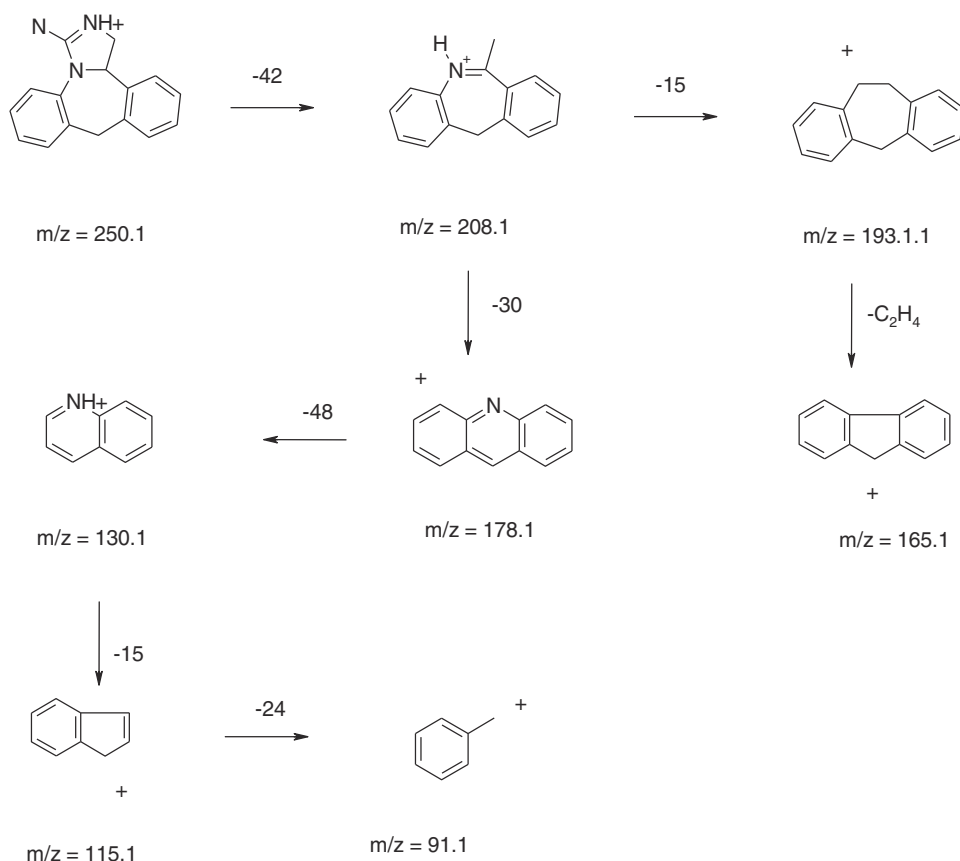
FIGURE 5.10 The fragmentation pathway of EPI.

When the hydrolysis was performed using lower sodium hydroxide concentration, the appearance of an additional product (**10**), ethyl(1-methyl-butyl)malondiamide, was detected. The independent hydrolysis of the diamide (**10**) yielded an acidic product (**11**) (Fig. 5.13).

The comparison of the two processes showed that the mechanistic pathways are different even if some of the products are common for both processes. The dealkylation process is the characteristic of photolytic degradation.

The study of photochemical degradation of barbituric acid derivatives was realized by UV irradiation of suspensions of barbiturate sodium salts in paraffin oil. The formation of an IR absorption peak at c. 2250 cm^{-1} was revealed, which was related with the formation of an isoyanate intermediate.[14]

During subsequent studies, another band at c. 2170 cm^{-1} attributable to the same reaction intermediate was detected. The intensity of the two bands depended on the kind of substituent present on the heterocyclic ring (Fig. 5.14).[15] Another work reported the photostability of barbiturates in aqueous solutions irradiated with UV light of 280 nm and a different result for the same samples irradiated with 254 nm light.[16,17]

Because of this, the stability of drugs against light needs to be formulated very carefully, as the stability of drugs with respect to sunlight may change its instability during sterilization with UV light.

5.4.2 Benzodiazepines

Among anxiolytic drugs, the photochemistry of benzodiazepines has been widely studied and found to be susceptible to photodegradation.

Alprazolam (benzodiazepines fused with a triazole ring, Fig. 5.14), for example, showed high susceptibility to photolytic conditions in an acidic medium.[18]
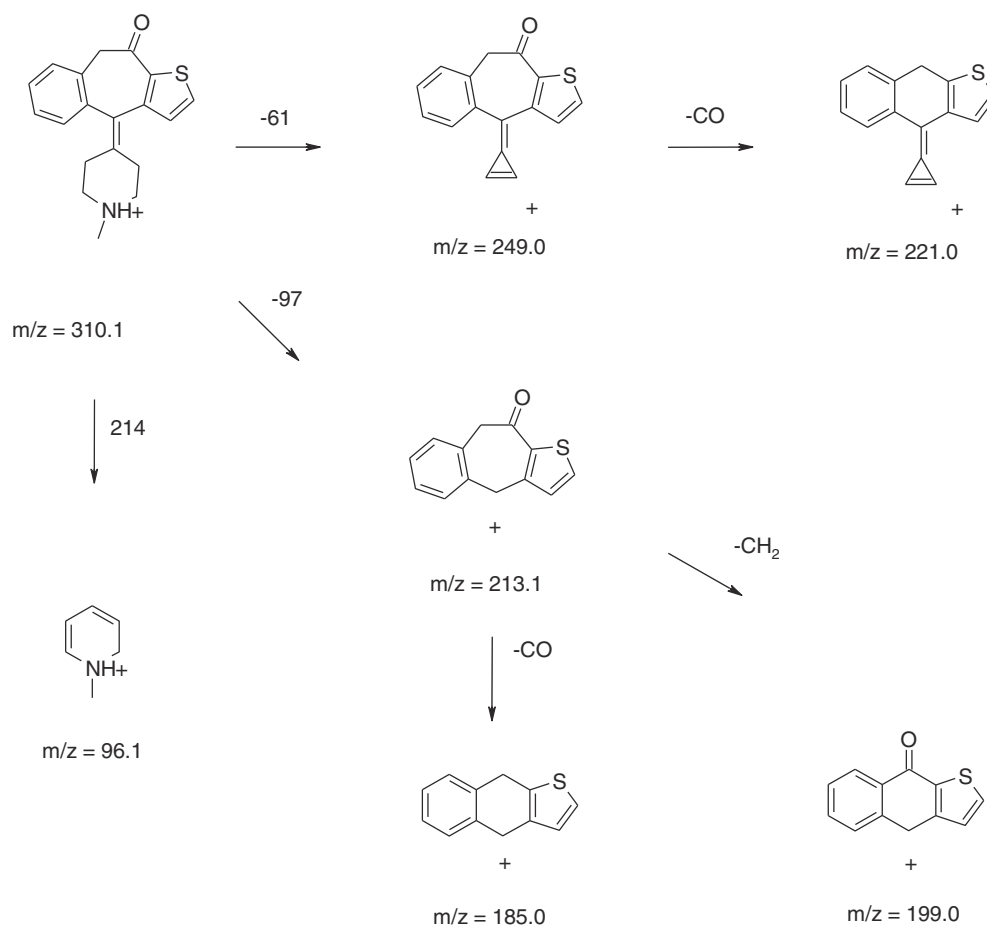
FIGURE 5.11   The fragmentation pathway of KET.

The photodegradation of AL was studied in aqueous and methanolic solutions. Characterization of the isolated products by 1 H and 13 C NMR and mass spectrometry revealed the occurrence of electron transfer, oxidation, and rearrangement reactions.

The photodegradation studies of alprazolam, carried out in solutions at different pH, showed that the photolability depends on pH, and it increases with the decrease in pH (at pH = 9 photodegradation does not even occur).

Characterization of the isolated products by ^{1}H and ^{13}C NMR and mass spectrometry revealed that electron transfer, oxidation, and rearrangement reactions take place. The main photodegradation products were isolated and characterized as triazolaminoquinoleine (**1**), 38-hydroalprazolam (**2**), and triazol-benzophenone (**3**) (Fig. 5.15). The photochemical studies also demonstrate that the photo-ability increases as the pH decreases.

Triazolaminoquinoleine was the main identified product. It is a highly fluorescent compound responsible for the photosensitivity observed in patients treated with alprazolam.[18]

The photodegradation of another benzodiazepine, diazepam (Fig. 5.16) and its metabolites in aqueous solutions have been thoroughly researched.[19]

Two diazepam photoproducts have been identified for the first time based on their ESI-Ms" fragmentation pathways and are proposed to be the acridinone derivatives, 4-chloro-10-methylacridin-9-one (4) and 4-chloro-10-acridinone (5) (Fig. 5.16).

Both direct and indirect photodegradation kinetics determined in the study for diazepam and its human metabolites were applied to UK river catchment models using a computer model. The overall results demonstrated that with photolysis half-lives ranging from 193 to 32 h, diazepam and its human metabolites are unlikely to be persistent in natural waters.
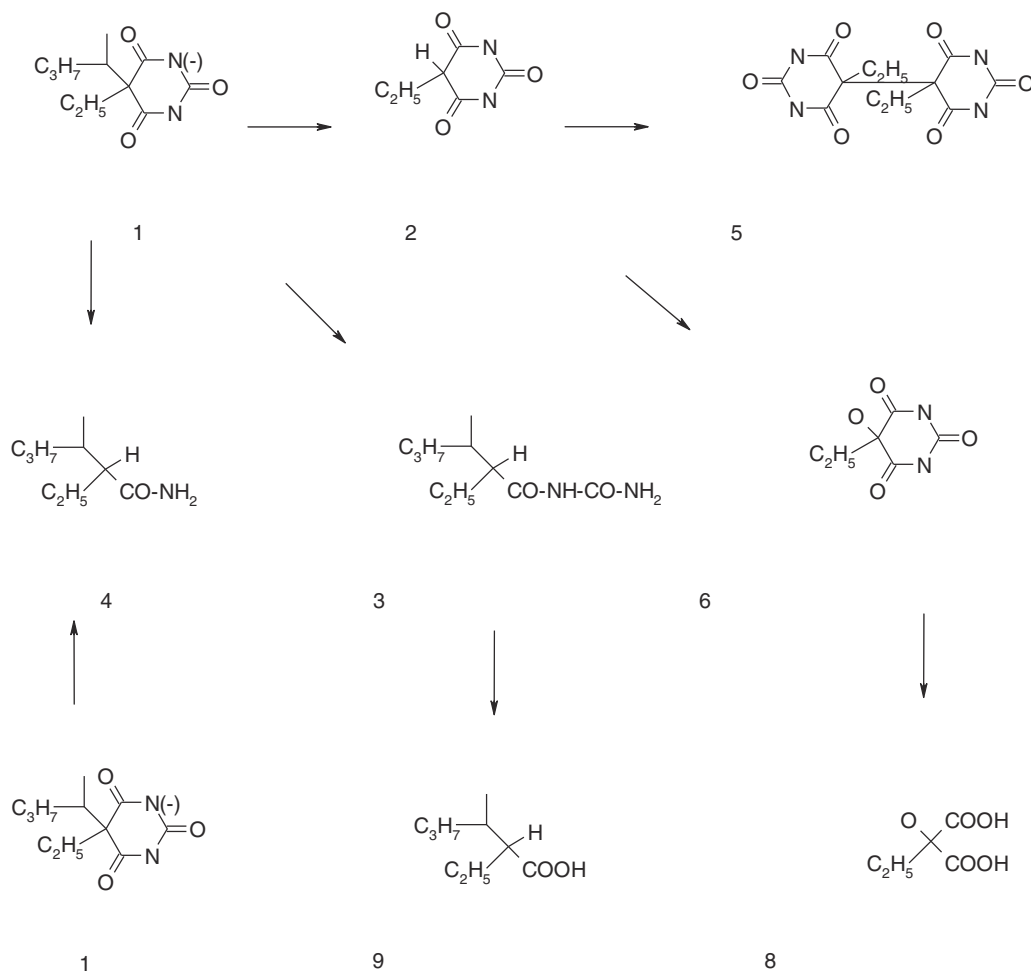
FIGURE 5.12 Pathways of photolysis of pentobarbital.

5.4.3 *Thioxanthene and phenothiazine psychotherapeutic agents*

Thioxanthene and phenothiazine are closely related chemically to each other, as can be seen from the chemical structures below:
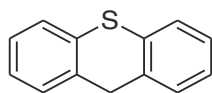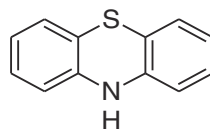
Thioxanthene   Phenothiazine

Chlorprothixene is the only representative of the thioxanthene group that was submitted for photostability testing. The main photoreaction pathway in the case of thioxanthene derivatives is photoisomerization, heteroaryl-conjugated alkenes can be isomerized between E and Z forms.[20]

Photostability of some derivatives of phenothiazine has also been studied, because they are well known for their phototoxic properties. In particular, the exposure of the skin to sunlight during therapy with antipsychotics belonging to this group results in phototoxic response, that is possible transformation of a compound resulting in the formation of genotoxic species and photoallergy. This is an immunologically mediated reaction because of the formation of an antigen by photoexcited molecules and proteins.[20]
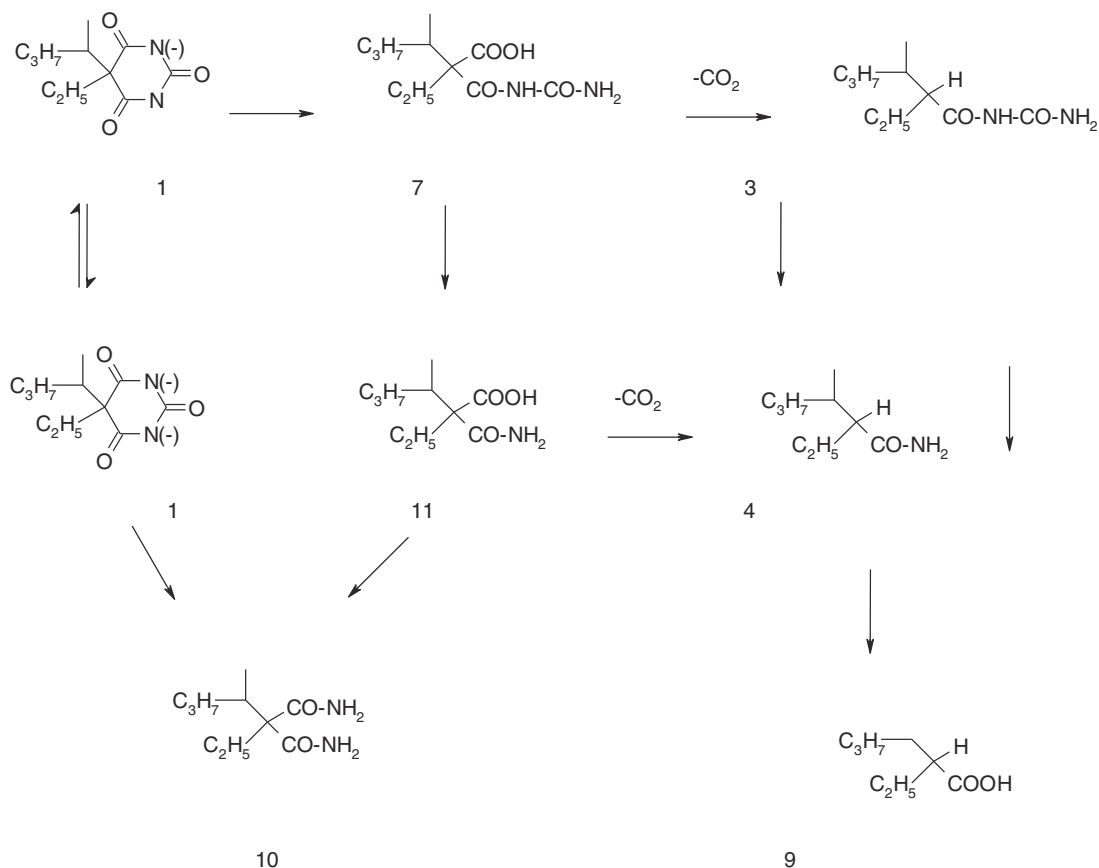
FIGURE 5.13   Pathways of hydrolysis of pentobarbital.
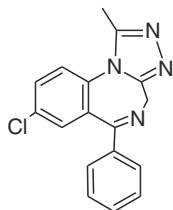
FIGURE 5.14   Alprazolam.

One of these studies, a short-term forced degradation study on chlorpromazine (a phenothiazine antipsychotic, which is often used in hospice and palliative care to treat hiccups, delirium, and nausea) was conducted under extreme pH, sunlight, ultraviolet (UV) light, and oxidative stress conditions. Significant degradation was observed in all conditions except 0.5 N NaOH. Because of that, in the recommended compounding procedure for the pharmacists, the following note is added: "It is important to use amber bottles or other light-resistant containers for long-term storage, because chlorpromazine is light sensitive."[21]

In another work, a forced photolytic degradation study (i.e., in UV and white light for 1.2 million lux hours) has been made on marketed tablet samples as well as on standards of chlorpromazine, through a method validated according to the International Harmonization Conference (ICH). In this case, only 4,5% of the drugs was degraded in UV light and 3,6% in white light.[22]
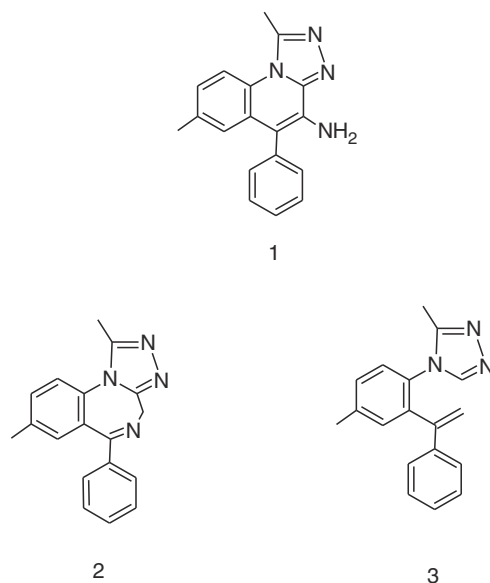
FIGURE 5.15   The main photodegradation products of Alprazolam.
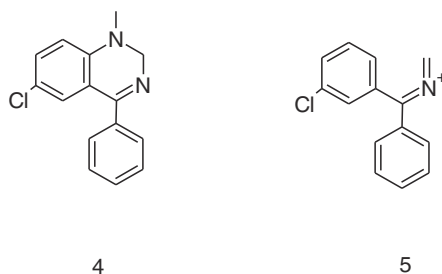
FIGURE 5.16   The photodegradation products of diazepam.

5.5 Cardiovascular drugs

5.5.1 Cardiac agents

Cardiovascular drug is any agent that affects the function of the heart and blood vessels. It means any drug indicated to treating hypertension, bradycardia, angina pectoris and so on. For this reason below we report the studies concerning some of them that is blood pressure regulating drugs, adrenergics and diuretics.

5.5.2 Blood pressure-regulating drugs

Among the most widely used antihypertensive drugs, 1, 4-dihydropyridine calcium channels β (DHPs) must certainly be mentioned.

These compounds are highly sensitive to light; therefore, their photodegradability has been extensively studied since the 80s, resulting in numerous publications and reviews in this regard.

The photodegradation process consists in the oxidation of the dihydropyridine ring to pyridine derivatives (Fig. 5.17), and in some cases the formation of secondary products has been observed due to a more complex degradation.

Owing to aromatization, drugs lose their pharmacological activity and, in some cases, products may even have toxic effects.

The process of degradation is started by proton transfer to the solvent. The presence of a nitro-group on the phenyl ring increases the process of aromatization because the delocalization of the negative charge is favorite, facilitating ionization and deprotonation. The nature of the substituents also has significant effect on the
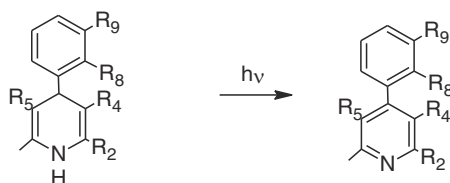
FIGURE 5.17 The photodegradation process of the dihydropyridine.
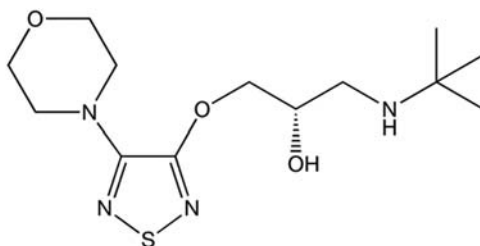
FIGURE 5.18 Chemical structure of timolol.
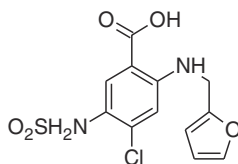
FIGURE 5.19 Furosemide.

photodegradation process; therefore, high stability was demonstrated when the fluorine group was in the position R1 of the phenyl ring or simultaneously present in R_1 and R_2 positions while the presence of chlorine in same positions R2 strongly increased the degradation process.[23]

Till now the DHPs drugs are sold as tablets (photodegradation is particularly fast in solution) in a dark container, but thanks to the numerous studies carried out on DHPs, for monitoring the stability of existing drugs as well as for synthesizing new molecules more stable to light, maybe it will be possible to overcome these traditional devices.

5.5.3 Adrenergics

Adrenergics are a class of drugs that bind to adrenergic receptors throughout the body and are usually used for the treatment of heart failure and cardiac arrhythmias. Between them, the most prescribed are ß-blocker medications.

The photodegradation of ß-blockers has been largely studied, but poorly understood until a few years ago when the photodegradation of ß-blocker timolol (Fig. 5.18) in fulvic acid (FA) solution was investigated under simulated sunlight.[24]

The triplet excited state of FA (^{3}FA*) and singlet oxygen ($^1O_2$) were responsible for the degradation of timolol in the aerated FA solutions. It was known that dissolved oxygen and halide ions are usually present in natural water (Cl$^-$, Br$^-$ and I$^-$) are the efficient quenchers of ^{3}FA*. The photodegradation is drastically accelerated after removing the dissolved oxygen, while chloride (Cl$^-$) and bromide (Br$^-$) exhibit less effect on the photodegradation of timolol than iodide (I$^-$). To study the reaction mechanism and the effect of halide ions, timolol was hardly degraded in one of the experiments reported[24] in deoxygenated and aerated FA solutions under simulated sunlight. Two reaction pathways were reported for the identified degradation products based on the LC-DAD chromatogram and the corresponding Ms, Ms/MS spectra (Fig. 5.19).

These results confirmed that photodegradation of timolol is an efficient way to remove it from natural waters.

5.5.4 Diuretics

Diuretics are used to reduce extra fluid in the body as well as to treat high blood pressure. Among them one frequently used is a 5-(aminosulfonyl)-4-chloro-2-[(2-furanylmethyl)-amino] benzoic acid, known as furosemide (Fig. 5.19).

Because of carboxylic group, this drug is photolabile under aerobic and anaerobic conditions. This phototoxic behavior is similar to those of other drugs with the same functional groups (i.e., nalidixic acid, tiaprofenic acid, and cinoxacin). Therefore, the photolysis of furosemide has been examined under conditions similar to those encountered in biological systems to characterize the degradation products and to determine the role of oxygen in the photodegradation process.[25]

Furosemide (1) was irradiated at room temperature for 72 h in methanol with an Osram HQL 250 Watt medium pressure Hg lamp in a Pyrex immersion-well photoreactor under an oxygen atmosphere for 48 h. The course of the reaction was followed by UV-Vis spectrophotometry and also by GC and TLC. By irradiation, three photodegradation products have been characterized (Fig. 5.20). A first process leads to the hydrogen abstraction product 1, the formation of 1 and 3 does not require oxygen, which was demonstrated by its detection under an argon atmosphere. Another photochemical process competes the reaction of the radical intermediate with oxygen to produce an unstable hydroperoxide that reduces in methanol to yield product 2. Product 1 is identified as the main product of the reaction (yield 82%). All three photoproducts have no phototoxic effects on red blood cells, but from photohemolysis test, it is possible to conclude that furosemide has its main phototoxic action only on biomembranes.

A similar process of photodegradation, induced from the generation of singlet oxygen radical, has also been verified for other types of diuretics such as acetazolamide, triamterene, and chlorthalidone (Fig. 5.21).[26]

Singlet oxygen is difficult to detect because of its short lifetime in solution. A way to confirm the involvement of oxygen is to demonstrate the reaction dependence on oxygen, but this does not necessarily imply the role of singlet oxygen. The influence of quenchers and D_2O is used to infer the intermediacy of singlet oxygen. In any case, the generation of singlet oxygen causes oxidation or superoxidation of membrane lipids. Oxidation of purine and pyrimidine bases has been overlooked.
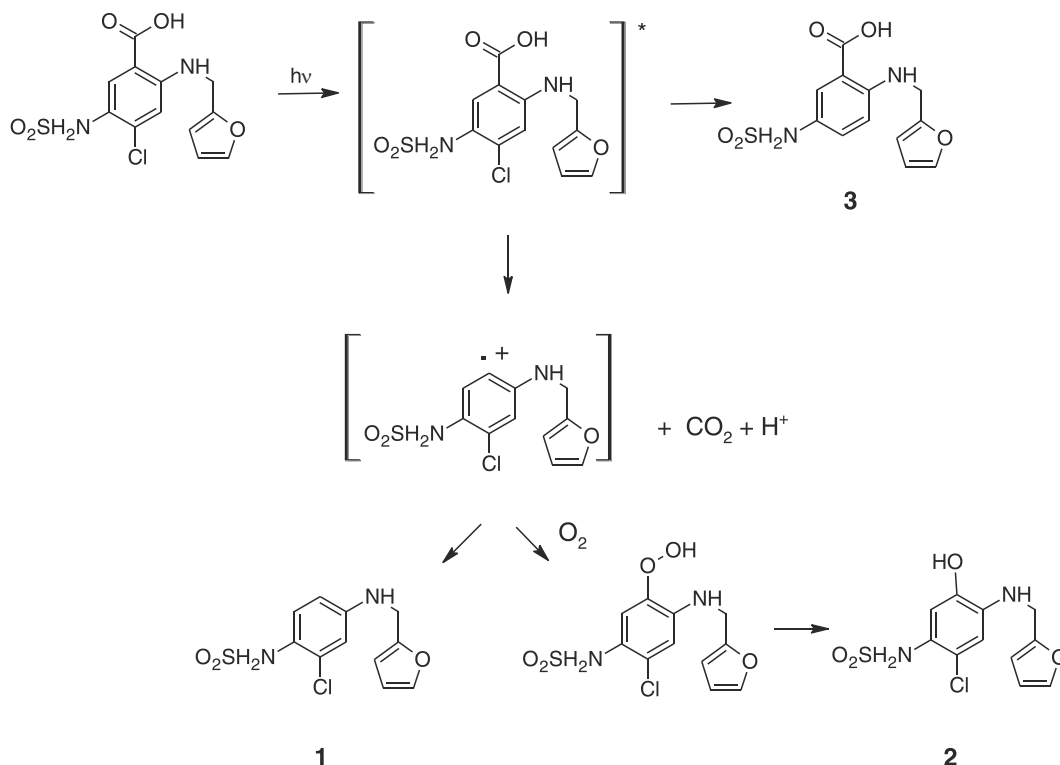
FIGURE 5.20   The photodegradation process of the Furosemide.
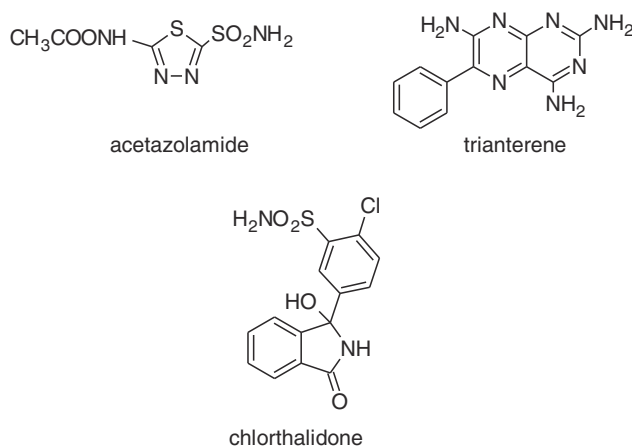
FIGURE 5.21 Others diuretics: acetazolamide, triamterene, and chlorthalidone.
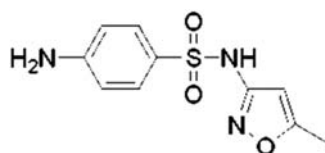
FIGURE 5.22 Sulfomethoxazole.

5.6 Chemotherapeutic agents

Specific chemotherapy drugs can have their effectiveness impaired by exposure to optical radiation. Several drugs were monitored to identify how light exposure can be maintained at levels that prevent photodegradation during the whole process of production, packaging, and distribution as well as during the drug administration phases, especially for drugs that required to be delivered by continuous infusion over time

5.6.1 Antibacterial drugs

Environmental occurrence of antibiotics in aquatic environment due to their incomplete elimination during wastewater treatment and their subsequent discharge in effluents from wastewater treatment plants, or derived from their application in cattle farming, agriculture, and aquaculture has been thoroughly documented.[27–32]

Photochemical degradation is likely to be the most important mechanism for many pharmaceutical pollutant losses. Photodegradation can occur by direct absorption of sunlight radiation (direct photolysis) or via reaction with transient reactive intermediates such as singlet oxygen, hydroxyl radicals, or other reactive species formed in natural waters (indirect photolysis).

Sulfamethoxazole (Fig. 5.22) is an antimicrobial sulfonamide component of o-trimoxazole, a 5:1 combination of sulfamethoxazole and trimethoprim. This formulation is applied in the treatment of respiratory tract such as bronchitis and Pneumocystis carinii pneumonia with AIDS,[33–35] severe urinary tract infections,[36] and enteric infections.[37]

The removal of sulfamethoxazole during sewage treatment is incomplete and concentrations varying from 0.01 and 2.0 ugL[1] have been detected in municipal sewage treatment plants effluents from different countries.[38–40]

The photodegradation showed a quantum yield of 0.47 at pH 3.4.[41] The main degradation product ($<D = 0.15$) was the product of the photoisomerization of the isoxazole ring (Fig. 5.23). A detailed description of photoisomerization reaction is provided in Chapter 2. It represents ca. 30% of the total products formed.

Other relevant degradation products were derived from the decomposition of the antibiotic. This way, 3-amino-5-methylisoxazole and 4-aminobenzensulfonic acid have been determined. The formation of the isoxazole isomer as the main product during photolysis has been confirmed in other works on the same compound. However, the oxidation products of both the aromatic part of the molecule and the isoxazole ring were observed. The results are summarized in Fig. 5.24.[42,43]

Furthermore, the degradation of sulfamethoxazole follows kinetics with a mean degradation rate of 0.05% min[1] under sunlight, and the degradation products showed an increased effect on the viability of murine fibroblasts L929.[44] However, in the case of a very similar compound, sulfisoxazole (Fig. 5.25), where substitutions on the isoxazole ring is different, no isomerization product was observed.[45]

The photodegradation, if performed at pH 4.0, where the neutral form of the substrate is prevalent, showed a $k = 5.4$ d[1]. However, the degradation does not fit pseudo first-order kinetics. In this case, the only determined photoproducts were derived from the cleavage of the isoxazole ring (Fig. 5.26).

A completely different behavior is observed in the photodegradation of sulfapyridine (Fig. 5.27).
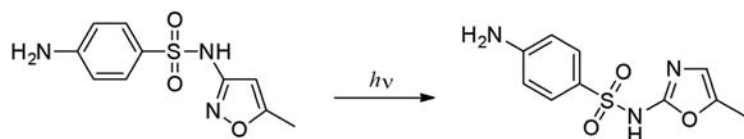
FIGURE 5.23 The photodegradation process of the sulfamethoxazole.
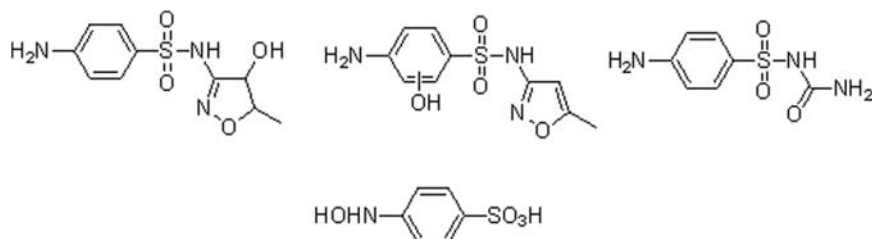
FIGURE 5.24 Minor degradation products of sulfamethoxazole.
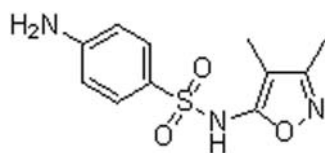
FIGURE 5.25 Sulfisoxazole.
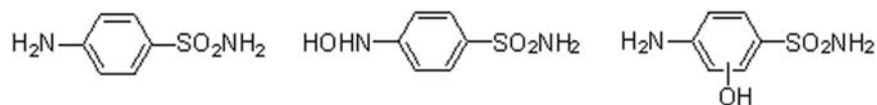
FIGURE 5.26 Degradation products of sulfisoxazole.
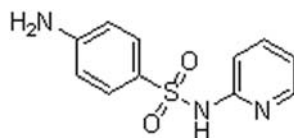
FIGURE 5.27 Sulfapyridine.

Sulfapyridine has been used for dermatological treatments and in veterinary medicine. In wastewaters, sulfapyridine has been observed at $65-95$ ngL[1].[46] Sulfapyridine showed an absorption at 309 nm (n^*). At pH 7.2 the degradation showed $k = 0.0072$ min.[1], while the degradation rate increased at pH 11.1 ($k = 0.022$ min.[1], $O = 0.013$). The main product observed was derived from SO_2 extrusion (Fig. 5.28).[47]

Other studies showed the presence of other photoproducts deriving from an oxidation process (Fig. 5.29).[48,49]

The same types of products were obtained in the treatment of sulfapyridine in the presence of both UV and H_2O_2.[50] Anyway, no photochemical reaction on the pyridine ring has been observed.

5.6.2 Antibacterials and antivirals: aromatic derivatives

Between the late eighties and early nineties, quinolones, a class of chemotherapeutic antibacterial agents, began to be extensively used. Their antibacterial activity is associated with the structure of quinolones (Fig. 5.30). Many of them have been reported to cause photosensitization reactions.

In 1991 a group of researchers showed that some quinolones, such as nalidixic acid (NA), rosoxacin (RS), and oxolinic acid (OA), induce the photosensitized hemolysis of erythrocytes.[51]
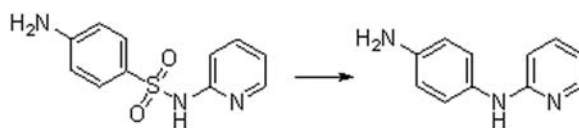
FIGURE 5.28   The main product of the photodegradation of sulfapyridine.
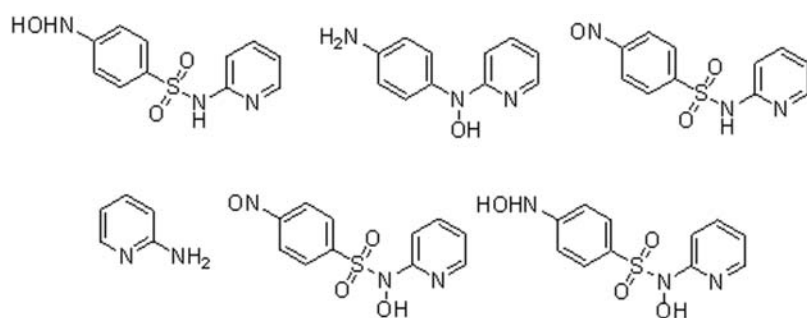
FIGURE 5.29   Minor degradation products of sulfapyridine.

NA

OA

RS

CP

NF

PA
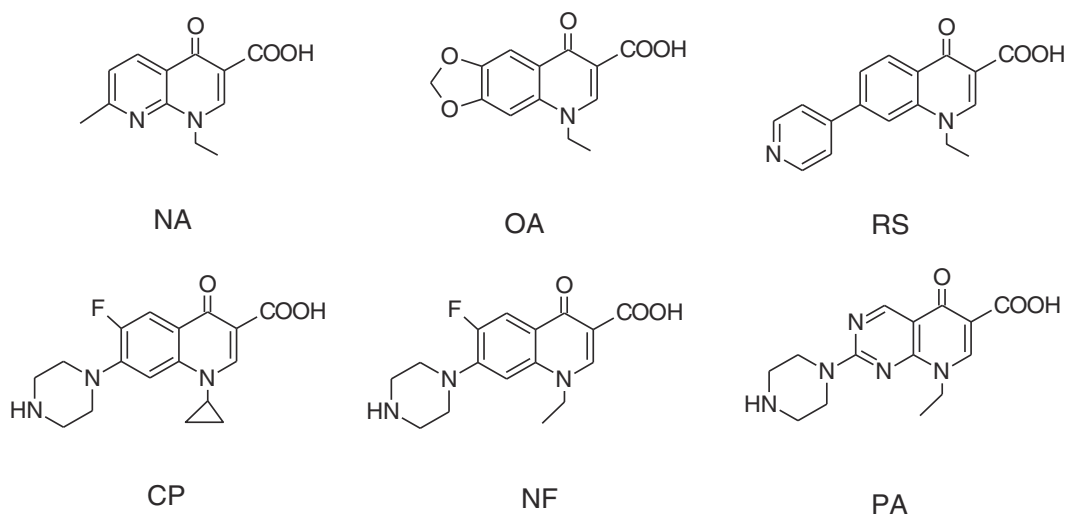
FIGURE 5.30   Structure of quinolones.

The same researchers studied the photodegradation kinetics of the quinolones OA, RS, ciprofloxacin (CP), NF norifloxacin, and pipemidic acid (PA) for obtaining an insight into the relationship between the structure and the photostability of these drugs.[52]

For these studies, a photoreactor equipped with 12 lamps was used. The lamps emit UVA radiation in the range 320–420 nm at pH 7,4 in phosphate-buffered saline solutions irradiated at a distance of 7 cm from the lamps. All these compounds exhibit moderate fluorescence, in the range 370,418 nm, when they are excited at the absorbance maximum. TLC analysis of the photoproducts showed the presence of at least five products.

PA, NF, and CP exhibit a higher photo consumption and higher fluorescence quantum yield, but they are not phototoxic to erythrocytes, whereas RS, NA and OA are photohemolytic agents.

Therefore, the presence of a piperazine group in position 7 is related to photostability. These drugs are more photolabile but without a phototoxic effect on cell membranes. This may be due to the greater hemolytic action of the unaffected drug when compared with the effect of the photoproducts.

Decarboxylation is the probable mechanism of photodegradation of the quinolones studied and this could be confirmed by the fact that in the case of CP, NF, and PA, this decarboxylation should be favored by the influence of the electron of free nitrogen, provided by the piperazine ring, resonating in the aromatic.

5.6.3 β-Lactam antibiotics

β-lactam antibiotics show antimicrobial properties due to the presence of a β-lactam ring. These are the most common group of chemotherapeutic drugs used in the treatment of bacterial infections.

These antibiotics are persistent and bioaccumulative contaminants by their nature and are found in large quantities in human-made environments such as sewage and waste-water treatment plants. Furthermore, they are biologically active compounds and have significant effect on organisms.

The environmental component of this issue has received an increased research interest in the last few years[53] and the development of purification methods of wastewater even in high concentrations of pollutants is a drastic effort.[54]

In this direction, the photodegradation of β-lactam antibiotics such as amoxicillin (AMO), ampicillin (AMP), penicillin G (PEG), penicillin V (PEV), and cloxacillin (CLX) (Fig. 5.31) has been studied in the presence of ZnS nanoparticles as photocatalyst.[55]

The photodegradation of antibiotic compounds catalyzed by ZnS nanoparticles was performed in a cylindrical glass reactor at 25°C. The degradation was carried out using a 500 W halogen lamp as the visible light source with UV cut-off filter. Each degradation experiment is repeated three times to study the reliability of the data. The concentration of antibiotic compounds was analyzed by a high-performance liquid chromatograph using a C18 column.
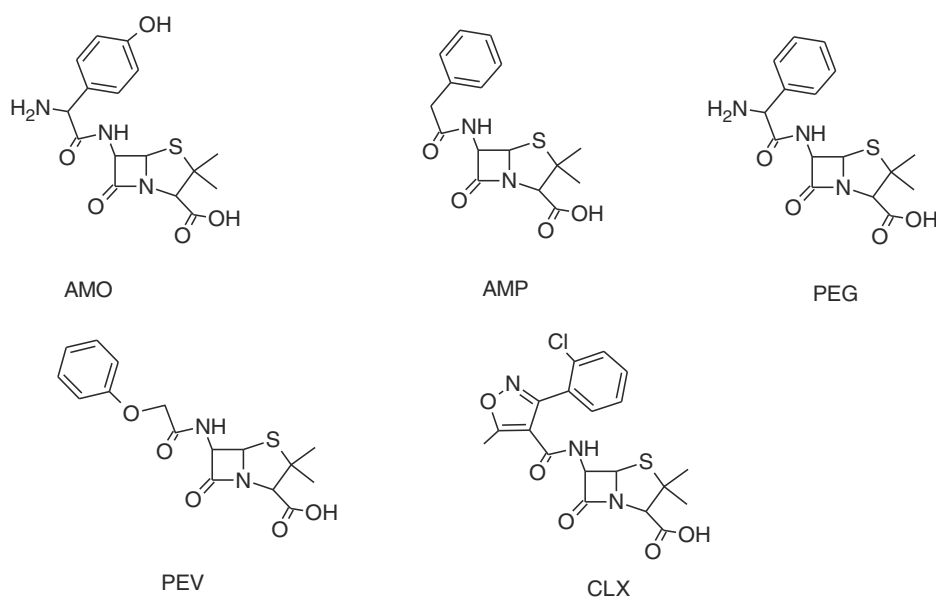
FIGURE 5.31 Structure of amoxicillin (AMO), ampicillin (AMP), penicillin G (PEG), penicillin V (PEV), and cloxacillin (CLX).

The study of the results obtained was followed by an optimization of the degradation process which led to the conclusion that the rate of degradation depends on the pH of samples, dosage of catalyst, initial concentration, and structure of β-lactam compounds.

The degradation rate increases with the decrease in the stability of antibiotic molecules. The degradation yield of 82%−100% is obtained for β-lactam compounds (50 mg/L) at a duration of 120 min at pH of 4.5 and 0.5 mg/L of ZnS nanoparticles.

5.6.4 Antiprotozoal, anti-amebic, antimycotic drugs

The significant worldwide impact of diseases caused by bacteria, fungi, and protozoa, which are among the most common and major causes of death, disability, social, and economic hindrance for millions of people, is reflected in the long-standing search for antiprotozoal, anti-amebic, and antimycotic chemotherapy. Most of the research done in this area predates the era of antibiotics; however, the same is still important today, especially in the case of the nosocomial pathogens that are resistant to many antibiotics.[56,57]

Owing to the sensitivity of some of these drugs to light their photodecomposition has been investigated.

Metronidazole (MTZ) (Fig. 5.32) is an anti-amebic, antiprotozoal, antibacterial, antiparasitic, and antitrichomonal agent.

In Sudan, it is widely used for the treatment of amebiasis, trichomoniasis, and giardiasis. Because of the strong sunlight and tropical conditions in Sudan, the photocomposition of MTZ has been investigated using not only a photochemical reactor but also sunlight.[58]

The sunlight-degraded and UV-irradiated samples of MTZ solution were analyzed using thin-layer chromatography (TLC), gas−liquid chromatography (GLC), UV and fluorescence spectroscopy. The photodecomposition reaction of the drug appears to follow pseudo-first-order kinetics. The rate of decomposition was found to increase with temperature, pH, and intensity of radiation and to decrease with an increase in drug concentration, while it is not affected from the presence of oxygen.

From this study, it can be concluded that metronidazole is a photolabile drug, and it should be protected from direct sunlight, especially in infusion forms.

The photodegradation of MTZ has been studied continuously in the years to come. In particular, a study on the degradation of metronidazole and different brands in active and different formulations by UV Spectroscopy has been reported.[59]

The different brands of metronidazole used for degradation study were: Flagyl "FGL," Metrozine "MNE," Klint "KNT" and the active metronidazole benzoate "MTZb." The solutions of the crushed tablets have been put in four different test tubes with 5 mL of DI water and left these test tubes in UV light of 320 nm for 30 min. Afterward, the absorbance of the solutions was analyzed separately at a wavelength max 278 nm. Only the MTZb showed decreased availability (25.68%) whereas all other three brands did not show any changes, which leads to the conclusion that moderate degradation actively occurs when exposed to UV light.

5.6.5 Antineoplastic drugs

Antineoplastic drugs are compounds used for anti-cancer treatment. They are delivered in the order of tons per year worldwide and are only poorly eliminated through conventional wastewater treatment. Because of that, they are considered as toxic, and numerous studies have been carried out to analyze their photostability and the toxicity of any photodegradation products.

In 2014, a study on photocatalytic degradation of two antineoplastic drugs, methotrexate, and doxorubicin (Fig. 5.33), in the aquatic environment was presented.

Doxorubicin and methotrexate were irradiated in Pyrex glass cells, filled with 5 mL of drug solution (15 mg/L) or of a suspension containing the drug (15 mg/L) and TiO$_2$ (200 mg/L) in a period of time from 2 min to 4 h.[60]
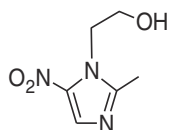
FIGURE 5.32   Structure of metronidazole.
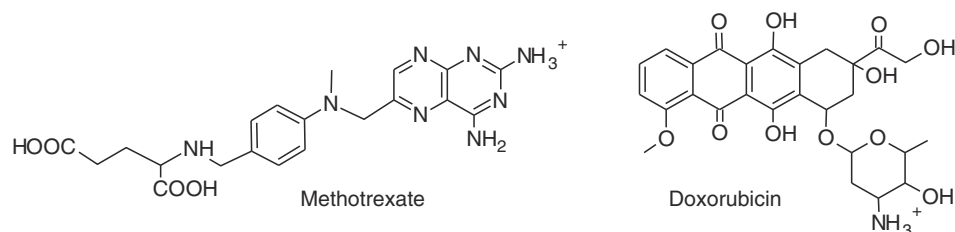
FIGURE 5.33 Two antineoplastic drugs :methotrexate and doxorubicin.
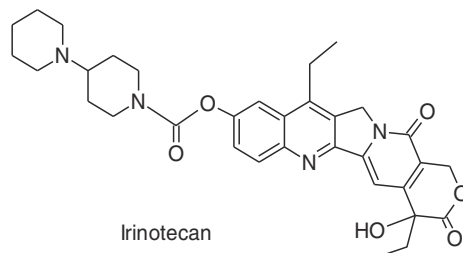
FIGURE 5.34 Irinotecan, IRI5-methoxypsoralen (5-MPO), 4′,5′-dimethyl-3,4-cyclohexyl psoralen (CS5) and 4′-methyl-3,4-cycloheptyl psoralen (CS4).

Methotrexate undergoes degradation both under UV-A irradiation and heterogeneous photocatalytic treatment, while doxorubicin is stable under UV-A irradiation. HPLC/HRMS analysis is used to identify and characterize products. The toxicity of all of them was evaluated with a Microtox Model 500 Toxicity Analyzer (Milan, Italy) by monitoring changes in the natural emission of the luminescent bacteria V. fischeri when challenged with toxic compounds.

In this way, it was possible to identify and characterize fourteen and eight toxic products from doxorubicin and methotrexate degradation, respectively.

In general, a reduction in toxicity was observed with increasing irradiation time and the more toxic compounds seemed to be those formed during the initial steps of drug transformation.

Recently, a new study on another antineoplastic drug irinotecan, IRI (Fig. 5.34) has been reported.[61]

Photocatalysis was carried out using commercial TiO$_2$ (Degussa P25) and several operational parameters were studied such as various pH levels (4−9) and different concentrations of TiO$_2$ catalyst (20−1000 mg/L).

Low-resolution mass spectrometry (LC-Ms/MS) and high-resolution mass spectrometry (LC-TOF-Ms) were used for the identification of toxic products from photolytic and photocatalytic degradation. The potential toxicity of irinotecan and its toxic products to aquatic organisms (bacteria) was measured by a Vibrio fischeri bioassay using a Microtox Model 500 Analyzer (SDI).

The results of this study pointed out that IRI can undergo photolysis under UV irradiation at pH 7 and photocatalytic degradation with UV-TiO$_2$ at pH 4.

During photodegradation, 19 toxic products were detected and 7 were structurally elucidated, using a combination of low- and high-resolution Ms techniques. For photocatalysis, the combination of high- and low- resolution LCMS techniques led to 32 toxic products and 12. were structurally elucidated.

The measurement of the aquatic toxicity of IRI and its toxic products using Vibrio fischeri bioassay showed a peak of toxicity at the beginning of the process which was then reduced during experiments.

5.6.6 Furocoumarins

Furocoumarins or psoralens usually used for psoriasis, vitiligo, and mycosis fungoides[62] are also used for phototherapy of cancer because of their ability to induce cancer cell apoptosis.[63,64]

The photodegradation of some of them (5-methoxypsoralen (5-MPO), 4′,5′-dimethyl-3,4-cyclohexyl psoralen (CS5) and 4′-methyl-3,4-cycloheptyl psoralen (CS4)) (Fig. 5.35) in ethanol under UV irradiation was recently studied. The photodegradation has been carried out in a XeBr excilamp, both in the presence of H$_2$O$_2$.[65]

From the results, it is possible to conclude that conversion values increase when the initial dye concentration decreases probably because with lower initial concentrations of substance, lower is the total mass irradiated and
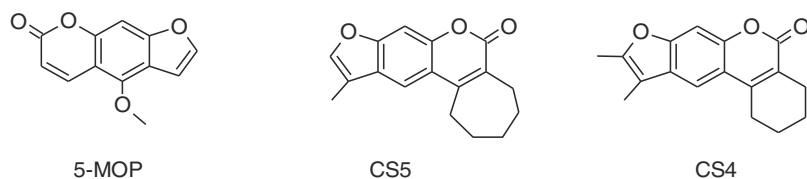
FIGURE 5.35 5-methoxypsoralen (5-MPO), 4′,5′-dimethyl-3,4-cyclohexyl psoralen (CS5) and 4′-methyl-3,4-cycloheptyl psoralen (CS4).

5-MOP   CS5   CS4
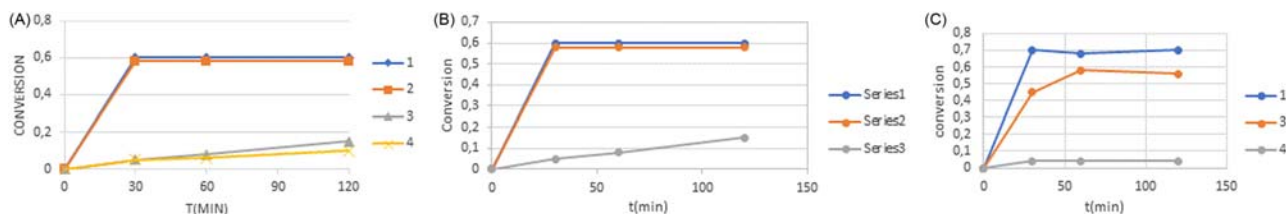
FIGURE 5.36 The conversion depends on irradiation time in ethanol of 2, 4 or 8 molecules of the compound with H_2O_2 (1−3) and without (4): (A) 5-MOP, (B) CS5, (C) CS4.[65]

higher is the density of radiation per mass unit and so the fraction of the total radiation received by the substance.

It is also important to underline that direct photolysis without hydrogen peroxide is negligible, while in the presence of the stoichiometric amount of hydrogen peroxide, total conversion to CO_2 and H_2O can be achieved (Fig. 5.36).

5.7 General mechanisms of photodegradation of crop protection products

For the European Commission, **plant protection products** are defined as 'pesticides' that protect crops or desirable or useful plants. They are primarily used in the agricultural sector but also in forestry, horticulture, amenity areas, and home gardens. They contain at least one **active substance** and have one of the following functions:

- protect plants or plant products against pests/diseases, before or after harvest
- influence the life processes of plants (such as substances influencing their growth, excluding nutrients)
- preserve plant products
- destroy or prevent the growth of undesired plants or parts of plants.

With the development of the agrochemical industry due to increasing global demand for vegetables, in recent decades an increase in the quantities of agrochemical pesticides dispersed in the environment and marine waters has also been noticed.

Some pesticides are resistant to chemical or photochemical degradation under typical environmental conditions,[66] while for some of them photodegradation is one of the most important abiotic transformations in the aquatic environment and the high energy of sunlight causes characteristic reactions such as bond scission, cyclization, and rearrangement, which are scarcely observed in hydrolysis and microbial degradation.[67]

Generally, photoproducts are less toxic to aquatic organisms, but sometimes enhanced toxicity has been reported. Because of this, many systematic studies have been carried out on the subject in the last few years.

The photochemical reaction mechanisms proposed are different:

1. *Photo-induced bond cleavage*
   a. *Carboxylic acid derivatives and carbamates*
   b. *Urea derivatives*
   c. *Ethers*
   d. *Organophosphorus (OP) esters*
   e. *Dehalogenation*
   f. *Denitration and deamination*
   g. *Hetero rings*

2. *Intramolecular bond formation-cyclization*
   a. *C—C bond formation*
   b. *C—O bond formation*
   c. *C—N bond formation*
3. *Rearrangement*
   a. *Isomerization*
   b. *Photo-Claisen and photo-Fries rearrangements*
4. *Oxidation*
5. *Reduction*

These reaction mechanisms for the direct photolysis of pesticides in water are described in Table 5.2.

5.7.1 Azole fungicides

At the beginning of 90s, the use of azole fungicides as plant protection products showed an increase and consequently the systematic study of their photochemical reactivity.

To examine the photostability of one of them, the fungicide penconazole (1-(2,4-dichloro-/β-propylphenethyl)-lH-1,2,4-triazole) (**1**) (Fig. 5.37) was irradiated in the presence of isopropanol, cyclohexane, and cyclohexene as representative model substances for the plant cuticle constituents.[68]

Photolysis on UV irradiation (2 > 280 nm) was much more efficient in isopropanol and cyclohexane than it was in cyclohexene. When irradiated in isopropanol or cyclohexane solution penconazole was degraded within 5—7 h by 50%, whereas in cyclohexene as solvent the half-life was 23 h.

TABLE 5.2 Reaction mechanisms in direct photolysis of pesticides in water.

Photo-induced hydrolysis			**Sulfonylurea (C-S, N-S), organophosphorus (P-O) chlorinated triazine herbicide (C-Cl)**
Homolytic cleavage of	C—O(S)	Norrish type-I	Pyrethroid[a'], thioester, O-aryl N-alkylcarbamate
C(=O)X (X = O, N, S)		β-Cleavage	Pyrethroid (type-II')
	C—N	Norrish type-I Norrish type-II	Aryl amide[a'], O-alkyl N-arylcarbamate[a'], benzoylurea[b'] aryl amide
Homolytic bond cleavage	C—O (ether)[c]		Diphenyl ether, phenoxyacetic acid sulfonamide, thioether[c'] oxime ether sulfonamide
	C—S		
	N—O		
	N—S		
Dehalogenation	Homolytic heterolytic		Organochlorine (DDT, methoxychlor) 2- or 3-halogenated phenol,[d] aniline & their derivatives Chloroacetanilide,[d] 4-halogenated aromatics[e]
Denitration, deamination	C—N		*Neo*-nicotinoid, triazinone herbicide
Isomerization	Geometrical valence		Pyrethroid, alkene, oxime ether pyridine, pyridazine & isoxazole rings
Cyclization	C—C[f]C—O[g]C—N		Pesticides having aromatic rings adequately oriented diamide insecticide, benzoyl-cyclohexanedione herbicide dinitroaniline herbicide
Rearrangement	Photo-Fries[a] Photo-Claisen Beckmann Thiono-thiolo[a]		O-alkyl N-arylcarbamate, O-aryl N-alkylcarbamate, phenylurea phenoxyacetic acid[a'], aryl benzyl ether oxime ether organophosphorus

[a]*Minor pathway in direct aqueous photolysis under sunlight.*
[b]*Norrish type II process followed by disproportionation is alternatively proposed.*
[c]*Het-erolytic bond cleavage is an alternative mechanism.*
[d]*Homolytic bond cleavage is an alternative mechanism.*
[e]*Formation of carbene is proposed for some compounds.*
[f]*Electrocyclic or oxidative process.*
[g]$S_N(ET)Ar^*$ *mechanism is most probable.*[67]
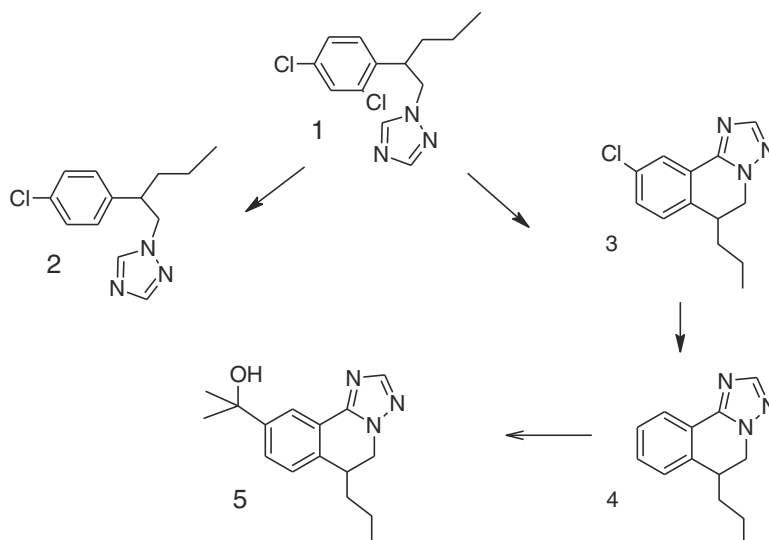
FIGURE 5.37   Photodegradation scheme of penconazole **1** in model solutions.

Photolysis of penconazole in isopropanol as irradiation medium mainly yielded **2** 1-(4-chloro-fl-propylphenethyl)-lH-1,2,4-triazole and **3** 5 H,6H-(1,2,4-triazole)-[5,1-a]-9-chloro-6-propyl-isoquinoline (Fig. 5.37), both new photoproducts of penconazole. After 8 h of irradiation, 42.1% of the degraded penconazole was converted to these photoproducts (29.8% of 2 and 12.3% of 3, respectively). On irradiation of penconazole in cyclohexane and cyclohexene as solvents, the photoproducts **2** and **3** were also formed, but in smaller quantities and different ratios than in the isopropanolic solution. In the presence of isopropanol, photodehalogenation of 3 competed with the substitution by a solvent molecule yielding **5** 5H, 6H-(1,2,4-triazolo)-[5,1-a]-9-(2-hydroxy-2-methylethyl)-6-propyl-isoquinoline (Fig. 5.37) as photoaddition product at a rather low level ($< 1\%$).

The photoreactivity of penconazole is mainly due to photodehalogenation and photocyclization; the photoinduced addition of penconazole to plant constituents of the cuticle seemed to play only a minor part.

The photodegradation of strobilurin fungicides have reported as an example of the most important groups of pesticides used to combat white mold, rot, early and late leaf spot, rust and rice outbreak.[69]

The photodegradation of benzothiostrobin in liquid media and on soil surface and glass surface were investigated under various experimental conditions including initial concentration of benzothiostrobin, and the water constituents such as NO_2^-, NO_3^-, Fe^{2+}, Fe^{3+}, H_2O_2, and turbidity were also evaluated. The degradation products in aqueous under xenon lamp irradiation were identified by ultra-performance liquid chromatography-tandem mass spectrometry (UPLC-Ms/MS) and the degradation pathways were proposed.[70]

The results showed that benzothiostrobin photodegradation followed first-order kinetics, and that the photodegradation rates decreased with the increase in the initial concentration of benzothiostrobin. The photodegradation of benzothiostrobin was studied in different organic solvents: benzothiostrobin was photodegraded at a faster rate in n-hexane, methanol, and acetonitrile, but slower in acetone. These results indicated that photolysis rates were not directly related to the polarity of organic solvent.

Regarding the effect of the aqueous environmental substances and turbidity, the results showed that the photodegradation of benzothiostrobin occurred more easily in the presence of Fe^{3+}, NO_2^-, and H_2O_2, whereas Fe^{2+} and turbidity reduced the photodegradation rates.

The four photodegradation products of benzothiostrobin in aqueous were identified by UPLC-Ms/MS and the presumed photodegradation pathways are shown in Fig. 5.38.

5.7.2 Dicarboximide fungicides

The broad-spectrum dicarboximide fungicides, including procymidone, iprodione, and vinclozolin, were commonly used to control *Botrytis* on vines, fruits, and vegetables in the 1980s. Fungicides of this class have been used since the mid-1970s mainly to control fungi of the related genera *Botrytis*, *Sclerotinia*, and *Monilinia*.[71]

To study the potential of vinclozin, 3-(3,5-dichlorophenyl)-5-methyl-5-vinyl-1,3-oxazolidine-2,4-dione, to undergo photochemical reactions on plant surfaces, the fungicide was irradiated in various organic solvents
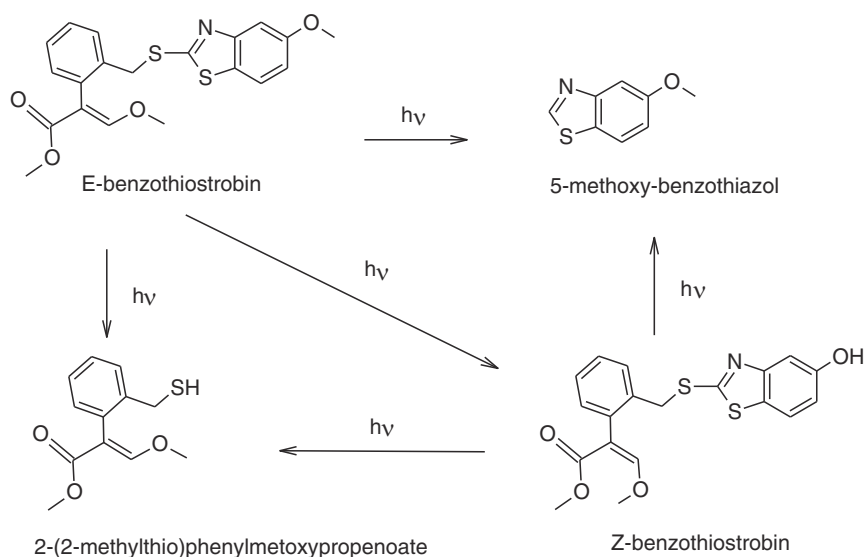
FIGURE 5.38   The presumed photodegradation pathways of benzothiostrobin.
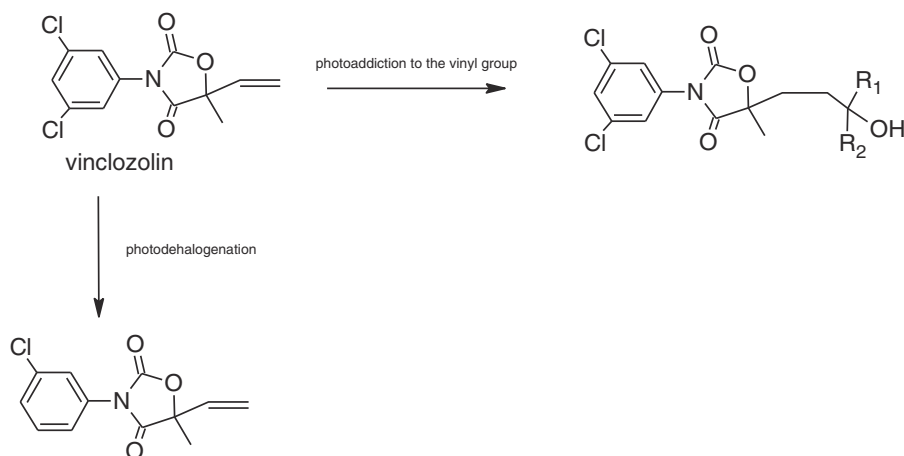
FIGURE 5.39   Photodegradation pathway of vinclozin in the presence of ethanol (R_1 = H, R_2 = CH$_3$), 2-propanol (R_1 = CH$_3$, R_2 = CH$_3$) or n-propanol (R_1 = H, R_2 = C$_2$H$_5$).

(cyclohexane, cyclohexene, 2-propanol, n-propanol, ethanol, methanol, and TBME) to simulate the plant cuticle environment.[72]

Vinclozolin was completely degraded in 2-propanol and n-propanol in 1 h, while the degradation in 5 h was lower in cyclohexane (13,6%), cyclohexene (21,5%), ethanol (61,4%), methanol (14,9%) and tert-butyl methyl ether (13,4%) possibly because of their H donor properties. When 2-propanol, n-propanol, and cyclohexane are used as solvents, the main reaction was photoaddition of the solvent molecules to the vinclozolin vinyl group (Figs. 5.39 and 5.40) followed by a dechlorination of the photoproducts. On the other hand, in the presence of ethanol, photodehalogenation of the fungicide competed with photoaddition (Fig. 5.39).

Pure photodehalogenation leading to the two photoproducts shown in Fig. 5.41 was observed on irradiation of vinclozolin in tert-butyl methyl ether and methanol after **17**h.

When vinclozolin was irradiated in cyclohexene, the main reaction was a substitution of C1 by solvent molecules, thus leading to cyclohexyl- and cyclohexenyl substituted products shown in Fig. 5.42.

The same authors studied the photoreactivity of two other dicarboximide fungicides that is procymidone, (3-(3,5-dichlorophenyl)-1,5-dimethyl-3-azabicyclo[3.1.0.]hexane-2,4-dione)[73] and iprodione (3-(3,5-dichlorophenyl)-N-(1-methylethyl)2,4-dioxo-1-imidazolidinecarboxamide)[74] (Fig. 5.43) in various organic solvents simulating the plant cuticle environment getting similar results.
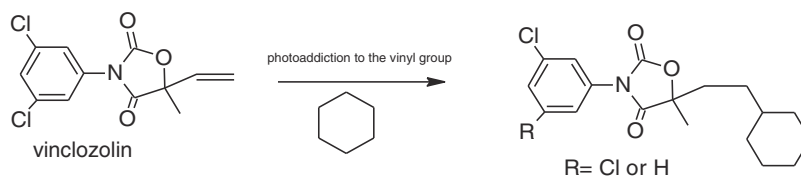
FIGURE 5.40 Photodegradation pathway of vinclozin in the presence of cyclohexane.
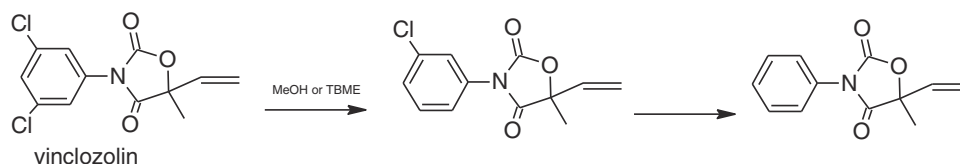
FIGURE 5.41 Photodegradation pathway of vinclozin in the presence of methanol or TBME.
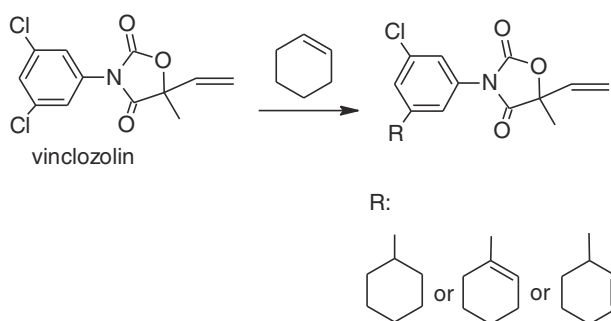
FIGURE 5.42 Photodegradation pathway of vinclozin in the presence of cyclohexene.
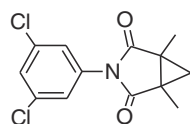
procymidone
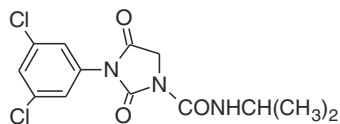
iprodione

FIGURE 5.43 Chemical structures of herbicides studied.

In conclusion, vinclozolin, procymidone, and iprodione showed a high potential to undergo photo-induced reactions with various types of chemical structures in different model environments. The photoproducts containing the solvent moiety indicate the possible formation of bound residues in plant cuticles where solvent molecules are replaced by constituents of plant waxes and the cutin polymer in such reaction pathways.[72−74]

5.7.3 Imidazolinone herbicides

Imidazolinone herbicides, which include imazapyr, imazapic, imazethapyr, imazamox, imazamethabenz, and imazaquin, control weeds by inhibiting the enzyme acetohydroxyacid synthase, which is a critical enzyme for the biosynthesis of branched-chain amino acids in plants. These herbicides control a wide spectrum of grass and broadleaf weeds, are effective at low application rates, have low mammalian toxicity, and possess a favorable environmental profile.[75]

The photodegradation of imazapyr, imazethapyr, and imazaquin (Fig. 5.44) was investigated under controlled conditions, because of their role in removing the herbicide from the environment.[76]
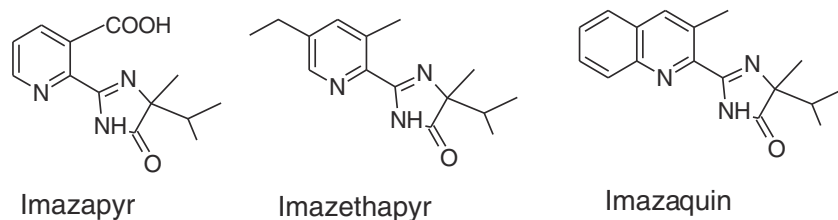
FIGURE 5.44 Chemical structures of herbicides studied.

Photodegradation of imazapyr, imazethapyr, and imazaquin was studied in the presence of different ratios of herbicide: humic acids (1:1, 1:2, and 1:3) and in sterilized Milli-Q water. The simulated solar irradiation was provided using a high-pressure mercury vapor lamp positioned 30 cm above the containers and with an irradiation intensity of 550 W/m^2 throughout the experiments. The herbicide solutions were adjusted to pH 7 and pH was maintained above 5.5 during the experiment. The temperature was kept constant at 25°C throughout the experiment. Photodegradation on the soil surface has been studied, too.

The results demonstrate that the photodegradation of imidazolinone herbicides in solution as well as on soil surface proceeded first-order reactions. The rate constants of photodegradation were decreased up to twofold in humic acid solutions compared with those determined in Milli-Q water. Photodegradation was further decreased when the herbicides were placed on the soil surface. The rank order of photodegradation was imazaquin > imazethapyr > imazayr with half-lives of 15.3, 24.6, and 30.9 days, respectively, on the soil surface.

In conclusion, photodegradation is an important way to remove herbicides from the environment only when they are exposed to light. While the biotic degradation could be much more important since these herbicides are into the soil profile.

5.7.4 Macrocyclic lactone insecticide

The avermectins are a class of macrocyclic lactones produced by the soil actinomycete *Streptomyces avermitilis*. They are widely used in agriculture due to the high biological efficiency against pests of crops. Many studies have shown that avermectins are easily oxidized and photodegradable. Because of that, photodegradation and the identification of photoproducts have been studied.

The use of Avermectin B1 or abamectin (80% of the B$_{1A}$ homolog and not more than 20% of the B$_{1B}$ homolog) (Fig. 5.45) had a rapid worldwide growth in use as an insecticide for several crops since the late 80s.

In that period, the photolysis of the B$_{1A}$ homolog (isolated from technical grade avermectin B1) thin films in vitro has been studied.[77]

To compare the effect of sunlight and artificial light, studies were conducted in parallel with both sources. In the first case, B$_{1A}$ was applied in ethyl acetate to the wells of a

Boerner slide, dried in the dark, was placed in sunlight for 8 h. In the second one, B$_{1A}$ was placed in uncovered 10-mL glass beakers or glass Petri dishes and dried under a stream of nitrogen at room temperature in the dark. The thin films were then placed near a bank of 10−12 General Electric 275-W Suntanner RS bulbs in a fume hood. In both cases, the residues were recovered by rinsing with methanol and then assayed by HPLC.

The C18 HPLC chromatograms of residues obtained after a 2 h photolysis of highly purified B$_{1A}$ under sunlamps as well as the chromatograms of residues obtained after a 8 h photolysis in sunlight indicate the presence of multiple identical photodegradants.

The observed photolability of avermectin B1, in the presence of oxygen and the apparent complexity of the resultant degradants, may be rationalized by the abundance of potentially oxygen-sensitive sites.

Several studies have shown that avermectin is easily oxidized and photodegradable, and this turns out to be a big disadvantage because of the short half-life under UV irradiation which means that, in practical application, not less than 90% of the applied conventional pesticide is lost because of its instability.

To solve this problem, a rapid and low-cost approach was reported on preparing avermectin microcapsules with anti-photodegradation and slow-release by the assembly of lignin derivatives.[78]

Alkyl chain-coupled lignosulfonate-based polymers (ALS) were prepared and dissolved in water, while avermectin (Av) was dissolved in ethanol solution. Afterward, the Av/ethanol solution was added to the ALS aqueous. Then, the mixed solution was stirred for 2.5 h at room temperature to obtain the Av@ALS microcapsules.
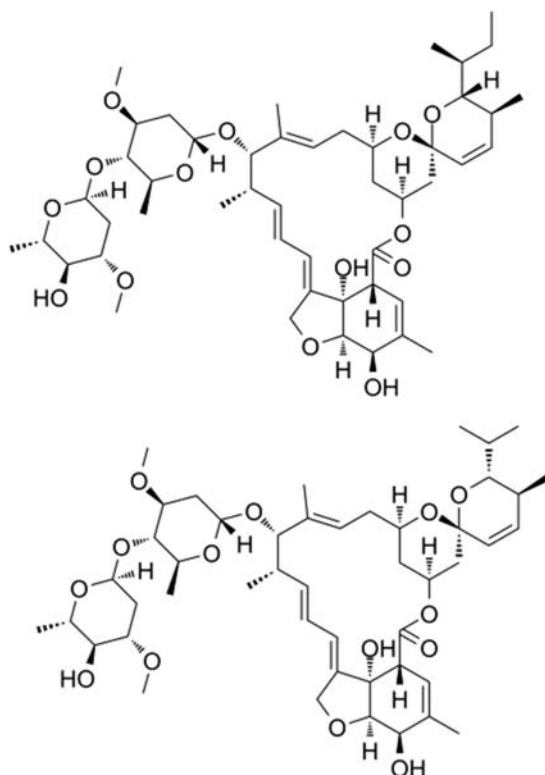
FIGURE 5.45   Chemical structures of B_{1A} i B_{1B} homologs.

To confirm the photostability of the microcapsules, samples of Av emulsifiable concentrate (Av-EC, 5% w/w), Av technical (Av-Tech) and Av@ALS microcapsules of products containing the same amount of Av, were prepared.

Samples were then exposed to UV light at room temperature with stirring. The remaining concentration of Av in the release medium after UV irradiation was measured immediately by UV-vis spectroscopy.

Av-Tech and Av-EC are completely decomposed by UV irradiation in 5 and 10 h, respectively. By contrast, Av remained detectable in the release medium of ALS carriers even after 55 h of UV irradiation.

These results demonstrate that the Av@ALS microcapsules have superior UV-shielding properties. Av@ALS microcapsules with excellent slow-release properties could improve the use rate of Av.

5.7.5 N-Methyl carbamate insecticides

In the late 50s and early 60s, carbamates were developed into commercial pesticides: insecticides, herbicides, and fungicides. Since then, the photodegradability of carbamates has been the subject of numerous studies.

For the carbamates are N-substituted esters of carbamic acid. Their general formula is:
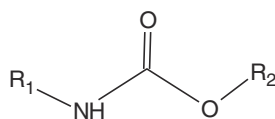
where R_2 is an aromatic or aliphatic moiety. Three main classes of carbamate pesticides are known:

1. carbamate insecticides; R_1 is a methyl group;
2. carbamate herbicides; R_1 is an aromatic moiety;
3. carbamate fungicides; R_1 is a benzimidazole moiety.

Specifically, below are reported only some of photodegradation studies carried out on an insecticide where R_2 is a heteroaromatic moiety ie the carbamate pesticide carbofuran (2,3-dihydro-2,2-dimethylbenzofuran-7-ol N-methylcarbamate) (Fig. 5.46).

The kinetic and mechanistic aspects of the photochemical degradation of carbofuran in aqueous solution and in the presence of various samples of dissolved organic matter (DOM) have been reported.[79]

Kinetic experiments are monitored with HPLC and found that the photodecomposition proceeds via first-order reaction kinetics and that the presence of various DOM samples inhibits the photolysis reaction of carbofuran probably because of different magnitudes of the binding interaction between carbofuran and DOM. To identify the photodecomposition products, the product mixture was analyzed with HPLC and GCMS.

Both techniques indicated that the mixture contained seven compounds, but only some products were identified due to insufficient evidence to propose structures for three of them.

The mechanism proposed is the following: carbofuran decomposes via direct photolysis. In the first step of the reaction, the carbamate group is cleaved forming carbamic acid and 2,3-dihydro-2,2-dimethylbenzofuran-7-ol. Carbamic acid readily decomposes to carbon dioxide and methylamine. The phenolic product decomposes upon irradiation into a substituted catechol. The ether linkage of the furan group is cleaved forming a tertiary alcohol side chain attached to catechol. This molecule also reacts photochemically, converting the alcoholic side chain to an alkene via a dehydration reaction (Fig. 5.47).

By comparing the results obtained, it can be concluded that the presence of DOM slows the rate of photolysis as well as the biological decomposition of carbofuran.

A new study on the photodegradation of carbofuran has been recently reported. In this case,

The photocatalytic degradation of a model compound of carbofuran in water was studied using polychromatic light and ZnO and TiO_2 catalysts.[80]

A solution of carbofuran in deionized water was irradiated using different types of photocatalysts (ZnO Merck and four commercial TiO_2) and polychromatic light.

Comparisons of photocatalytic performances of catalysts of different origin showed that ZnO Merck was the best catalyst for 315−400 nm carbofuran oxidative degradation as shown in Table 5.3.

Kinetics of carbofuran degradation with 2 g/L of catalysts(C_0 (carbofuran) = 88.4 mg/L, pH = 5.9)

The results also showed that the photodegradation was affected by the initial concentration of carbofuran (a decrease in photodegradation with increasing initial concentration) and that was almost complete within 2 h. A pseudo-first-order kinetic model was established also in this work.
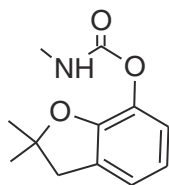
FIGURE 5.46   Carbofuran structure.
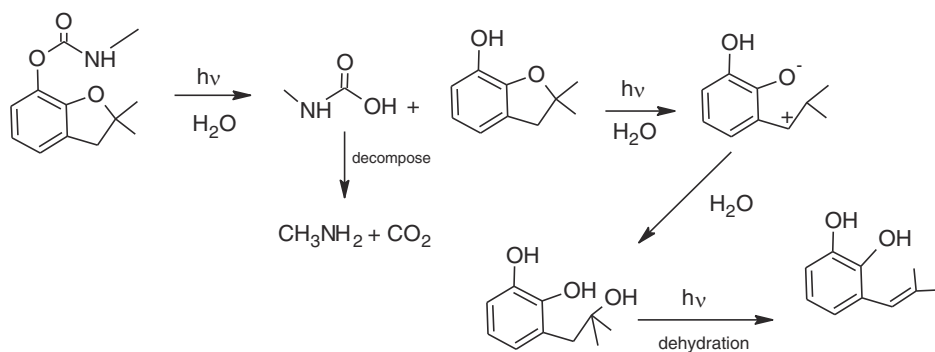
FIGURE 5.47   Photodegradation of carbofuran.

TABLE 5.3 Kinetics of carbofuran degradation with 2 g L−1 of catalysts (C_0 (carbofuran) = 88.4 mg L−1, pH 5.9).

Catalyst	k (min^{-1})	$t_{1/2}$ (min)	R
ZnO Merck	0.1072	6.47	0.9836
TiO$_2$ Degussa P-25	0.0822	8.43	0.9824
TiO$_2$ Merck Eusolex® T	0.0268	25.86	0.9836
TiO$_2$ Merck anatase	0.0179	38.72	0.9784
TiO$_2$ Merck R-706 rutile	0.0143	48.47	0.9786
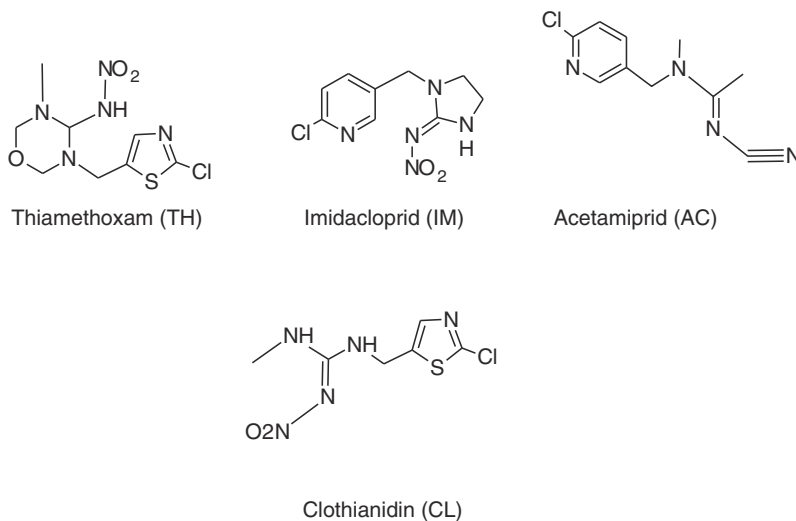
FIGURE 5.48 Structures of thiamethoxam (TH), imidacloprid (IM), acetamiprid (AC) and clothianidin (CL).

5.7.6 Neonicotinoid insecticides

Neonicotinoids (NIs), so named for the nicotine-like structure, are a relatively new group of insecticides that have also the common mode of action of nicotine on the nervous system of insects.

Thiamethoxam (TH), imidacloprid (IM), and acetamiprid (AC) (Fig. 5.48) are three commercial neonicotinoids used extensively as treatment of agricultural crop pests.

The photocatalytic degradation of these three neonicotinoid insecticides (TH, IM and AC), in pure water has been studied using zinc oxide (ZnO) and titanium dioxide (TiO$_2$) as photocatalysts under natural sunlight and artificial light irradiation.[81]

For artificial light irradiation, a photochemical reactor equipped with a magnetic stirring bar and a 8-W low-pressure mercury lamp were used. Different samples were prepared with or without chalcogenide oxides but also with each of them in combination with oxidant Na$_2$S$_2$O$_8$.

The results are different for the three types of samples:

- the photocatalytic degradation of all NIs in the presence of the semiconductor oxides (ZnO or TiO$_2$) leads to the disappearance of these substances,
- in the absence of oxides, the photolytic decomposition occurs at a very slow rate and only a 30% reduction of Nis' concentration is achieved after 120 min of irradiation,
- in the presence of ZnO/ Na$_2$S$_2$O$_8$ and TiO$_2$/Na$_2$S$_2$O$_8$, complete disappearance was achieved after 10 and 30 min of irradiation, respectively.

For the natural sunlight irradiation, the same types of samples were irradiated during July, 2013 in Murcia, SE Spain receiving more than 3000 h of sunlight per year.

In this case, complete disappearance was achieved after 5 and 30 min of illumination using ZnO/Na$_2$S$_2$O$_8$ and TiO$_2$/Na$_2$S$_2$O$_8$, respectively.

In addition, the main photocatalytic intermediates were identified by HPLC-Ms/MS during the experiments under solar irradiation and the DOC analyses confirmed a very low mineralization rate indicating that several nondegradable organic intermediates were formed.

The photodegradation of the same INs (TH, IM, and AC) but also of clothianidin (CL) (Fig. 5.48) was investigated in Bamboo vinegar (a brown liquid with unique smoky taste collected via condensation of gases during bamboo pyrolysis or distillation) as a synergistic agent for improved functional duration.[82]

All NIs were dissolved in methanol to prepare standard solutions and analyzed using high-performance liquid chromatography (HPLC) with variable-wavelength ultraviolet detection to obtain standard curves.

All samples were irradiated using a high-pressure mercury lamp or sunlight to determine the influence of different light sources and as control, parallel darkness experiments were carried out. In addition, samples of NIs dissolved in methanol and combined with bamboo vinegar were also irradiated with a high-pressure mercury lamp.

The initial concentration, light source, water quality, and pH were employed as parameters to systematically determine the photodegradation characteristics of the neonicotinoids in water.

It was detected that:

- the photodegradation half-lives of the NIs increased by nearly onefold when the initial neonicotinoid concentration decreased from 20 to 5 mg/L,
- the photodegradation rates under high-pressure mercury lamp irradiation were comparably higher than those under sunlight irradiation,
- the photodegradation rates were also different depending on the type of employed aqueous media and the highest one was in ultra-pure water,
- the photodegradation rates were also influenced by pH, the lowest was in acidic buffer solution and relatively high in alkaline and neutral buffer solutions.

In addition, Bamboo vinegar exhibited a quenching effect on photodegradation, especially when the vinegar concentrations were high.

These results showed the environmental friendliness of pesticides in addition of bamboo vinegar at the appropriate concentration.

5.7.7 Organophosphate insecticides

Organophosphates (Ops) are the most widely used insecticides today. They work by damaging the enzyme acetylcholinesterase (AChE), that is critical for controlling nerve signals in the body. The damage to this enzyme kills pests but may also cause unwanted side effects in exposed humans. In addition, the extensive use of these kinds of pesticides to enlarge the production in agriculture has dramatically increased their presence in the environment.

For this reason, all the possible degradation mechanisms of the same have been and continue to be the object of study. Even if the first studies on photodegradation date back to the early 1980s, only in 2007 a more general investigation of OPs photodegradation processes has been reported.[83]

Four OPs among which chlorpyrifos and azinphos-methyl in aqueous solution were degraded by using a 125 W xenon parabolic lamp. During the photoprocess, several intermediates were identified by GC−Ms, suggesting the pathway of OP degradation and their toxicity. The toxicity of photodegraded OPs was determined using a flow-injection analysis manifold (FIA-AChE-TLS).

The photodegradation of chlorpyrifos was completed within 120 min of irradiation. From the analysis, it has been found that the photodecomposition proceeds via first-order reaction kinetics and that chlorpyrifos-oxon is identified as the main photoproduct (Fig. 5.49).

The AChE-TLS bioassay measurements of irradiated samples indicate a 60% decrease of initial AChE activity. In any case, after 120 min of irradiation, AChE inhibition was still observed, which means that longer irradiation is required for the complete removal of toxic degradation products.

The photodegradation of azinphos-methyl also proceeds via first-order reaction kinetics. The complete degradation of the starting compound was achieved within the first 15 min and the GC−Ms analysis of irradiated samples indicates the formation of several photoproducts (Fig. 5.50).

The results obtained in AChE-TLS bioassay measurements indicate a 30% decrease of initial AChE activity. The reduced activity of the enzyme can be attributed mainly to formed trimethyl phosphate esters 1 and 4 in Fig. 5.50. Also, in this case, the complete removal of toxic compounds required longer irradiation times compared to those needed for the complete removal of parent pesticides.
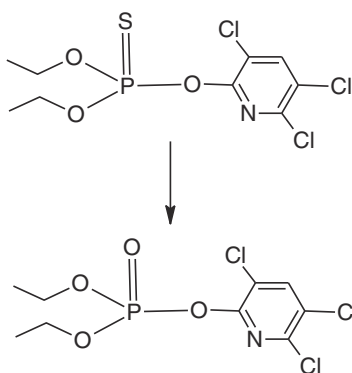
FIGURE 5.49 Main photodegradation product of chlorpyrifos.
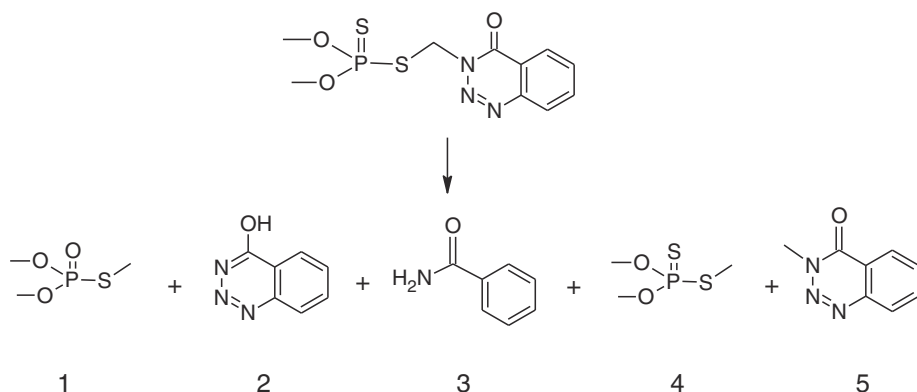
FIGURE 5.50 Main photodegradation products of azinphos-methyl.

These results demonstrate the importance of toxicity monitoring during the degradation of OPs in processes of waste-water remediation, before releasing it into the environment.

5.7.8 Triazine herbicides

Triazine herbicides are classified as persistent organic compounds because their biological and chemical degradation are very slow. This finding has led to their degradation into environmentally compatible compounds by photochemical methods. Numerous studies have been reported in this regard for the last 30 years.

The photodegradation of the unsaturated triazine derivatives has been investigated.[84]

	R=
1	-NHCH(CH$_3$)$_2$
2	-N(C$_2$H$_5$)$_2$
3	-N(CH$_3$)$_2$
4	-N(CH$_2$CH=CH$_2$)$_2$
5	-NHC$_2$H$_5$
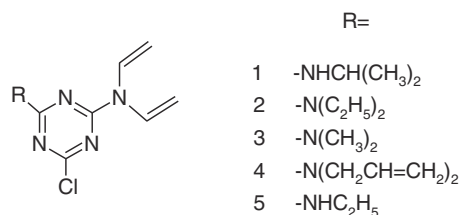
The course of the photodegradation in water solution was followed by HPLC. From analysis, the most stable triazine resulted to be 5, which reached appr. 70% degradation after 12 h.

The photodegradation rate, depending on the chemical structure of the compound, was decreasing in the order: 4 > 2 > 3 > 1 > 5.

In all cases, the photodegradation was relatively rapid, which was promising for their ecological behavior.

The photodegradation of other three triazines (atrazine, simazine, and prometryn) in aqueous solutions and natural waters using UV radiation has been studied, too.[85]

Photolysis experiments for the aqueous solutions and surface waters were carried out in a 500 mL Pyrex UV reactor, equipped with a diving Philips HPK 125 W high-pressure mercury lamp, accompanied by dark reaction controls.

All the studied pesticides disappeared by more than 90% after 25 h of UV radiation in the examined water systems, while dark decomposition was negligible.

The indirect photolysis (UV with H_2O_2) has been also studied. In this case, all the studied pesticides disappeared by more than 80% after only 6 h of radiation, which means that hydrogen peroxide in combination with UV light can significantly enhance the degradation efficiency. The reason is probably a radical mechanism.

In both cases, the rate of photodecomposition of aqueous solutions depends on the nature of the triazines and follows first-order kinetics.

The number of compounds detected during the degradation depends on the structure of the triazin (Fig. 5.51) and suggests the existence of different degradation pathways.

The photodegradation of prometryn has been also studied as residue in soil by exploring a variety of factors such as soil moisture, temperature, and light exposure that potentially affect prometryn photodegradation.[85]

Four moisture levels (0%, 40%, 60%, and 90%) were set to investigate the effect of soil moisture on photodegradation of prometryn. The effect of different moisture levels was confirmed for photodegradation, while it was insignificant under darkness. Specifically, when the soil moisture was 60%, the photodegradation was most effective and was increased with temperature and prometryn concentrations.

The degraded products of prometryn under UV light characterized using ultra high-performance liquid chromatography coupled to a linear ion trap-orbitrap hybrid mass spectrometer are reported in Fig. 5.52.

5.7.9 Triazinone herbicides

Metribuzin and metamitron are the widely used triazinone herbicides, and photodegradation studies about them are reported.

For example, the photodegradation of metribuzin in aqueous solution under simulated solar light irradiation was studied.[86] Irradiation of the aqueous solution (200 mL) was carried out in a cylindrical reactor equipped with a mercury lamp, and the concentrations of metribuzin were analyzed by high-performance liquid chromatography.
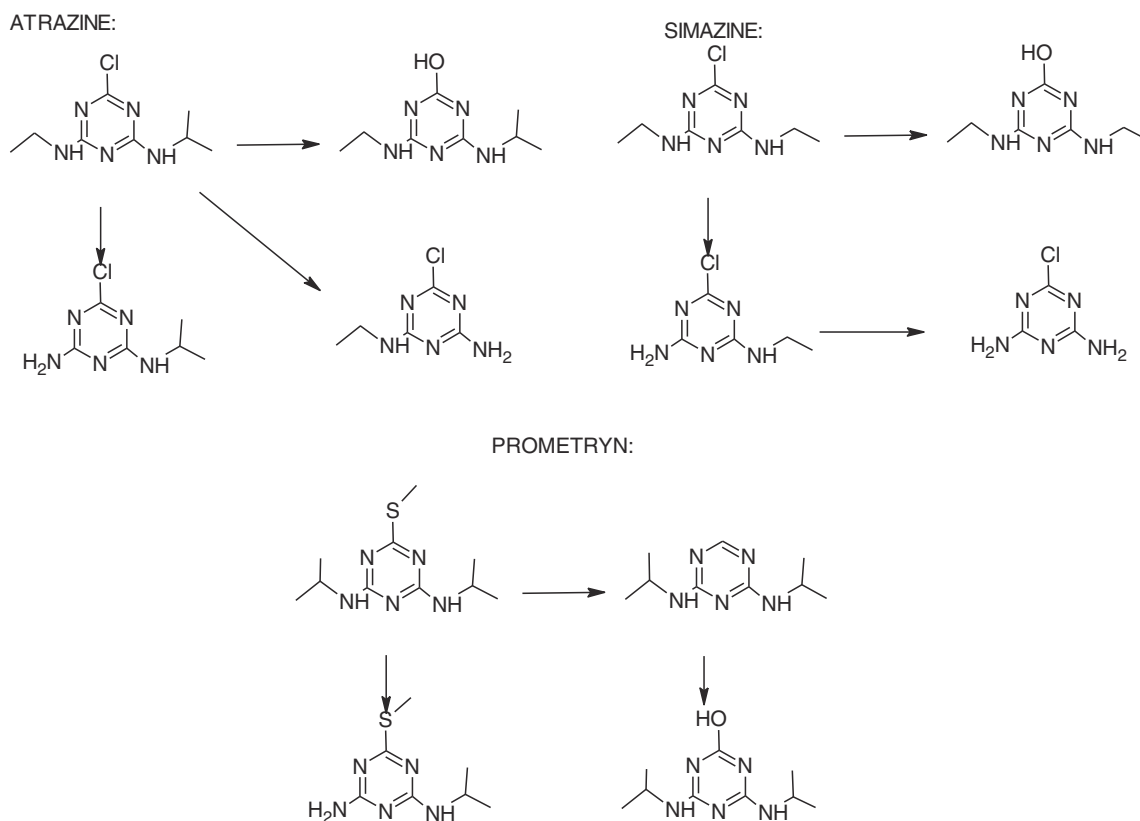
FIGURE 5.51   Main photoproducts of atrazine, simazine, and prometryn after photochemical degradation in natural waters.
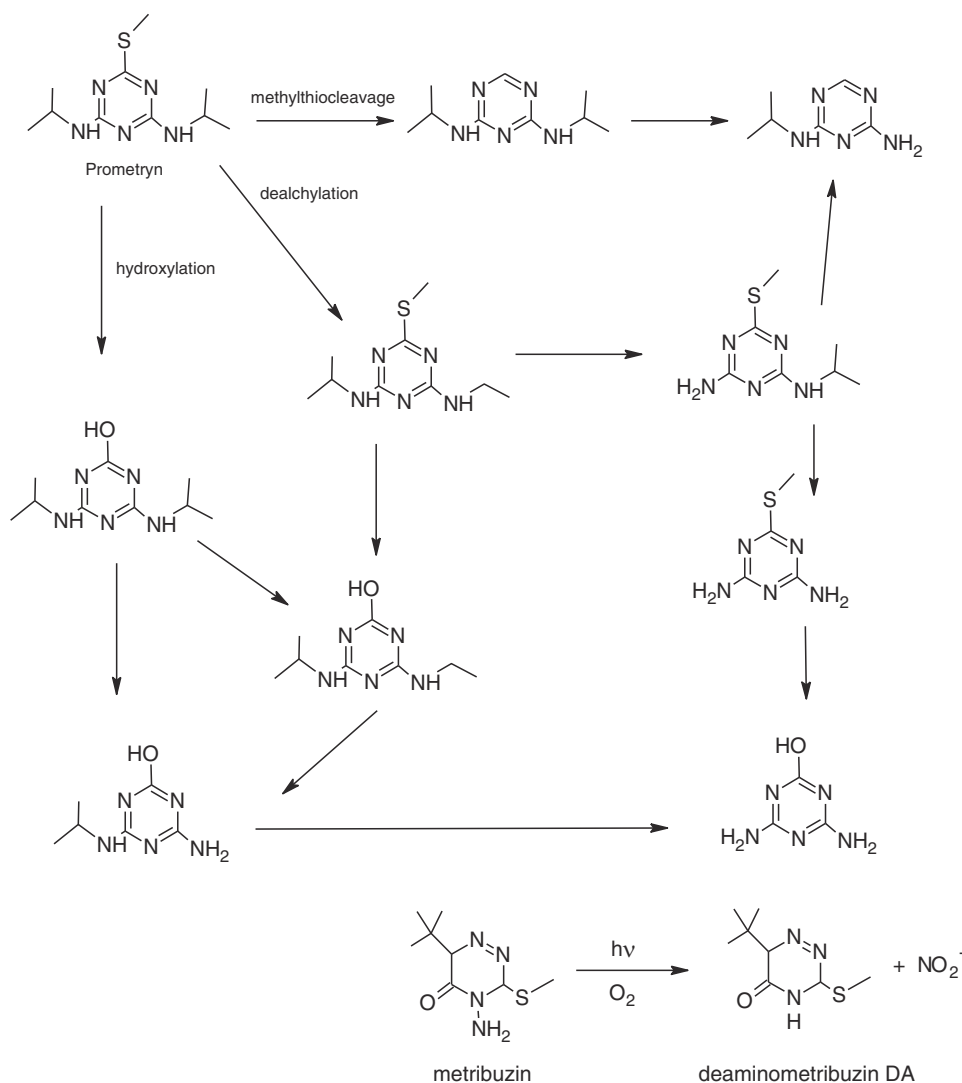
FIGURE 5.52   Proposed pathways of prometryn photodegradation in soil.

FIGURE 5.53   The major pathway for metribuzin degradation.

The photodecomposition of metribuzin was examined with different light intensities but also in the dark control experiment. In the first cases, metribuzen underwent obvious decomposition while in dark control experiment no significant change was observed even over 100 min.

In addition, the metribuzin was irradiated in N_2-saturated or in air-saturated solution, and the results showed that oxygen was an important factor for the photochemical transformation process due to the inhibiting effect of nitrogen.

The main photoproduct was identified as deaminometribuzin (DA) that means that the major pathway for metribuzin degradation was deamination to DA and nitrite (Fig. 5.53).

The influence of different pH was also examined, and the results showed that the reaction rate was higher in acidic and neutral than in alkaline solutions that is proton-donating solvents are necessary for deamination.

The effect of DOM by performing the irradiation experiment of metribuzin in the river water was also investigated. the presence of DOM lowered the degradation because of the DOM in the river water could compete with metribuzin to absorb the limited photons in the solution.

The photocatalytic degradation of metamitron was carried out using combustion synthesized nano-TiO_2.[87]

The photocatalytic degradation of metamitron using combustion synthesized TiO_2 (CS TiO_2) was compared with the same process using commercial TiO_2.

The photocatalytic activity of CS TiO_2 was superior compared to commercial TiO_2, and was attributed to its superior properties such as the presence of pure anatase phase, lesser crystallite size, better surface area and narrower band-gap compared to commercial TiO_2.

In both cases, the degradation of metamitron followed pseudo-first-order kinetics and the percentage of degradation of metamitron increased with increasing pH of the solution and a maximum 97% degradation was observed at a natural pH of the solution (pH = 8.4).

The by-products formed during the photocatalytic degradation of metamitron using CS TiO$_2$ were identified using LC/Ms analysis, and the mechanism shown in Fig. 5.54 was proposed.

5.7.10 Triazolopyrimidine herbicide

The triazolopyrimidine scaffold represents one of the privileged structures in chemistry, and there has been an increase in the number of studies utilizing this scaffold and its derivatives. The triazolopyrimidine ring has been extensively used as a template in medicinal chemistry as well as in herbicide chemistry with potential antifungal agents.

Florasulam (Fig. 5.55), for example, is a systemic herbicide used for the control of broadleaf weeds in cereals and pasture. Its mode of action is through acetolactate synthase (ALS) inhibition.

Although florasulam is rapidly degraded by microorganisms in soil,[88] abiotic degradation by photolysis has been also studied to determine the impact of florasulam on the environment.[89]

The photodegradation studies were carried out in both soil and water. In the first case, florasulam was applied to a moist viable and exposed to natural sunlight for up to 30 days. In the second one, florasulam was applied to a sterile pH 5 buffer at a rate of 100 ppb and exposed to natural sunlight for up to 32 days. Dark control samples were treated identically.

The results showed that florasulam degraded quickly in the soil systems, forming two degradants that reached significant concentrations (Fig. 5.56).

The same degradants were observed both in the exposed and the dark control samples, indicating that the degradants were formed by nonphotolytic degradation.

In the buffered water aqueous photolysis study, only one degradant (triazolopyrimidine sulfonic acid (TPSA)) was found at greater than 10% of the applied radioactivity.
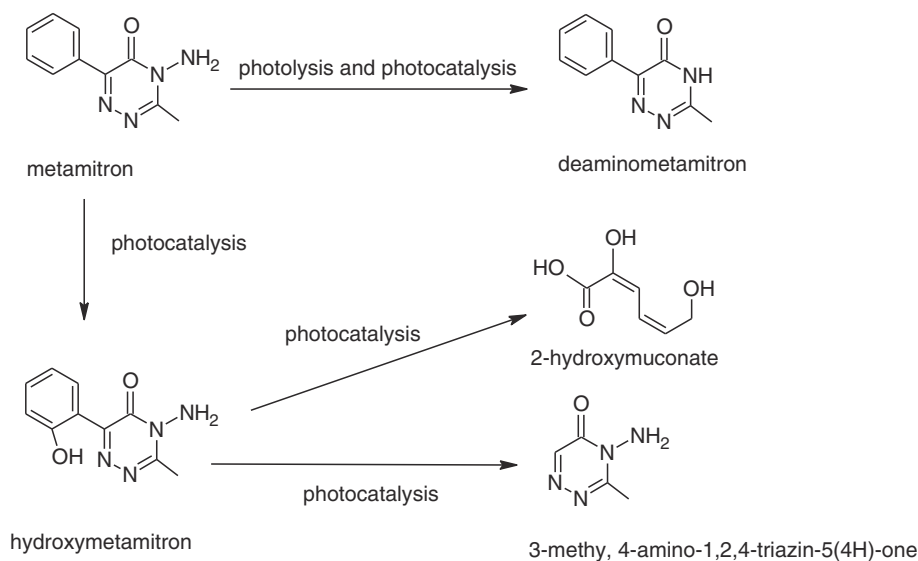
FIGURE 5.54 Proposed pathway for photocatalytic degradation of metamitron using combustion synthesized TiO$_2$.
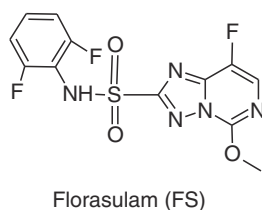
FIGURE 5.55 Structure of florasulam.
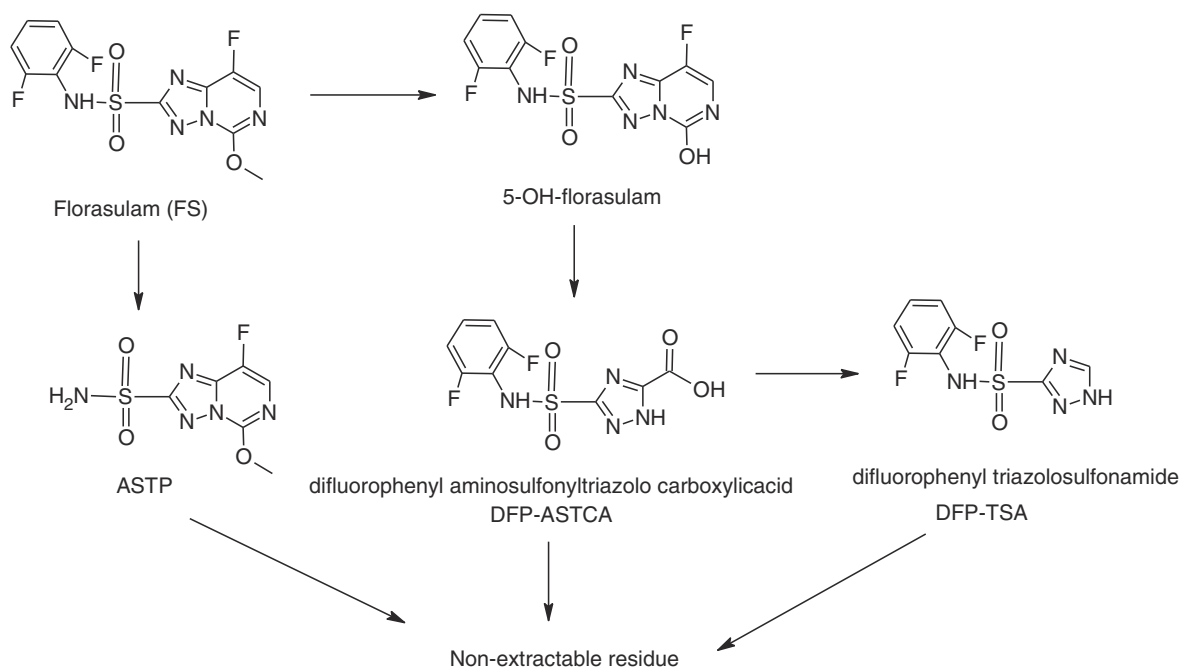
FIGURE 5.56 Proposed pathway for the degradation of florasulam in moist after exposure to natural sunlight.
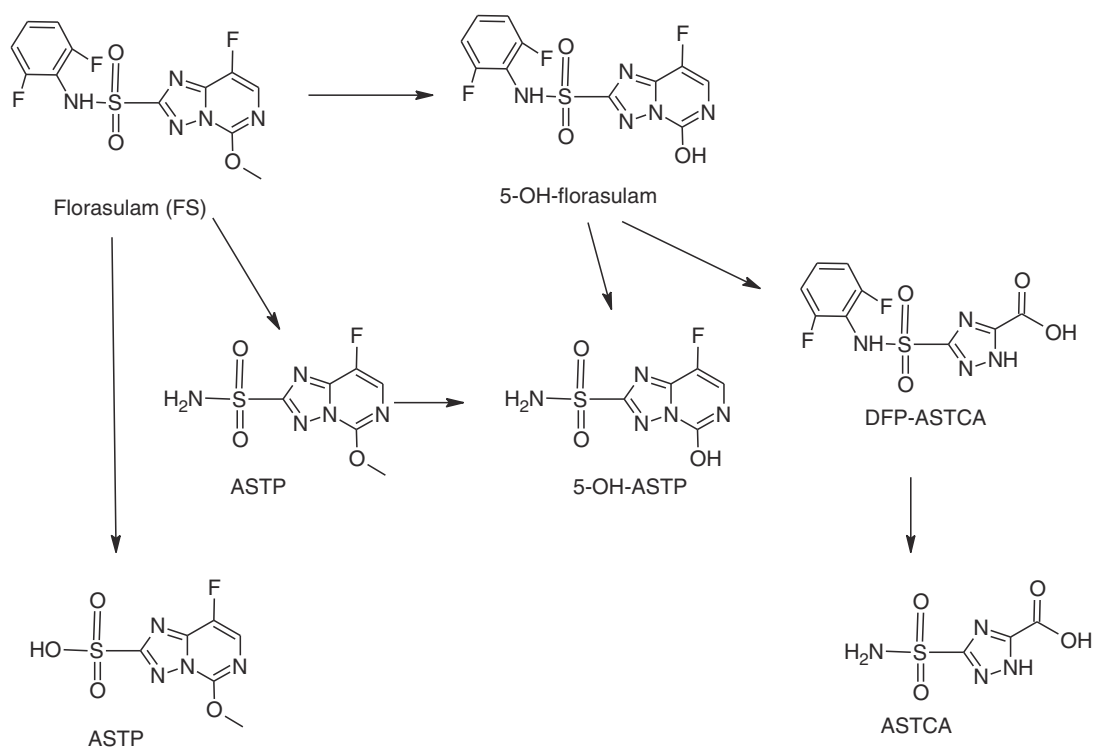
FIGURE 5.57 Proposed pathway for the degradation of florasulam in water after exposure to sunlight.

A substantially different route of degradation was observed in the natural water system: TPSA was not observed in any sample, and florasulam was transformed to two different degradation products (Fig. 5.57).

From the results, it is evident that indirect photolytic processes could be important contributors to the photolytic degradation of florasulam in aqueous environments.

Another triazolopyrimidine used as rice herbicide is penoxsulam (Fig. 5.58).

The phototransformation of penoxsulam was studied under UV and sunlight in aqueous methanol and acetonitrile in both the presence and absence of titanium dioxide (TiO$_2$) as sensitizer.[90]

A total of six photoproducts were identified and characterized based on the Q–T of micromass spectral data, and a probable mechanism of formation has been proposed. The plausible pathway of photodegradation is hydrolysis, photo oxidation of the sulfonamide group, breaking of sulfonamide bond, loss of amino and sulfonic acid group (Fig. 5.59).

Although the conditions used in the work differ from those in the practical use of penoxsulam, it is possible to conclude that the degradation products reported may occur in soil, water and plants, which have been exposed to the material in practical situations.

5.7.11 Unclassified pesticides

Unclassified or miscellaneous means it can not cause harm to humans or the environment. The reason is their disappearance in drinking or surface water under natural sunlight. Because of that, these pesticides are much less studied than the others. Despite this, it is possible to find some works in which the photocatalytic degradation of some has been studied.

Penoxsulam (PS)

FIGURE 5.58 Structure of penoxsulam.

FIGURE 5.59 Plausible pathway of photodegradation of penoxsulam in different solvent systems.

FIGURE 5.60 Molecular structures of the studied heterocyclic pesticides.

For example, the photodegradation of eight miscellaneous pesticides, including two heterocyclics (Fig. 5.60), has been reported.[91] Particularly, photolysis and photocatalysis with different semiconductors (ZnO, TiO_2, SnO_2, WO_3, and ZnS) have been studied to evaluate the effectiveness on disappearance of these pollutants in drinking water under natural sunlight.

The photolysis in the absence of the photocatalysts showed very low efficiencies as compared to the reactions in the presence of semiconductors and between them ZnO showed to be the most efficient and in this case the photodegradation followed a pseudo, first-order kinetics.

The effect of photocatalyst loading, $Na_2S_2O_8$ concentration, and pH has also been studied to optimize the process. Finally, the ZnO/ $Na_2S_2O_8$ system in combination with sunlight has been shown as the most advantageous system to remove these compounds from water.

References

1. Gomtsyan, A. Heterocycles in Drugs and Drug Discovery. *Chem. Heterocycl. Compd.* **2012,** *48.*
2. Lamberth, C. Heterocyclic Chemistry in Crop Protection. *Pest. Manag. Sci.* **2013,** 3615.
3. Albini, A.; Fasani, E. *Drugs Photochem. Photostab.* **1998.**
4. Moore, D. E. *Drugs Saf.* **2002,** *25* (5), 345−372.
5. Elghamry, I.; Letzel, M. C.; Mattay, J. *Trends Photochem. Photobiol.* **2012,** *14,* 21−25.
6. Nascimento, A.; Escobar, J.; Cilento, G. *Photochem. Photobiol.* **1993,** *57,* 362.
7. Elghamry, I.; El-Ayaan, U.; Youssef, M. M., et al. *Monatsh Chem.* **2017,** *148,* 257−262.
8. Volz, M.; Kellner, H. M. *J. Clin. Pharmac.* **1980,** *10,* 299S−308S.
9. Favier, M.; Van Schepdael, A.; Cabooter, D. *Chromatographia* **2019,** *82,* 261−269.
10. Sami, N. *Autoimmune Bullous Diseases: Approach and Management;* Springer, 201683.
11. Sahasranaman, S.; Howard, D.; Roy, S. *Eur. J. Clin. Pharmacol.* **2008,** *64,* 753−767.
12. Smarandaa, I.; Nilaa, A.; Mantab, C. B.; Samohvalovb, D.; Ghercab, D.; Baibaraca, M. *Result. Phys.* **2019,** *14.*
13. Gumieniczek, A.; Berecka-Rycerz, A.; Hubicka, U.; Zmudzki, P.; Lejwoda, K.; Kozyra, P. *Pharmaceutics* **2020,** *12,* 560.
14. Jochym, K.; Barton, H.; Bojarski, J. *Pharmazie* **1988,** *43* (9), 621−624.
15. Barton, H.; Bojarski, J.; Mokrosz, J. *Tetrahedron lett.* **1982,** 2133.
16. Thoma, K.; Struve, M. *Dtsch. Apoth. Ztg.* **1985,** *125,* 2062.
17. Bojarski, J.; Mokrosz, B. H.; Palachowska, M. *Adv. Heterocycl. Chem.* **1985,** *38,* 282.
18. Cabrera, C. G.; Goldberg, D. W.; Nudelman, N. S. *J. Phys. Org. Chem.* **2005,** *18,* 156−161.
19. The Photodegradation of Diazepam and its Human Metabolites in Water By Charles Edward West A thesis submitted to the University of Plymouth In partial fulfilment for the degree of DOCTOR (i)F PHILOSOPHY School of Earth, Ocean and Environmental Sciences Faculty ofScience University of Plymouth In collaboration with AstraZeneca Brixham Environmental Laboratory.
20. Trawiński, J.; Skibiński, R. *Environ. Sci. Pollut. Res.* **2017,** *24,* 1152−1199.
21. Prohotsky, D. L.; Juba, M. K.; Zhao, F. *J. Pain. Palliat. Care Pharmacotherapy* **2014,** *28* (4), 367−370.
22. Shetti, P.; Venkatachalam, A. *E-J Chem.* **2010,** *7,* S299−S313.
23. De Luca, M. D.; Ioele, G.; Spatari, C.; Ragno, G. *Int. J. Pharm. Pharm. Sci.* **2018,** *10* (1), 8.
24. Yong, C.; Qi Liang, B.; Danna, Z.; Zongping, W.; Tao, T.; Yuegang, Z. *J. Hazard. Mater.* **2013,** 252−253, 220−226.
25. Vargas, F.; Martinez Volkmar, I.; Sequera, J.; Mendez, H.; Rojas, J.; Fraile, G.; Velasquez, M.; Medina, R. *J. Photochem. Photobiol. B* **1998,** *42* (3), 219−225.
26. Vargas, F.; Mendez, H.; Sequera, J.; Rojas, J.; Fraile, G.; Velasquez, M. *Toxic. Substance Mech.* **1999,** *18* (2), 53−65.
27. Batt, A. L.; Kim, S.; Aga, D. S. *Chemosphere* **2007,** *68,* 428−435.
28. Kim, S. C.; Carlson, K. *Environ. Sci. Technol.* **2007,** *41,* 50−57.
29. Ibañez, M.; Guerrero, C.; Sancho, J. V. *J. Chromatogr. A* **2009,** *1216,* 2528−2539.
30. Kümmerer, K. *Chemosphere* **2009,** *75,* 417−434.
31. García-Galán, M. J.; Díaz-Cruz, M. S.; Barceló, D. *Environ. Int.* **2011,** *37,* 462−473.
32. Xu, L.; Ouyang, W.; Qian, Y.; Su, C.; Su, J.; Chen, H. *Environ. Pollut.* **2016,** *273,* 119−126.

33. Hughes, D. T.; Russell, N. J. *Rev. Infect. Dis.* **1982,** *2,* 528−532.
34. Amyes, S. G. B.; Doherty, C. J.; Wonnacott, S. *Scand. J. Infect. Dis.* **1986,** *18,* 561−566.
35. Fischl, M. A.; Dickinson, G. M.; La, V. L. *J. Am. Med. Assoc.* **1988,** *259,* 1185−1189.
36. Lude, H. *Infection* **1987,** *15,* S222−S226.
37. Yunus, M.; Mizanur Rahman, A. S.; Farooque, A. S.; Glass, R. I. *J. Trop. Med. Hyg.* **1992,** *85,* 195−198.
38. Hirsch, R.; Ternes, T.; Haberer, K.; Katz, K.-L. *Sci. Total Environ.* **1999,** *225,* 109−118.
39. Andreozzi, R.; Rafaele, M.; Paxeous, N. *Chemosphere* **2003,** *50,* 1319−1330.
40. Bueno, M. J. M.; Agüera, A.; Gómez, M. J.; Hernando, M. D.; García-Reyes, J. F.; Fernández-Alba, A. R. *Anal. Chem.* **2007,** *79,* 9372−9384.
41. Zhou, W.; Moore, D. L. *Int. J. Pharm.* **1994,** *110,* 55−63.
42. Trovó, A. G.; Nogueira, R. F. P.; Agüera, A.; Sirtori, C.; Fernández-Alba, A. *Chemosphere* **2009,** *77,* 1292−1298.
43. Ao, X.; Liu, W.; Sun, W.; Yang, C.; Lu, C. Y.; Lu, Z.; Li, C. *Chemosphere* **2018,** *212,* 365−375.
44. Zessel, K.; Mohring, S.; Hamscher, G.; Kietzmann, M.; Stahl, J. *Chemosphere* **2014,** *100,* 167−174.
45. Fabiańska, A.; Ofiarska, A.; Władyka, M.; Białk-Bielińska, A.; Kumirska, J.; Siedlecka, E.M. *Proceed. 4th Int. Conf. Environ. Pollut. Remed.* Prague, **2014,** 97-1/97-7.
46. Göbel, A.; McArdell, C. S.; Suter, M. J.-F.; Giger, W. *Anal. Chem.* **2004,** *76,* 4756−4764.
47. Challis, J. K.; Carlson, J. C.; Friesen, K. J.; Hanson, M. L.; Wong, C. S. *J. Photochem. Phobiol. A: Chem.* **2013,** *262,* 14−21.
48. García-Galan, M. J.; Díaz-Cruz, M. S.; Barceló, D. *Water Res.* **2012,** *46,* 711−722.
49. Xu, J.; Hao, Z.; Guo, C.; Zhang, Y.; He, Y.; Meng, W. *Chemosphere* **2014,** *99,* 186−191.
50. García-Galan, M. J.; Anfruns, A.; Gonzales-Olmos, R.; Rodriguez-Mozaz, S.; Comas, J. *Chemosphere* **2016,** *147,* 451−459.
51. Cbrdenas, A. M.; Vargas, F.; Femendez, E.; Hidalgo, M. E. *J. Photochem. Photobiol. B: Biol.* **1991,** *10,* 249−255.
52. Hidalgo, M. E.; Pessoa, C.; Fernandez, E.; Grdenas, A. M. *Photochem. Photobiol. A: Chem.* **1993,** *73,* 135−138.
53. Kraemer, S. A.; Ramachandran, A.; Perron, G. G. *Microorganisms* **2019,** *7* (6), 180.
54. Homem, V.; Alves, A.; Santos, L. *Sci. Total Environ.* **2010,** *408,* 6272−6280.
55. Pouretedal, H. R.; Hasanal, M. A. *Desalin Water Treat.* **2013,** *51,* 2617−2623.
56. Peleg, A. Y.; Hooper, D. C. *N. Engl. J. Med.* **2010,** *362,* 1804−1813.
57. Talbot, G. H.; Bradley, J.; Edwards, J. E.; Gilbert, D.; Scheld, M.; Bartlett, J. G. *Clin. Infect. Dis.* **2006,** *42,* 657−668.
58. Elfatih, I. A. K.; Kamal, E. I.; Mohamed, E. A. *Int. J. Pharm.* **1991,** *76* (3), 261−264.
59. Naveed., et al. *J. Bioequiv. Availab.* **2014,** *6,* 4.
60. Calza, P., et al. *J. Chromatogr. A* **2014.**
61. Chatzimpaloglou, A.; Christophoridis, C.; Fountoulakis, I.; Antonopoulou, M.; Vlastos, D.; Bais, A.; Fytianos, K. *Chem. Eng. J.* **2021,** 405.
62. Varanda, E. A.; Pozetti, G. L.; Lourenc, M. V.; Vilegas, W.; Raddi, M. S. G. *J. Ethnopharmacol.* **2002,** *81,* 257−264.
63. Thakur, A.; Sharma, R.; Jaswal, V. S.; Nepovimova, E.; Chaudhary, A.; Kuca, K. P. *Mini Rev. Med. Chem.* **2020,** *20* (18), 1838−1845.
64. Panno, M. L.; Giordano, F.; Rizza, P.; Pellegrino, M.; Zito, D.; Giordano, C.; Mauro, L.; Catalano, S.; Aquila, S.; Sisci, D., et al. *Breast Cancer Res. Treat.* **2012,** *136* (2), 443−455.
65. Bryantseva, N. G., et al. *Key Eng. Mater.* **2016,** *683,* 402−405.
66. Grover, R.; Cessna, A. J. *Environmental Chemistry of Herbicides;* CRC Press: Boca Raton, FL, 1991.
67. Katagi, T. *J. Pestic. Sci.* **2018,** *43* (2), 57−72.
68. Schwack, W.; Hartmann, M. Z. *Lebensm. Unters. Forsch.* **1994,** *198* (1), 11−14.
69. Bartett, D. W.; Clough, J. M.; Godfrey, C. R. A.; Godwin, J. R.; Hall, A. A.; Heaney, S. P., et al. *Pestic. Outlook* **2001,** *12,* 143−148.
70. Zhou, Z.; Yang, Y.; Zheng, Z.; Wang, M. *Water Sci. Technol.* **2017,** *76* (2), 364−372.
71. Correia, M.; Rodrigues, M.; Paíga, P.; Delerue-Matos, C. *Encyclopedia of Food and Health;* Academic Press, 2016169−176.
72. Schwack, W.; Walker, F.; Bourgeois, B. *J. Agric. Food Chem.* **1995,** *43* (12), 3088−3092.
73. Schwack, W.; Bourgeois, B.; Walker, F. *Chemosphere* **1995,** *31* (9), 4033−4040.
74. Schwack, W.; Bourgeois, B.; Walker, F. *Chemosphere* **1995,** *31* (9), 2993−3000.
75. Tan, S.; Evans, R. R.; Dahmer, M. L.; Singh, B. K.; Shaner, D. L. *Pest. Manage. Sci.* **2005,** *61* (3), 246−257.
76. Ramezani, M.; Oliver, D. P.; Kookana, R. S.; Gill, G.; Preston, C. *J. Environ. Sci. Health B* **2008,** *43* (2), 105−112.
77. Crouch, L. S.; Feely, W. F.; Arison, B. H.; VandenHeuvel, W. J. A.; Colwell, L. F.; Stearns, R. A.; Kline, W. F.; Wislocki, P. G. *J. Agric. Food Chem.* **1991,** *39* (7), 1310−1319.
78. Liu, Z.; Qie, R.; Li, W.; Hong, N.; Li, Y.; Li, C.; Wang, R.; Shi, Y.; Guo, X.; Jia, X. *N. J. Chem.* **2017,** *41,* 3190−3195.
79. Bachman, J.; Patterson, D. H. *Environ. Sci. Technol.* **1999,** *33,* 874−888.
80. Tomašević, A., et al. *Pestic. Phytomed. (Belgrade)* **2019,** *34* (3−4), 193−200.
81. Fenoll, J.; Garrido, I.; Hellín, P.; Flores, P.; Navarro, S. *Environ. Sci. Pollut. Res. Int.* **2015,** *22* (19), 15055−15066.
82. Liang, R.; Tang, F.; Wang, J.; Yue, Y. *PLoS One* **2019,** *14* (10), e0223708.
83. Bavcon Kralj, M.; Franko, M.; Trebse, P. *Chemosphere* **2007,** *67* (1), 99−107.
84. Korte, F.; Konstantinova, T.; Mansour, M.; Ilieva, P.; Bogdanova, A. *Chemosphere* **1997,** *35* (1/S), 51−54.
85. Jiang, C.; Li, X. J.; Wang, Y. R., et al. *Water Air Soil Pollut.* **2017,** *228,* 135.
86. Liu, H.; Guan, L. *Adv. Mater. Res.* **2012,** *518−523,* 436−439.
87. Prabhudesai, V. S.; Meshram, A. A.; Vinu, R.; Sontakke, S. M. *Chem. Eng. J. Adv.* **2021,** *5,* 100084.
88. Krieger, M. S.; Pillar, F.; Ostrander, J. A. *J. Agric. Food Chem.* **2000,** *48* (10), 4757−4766.
89. Krieger, M. S.; Yoder, R. N.; Gibson, R. *J. Agric. Food Chem.* **2000,** *48* (8), 3710−3717.
90. Pramanik, S. K.; Das, S.; Bhattacharyya, A. *J. Environ. Sci. Health B* **2008,** *43* (7), 569−575.
91. Fenoll, J.; Flores, P.; Hellín, P.; Martínez, C. M.; Navarro, S. *Chem. Eng. J.* **2012,** *204−206,* 54−64.

Index

Note: Page numbers followed by "*f*" and "*t*" refer to figures and tables, respectively.

Photochemistry of Heterocycles

A comprehensive review including photooxidation, photoreduction and photoaddition, as well as industrial aspects of heterocyclic photochemistry

By

Maurizio D'Auria
Professor, University of Basilicata, Potenza, Italy

Ambra Guarnaccio
Researcher, Institute of Structure of Matter (ISM) at the CNR-ISM, Tito Scalo, Italy

Rocco Racioppi
Associate Professor, University of Basilicata, Potenza, Italy

Sonia Stoia
Chemistry teacher, ITT "16 Agosto 1860", Corleto Perticara, Potenza, Italy

Lucia Emanuele
Associate Professor, Department of Art and Restoration, University of Dubrovnik, Dubrovnik, Croatia

Heterocyclic compounds are widely used in the modern world, and most of the drugs currently in use have heterocyclic nuclei among their constituents. These compounds are subject to a photochemical degradation processes which must be known and prevented. *Photochemistry of Heterocycles* is a comprehensive review of the topic, including photooxidation, photoreduction and photoaddition reactions as well as industrial aspects of heterocyclic photochemistry. Many materials used for the manufacturing of OLEDs and other electrooptical switches contain heterocycles, and the use of small molecules or polymers containing heterocyclic substances are being studied as new photovoltaic materials. This reference is ideal for synthetic organic chemists, specifically researchers working in organic photochemistry, as well as medicinal chemists and material scientists.

Key Features:

- Presents an authoritative and comprehensive review of the photochemistry of heterocycles

- Covers the full spectrum of photochemical reactivity

- Includes industrial aspects of heterocyclic photochemistry and materials used to manufacture OLEDs and other electrooptical switches